

This document was produced
by scanning the original publication.

Ce document est le produit d'une
numérisation par balayage
de la publication originale.



GEOLOGICAL SURVEY OF CANADA
COMMISSION GÉOLOGIQUE DU CANADA

**CURRENT RESEARCH 1994-A
CORDILLERA AND PACIFIC MARGIN**

**RECHERCHES EN COURS 1994-A
CORDILLÈRE ET MARGE DU PACIFIQUE**



1994



Natural Resources Canada
Ressources naturelles Canada

JAN 14 1994

\$ 14.95

\$ 16.98

Canada

NOTICE TO LIBRARIANS AND INDEXERS

The Geological Survey's Current Research series contains many reports comparable in scope and subject matter to those appearing in scientific journals and other serials. Most contributions to Current Research include an abstract and bibliographic citation. It is hoped that these will assist you in cataloguing and indexing these reports and that this will result in a still wider dissemination of the results of the Geological Survey's research activities.

AVIS AUX BIBLIOTHÉCAIRES ET PRÉPARATEURS D'INDEX

La série Recherches en cours de la Commission géologique contient plusieurs rapports dont la portée et la nature sont comparables à ceux qui paraissent dans les revues scientifiques et autres périodiques. La plupart des articles publiés dans Recherches en cours sont accompagnés d'un résumé et d'une bibliographie, ce qui vous permettra, on l'espère, de cataloguer et d'indexer ces rapports, d'où une meilleure diffusion des résultats de recherche de la Commission géologique.

GEOLOGICAL SURVEY OF CANADA
COMMISSION GÉOLOGIQUE DU CANADA

**CURRENT RESEARCH 1994-A
CORDILLERA AND PACIFIC MARGIN**

**RECHERCHES EN COURS 1994-A
CORDILLÈRE ET MARGE DU PACIFIQUE**

1994

© Minister of Energy, Mines and Resources Canada 1994

Available in Canada through
authorized bookstore agents and other bookstores

or by mail from

Canada Communication Group - Publishing
Ottawa, Canada K1A 0S9

and from

Geological Survey of Canada offices:

601 Booth Street
Ottawa, Canada K1A 0E8

3303-33rd Street N.W.,
Calgary, Alberta T2L 2A7

100 West Pender Street
Vancouver, B.C. V6B 1R8

A deposit copy of this publication is also available for reference
in public libraries across Canada

Cat. No. M44-1994/1

ISBN 0-660-58982-6

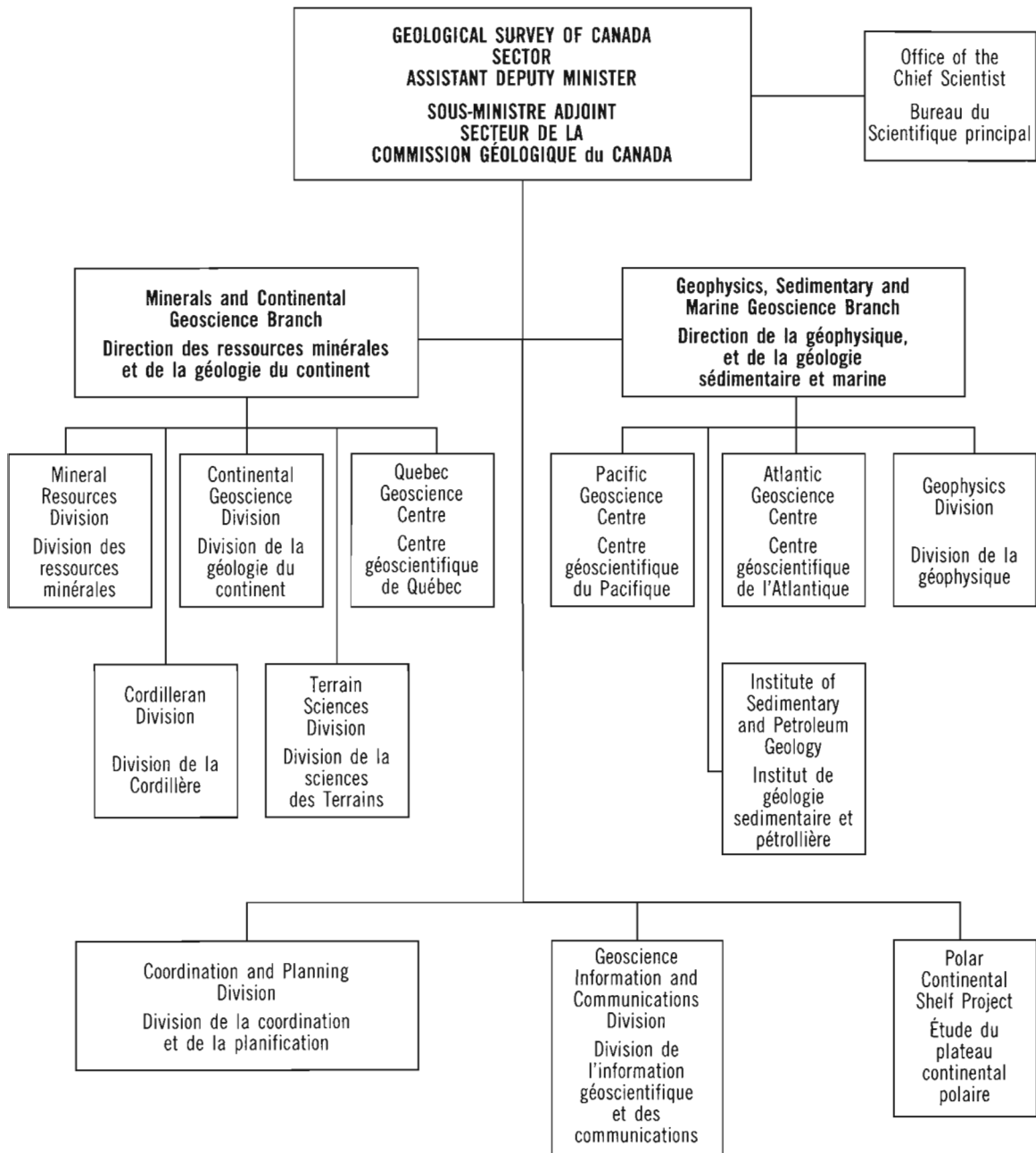
Price subject to change without notice

Cover description

View north across Iskut River to Hoodoo Mountain. Its distinctive domical shape and relatively flat summit suggest the origin of the Hoodoo Mountain volcanic centre as a tuya, or subglacial volcano comprising trachyte lava flows and domes interlayered with pyroclastic rocks and deposits erupted over the past 110 000 years. For more information on the Hoodoo Mountain centre see the report by Edwards and Russell on pages 67-76. (photo by R.G. Anderson, 1993; GSC 1993-304).

Description de la photo couverture

Le mont Hoodoo, vu vers le nord de l'autre côté de la rivière Iskut. La forme caractéristique en dôme et le sommet relativement plat du mont donnent à penser que le centre volcanique de Hoodoo Mountain était à l'origine un tuya, ou volcan sous-glaciaire, comportant des dômes et des coulées de laves trachytiques interstratifiés de roches et de dépôts pyroclastiques épanchés au cours des 110 000 dernières années. Pour de plus amples renseignements sur le centre volcanique de Hoodoo Mountain, voir le rapport par Edwards et Russell aux pages 67-76 (photo de R.G. Anderson, 1993; GSC 1993-304).



Separates

A limited number of separates of the papers that appear in this volume are available by direct request to the individual authors. The addresses of the Geological Survey of Canada offices follow:

601 Booth Street
OTTAWA, Ontario
K1A 0E8
(FAX: 613-996-9990)

Institute of Sedimentary and Petroleum Geology
3303-33rd Street N.W.
CALGARY, Alberta
T2L 2A7
(FAX: 403-292-5377)

Cordilleran Division
100 West Pender Street
VANCOUVER, B.C.
V6B 1R8
(FAX: 604-666-1124)

Pacific Geoscience Centre
P.O. Box 6000
9860 Saanich Road
SIDNEY, B.C.
V8L 4B2
(Fax: 604-363-6565)

Atlantic Geoscience Centre
Bedford Institute of Oceanography
P.O. Box 1006
DARTMOUTH, N.S.
B2Y 4A2
(FAX: 902-426-2256)

Québec Geoscience Centre
2700, rue Einstein
C.P. 7500
Ste-Foy (Québec)
G1V 4C7
(FAX: 418-654-2615)

When no location accompanies an author's name in the title of a paper, the Ottawa address should be used.

Tirés à part

On peut obtenir un nombre limité de «tirés à part» des articles qui paraissent dans cette publication en s'adressant directement à chaque auteur. Les adresses des différents bureaux de la Commission géologique du Canada sont les suivantes:

601, rue Booth
OTTAWA, Ontario
K1A 0E8
(facsimilé : 613-996-9990)

Institut de géologie sédimentaire et pétrolière
3303-33rd St. N.W.,
CALGARY, Alberta
T2L 2A7
(facsimilé : 403-292-5377)

Division de la Cordillère
100 West Pender Street
VANCOUVER, British Columbia
V6B 1R8
(facsimilé : 604-666-1124)

Centre géoscientifique du Pacifique
P.O. Box 6000
9860 Saanich Road
SIDNEY, British Columbia
V8L 4B2
(facsimilé : 604-363-6565)

Centre géoscientifique de l'Atlantique
Institut océanographique Bedford
B.P. 1006
DARTMOUTH, Nova Scotia
B2Y 4A2
(facsimilé : 902-426-2256)

Centre géoscientifique de Québec
2700, rue Einstein
C.P. 7500
Ste-Foy (Québec)
G1V 4C7
(facsimilé : 418-654-2615)

Lorsque l'adresse de l'auteur ne figure pas sous le titre d'un document, on doit alors utiliser l'adresse d'Ottawa.

CONTENTS

| | |
|--|----|
| Preliminary stratigraphy from Lansing map area, Yukon Territory C. Roots and D. Brent | 1 |
| Tectonic framework of the Teslin region, southern Yukon Territory S.P. Gordey and R.A. Stevens | 11 |
| Operation Bouguer – the final phase of a gravity survey in the northern Cordillera C. Lowe, D.A. Seemann, D.B. Hearty, and D.W. Halliday | 19 |
| New sulphide occurrences in the northeastern part of Iskut River map area and southeastern part of Telegraph Creek map area, northwestern British Columbia M.H. Gunning, K. Patterson, and D. Green | 25 |
| Stratigraphic and structural setting of mineral deposits in the Brucejack Lake area, northwestern British Columbia A.G.S. Davies, P.D. Lewis, and A.J. Macdonald | 37 |
| Geology of the Cambria Icefield: regional setting for Red Mountain gold deposit, northwestern British Columbia C.J. Greig, R.G. Anderson, P.H. Daubeny, K.F. Bull, and T.K. Hinderman | 45 |
| Recent basaltic volcanism in the Iskut-Unuk rivers area, northwestern British Columbia S. Hauksdóttir, E.G. Enegren, and J.K. Russell | 57 |
| Preliminary stratigraphy of Hoodoo Mountain volcanic centre, northwestern British Columbia B.R. Edwards and J.K. Russell | 69 |
| Geology and origins of the Zippa Mountain igneous complex with emphasis on the Zippa Mountain pluton, northern British Columbia B.A. Lueck and J.K. Russell | 77 |
| Northern continuation of the Eastern Waddington Thrust Belt and Tyaughton Trough, Tatla Lake-Bussel Creek map areas, west-central British Columbia P. van der Heyden, P.S. Mustard, and R. Friedman | 87 |
| Stratigraphy and sedimentology of the Tatla Lake-Bussel Creek map areas, west-central British Columbia P.S. Mustard and P. van der Heyden | 95 |

| | |
|---|-----|
| Preliminary study of Tertiary volcanic stratigraphy in the Clisbako River area, central British Columbia P. Metcalfe and C.J. Hickson | 105 |
| The geology and structure of the Coryell Batholith, southern British Columbia P. Stinson and P.S. Simony | 109 |
| A new regional mapping project in Vernon map area, British Columbia R.I. Thompson and K.L. Daughtry | 117 |
| Was the depositional environment of the Sullivan Zn-Pb deposit in British Columbia marine or lacustrine and how saline was it?: a summary of the data F.W. Chandler and G.A. Zieg | 123 |
| Field evidence for Early Proterozoic tectonism in core gneisses of Frenchman Cap dome, Monashee complex, southern Canadian Cordillera J.L. Crowley and P.M. Schaub | 131 |
| Geology of Big Bar map area, British Columbia: facies distribution in the Jackass Mountain Group C.J. Hickson, J.B. Mahoney, and P. Read | 143 |
| Preliminary studies of Recent volcanic deposits in southwestern British Columbia using ground penetrating radar M.V. Stasiuk and J.K. Russell | 151 |
| Turonian (Upper Cretaceous) strata and biochronology of southern Gulf Islands, British Columbia J.W. Haggart | 159 |
| Cayoosh Assemblage: regional correlations and implications for terrane linkages in the southern Coast Belt, British Columbia J.M. Journeay and J.B. Mahoney | 165 |
| Late Cretaceous to Paleogene cooling adjacent to strike-slip faults in the Bridge River area, southern British Columbia, based on fission-track and ⁴⁰ Ar- ³⁹ Ar analyses J.I. Garver, D.A. Archibald and W.F. Van Order, Jr. | 177 |
| The Ice River Complex, British Columbia T.D. Peterson and K.L. Currie | 185 |
| A gravitational origin for the Hell Creek 'fault', British Columbia J.J. Clague and S.G. Evans | 193 |
| An overview of the Vancouver-Fraser Valley hydrogeology project, southern British Columbia B.D. Ricketts and L.E. Jackson, Jr. | 201 |

| | |
|---|-----|
| A digital database for groundwater data, Fraser Valley, British Columbia G.J. Woodsworth and B.D. Ricketts | 207 |
| Ground-penetrating radar survey of the Brookwood aquifer, Fraser Valley, British Columbia J. Rea, R. Knight, and B.D. Ricketts | 211 |
| Preliminary studies of currents on Sturgeon Bank, Fraser River delta, British Columbia T.D. Feeney | 217 |
| Two centimetre-level Global Positioning System surveys of intertidal habitat, Fraser River delta, British Columbia J.A. Aitken and T.D. Feeney | 225 |
| Regional geology of the Cardston map area, Alberta D. Lebel | 231 |
| Quaternary geology and terrain inventory, Foothills and adjacent plains, southwestern Alberta: some new insights into the last two glaciations L.E. Jackson, Jr. | 237 |
| Author Index | 234 |

Preliminary stratigraphy from Lansing map area, Yukon Territory¹

C. Roots and D. Brent²
Cordilleran Division, Vancouver

Roots, C. and Brent, D., 1994: Preliminary stratigraphy from Lansing map area, Yukon Territory; in Current Research 1994-A; Geological Survey of Canada, p. 1-9.

Abstract: Lansing map area (105N) in Selwyn Basin of central Yukon Territory is separated into two structural domains by a southeasterly trending fault that appears to be the continuation of the Robert Service and Tombstone thrusts. The fault is bound to the southwest by isoclinally folded southwest-plunging, Proterozoic to Cambrian Hyland Group metasandstone and argillite. It is bound to the northeast for 40 km by Hyland Group, Ordovician to Devonian Road River Group and Devono-Mississippian Earn Group strata. In the northern and eastern parts of the map area, Hyland Group and lower Paleozoic off-shelf rocks are exposed in anticlines and thrust panels and are bounded by Road River Group rocks. Structures in southwest Lansing map area are similar to those in adjacent Mayo map area, while the strata in the northeast are continuous with units of adjacent Niddy Lake map area.

Résumé : La région cartographique de Lansing (105N), dans le bassin de Selwyn du centre du Yukon, est divisée en deux domaines structuraux par une faille de direction sud-est qui semble être le prolongement des failles de chevauchement de Robert Service et de Tombstone. La faille marque la limite nord-est de métagrès et d'argilite du Groupe de Hyland (Protérozoïque à Cambrien), déformés par des plis isoclinaux plongeant vers le sud-ouest. Sur une distance de 40 km, elle constitue la limite sud-ouest de couches du Groupe de Hyland, du Groupe de Road River (Ordovicien-Dévonien) et du Groupe d'Earn (Dévonien-Mississippien). Dans les parties nord et est de la région cartographique, les roches du Groupe de Hyland, ainsi que des roches du Paléozoïque inférieur qui représentent des milieux situés au large de la plate-forme continentale, affleurent dans des anticlinaux et des panneaux de charriage et sont encadrées par des roches du Groupe de Road River. Les éléments structuraux de la partie sud-ouest de la région cartographique de Lansing sont similaires à ceux de la région cartographique adjacente de Mayo, alors que les strates de la partie nord-est se situent dans la continuité des unités de la région cartographique adjacente du lac Niddy.

¹ Contribution to Canada-Yukon Mineral Resource Development Cooperation Agreement (1991-1996), a subsidiary agreement under the Canada-Yukon Economic Development Agreement.

² Canada-Yukon Mineral Development Agreement Geoscience Office, 2099-2nd Avenue, Whitehorse, Yukon Territory Y1A 1B5

INTRODUCTION

In recent years, ongoing regional mapping by the Geological Survey of Canada has resulted in new geological maps for areas adjacent to Lansing map area on the south (Tay River, 105I; Gordey and Irwin, 1987), west (Mayo, 105M; Roots and Murphy, 1992b), and east (Niddery Lake, 105O; Cecile and Abbott, 1992) sides (Fig. 1). In addition, the recent release of the Nahanni memoir (Gordey and Anderson, 1993) with formal descriptions of the Hyland Group (Precambrian to Lower Cambrian) and new Paleozoic units allows the stratigraphy of the northwestern Selwyn Basin to be defined with a new level of certainty. These advances in regional geology and stratigraphy provide the opportunity to improve Blusson's (1974) map of the Lansing area.

In 1993 a 3-year project toward a new 1:250 000 scale geological map for Lansing (105N) was initiated in partnership with the Canada-Yukon Geoscience Office (Government of Yukon) under the Economic Development Agreement (1991-1996). The first season consisted of 1:50 000 scale mapping of well-exposed areas. This note outlines the Selwyn Basin strata and large structures in Lansing map area.

REGIONAL SETTING

Lansing map area lies near the northern edge of the Selwyn Basin, which flanks the Mackenzie Platform rocks that are exposed in the Ogilvie and Wernecke mountains. Within the Selwyn Basin are late Proterozoic to Triassic off-shelf strata that were imbricated and thrust northward during the Mesozoic. The resulting Selwyn Fold Belt includes three regional thrust panels that overlie the Dawson, Tombstone, and Robert Service thrusts respectively.

The Robert Service Thrust extends eastward from north of Dawson for 200 km to northeastern Mayo map area (Gordey, 1990) and continues southeast across Lansing map area (Fig. 2). The Robert Service Thrust panel (RSTP) which was defined in Mayo map area (Roots and Murphy, 1992a) underlies the southwest third of Lansing map area. It comprises isoclinally folded Hyland Group overlain by open-folded Road River Group strata.

The northeastern two-thirds of Lansing map area is underlain by Hyland Group and a lower Paleozoic succession that probably extends southwest to correlate with strata in Niddery Creek map area. These strata, less deformed than those in the Robert Service Thrust panel, have also been transported northward, but this area is not a far-transported panel like the Robert Service Thrust panel. Although the Dawson Thrust lies 15 km north of Lansing map area, it does not extend further eastward, where shortening is probably accommodated by internal thickening of the sedimentary units.

The Tombstone Thrust has not been identified east of Mayo map area. Its identification is in part based upon the existence of Carboniferous Keno Hill Quartzite above the thrust. This unit was not recognized during 1993 in Lansing map area. It is possible that the Tombstone Thrust either: a) is not present because its northwest movement (Roots and

Murphy, 1992a) did not result in significant displacement in this area, or b) has been overthrust by the Robert Service Thrust.

STRATIGRAPHY

Five broad lithostratigraphic units and Cretaceous granitic rocks are present in Lansing map area (Fig. 2). From oldest to youngest the stratigraphic units are: Hyland Group, lower Paleozoic provisional units 1 and 2 (probable equivalents of Gull Lake and Rabbitkettle formations respectively), Road River Group, and Earn Group. We were able to identify only a few rock types that are unique to these units (such as maroon shale in Hyland Group and chert pebble conglomerate of the Earn Group) and lack the palaeontological control and understanding of the facies transitions needed to map the distribution of formations within these groups. The following is therefore a preliminary Lansing stratigraphy.

Hyland Group

The Hyland Group occurs in both the Robert Service Thrust panel and the northern and eastern regions (hereafter referred to as the Tasin Range and Surveys Range respectively) and

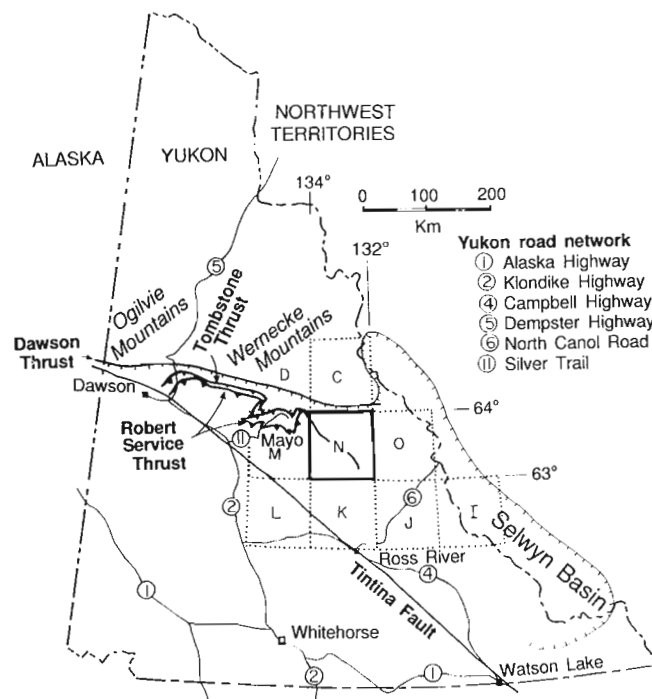


Figure 1. Lansing map area (box) within Selwyn Basin. The three major thrust faults (Dawson, Tombstone, and Robert Service) are shown. Letters denote map areas, as follows: 105I: Nahanni (Gordey and Anderson, 1993); 105J: Sheldon Lake, and 105K: Tay River (Gordey and Irwin, 1987); 105L: Glenlyon (Campbell, 1967); 105M: Mayo (Roots and Murphy, 1992b); 105N: Lansing (Blusson, 1974); 105O: Niddery Lake (Cecile and Abbott, 1992); 106C: Nadaleen River (Blusson, 1974); 106D: Nash Creek (Green, 1972).

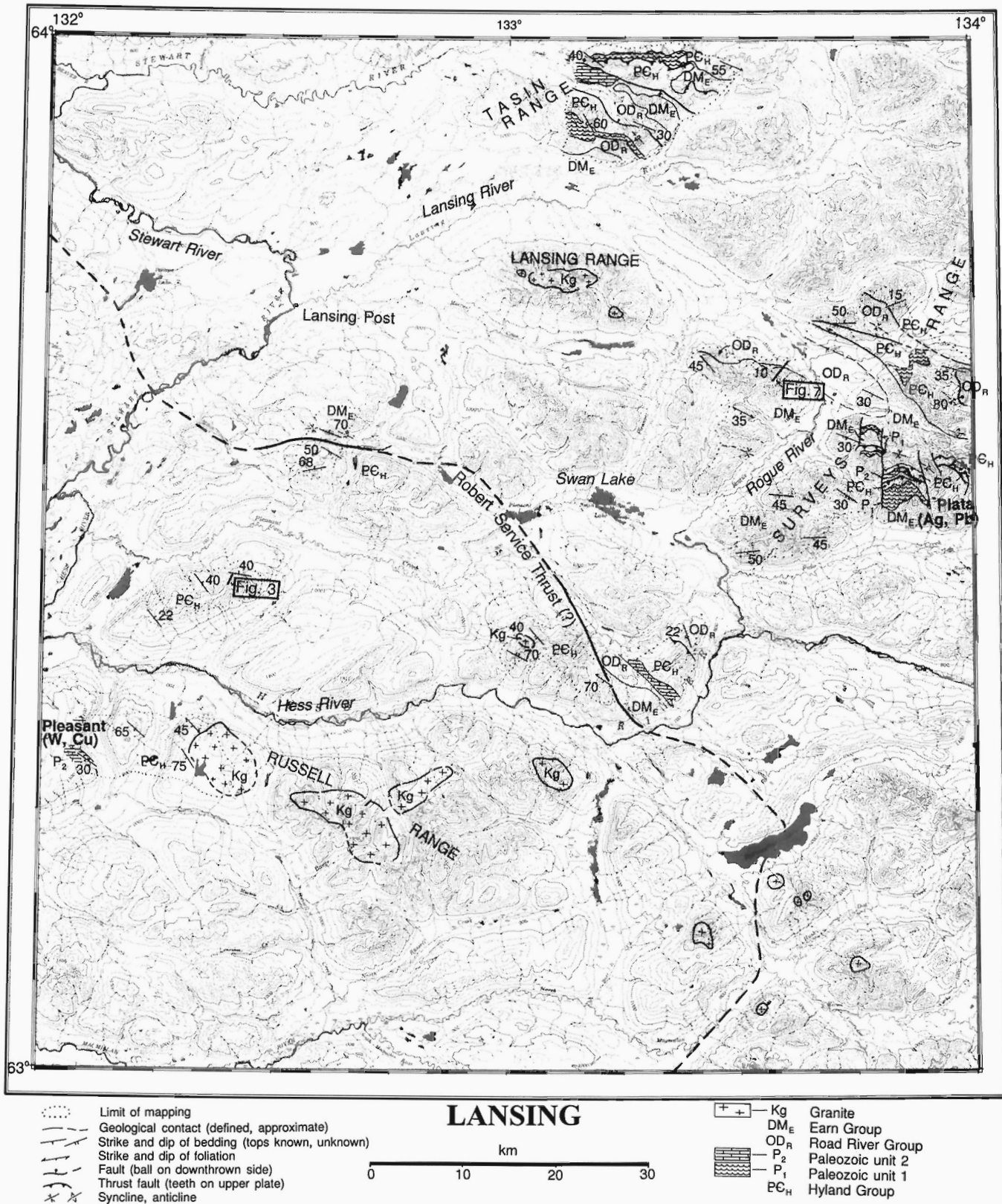


Figure 2. Lansing map area showing areas examined in 1993 and location of sections depicted in Figures 3 and 7. The distribution of granitic intrusions and approximate trace of the Robert Service Thrust are modified from Blusson (1974).

its base is not exposed. Metamorphosed grit and sandstone predominate in the Robert Service Thrust panel with a few localities of maroon argillite and limestone lenses. These rocks are unconformably overlain by, or more commonly faulted against, younger units. In the Surveys and Tasin ranges, the Hyland Group consists of medium- and thin-bedded sandstone overlain by a carbonate interval and maroon argillite. The upper part of the Hyland Group is intercalated with, and conformably overlain by, mafic volcanic rocks and shales of Paleozoic units 1 and 2. The Hyland Group is everywhere structurally thickened by internal folding and minor thrusts.

In the Robert Service Thrust panel the monotonous meta-grit succession consists of resistant beds from 5 to 20 m thick, separated by recessive intervals of green or brown meta-siltstone and phyllitic mudstone. South of Swan Lake well-exposed lenticular and branching grit bodies suggest sediment gravity flows, as described by Gordey and Anderson (1993, p. 47).

An unusual fine grained succession was measured (Fig. 3) 30 km south of Lansing Post. At least 460 m of sandstone with phyllitic interbeds is overlain by 400 m of siltstone and argillite with thin sandstone beds. In this upper succession is a prominent grey-weathering limy siltstone interval 90 m thick. Chloritic sandstone, the top of which is not preserved, caps the succession.

Limestone lenses are sparse although widely distributed in Robert Service Thrust panel. Most are strongly recrystallized and less than 15 m thick. Maroon argillite is likewise rare and discontinuous, in contrast to the mappable belts across southern Mayo map area. One tectonically thickened exposure of maroon argillite underlies Paleozoic unit 2 at the Pleasant (Cu,W) showing.

In the Tasin and Surveys ranges four units comprise the Hyland Group: a lower sandstone, an upper maroon argillite, and two thinner units in between them. One of these is dominantly limestone, the other includes alternating sandstone and argillite. These four units are described below.

The oldest exposed rocks in northern Lansing map area are light brown fissile sandstone, medium brown weathering grit, and interbedded brown and khaki mudstone. In contrast to the siliciclastic Hyland Group rocks in the Robert Service Thrust panel, these northern successions contain minor grit-size sediment, and are commonly thin- or medium-bedded. Limy quartz arenite is most abundant in beds 5-20 cm thick with recessive partings (Fig. 4) that have a pink-weathering hue. Wavy bedding is very common and planar cross-stratification was observed in two places.

This unit resembles the Yusezyu Formation described by Gordey and Anderson (1993) and is continuous with map unit Hq (Cecile and Abbott, 1992) in the adjacent Nidderly Lake map area.

In the northern Surveys Range, beige-weathering limestone overlies the sandstone, but in other areas and the Tasin Range the limestone is enclosed by maroon argillite. The limestone is grey and finely crystalline, in thick beds with dark mudstone partings, and estimated to be about 50 m thick.

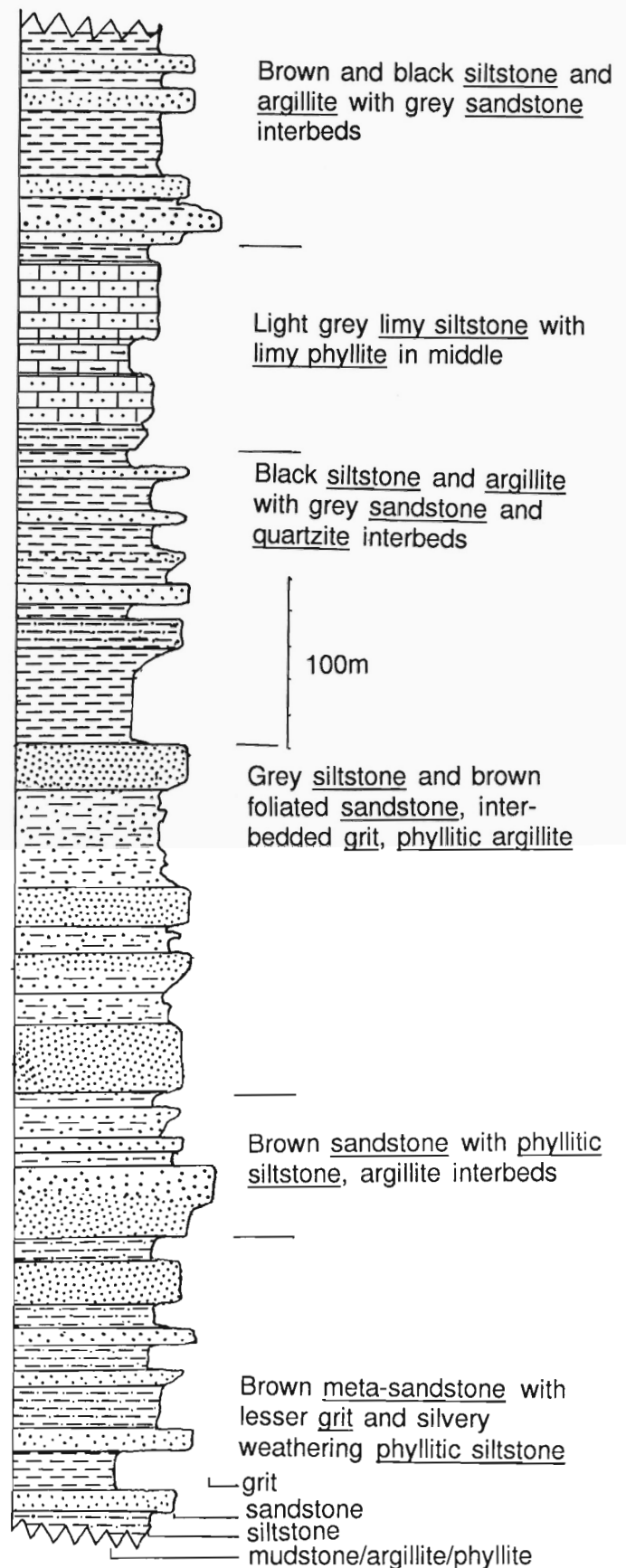


Figure 3. Stratigraphic section of Hyland Group strata (63°29'N, 133°33'W).

This unit adjoins map unit H1_b (Cecile and Abbott, 1992) at the east edge of Lansing map area where it separates sandstone from maroon argillite.

The third unit in Hyland Group consists of sandstone beds 20-80 cm thick interbedded with maroon argillite. This formation is prominent in the northern part of the Surveys Range where it is at least 45 m thick, but also occurs in the south-western Tasin Range. It is distinguished by beige-weathering beds of limy laminated siltstone. This unit probably correlates with map unit Hma of Cecile and Abbott (1992).

Maroon to wine-red argillite is widely exposed in the Surveys and Tasin ranges. This unit also includes green and brown argillite and siltstone. The maroon argillite contains single beds of grey- or beige-weathering, fine grained sandstone, and dark brown quartz grit 1-6 cm thick. A few top determinations have been obtained from load casts at the base of the sandstone, and burrowing marks are present where slaty cleavage has not destroyed sedimentary textures. The trace fossil *Oldhamia* occurs among indurated green-brown slate in the southeastern Surveys Range. This fine grained clastic unit corresponds to map unit ICma (Cecile and Abbott, 1992) in Niddery Lake map area.

Lower Paleozoic unit 1

Mafic volcanic flows, volcanoclastic conglomerate, and mudstone comprise this unit. All components of this unit contain chlorite which generally appears to have resulted from the breakdown of ferromagnesian minerals. The flows and tuffs form resistant knobs and buttresses with cliff sections coated by white calcareous precipitate. Volcanoclastic and mudstone successions are thickly layered and appear dark grey with lighter-weathering bands (Fig. 5).

This unit occurs in discrete bands in the northern parts of both the Surveys and Tasin ranges. Volcanic flows and interbedded tuffs form discontinuous accumulations up to 300 m thick near the Rogue River. Volcanoclastic conglomerate is the ubiquitous lithology; is found in most exposures less than 50 m thick but a 1300 m succession is exposed about 6 km southwest of the Plata property. At this locality the

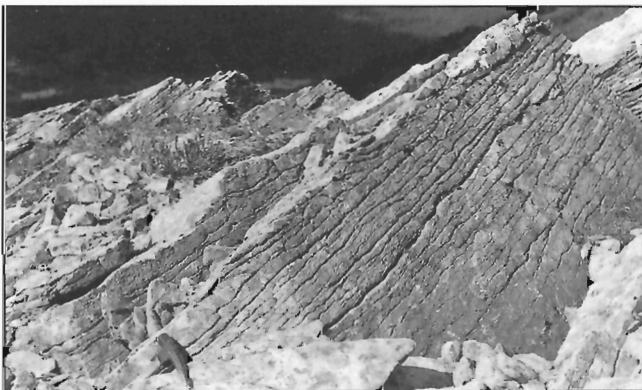


Figure 4. Yusezyu Formation in the Surveys Range. The thin-bedded sandstone contains 15% quartz grains of greater than 0.5 mm diameter in limy cement.

lowest 25 m consists of parallel laminated grey and black siltstone and intercalated laminated limestone, both of which weather light orange. Throughout the Surveys Range are numerous occurrences (too thin to depict on Fig. 2) of dark grey and rusty shale and mudstone with fine sandstone interbeds. In the Tasin Range, however, a layered succession of volcanic siltstone and sandstone is over 400 m thick.

Each occurrence overlies maroon argillite although a conformable contact has not been confirmed. Some volcanic tuffs appear interbedded with maroon argillite although interleaving by low-angle faults cannot be discounted.

Flows are massive, from 3 m to more than 10 m thick, with zones of calcite-filled vesicles. Pillow structures appear locally, but are generally obscured by closely spaced brittle fractures. The chloritic sandstone-siltstone successions are well bedded at decimetre scale, with ripple laminations and grey quartzite interbeds. The 400 m succession in the Tasin Range consists of dark green, indurated sandstone layers 1-5 m thick, separated by a few centimetres of siltstone and several 10 m thick bands of light-weathering quartz grit in the upper half of the succession. These beds contain concretions.

The mudstone successions included in this unit are thick bedded, locally laminated, and typically mottled, perhaps as a result of bioturbation. A common characteristic is a purple or indigo weathering patina on the crumbly mudstone. The volcanoclastic conglomerate has similar mudstone as framework support for green siliceous clasts. Most clasts are subrounded, smooth-surfaced lumps, and some are 1.5 m in diameter, although small cobble size is most common. At the top of an 800 m thickness of volcanoclastic mudstone is at least 50 m (top not preserved) of light green claystone which forms smooth, thin plates in contrast to the crumbly mudstone below.



Figure 5. Thickly bedded mafic tuff layers in the Tasin Range. The light coloured layers have limy matrix.

Light weathering quartzite, typically mauve on fresh surface, is present as lenticular beds within the mudstone. In the 1920 m peak section two lenses are more than 100 m long and up to 15 m thick. In addition, blocks of pebbly grit with abundant white quartz clasts occur at the base of the mudstone in two localities.

Paleozoic unit 1 represents a period of volcanism and renewed coarse clastic input following deposition of the Hyland Group. Volcanic source areas probably existed in the northern Surveys Range, and in Nidderly map area where map unit Cav of Lower to Upper(?) Cambrian age is extensive (Cecile and Abbott, 1992). The age and extent of the thick volcanoclastic succession in the Tasin Range is unknown.

This unit in both map areas is in the equivalent stratigraphic position to the Gull Lake Formation described by Gordey and Anderson (1993), although volcanic rocks are not present in the formation. Furthermore, the diagnostic basal carbonate conglomerate has not been found in Lansing map area.

Lower Paleozoic unit 2

This unit consists of four different lithological successions occupying the same stratigraphic interval at four widely separated localities (Fig. 2). In the Surveys Range, it consists of thin-bedded limestone, grey mudstone and wispy laminated siltstone. In the Tasin Range, brown-weathering green argillite and siltstone containing thin-bedded limy siltstone is capped by a light grey limestone more than 50 m thick. South of Swan Lake, graded limy siltstone is overlain by tan-weathering brown shale with pods of grey limestone. At the Pleasant (Cu,W) occurrence in the Robert Service Thrust panel, a section of thick-bedded limestone is overlain by thin-bedded limestone and limy siltstone. Each locality is distinguished by light-weathering carbonate cliff bands above maroon argillite (Hyland Group) but the intervening lithological sequence varies.

The best exposure of unit 2 in the Surveys Range overlies 20 m of black shale and calc-phyllite (Lower Paleozoic unit 1) with apparent conformity, and therefore the lowest limestone bed is designated the base of the unit. The limestone beds are irregular in thickness and locally nodular (Fig. 6). Fresh surfaces of the limestone are smooth and grey but weather beige, with brown ochre along the mudstone partings. Intercalated mudstone is dark grey with lighter silty streaks.

At the Pleasant (Cu,W) showing the basal white crystalline limestone is about 40 m thick and conformably overlies maroon argillite. This massive carbonate is succeeded by olive-brown-weathering shale (at least 50 m), and in turn conformably overlain by brown limestone interbedded with mauve and green limy siltstone. Planar crossbeds are common in the limy siltstone.

Some lower Paleozoic unit 2 occurrences resemble the Cambro-Ordovician Rabbitkettle Formation; in particular the nodular limestone and thin-bedded mauve and green siltstone in the Surveys Range. In the Robert Service Thrust panel, the white limestone at Pleasant (Cu,W) showing is probably the same carbonate marker traced by Blusson (1974) about 15 km

southeast, and may correlate with thick-bedded Cambro-Ordovician limestone in adjacent Tay River map area (map unit CO_r; Gordey and Irwin, 1987).

Road River Group

In Lansing map area the Road River Group consists of chert and mudstone with lesser black quartzite and siltstone. This unit can only be unambiguously distinguished from overlying Earn Group with fossils. *Monograptids* were found in the northern Surveys Range and therefore the associated dark-weathering, thick bedded chert has provisionally been used to define areas of Road River Group rocks. They occur in broad belts across the Tasin Range, mountains southeast of the Lansing Range, and along the north side of the Robert Service Thrust.

The chert with shale interbeds is commonly thickened by structural repetition. The base is rarely exposed because thrusts bring this unit over less competent shales. Locally, the Road River unconformably overlies maroon argillite of the Hyland Group. The top of Road River is not clearly defined except where chert pebble conglomerate, a diagnostic lithology of the Earn Group, occurs at the base of that unit.

A measured section southeast of the Lansing Range consists of black mudstone and thin bedded chert (at least 310 m), overlain by 120 m of black quartzite in thin beds with fine laminations (Fig. 7). The chert forms massive, uneven beds several metres thick separated by grey-weathering black



Figure 6. Thin bedded and nodular grey limy siltstone with dark brown mudstone interbeds in lower Paleozoic unit 2. This lithology is 15 m thick and may correlate with the Rabbitkettle Formation.

shale. Chert is mottled grey and locally altered to dark blue or green, with nobby bedding planes suggestive of bioturbation. Grey-weathering, parallel laminated black quartzite beds in association with thick bedded chert are traceable for 12 km toward the Surveys Range.

This unit matches map unit ImOc of Nidderly Lake map area but the Sa division of Road River Group there (Cecile and Abbott, 1992) has not been recognized in Lansing map area.

Earn Group

This unit contains black siliceous siltstone, chert pebble conglomerate, dark coloured shales with lesser quartzite, and limestone. The first two rock types are distinctive of the Earn Group throughout the Selwyn Basin, as is the pronounced light blue weathering of the carbonaceous siltstone.

The Earn Group rocks probably dominate a 40 km wide belt across Lansing map area north of the Robert Service Thrust. The contact with the underlying Road River rocks is not defined. Strata overlying the Earn Group have not yet been encountered in Lansing map area. In all localities the unit has been repeated by folds and minor thrusts so that its true thickness is unknown.

The black siltstone is thin bedded, with black argillite intercalations. Concretions, which weather out as 2-4 cm spheres, are abundant in several places, and diagenetic pyrite cubes are common.

The conglomerate occurs in lenses up to 500 m thick. These lenticular bodies are thickly bedded or massive and consist mostly of cobbles of grey chert and dark grey argillite, framework supported in a sand or silt matrix. In the Surveys Range some conglomerate is prominently white-weathering as a result of bleaching and crumbling of the silicified matrix. Similar alteration and intense fracturing were noted in a chert succession west of the Rogue River, generally along strike and believed correlative with the conglomerate.

Thin bedded black chert is provisionally included in Earn Group, although fossil confirmation is needed. The chert forms orange-brown bands up to 100 m thick that locally exhibit bright yellow and orange oxide streaks. Some chert beds exhibit internal layering revealed by convoluted boundaries of bleached and unbleached chert. Two barite horizons have been located.

A succession of brown and black siltstone also contains widely spaced chert bands 5-10 m thick, sandstone, medium bedded grey limestone, and a single massive white quartzite bed. All these layers can be traced across the southwestern Surveys Range and may be useful markers in the central part of Lansing map area. The Earn Group strata reflect facies changes not yet understood in Lansing map area because both the conglomerate and the chert occur near the base of the unit in different places. These strata match the lithological descriptions of many map units described by Cecile and Abbott (1992) in adjacent Nidderly Lake map area.

Igneous rocks

Five granitic stocks in the Lansing and Russell ranges, and numerous plugs are part of the west-trending Selwyn Plutonic Suite (Woodsworth et al., 1991). Only the westernmost stock in the Russell Range was examined in 1993. It consists of medium grained, equigranular and unfoliated biotite granite.

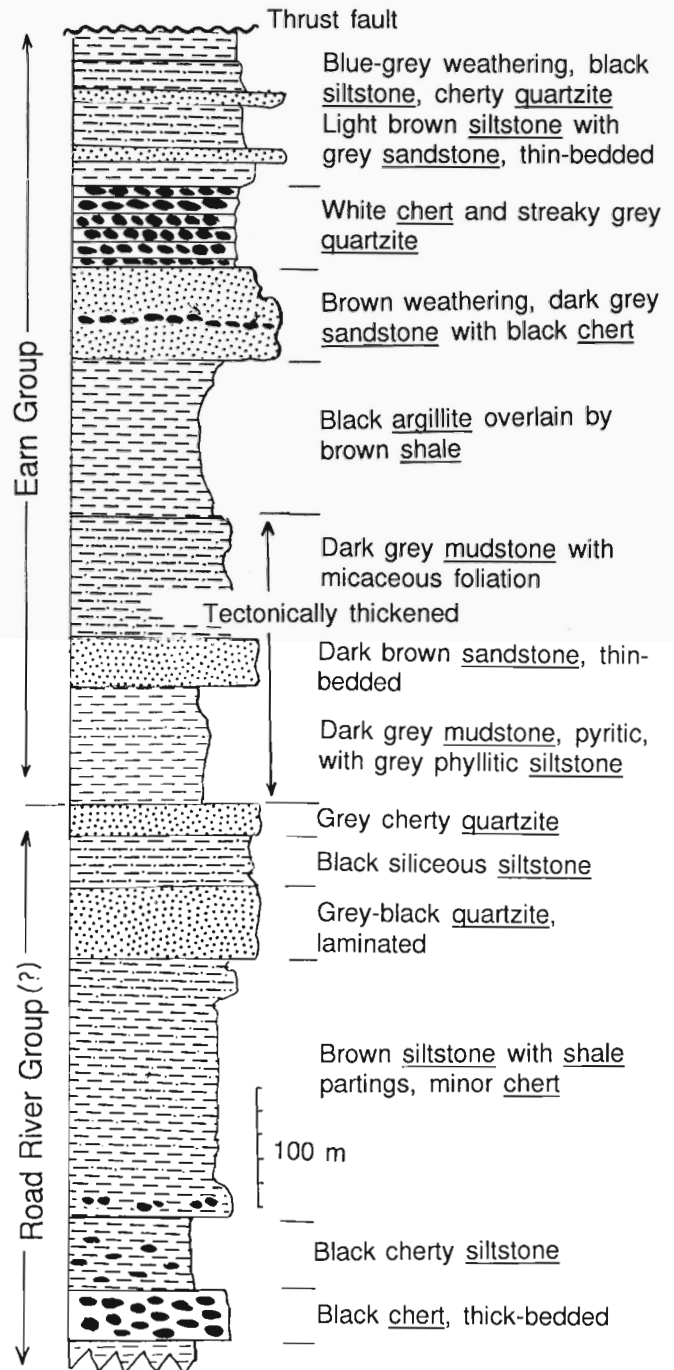


Figure 7. Stratigraphic section of Road River and Earn Group strata, west of Rogue River (63°42'N, 132°27'W).

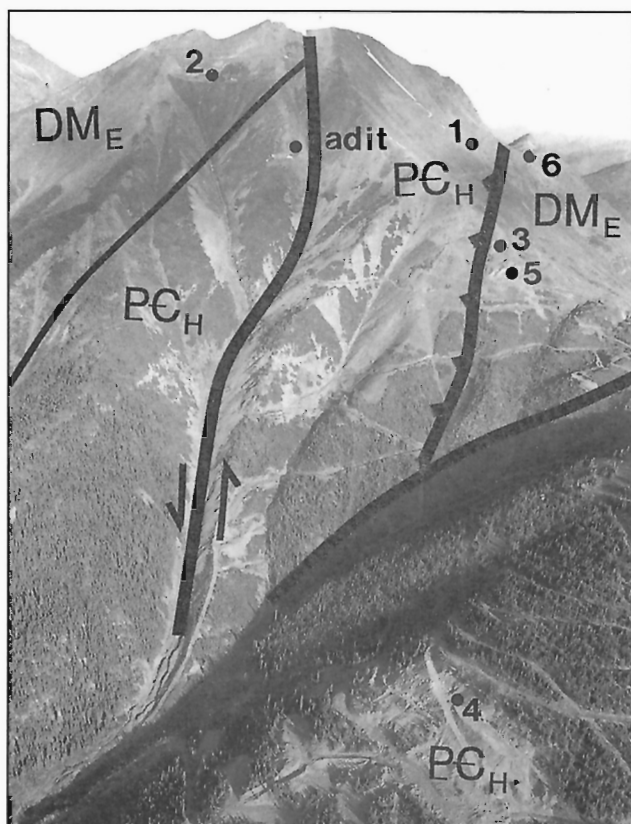


Figure 8. Aerial view looking northwest at the PLATA property. Numbers denote silver-lead veins that were mined between 1976 and 1985. Maroon argillite of the Hyland Group (PCH) is thrust over black shales and chert of the Earn Group (DM_E) and offset by steep normal faults.

These intrusions are likely to be coeval with the Two Buttes stock in Mayo map area which has yielded a 92.4 Ma U-Pb zircon age (J.K. Mortensen, written comm., 1993).

Quartz-feldspar dykes up to 20 m thick in the Surveys Range trend 300° and dip steeply south. Their white-weathering, kaolinized matrix contains up to 15% feldspar and 10% quartz phenocrysts. The dykes might be offshoots of Cretaceous stock exposed in Niddery Lake map area near the north end of the Surveys Range.

LARGE SCALE STRUCTURES

In the Robert Service Thrust panel the pervasively foliated Hyland Group rocks are southwest-dipping, although some areas, such as the succession at Figure 3, dip northward. Map-scale isoclinal folds exposed in the Russell Range demonstrate that the great thickness of uniformly dipping rocks results from layer-parallel folds and faults. The few minor folds encountered are northward-verging with axes plunging gently northwest. In each locality, foliation appeared to parallel to primary bedding. In Mayo map area, study of rock

fabrics revealed that the Robert Service Thrust panel underwent at least two deformation phases (Roots and Murphy, 1992a). A second, overprinted fabric has not yet been recognized in Lansing map area.

In the Surveys and Tasin ranges, open folds are outlined by Hyland Group sandstone. Box anticlines that plunge gently southeastward typify the Tasin Range, and some steeply overturned limbs expose more than 1 km of stratigraphy. Some of these anticlines of Hyland Group rocks are clearly the leading edges of shallow thrusts over black Earn Group siltstone. In the Surveys Range, moderately south-dipping thrusts lift the Hyland Group over Earn Group. These thrusts are truncated by west-trending vertical and north-trending tear faults (Fig. 8).

The major fault trending southeast across Lansing map area is probably the Robert Service Thrust because it marks the northeastern limit of penetratively deformed Hyland Group rocks. South of Swan Lake this fault crosscuts contacts between units on the north side but is parallel to foliation of the adjacent Robert Service Thrust panel on the south side. South of Lansing Post it is a vertical zone of brittle deformation. The deeper structural level exposed in the Robert Service Thrust panel is consistent with either a normal fault or a south-dipping thrust fault interpretation of this major break.

MINERALIZATION

Two metallic mineral prospects were examined in 1993. The Plata (Ag, Pb) property is in carbonaceous siltstone and chert of the Earn Group (Abbott, 1986) where it is overthrust by Hyland Group limestone and maroon argillite. At least six quartz veins were mined for silver minerals associated with galena. Productive veins have also been located in adjacent Niddery Lake map area. Prospective Earn Group strata extend westward to the Rogue River, and gossans and oxidized stream beds are common in this area. Barite within carbonate of the Earn Group was noted on a ridge at 63°23'N, 132°08'W in the Surveys Range, and another barite horizon was noted by Abbott (1986) 5 km north-northeast of this locality.

The Pleasant (Cu,W) showing is a minor chalcopyrite-scheelite occurrence where limestone (lower Paleozoic unit 2) is intruded by diorite. No other diorite intrusions were located. Most copper and tungsten mineralization that has been found in Lansing map area is skarn-related around Cretaceous intrusions.

The 1993 mapping provides a solid basis for focused study and wide-ranging mapping in subsequent years. In conjunction with the Regional Stream Sediment Survey (Friske et al., 1991), the new map will provide a new basis for mineral exploration in this remote area. In addition, mapping of rocks and structures has the potential to elucidate several key questions along the northern edge of the Selwyn Basin.

ACKNOWLEDGMENTS

This project was funded by the Canada-Yukon Mineral Development Agreement (1991-1996), jointly administered by the federal Department of Indian and Northern Affairs and the Department of Economic Development, Government of Yukon. We are grateful for the support of the Canada-Yukon Geoscience Office (especially Dianne Carruthers and Will van Randen for regular radio contact), prompt transport by Brian Macpherson of Capital Helicopters, Ltd., and discussions during a field visit by Don Murphy. Bert Struik and Grant Abbott edited, and Bev Vanlier greatly improved the manuscript.

REFERENCES

- Abbott, J.G.**
1986: Geology of the Plata-Inca property, Yukon; in *Yukon Geology*, Vol. 1; Exploration and Geological Services Division, Yukon, Indian and Northern Affairs Canada, p. 109-112.
- Blusson, S.L.**
1974: Geology of Nadaleen River, Lansing, Niddery lake, Bonnet Plume Lake and Mount Eduni map areas, Yukon Territory; Geological Survey of Canada, Open File 205, scale 1:250 000.
- Campbell, R.B.**
1967: Geology of Glenlyon map area, Yukon; Geological Survey of Canada, Memoir 352 (includes Map 1221A, scale 1:253 440).
- Cecile, M.P. and Abbott, J.G.**
1992: Geology of Niddery Lake map area (1050), Yukon; Geological Survey of Canada, Open File 2465, scale 1:125 000.
- Friske, P.W.B., Hornbrook, E.H.W., Lynch, J.J., McCurdy, M.W., Gross, H., Galletta, A.C., and Durham, C.C.**
1991: National geochemical reconnaissance stream sediment and water data, east-central Yukon (NTS 105N); Geological Survey of Canada, Open File 2363.
- Gordey, S.P.**
1990: Geology and mineral potential, Tiny Island Lake map area, Yukon; in *Current Research, Part E*; Geological Survey of Canada, Paper 90-1E, p. 23-29.
- Gordey, S.P. and Anderson, R.G.**
1993: Evolution of the northern Cordilleran miogeocline, Nahanni map area (1051), Yukon and Northwest Territories; Geological Survey of Canada, Memoir 428.
- Gordey, S.P. and Irwin, S.E.B.**
1987: Geology, Sheldon Lake and Tay River map area, Yukon Territory; Geological Survey of Canada, Map 19-1987 (3 sheets), scale 1:250 000.
- Green, L.H.**
1972: Geology of Nash Creek, Larsen Creek and Dawson map-areas, Yukon Territory; Geological Survey of Canada, Memoir 364.
- Roots, C.F. and Murphy, D.C.**
1992a: New developments in the geology of Mayo map area, Yukon Territory; in *Current Research, Part A*; Geological Survey of Canada, Paper 92-1A, p. 163-171.
1992b: Geology, Mayo map area; Geological Survey of Canada, Open File 2483 and Indian and Northern Affairs, Exploration and Geological Services, Yukon Region, Open File 1992-4 (scale 1:250 000).
- Woodsworth, G.J., Anderson, R.G., and Armstrong, R.I.**
1991: Plutonic regimes, Chapter 15; in *Geology of the Cordilleran Orogen in Canada*, (ed.) H. Gabrielse and C.J. Yorath; Geological Survey of Canada, Geology of Canada, no. 4, p. 491-531 (also Geological Society of America, *The Geology of North America*, v. G-2).

Geological Survey of Canada Project 900035

Tectonic framework of the Teslin region, southern Yukon Territory

S.P. Gordey and R.A. Stevens¹
Cordilleran Division, Vancouver

Gordey, S.P. and Stevens, R.A., 1994: Tectonic framework of the Teslin region, southern Yukon Territory; in Current Research 1994-A; Geological Survey of Canada, p. 11-18.

Abstract: Results of revision geological mapping in Teslin map area (105C) compel a reinterpretation of the tectonic framework for southern Yukon Territory. Significant revelations include the discovery of a thick section of mafic volcanics in North American margin strata, that Kootenay terrane forms a flat sheet above North American margin strata within which is exposed a window of these same volcanics, and that the Cache Creek terrane, probably soled on the Nahlin fault, rests as a thrust sheet above Stikine terrane. Five varieties of post-tectonic plutonic rocks are recognized.

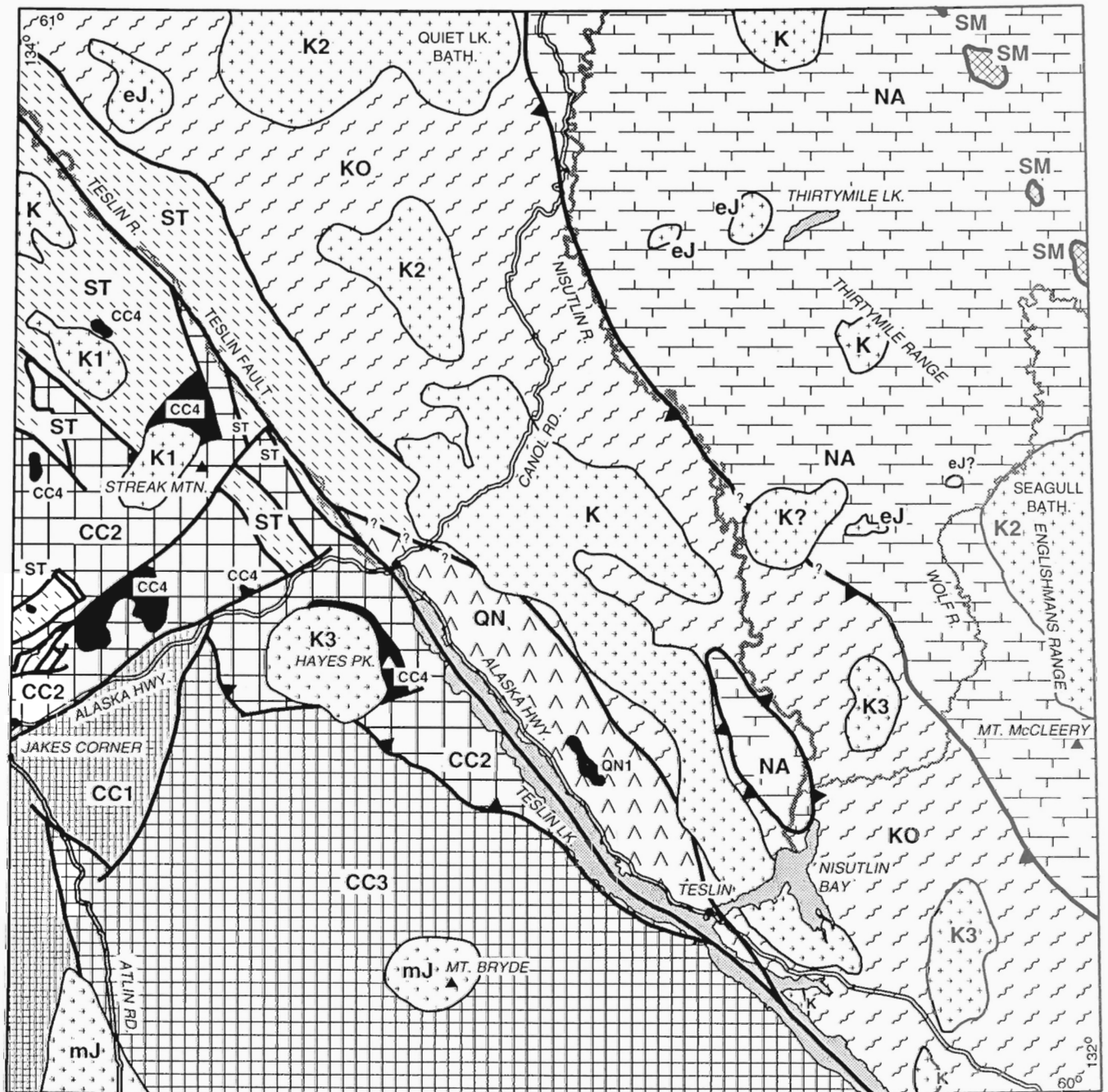
Résumé : Les résultats de la cartographie géologique de révision dans la région cartographique de Teslin (105C), nécessitent une réinterprétation du cadre tectonique du sud du Yukon. D'importantes découvertes ont été faites : un épais empilement de roches volcaniques mafiques a été identifié dans les strates de la marge nord-américaine; le terrane de Kootenay forme une nappe plane sur les strates de la marge nord-américaine et les volcanites mentionnées précédemment y sont observées dans une fenêtre; et le terrane de Cache Creek, probablement limité à sa base par la faille de Nahlin, forme une nappe de charriage sur le terrane de Stikine. Cinq variétés de roches post-tectoniques ont été reconnues.

¹ Department of Geology, University of Alberta, Edmonton, Alberta T6G 2E3

INTRODUCTION

Fieldwork in 1993 constituted the third season of a project to remap the geology of Teslin map area (NTS 105C; 60-61°N; 132-134°W) in southern Yukon Territory (Fig. 1). The aim

of this project is to produce a revised 1:250 000 scale map and reports, as well as 1:50 000 scale maps of selected areas, to understand the regional stratigraphic, structural, and tectonic context of the area's mineral resources and its environmental geological framework. The fieldwork of Mulligan in the



TESLIN (105C)



Figure 1. Tectonic framework of Teslin map area (105C).

early 1950s (Mulligan, 1963) established a broad geological framework, but little other work has been done until recently (Cordey et al., 1991; Gareau, 1992; Gordey, 1991, 1992; Harms, 1992; Jackson, 1990; Stevens, 1991, 1992, 1993; Stevens and Erdmer, 1993; and Stevens et al., in press). The reader is referred to Mulligan (1963) and these later works for stratigraphic and lithological descriptions. This report presents a synopsis of previous fieldwork supplemented by current results that focuses on the interpretation of plutonic and terrane relationships.

SETTING AND TERRANE DESCRIPTIONS

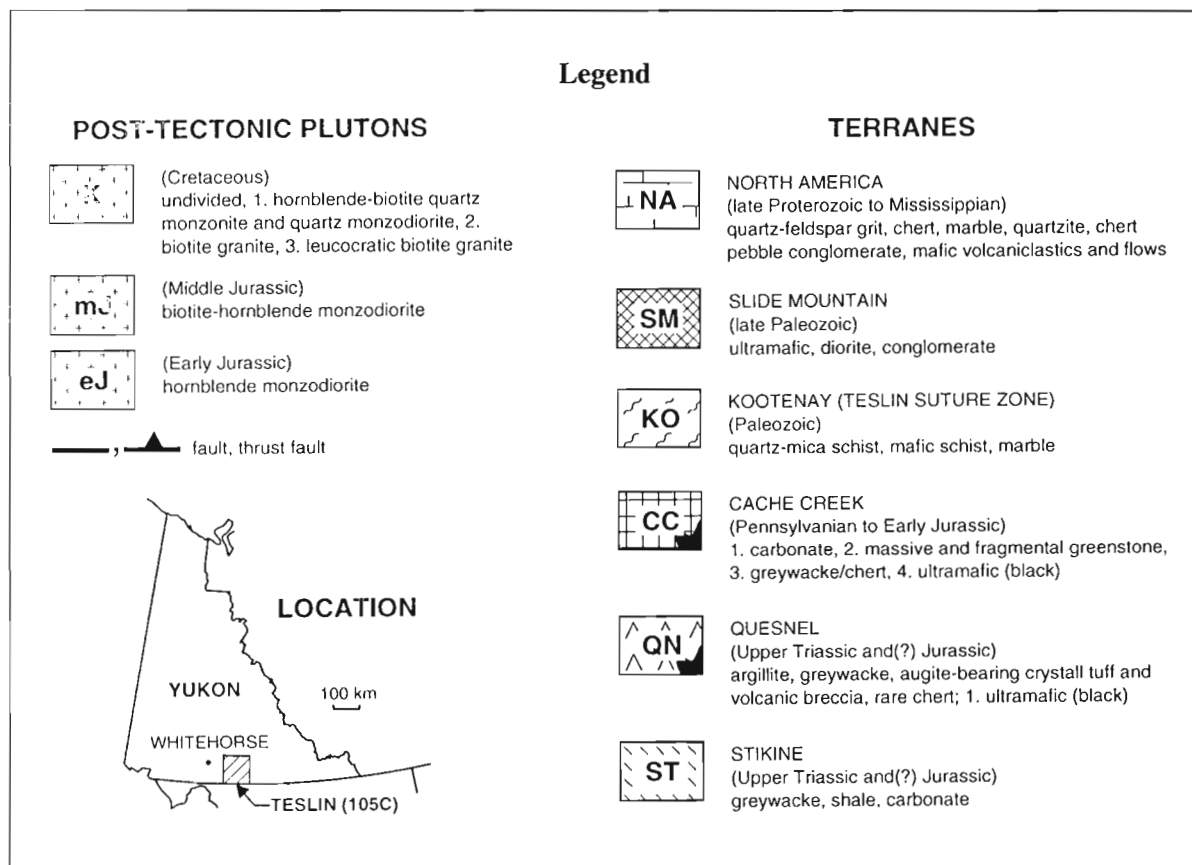
The Teslin area is underlain by six terranes of contrasting sedimentary and structural histories that were juxtaposed in the Jura-Cretaceous and intruded by at least five varieties of post-tectonic plutonic rocks grouped into three main suites (Fig. 1).

North America Margin (NA)

The northeast part of the area (NA, Fig. 1) is underlain by quartz sandstone and quartz-feldspar grit, chert, chert pebble conglomerate, andesite, quartzite, and carbonate. These strata are disrupted by variable and locally intense bedding parallel mylonitization and steep normal faults. Foliation and bedding dip gently, but the nature of contacts is obscured by deformation. A tentative stratigraphic framework has been

erected from locally exposed relationships in different parts of the area (see Gordey, 1992). The only fossiliferous unit is a regional limestone/quartz arenite marker containing corals of probable Carboniferous age (Mulligan, 1963, unit 2). This is thickest and best developed in the southeast part of the Thirtymile Range. West and northwest of Thirtymile Lake, the formation gradually changes facies to discontinuous limestone lenses enclosed within calcareous graphitic phyllite, graphitic quartzite, and siliceous muscovite phyllite. In addition to isolated volcanics reported previously in the Thirtymile Range (Gordey, 1991, 1992; Harms, 1992), thick (200+? m), extensive exposures of aphyric massive andesite/basalt flows(?) and tuffaceous volcanoclastics occur in the Englishmans Range south and northwest of Mount McCleery, and at the same latitude on the west side of the Wolf River. Near Mount McCleery the volcanics form a member within(?) the regional carbonate marker. Identical volcanics and volcanoclastics form the structural window of North American margin strata north of Nisutlin Bay.

The above mentioned strata are assigned to the Dorsey and Slide Mountain terranes by Wheeler et al. (1991) on the basis of their nonvolcanic or volcanic character respectively. However, all components of the stratigraphic succession have lithologic counterparts in the Proterozoic Ingenika, Early Paleozoic Road River(?), and Devon-Mississippian Earn Groups that typify North American margin strata (Fig. 3 of Gordey, 1992). A Mississippian age for volcanism and block faulting recognized in the Thirtymile (Gordey, 1992) and Englishmans ranges is in keeping with Devon-Mississippian



tectonism elsewhere along the North American margin. At that time, the margin was regionally characterized by block-faulting, local volcanism, sedimentary exhalative Pb-Zn-Ag-barite deposition, and accumulation of chert-rich clastic rocks and local carbonate (Gordey, 1988).

Slide Mountain (SM)

Rocks tentatively interpreted as Slide Mountain terrane (after Wheeler et al., 1991) include isolated exposures of ultramafic, diorite, and conglomerate (units 6, 11, and 12 of Mulligan, 1963) in the northeast corner of the Teslin area. These have yet to be examined for this study.

Kootenay (KO)

The Kootenay terrane (Teslin suture zone, Hansen et al., 1989; or Yukon Tanana terrane, Mortensen, 1992) trends northwest across the central part of the map area. Northwest of Canol Road it consists of metamorphosed and ductile-deformed S-, L-S-, and L-tectonites derived from sedimentary, volcanic, and plutonic rocks (Stevens, 1993) that form three lithotectonic assemblages. The oldest consists pre-early Mississippian metasedimentary rocks including quartz-muscovite±chlorite schist, muscovite-chlorite quartzite, muscovite graphite phyllite, calcareous schist, and minor marble. Intrusive into these strata are foliated hornblende-bearing metagranitoids of early Mississippian age. The last assemblage consists of mafic schist, greenstone, amphibolite, and metagabbro of late Paleozoic age. Contacts between rock units are dominantly structural with rare preservation of primary depositional and intrusive relationships. Metamorphic grade is greenschist to amphibolite facies (Stevens, 1991, 1992, 1993; Stevens and Erdmer, 1993).

Between Canol Road and Nisutlin River the terrane comprises biotite quartzite to semi-schist, hornblende gneiss, biotite±hornblende metaplutonic rock, and mylonite of greenschist to lower amphibolite facies (Gareau, 1992). Immediately east of Nisutlin Bay variably sheared originally hornblende(?) bearing metaplutonic rock with lesser amphibole-rich schist (metavolcanic?) are dominant.

Cache Creek (CC)

The Cache Creek terrane occurs southwest of Teslin valley where four main fault-bounded assemblages are recognized. Late Paleozoic (mostly(?) Permian) massive to locally crinoidal carbonate (CC1) occurs near Jakes Corner. The second assemblage (CC2) comprises Late Paleozoic volcanics that have been subdivided into two units (see Gordey, 1992) of uncertain original stratigraphic relationship. One unit comprises massive greyish-green to dark grey aphyric andesite/basalt in which spherulites are common and pillows are locally well developed. The second consists of massive grey-green to chrome-green, highly fractured and poorly indurated rocks of probable fragmental origin. This unit is distinguished by blocks of bedded chert and carbonate from fist-size to up to 30 m across.

Extensive ribbon chert and greywacke with minor shale (Gordey, 1992) form the third assemblage (CC3) in the southwest part of the map area. The greywacke is well indurated, medium grey, and fine- to coarse-grained. Angular lithic clasts are locally abundant, range up to 5 cm in diameter, and are dominated by grey- to white-weathering chert and argillite. Some of the chert contains radiolarians. Framework grains consist of subequal proportions of quartz and plagioclase, and minor orthoclase, hornblende, and lithic clasts. The chert and greywacke occur in alternating members 10 m to 200 m thick. Chert members range from being weakly deformed to intensely crumpled, whereas the greywacke-dominated clastic members lack internal deformation and cleavage. For both rock types near-vertical dips are commonplace. Although greywacke and chert are locally interbedded, the alternation of these rock types over large areas results from structural imbrication. This structural style persists across strike (ie., west-southwesterly) for about 60 km, the width across which these strata are exposed. Radiolaria recovered from chert and argillite range from Middle Triassic (Ladinian) to Early Jurassic (Pliensbachian or early Toarcian) (Cordey et al., 1991).

Ultramafic rocks of the Cache Creek terrane (CC4, Fig. 1) consist of massive to foliated peridotite and variably serpentized equivalents. The foliation is defined by concentrations of large pyroxene crystals up to a few centimetres thick within a matrix of finer grained olivine and pyroxene. Irregular shaped, metre-sized masses of dunite with gradational boundaries are found locally in which occur scattered euhedral black oxides (chromite?) to about a millimetre across.

Ultramafic bodies in the Teslin area were tentatively considered intrusive on the basis of locally steep but unexposed contacts (Gordey, 1991). Further examination has shown such contacts (e.g., the body north of Streak Mountain) to be post-emplacement normal faults. Also, more bodies have since been examined and all display a degree of serpentinization, uniformity of lithology, and lack of zoning more typical of alpine rather than alaskan ultramafics. Ultramafics in the Teslin area have the mineralogical and structural hallmarks of mantle tectonites as described for the ultramafic bodies near Atlin, British Columbia by Ash and Arksey (1990).

Quesnel (QN)

Quesnel terrane forms a fault-bounded panel east of Teslin Lake that includes as much as 600(?) m of clastic and minor volcanic rocks and chert. These are intruded by dunite and highly altered diorite (Gordey, 1992).

The most common rock types are siliceous argillite, siltstone, and sandstone. The sandstone occurs as massive, fine- to coarse-grained members from 1 m to at least 50 m thick containing quartz, much feldspar, and as much as 10% fresh, in places euhedral, augite (±hornblende?). Volcanic breccia consisting of augite and rare feldspar porphyry blocks to 20 cm across occurs locally, as do augite porphyry dykes and sills up to 10 m thick. The freshness, abundance, and euhedral

character of the augite suggests much of the clastics may be resedimented, poorly indurated pyroclastic deposits. Some sandstones resemble crystal lithic tuff. Thick bedded chert that occurs low in the stratigraphic succession has yielded Upper Triassic (Norian) conodonts (Gordey, 1992).

The sedimentary strata are weakly folded, and for the most part form a moderate northeast-dipping homocline. Overall southwest vergence of folds with long, moderate northeast-dipping limbs and short near vertical southwest-facing limbs is consistent with bedding attitudes and rare northeast-dipping slaty cleavage within mudrocks.

An ultramafic body about 5.5 km long and 1.3 km across that flanks either side of Lone Tree Creek (QN1) consists of fresh, dark green dunite and minor fresh coarse grained pyroxenite/peridotite. It differs from the ultramafics of the Cache Creek terrane both in composition and in lack of alteration (Gordey, 1992). Its contacts are not exposed, but its composition and lack of alteration to the limits of its exposure suggest an intrusive origin and probable Mesozoic age.

Stikine (ST)

Early Jurassic clastic and minor volcanic strata of Stikine terrane (ST, Fig. 1) outcrop in the northwest part of the area. The sediments consist predominantly of sandstone and lesser interbedded argillite. The sandstone is well indurated and occurs as individual thin to thick beds sharply bounded by argillite, as well as in uniformly fine- to medium-grained packets from 10 m to as much as 150 m thick. The sands are composed mostly of plagioclase, lesser monocrystalline quartz, and minor orthoclase, hornblende, pyroxene, and rock fragments, the last including chert(?) and aphanitic volcanics. Thinly interbedded grey, green, and tan laminated argillite and siltstone form members up to 100 m thick. Conglomerate members from a few metres to up to 200 m thick contain pebble-, to cobble-sized clasts of limestone, granitic rock, feldspar porphyry, green to grey-green volcanic(?) and argillite(?), chert, and dark grey argillite. A second type contains rounded, largely limestone clasts to 1.5 m across and minor granitoid and volcanic clasts within black calcareous mudstone.

Volcanic rocks are rare. Pillowed andesite, estimated at up to 200 m thick, was seen at one locality but could not be traced more than a few kilometres along strike.

Several hundred metres of massive carbonate of Late Triassic (Norian) age occurs within the fault bounded panels 8.9 km and 14.7 km north-northeast of Jakes Corner (unit 8a of Mulligan, 1963).

The structure of the clastic rocks is relatively simple. Dips of bedding range from shallow to up to 70 degrees, and reversals of dip direction indicate northwest-trending, upright folds with wavelengths of a kilometre or more. Slaty cleavage is not developed and small- to outcrop-scale folds are absent.

Plutonic suites

A tentative subdivision of plutonic rocks into three main suites comprising five main types (Fig. 1) is based on mineralogy and preliminary results from radiometric dating (unpublished unless otherwise cited). Large bodies of plutonic rock remain to be characterized and dated. For example, the large body underlying the central part of the map area may be composite and have several Cretaceous and/or Tertiary(?) components. As well, the body apparently straddling the North America-Kootenay terrane contact is largely unstudied.

Early Jurassic plutons (eJ) intrude the Kootenay terrane and North American margin and consist of unfoliated, medium grained monzodiorite and quartz monzodiorite, and minor hornblende. Hornblende, up to 25%, is the dominant mafic mineral. It is rarely accompanied by up to a few per cent biotite. A faint pistachio-coloured stain and trace amounts of very fine grained granular epidote are seen in places. The weak alignment of hornblende seen locally is likely an igneous flow fabric. Preliminary ages on this suite include 185 ± 3 Ma (^{40}Ar - ^{39}Ar , hornblende) from the body west of Wolf River, and 188.0 ± 2.7 – 5.4 Ma (U-Pb, zircon) from the body near the northwest corner of the map area (Stevens et al., in press).

The Middle Jurassic suite (mJ) intrudes the Cache Creek terrane and is exemplified by the Mt. Bryde pluton composed of unfoliated, medium- to coarse-grained monzodiorite and quartz monzodiorite, and minor hornblende. The monzodiorite commonly contains about 20%, but locally up to 40%, hornblende, and occurs at the east and west margins of the body. The quartz monzodiorite is more leucocratic and characterized by hornblende at about twice the abundance of biotite, the mafics in total ranging up to about 15%. Inclusions, veins, and dykes in the pluton are rare. The closest exposures of country rock to the pluton, about 150 m distant, display minimal contact metamorphism. Radiometric ages on the Mt. Bryde pluton include 173 ± 3 Ma (^{40}Ar - ^{39}Ar , hornblende) and 169 ± 2 Ma (^{40}Ar - ^{39}Ar , biotite). The Fourth of July Creek batholith in the southwest corner of the area, dominantly granite with biotite- to hornblende-rich and K-feldspar megacrystic to equigranular phases, has yielded an age of 171.7 ± 3 (U-Pb, zircon) (Mihalynuk et al., 1992).

Plutons grouped as the Cretaceous (K) suite are of three main types (Fig. 1). The first type (K1) is dominated by medium grained, hornblende-biotite quartz monzonite and quartz monzodiorite. Hornblende and biotite occur in subequal proportions in amounts totalling up to 25%. Examples include the pluton near Streak Mountain which has yielded an age of 118.1 ± 3 Ma (K-Ar, biotite), and the body immediately to the north-northwest with ages of 120.2 ± 2.2 (^{40}Ar - ^{39}Ar , hornblende) and 119.8 ± 1.3 (^{40}Ar - ^{39}Ar , biotite). A preliminary age of 123.1 ± 1.7 Ma (U-Pb, zircon) (as quoted in Gordey, 1992) was determined on similar but foliated hornblende-biotite granite 30.1 km north-northwest of Teslin.

The second main type (K2) contains biotite as the sole mafic mineral and is exemplified by the Seagull and Quiet Lake batholiths. The former, underlying the Englishmans Range, consists of homogeneous coarse grained granite distinguished by up to 40% pink K-feldspar crystals to about 2 cm long and by about 5% small fresh biotite flakes. Three ages from the Seagull batholith east of the Teslin area range from 92 to 98 Ma (K-Ar, biotite, Wanless et al., 1972). The Quiet Lake batholith, the large body at the north margin of the map area, comprises homogeneous, medium grained biotite granite with up to 15% biotite, and local phenocrysts of pinkish K-feldspar up to 10-15%. Two ages from the Quiet Lake batholith north of the Teslin area are 70 and 85 Ma (K-Ar, biotite, Wanless et al., 1979). The third type of Cretaceous pluton (K3) consists of unfoliated, medium- to coarse-grained, leucocratic, biotite granite. The biotite occurs as small flakes, comprising up to 5% of the rock. Plutons of this suite are massive and homogeneous as typified by the bodies 25 km east of Teslin and 25 km northeast of Teslin. Compositionally they resemble the Seagull batholith but lack the distinctive pink K-feldspar of that body. A third example of this type, the Hayes Peak intrusion, contains abundant screens and inclusions of hornblende monzodiorite that may be remnants of the Middle Jurassic suite. Plutons of the third type are as yet undated; a Late Cretaceous or Tertiary age for these is possible. Dating is required to determine whether the hornblende-free plutons (K2) of this suite are consistently younger than hornblende-bearing varieties (K1). Except for fabric within part of the plutonic body mentioned above (Gordey, 1991, 1992; Gareau, 1992), plutons of the Cretaceous suite are unfoliated.

TERRANE RELATIONSHIPS

Kootenay-North America

Across the contact of Kootenay terrane with strata of the North American margin there is a marked contrast in metamorphic grade and degree of deformation. Rocks of the former are greenschist to amphibolite facies and penetratively ductile-deformed whereas those of the North America margin are of subgreenschist to greenschist grade, locally slaty-cleaved and affected by inhomogeneous spaced shear. A northeast vergent thrust contact reconciles these differences and explains the topographically low exposures of low-grade, little-deformed rocks north of Nisutlin Bay as a window of North American margin strata. Fabrics within Kootenay terrane both near the window and at the thrust front near Wolf River are steeply dipping and apparently truncated at the thrust. On the basis of ^{40}Ar - ^{39}Ar cooling ages, Hansen et al. (1991) implied overthrusting of Teslin-Taylor Mountain allochthons (Kootenay terrane of this report) above North American margin at ~190 Ma. Consistent with this, the undeformed Early Jurassic intrusions form a "stitching" plutonic suite implying proximity of the two terranes by ~186 Ma. The degree of post-Jurassic displacement along the terrane-bounding thrust is uncertain.

Quesnel-Stikine-Kootenay-Cache Creek

Quesnel and part of Stikine terrane are bounded by two steep faults which merge south of Teslin (Fig. 1) and are contiguous with the Thibert fault in northern British Columbia. For the latter structure Gabrielse (1985) proposed 75 km of pre-Late Cretaceous dextral offset, but how this offset is partitioned along the two splays in Teslin area is unclear. One possibility is to have all displacement taken up along the eastern splay. Restoration of 75 km of dextral slip along this structure and the Thibert fault adjoins Quesnel terrane of the Teslin area with similar and partly correlative Quesnel strata of the Nazcha and Shonektaw formations in Jennings River map area. In this instance the western strand along Teslin valley (the structure traditionally called the Teslin fault) has little strike-slip offset. Alternately most dextral displacement occurred along Teslin fault. Restoration of 75 km of offset in this case does not realign similar elements. Rather Quesnel strata of the Teslin area are restored adjacent to Stikine terrane.

Based on present terrane assignments, the first possibility presented above is most appealing as it restores continuity to disconnected elements. However, assignment of strata to the Quesnel terrane in the Teslin area is a "best guess" rather than proven. If strata of Quesnel terrane have been misassigned and actually represent an older part of the Stikine succession (e.g., volcanics and volcanoclastics of the Lewes River Group (Wheeler, 1961)), the alternate scenario presented above is plausible. Better fossil and age control on the Quesnel succession would constrain these options. If Quesnel strata could be shown to extend into the Jurassic, and hence be proven age-equivalent to Stikine strata, the present terrane assignment would be confirmed.

The fault indicated between Quesnel and Stikine terranes near the Canol Road (Fig. 1) is assumed. Exposure in this area is poor and contact relationships unclear.

Cache Creek-Stikine

Traditional interpretation of the relationship of Cache Creek and Stikine terranes (e.g., Wheeler and McFeely, 1991) portrays Cache Creek strata to plunge beneath, and form the basement to, Stikine. However, relationships in western Teslin area indicate the opposite; the Cache Creek terrane forms a large thrust sheet above Stikine terrane. Steep northeast- and northwest-trending normal faults have broken both the sheet and its footwall so that horsts of Stikine strata have locally popped up through the overlying Cache Creek. Examples include the block southeast of Streak Mountain and that north of Jakes Corner.

Mesozoic radiolarian ribbon chert and greywacke in the Cache Creek are the same age as the chert-free clastic succession of Stikine found along strike to the northwest. Westerly overthrusting of the Cache Creek terrane explains the juxtaposition of proximal (Stikine) and distal (Cache Creek) facies and intimates that before thrusting both were deposited within the same basin.

Mutual contacts of Stikine and Cache Creek terranes are largely defined by late steep normal faults, so little of the thrust at the base of the Cache Creek is potentially exposed. One possibility is in the irregular contact north-northwest of Streak Mountain. However, outcrop in this area is poor and the position of the contact poorly constrained. Most ultramafic bodies within the Cache Creek occur as fault slice(s) within the volcanics. However, two bodies, one 17.7 km northwest of Streak Mountain and another in adjacent Whitehorse map area 26.4 km west-northwest of Streak Mountain (Wheeler, 1961) are surrounded by, and presumably rest directly above, Stikine clastics.

The Cache Creek terrane is likely floored by the west-directed Nahlin fault (e.g., Wheeler and McFeely, 1991), a large thrust fault with ultramafic bodies near and at its base that surfaces to the south and west in the Atlin area. The age of structural duplication within the Cache Creek terrane and its time of emplacement above Stikine is constrained as pre-170 Ma (pre-mid-Bajocian (time scale of Harland et al., 1989)), the age of the posttectonic Mt. Bryde pluton, and post-Pliensbachian or early Toarcian, the age of the youngest Cache Creek beds involved in deformation.

ECONOMIC GEOLOGY FRAMEWORK

Two terranes within the map area host showings and have potential deposit types that are terrane specific. Ultramafic bodies in the Cache Creek terrane locally carry asbestos, and one small body of podiform dunitite is known to host small concentrations of chromite (Squanga occurrence, DIAND, 1993). Carbonate alteration zones within the ultramafics (listwanite) that might carry gold-quartz veins, as seen in similar ultramafics of the Atlin camp in British Columbia (Ash and Arksey, 1990), have yet to be noted. Potential deposit types in strata of the North American margin include sedimentary exhalative barite-Pb-Zn-Ag (e.g., Bar occurrence, DIAND (1993)) and/or volcanogenic massive sulphide deposits. Both are expected in association with Mississippian block faulting and volcanism.

The majority of the twenty-two known mineral occurrences in the Teslin area (DIAND, 1993) include Ag-Pb-Zn vein deposits as well as Pb-Zn, Cu-Fe, and Sn-W skarns. These are hosted by Kootenay and North American margin rocks and all of these occurrences are likely related to Cretaceous plutonism. Tin-bearing skarns are genetically associated with the Seagull batholith (Abbott, 1981). The most intensively explored property in the map area, the Red Mountain porphyry Mo prospect, is hosted in a small intrusion of quartz monzonite porphyry about 95 Ma old (Brown and Kahlert, 1986; Stevens et al., 1982).

ACKNOWLEDGMENTS

Rahim Ismaili and Lars Bartholsen provided superb assistance in the field. Excellent air support was provided by Trans North Air (Whitehorse), Discovery Helicopters (Atlin), and

Coyote Air Service (Teslin). Steve Morison kindly allowed use of the facilities of Geological and Exploration Services (Indian and Northern Affairs Canada) in Whitehorse.

REFERENCES

- Abbott, J.G.**
1981: Geology of Seagull tin district; in Yukon Geology and Exploration 1979-80, Geology Section, Department of Indian and Northern Affairs Canada, Whitehorse, p. 32-44.
- Ash, C.H. and Arksey, R.L.**
1990: The Atlin ultramafic allochthon: ophiolitic basement within the Cache Creek terrane; tectonic and metallogenic significance (104N/12); in Geological Fieldwork 1989; British Columbia Ministry of Energy, Mines and Petroleum Resources, Geological Survey Branch, Paper 1990-1, p. 365-374.
- Brown, P. and Kahlert, B.**
1986: Geology and mineralization of the Red Mountain porphyry molybdenum deposit, south-central Yukon; in Mineral Deposits of the Northern Cordillera, (ed.) J. Morin; Canadian Institute of Mining and Metallurgy, Special Volume 37, p. 288-297.
- Cordey, F., Gordey, S.P., and Orchard, M.J.**
1991: New biostratigraphic data for the northern Cache Creek Terrane, Teslin map area, southern Yukon; in Current Research, Part E; Geological Survey of Canada, Paper 91-1E, p. 67-76.
- DIAND (Department of Indian Affairs and Northern Development, Canada)**
1993: Yukon Minfile (area 105C), Northern Cordillera Mineral Inventory; Exploration and Geological Services, Whitehorse.
- Gabrielse, H.**
1985: Major dextral displacements along the Northern Rocky Mountain Trench and related lineaments in north-central British Columbia; Geological Society of America, Bulletin, v. 96, p. 1-14.
- Gareau, S.**
1992: Report on fieldwork in the southern Big Salmon metamorphic complex, Teslin map area, Yukon Territory; in Current Research, Part A; Geological Survey of Canada, Paper 92-1A, p. 267-277.
- Gordey, S.P.**
1988: Devonian-Mississippian clastic sedimentation and tectonism in the Canadian Cordilleran miogeocline; in Devonian of the World, (ed.) N.J. McMillan, A.F. Embry, and D.J. Glass; Canadian Society of Petroleum Geologists, Memoir 14, v. II, p. 1-14.
1991: Teslin map area, a new geological mapping project in southern Yukon; in Current Research, Part A; Geological Survey of Canada, Paper 91-1A, p. 171-178.
1992: Geological fieldwork in Teslin map area, southern Yukon Territory; in Current Research, Part A; Geological Survey of Canada, Paper 92-1A, p. 279-286.
- Hansen, V.L., Heizler, M.T., and Harrison, T.M.**
1991: Mesozoic thermal evolution of the Yukon-Tanana composite terrane: new evidence from ⁴⁰Ar-³⁹Ar data; Tectonics, v. 10, no. 1, p. 51-76.
- Hansen, V.L., Mortensen, J.K., and Armstrong, R.L.**
1989: U-Pb, Rb-Sr, and K-Ar isotopic constraints for ductile deformation and related metamorphism in the Teslin suture zone, Yukon-Tanana terrane, south-central Yukon; Canadian Journal of Earth Sciences, v. 26, p. 2224-2235.
- Harland, W.B., Armstrong, R.L., Cox, A.V., Craig, L.E., Smith, A.G., and Smith, D.G.**
1989: A geologic time scale, 1989; Cambridge University Press.
- Harms, T.A.**
1992: Stratigraphy of the southern Thirtymile Range, Teslin map area, southern Yukon Territory; in Current Research, Part A; Geological Survey of Canada, Paper 92-1A, p. 297-302.
- Jackson, J.**
1990: Geology and Nd isotope geochemistry of part of the northern Cache Creek terrane, Yukon: implications for tectonic relations between Cache Creek and Stikine; in Geological Association of Canada and Mineralogical Association of Canada Joint Annual Meeting, Program with Abstracts, v. 15, p. A64.

Mihalynuk, M.G., Smith, M.T., Gabites, J.E., Runkle, D., and LeFebure, D.

1992: Age of emplacement and basement character of the Cache Creek terrane as constrained by new isotopic and geochemical data; *Canadian Journal of Earth Sciences*, v. 29, no. 11, p. 2463-2477.

Mortensen, J.K.

1992: Pre-mid-Mesozoic tectonic evolution of the Yukon-Tanana terrane, Yukon and Alaska; *Tectonics*, v. 11, no. 4, p. 836-853.

Mulligan, R.

1963: Geology of Teslin map area, Yukon Territory (105C); Geological Survey of Canada, Memoir 326.

Stevens, R.A.

1991: The Teslin suture zone in northwest Teslin map area, Yukon; in *Current Research, Part A*; Geological Survey of Canada, Paper 91-1A, p. 271-277.

1992: Regional geology, fabric and structure of the Teslin suture zone in northwest Teslin map area, Yukon Territory; in *Current Research, Part A*; Geological Survey of Canada, Paper 92-1A, p. 287-295.

1993: Teslin suture zone; in *Field Guide to Accompany the 1993 Nuna Conference on The Northern Intermontane Superterrane*, (ed.) Johnson et al., p. 44-45.

Stevens, R.A. and Erdmer, P.

1993: Geology and structure of the Teslin suture zone and related rocks in parts of Laberge, Quiet Lake, and Teslin map area, Yukon Territory; in *Current Research, Part A*; Geological Survey of Canada, Paper 93-1A, p. 11-20.

Stevens, R.D., Delabio, R.N., and Lachance, G.

1982: Age determinations and geologic studies, K-Ar isotopic ages, Report 16; Geological Survey of Canada, Paper 82-2, 56 p.

Stevens, R.A., Mortensen, J.K., and Hunt, P.A.

in press: U-Pb and ^{40}Ar - ^{39}Ar geochronology of plutonic rocks from the Teslin suture zone, Yukon Territory; in *Radiogenic Age and Isotopic Studies: Report 7*; Geological Survey of Canada, Paper 93-2.

Wanless, R.K., Stevens, R.D., Lachance, G.R., and Delabio, R.N.

1972: Age determinations and geological studies, K-Ar isotopic ages, Report 10; Geological Survey of Canada, Paper 71-2.

Wanless, R.K., Stevens, R.D., Lachance, G.R., and Delabio, R.N.

1979: Age determinations and geological studies, K-Ar isotopic ages, Report 14; Geological Survey of Canada, Paper 79-2.

Wheeler, J.O.

1961: Whitehorse map area (105D), Yukon Territory; Geological Survey of Canada, Memoir 312, 156 p.

Wheeler, J.O. and McFeely, P.

1991: Tectonic assemblage map of the Canadian Cordillera and adjacent parts of the United States of America; Geological Survey of Canada, Map 1712A, scale 1:2 000 000.

Wheeler, J.O., Brookfield, A.J., Gabrielse, H., Monger, J.W.H.,

Tipper, H.W., and Woodsworth, G.J.

1991: Terrane map of the Canadian Cordillera; Geological Survey of Canada, Map 1713A, scale 1:2 000 000.

Geological Survey of Canada Project 900036

Operation Bouguer – the final phase of a gravity survey in the northern Cordillera

C. Lowe, D.A. Seemann, D.B. Hearty¹, and D.W. Halliday¹
Pacific Geoscience Centre, Sidney

Lowe, C., Seemann, D.A., Hearty, D.B., and Halliday, D.W., 1994: Operation Bouguer – the final phase of a gravity survey in the northern Cordillera; in Current Research 1994-A; Geological Survey of Canada, p. 19-24.

Abstract: Reconnaissance gravity mapping of the Canadian Cordillera was completed this year with the acquisition of 1553 new measurements. The measurements, spaced approximately 10 km apart, were acquired in the western and northern Cordillera, in regions of very rugged relief. Station positions, determined using a Global Positioning System, are considered accurate to ± 2.5 m in each of latitude, longitude, and elevation. The new data have been reduced to simple Bouguer anomalies, but terrain corrections remain to be applied. Significant (tens of mGal) terrain corrections are anticipated for many observations in the St. Elias and Coast Mountains. Once processing is complete the new data will be added to the National Gravity Database in Ottawa and used to upgrade geoid models, improve inertial navigation systems, and aid structural and tectonic interpretations of the northern Canadian Cordillera.

Résumé : La cartographie gravimétrique de reconnaissance de la Cordillère canadienne s'est terminée cette année par l'acquisition de 1 553 nouvelles mesures. Celles-ci ont été faites à des intervalles approximatifs de 10 km dans l'ouest et le nord de la Cordillère, dans des régions au relief très accidenté. Les positions des stations, établies au moyen d'un système de positionnement global, sont considérées précises à $\pm 2,5$ m pour la latitude, la longitude et l'altitude. Les nouvelles données ont été corrigées pour obtenir la simple anomalie de Bouguer, mais les corrections topographiques (de relief) n'ont pas encore été faites. Des corrections topographiques significatives (dizaines de mGal) sont prévues pour de nombreuses observations dans le massif St. Elias et la chaîne Côtière. Lorsque le traitement sera terminé, les nouvelles données seront ajoutées à la base de données gravimétriques nationale, à Ottawa, et utilisées pour améliorer les modèles du géoïde, perfectionner les systèmes de navigation par inertie et faciliter les interprétations structurales et tectoniques du nord de la Cordillère canadienne.

¹ Geophysics Division, Ottawa

INTRODUCTION

Operation Bouguer, a three year program of reconnaissance gravity surveying, is a joint venture involving the Geological Survey of Canada, the Canadian Department of National Defence, and the United States Defence Mapping Agency. The program was initiated in 1991 as a consequence of a Canada-United States agreement on gravity. During the first two years of the program, 3637 measurements were acquired in the southern Yukon and Northwest Territories (see Fig. 1), at a station interval of 10 km. These measurements have been used to significantly improve inertial guidance systems and geoid models (Veronneau and Mainville, 1992). In addition, they have provided valuable insight into the nature of the deep crust beneath the northern Cordillera (Seemann et al., 1993; Lowe et al., in press). Where available, outcrop samples were also collected at gravity stations, analyzed for density, and used in tectonic analyses and gravity models (Lowe et al., in press). In this, the final phase of Operation Bouguer, 1553 new measurements were acquired in northwestern British

Columbia and the southwestern Yukon in regions of very rugged relief. This paper describes the acquisition and processing procedures used and presents some preliminary comments on observed variations in the Bouguer field.

TECTONIC SETTING

Figure 1 shows the three regions surveyed during Operation Bouguer and locates the 1553 new gravity measurements acquired this year. In addition to stations along the Alaska panhandle, measurements between 58°N and 60°N, to the east of Dease Lake, were taken to infill a region of sparse gravity coverage. The entire survey area is underlain by a collage of fault-bounded terranes and onlapping sedimentary assemblages (Wheeler et al., 1991). The terranes were juxtaposed by the processes of subduction, compression, accretion, magmatism, and transcurrent fault movements. These processes began in the Mesozoic, and many continue to shape the region

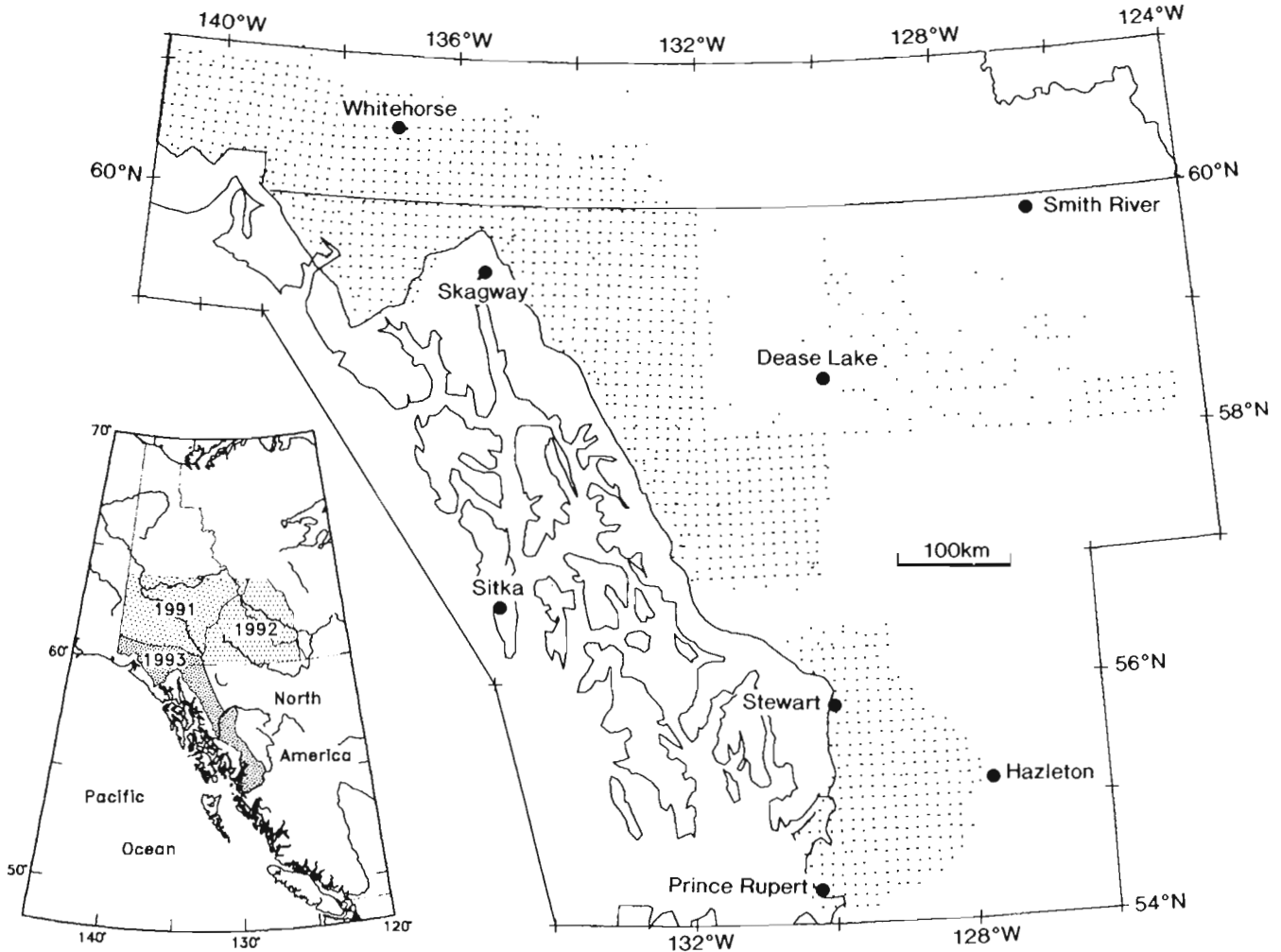


Figure 1. Location of gravity stations occupied during phase 3 (the final phase) of Operation Bouguer. Diagram in lower left outlines the regions surveyed during phases 1 (1991) and 2 (1992) of Operation Bouguer.

today. The St. Elias Mountains in the extreme southwest Yukon are the most tectonically active and rapidly uplifting region in Canada.

Although the regional framework has been established, through 1:250 000 scale geological mapping, little is known of the subsurface geology. Drillholes are few and invariably shallow, and the region has received little geophysical attention to date. In 1996 however, the Slave Northern Cordillera Lithospheric Experiment (SNORCLE), an approved Lithoprobe multidisciplinary transect, will commence. This experiment is designed to investigate the deep architecture and evolution of the lithosphere in northern Canada along three primary profiles (Fig. 2). With the exception of Great Bear Lake (Northwest Territories), reconnaissance gravity surveying within the SNORCLE corridor is now complete. Interpretation of the recently acquired gravity data will form an important component of the SNORCLE.

DATA ACQUISITION

Gravity data

Gravity data were obtained using Lacoste and Romberg (model G) gravity meters. Daily gravity traverses began and ended at national gravity control points, established throughout the survey area. The maximum accepted closure error on a traverse

was 0.5 mGal, and all traverses were well below this limit. Accuracy checks were performed by repeating gravity measurements at selected stations. The mean gravity difference was 0.059 mGal for 171 repeat measurements.

Positioning data

Stations were located using the Global Positioning System (GPS). Approximately 15 minutes of satellite data were recorded on Ashtech XII 12 channel, dual frequency, P-code receivers. The receivers were operated in differential mode, i.e., data were recorded simultaneously at the gravity station and at two base-stations deployed in the area. An antenna, mounted on the tail-fin of a Hughes 500E helicopter, was used to provide station coordinates and to navigate between stations. For station positioning, the horizontal and vertical offsets between the antenna and the gravity station were accurately determined and a correction was applied in the subsequent processing.

DATA PROCESSING

Gravity data

The gravity data were reduced to the International Gravity Standardization Net 1971 (Morelli, 1974) and theoretical gravity values were calculated using the Geodetic Reference

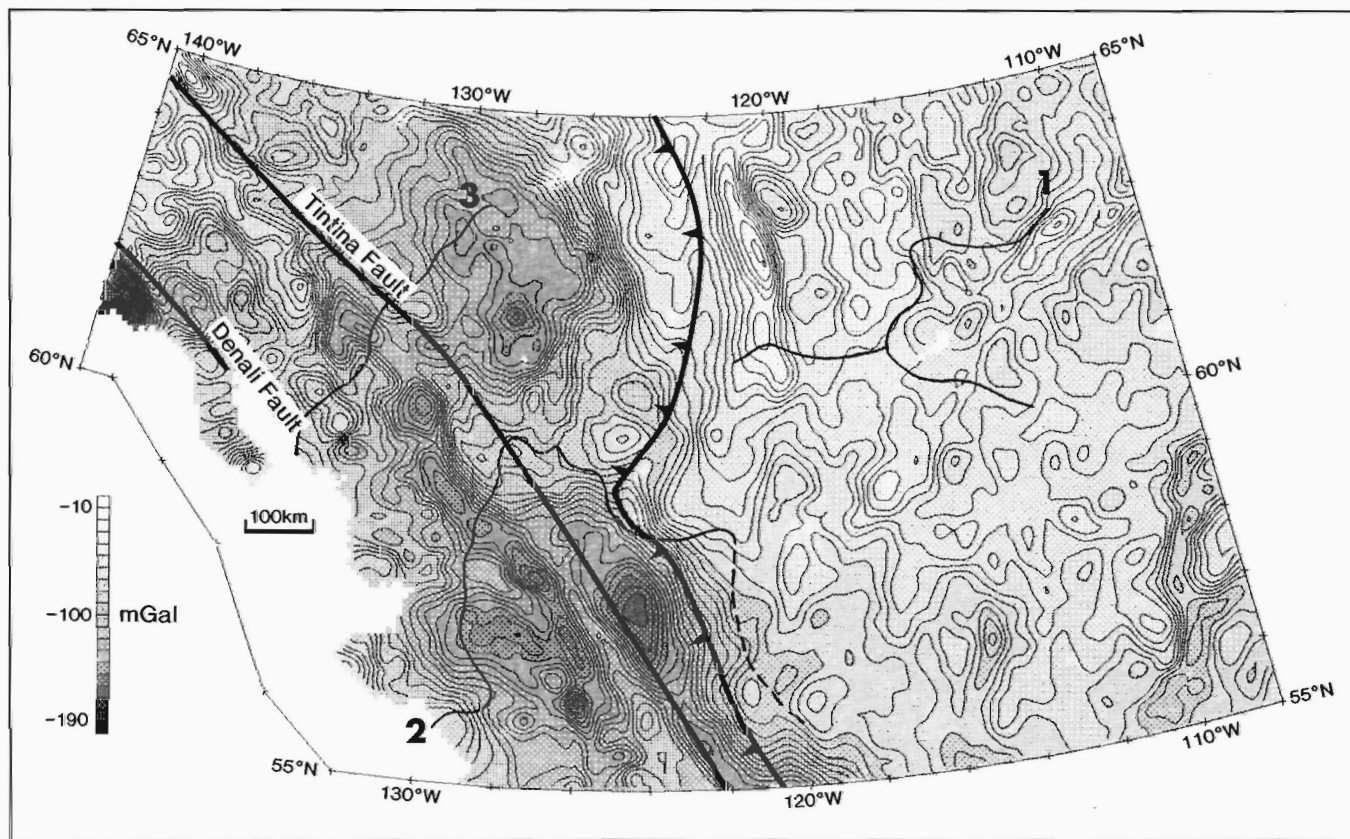


Figure 2. Bouguer anomaly map of the northern Canadian Cordillera (does not include Operation Bouguer 1993 data), showing the Tintina and Denali faults (solid lines) and the eastern limit of Cordillera deformation (spiked line). Thin lines labelled 1, 2, and 3 are the location of SNORCLE profiles.

System 1967 gravity formula. Simple Bouguer anomalies were calculated using a standard density of $2670 \text{ kg}\cdot\text{m}^{-3}$ and are presented as a contour map in Figure 3. Terrain encountered during this survey is the most extreme in Canada (Fig. 4) and in order that variations in the Bouguer field be uniquely ascribed to geological sources, terrain corrections must be calculated.

Terrain corrections will be computed using the program "TRITER" (Rupert, 1988), which calculates the cumulative effect of all terrain out to a distance of 25 km from each gravity station, using a digital elevation file and triangular, sloping-topped vertical prisms. Figure 5 shows the terrain correction of a 1992 station in a region of moderate relief. Observe that terrain within a 1 km radius of the station contributes more than 48% of the total correction. Given the extreme terrain encountered in the St. Elias and Coast Mountains this year, corrections of several tens of milliGals

are anticipated. Caution must be exercised when speculating on the geological significance of variations in the simple Bouguer field as these data have not yet been terrain corrected (Fig. 3).

Positioning data

All GPS data were processed in the field using Ashtech software. Stations with positioning error estimates in excess of $\pm 2.5 \text{ m}$ were repeated. The geoidal undulation was calculated using the GSD93A model (M. Veronneau, pers. comm., 1993), and used to transform GPS (ellipsoidal) elevations to orthometric (geoidal) elevations. This model, which is similar to the GSD91 model of Veronneau and Mainville (1992) incorporates gravity data collected during the first two phases of Operation Bouguer, and consequently is a significant improvement over previous models.

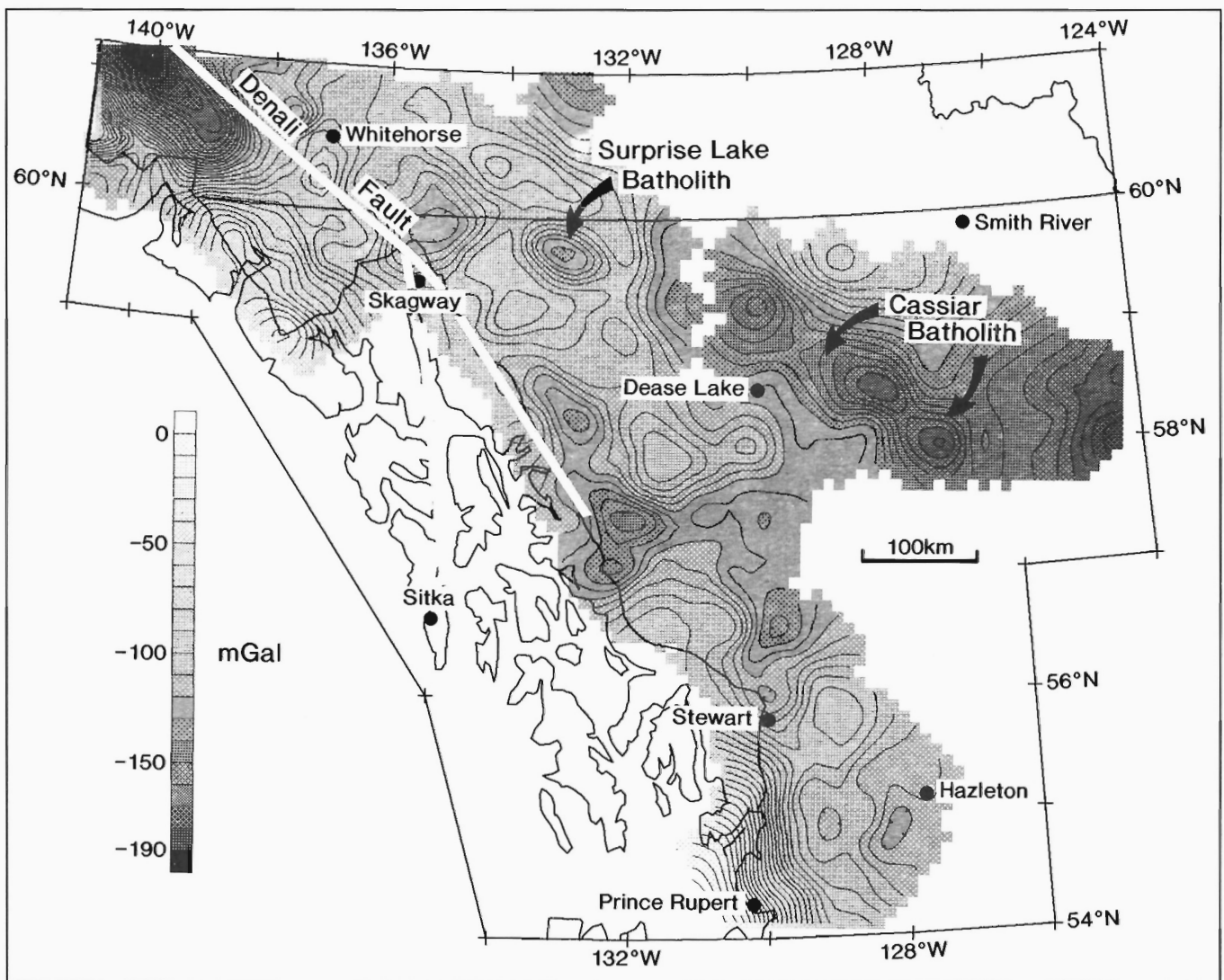


Figure 3. Simple Bouguer anomaly map of Operation Bouguer 93 gravity data. Contour interval is 5 mGal, colour interval is 10 mGal. Note: terrain corrections have not been applied to the data.

Other

Where possible, samples of outcrop were collected at each gravity station. The density of these samples will be determined during the next few months and used in the quantitative analysis and modelling of the new gravity data. In addition, the magnetic susceptibility of each sample will be measured, and both measurements will be added to an ORACLE database of similar measurements, which is being compiled at the Pacific Geoscience Centre, on Cordilleran rock samples.



Figure 4. Much of the survey area was in high-relief terrain. This picture (courtesy of M. Schmidt) shows the north face of Mount Logan (5959 m) in the St. Elias Range. Vertical relief is approximately 3000 metres.

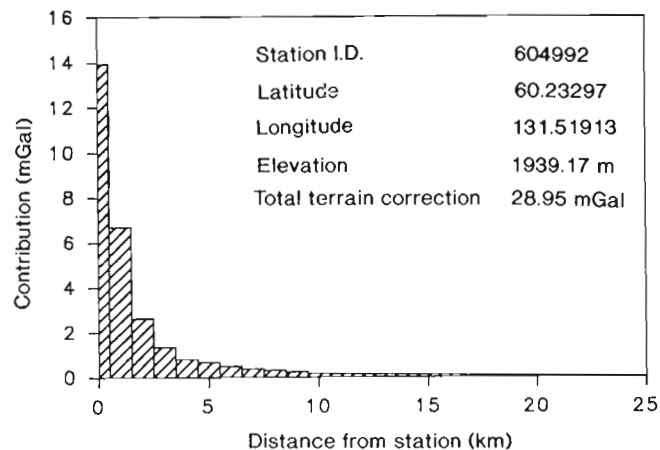


Figure 5. Terrain correction for a gravity station located in the Operation Bouguer 1992 survey region. Note that terrain within a 1 km radius constitutes more than 48% of the total correction.

SOME PRELIMINARY COMMENTS

As mentioned earlier, until terrain corrections are applied, caution must be exercised when speculating on the geological significance of anomalies recognized in the simple Bouguer data. Some features of the new data (Fig. 3), unlikely to change when these corrections are applied, are:

1. A strong northwesterly trend parallel to the tectonic fabric. This trend indicates the control which tectonic activity has played on the distribution of density (i.e., rock units) in the area.
2. Pronounced sub-oval Bouguer lows associated with mapped granitic rocks, for example, the Surprise Lake (a Lower Cretaceous leucocratic alaskite and quartz monzonite) and the Cassiar (a Middle Cretaceous biotite quartz monzonite and granodiorite) batholiths (Fig. 3). Granitic rocks typically have low values of density relative to their host rocks, a feature which can be exploited in quantitative gravity models to determine the geometry of the bodies.
3. A zone of high Bouguer values over coastal regions near Prince Rupert. These high values are continuous with a coast-parallel zone of high values in western British Columbia and Alaska. Lack of deep crustal information limits our understanding of the nature of the source of this anomaly.
4. A region of very low Bouguer values west of Whitehorse, and south of the Denali Fault. Low values are also mapped in adjacent regions of Alaska, where they are thought to be related to tectonically thickened continental crust (Brew et al., 1991).

CONCLUSIONS

In the final phase of a three year program of enhanced gravity mapping, 1553 new gravity measurements were acquired in the western and northern Canadian Cordillera. The measurements, spaced approximately 10 km apart, were located using the Global Positioning System. Positions are considered accurate to ± 2.5 m in latitude, longitude, and elevation. Simple Bouguer anomalies have been calculated, but terrain corrections have not yet been applied. These latter corrections are in progress and once completed the new measurements will be added to the National Gravity Database in Ottawa. They will be used to improve inertial guidance systems, update geoid models, and provide insight into the tectonic framework of the region.

ACKNOWLEDGMENTS

Funding for the field program was provided by the United States Defence Mapping Agency and the Geological Survey of Canada. Field surveying was carried out by personnel from the Canadian Department of National Defence (Mapping and Charting Establishment), under the capable direction of

Capt. M.K. Walker. The participation of all field staff is gratefully acknowledged. We thank Richard Franklin and Brian Sawyer for drafting assistance.

REFERENCES

Brew, D.A., Karl, S.M., Barnes, D.F., Jachens, R.C., Ford, A.B., and Horner, R.B.

1991: A northern Cordilleran ocean-continent transect: Sitka Sound, Alaska, to Atlin Lake, British Columbia; *Canadian Journal of Earth Sciences*, v. 28, p. 840-953.

Lowe, C., Horner, R.B., Mortensen, J.K., Johnston, S.T., and Roots, C.F.

in press: New geophysical data from the Northern Cordillera: preliminary interpretations and implications for the tectonics and deep geology; *Canadian Journal of Earth Sciences*.

Morelli, C. (comp.)

1974: International Gravity Standardisation Net 1974; International Association of Geodesy, Special Publication No. 4, Paris.

Rupert, J.

1988: TRITER: A gravitational terrain correction program for IBM compatible personal computers; Geological Survey of Canada, Open File 1834.

Seemann, D.A., Lowe, C., Halliday, D.W., and Hearty, D.B.

1993: Enhanced gravity mapping project in the Canadian Cordillera; Society of Exploration Geophysicists 63rd Annual Meeting, Washington, D.C., Expanded abstract, p. SS2.26.

Veronneau, M. and Mainville, A.

1992: Computation of a Canadian geoid model using the FFT technique to evaluate Stokes' and Vening-Meinesz formulas in a planar approximation; Internal Report, Geodetic Survey Division, Energy, Mines and Resources, Ottawa, p. 11.

Wheeler, J.O., Brookfield, A.J., Gabrielse, H., Monger, J.W.H.,

Tipper, H.W., and Woodsworth, G.J. (comp.)

1991: Terrane map of the Canadian Cordillera; Geological Survey of Canada, Map 1713A.

Geological Survey of Canada Project 910027

New sulphide occurrences in the northeastern part of Iskut River map area and southeastern part of Telegraph Creek map area, northwestern British Columbia

M.H. Gunning¹, K. Patterson², and D. Green²
Cordilleran Division

Gunning, M.H., Patterson, K., and Green, D., 1994: New sulphide occurrences in the northeastern part of Iskut River map area and southeastern part of Telegraph Creek map area, northwestern British Columbia; in Current Research 1994-A; Geological Survey of Canada, p. 25-36.

Abstract: Six new sulphide occurrences were found during geological mapping of Paleozoic rocks in the More Creek area.

A zone more than 100 m long of massive seams and concentrated veinlets of pyrite northeast of Alexander Glacier is named the Broken Antler sulphide occurrence. It is within one of at least 3 rhyolite bodies in a thick, basalt-dominated, subaqueous volcanic succession believed to be mid-Early Carboniferous or older. Base metal abundances are low, and precious metal and trace element abundances are variable (e.g., <5-200 ppb Au, 2-3980 ppm As, <2-108 ppm Sb). The geological setting and lack of previous work warrant thorough exploration for volcanic-hosted base metal sulphide deposits.

An occurrence of auriferous quartz veins in a mid-Carboniferous or older metavolcanic succession, two occurrences of copper sulphide and gold in mid-Carboniferous or older limestone, and one occurrence of specular hematite and gold in Permian limestone are also described.

Résumé : Six nouveaux indices de sulfures ont été découverts pendant la cartographie géologique des roches paléozoïques de la région du ruisseau More.

Une zone de plus d'un centaine de mètres de veines massives et de filonnets concentrés de pyrite, au nord-est du Glacier Alexander, est appelée l'indice de sulfures de Broken Antler. Elle est contenue dans l'un d'au moins trois massifs rhyolitiques encaissées dans une épaisse succession volcanique subaquatique à prédominance de basalte qui daterait du milieu du Carbonifère précoce ou d'avant. Les concentrations de métaux communs sont faibles et celles des métaux précieux et des éléments traces sont variables (p. ex. <5-200 ppb d'Au, 2-3980 ppm d'As, <2-108 ppm de Sb). La cadre géologique et l'absence de travaux antérieurs justifient une prospection approfondie de cette succession volcanique pour la découverte de gisements de sulfures de métaux communs.

Un indice de filons de quartz aurifères dans une succession métavolcanique du Carbonifère moyen ou plus ancienne, deux indices de sulfures cuprifères et d'or dans un calcaire du Carbonifère moyen ou plus ancien et une occurrence d'hématite spéculaire et d'or dans un calcaire permien sont également décrites.

¹ Department of Earth Sciences, University of Western Ontario, London, Ontario, N6A 5B7

² Department of Geological Sciences, University of British Columbia, Vancouver, British Columbia V6T 1Z4

INTRODUCTION

The middle to upper Paleozoic Stikine assemblage is the foundation for extensive early Mesozoic volcano-sedimentary successions that underlie much of northwestern Stikinia. Volcanic rocks are predominant in sub-Permian strata but there has been little exploration for syngenetic or epigenetic, volcanic-hosted, base-metal sulphide deposits, particularly in comparison to the amount of exploration in Mesozoic volcanic successions. This report documents the character of new sulphide occurrences in Paleozoic strata, and highlights the potential for volcanic-hosted base metal deposits in the Stikine assemblage.

The study area is in the northwestern part of Stikinia, near the western margin of the Intermontane Belt (Fig. 1). It straddles the boundary between 1:250 000 NTS map areas 104B (Iskut River) and 104G (Telegraph Creek). New sulphide occurrences are hosted in Paleozoic strata (Fig. 2). Trace element analyses of grab samples obtained during cursory examination of the occurrences during regional geological mapping and UTM locations are in Table 1.

Sulphide occurrence 1 is named Broken Antler, and occurrences 2 to 6 are not named. Occurrence descriptions are grouped by area: Alexander Glacier, Iskut Icefield, and Mess Creek headwater. Occurrence 3 is massive and semimassive pyrite in a 20-50 centimetre-wide, steeply east-dipping quartz-carbonate alteration zone about 10 m long within basalt, and is not described in detail.

Data in this report are from geological mapping in 1992 and 1993 that is part of a PhD study on the nature of subaqueous volcanic successions of the middle to upper Paleozoic Stikine assemblage in the Forrest Kerr Creek-More Creek-Mess Creek area (e.g., Gunning, 1992, 1993). Fieldwork for the thesis was done in conjunction with ongoing regional mapping of the Iskut River map area by R.G. Anderson (e.g., Anderson, 1989).

GENERAL GEOLOGICAL SETTING

The new sulphide occurrences are within a continuous, north-trending belt of Paleozoic strata over 80 km long between the Iskut River and Mess Lake. The Late Devonian Forrest Kerr pluton (Logan et al., 1992a, b, 1993; Gunning, 1993) is the east boundary to the belt in the More Creek area (Fig. 2). The polyphase pluton underlies more than 500 km². Mafic phases are common near pluton margins; medium- to coarse-grained granite is the most extensive, and granite and aplite intrude mafic rocks in complex mixed zones of diorite and granite (Fig. 3). An intermediate phase of the pluton in the Forrest Kerr area yielded a Late Devonian date from U-Pb geochronology on zircon (Logan et al., 1992a, 1993).

Occurrences 1 and 3-6 are in metavolcanic successions. Strata are likely mid-Carboniferous or older based on their down-section position relative to a skeletal wackestone interval at occurrence 5 which resembles well-dated, mid-Lower

Carboniferous limestone to the south (Logan et al., 1990a, b; Gunning, 1992). Occurrence 2 is in Permian(?) limestone associated with Upper Triassic intrusive and extrusive rocks on a nunatak in the eastern part of the Iskut Icefield.

PREVIOUSLY KNOWN SHOWINGS

There are less than 20 assessment reports filed for 1:50 000 NTS map areas 104G/2 and 3, and there are only three BC MEMPR MINFILE mineral showings in Paleozoic strata in the More Creek area; there is no previous work on the sulphide occurrences reported here. Previous work relevant to this report includes exploration on the BIK showing by Silver Standard Mines (MINFILE #104G-49) and the BJ showing (MINFILE #104G-70) by Teck Exploration Ltd. in the Mess Creek area, and evaluation of mineralized boulders and geophysical anomalies in the More Glacier area (Foremore Property; FM on Fig. 2) by Cominco Limited. The character of showings of stratabound veins, stratiform massive sulphides, porphyry copper-gold occurrences, and skarns in Paleozoic and Mesozoic strata and plutons in the More Creek area are reviewed by Logan et al. (1992a).

BIK showing

The BIK showing is similar to the newly found sulphide occurrences 5 and 6 that are located about 1 and 4 km to the south, respectively (Fig. 2). Stringers and blebs of tetrahedrite in limestone breccia, and malachite on fractures, are in fossiliferous, recrystallized, siliceous limestone. Sulphides are commonly associated with subhorizontal quartz vein and fracture sets. Grab samples have up to 819 g/t silver, 13% copper, 2.8% zinc, and trace gold (BC MEMPR MINFILE 104G-049). The limestone dips west-northwest, and is within an undifferentiated succession of massive and foliated basalt and dolerite, and dark green phyllite.

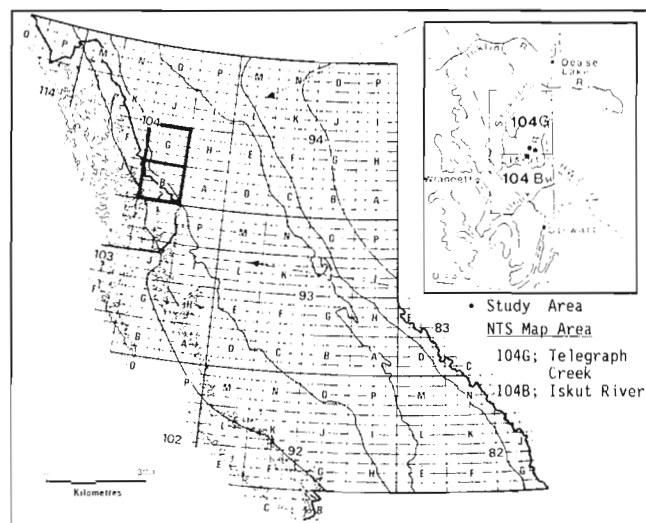


Figure 1. Location of new sulphide occurrences in the More Creek area.

BJ showing

Quartz-sulphide veins at the BJ showing are similar to veins at the newly found sulphide occurrence 4 located about 5 km to the southwest. The showing is at the contact between Paleozoic, foliated diorite and a metavolcanic succession of basalt, foliated basalt, microdolerite sills, and chlorite and

quartz-sericite schist. Metamorphic quartz segregations are tightly folded with dark green chlorite schist, and contain stringers and blebs of pyrite and rare chalcopyrite (BC MEMPR MINFILE 104G-070). Veins grade into siliceous and potassic alteration halos. One auriferous vein is >180 m long and contains trace base metal sulphides and sporadic gold. Limonitic and sideritic, brown-weathered carbonate

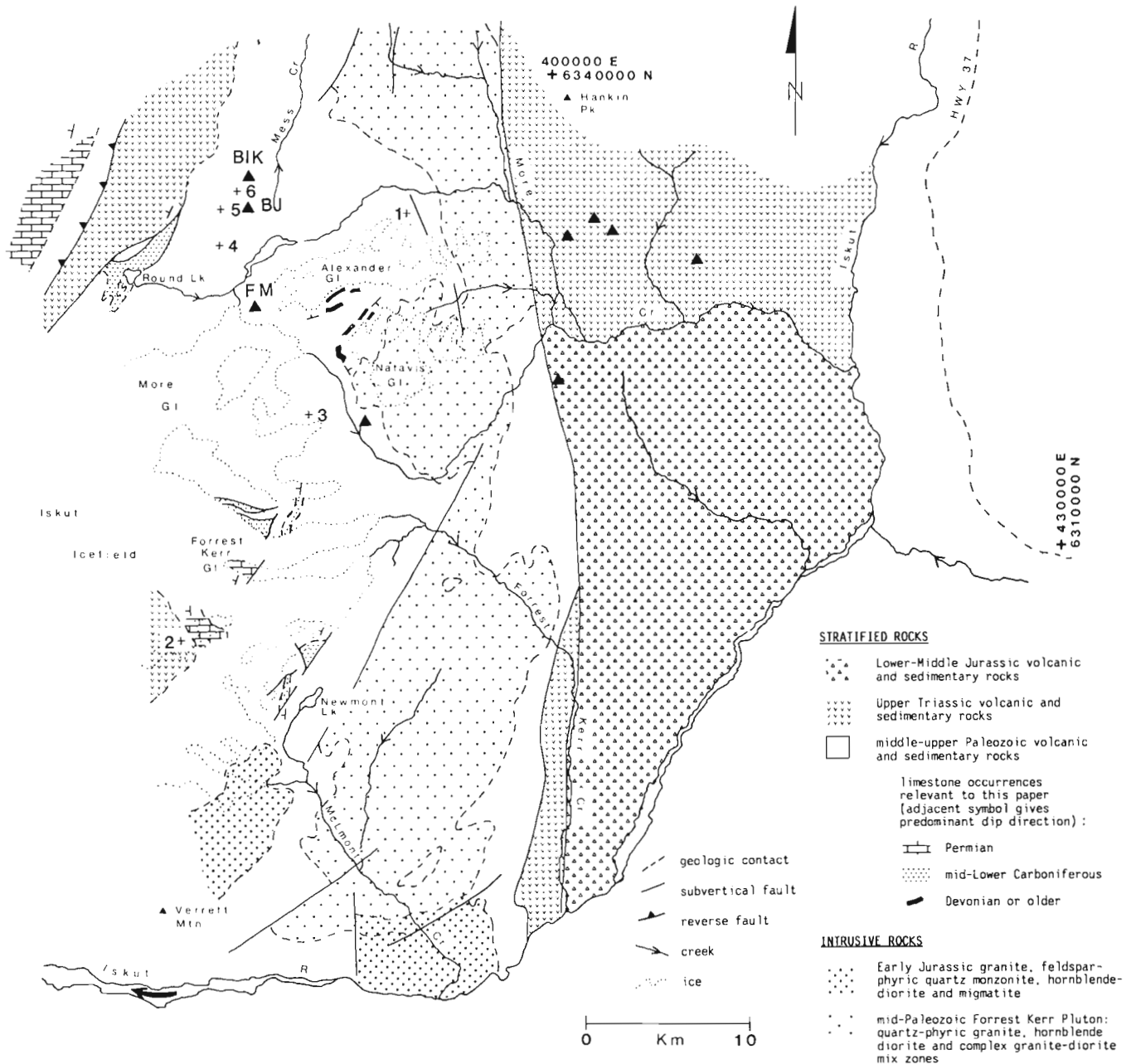


Figure 2. General distribution of Paleozoic, Upper Triassic, and Lower-Middle Jurassic volcano-sedimentary successions and plutons, in the Forrest Kerr Creek-More Creek area. Some data from Geological Survey of Canada (1957), Read et al. (1989), Souther (1972), and Logan et al. (1990b, 1992b) are included. Crosses are at new sulphide occurrences (UTM locations are in Table 1). Solid triangles are at previously discovered showings in the southwestern part of the Telegraph Creek map area; letters abbreviate names of showings discussed in text.

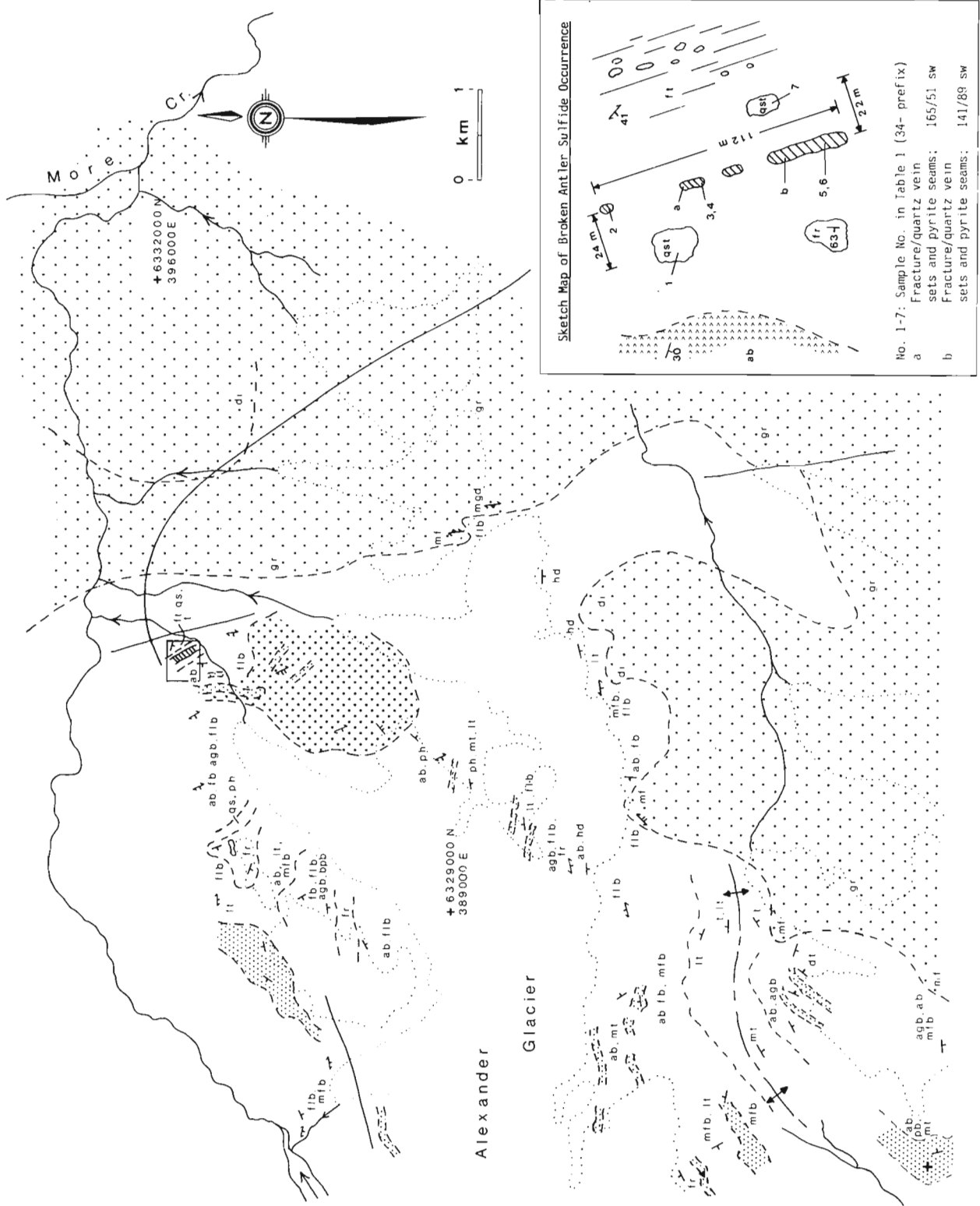


Figure 3. Geological sketch map of the Alexander Glacier area, and sketch map of the Broken Antler sulphide occurrence. The cross and solid triangle are locations of fossils assigned Late Silurian to Early Devonian age.

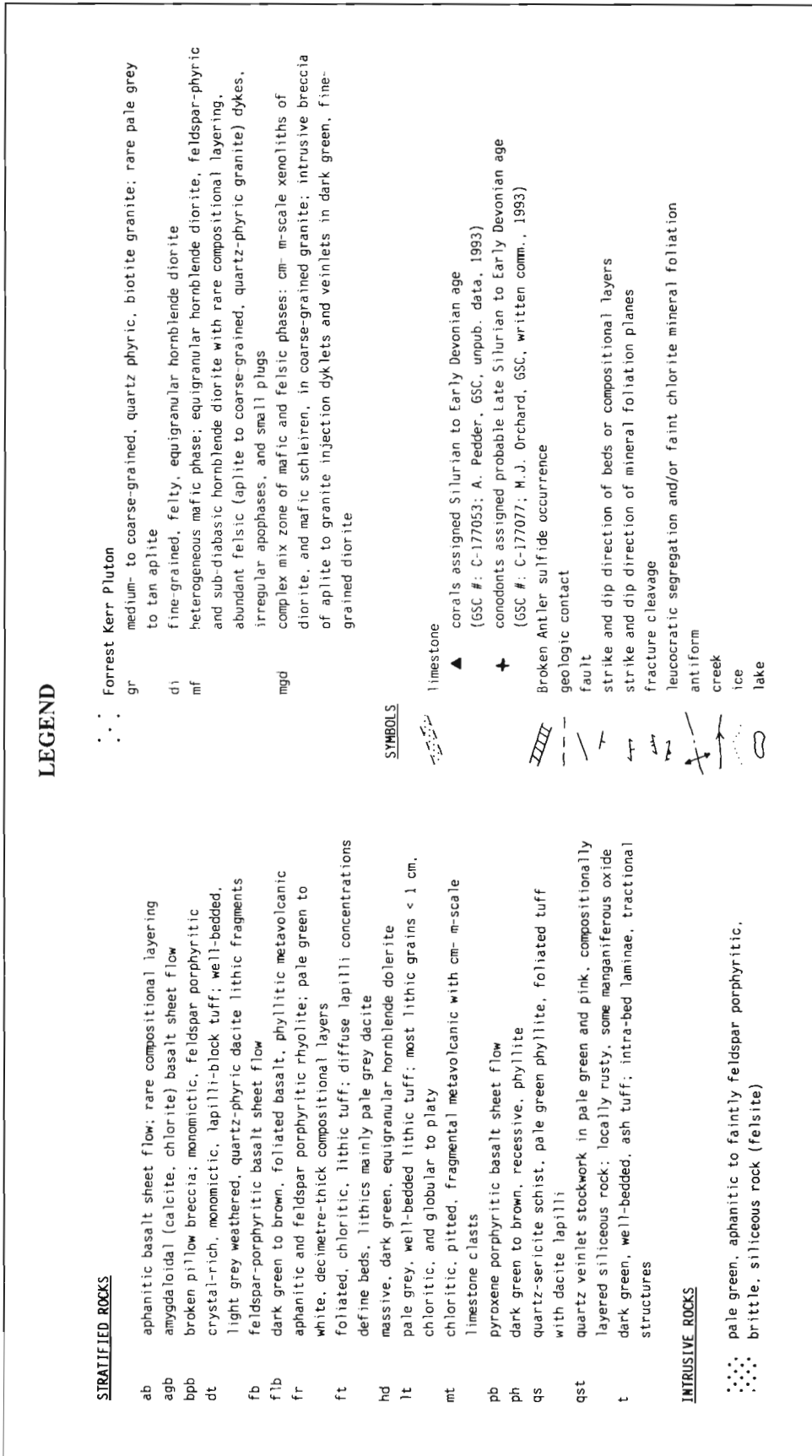


Table 1. Trace element abundances in grab samples from new sulphide occurrences.

| Sample No.: | 34-1 | 34-2 | 34-3 | 34-4 | 34-5 | 34-6 | 34-7 | 333-2 | 294 | 49 | 50 | 82 (Base) | 82-2 | 98 |
|-----------------------|---------|---------|---------|---------|---------|---------|---------|---------|---------|---------|---------|-----------|----------|---------|
| Location on Figure 2: | 1 | 1 | 1 | 1 | 1 | 1 | 1 | 2 | 3 | 4 | 4 | 5 | 5 | 6 |
| Map Area: | 104G/2 | 104G/2 | 104G/2 | 104G/2 | 104G/2 | 104G/2 | 104G/2 | 104B/14 | 104G/2 | 104G/2 | 104G/2 | 104G/2 | 104G/2 | 104G/2 |
| UTM N: | 6331790 | 6331790 | 6331790 | 6331790 | 6331790 | 6331790 | 6331790 | 6305860 | 6319470 | 6330220 | 6330480 | 6338120 | 6338120 | 6340610 |
| UTM E: | 391840 | 391840 | 391840 | 391840 | 391840 | 391840 | 391840 | 376210 | 384810 | 379790 | 380000 | 380180 | 380180 | 381290 |
| Au (ppb) | < 5 | 15 | 30 | 15 | 200 | 40 | < 5 | 515 | < 5 | 43 | 150 | 5 | < 5 | 5 |
| Ag (ppm) | < 0.2 | 0.2 | < 0.2 | 0.4 | < 0.2 | 0.4 | < 0.2 | 1.4 | | | | < 0.2 | > 200 | 1.2 |
| Al (%) | 0.46 | 0.35 | 0.22 | 0.36 | 0.53 | 0.41 | 0.37 | 0.71 | | | | 0.10 | 0.10 | 0.11 |
| As (ppm) | 2 | 112 | 3230 | 200 | 3980 | 958 | 28 | 54 | 210 | 25 | 17 | < 2 | 2320 | < 2 |
| Ba (ppm) | 190 | 140 | < 10 | 40 | < 10 | 10 | 90 | 10 | | | | 10 | 290 | 30 |
| Be (ppm) | < 0.5 | < 0.5 | < 0.5 | < 0.5 | < 0.5 | < 0.5 | < 0.5 | < 0.5 | | | | 0.5 | 0.5 | < 0.5 |
| Bi (ppm) | < 2 | < 2 | < 2 | < 2 | < 2 | < 2 | < 2 | < 2 | | | | < 2 | < 2 | < 2 |
| Cd (ppm) | < 0.5 | < 0.5 | 3.5 | < 0.5 | < 0.5 | 0.5 | < 0.5 | < 0.5 | | | | < 0.5 | 69.5 | 0.5 |
| Co (ppm) | < 1 | 1 | < 1 | 3 | < 1 | 1 | < 1 | 34 | 20 | < 5 | 17 | 4 | 28 | 3 |
| Cr (ppm) | 151 | 159 | 134 | 142 | 156 | 190 | 171 | 80 | 98 | < 5 | < 5 | 18 | 10 | 14 |
| Cu (ppm) | 1 | < 1 | 16 | < 1 | 35 | < 1 | < 1 | 501 | 18 | 15 | 27 | 32 | > 10,000 | 204 |
| Ga (ppm) | < 10 | < 10 | < 10 | < 10 | < 10 | < 10 | < 10 | < 10 | | | | 10 | < 10 | < 10 |
| Hg (ppm) | < 1 | < 1 | < 1 | < 1 | 10 | < 1 | < 1 | 1 | | | | < 1 | 154 | < 1 |
| La (ppm) | 20 | 10 | < 10 | 10 | < 10 | 10 | 20 | 30 | | | | < 10 | < 10 | < 10 |
| Mb (ppm) | < 1 | 7 | 82 | 4 | 101 | 17 | < 1 | 8 | | | | < 1 | < 1 | 2 |
| Ni (ppm) | 2 | 2 | 4 | 3 | < 1 | 3 | 2 | 8 | 51 | 22 | 19 | 56 | 40 | 35 |
| P (ppm) | 70 | 30 | < 10 | 10 | 60 | < 10 | 30 | 170 | | | | 50 | 10 | 150 |
| Pb (ppm) | 38 | 12 | 16 | 30 | 20 | 12 | 6 | 30 | < 5 | < 5 | < 5 | 12 | 20 | 6 |
| Sb (ppm) | < 2 | < 2 | 88 | < 2 | 108 | 12 | < 2 | 8 | | | | 12 | > 10,000 | 124 |
| Sc (ppm) | < 1 | < 1 | 1 | < 1 | 1 | < 1 | < 1 | 3 | | | | < 1 | 2 | 1 |
| Sr (ppm) | 5 | 6 | 1 | 3 | 2 | 6 | 7 | 19 | | | | 47 | 57 | 36 |
| Ti (%) | < 0.01 | < 0.01 | < 0.01 | < 0.01 | < 0.01 | < 0.01 | < 0.01 | 0.04 | | | | < 0.01 | < 0.01 | < 0.01 |
| Tl (ppm) | 10 | < 10 | 60 | < 10 | 30 | 10 | 10 | < 10 | | | | 20 | < 10 | 20 |
| U (ppm) | < 10 | < 10 | < 10 | < 10 | < 10 | < 10 | < 10 | < 10 | | | | < 10 | < 10 | < 10 |
| V (ppm) | 2 | 1 | < 1 | 1 | < 1 | < 1 | 1 | 23 | 249 | 22 | 41 | 2 | 1 | < 1 |
| W (ppm) | < 10 | < 10 | < 10 | < 10 | 20 | < 10 | < 10 | 40 | | | | < 10 | < 10 | < 10 |
| Zn (ppm) | 48 | 8 | 42 | 14 | 34 | 20 | 12 | 76 | 124 | 94 | 17 | 26 | 5760 | 62 |

veins are also within chlorite schist. They have potassic and carbonate alteration envelopes, and contain stringers of pyrite and arsenopyrite, and scattered blebs of sphalerite, chalcopyrite, and galena; sporadic gold content is up to 2.06 g/t. North- to northwest-trending veins and alteration zones are crosscut by barren, light brown-weathered, northeast-trending quartz-carbonate veinlet sets (Holbek, 1988).

Quartz veins and quartz-barite breccia are at a north- to northeast-trending fault between quartz-sericite schist and foliated, fine grained diorite in one area. Disseminations and blebs of pyrite, galena and sphalerite are scattered throughout breccia. The sulphide occurrence is more than 450 m long and gold content is sporadic (up to 0.34-1.36 g/t; Folk, 1986). Quartz-chalcopyrite veins in limonitic, brown-weathered iron-carbonate alteration zones peripheral to breccia zones contain narrow, sinuous, discontinuous stringers of tetrahedrite.

Foremore property

The Foremore claim group was explored by Cominco Limited to locate the source of thousands of boulders of massive sphalerite and pyrite in moraine of the north and east forks of More Glacier (Fig. 2; Barnes, 1989). Float distribution is indicative of a subglacial source, possibly coincident with an electromagnetic conductor below the confluence of the east and north lobes of the glacier. In order of decreasing abundance, pyrite, sphalerite, galena, barite, and chalcopyrite occur as massive seams and stringers in rusty, manganiferous, siliceous, hematitic rock.

A sulphide-bearing, felsic volcanoclastic interval within a north-trending belt of steep east-dipping graphite and chlorite schist east of the north fork of More Glacier was also examined by Cominco. The quartz-eye bearing rock has laminations and disseminations of fine grained pyrite, galena, and sphalerite. The mafic succession in the More Glacier area, including scattered limestone of Early Devonian age, forms the western and southwestern part of the basalt- and dolerite-dominated metavolcanic facies that underlies the Mess Creek headwater and Alexander Glacier area.

NEW SULPHIDE OCCURRENCES

Alexander Glacier area

Sulphide occurrence 1: Broken Antler

A discontinuous belt of rusty, brittle, siliceous rock about 110 m long and 10 m wide with abundant decimetre-thick seams of massive pyrite, and metre-thick zones of concentrated pyrite stringers occurs just northeast of a northeast fork of Alexander Glacier (1:50 000 NTS map area 104G/2; UTM coordinates: 6331790N, 391840E; sulphide occurrence 1 on Fig. 2, Fig. 3 inset, and Fig. 4). Rusty and manganiferous patches are scattered throughout pale green, mottled grey-white and tan siliceous rock (Fig. 4b). There are at least three stages of quartz veins and one stage of carbonate veins which predate seams and stringers of massive, fine grained pyrite. Outcrops of dense stockworks of millimetre-thick, sinuous, milky quartz veinlets in pale grey and pink siliceous rock are

similar to quartz vein stockworks in siliceous rock immediately west and east of the sulphide occurrence, and to stockworks in the rhyolite body about 2 km southwest of the sulphide occurrence (Fig. 5c). Two tabular, concordant, 30-50 centimetre wide seams of massive pyrite more than 5 m long occur in the central and south part of the occurrence. Narrower, centimetre-thick, sinuous, broadly concordant seams of massive pyrite are throughout the occurrence (Fig. 4b). A 2.8 m wide, concordant zone of >80% sinuous pyrite veinlets in a white, siliceous, sintery matrix outcrops in the northern part of the showing. Medium grained pyrite lines fracture and vug surfaces throughout the central part.

Base metal contents in the sulphide occurrence are low, and there are no base or precious metal anomalies in stream sediment samples from two streams that drain the glacial

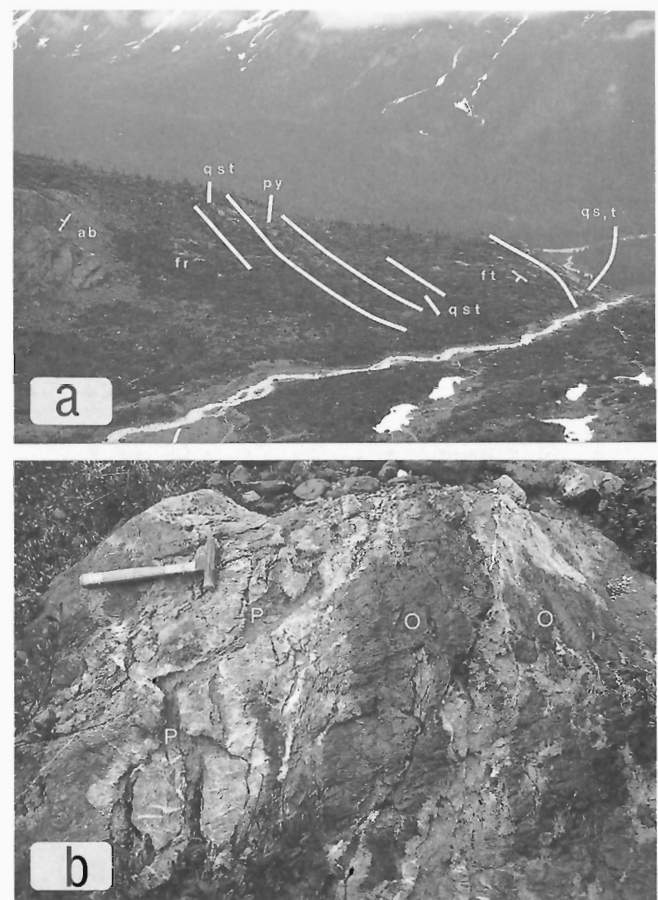


Figure 4. (a) View north at the Broken Antler sulphide occurrence. Beds, mineral foliation planes, and sulphide zones in the field of view are southwest-dipping (Fig. 3). Dimensions of the occurrence are in Figure 3 inset. All labels except "py", the zone of extensive pyrite, correspond to Figure 3 map legend. (b) South end of the sulphide occurrence is brittle, fractured, light-coloured siliceous rock which contains irregular patches of rusty and manganiferous oxide (dark zones labelled "O"), quartz veinlet stockworks (lower left), and tabular and irregular seams of massive pyrite (P) and wider zones of concentrated pyrite stringers.

valley south of the showing (Table 1; Geological Survey of Canada, 1988). Precious metal and trace element contents in massive pyrite seams are variable (e.g., 15-200 ppb Au, 112-3980 ppm As, <1-10 ppm Hg, and <2-108 ppm Sb).

Quartz veinlet stockworks, rusty patches and trace disseminated pyrite are in pale grey and pale pink rhyolite immediately southwest and northeast of the occurrence (Fig. 3 inset). This rock grades into, and is overlain by, pale green, compositionally layered rhyolite west of the sulphide occurrence, and is underlain by foliated tuff and lapilli tuff east of the occurrence. Rhyolite east and west of the sulphide occurrence has high Ba and K, and low base metal (excluding Pb), precious metal and trace element contents compared to seams and stringers of pyrite from the sulphide occurrence (Samples 34-1 and 34-7 in Table 1; e.g., Ba 90-190 ppm, As 2-28 ppm, and Au and Sb below detection).

Geological setting

The sulphide occurrence is within an extensive, compositionally bimodal but predominantly mafic, metavolcanic succession that underlies the Mess Creek headwater-Alexander Glacier-Natavis Glacier-More Glacier area (Fig. 3). It is believed to be in the lowermost part of the succession. Intercalated phyllite, graphite, chlorite and quartz-sericite schist, and tightly folded, thin-bedded ash and lapilli tuff, chert, and medium to dark grey limestone are intercalated with mafic volcanic rocks throughout the succession. Beds and mineral foliation planes dip west-southwesterly and a second phase, crenulation cleavage is common in phyllite and schist.

Age of the succession is equivocal. Limestone on the south limb of a northeast- to east-trending antiform south of Alexander Glacier has conodonts assigned a probable

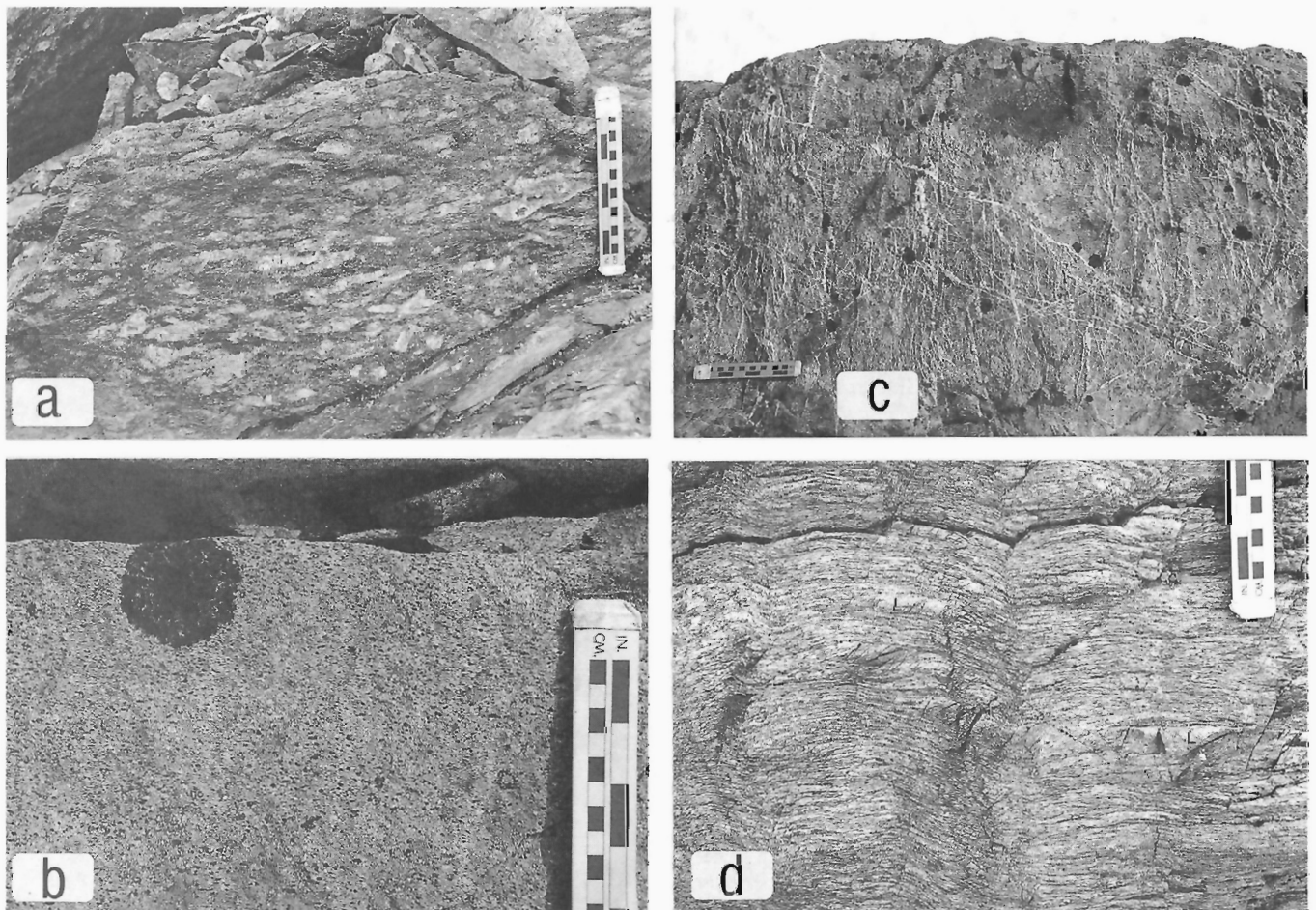


Figure 5. Rock types characteristic of the metavolcanic succession that hosts the Broken Antler sulphide occurrence. Monomictic, aphanitic and feldspar porphyritic mafic volcanic breccia (a), and thin interbeds of pale grey weathered lithic tuff with globular and platy, chloritic fragments (b) intercalated with basalt, and compositionally layered, aphanitic and feldspar porphyritic rhyolite with abundant quartz veinlet stockwork zones (c) are common west of the sulphide occurrence. Tightly folded and crenulated, pale grey quartz-sericite schist (d) with scattered fragments of aphanitic rhyolite (L) is east of the occurrence.

M.J. Orchard, GSC, written comm., 1993) and limestone on the north limb has small dendroid corals assigned Silurian to Early Devonian age (GSC #: C-177053; A.E. Pedder, GSC, unpub. data, 1993). Similar, but nonfossiliferous limestone is within the mafic volcanic succession north of Alexander Glacier, but the stratigraphic position, and hence age of the Broken Antler sulphide occurrence is equivocal because of folds, faults, and abrupt facies changes. Mid-Lower Carboniferous limestone is within successions of mafic flows and monomictic breccia, felsic tuff, and coarse grained volcanoclastic rocks in the Round Lake and Forrest Kerr Glacier areas, up-section according to regional dip-directions (Fig. 2). The Late Devonian Forrest Kerr Pluton bounds the succession to the east.

Steep south to southwest dips reveal a thick stratigraphic section north of Alexander Glacier. Rock types in the succession in order of decreasing abundance are: aphanitic and feldspar porphyritic basalt sheet flows, some with planar compositional layering; monomictic, pitted, dark green basalt flow breccia; isolated pillow breccia; amygdaloidal basalt sheet flows; lithic tuff; compositionally layered rhyolite; and rare dark green and brown phyllite, sericite, and quartz-sericite schist and dark to medium grey, nonfossiliferous limestone.

Mafic fragmental volcanic rocks are massive to crudely bedded with diffuse, decimetre-thick fragment concentrations; they are commonly feldspar porphyritic and generally matrix-supported (Fig. 5a). Fragments are 20-40% of the breccia and generally less than 10 cm in size. Alignment of fragments in the plane of a faint, but pervasive chlorite mineral foliation is common (Fig. 5a). Isolated pillow breccia with imbricated, amoeboid-shaped pillows is rare. Lithic tuff is volumetrically minor but distinctive in outcrop because platy to globular, chloritic fragments generally <1 cm in size contrast to a pale grey ash matrix (Fig. 5b). Tuff forms metre-thick intervals intercalated with mafic sheet flows and flow breccias. A small rhyolite body is about 2 km southwest of the occurrence, and there is a large, dome-like, nondescript felsic intrusion (felsite) south of the sulphide occurrence. Rhyolite is aphanitic to faintly feldspar-porphyritic. Decimetre-thick, nontabular compositional layers with sharp, coherent contacts are common, and rusty quartz veinlet stockwork zones are scattered throughout (Fig. 5c).

East of the sulphide occurrence, from west to east are foliated lapilli tuff, crenulated and chaotically folded quartz-sericite schist (Fig. 5d), and dull green, thin-bedded ash tuff with tractional sedimentary structures. There are rare rhyolite fragments with quartz vein stockwork in lapilli tuff. High length-to-width ratios, and well-developed strain shadows are characteristic of felsic lapilli in foliated tuff, and there is a pervasive crenulation cleavage in schist.

Iskut Icefield area

Occurrence 2

Auriferous specular hematite is in limestone on a nunatak in the eastern part of the Iskut Icefield, southwest of Forrest Kerr Glacier (1:50 000 NTS map area 104G/2; UTM coordinates: 6331790N, 391840E; occurrence 2 on Fig. 2). A tabular interval of light grey limestone hosts fine- to medium-grained, dull brown and dark grey to steel grey hematite in irregular patches and in massive to semimassive, tabular and sinuous veins in concordant, metre-wide zones. Hematite is in a brown, friable, calcareous Fe-oxide matrix; Fe-rich zones account for about 10% of the limestone interval. Regular centimetre-spaced hematite-lined fractures are common. There are traces of a pale blue to blue-grey oxide mineral within darker grey hematite in some outcrops. Hematite-rich zones have sharp margins and although locally irregular they are broadly concordant to bedding in limestone. A grab sample of hematite and calcareous, brown oxide has 515 ppb Au, 501 ppm Cu, 30 ppm Pb, and 76 ppm Zn (Sample 333-2 in Table 1).

Geological setting

Specular hematite and limestone are within an Upper Triassic volcanic succession near the contact with Permian limestone in the central part of the nunatak (Fig. 2). The east end of the nunatak is underlain by a volcanoclastic unit that overlies a columnar jointed rhyolite dome. Volcanoclastic rocks form dark purple, grey, and maroon, crudely bedded, polyolithic deposits with abundant decimetre- to metre-size, rounded blocks of fossiliferous limestone and rhyolite joint fragments, supported in a crystal-rich matrix. Volcanic rocks are interpreted to be mid-Early Carboniferous or younger.

A thick, well-bedded succession of Permian skeletal wackestone conformably overlies the coarse grained volcanoclastic strata but the contact is locally faulted. Tabular, concordant concentrations of large, strophic brachiopods, and ceratoid, cylindrical, and dendroid rugose corals are common in limestone. The west half of the nunatak is underlain by Upper Triassic(?) pyroxene-phyric basalt, aphanitic dacite, crystal tuff with pale grey dacite lapilli and blocks, trachytic and equigranular, potassium feldspar megacrystic syenite(?), and potassium feldspar megacrystic intrusive breccia. Flows and tuff dip moderately west-southwest. The contact with Paleozoic strata is, in one place, a north-trending fault, and at another locality, a pyroxene crystal-rich, well-bedded volcanoclastic unit with local tractional sedimentary structures and abundant pyroxene-phyric basalt fragments conformably overlies Permian limestone. Potassium feldspar megacrystic, trachytic to equigranular syenite(?) dykes intrude Permian limestone in the central part of the nunatak.



Figure 6. View north at the headwater valley of Mess Creek (right-center of photo) from the north fork of More Glacier. The black arrow points to new sulphide occurrence 5, the interval of recrystallized, skeletal wackestone believed to mid-Early Carboniferous in age that hosts copper minerals, and contains free gold obtained from a conodont separate.

Decimetre-thick beds of light grey skeletal wackestone which host hematite dip moderately west-northwest. Limestone is light grey, and contains scattered echinoderm columnals and small, ceratoid corals. Limestone is believed to be Permian in age, and if so, it must be a raft associated with the construction of a Late Triassic intrusive/extrusive complex.

Mess Creek headwater area

Sulphide occurrence 4

Sulphide-bearing quartz veins are within a northwest-trending belt of graphite, chlorite, graphite-chlorite, and graphite-chlorite-talc schist northeast of Round Lake (1:50 000 NTS map area 104G/2; UTM coordinates: 6330220N, 379790E; occurrence 4 on Fig. 2). The schist belt is well exposed on the east flank of a north-trending creek valley (Fig. 6). Abundant veins define a zone about 2 km long and about 300 m wide that grades into barren schist; vein distribution within the zone is erratic. Most veins are parallel to subparallel to a steep east-dipping to subvertical S_1 mineral foliation and are locally folded with the schist in north- and east-trending minor folds. Some are tabular and laterally continuous for tens of metres, and others are discontinuous, anastomosing boudins and sigmoids, elongate parallel to S_1 mineral foliation.

Sharp-walled veins are cloudy to milky bull quartz from 1 to 50 cm wide. Quartz vein breccia with angular, vein-margin xenoliths of dark green wall rock chlorite schist is common. Pyrite-lined vugs, and 2-5 cm long quartz cockscombs are common. Scattered veins have concordant seams of graphite in vein centres, and rare veins have marginal graphite/pyrite zones. Centimetre-wide, pale grey to brown, quartz-carbonate alteration zones are peripheral to some veins. Most veins are metamorphogenic in nature and predate formation of

north- and east-trending folds; similar timing is inferred for mineralized quartz veins farther north in the Mess Creek area (i.e. BJ showing).

A sample of a quartz vein and pyrite-lined vug contains 43 ppb Au (sample 49; Table 1), and a sample from a boulder within the vein system of rusty, manganiferous, siliceous, hematitic rock with disseminations, blebs, stringers, and massive seams of fine grained pyrite contains 150 ppb Au (sample 50; Table 1). Abundances of Au, Co, As, Ba, and Hg in a regional stream sediment sample from the river that drains the valley immediately west of the vein system, are anomalous for the Telegraph Creek map area (95th percentile; Geological Survey of Canada, 1988).

Sulphide occurrences 5 and 6

Copper sulphides are in massive and brecciated, distinctive pale orange to buff weathered limestone at the south end of an exposure of well-bedded, fossiliferous limestone at the east edge of a snowfield west of the headwater area of Mess Creek (1:50 000 NTS map area 104G/2; UTM coordinates: 6338120N, 380180E; occurrence 5 on Fig. 2). The limestone forms a tabular deposit at least 30 m thick that conformably overlies basalt; the upper contact is in the snowfield (Fig. 6). Sulphide occurrence 6 is at a similar interval of recrystallized, fractured, brecciated copper sulphide-bearing limestone about 2 km to the northeast.

The limestone interval at occurrence 5 is mainly coarse-grained, sparry floatstone with centimetre-scale echinoderm ossicles and concordant, but randomly oriented stem pieces. Lithologies are correlative to mid-Lower Carboniferous limestone to the south (Gunning, 1992). Decimetre-thick beds are defined by elongate and coalesced, pale tan chert nodules, and wavy stylo-bedding fracture partings. Copper minerals are most abundant in blocky, friable, highly fractured outcrops with abundant open spaces. Malachite and azurite occur as vug and fracture linings, and dull grey chalcocite is in discontinuous, millimetre- to centimetre-scale veinlets in pale orange-brown ankerite breccia. Breccia consists of angular, centimetre-scale, pale grey sparry floatstone fragments supported in a dull-brown ankerite matrix. A sample of limestone breccia at occurrence 5 contains >200 ppm Ag, 2320 ppm As, >10 000 ppm Cu, 154 ppm Hg, >10 000 ppm Sb, and 5760 ppm Zn (Sample 82-2; Table 1). Separates from conodont microfossil collections from both occurrences 5 and 6 contain free gold, but gold contents are below detection limits in grab samples from mineralized breccia zones (Table 1).

Geological setting

Sulphide occurrences 4 to 6 are within a thick, mafic, meta-volcanic succession well exposed on the west side of the headwater valley of Mess Creek (Fig. 6). Thin intervals of recrystallized, fossiliferous wackestone, such as those at occurrences 5 and 6, are throughout. Beds and mineral foliation planes are predominantly west- to southwest-dipping.

Rocks, in order of decreasing abundance are aphanitic and feldspar porphyritic, massive and faintly foliated basalt sheet flows, mafic lapilli tuff, mafic, monomictic volcanic breccia, massive microdolerite, and metre-thick intervals of pale green phyllite and dark green chlorite schist. Limestone is commonly spatially associated with phyllite. Phyllite commonly grades into thin-bedded ash tuff, and chlorite schist commonly grades into foliated and massive basalt.

DISCUSSION

The vein system at occurrence 4 is unexplored, and the extent of copper and precious metals in limestone at occurrences 5 and 6 is unknown. No evidence of previous prospecting was seen at any of the occurrences. The belt of schist and quartz veins at occurrence 4 warrants a thorough evaluation based on gold content in quartz veins and in pyrite-rich, siliceous, hematitic rock, and abundances of Au, Co, As, Ba, and Hg in a regional stream sediment sample in the river that drains the valley immediately west of the vein system (Geological Survey of Canada, 1988). Laminated pyrite and base metal sulphide in felsic tuff within the same belt of schist east of the north fork of More Glacier (Fm in Fig. 2) are further incentive for thorough exploration of the entire belt. The proximity, and similarity of previously discovered and newly found sulphide occurrences in the area is evidence of an extensive hydrothermal fluid system; precious metal abundances, and abundances of trace elements commonly abundant in epithermal deposits, in some sulphide occurrences and in one stream sediment sample, highlight the potential for epigenetic, strat-
abound, or structurally-controlled metal deposits.

Alexander Glacier area

There is potential for volcanic-hosted base metal sulphide deposits in the mid-Carboniferous or older metavolcanic succession in the More Creek area, yet previous mineral exploration work is limited. There is no evidence of previous prospecting at the Broken Antler sulphide occurrence, or at any of the other rhyolite bodies in the area. Logan et al. (1990a) emphasize the potential for massive sulphide deposits in mid-Carboniferous or older mafic volcanic successions west of Forrest Kerr Creek based on the discovery of layer-parallel pyrite zones in foliated, felsic volcanoclastic rocks, and Logan et al. (1992a) also suggest that the sulphide-rich boulders on the Foremore claim group are similar to Kuroko-style volcanogenic massive sulphide ore.

There are copper-zinc volcanogenic massive sulphide deposits in an Upper Carboniferous, compositionally bimodal but mafic-dominated metavolcanic succession north of the junction of the Taku and Tulsequah rivers in northwestern British Columbia (Nelson and Payne, 1984; Gunning, 1988). Sulphide occurrences and quartz vein stockwork zones are associated with rhyolite bodies in the Alexander Glacier area; the association of base metal massive sulphide deposits with felsic rocks in a lithologically correlative, upper Paleozoic metavolcanic succession at

Tulsequah underscores the potential for a base metal massive sulphide deposit in the Alexander Glacier area. Abundances of As, Sb, and Hg in one sample of massive pyrite in the south part of the sulphide occurrence (34-5; Table 1) could be indicative of an epithermal component to mineralization, and if so, structurally-controlled fluid migration could be an important aspect of the Broken Antler sulphide occurrence.

ACKNOWLEDGMENTS

Gunning thanks Bob Anderson (Project 840046) for support of the Stikine assemblage thesis project, and Rod Kirkham and Bob Hodder for instructive guidance and support. New sulphide occurrences described here are a credit to the regional mapping program of the Cordilleran Division; additional support from the NSERC/EMR Research Agreement Program (Grant #190 4 92), and from the Hirschhorn Bursary administered by Dr. R.W. Hodder at the University of Western Ontario, made completion of fieldwork in the remote area possible. Wayne Bamber, Mike Orchard, and Allan Pedder are thanked for preliminary fossil identifications. This article has been improved by comments from Bob Anderson and Bob Hodder.

REFERENCES

- Anderson, R.G.**
1989: A stratigraphic, plutonic and structural framework for the Iskut River map area, northwestern British Columbia; in *Current Research, Part E*; Geological Survey of Canada, Paper 89-1E, p. 145-154.
- Barnes, D.R.**
1989: Geological, Geochemical Report, Foremore Group, Liard Mining Division; British Columbia Ministry of Energy, Mines and Petroleum Resources, Assessment Report 19379.
- Folk, P.**
1986: Report on the geology and geochemistry of the Bee Jay group of claims; British Columbia Ministry of Energy, Mines and Petroleum Resources, Assessment Report 14982.
- Geological Survey of Canada**
1957: Operation Stikine; Geological Survey of Canada, Map 9-1957.
1988: National Geochemical Reconnaissance 1:250,000 Map Series, Sumdum-Telegraph Creek map areas; Geological Survey of Canada, Open File 1646.
- Gunning, M.H.**
1988: Tulsequah Chief Deposit; in *Exploration in British Columbia 1987*, British Columbia Ministry of Energy, Mines and Petroleum Resources, B78-83.
1992: Carboniferous limestone, Iskut River region, northwest British Columbia; in *Current Research, Part A*; Geological Survey of Canada, Paper 92-1A, p. 315-322.
1993: Lower to upper Paleozoic strata and plutons, lower Forest Kerr Creek area, northwestern British Columbia; in *Current Research, Part A*; Geological Survey of Canada, Paper 93-1A, P. 27-36.
- Holbek, P.M.**
1988: Geology and mineralization of the Stikine assemblage, Mess Creek area, northwestern British Columbia; M.Sc. thesis, University of British Columbia, Vancouver, British Columbia, 184 p.
- Logan, J.M., Koyanagi, V.M., and Drobe, J.R.**
1990a: Geology of the Forest Kerr Creek area, northwestern British Columbia (104G/15); in *Geological Fieldwork 1989*, British Columbia Ministry of Energy, Mines and Petroleum Resources, Paper 1990-1, p. 127-140.

Logan, J.M., Koyanagi, V.M., and Drobe, J.R. (cont.)

1990b: Geology and mineral occurrences of the Forest Kerr-Iskut River Area, northwestern British Columbia (104G/15); British Columbia Ministry of Energy, Mines and Petroleum Resources, Open File 1990-2.

Logan, J.M., Drobe, J.R., and Elsby, D.C.

1992a: Geology of the More Creek area, northwestern British Columbia; in Geological Fieldwork 1991, British Columbia Ministry of Energy, Mines and Petroleum Resources, Paper 1992-1, p. 161-178.

1992b: Geology, geochemistry, and mineral occurrences of the More Creek area, northwest British Columbia; British Columbia Ministry of Energy, Mines and Petroleum Resources, Open File 1992-5.

Logan, J.M., Drobe, J.R., McClelland, W.C., and Anderson, R.G.

1993: Devonian intraoceanic arc magmatism in northwestern Stikinia; (abstract), Geological Association of Canada Mineralogical Association of Canada, Program with Abstracts, v. 20, p. A60.

Nelson, J. and Payne, J.G.

1984: Paleozoic volcanic assemblages and volcanogenic massive sulfide deposits near Tulsequah, British Columbia; Canadian Journal of Earth Sciences, v. 21, p. 379-381.

Read, P.B., Brown, R.L., Psutka, J.F., Moore, J.M., Journeay, M., Lane, L.S., and Orchard, M.J.

1989: Geology of Parts of Snippaker Creek (194B/10), Forest Kerr Creek (104B/15), Bob Quinn Lake (104B/16), Iskut River (104G/1) and Moore Creek (104G/2); Geological Survey of Canada, Open File 2094.

Souther, J.G.

1972: Telegraph Creek map area, British Columbia; Geological Survey of Canada, Paper 71-44, 68 p.

Geological Survey of Canada Project 840046

Stratigraphic and structural setting of mineral deposits in the Brucejack Lake area, northwestern British Columbia

A.G.S. Davies¹, P.D. Lewis¹, and A.J. Macdonald¹
Cordilleran Division

Davies, A.G.S., Lewis, P.D., and Macdonald, A.J., 1994: Stratigraphic and structural setting of mineral deposits in the Brucejack Lake area, northwestern British Columbia; in Current Research 1994-A; Geological Survey of Canada, p. 37-43.

Abstract: Upper Triassic to Lower Jurassic Stuhini and Hazelton groups in the Brucejack Lake area, northwestern British Columbia (104B/8) host several precious metal vein deposits and showings. Oldest strata in the map area are Upper Triassic(?) heterolithic volcanoclastic conglomerate-breccia and sedimentary rocks, overlain by Lower Jurassic(?) sedimentary rocks. This sedimentary succession is overlain by intermediate volcanoclastic rocks dominated by feldspar-amphibole-bearing volcanic breccia. Uppermost rocks are dacitic and include both flows and volcanoclastic rocks. The stratigraphic succession is intruded successively by (1) plagioclase-hornblende diorite porphyry, (2) plagioclase-hornblende-phyric, potassium feldspar megacrystic porphyry, (3) flow-layered plagioclase porphyry. Field relationships suggest that precious metal mineralization may be associated with the second of these intrusive suites. Principal folds and associated cleavage overprint precious metal-bearing veins and associated alteration, and likely formed during Cretaceous contractional deformation.

Résumé : Les groupes de Stuhini et de Hazelton du Trias supérieur-Jurassique inférieur dans la région du lac Brucejack, dans le nord-ouest de la Colombie-Britannique (104B/8), recèlent plusieurs gisements filoniens et indices de métaux précieux. Les couches les plus anciennes dans la région cartographiée sont des roches sédimentaires et des roches volcanoclastiques hétérolithiques (conglomérat-brèche) du Trias supérieur(?), sur lesquelles reposent des roches sédimentaires du Jurassique inférieur(?). Cette succession sédimentaire est surmontée de roches volcanoclastiques intermédiaires où prédomine une brèche volcanique à feldspath-amphibole. Les roches sommitales sont dacitiques et renferment des coulées et des roches volcanoclastiques. La succession stratigraphique est recoupée successivement par 1) un porphyre de diorite à plagioclase-hornblende, 2) un porphyre à phénocristaux de plagioclase-hornblende et à mégacristaux de feldspath potassique, et 3) un porphyre à plagioclase, à rubanement de coulée. Les relations établies sur le terrain indiquent que la minéralisation de métaux précieux pourrait être associée à la deuxième suite de roches intrusives. Les plis principaux et le clivage associé se surimpriment aux filons renfermant les métaux précieux et à l'altération associée et ils se sont probablement formés durant la déformation par compression du Crétacé.

¹ Mineral Deposit Research Unit, Department of Geological Sciences, University of British Columbia, 6339 Stores Road, Vancouver, British Columbia V6T 1Z4

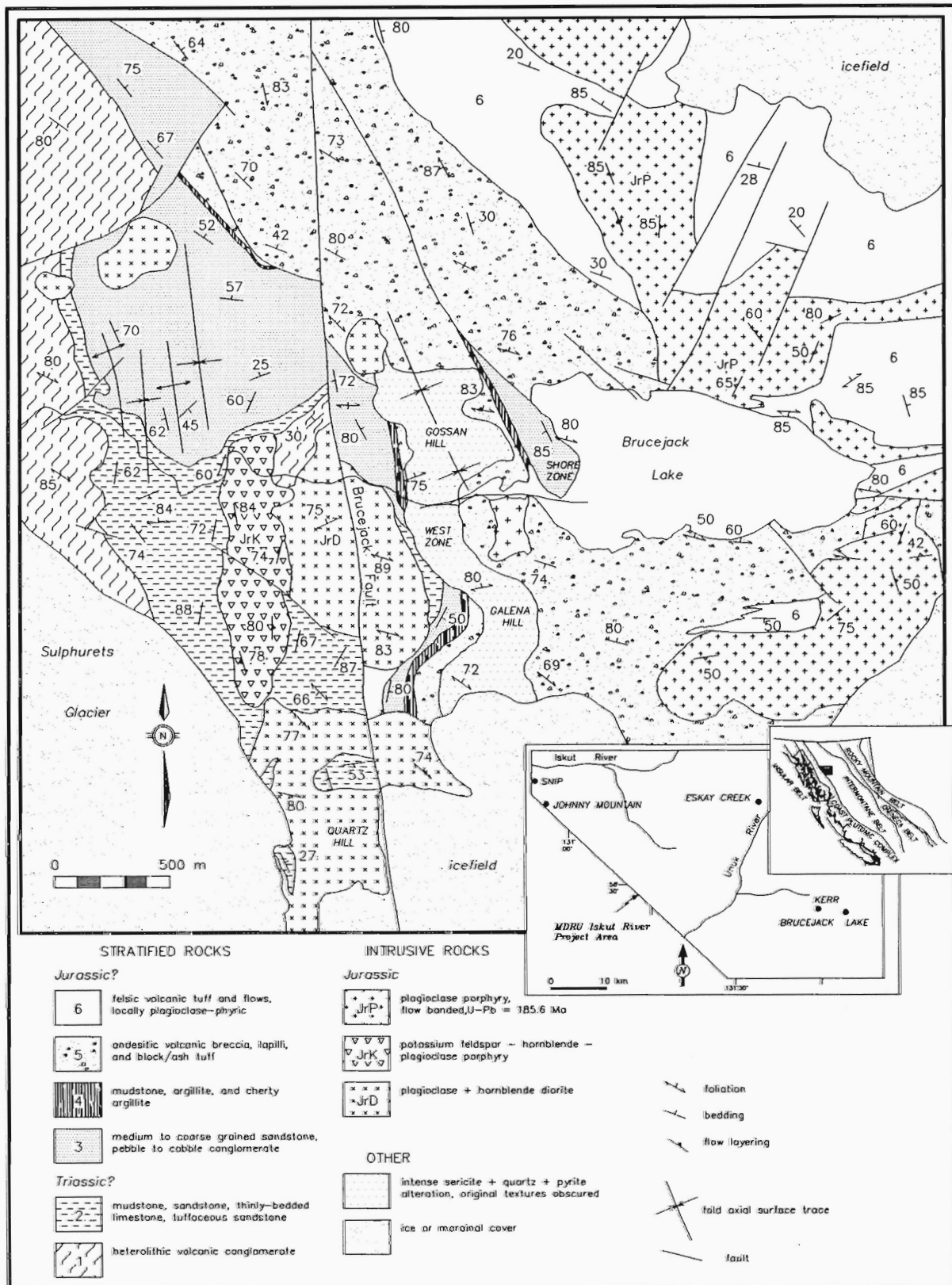


Figure 1. Geology of the Brucejack Lake area, northwestern British Columbia, based upon and simplified from 1:5000 mapping by the authors in 1993. Inset shows regional location.

INTRODUCTION

Widespread alteration and abundant mineral showings near Brucejack Lake in the Iskut River map sheet, northwestern British Columbia (Fig. 1) have attracted exploration to the area for over 30 years. Despite this focused interest, efforts to equate stratified host rocks with regionally defined sections elsewhere have been thwarted by alteration and plutonism in the area, and poor chronologic control. Documentation of a 185.6 Ma dacitic flow-dome complex in the east part of the area (Macdonald, 1993) demonstrates that at least some of the area contained rocks coeval with parts of the Hazelton Group, but the rock type distribution and stratigraphic relationships within the area remained poorly known. Mineral Deposit Research Unit (University of British Columbia) 1:5000 scale mapping completed during the 1993 field season (Fig. 1) identified a stratigraphic succession over 750 m thick which contains the upper part of the Stuhini Group and a thick Hazelton Group section. This report outlines six units defining this stratigraphic succession and three plutonic rock types which intrude these units, discusses new constraints on the structural history of the area, and briefly addresses how these aspects relate to alteration and mineralization near Brucejack Lake.

PREVIOUS GEOLOGICAL WORK

Earliest mapping in the Brucejack Lake area was completed as part of an M.Sc. thesis by Kirkham (1963). Subsequent exploration of the property by Granduc Mines Ltd. and Esso Resources Canada was reported by, for example, Bridge et al. (1981). Results of British Columbia Geological Survey Branch mapping have been reported by Alldrick and Britton (1988), Britton and Alldrick (1988), and Alldrick and Britton (1991); Geological Survey of Canada Open File maps have been published by Kirkham (1991, 1992). Henderson et al. (1992) described stratigraphy and structure to the north of the Brucejack Lake area. Mapping by Newhawk Gold Mines Ltd. has focused on the geology in the vicinity of mineral showings that are the subject of active exploration (e.g., Roach, 1990). Earlier work by Mineral Deposit Research Unit personnel and co-workers include a discussion of mineralization in the West Zone (Roach and Macdonald, 1992) and the stratigraphy south and east of Brucejack Lake (Macdonald, 1993).

STRATIGRAPHY

Strata exposed at Brucejack Lake comprise six mappable sedimentary and volcanic rock units. Moderate to steep eastward regional dips and facing directions, although locally complicated by folds and faults, indicate an eastward younging progression of these units. Contacts between these map units are sharp to gradational over several metres; all non-faulted contacts are parallel to bedding in units both above and below, and no unconformities are identified. Detailed lithostratigraphic descriptions for all rock units are provided

in Table 1 and photographs of representative examples are given in Figures 2-8. Lowest rocks, assigned to unit 1, comprise heterolithic mafic to intermediate volcanic breccia and conglomerate. Units 2 through 4 are sedimentary units consisting primarily of interbedded siltstone and sandstone, coarse grained sandstone to conglomerate, and thinly bedded argillite and mudstone, respectively. Andesitic rocks of unit 5, dominated by plagioclase-hornblende volcanic breccia, mark a transition to more active volcanic environments characterizing the central part of the exposed sequence. Rocks of unit 6 are dacitic (Macdonald, 1992) and include both flow and volcanoclastic rocks, and minor sedimentary rocks.

Although absolute age control is lacking at Brucejack Lake, similarities of units 1 through 6 to strata elsewhere in the Iskut River area (e.g., Alldrick and Britton, 1988; Anderson and Thorkelson, 1990; Anderson, 1993) suggest equivalence to Upper Triassic and Lower Jurassic Stuhini and Hazelton Group rocks. The boundary between Stuhini and Hazelton groups elsewhere in the region is an angular unconformity to disconformity, overlain by coarse clastic sedimentary strata (Henderson et al., 1992) followed by andesitic volcanic breccia. Stratigraphically higher rocks typically include intercalated sedimentary and felsic volcanic rocks, with local basaltic flows. Units 3 through 6 at Brucejack Lake are similar to this regional Jurassic succession, although detailed correlation to specific sections elsewhere are not possible. Rock types present in units 1 and 2 are consistent with Triassic Stuhini Group strata elsewhere in the region (Anderson, 1993).

Intrusive rocks at Brucejack Lake can be grouped into three map units: (1) a plagioclase-hornblende-phyric diorite (Macdonald, 1992), (2) a potassium feldspar megacrystic plagioclase-hornblende porphyry, and (3) a plagioclase and (rarely) potassium feldspar porphyry of dacitic composition. Minor, fine grained, green andesitic and felsic (quartz monzonitic composition; Macdonald, 1992) dykes cut these units, and are not differentiated in Figure 1. Lithological similarities and contact relationships suggest that some of the intrusive rocks are cogenetic with upper parts of the volcanic sequence; the plagioclase porphyry exhibits both intrusive and extrusive contacts with supracrustal rocks to the north and south of Brucejack Lake, and forms a flow dome south of the lake (Macdonald, 1993). The potassium feldspar megacrystic porphyry may be the subvolcanic equivalent of volcanic rocks of unit 6 (Table 1) on Mount John Walker; petrographical and geochronological analyses to evaluate this proposition are in progress. Intrusive rocks similar to the megacrystic porphyry elsewhere in the Iskut River area have yielded Early Jurassic U-Pb dates ranging from 185-195 Ma (Anderson, 1993).

The rock units presented in Table 1 and diagram shown in Figure 1 include several modifications to previously published geological maps (e.g., Alldrick and Britton, 1988; Kirkham, 1992) that include the Brucejack Lake area:

1. Jurassic Hazelton Group strata are divided into four mappable units (units 3 to 6; Table 1), comprising from the base upwards two distinct sedimentary units (units 3 and 4), an intermediate volcanoclastic unit (5) and an upper felsic, mixed flow and volcanoclastic unit (6).

Table 1. Map units identified in the Brucejack Lake area.**Stratified Rocks:**

| Unit | Thickness | Lithology |
|---------------------|------------------------|---|
| Jurassic | | |
| 6 | 250-450 m | Flow and volcanoclastic rocks, minor sedimentary rocks. Flows: dominantly plagioclase phyric, laterally discontinuous plagioclase and potassium feldspar phyric; Volcanoclastic rocks: range from plagioclase ash and crystal tuffs to felsic breccias - clast size may attain several metres. Conglomerate: similar to felsic volcanoclastic breccias with rounded clasts of flow-layered plagioclase porphyry but with matrix component of hematitically altered mud, locally stratified; also includes volumetrically insignificant argillaceous and limy sedimentary rocks at top of exposed section, not differentiated in Figure 1. |
| 5 | 200-300 m | Massive, green, monolithologic andesitic volcanic breccia to block and ash tuff and minor polyolithic volcanoclastic conglomerate. Moderately porphyritic with abundant plagioclase and hornblende phenocrysts up to 2-3 mm long in both clasts and matrix. Clasts are very angular and range in longest dimension from less than 1 cm to almost 1 m. Lowest rocks in section are completely clast supported, and in highest rocks irregularly shaped clasts are supported by a fine- to medium-grained tuffaceous matrix. |
| 4 | approx. 75 m | Thin- to medium-bedded dark grey to black mudstone and argillite. Typically highly altered; mudstone is typically highly siliceous or cherty in appearance. |
| 3 | 50-100 m | Medium- to thick-bedded, medium- to coarse-grained sandstone and pebble to cobble conglomerate. Sandstone is medium- to coarse- grained, moderately to well-sorted. Conspicuous internal planar laminations and rare cross-stratification. Conglomeratic portions are clast supported by rounded to subangular pebbles to cobbles. Clasts are dominantly intermediate composition porphyritic rocks and subordinate argillite and mudstone clasts. Rare, cross-stratified approximately mud chip conglomerate near middle of unit. |
| Triassic (?) | | |
| 2 | uncertain, > 200 m? | Thin- to medium- bedded black argillite, siltstone, and fine-grained sandstone. Minor medium-bedded dark grey limestone, tuffaceous mudstone, feldspathic sandstone, and tuffaceous pebble conglomerate. |
| 1 | > 150 m | Heterolithic volcanic conglomerate. Massive outcrops, stratification and sorting not visible. Subangular to rounded clasts are dominantly porphyritic (plag, hb, cpx) mafic to intermediate composition volcanic rocks. Clast-supported. Matrix consists of feldspathic wacke. |

Intrusive Rocks:

| Unit | Lithology |
|---------------------|--|
| Jurassic (?) | |
| JrP | Plagioclase porphyry, typically flow layered and flow folded intrudes unit 5 north of Brucejack Lake and flows and volcanoclastic rocks of unit 6; plagioclase phenocrysts (30-40%) to 4 mm exhibiting minor sericite alteration along fractures, and local epidote and hematite alteration; rare potassium feldspar megacrysts; conspicuous, trace apatite (<0.2%) needles to 400 microns; groundmass (60-70%) of quartz±feldspar±clay±sericite±carbonate. |
| JrK | Megacrystic potassium feldspar, hornblende+plagioclase porphyry, probably intrudes the hornblende-plagioclase diorite. Potassium feldspar megacrysts up to 4 cm long, less common megacrystic hornblende up to 2 cm, and widespread smaller (<5 cm) plagioclase+hornblende phenocrysts, all set in a fine-grained groundmass. Conspicuous flow layering defined by crystal size, composition is subparallel to intrusive contacts. Intrusive contacts with unit 1 argillites have only thin (<10 cm) chilled margins and wall rock hornfels zones. |
| JrD | Plagioclase-hornblende diorite, fine grained, massive; plagioclase and hornblende phenocrysts up to 4 mm in longest dimension. Extensively altered and veined west of Galena Hill and the West Zone, but in some exposures relic feldspar phenocryst outlines allow positive identification. |

2. A potassium feldspar megacrystic intrusion is recognized west of the major mineralized zones, where previous maps indicate Triassic volcanic strata. An intrusive origin for this unit is supported by exposed contacts which cut across bedding in adjacent sedimentary country rock, narrow (<10 cm) contact aureoles, and the presence of well-developed flow layering following irregular intrusive contacts.

STRUCTURAL GEOLOGY

Major structures at Brucejack Lake include several orientations of mappable faults and folds, a regional penetrative foliation, and zones of extensive veining and alteration. The dominant structure in the area is the Brucejack Fault, which

forms a north-striking lineament extending northward from the Sulphurets-Knipple icefield (Kirkham, 1963). This fault cuts all stratigraphic and intrusive contacts, alteration zones, and vein systems that contact it, indicating that latest motion postdates all rocks and alteration in the area. A vertical to steep westerly fault dip is constrained by outcrop distribution in the northern part of the map area, and is consistent with orientations of both minor adjacent fault surfaces and the exposed Brucejack Fault north of the map area. Previous attempts to estimate movement on the Brucejack Fault have indicated a combination of right lateral and normal (east-side-down) motion to the north of the map area (e.g., J. Margolis, pers. comm.). From our work to the northwest of Brucejack Lake, the fault surface preserves slickenside and clast elongation lineations indicating at least a late period of dip-slip offset. If these linear features represent the net slip direction,

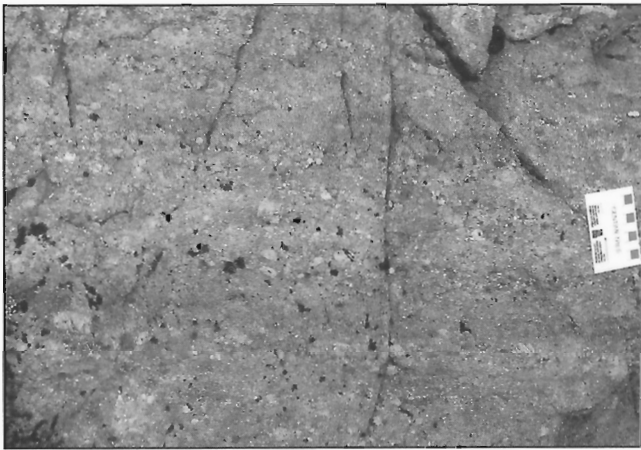


Figure 2. Pebble to cobble conglomerate bed within medium- to coarse-grained feldspathic wacke, 1 km west-northwest of Brucejack Lake. Matrix is coarse and well-sorted lithic sand, unit 3.



Figure 4. Intermediate lapilli tuff and block tuff, 1 km northwest of Brucejack Lake, unit 5.



Figure 3. Trough cross-stratified quartz-feldspar arenite, interbedded with mud-chip conglomerate beds, west of the Catear mine site, unit 3.



Figure 5. Potassium feldspar-megacrystic, plagioclase phyric flow, 400 m south of Brucejack Lake, unit 6.



Figure 6. Flow fold in flow-layered dacitic intrusion, 750 m north of Brucejack Lake, JrP.

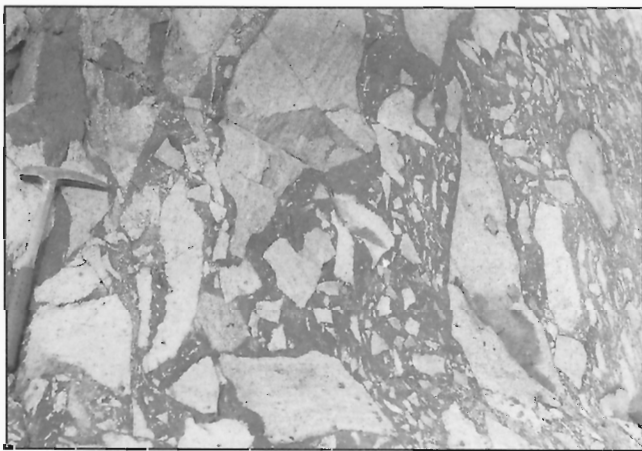


Figure 7. Breccia of flow-layered dacitic flow (extrusive equivalent of rock in Fig. 6) in hematitic mud matrix, 1.35 km north-northwest of Brucejack Lake, unit 6.



Figure 8. Medium- to coarse-grained ash tuff and lapilli tuff, 550 m south of Brucejack Lake, unit 6.

displacement of 700-800 m of reverse (west-side-up) motion is constrained from offset faulted and stratigraphic contacts. One kilometre northwest of Brucejack Lake, contacts show 200 to 300 m of strike separation, and displacement is likely less than in the north.

Other mappable faults in the map area strike northeasterly and northwesterly. Northeast-striking faults dip steeply to the northwest, have steep north-plunging striations, and have tens of metres of normal-dextral oblique displacement. Northwest-striking faults have unknown dips and displacement directions, but displace steep contacts a few tens of metres dextrally.

Folds in the map area are best developed in thinly- to medium-bedded sedimentary strata of units 1 and 2, exposed in Brucejack Creek west of the potassium feldspar megacrystic porphyry. Axial trends in this region vary from northerly to northwesterly. Folds are tight to open, have subangular to rounded hinges, and wavelengths of several tens of metres. Limb thrusts are common, prohibiting estimates of shortening represented by the folds. Facing directions and stratigraphic distribution patterns north of Brucejack Creek outline two larger-scale, northwesterly-trending open synforms (Fig. 1). These two folds have rounded hinges and wavelengths of 700 to 1000 m, and are separated by the Brucejack Fault.

West- to northwest-striking penetrative foliation is present to varying degrees in most map units, but is most strongly developed in areas of sericitic alteration associated with vein-style mineralization, and in unit 2 argillites. Foliation is defined by parallel preferred orientation of fine grained phyllosilicates, and by flattened clast shapes in fragmental rocks. Flattened clasts are most apparent in units 1 and 5 and have oblate to moderately prolate shapes indicative of dominantly flattening strain. In much of the area, the regional cleavage is subparallel to fold axial surfaces and likely formed during the same deformation event.

Shortening directions implied by folds and cleavage at Brucejack Lake are consistent with formation during the Cretaceous development of the Skeena Fold and Thrust Belt (Evenchick, 1991), and are similar to those in the westerly adjacent Kerr Deposit (D.J. Bridge, pers. comm., 1993). Large competency contrasts between intrusive rocks, bedded sedimentary rocks, and altered volcanic and intrusive rocks led to heterogeneous strain partitioning and irregular trends of structural features. The Brucejack Fault and other mappable faults are younger, local features with relatively small offsets, and are probably not formed during a regional deformation event.

ALTERATION AND MINERALIZATION

This study did not include a detailed analysis of mineralization and alteration, but several general observations suggest stratigraphic control on the present geometry and distribution of alteration/mineralization:

1. Extensive alteration at the West Zone, the Shore Zone, Galena Hill, Old Yeller, and Quartz Hill overprints rocks belonging to units 2, 3, and 4, and the hornblende-plagioclase porphyry (JrD), but is most prevalent in the porphyry and the base of unit 5.
2. Quartz+carbonate sheeted veins, massive veins, stock-work veins, and breccia veins within and stratigraphically below this alteration have variable orientations, but on average have steep dips and southwesterly to northwesterly strikes, at moderate to high angles to regional stratigraphic contacts. These veins and localized alteration extend westward as far as, and locally into, the potassium feldspar megacrystic porphyry.
3. Most veins and alteration are deformed by both folds and foliation. Deformation within altered and mineralized zones is characterized by buckle folds of veins with axial surfaces parallel to regional foliation, and locally intense foliation development. However, cleavage is locally folded (e.g., West Zone and Old Yeller Zone; Roach and Macdonald, 1992) and quartz-carbonate veins cut the folded cleavages suggesting more complex timing relationships between veins and the development of penetrative fabrics in the Brucejack Lake area.

The postulated equivalence between the potassium feldspar porphyry and unit 6, the style and orientation of veins, and the stratigraphic localization of veins and alteration all imply that alteration and mineralization at Brucejack Lake resulted from a shallow hydrothermal system associated with the megacrystic porphyry. Stratigraphic distribution and interpreted thicknesses suggest a depth of porphyry emplacement of not more than a kilometre or two, with most extensive mineralization and alteration (West Zone, Galena Hill, etc.) focused approximately 500 m above the intrusion in lower parts of the mixed volcanic-sedimentary sequence.

ACKNOWLEDGMENTS

This work was conducted as part of the Mineral Deposit Research Unit project "Metallogenesis of the Iskut River area, Northwestern B.C." in the Department of Geological Sciences at the University of British Columbia that commenced in June 1990. Funding for the research has been received from the Federal Government (NSERC Collaborative Research and Development Grant #102437), several exploration and mining companies, and the Government of British Columbia (Science Council of British Columbia Technology B.C. Grant #119(T-2)).

We are grateful to Rod Kirkham (GSC, Vancouver) for editing earlier versions of the manuscript.

We are indebted to the hospitality provided us by Newhawk Gold Mines Ltd. of Vancouver, B.C.; in particular we wish to thank Fred Hewett, Dave Visagic, and Steve Roach of Newhawk for their continued support of our work.

At Brucejack Lake, we received logistic support from Vancouver Island Helicopters; a special word of thanks is due to Pilot Mario Chandler for his skills, sense of safety and finely tuned wit.

This Paper is MDRU Contribution No. 31.

REFERENCES

- Alldrick, D.J. and Britton, J.M.**
1988: Geology and mineral deposits of the Sulphurets area; British Columbia Ministry of Energy, Mines and Petroleum Resources, Open File Map 1988-4.
1991: Sulphurets area geology; British Columbia Ministry of Energy, Mines and Petroleum Resources, Open File 1991-21.
- Anderson, R.G.**
1993: A Mesozoic stratigraphic and plutonic framework for Northwestern Stikinia (Iskut River area), northwestern British Columbia, Canada; in *Mesozoic Paleogeography of the Western United States -- II*, (ed.) G. Dunne and K. McDougall; Society of Economic Paleontologists and Mineralogists, Pacific Section, v. 91, p. 477-494.
- Anderson, R.G. and Thorkelson, D.J.**
1990: Mesozoic stratigraphy and setting for some mineral deposits in Iskut River map area, northwestern British Columbia; in *Current Research, Part E*; Geological Survey of Canada, Paper 90-1E, p. 131-159.
- Bridge, D.A., Ferguson, L.J., and Brown, M.G.**
1981: 1980 exploration report on the Sulphurets property, Skeena Mining Division, B.C.; unpublished internal report, Granduc Mines Ltd., Esso Resources Canada Ltd. and Sidney F. Ross., 152 p.
- Britton, J.M. and Alldrick, D.J.**
1988: Sulphurets map area (104A/5W, 12W; 104B/8E, 9E); in *Geological Fieldwork 1987*; British Columbia Ministry of Energy, Mines and Petroleum Resources, Paper 1988-1, p. 199-209.
- Evenchick, C.A.**
1991: Structural relationships of the Skeena Fold Belt west of the Bowser Basin, northwest British Columbia; *Canadian Journal of Earth Sciences*, v. 28, p. 973-983.
- Henderson, J.R., Kirkham, R.V., Henderson, M.N., Payne, J.G., Wright, T.O., and Wright, R.L.**
1992: Stratigraphy and structure of the Sulphurets area, British Columbia; in *Current Research, Part A*; Geological Survey of Canada, Paper 92-1A, p. 323-332.
- Kirkham, R.V.**
1963: The geology and mineral deposits in the vicinity of the Mitchell and Sulphurets Glaciers, northwestern British Columbia; M.Sc. thesis, University of British Columbia, Vancouver, British Columbia, 122 p.
1991: Provisional geology of the Mitchell-Sulphurets region, northwestern British Columbia (104B/8,9); Geological Survey of Canada, Open File 2416.
1992: Preliminary geological map of the Brucejack Creek area, British Columbia (part of 104B/8); Geological Survey of Canada, Open File 2550.
- Macdonald, A.J.**
1992: Eskay Porphyry, Section 3.2, in MDRU Iskut Project Annual Report, May 1992; Mineral Deposit Research Unit, University of British Columbia, Vancouver, British Columbia.
1993: Lithostratigraphy and geochronometry, Brucejack Lake, northwestern British Columbia (104B/8E); in *Geological Fieldwork 1992*; British Columbia Ministry of Energy, Mines and Petroleum Resources, Paper 1993-1, p. 315-323.
- Roach, S.**
1990: 1989 surface exploration program; unpublished internal report, Newhawk Gold Mines Ltd., 12 p.
- Roach, S. and Macdonald, A.J.**
1992: Silver-gold mineralization, West Zone, Brucejack Lake, northwestern British Columbia; in *Geological Fieldwork 1991*; British Columbia Ministry of Energy Mines and Petroleum Resources, Paper 1992-1, p. 503-511.

Geology of the Cambria Icefield: regional setting for Red Mountain gold deposit, northwestern British Columbia

C.J. Greig¹, R.G. Anderson, P.H. Daubeny², K.F. Bull³, and T.K. Hinderman⁴

Cordilleran Division, Vancouver

Greig, C.J., Anderson, R.G., Daubeny, P.H., Bull, K.F., and Hinderman, T.K., 1994: Geology of the Cambria Icefield: regional setting for Red Mountain gold deposit, northwestern British Columbia; in Current Research 1994-A; Geological Survey of Canada, p. 45-56.

Abstract: Lower Jurassic (LJr) Hazelton Group (HG) volcanic and volcanoclastic rocks underlie much of the Cambria Icefield area and host LAC Minerals' Red Mountain Au deposit. They occur with similar Upper Triassic and older rocks in a structural culmination outlined by the contact between competent felsic and mafic volcanic rocks of uppermost Hazelton Group and overlying, relatively incompetent late Lower Jurassic and younger, westerly-derived clastic rocks. Stratigraphy of Hazelton Group is complex, but locally traceable units show that Lower Jurassic stratigraphy helped localize mid-Cretaceous(?) structure. The newly-recognized mafic-felsic association in upper Hazelton Group has significant exploration and tectonic implications. Plutonic styles suggest the age and exploration potential of plutons be reconsidered. Genesis of the Red Mountain deposit has yet to be firmly established, but the main mineralizing event predated regional deformational events, implying significant stratigraphic control and potential in the area mapped, and areas nearby, for similar deposits.

Résumé : Les roches volcaniques et volcanoclastiques du Groupe de Hazelton du Jurassique inférieur forment le substratum rocheux de la plus grande partie du champ de glace de Cambria et contiennent le gisement d'or de Red Mountain de LAC Minerals. Elles apparaissent avec des roches semblables du Trias supérieur et de temps plus anciens dans une culmination structurale délimitée par le contact entre les volcanites felsiques et mafiques compétentes du sommet du Groupe de Hazelton, et les roches clastiques à source occidentale, relativement incompétentes, du sommet du Jurassique inférieur et plus hautes. La stratigraphie du Groupe de Hazelton est complexe, mais des unités retraçables par endroits révèlent que la stratigraphie du Jurassique inférieur a joué un rôle dans la localisation des structures du Crétacé moyen(?). La découverte récente de l'association mafique-felsique dans la partie supérieure du Groupe de Hazelton a des répercussions importantes du point de vue de l'exploration minérale et de la tectonique. Les styles plutoniques indiquent qu'il faut réévaluer l'âge et le potentiel en termes d'exploration minérale des plutons. La genèse du gisement de Red Mountain n'est pas encore fermement établie, mais le principal épisode minéralisateur a précédé la déformation régionale, ce qui laisse supposer un contrôle stratigraphique et un potentiel importants dans la région cartographiée et dans les régions avoisinantes, relativement à des gisements semblables.

¹ Department of Geosciences, University of Arizona, Building #77, Tucson, Arizona, U.S.A. 85721

² LAC Minerals Ltd., P.O. Box 337, Stewart, British Columbia VOT 1W0

³ Dihedral Exploration, P.O. Box 81418, Fairbanks, Alaska, U.S.A. 99708

⁴ Alaska Earth Sciences, 11341 Olive Lane, Anchorage, Alaska, U.S.A. 99515

INTRODUCTION

An Industrial Partners Program project involving the Cordilleran Division of the Geological Survey of Canada and Lac Minerals Ltd. in 1993-94 encompassed mapping a little-known but highly prospective region east of Stewart and between Kitsault River and American Creek in northwestern British Columbia. Mineral potential in the region is high, as manifested in LAC's Red Mountain Au deposit, which is in the initial stages of underground exploration. The work will help place the Red Mountain precious and base metal deposit into a district-wide geological context and facilitate more effective mineral exploration.

This paper presents preliminary results of 1:50 000 scale mapping in the Cambria Icefield area, including parts of 103P/13, 103P/14, 104A/3, and 104A/4 NTS map areas (Fig. 1). The new work links recent mapping to the southeast (Greig, 1991, 1992; Alldrick et al., 1986) with that to the

northwest (Grove, 1971; Alldrick, 1993). Reconnaissance scale maps encompassing the Cambria Icefield (McConnell, 1913; Hanson, 1929, 1935; Grove, 1986), and recent new stratigraphic and structural data from adjacent areas (Evenchick et al., 1992; Greig and Evenchick, 1993; Anderson, 1993) proved useful. The present mapping incorporates more detailed, unpublished work from the Cambria Icefield area by Bull et al. (LAC Minerals, 1991). Permanent ice and high relief characterize the Cambria Icefield area, and except for vehicle access along Highway 37A, the easiest access is by helicopter.

REGIONAL GEOLOGY AND STRATIGRAPHY

The Cambria Icefield area lies near the boundary of the Intermontane and Coast belts in northwestern Stikinia, along the southwestern margin of the Bowser Basin. Uppermost

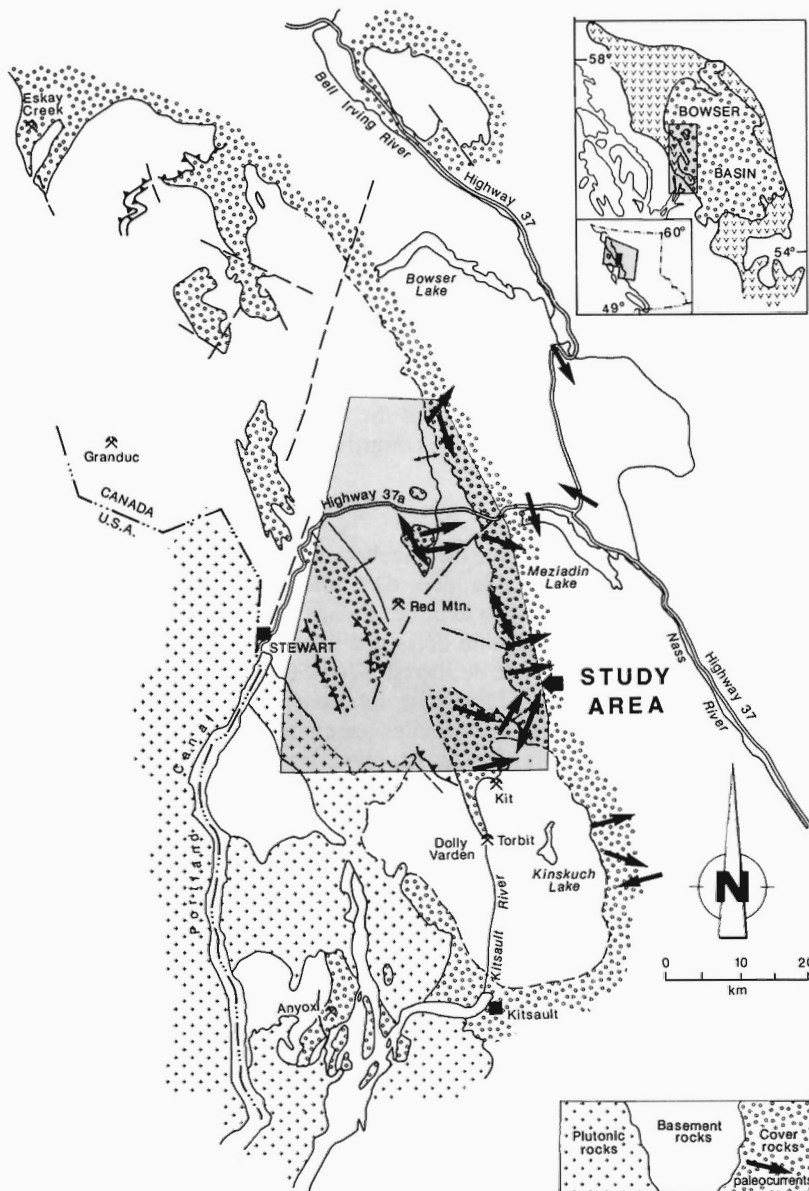


Figure 1.
Location of study area.

Lower Jurassic to Upper Jurassic well-bedded marine clastic rocks stratigraphically overlie and form the less competent structural cover to a generally more massive and competent basement of Paleozoic to Lower Jurassic oceanic arc volcanic and volcanoclastic rocks (see Anderson, 1993) exposed in structural culminations of the latest Jurassic or Early Cretaceous to Tertiary Skeena Fold Belt (Evenchick, 1991).

Cambria Icefield area strata are mainly Jurassic (Fig. 2). The central and higher parts of the area, coinciding with the major icefields, are underlain by resistant Lower Jurassic felsic and mafic pyroclastic and subordinate flows and volcanoclastic rocks which mark the top of both the structural basement and the volcanic part of the Hazelton Group. The less rugged eastern part is underlain by upper Lower Jurassic to Upper Jurassic clastic rocks correlative to the Salmon River Formation (of the Hazelton Group) and Bowser Lake Group. Upper Triassic clastic rocks and Triassic or older basalt occur locally.

Hazelton Group clastic rocks were divided into three units by inferred stratigraphic position and sedimentological maturity. The uppermost unit (MUJ, Salmon River Formation) is the best stratified and sorted and finest grained. The common debris flow conglomerate and ash tuff of the middle unit (Jdf) is least mature; the lowest unit (Jvc) is intermediate in these characteristics. Stratigraphic relationships of the three units are poorly known because they contain few fossils, their contacts are gradational and/or structurally modified (Fig. 3, 4), and locally they resemble each other and other units. It is likely that rocks mapped as one unit include rocks of another, particularly where traverse density was low. All three units are at least partial facies equivalents of volcanic units (e.g., Fig. 5), and commonly include pyroclastic rocks or flows.

Basement rocks

Crowded feldspar-phyric basalt (unit PTb)

Crowded feldspar-phyric basalt of probable Late Triassic or older age underlies an area between the Nelson glaciers and South Willoughby Creek. Typically, aligned feldspar phenocrysts outline discontinuous centimetre- to decimetre-sized irregular to subround shapes (Fig. 6) but the unit is otherwise massive. Contacts with bounding Upper Triassic and/or Lower Jurassic clastic units are faulted and the age of the unit is inferred from the presence of distinctive basalt clasts of unit PTb in conglomerate of the bounding units, and from probable interfingering of the volcanic and Upper Triassic clastic rocks north of Willoughby Glacier.

Upper Triassic volcanoclastic rocks (unit Tv)

A belt of Upper Triassic volcanoclastic rocks bounds the feldspar-phyric basalt to the west. Rocks near the Cambria fault at Entrance Peak may be dextrally-offset equivalents. Silty mudstone, siltstone, sandstone, and local conglomerate and debris flow conglomerate are typical but locally are difficult to distinguish from Jurassic rocks. Contacts between Triassic and Jurassic rocks have been structurally modified.

Bedding across these contacts is discordant, and north of Willoughby Glacier, stratigraphic facing directions are opposed (Fig. 4, section OP). The contact is likely an unconformity or a normal fault, but the data are equivocal.

It is possible that the unit is partly equivalent to the lower Lower Jurassic clastic unit. If so, the Upper Triassic unit may be slightly older than, but correlative with, the Jack formation of Henderson et al. (1992). Bivalves of probable Late Norian age (H.W. Tipper, pers. comm., 1993) were collected from two localities near Willoughby Glacier.

Andesite/dacite lapilli and ash tuff (unit Jt)

A thick (>1000 m) and very weakly stratified, dark greenish-grey, lapilli and ash crystal-lithic tuff underlies the lower slopes of Bear River Pass. It contains common intermediate to felsic volcanic lithic lapilli and chloritized fiamme, and is dacitic to andesitic (Fig. 7). Its base is not exposed but it is conformable with overlying felsic volcanic rocks. The tuff is not recognized southwest or northeast of the Bear River Pass, across the Bitter Creek and Cornice Mountain antiforms. Its distribution to the northwest is unknown. Much thinner, muddy debris flow conglomerates common within Hazelton Group on the limbs of the Bitter Creek and Cornice Mountain structures (parts of units Jdf and Jd) may be facies equivalents because they contain angular intermediate to felsic volcanic clasts. If so, the locus of facies change coincides with and localized regional structures. Tuff deposition probably also reflects pronounced local subsidence; overlying upper Lower and Middle Jurassic clastic rocks suggest deposition in an environment of subdued local relief. The Bear Pass tuff represents a restricted, synvolcanic basin rather than a constructional volcanic edifice.

Lower Jurassic volcanoclastic rocks (unit Jvc)

The unit occurs in two belts: one bounds Triassic or older basalts on the east, and the other occurs in the core of the Bitter Creek antiform. Weakly calcareous arkosic sandstone, siltstone, muddy debris flows and volcanic debris flows, and local limestone and polymict conglomerate are typical, and the rocks are commonly Fe-carbonate altered. Conglomerate is discontinuous and minor but widespread, and its diverse clast compositions distinguish it from conglomerate in other units. It contains abundant feldspar-phyric volcanic clasts, probably derived from the Triassic or older basalt, common coralline limestone boulders, and scattered plutonic cobbles. The conglomerate may be the expression of latest Triassic-earliest Jurassic deformation and uplift recognized elsewhere in Stikinia (e.g., Brown and Greig, 1990; Greig, 1992; Greig and Gehrels, 1992; Henderson et al., 1992; Anderson, 1993).

Maroon feldspathic pyroclastic and epiclastic rocks (unit Jm)

Interbedded maroon, lavender, purple, or green feldspathic pyroclastic and volcanoclastic rocks locally are useful marker units. Where traverse density allowed, pyroclastic (unit Jmp) and epiclastic (unit Jme) facies were recognized.

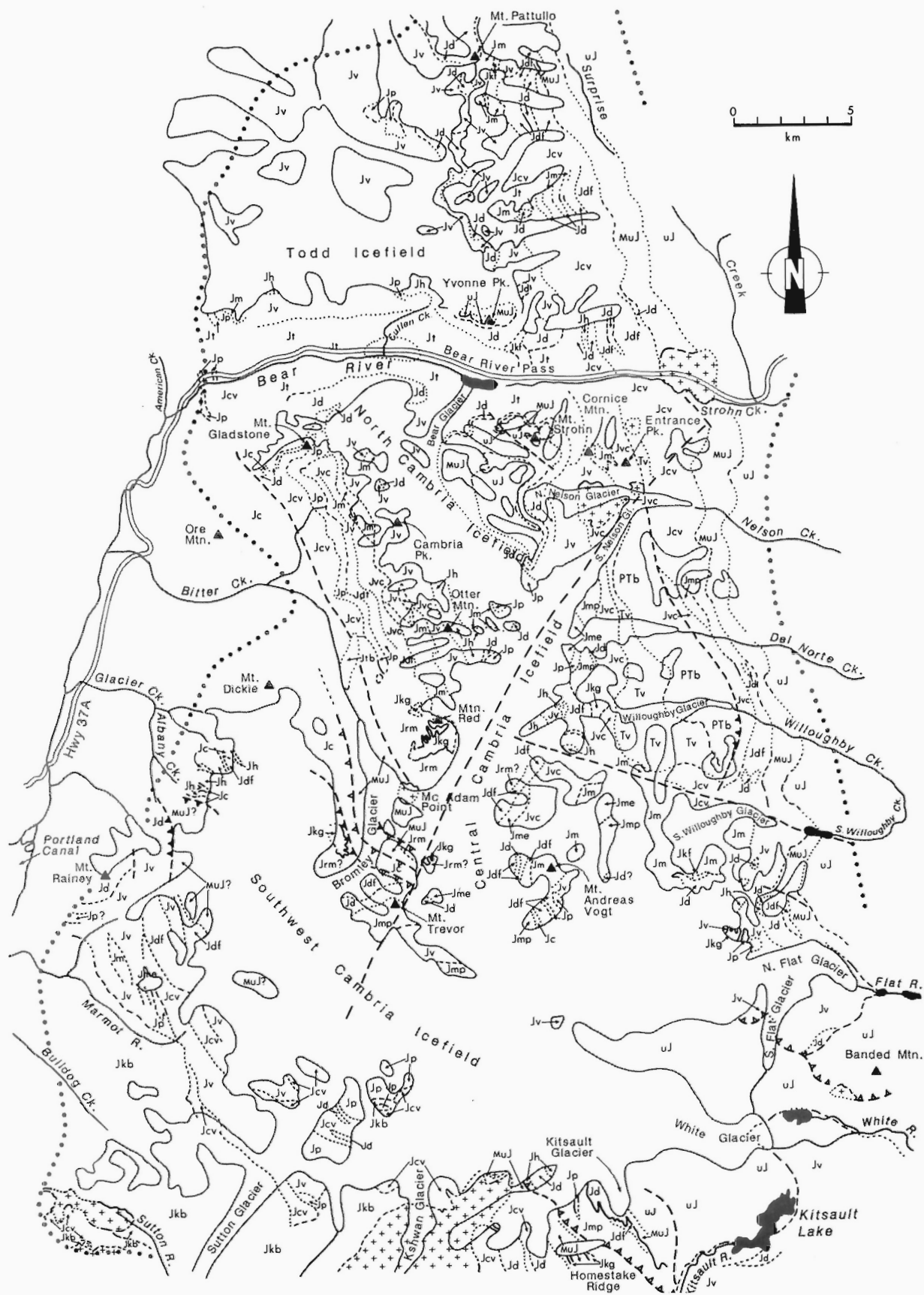


Figure 2. Geology of the Cambria Icefield area.

LEGEND FOR FIGURE 2**STRATIFIED ROCKS****COVER**

Middle to Upper Jurassic

| | |
|----|------------------------------|
| UJ | Upper Jurassic clastic rocks |
|----|------------------------------|

| | |
|-----|---|
| MUJ | Middle and Upper Jurassic clastic rocks |
|-----|---|

| | |
|----|---|
| Jc | Lower to Middle(?) Jurassic clastic rocks |
|----|---|

BASEMENT

Lower to Middle(?) Jurassic

| | |
|-----|--|
| Jdf | debris flow conglomerate and volcanic debris flows |
|-----|--|

| | |
|-----|-----------------------|
| Jrm | Red Mountain sequence |
|-----|-----------------------|

Lower Jurassic

| | |
|----|---|
| Jh | hornblende-feldspar-phyric volcanic rocks |
|----|---|

| | |
|----|-----------------------|
| Jd | felsic volcanic rocks |
|----|-----------------------|

| | |
|----|--|
| Jp | pyroxene-bearing volcanic and volcanoclastic rocks |
|----|--|

| | |
|-----|--------------------------|
| Jmp | maroon pyroclastic rocks |
|-----|--------------------------|

| | |
|-----|-------------------------|
| Jme | maroon epiclastic rocks |
|-----|-------------------------|

| | |
|----|---|
| Jm | maroon feldspathic pyroclastic and epiclastic rocks |
|----|---|

| | |
|-----|----------------------|
| Jvc | volcanoclastic rocks |
|-----|----------------------|

| | |
|----|--|
| Jt | andesite / dacite lapilli and ash tuff |
|----|--|

| | |
|-----|--------------------------------------|
| Jcv | undivided clastic and volcanic rocks |
|-----|--------------------------------------|

| | |
|----|--------------------------|
| Jv | undivided volcanic rocks |
|----|--------------------------|

Upper Triassic


| | |
|----|----------------------|
| Tv | volcanoclastic rocks |
|----|----------------------|

Triassic or older

| | |
|-----|--------------------------------|
| PTb | crowded feldspar-phyric basalt |
|-----|--------------------------------|

PLUTONIC ROCKS

Tertiary(?)

| | |
|---|-----------------------------|
|  | quartz monzonite to diorite |
|---|-----------------------------|

Middle or Late Jurassic to Tertiary

| | |
|-----|------------------------|
| Jtb | Bromley Glacier pluton |
|-----|------------------------|

Middle Jurassic to Cretaceous

| | |
|-----|-------------------|
| JKf | felsic intrusions |
|-----|-------------------|


| | |
|------|------------------|
| JKbp | Bear Pass pluton |
|------|------------------|


| | |
|-----|----------------------|
| JKb | Bulldog Creek pluton |
|-----|----------------------|

| | |
|-----|---------------------|
| JKg | Goldslide intrusion |
|-----|---------------------|

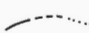
 Highway

 limit of mapping

 limit of permanent ice

 thrust or reverse fault

 high angle fault

 geological contact: known, inferred, assumed

Epiclastic rocks consist of poorly to moderately well stratified and sorted conglomerate (Fig. 8), sandstone, siltstone, and mudstone, all cemented by patchy carbonate. Clast compositions are dominantly volcanic, with very fine grained felsic volcanic clasts conspicuous and common. Andesitic or basaltic, hornblende- or pyroxene-phyric pyroclastic rocks are massive, crystal-lithic lapilli tuff-breccia, coarse to fine lapilli tuff and ash. Oxidization and alteration of the unit are common.

The epiclastic rocks resemble the Betty Creek Formation of Grove (1986), but unlike these rocks in eastern Iskut map area (Anderson, 1993), the Cambria Icefield equivalents have no unique stratigraphic position within the Lower Jurassic succession.

Pyroxene-bearing volcanic and volcanoclastic rocks (unit Jp)

Dark green, pyroxene- and plagioclase-phyric pyroclastic and volcanoclastic rocks are common and distinctive in the upper Hazelton Group. They are locally interbedded with felsic volcanic rocks (unit Jd) and are a significant component of the maroon unit (unit Jm). Commonly amygdaloidal lapilli tuff-breccia (Fig. 9), lapilli and ash tuff, as well as local flows, volcanic debris flows, and rare pillowed basalt make up the unit. Pyroxene phenocrysts are typically 2-3 mm in diameter but reach 0.5 cm. Clastic rocks include pyroxene arkosic litharenite, mafic siltstone, and local volcanic conglomerate. Northeast of Sutton Glacier, coarse lapilli tuff contains mafic plutonic fragments.

Near Mount Gladstone, the mafic volcanic unit is traceable across the Bitter Creek antiform to a mainly clastic section to the west. This suggests that the clastic rocks on the west flank of the Bitter Creek structure (and east of Bitter Creek) are a facies equivalent of volcanic rocks east of the structure and constrains kinematics on associated structures.

Felsic volcanic rocks (unit Jd)

Dacite, dacitic andesite, and rhyolite correlated with the Mount Dilworth Formation (Alldrick, 1993) occur near the top of the volcanic part of the Hazelton Group, where they commonly delineate the basement-cover contact. They are widespread, commonly interfingering with limy mudrocks of units Jdf and Jc, but in bodies too small to show on Figure 2. The felsic rocks weather distinctively pale grey to white and are commonly rusty due to disseminated pyrite. Lithic lapilli tuff and lapilli tuff-breccia are most common. Ash and dust tuff, and flow-foliated and flow-folded flows and flow breccias occur locally. Pillowed flows are rare. About 6 km east of Mount Andreas Vogt, felsic flows and flow-breccias are continuous with their intrusive counterparts.

Hornblende feldspar-phyric volcanic rocks (unit Jh)

In many places, very resistant, massive (amygdaloidal) hornblende feldspar-phyric dacitic andesite or andesite flows, flow-breccias and coarse crystal lithic lapilli to lithic crystal ash tuff are associated with the felsic volcanic rocks described

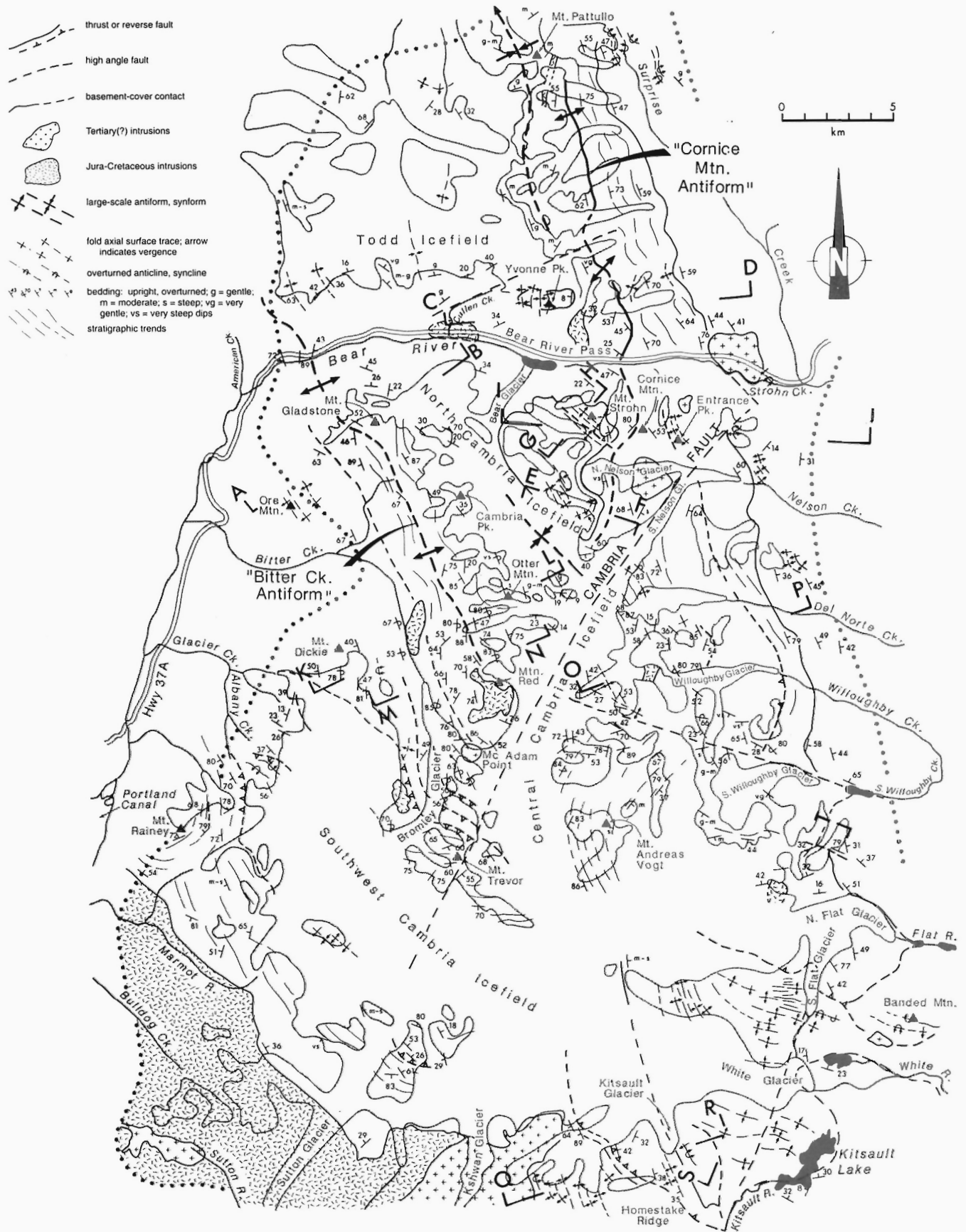


Figure 3. Structural elements of the Cambria Icefield area.

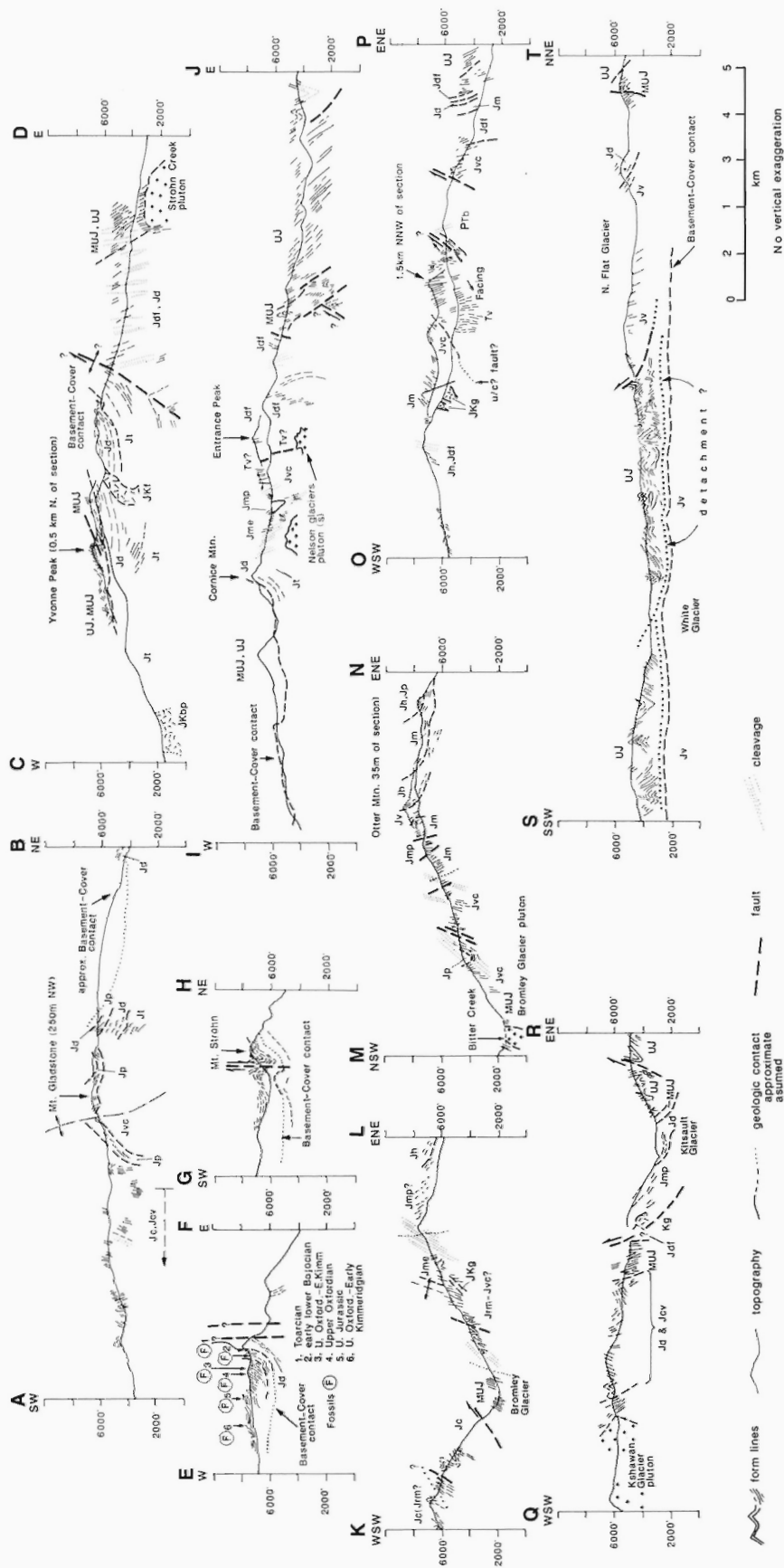


Figure 4. Geological cross-sections.

above. They are also commonly pyritic and interfinger with clastic rocks, locally producing striking hyaloclastite matrix breccias and syndepositional loading structures. Some breccias grade into and interfinger with volcanic debris flows, and compose a significant proportion of the overlying debris flow unit (Jdf).

Red Mountain sequence (unit Jrm)

The Red Mountain sequence is steeply west-dipping, probably west-facing, and consists of thin bedded (1-10 cm, average 3 cm beds) to very thickly bedded, well-indurated felsic(?) to mafic(?) dust, ash, and subordinate lithic crystal (hornblende and feldspar) lapilli tuff, and siliceous (cherty) argillite, and rare bedded radiolarian chert. Much of the sequence is pyritic and strikingly rusty weathering, giving Red Mountain its name. Massive tuff contains scattered fine lapilli compositionally similar to matrix ash. Centimetre- to decimetre-scale, syndimentary deformation structures are not uncommon. Sills and dykes of (biotite quartz) hornblende feldspar porphyry (Goldslide intrusions) intruded the sequence, which itself may contain their extrusive equivalents.

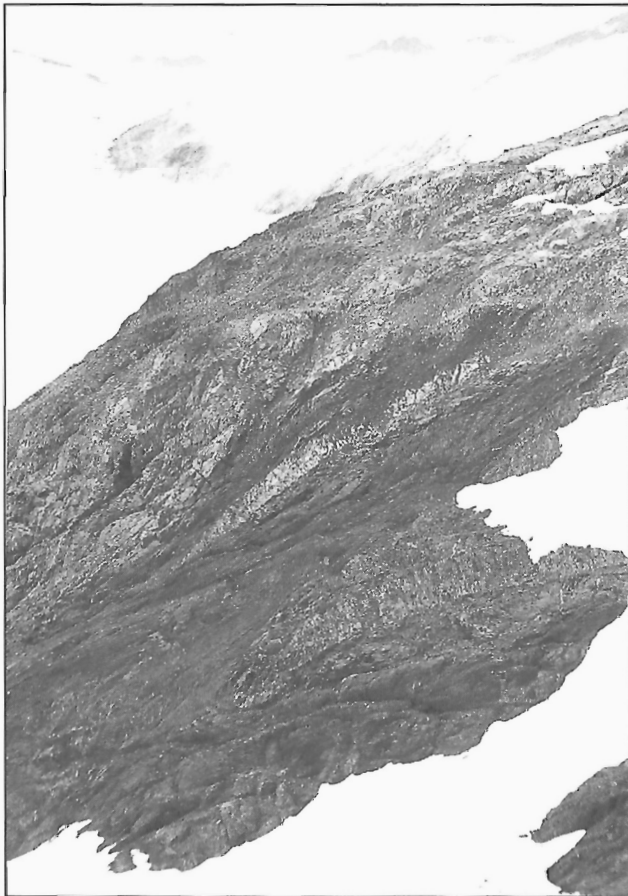


Figure 5. Facies change units Jcv and Jd (pale, capping ridge and as tongues in darker rocks) west of Homestake Ridge; view to west, elevation gain on ridge 200 m.

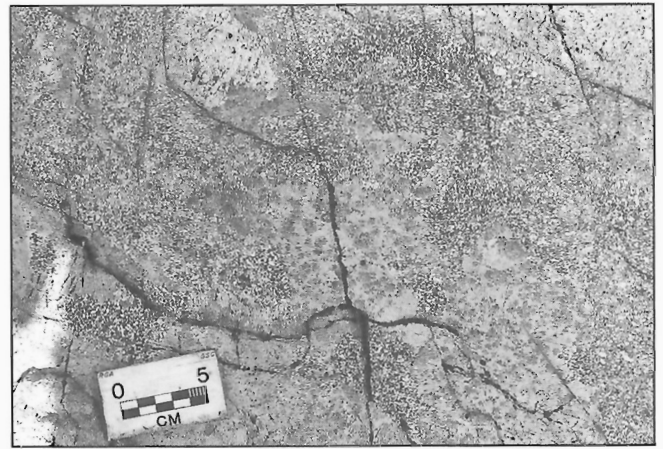


Figure 6. Basalt of unit Ptb, showing characteristic grain size variation.

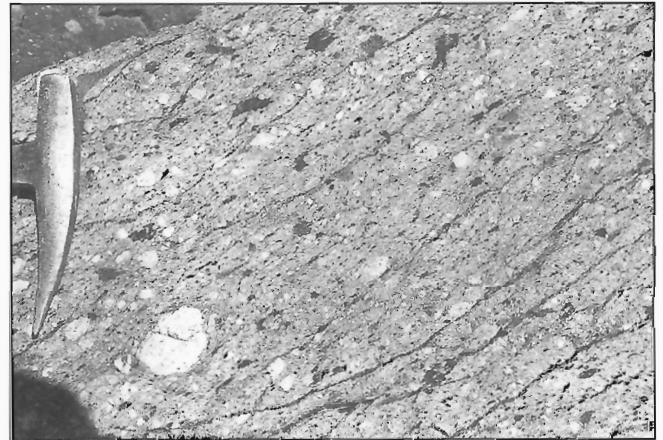


Figure 7. Crystal lithic tuff of unit Jt.



Figure 8. Conglomerate of unit Jme; note very large clast and crude stratification.

The Red Mountain sequence is continuous with volcanic units to the north (Jdf, Jvc, Fig. 2), but is generally more siliceous or altered. Radiolarian fauna from chert in the various successions may help to corroborate these correlations. Clastic rocks, chert, and fine grained tuffaceous rocks with close similarities to, but less altered than, those at Red Mountain also occur to the southwest and south.

Debris flow conglomerate and volcanic debris flows (unit Jdf)

Very poorly stratified muddy debris flow conglomerate (Fig. 10) and subordinate volcanic debris flows typify the unit; less common silty mudstone, siltstone, sandstone, pebble conglomerate, and limestone are partly correlative with and indistinguishable from Lower to Middle Jurassic(?) clastic rocks (unit Jc). Most rocks in the unit are weakly carbonate-cemented. Discontinuous limestone pods are typically sandy or pebbly and locally contain bivalves. North of Willoughby Glacier, colonial corals occur in limestone several metres thick. Debris flows are typically feldspathic and tuffaceous and clasts are angular to subrounded, fine grained clastic rocks and intermediate to felsic, commonly pyritic volcanic rocks. Uncommon, centimetre-scale, massive pyrite fragments in the debris flows, along with the pyritic felsic fragments and the general pyrite-rich, rusty weathering character, are important because they suggest a widespread Early Jurassic mineralizing event occurred.

Cover rocks

Lower to Middle(?) Jurassic clastic rocks (unit Jc)

Thin-bedded silty mudstone and siltstone, with local thin-bedded sandstone and carbonate mudstone lenses, occur only in the southwest. They were not differentiated from clastic rocks of probable older age in much of that area (hence unit Jcv). Unit Jc is probably partly correlative to the Red Mountain sequence (unit Jrm), the debris flow unit (Jdf), and to the Middle to Upper Jurassic clastic rocks (unit MUJ). It is better stratified than the debris flow unit and less siliceous than either the Red Mountain sequence or unit MUJ.

Middle to (Upper?) Jurassic clastic rocks (unit MUJ)

Fine grained, clastic rocks of Middle (to Late?) Jurassic age are exposed nearly continuously in a narrow belt to the east and in an outlier near Mount Strohn. Similar rocks occur in outliers near Bitter Creek and near Yvonne Peak. In the east the rocks are characteristically thin bedded and siliceous or less commonly limy; near Bitter Creek, thick bedded to very thick bedded (3-6 m, on average) massive to laminated silty mudstone and local muddy debris flow conglomerate containing exclusively sedimentary clasts are typical. The general siliceous nature and association with very thin bedded (2 cm on average) and laminated, varicoloured tuffaceous chert, chert, and cherty argillite are characteristic. Fossils collected from the unit suggest Toarcian, Bajocian, and Callovian ages (H.W. Tipper, G. Jakobs, E. Carter, pers. comm., 1990), but near Bitter Creek, the unit may include Upper Jurassic rocks.

In the east, unit MUJ corresponds to the lower part of the Surprise Creek facies of the Middle Jurassic Salmon River Formation, as mapped by Evenchick et al. (1992). The laminated and siliceous beds are likely equivalent to Anderson's (1993) Troy Ridge facies of the Salmon River Formation.

Upper Jurassic clastic rocks (unit UJ)

This unit conformably overlies unit MUJ (Fig. 4, section EF; Fig. 11) and is similarly distributed. Silty mudstone and metre-scale (1-6 m) arkosic litharenite A-E turbidites predominate. The thicker sandstone beds and the less siliceous and thicker-bedded character of the mudstone distinguish rocks of unit UJ from those of unit MUJ. Unit UJ resembles the upper member of the Salmon River Formation to the south (Greig, 1991), and coincides in the northeast with the upper part of the Surprise Creek facies (Evenchick et al., 1992). However, an improved paleontological database suggests that the rocks are Upper Jurassic and equivalent in age to nearby Bowser Lake Group. Greig (1991) and Evenchick et al. (1992)

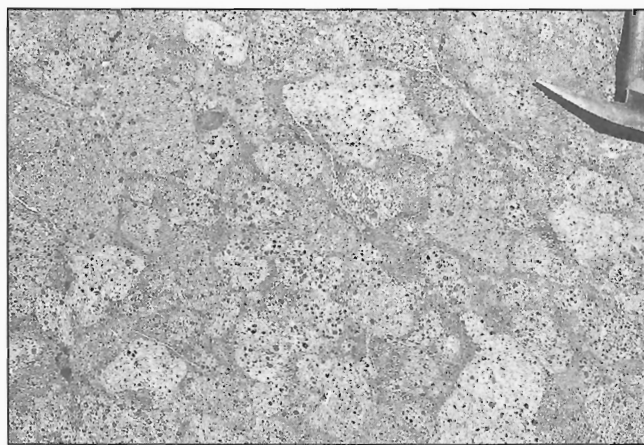


Figure 9. Mafic pillow breccia/coarse lapilli tuff of unit Jp.



Figure 10. Debris flow conglomerate with felsic volcanic rock fragments in muddy matrix; unit Jdf.

have pointed out that they are distinctly different than nearby Bowser Lake Group rocks. East-trending paleocurrent indicators (Fig. 1) suggest at least a local western source for these westernmost Upper Jurassic Bowser Basin sedimentary rocks.

INTRUSIONS

Previously, plutonic rocks in much of the area were undivided and considered Tertiary and older(?) (Carter, 1981; Grove, 1986). Five Middle Jurassic and younger and Tertiary(?) suites of plutons were distinguished by composition and mineralogy, alteration, intrusive relationships, and internal fabrics. Only the Goldslide and related intrusions are described in detail because of their close association with the Red Mountain deposit. The Tertiary suite, similar to Middle Eocene Hyder plutonic suite intrusions (Grove, 1986) vary in composition from quartz monzonite and monzogranite to granodiorite or quartz diorite, commonly contain scattered pink potassium feldspar megacrysts, and are typically medium grained and unfoliated.

Two prominent dyke swarms also occur: the west-southwest-dipping Portland Canal swarm (lamprophyre and basalt to dacite, rhyolite, and granite), which underlies Bitter Creek, Mount Dickie, and Ore Mountain; and the subvertical, northwesterly-striking Nelson glaciers swarm (homogeneous (biotite-quartz-) hornblende-feldspar porphyry) (Fig. 12). The Portland Canal dykes likely were emplaced along pre-existing bedding and cleavage in the host rocks (see Grove, 1986).

Middle Jurassic and younger intrusive rocks

Goldslide pluton and related intrusions (unit Jkg)

The Goldslide intrusions comprise small plutons and related sills and dykes of hornblende plagioclase porphyritic to seriate quartz monzodiorite, granodiorite or diorite, locally

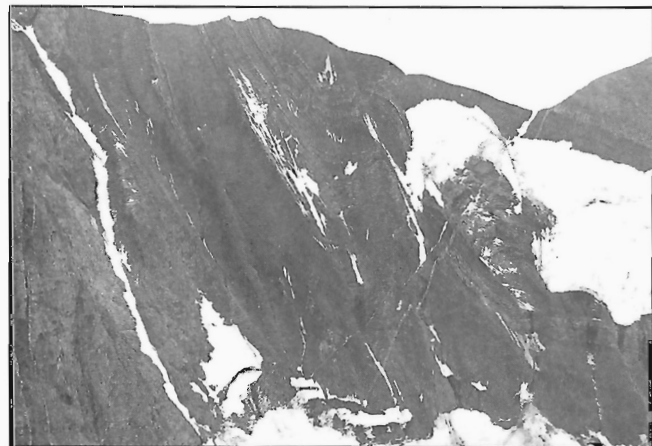


Figure 11. View south-southwest of basement-cover contact and fossiliferous cover succession 3.5 km south of Cornice Mountain; see section EF, Figure 4.

containing phenocrysts of quartz, biotite, or potassium feldspar. They include the main intrusion on Red Mountain (Goldslide pluton, 160 and 200 Ma $^{40}\text{Ar}/^{39}\text{Ar}$; LAC Minerals Ltd., unpub. data cited in Schroeter et al., 1992) and similar bodies 6-7 km south and southwest of Red Mountain, north of Homestake Ridge, northwest of North Flat Glacier, and west of Willoughby Glacier. They intrude probable upper Lower Jurassic rocks and are commonly dyked, veined, and altered. Locally they have the regional cleavage prominent in their hosts and are likely pre-Cretaceous. At Red Mountain, and locally elsewhere, contact relations between the Goldslide intrusions and their country rocks are equivocal and the bodies have been interpreted as flows or as sills and dykes. Their discordant map pattern at the property scale at Red Mountain is consistent with an intrusive origin. Host tuffaceous rocks are locally highly disrupted, with common plastically-deformed fragments suspended in a compositionally-similar ash matrix. These textures are interpreted to indicate intrusion into unlithified or poorly lithified host rocks.



Figure 12. Nelson glaciers pluton and related dyke swarm; pluton in foreground and lowermost part of ridge in background; view northwest, Cornice Mountain upper right (relief 1200 m).

STRUCTURE

Several domains and their bounding structures are distinguished on the map of structural elements (Fig. 3) and on cross-sections (Fig. 4). The northeast-trending Cambria fault separates domains containing structures of different vergence. The fault probably was the locus of limited pre-Tertiary(?) right lateral displacement; the crosscutting Tertiary(?) Nelson glaciers dyke swarm is apparently not offset across it.

Northwest of the fault, the domain is characterized by structures with southwest vergence on the northeast and northeast vergence on the southwest. It is a broad structural culmination comprising a central, relatively undeformed area underlain primarily by volcanic rocks (North Cambria and Todd icefields), and flanking, more strongly deformed areas (limbs) to the southwest and northeast underlain by clastic, well-bedded rocks. In the central area, gentle to moderate dips prevail and the basement-cover contact is deformed into broad, open folds. On the limbs, typical smaller-scale, tight and overturned folds are parasitic to the larger scale, basement-cored, central structure. Although the magnitude of shortening on the limbs is difficult to estimate, it appears to be much greater on the southwest, where overturned folds and thrust (or reverse) faults duplicate stratigraphy. On the northeast, folds are less common and stratigraphic overlap is small. The boundaries between the central culmination and the limbs are coincident with faulted antiforms, the Bitter Creek and Cornice Mountain antiforms (Fig. 4). Correlations of pyroxene-bearing volcanic rocks, discussed above, suggest that strike-slip displacement on the Bitter Creek structure, manifested in small-scale structures, is minimal. Alternatively, if a large scale structure is present, it lies west of the mafic volcanic rocks.

Southeast of the Cambria fault, southwest-verging structures dominate. In the northeasternmost part (section OP, Fig. 4), partly underlain by Upper Triassic and older rocks, structures are complex and may record a polyphase history, perhaps involving Triassic-Jurassic deformation similar to that observed near Kinskuch Lake (Greig, 1992). In this area, however, Hazelton Group rocks have also been affected by both northeast- and younger(?) southwest-vergent structures (Fig. 3). Southwest-directed shortening dominates here, compared to the domain on the northwest (cf. sections IJ and ST). The reason for this is uncertain, but speculatively, the Cambria fault may be a tear fault separating fold-thrust subsystems within the Skeena fold belt.

Basement and cover structural styles are dissimilar. The apparent disparity in magnitude of shortening is probably accommodated by detachments within the lower part of the cover sequence (e.g., section ST), by thrust faults within the basement (e.g., the thrust near the South Flat Glacier), and by detachments beneath basement culminations (Evenchick, 1991).

DISCUSSION

The stratigraphic position and distribution of the mafic volcanic rocks (e.g., units Jp and Jd) are important in mineral exploration and for Early Jurassic tectonics. Their discontinuous distribution down the southwest margin of the icefield to west of Homestake Ridge permits a speculative correlation with mafic volcanic rocks mapped by Alldrick et al. (1986) along strike west of Kitsault River valley (Fig. 1). Although Alldrick et al. (1986) correlated them with mafic rocks east of the Kitsault Valley, mafic rocks there occur at the base of a very thick section of Hazelton Group rocks and may be as old as Upper Triassic (Cordey et al., 1992). Mafic rocks west of the valley are likely much younger.

If so, the area underlain by upper Hazelton Group volcanic rocks is considerably expanded. The strata host the nearby Torbrit, Dolly Varden, and Kit stratiform base metals deposits, and more precious metals-rich occurrences such as Red Mountain and Homestake Ridge. If the mafic rocks west of Kitsault River are part of the upper Hazelton Group, it would support the view that the Anyox pendant, which includes mafic volcanic and Jurassic (Goutier et al., 1990) clastic rocks, is part of Stikinia. It follows that the Anyox massive sulphide deposit might be similar in age to the Torbrit, Dolly Varden, and Kit deposits, and (or) to those at Granduc(?) and Eskay Creek (Anderson et al., 1993).

CONCLUSIONS

1. Lower Jurassic Hazelton Group volcanic and volcanoclastic rocks, with a common bimodal composition, underlie much of the Cambria area and possibly overlie previously deformed Upper Triassic and older volcanic and clastic rocks. A shallow marine arc or extensional arc setting is indicated.
2. Mafic, pyroxene-rich volcanic rocks are an important part of the succession and their recognition has consequences for regional metallogeny and tectonics.
3. The volcanic rocks are overlain by a Middle and Upper Jurassic clastic succession characterized by increasing sedimentological maturity upsection and a westerly provenance.
4. Middle Jurassic and younger and Tertiary plutons intrude the successions; the Jurassic plutons, particularly the porphyritic Goldslide intrusions, are altered and associated with mineral deposition (such as at Red Mountain), and predate inception of the Cretaceous Skeena Fold Belt.
5. Apparent disparity in magnitude of shortening between cover and basement reflects differences in structural style that are attributable to contrasts in lithologic competency.
6. Mineral deposition at Red Mountain is Early Jurassic based on: intrusive relations and age of the spatially associated Goldslide pluton; occurrence of pyritic

volcanic rock fragments and sulphide clasts in Lower to Middle Jurassic clastic units; and pre-kinematic structural setting of host rocks and mineralization. An Early Jurassic age for the deposit is consistent with its setting in a mining district characterized by a widespread Early Jurassic mineralizing event.

ACKNOWLEDGMENTS

We acknowledge the geological input of LAC Minerals geologists, the hospitality of LAC and J.T. Thomas Diamond Drilling at the Red Mountain camp, and the flying skills of the pilots of Vancouver Island Helicopters Ltd., particularly Thanh Pham and Tom Schneider. Carol Evenchick and Glenn Woodsworth provided helpful reviews, Bev Vanlier helped in preparation of the final manuscript, and Tonia Williams drafted the figures.

REFERENCES

- Alldrick, D.A.**
1993: Geology and metallogeny of the Stewart Mining Camp, northwestern British Columbia; British Columbia Ministry of Energy, Mines and Petroleum Resources, Bulletin 85, 105 p.
- Alldrick, D.A., Dawson, G.L., Boshier, J.A., and Webster, I.C.L.**
1986: Geology of the Kitsault River area; British Columbia Ministry of Energy, Mines and Petroleum Resources, Open File Map 1986/2.
- Anderson, R.G.**
1993: A Mesozoic stratigraphic and plutonic framework for northwestern Stikinia (Iskut River area), northwestern British Columbia, Canada; in *Mesozoic Paleogeography of the Western United States--II*, (ed.) G. Dunne and K. McDougall; Society of Economic Palaeontologists and Mineralogists, Pacific Section, v. 71, p. 477-494.
- Anderson, R.G., Bevier, M.L., Nadaraju, G., Lewis, P., and Macdonald, J.**
1993: Jurassic arc setting for Stikinia's "Golden Triangle"; (abstract), Geological Association of Canada-Mineralogical Association of Canada, Program with Abstracts, v. 18, p. A3.
- Brown, D.A. and Greig, C.J.**
1990: Geology of the Stikine River-Yehiniko Lake area, northwestern British Columbia (104G/11W and 12E); in *Geological Fieldwork 1989*; British Columbia Ministry of Energy, Mines and Petroleum Resources, Paper 1990-1, p. 141-151.
- Carter, N.C.**
1981: Porphyry copper and molybdenum deposits of west-central British Columbia; British Columbia Ministry of Energy, Mines and Petroleum Resources, Bulletin 64, 150 p.
- Cordey, F., Greig, C.J., and Orchard, M.J.**
1992: Permian, Triassic, and Middle Jurassic microfaunal associations, Stikine Terrane, Oweegee and Kinskuch areas, northwestern British Columbia; in *Current Research, Part E*; Geological Survey of Canada, Paper 92-1E, p. 107-116.
- Evenchick, C.A.**
1991: Geometry, evolution, and tectonic framework of the Skeena Fold Belt, north-central British Columbia; *Tectonics*, v. 10, no. 3, p. 527-546.
- Evenchick, C.A., Mustard, P.S., Porter, J.S., and Greig, C.J.**
1992: Regional Jurassic and Cretaceous facies assemblages, and structural geology in Bowser Lake map area (104A) B.C.; Geological Survey of Canada, Open File 2582, 17 p.
- Goutier, J., Marcotte, C., and Wares, R.**
1990: Deformation of the Anyox massive sulfide deposit, British Columbia; (abstract), Geological Association of Canada-Mineralogical Association of Canada, Program with Abstracts, v. 15, p. A50.
- Greig, C.J.**
1991: Stratigraphic and structural relations along the west-central margin of the Bowser Basin, Oweegee and Kinskuch areas, northwestern British Columbia; in *Current Research, Part A*; Geological Survey of Canada, Paper 91-1A, p. 197-205.
1992: Fieldwork in the Oweegee and Snowslide ranges and Kinskuch Lake area, northwestern British Columbia; in *Current Research, Part A*; Geological Survey of Canada, Paper 92-1A, p. 145-155.
- Greig, C.J. and Evenchick, C.A.**
1993: Geology of Oweegee Dome, Delta Peak (104A/12) and Taft Creek (104A/11W) map areas; Geological Survey of Canada, Open File Map 2688, 3 sheets.
- Greig, C.J. and Gehrels, G.E.**
1992: Latest Triassic-earliest Jurassic orogenesis, Stikine terrane, northwestern British Columbia; (abstract), Geological Society of America, Abstracts with Programs, v. 24, no. 5, p. 28.
- Grove, E.W.**
1971: Geology and mineral deposits of the Stewart area; British Columbia Department of Mines and Petroleum Resources, Bulletin No. 58, 219 p.
1986: Geology and mineral deposits of the Unuk River-Salmon River-Anyox area; British Columbia Ministry of Energy, Mines and Petroleum Resources, Bulletin 63, 152 p.
- Hanson, G.**
1929: Bear River and Stewart map-areas, Cassiar District, B.C.; Geological Survey of Canada, Memoir 159, 84 p.
1935: Portland Canal Area, British Columbia; Geological Survey of Canada, Memoir 175, 179 p.
- Henderson, J.R., Kirkham, R.V., Henderson, M.N., Payne J.G., Wright, T.O., and Wright, R.L.**
1992: Stratigraphy and structure of the Sulphurets area, British Columbia; in *Current Research, Part A*; Geological Survey of Canada, Paper 92-1A, p. 323-332.
- McConnell, R.G.**
1913: Portions of Portland Canal and Skeena Mining Divisions, Skeena District, B.C.; Geological Survey of Canada, Memoir 32, 101 p.
- Schroeter, T., Lane, B., and Bray, A.**
1992: Red Mountain (103P 086); in *Exploration in B.C. 1991*, British Columbia Ministry of Energy, Mines and Petroleum Resources, Paper 1992-1, p. 117-125.

Recent basaltic volcanism in the Iskut-Unuk rivers area, northwestern British Columbia

S. Hauksdóttir¹, E.G. Enegren², and J.K. Russell¹

Cordilleran Division

Hauksdóttir, S., Enegren, E.G., and Russell, J.K., 1994: Recent basaltic volcanism in the Iskut-Unuk rivers area, northwestern British Columbia; in Current Research 1994-A; Geological Survey of Canada, p. 57-67.

Abstract: The Iskut-Unuk rivers area contains eight Recent volcanic centres comprising alkali-basalt lava flows, pillow lava, hyaloclastite and cinder cones, including: the Iskut River, Tom MacKay Creek, Snippaker Creek, Cone Glacier, Cinder Mountain, King Creek, Second Canyon and Lava Fork centres. Lava flows range from 70 000 to ~150 years. The oldest volcanic rocks underlie the Iskut River Lava Flats and the youngest occur at the Lava Fork centre. The lavas erupted from each centre are similar in mineralogy. Most contain plagioclase and olivine phenocrysts and clinopyroxene occurs as a groundmass phase. Plagioclase megacrysts characterize lavas from a number of volcanic centres, but are particularly abundant in lavas from Snippaker Creek and Cone Glacier. Crustal xenoliths are abundant in Lava Fork and Cone Glacier lavas but less common elsewhere. Many of the volcanological features are attributable to volcanic eruptions occurring near and beneath glaciers.

Résumé : La région des rivières Iskut et Unuk renferme huit centres volcaniques actifs à l'Holocène ayant émis des basaltes alcalins sous forme de coulées massives, de coulées en coussins, d'hyaloclastites et de cônes de scories. Ces centres ont pour nom : Iskut River, Tom MacKay Creek, Snippaker Creek, Cone Glacier, Cinder Mountain, King Creek, Second Canyon et Lava Fork. L'âge des coulées de lave varie de 70 000 à environ 150 ans. Les roches volcaniques les plus anciennes gisent sous les plaines de lave de la rivière Iskut et les plus récentes se trouvent au centre de Lava Fork. Les laves éjectées de chaque centre ont des minéralogies semblables. La plupart contiennent des phénocristaux de plagioclase et d'olivine sertis dans une matrice à clinopyroxène. Des mégacristsaux de plagioclase caractérisent les laves de plusieurs centres volcaniques, mais sont particulièrement abondants dans les laves des centres de Snippaker Creek et de Cone Glacier. Des xénolites de matériel crustal abondent dans les laves de Lava Fork et de Cone Glacier, mais sont plus rares ailleurs. Un grand nombre de caractéristiques volcanologiques sont attribuables à des éruptions volcaniques se produisant à proximité ou au-dessous de glaciers.

¹ Department of Geological Sciences, University of British Columbia, 6339 Stores Road, Vancouver, British Columbia V6T 2B4

² Hydroelectric Engineering Division, B.C. Hydro, 6911 Southpoint Drive, Podium A02, Burnaby, British Columbia V3N 4X8

INTRODUCTION

The Stikine Volcanic Belt includes a number of relatively small Recent cones and related lava fields along with three large compositionally diverse volcanic complexes: Level Mountain (Hamilton, 1981), the Edziza-Spectrum Complex (Souther, 1989) and Hoodoo Mountain (Souther, 1990a; Edwards and Russell, 1994). Souther (1990b) named the Recent cinder cones and lava flows scattered south of the Iskut River the Iskut-Unuk River Cones (Fig. 1). Volcanoes within the Stikine Volcanic Belt are disposed along several short en échelon segments. Souther (1990a) suggested that the southern part of the belt where the Iskut-Unuk rivers volcanic rocks are located is associated with north-trending

extensional structures. These structures probably developed in response to shear along the adjacent, transcurrent boundary between the continent and the Pacific plate.

The Iskut-Unuk rivers volcanic assemblage includes eight volcanic centres named after their geographic locations: the Iskut River, Tom MacKay Creek, Snippaker Creek, Cone Glacier, Cinder Mountain, King Creek, Second Canyon and Lava Fork centres. These Recent lava flows and pyroclastic deposits mostly occupy topographic lows (e.g., stream valleys) and mineralogically and chemically are alkali-olivine basalts (Grove, 1974; D.A. Brew, pers. comm., 1990). Recent volcanism in the Iskut-Unuk rivers area spanned 70 000 to ~150 B.P. (B.C. Hydro, 1985).

In 1989 Stasiuk and Russell (1990) visited and sampled most of the Iskut-Unuk rivers volcanic centres. We designed the 1993 field season to complete the sample collection and to ascertain field relationships among volcanic units within each centre. Appendix 1 lists the representative samples and their locations. Crustal xenoliths are common in these volcanic rocks and special efforts were made to collect samples of these diverse materials (Appendix 2). Lastly, unconsolidated basaltic ash was sampled at three locations; pertinent details are given in Appendix 3.

Based on these samples and those collected previously (Stasiuk and Russell, 1990), we are directing future research towards: i) characterizing the chemistry and mineralogy of each centre; ii) investigating source-region processes related to the Iskut-Unuk rivers magmatism; iii) identifying the styles of magmatic differentiation within and between each volcanic centre; and iv) evaluating the role and mechanisms of assimilation.

PREVIOUS WORK

The two southernmost centres, Lava Fork and Second Canyon were briefly noted by workers in the early part of this century (Wright, 1906). Regional mapping programs provided first descriptions for the majority of volcanic centres in the Iskut-Unuk rivers area. Kerr (1948) mapped the Recent flows occurring along Iskut River. Grove (1974) visited and sampled most of the Recent volcanic centres. His work currently represents the only published chemical analyses for Iskut-Unuk rivers volcanic rocks; he published major and trace element data for volcanic rocks from six centres. Grove's (1986) compilation for the Unuk River-Salmon River-Anyox area also gave distributions of Recent volcanic rocks, for the Iskut-Unuk rivers area and beyond.

The most detailed mapping of Iskut-Unuk rivers volcanic centres was conducted by B.C. Hydro, between 1982 and 1984, as a part of their Iskut Canyon and More Creek projects (B.C. Hydro, 1985). This largely unpublished work mainly concerned the Recent volcanic stratigraphy of the area and included 1:50 000 and 1:10 000 scale geological mapping, ^{14}C and K-Ar dating of units and diamond drilling of the Iskut River lava flows. Later regional geological maps (Britton et al., 1988, 1989; Read et al., 1989) include distributions of Recent volcanic rocks in the Snippaker Creek and Unuk River

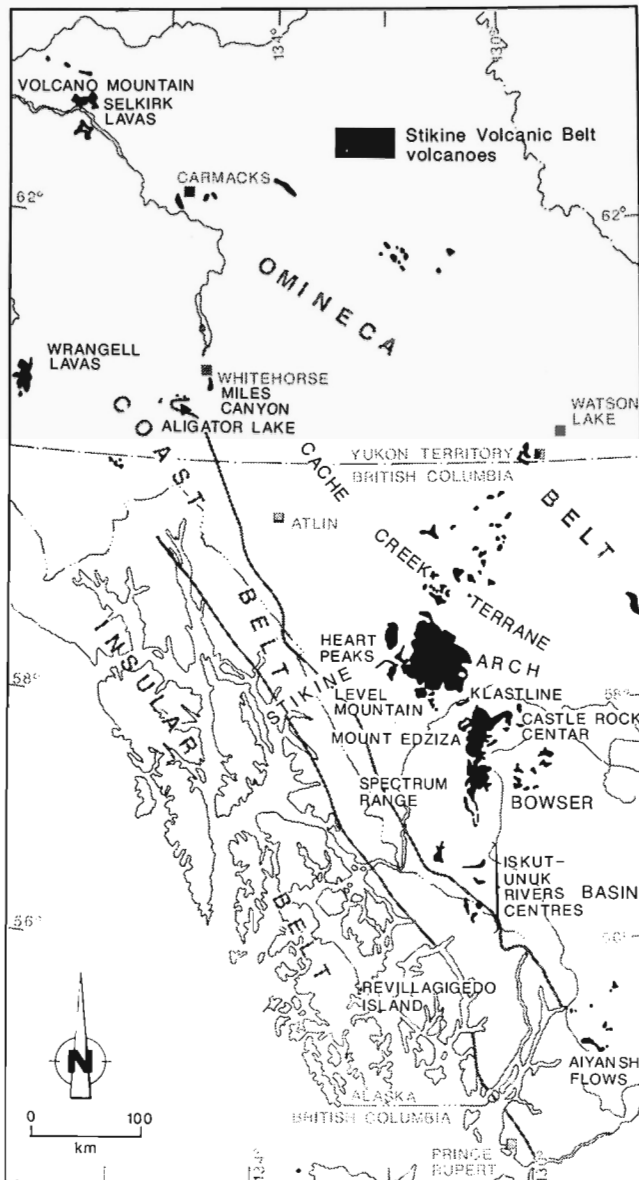


Figure 1. Location of the Iskut-Unuk rivers volcanic centres within the Stikine Volcanic Belt (after Souther and Yorath, 1991).

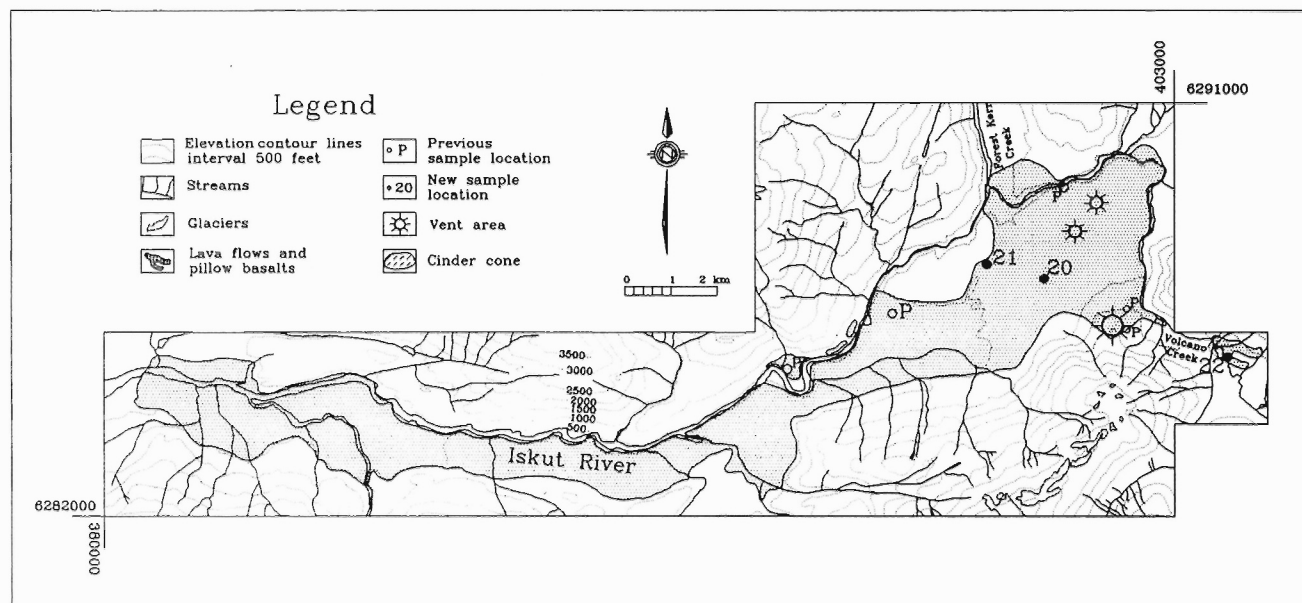


Figure 2. Distribution of volcanic material in the Iskut River and Tom MacKay Creek volcanic centres. Legend distinguishes between lava flows or pillow basalt and cinder cones.

areas. Finally, Elliott et al. (1981) and D.A. Brew (pers. comm., 1990) described lava flows and stratigraphic relationships from the Lava Fork centre. Souther (1990b) compiled and summarized much of the information described above. Stasiuk and Russell (1990) used the maps of previous workers (Kerr, 1948; Grove, 1986; Elliott et al., 1981) when they collected samples.

THE ISKUT-UNUK RIVERS CENTRES

This report is a compilation of fieldwork results derived from the 1993 field season and B.C. Hydro's Iskut Canyon and More Creek projects. In particular the ages of the volcanic units and most of the distributions result from B.C. Hydro's research (B.C. Hydro, 1985) and this paper largely corroborates the existing maps with few exceptions (e.g., Cone Glacier and Cinder Mountain centres).

Iskut River

Figure 2 shows the distribution of Recent lava flows along Iskut River and three proposed vents which have produced both lavas and cinder. The Iskut River canyon cuts down through at least 10 thick, subaerial lava flows and immediately south of the canyon, these flows form the Iskut River Lava Flats (B.C. Hydro, 1985). At least two younger lava flows can be traced across the Lava Flats (i.e., they overlie older flow surfaces) (B.C. Hydro, 1985). Contacts between these younger lavas and those making up the majority of the Lava Flats are partly marked by differences in vesicularity between the base of one flow and the top of the other. All of the flows observed are porphyritic with plagioclase and olivine phenocrysts, a feature that makes separation of flows in

the field difficult. The surfaces of both these younger flows and the Lava Flats are vegetated and characteristically cindery, blocky and hummocky which hindered collection of fresh material (e.g., Sta. 20 and 21).

Flows at the base of the Iskut River Lava Flats are about 70 000 years old, based on K-Ar dating; the overlying basalt flows are dated (^{14}C) at 8730 years (Table 1, B.C. Hydro, 1985). Three cinder cones are identified (Fig. 2). The youngest cone lies to the south and appears to have fed the two youngest flows. It appears to have repeatedly erupted lava which dammed both Tom MacKay and Forrest Kerr creeks (B.C. Hydro, 1985). This inference is based on ^{14}C dating of plant remains in lake sediments associated with these ephemeral dams. These age determinations (Table 1, B.C. Hydro, 1985; Read et al., 1989) suggest lava effusion occurred 3800, 5600 and 6500-6800 years ago; the Iskut River Canyon was eroded to its present configuration in the last 3600 to 3800 years (B.C. Hydro, 1985). The two youngest flows have not been successfully dated.

Tom MacKay Creek

Volcanic rocks in the Tom MacKay volcanic centre occur just east of the Iskut River Lava Flats (Fig. 2) and make up a single flow unit composed of highly weathered, fragmented pillow basalt. Individual pillows (Sta. 22) are 20-40 cm in diameter, very vesicular, radially jointed and commonly have glassy rinds. The pillow lava locally forms 20-30 m high cliffs. These thick, restricted accumulations of pillow lava have probably resulted from volcanic eruption against or close to ice. No samples were previously collected from this centre (e.g., Stasiuk and Russell, 1990).

Snippaker Creek

Recent lava distributions within the Snippaker Creek drainage are shown in Figure 3. The lavas outcrop from stream level to approximately the 1000 foot contour. Representative samples were collected from three localities including: i) the southern terminus (Sta. 17), ii) along Memorial Creek (Sta. 1), and iii) within the Snippaker creekbed towards the northern terminus (Sta. 16). Two flow units were sampled at each location although more flows were observed in the last locality. Here (Sta. 16), Snippaker Creek has incised a narrow, steep-sided canyon through the flow sequence where at least 6 flow units are exposed, each 3-5 m thick. Contacts between flow units are marked by changes in vesicularity between flow tops and scoriaceous flow bases.

Flows from the three localities are indistinguishable. They have grey, vesicular fresh surfaces and are plagioclase and olivine porphyritic; phenocrysts range in size from 0.1 to 1 cm. Previous work has suggested that the vent to these lavas lies upstream of the confluence of Memorial Creek and Snippaker Creek (B.C. Hydro, 1985). The northern terminus of these flows abuts against lavas of the Iskut River Lava Flats and both sets of lavas are plagioclase and olivine porphyritic and indistinguishable in hand sample (B.C. Hydro, 1985).

Cone Glacier

The Cone Glacier volcanic centre comprises two prominent cones and several lava flows (Fig. 4). Lava flows emanate from the Cone Glacier area, cover a portion of Snippaker Creek (to the west) and underlie Julian Lake and the King Creek drainage (to the south). Near the western terminus of the flows only 1-3 flows are exposed and some overlie till or river gravel (B.C. Hydro, 1985). Lava flow surfaces are

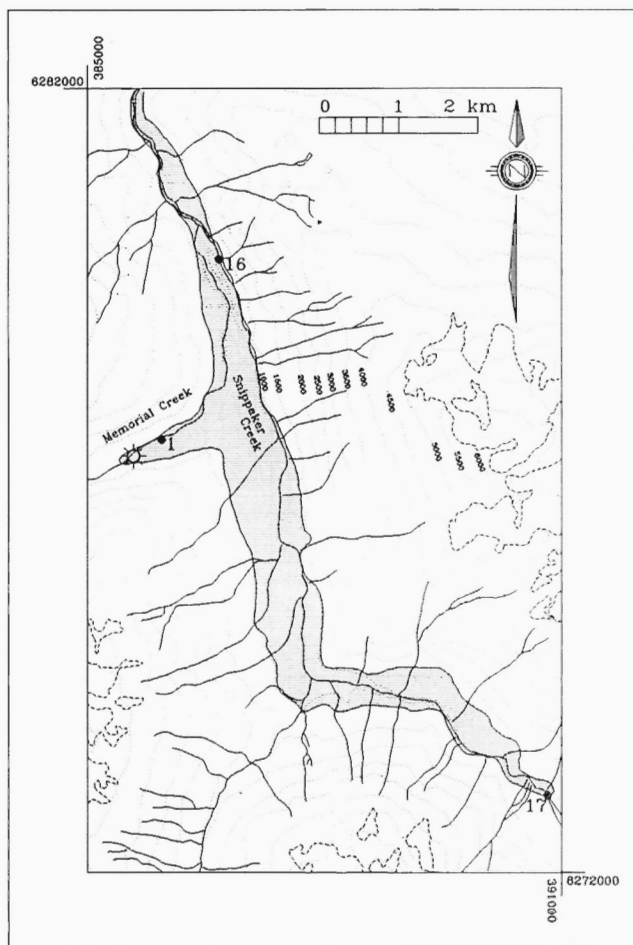


Figure 3. Distribution of Recent volcanic rocks for the Snippaker Creek centre. Legend is as in Figure 2.

Table 1. Summary of radiometric age determinations of Iskut-Unuk rivers volcanic centres.

| Centre | Date (yrs) | Method | Notes | Reference |
|-----------------|---------------|-----------------|------------------------------|-----------------------|
| Iskut River | 70,000±30 000 | K-Ar | Basal flow 1 from Lava Flats | B.C. Hydro (1985) |
| Iskut River | 10,000±10 000 | K-Ar | Flow 2 on top of flow 1 | B.C. Hydro (1985) |
| Iskut River | 8780±150 | ¹⁴ C | Cinder on top of flow 2 | Read et al. (1989) |
| Iskut River | 8730±600 | ¹⁴ C | Cinder on top of flow 2 | B.C. Hydro (1985) |
| Iskut River | 6800±160 | ¹⁴ C | Damming Tom MacKay Creek | B.C. Hydro (1985) |
| Iskut River | 6500±160 | ¹⁴ C | Damming Tom MacKay Creek | B.C. Hydro (1985) |
| Iskut River | 5400±160 | ¹⁴ C | Damming Tom MacKay Creek | B.C. Hydro (1985) |
| Iskut River | 3970±120 | ¹⁴ C | Damming Forrest Kerr Creek | B.C. Hydro (1985) |
| Iskut River | 3930±80 | ¹⁴ C | Damming Forrest Kerr Creek | Read et al. (1989) |
| Iskut River | 3800±160 | ¹⁴ C | Damming Tom MacKay Creek | B.C. Hydro (1985) |
| Iskut River | 3660±90 | ¹⁴ C | Damming Forrest Kerr Creek | B.C. Hydro (1985) |
| Iskut River | 3540±70 | ¹⁴ C | Damming Forrest Kerr Creek | Read et al. (1989) |
| Iskut River | 2610±70 | ¹⁴ C | Damming Forrest Kerr Creek | Read et al. (1989) |
| Iskut River | 2535±75 | ¹⁴ C | Youngest ash deposit | B.C. Hydro (1985) |
| Iskut River | 2555±60 | ¹⁴ C | Youngest ash deposit | B.C. Hydro (1985) |
| Cinder Mountain | 33,000±2400 | ¹⁴ C | A single lava flow | B.C. Hydro (1985) |
| Lava Fork | >70, ~150 | Tree ring | An estimate of top flow | B.C. Hydro (1985) |
| Lava Fork | >350 | Tree ring | An estimate of second flow | B.C. Hydro (1985) |
| Lava Fork | 360±60 | ¹⁴ C | On surface of one of flows | Elliott et al. (1981) |
| Lava Fork | ~130 | ¹⁴ C | On "the lower flows" | Grove (1986) |

blocky and heavily vegetated except above 3500 feet on the saddle immediately in front of Cone Glacier. The recent retreat of Cone Glacier has left the lava exposed and striated.

Cone Glacier takes its name from a 300 m high, well-exposed volcanic cone (west cone) of grey cinder, hyaloclastite and basaltic ash (Appendix 3). At the northern side of west cone the lowest unit is pillow lava. The pillows are radially jointed and have glassy rinds and a concentric distribution of vesicles. Hyaloclastite breccia overlies the pillowed lava and consists of fragments of lava and glass in a brown-gold coloured, devitrified basaltic glass matrix (palagonitized sideromelane). The majority of pyroclastic material making up the cone is cinder which represents sub-aerial eruptions. There are no flows observed which definitely originate from the vent. The majority of lavas in the Snippaker Creek drainage probably have a source to the east of west cone.

Another well-dissected and nearly vegetation-free cone of red cinder and scoria (east cone), northeast of Cone Glacier, may be the source to the lavas in the Snippaker Creek drainage. North of Cone Glacier on the south side of Snippaker Creek (Sta. 6-9) a cliff provides exposure of up to seven different flow units. They are generally 2-3 m thick with scoriaceous and brecciated bottoms and tops. All of the lava flows are characterized by abundant, coarse (up to 4 cm long) megacrysts of euhedral glassy feldspar. The lavas also contain phenocrysts of feldspar and olivine, 2-3 mm in diameter. Cinder and scoria derived from both west and east cones are mineralogically similar. Diverse crustal xenoliths are found in most of the lava flows (Fig. 5); the majority are granitic. For example, the lava flow at Station 15 contains abundant xenoliths ranging from granitic to grey aphanitic igneous clasts. The latter suite of clasts is concentrated at the base of the flow and, therefore, probably was incorporated into the lava after it was erupted.



Figure 4. Cone Glacier and Cinder Mountain volcanic centres. Map delineates three vent areas and lava distributions associated with the two centres. Legend is as in Figure 2.

Remnants of three lava flows are found on the eastern margin of east cone. The provenance of these lavas is somewhat ambiguous because they are equidistant to the Cinder Mountain centre (see below). Based on the presence of abundant large feldspar phenocrysts and the fact that these lavas occur at an elevation below or equal to the remnant of east cone, these lavas are interpreted as part of the Cone Glacier centre.

Cinder Mountain

Cinder Mountain volcanic centre is east and northeast of Cone Glacier (Fig. 4). The distribution of volcanic units shown in Figure 4 is an estimate because ice, snow, talus and minor vegetation obscure the rocks. Cinder Mountain lava flows and hyaloclastite breccia are mainly exposed on the south and west slopes of Cinder Mountain and as a single outcrop to the north near Copper King Glacier.

Hyaloclastite breccia is the most voluminous unit found at Cinder Mountain (Fig. 6a, b). It is a golden-brown volcanic breccia comprising basaltic fragments and basaltic glass in a matrix of palagonitized sideromelane. The hyaloclastite varies from basaltic rock fragment-dominated breccia with very little matrix to breccia that is dominantly basaltic glass fragments (Fig. 6a). These variations define the prominent 10-50 cm scale layering observed in the hyaloclastite (Sta. 13). Basaltic dykes with chilled margins commonly cut the hyaloclastite breccia. Elsewhere massive basalt bodies apparently intrude the hyaloclastite and grade into pillow-like bodies with glassy rinds. These dykes are light-grey in colour, very massive and have rare, small feldspar crystals and are distinct from lavas erupted from the Cone Glacier centre.

The breccia is more finely and regularly layered (Fig. 6b) where the hyaloclastite breccia is in contact with basement rocks (plutonic and metamorphic rocks) (e.g., Sta. 19). The

layers comprise different basaltic glass contents and internal planar and cross-laminations suggest significant transport and reworking (Fig. 6b). Layering parallels depositional surfaces which dip up to 30° to the north, and probably reflects the paleoslopes along which the hyaloclastite debris was transported.

Close to Copper King Glacier, near the head of Harrymel Creek, the remnant of a single flow is exposed. It overlies till and itself is overlain by an ablation moraine (B.C. Hydro, 1985). The flow forms a 15-20 m high wall of columnar jointed basalt (e.g., Sta. 18). ¹⁴C dating of a sample recovered from the underlying till-basalt contact gives an age of 33 000 ± 2000 years (Table 1, B.C. Hydro, 1985). The lack of megacrystic feldspar and xenoliths and overall paucity of phenocrysts suggest the lava was erupted from the Cinder Mountain centre.

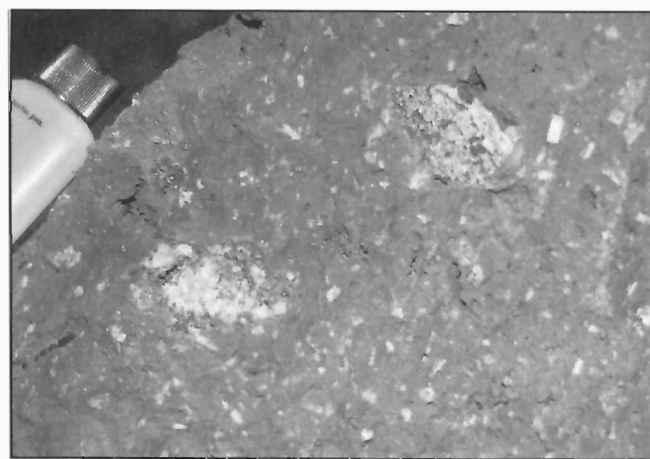


Figure 5. Large (5-7 cm) xenoliths found in uppermost flow at Cone Glacier. Also visible are large (0.5-1 cm) feldspar phenocrysts characteristic of Cone Glacier lavas.

Figure 6. Hyaloclastite breccias from Cinder Mountain: upper photograph (6a) shows massive lava (right side) intruding layered coarse- and fine-grained hyaloclastite breccias; lower photograph (6b) shows finer scale layering and internal structure of hyaloclastite deposits immediately overlying bedrock.

King Creek

The King Creek centre dominantly comprises pillow lava and associated breccia. The lavas are exposed in a steep narrow creek south of Cone Glacier (Fig. 7) where they form a 40-50 m cliff. The pillow lava and overlying breccia are exposed from stream-level to about 1070 m elevation (Stasiuk and Russell, 1990). Individual pillows are commonly surrounded by scoriaceous breccia (Sta. 14). A 1-2 m wide vertical dyke crosscuts the pillow lavas. As at Tom MacKay Creek, the restricted extent of thick pillowed lava and associated breccia suggest that the lava was erupted against or close to ice.

Second Canyon

The Second Canyon centre comprises a single blocky lava flow where eruption forced the Unuk River against its eastern bank (Fig. 8). Subsequent dissection of the lava formed Second and Third canyons. The walls to these canyons are 15 m high cliffs of columnar jointed basalt lava (B.C. Hydro, 1985). The lava flow overlies fluvial sediments and the presence of a scoriaceous, flow-structured lava surface suggests that the eruption was postglacial (B.C. Hydro, 1985). The source to the lava flow is either a tree-covered cone located at the confluence of Unuk River and Canyon Creek or on the slope immediately above Canyon Creek, about 4 km upstream from the same confluence (Fig. 8, B.C. Hydro, 1985). A sample of the flow collected in 1989 (Stasiuk and Russell, 1990) suffices because all sources agree that there is only a single flow unit (e.g., B.C. Hydro, 1985; Stasiuk and Russell, 1990).

Lava Fork

The Lava Fork volcanic centre comprises basaltic ash and at least three flows, which are exposed at the confluence of Blue River and Unuk River. Dissection by the Unuk River at the

southern terminus formed the First Canyon (B.C. Hydro, 1985). The distribution of volcanic material shown in Figure 9 includes undifferentiated cinder and ash deposits as well as lava flows. A layer of basaltic cinder and glassy ash covers the lava flows as well as the area to the east towards Leduc Glacier and Twin John Peaks (Grove, 1986). The youngest flow erupted from a vent located on a ridge on the eastern side of Lava Fork valley. The lava flowed south, along the valley and southeast along Blue River valley, damming the river and forming Blue Lake. Near the main vent, the volcanic rocks overly basement rocks, including foliated biotite-quartz-schist intruded by granodiorite. A possible vent for the older flows is a tree-covered cinder cone located 4 km downstream of Blue Lake (B.C. Hydro, 1985).

Near its source, the youngest lava flow has ropey pahoehoe surfaces and forms well-developed small lava channels and lava tubes. Spatter, cinder and ash are abundant around the vent. Downslope and away from the vent, the flow surface abruptly changes to aa and splits into two main streams (north and south forks). The lava streams form large channels (Fig. 10) with several generations of prominent levees. Accretionary lava balls are common on the flow surface of the north fork lava (Sta. 23). They are approximately 5 m in diameter and consist of a red cinder breccia coated by massive flow which exhibits radially oriented irregular jointing. Xenoliths of basement rocks occur in both the interior and exterior portions of the lava balls.

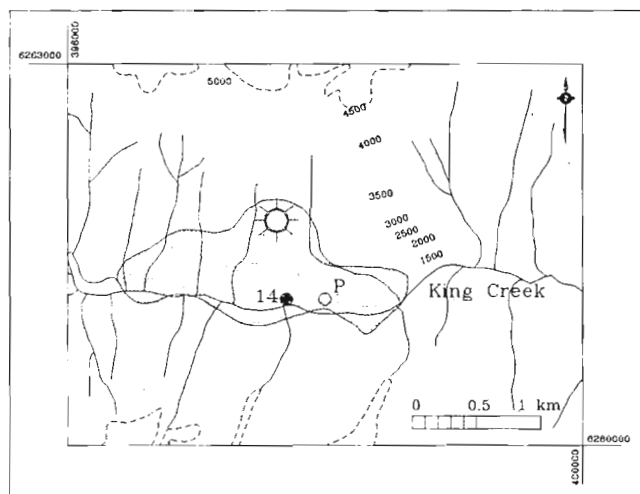


Figure 7. Distribution of King Creek volcanic rocks. Legend as in Figure 2.

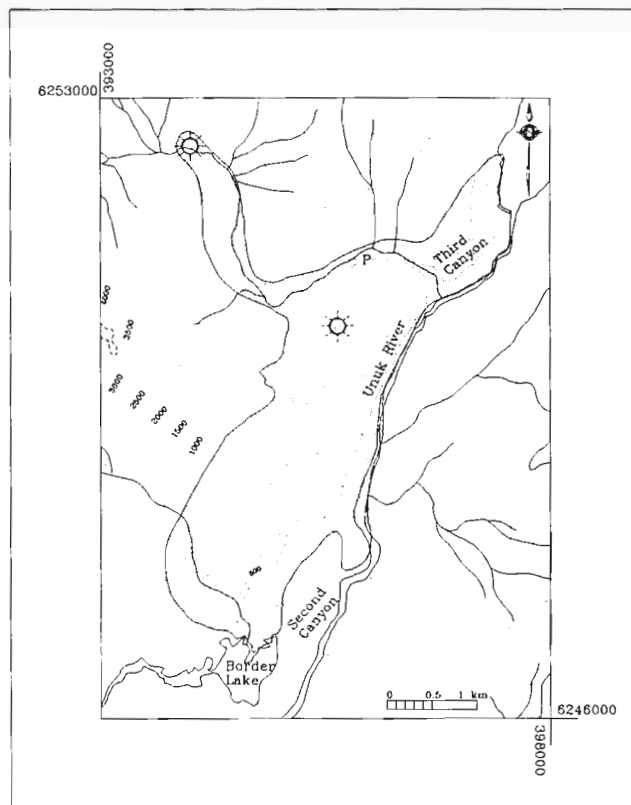


Figure 8. Distribution of volcanic rocks from the Second Canyon centre. Legend as in Figure 2.

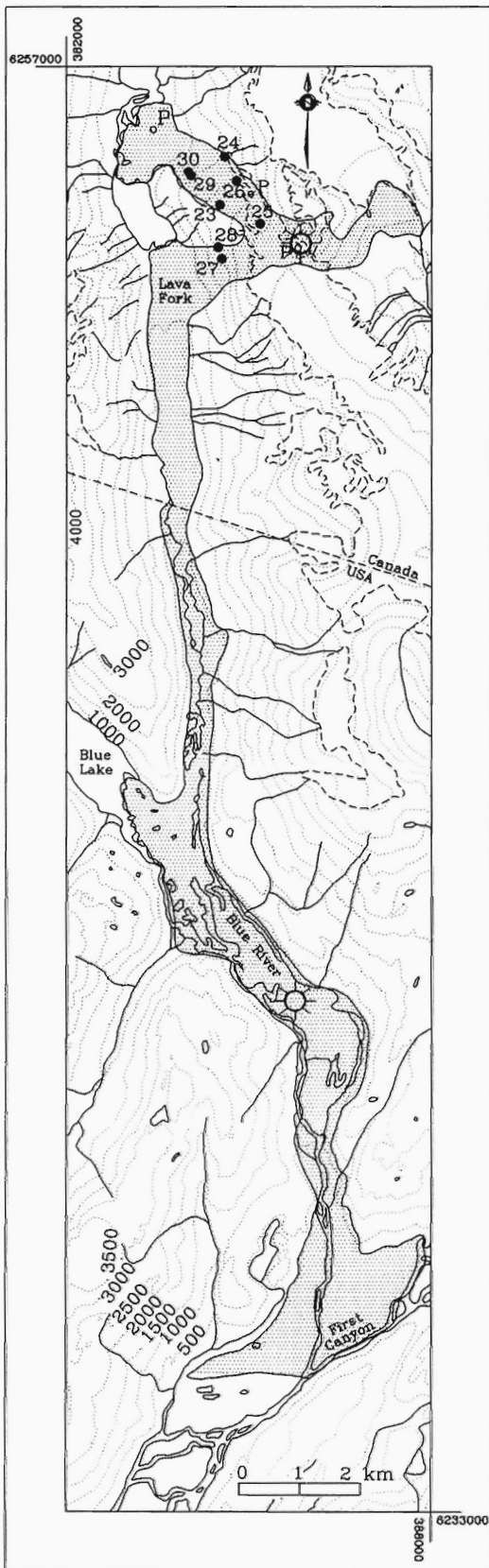


Figure 9. Distribution of lavas and cinder associated with the Lava Fork centre. Legend as in Figure 2.

Crustal xenoliths are common throughout the lava and are mainly granitic rocks or metamorphic schist. The xenoliths are mainly angular, range from 1 to 30 cm in diameter, and resemble the basement rocks underlying the main vent area. The degree of reaction between lava and xenolith is highly variable. Many show no signs of reaction (e.g., reaction rims) whereas others are porous, granular and friable. Commonly, the host basaltic melt has invaded these latter xenoliths along thin fractures.

^{14}C dating of a partly charred conifer log from the surface of one of the flows yielded an age of 360 ± 60 BP (Table 1, Elliott et al., 1981). Grove (1986) argued for an age of 130 BP based on ^{14}C dating of material associated with the lower flows. Subsequent dating, using tree-ring counts, gives a minimum age of 70 years old for the youngest flow (B.C. Hydro, 1985). Based on tree ring counts on living trees, and observations of the lava flow surface it is estimated to be around 150 years old. Living trees on the surface of an underlying flow give a minimum age of 350 years (B.C. Hydro, 1985).



Figure 10. Typical lava channel with well-developed levees from the Lava Fork volcanic centre.

DISCUSSION

Recent volcanic rocks within the Iskut-Unuk rivers area are alkali-olivine basalt lava flows and pyroclastic material. They are petrographically similar, generally being fine grained, porphyritic basalts containing phenocrysts of plagioclase and olivine. Megacrysts (0.5-4 cm) of glassy plagioclase are common; to date they are recognized in lavas from every centre except Second Canyon and Cinder Mountain. The groundmass comprises plagioclase, olivine, opaque minerals, glass and titanite. Clinopyroxene is conspicuously rare as a phenocryst. There are few mineralogical differences between lavas from different centres. The Cinder Mountain lavas are distinct in that they typically contain few phenocrysts, have a trachytic groundmass, and apparently lack xenoliths.

The diversity of feldspar habits in the lavas is one of the more remarkable features of these volcanic rocks. They occur in a wide variety of sizes (megacryst to microphenocryst), forms (euhedral to corroded), and compositional zonation (strong oscillatory zoning to unzoned). The extent to which they are cognate versus xenocrystic is not immediately obvious, although given the pervasive occurrence of crustal xenoliths some of the populations probably relate to assimilation processes.

ACKNOWLEDGMENTS

The field work component of this research was funded by the Geological Survey of Canada (Project 840046). Ancillary funding was provided by a 1993 Geological Society of America Research Grant to the senior author and NSERC operating grant 589820 (JKR). Field assistance was provided by Lori Snyder, Ben Edwards, Darwin Green and Sean Galway. We thank R.G. Anderson, C.E. Evenchick for reviewing and editing earlier versions of the manuscript and Bev Vanlier for manuscript preparation for final publication. B.C. Hydro generously provided access to all information compiled during the Iskut Canyon and More Creek projects in 1979-1984.

REFERENCES

- B.C. Hydro**
1985: Stikine-Iskut Development, Iskut Canyon and More Creek Projects, 1982-1984; Geotechnical Investigations, Main Report, Volume 1, Report No. H1614. B.C. Hydro Information Centre.
- Britton, J.M., Webster, L.C.L., and Alldrick, D.J.**
1988: Unuk map area (104B/7E, 8W, 9W, 10E); in Geological Fieldwork 1988; British Columbia Ministry of Energy, Mines and Petroleum Resources, Paper 1989-1, p. 241-250.
- Britton, J.M., Fletcher, B.A., and Alldrick, D.J.**
1989: Snippaker map area (104B/6E, 7W, 10W, 11E); in Geological Fieldwork 1989; British Columbia Ministry of Energy, Mines and Petroleum Resources, Paper 1990-1, p. 115-125.
- Edwards, B.R. and Russell, J.K.**
1994: Preliminary stratigraphy of Hoodoo Mountain volcanic centre, northwestern British Columbia; in Current Research 1994-A; Geological Survey of Canada.
- Elliott, R.L., Koch, R.D., and Robinson, S.W.**
1981: Age of basalt flows in the Blue River Valley, Bradfield Canal Quadrangle; in The United States Geological Survey of Alaska, Accomplishments during 1979, United States Geological Survey Circular 823-B, p. B115-B116.
- Grove, E.W.**
1974: Deglaciation - A possible triggering mechanism for Recent volcanism; International Association of Volcanology and Chemistry of the Earth's Interior, Proceedings of the Symposium on Andean and Antarctic Volcanology Problems, Santiago, Chile, September 1974, p. 88-97.
1986: Geology and mineral deposits of the Unuk River - Salmon River - Anyox Area; British Columbia Ministry of Energy, Mines and Petroleum Resources, Bulletin 63, 152 p.
- Hamilton, T.S.**
1981: Late Cenozoic alkaline volcanics of the Level Mountain Range, northwestern British Columbia: geology, petrology and paleomagnetism; Ph.D. thesis, University of Alberta, Edmonton.
- Kerr, A.**
1948: Lower Stikine and western Iskut River areas, British Columbia; Geological Survey of Canada, Memoir 246, 94 p.
- Read, P.B., Brown, R.L., Psutka, J.F., Moore, J.M., Journeay, M., Lane, L.S., and Orchard, M.J.**
1989: Geology of parts of Snippaker Creek (104B/10), Forrest Kerr Creek (104B/15), Bob Quinn Lake (104B/16), Iskut River (104G/1) and More Creek (104G/2); Geological Survey of Canada, Open File 2094.
- Souther, J.G.**
1989: The Late Cenozoic Mount Edziza Volcanic Complex, British Columbia; Geological Survey of Canada, Memoir 420, 320 p.
1990a: Volcano tectonics of Canada; in Volcanoes of North America, United States and Canada, C.A. Wood and J. Kienle (ed.); Cambridge University Press, p. 111-116.
1990b: Iskut-Unuk River Cones, Canada; in Volcanoes of North America, United States and Canada, C.A. Wood and J. Kienle (ed.); Cambridge University Press, p. 128-129.
- Souther, J.G. and Yorath, C.J.**
1991: Neogene assemblages, Chapter 10; in Geology of the Cordilleran Orogen in Canada, H. Gabrielse and C.J. Yorath (ed.); Geological Survey of Canada, Geology of Canada, no. 4, p. 373-401 (also Geological Society of America, The Geology of North America, v. G-2).
- Stasiuk, M.V. and Russell, J.K.**
1990: Quaternary volcanic rocks of the Iskut River region, northwestern British Columbia; in Current Research, Part E; Geological Survey of Canada, Paper 90-1E, p. 153-157.
- Wright, F.E.**
1906: The Unuk River mining region of British Columbia; in Geological Survey of Canada, Summary Report of the Year 1905, p. 68-74.

Geological Survey of Canada Project 840046

APPENDIX 1

Summary of samples collected for bulk chemical analysis.

| Sample | Station | Centre | Type | UTM | Notes |
|--------|---------|------------------|---------------|-----------------|------------------------|
| SH9301 | 1 | Snippaker Creek | Lava flow | 385940, 6277520 | |
| SH9302 | 1 | Snippaker Creek | Lava flow | 385940, 6277520 | |
| SH9304 | 3 | Cone Glacier | Lava flow | 398370, 6270050 | Cindery flow |
| SH0307 | 4 | Cone Glacier | Lava flow | 398310, 6270050 | Cindery flow |
| SH9309 | 6 | Cone Glacier | Lava flow | 397650, 6270000 | |
| SH9310 | 6 | Cone Glacier | Lava flow | 397650, 6270000 | |
| SH9312 | 8 | Cone Glacier | Lava flow | 397620, 6269960 | |
| SH9313 | 8 | Cone Glacier | Lava flow | 397620, 6269960 | |
| SH9314 | 9 | Cone Glacier | Lava flow | 397550, 6269900 | |
| SH9315 | 9 | Cone Glacier | Lava flow | 397550, 6269900 | |
| SH9316 | 9 | Cone Glacier | Lava flow | 397550, 6269900 | |
| SH9317 | 9 | Cone Glacier | Lava flow | 397550, 6269900 | Same as SH9309 |
| SH9318 | 9 | Cone Glacier | Lava flow | 397550, 6269900 | Same as SH9312 |
| SH9319 | 10 | Cinder Mountain | Lava flow | 400380, 6270030 | Fractured flow |
| SH9321 | 12 | Cinder Mountain | Dyke | 400120, 6269370 | Cuts hyaloclastite |
| SH9322 | 13 | Cone Glacier | Lava flow | 398580, 6269810 | |
| SH9324 | 14 | King Creek | Pillow lava | 397700, 6261150 | |
| SH9326 | 13 | Cone Glacier | Lava flow | 398580, 6269810 | |
| SH9328 | 13 | Cinder Mountain | Hyaloclastite | 398580, 6269810 | Above station 13 |
| SH9331 | 16 | Snippaker Creek | Lava flow | 386670, 6272820 | |
| SH9332 | 16 | Snippaker Creek | Lava flow | 386670, 6272820 | |
| SH9334 | 17 | Snippaker Creek | Lava flow | 390820, 6272970 | |
| SH9335 | 18 | Cinder Mountain | Lava flow | 403140, 6274330 | |
| SH9336 | 12 | Cinder Mountain | Dyke | 400120, 6269370 | Cuts hyaloclastite |
| SH9337 | 20 | Iskut River | Lava flow | 400220, 6287170 | |
| SH9338 | 21 | Iskut River | Lava flow | 398970, 6287480 | |
| SH9339 | 22 | Tom MacKay Creek | Pillow lava | 404130, 6285420 | |
| SH9344 | 24 | Lava Fork | Lava flow | 384600, 6255500 | Early channel |
| SH9345 | 25 | Lava Fork | Lava flow | 385180, 6254380 | Thin flow near vent |
| SH9346 | 25 | Lava Fork | Lava flow | 385180, 6254380 | Thin flow near vent |
| SH9347 | 25 | Lava Fork | Lava flow | 385180, 6254380 | Thin flow near vent |
| SH9353 | 26 | Lava Fork | Lava flow | 384790, 6255100 | Lava channel |
| SH9354 | 27 | Lava Fork | Lava flow | 384480, 6254030 | Thin flows in cliff |
| SH9355 | 28 | Lava Fork | Lava flow | 384450, 6254380 | Levee in Southern Fork |
| SH9358 | 30 | Lava Fork | Lava flow | 384000, 6255250 | Older channel levee |
| SH9359 | 30 | Lava Fork | Lava flow | 384000, 6255250 | Younger channel levee |
| SH9360 | 30 | Lava Fork | Lava flow | 384000, 6255250 | Lava channel |

APPENDIX 2

Summary of bulk samples containing abundant or distinctive xenoliths and xenocrysts.

| Sample | Station | Centre | Type | UTM | Notes |
|--------|---------|-----------------|----------------------|-----------------|---------------------|
| SH9305 | 3 | Cone Glacier | Lava flow | 398370, 6270050 | Talus from flow |
| SH9306 | 4 | Cone Glacier | Lava flow | 398310, 6270050 | |
| SH9308 | 5 | Cone Glacier | Pyroclastic material | 398380, 6270160 | Green cinder |
| SH9311 | 7 | Cone Glacier | Lava flow | 397570, 6269980 | Scoriaceous cinder |
| SH9320 | 11 | Cinder Mountain | Hyaloclastite | 400040, 6269420 | Talus |
| SH9323 | 14 | King Creek | Pillow lava | 397700, 6261150 | |
| SH9325 | 15 | Cone Glacier | Lava flow | 398170, 6269920 | Block on top flow |
| SH9327 | 13 | Cone Glacier | Lava flow | 398580, 6269810 | |
| SH9329 | 13 | Cinder Mountain | Dyke | 398580, 6269810 | Cuts hyaloclastite |
| SH9330 | 13 | Cinder Mountain | Pillow lava | 398580, 6269810 | |
| SH9340 | 23 | Lava Fork | Lava ball | 384520, 6254700 | |
| SH9341 | - | Lava Fork | Bomb | 384520, 6254700 | Close to station 23 |
| SH9342 | - | Lava Fork | Bomb | 384520, 6254700 | Close to station 23 |
| SH9343 | var. | Lava Fork | Lava flow | - | North fork |
| SH9348 | var. | Lava Fork | Lava flow | - | North fork |
| SH9351 | - | Lava Fork | Granodiorite | - | Basement rock |
| SH9352 | - | Lava Fork | Bt-qtz-schist | - | Basement rock |
| SH9356 | 29 | Lava Fork | Lava ball | 384040, 6255190 | Cinder blocks |
| SH9357 | 29 | Lava Fork | Lava ball | 384040, 6255190 | Cinder blocks |
| SH9361 | 30 | Lava Fork | Lava flow | 384000, 6255250 | Same as SH9360 |

APPENDIX 3

Summary of unconsolidated basaltic ash samples.

| Sample | Description | UTM | Location Notes |
|--------|--|-----------------|--|
| SH9303 | Reworked by glacial outwash | 398090, 6269720 | Station 2 at front of Cone Glacier |
| SH9350 | In situ ash fall deposit | - | Northwest of Lava Fork vent |
| JKR1 | Loose reworked ash on surface of a Nickel Mountain glacier | 397325, 6271075 | Surface of a southeast facing glacier on Nickel Mountain |

Preliminary stratigraphy of Hoodoo Mountain volcanic centre, northwestern British Columbia

B.R. Edwards¹ and J.K. Russell¹

Cordilleran Division

Edwards, B.R. and Russell, J.K., 1994: Preliminary stratigraphy of Hoodoo Mountain volcanic centre, northwestern British Columbia; in Current Research 1994-A; Geological Survey of Canada, p. 69-76.

Abstract: Hoodoo Mountain volcanic centre is a complex edifice consisting of multiple trachyte lava flows and domes interlayered with pyroclastic rocks and deposits. Aphanitic trachyte flows and hyaloclastite are the oldest volcanic units; they underlie sequences of welded and unwelded pyroclastic flows, and aphanitic domes and lavas. Porphyritic trachyte lavas with up to 20% anorthoclase phenocrysts cap the entire volcanic sequence. Little Bear mountain volcanic centre lies immediately north of Hoodoo Mountain and consists of basalt, basaltic breccia, hyaloclastite, and crystal lithic tuff. Stratigraphy and radiometric dates (Souther and Yorath, 1991) suggest volcanic activity was interspersed with glacial activity over at least the past 110 000 years. The youngest lava flows erupted after the last major glaciation in this region. Hyaloclastite deposits at Hoodoo Mountain and at Little Bear mountain are interpreted as products of subglacial eruptions.

Résumé : Le centre volcanique de Hoodoo Mountain est un édifice complexe composé de multiples dômes et coulées de trachyte interstratifiés avec des roches et des sédiments pyroclastiques. Les coulées de trachyte aphanitique et les hyaloclastites sont les unités volcaniques les plus anciennes; elles sont sous-jacentes à des séquences de coulées pyroclastiques soudées et non soudées, et à des dômes et laves aphanitiques. Des trachytes porphyriques contenant jusqu'à 20 % de phénocristaux d'anorthose constituent l'unité sommitale de la séquence volcanique. Le centre volcanique de Little Bear Mountain se situe immédiatement au nord du mont Hoodoo et se compose de basalte, de brèche basaltique, d'hyaloclastite et de tuf lithique à cristaux. La stratigraphie et les datations radiométriques (Souther et Yorath, 1991) suggèrent que l'activité volcanique alterne avec l'activité glaciaire depuis 110 000 années au moins. Les plus récentes coulées ont été mises en place après la dernière grande glaciation de cette région. On considère les dépôts d'hyaloclastites des centres de Hoodoo Mountain et de Little Bear Mountain comme le produit d'éruptions sous-glaciaires.

¹ Department of Geological Sciences, University of British Columbia, 6339 Stores Road, Vancouver, British Columbia V6T 2B4

INTRODUCTION

Hoodoo Mountain and Little Bear mountain are situated 120 km northwest of Stewart, British Columbia, near the Alaskan border. Hoodoo Mountain (UTM centre 360000E/6295000N) is a symmetrical volcanic dome rising 1800 m above the north bank of the Iskut River, 30 km east of its junction with the Stikine River, in northwestern British Columbia (Fig. 1). It is 6 km in diameter and has an ice cap 4 km in diameter. Valley glaciers bound Hoodoo Mountain on both sides: Hoodoo Glacier on the west and Twin Glacier on the east (Fig. 2). The edifice is forested on its lower slopes except on the northeastern corner. Because of its relatively flat summit, Hoodoo Mountain has been described as a tuya, or subglacial volcano (Souther, 1990).

Little Bear mountain (UTM centre 359500E/6297500N) lies immediately north of Hoodoo Mountain and forms the southeastern end of a ridge separating the northwestern portions of Twin and Hoodoo glaciers. It is an asymmetric volcanic edifice trending 20 degrees west of north, is 2 km along its axis, and rises 120 m above the surface of Twin Glacier to an elevation of 1220 m. It has a narrow summit on the northern end which broadens to a flat saddle in the middle and slopes gradually down to the south fork of the upper Hoodoo River. It is forested on its lower western flank, but has only minor vegetative cover above 900 m.

Little previous geological mapping has been done on these volcanic features, although Kerr (1948) described Hoodoo Mountain as "...one of the most magnificent and interesting mountains in northern B.C." in his memoir on the Lower Stikine and Iskut rivers. He recognized an older series of aphyric lavas, voluminous sanidine-porphyrific lavas, and younger aa flows. He also described pyroclastic rocks, glacial till, and fluvial/lacustrine deposits interlayered with some of the lava flows, although none of these units were distinguished on his map of the Iskut area. Hoodoo Mountain lavas were also studied by Souther (1990), who recognized pantellerite and comenditic trachyte as important rock types. Two samples analyzed for major and trace element geochemistry by M.L. Bevier and B. Cousens (unpub. data, 1992) are peralkaline (normative acmite), undersaturated (normative nepheline) trachytes. No work has been done on the basaltic units at Little Bear mountain.

REGIONAL SETTING

Both the Hoodoo Mountain and Little Bear mountain volcanic centres are built upon a basement of Jurassic metamorphic rocks. The older country rocks are dominantly intermediate to mafic metavolcanic rocks with minor meta-sedimentary rocks and small intrusions (Kerr, 1948; Phillipone and Ross, 1989; Anderson, 1993). They are representative of the Stuhini arc assemblage, part of Stikinia (Phillipone and Ross, 1989; Anderson, 1993). The basement rocks form a ridge to the north of both mountains, separating the northwestern ends of Twin and Hoodoo glaciers (Fig. 2). Phillipone and Ross (1989) mapped the basement rocks on the ridge as

mainly mafic to intermediate volcanic rocks and recognized basalt, trachyte, and agglomerate as part of the Hoodoo volcanic rocks. Fragments of these rocks rarely occur as xenoliths in volcanic rocks from both centres.

The Hoodoo Mountain and Little Bear mountain volcanic centres define the southwestern edge of the Stikine Volcanic Belt (Fig. 1). The Stikine Belt extends north from the Iskut River area up to Level Mountain and includes Mount Edziza and the Spectrum Range volcanic rocks (Souther and Yorath, 1991). The largest volcanoes of the belt, Level Mountain and Mount Edziza, comprise volcanic plateaus of valley-filling basalt lava flows capped by smaller silicic volcanoes (Hamilton, 1981; Souther, 1992).

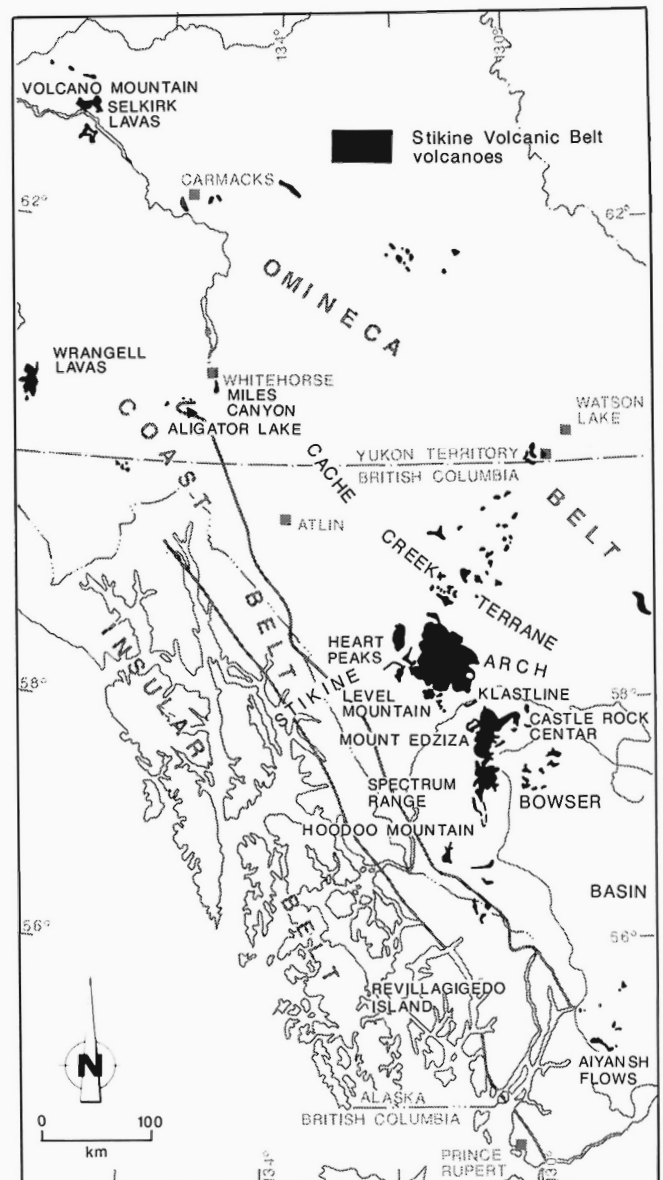


Figure 1. Location of Hoodoo Mountain in the southern Stikine Volcanic Belt (after Fig. 10.14, Souther and Yorath, 1991).

GEOLOGICAL MAPPING

The geology of Hoodoo and Little Bear mountains (Fig. 2) was mapped, compiled and produced at 1:25 000 scale. Several geographic localities were given informal names (Fig. 2 inset). These include: NW flow, SW flow, Slide canyon, the bowl, the hook, valley of the hook, Pointer ridge, Ship rock, Long valley, lake Hoodoo, south fork of upper Hoodoo River, and Little Bear mountain.

The results reported here are based on field work completed between July and August of 1993 as part of the Iskut map area regional mapping project. The geological map and stratigraphic relationships between volcanic units form the basis for future petrogenetic-oriented studies of the Hoodoo Mountain volcanic centre. One-hundred and eighty samples were collected for petrographic and geochemical analysis.

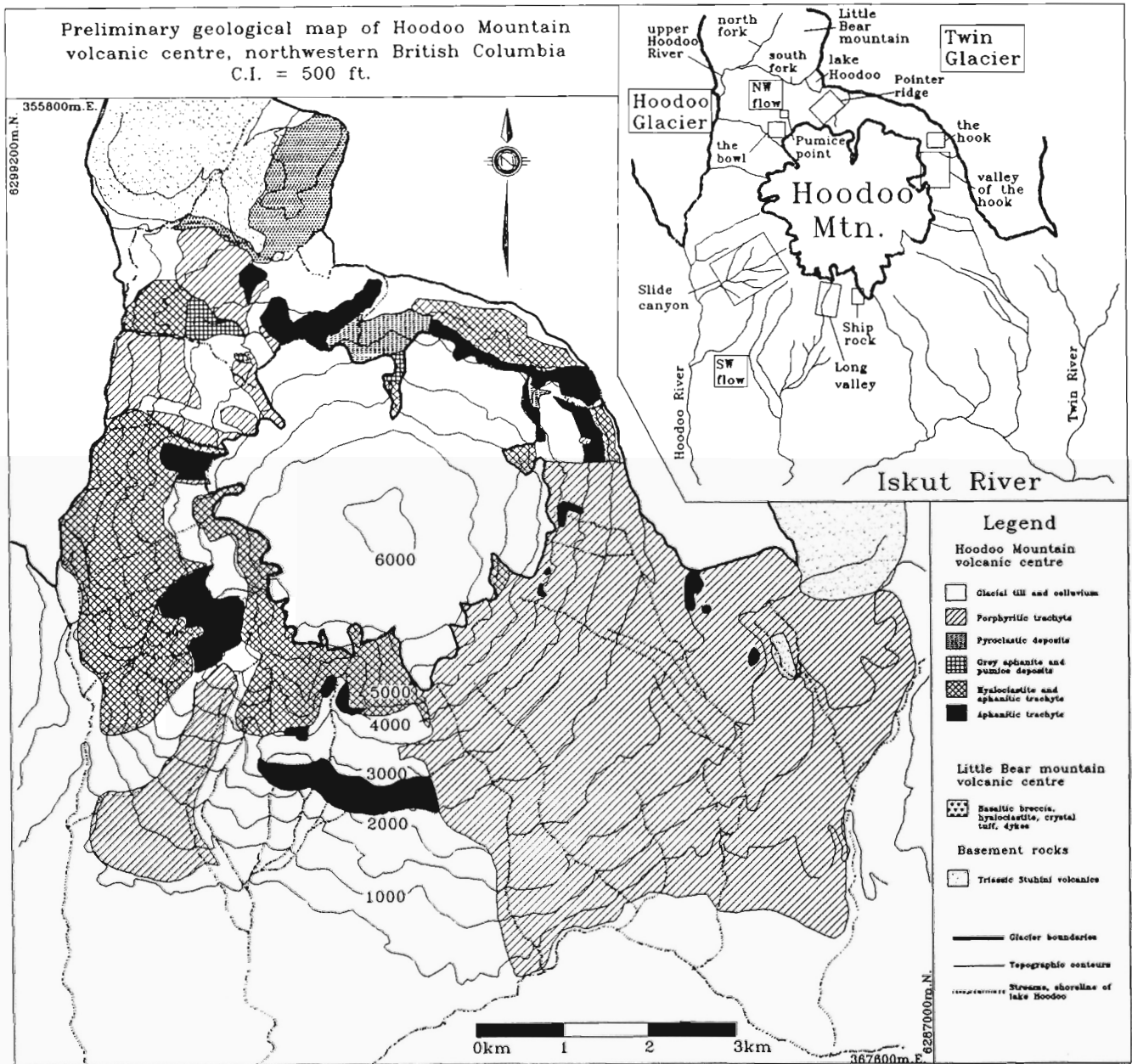


Figure 2. Geological map of Hoodoo Mountain volcanic centre. Inset map gives location names referred to in the text.

STRATIGRAPHY OF HOODOO MOUNTAIN VOLCANIC CENTRE

Hoodoo Mountain volcanic centre contains a variety of volcanic material including: 1) lava domes and flows, 2) hyaloclastite, and 3) thick sequences of pyroclastic flows. The oldest units deduced from field relationships are the lower aphanitic trachyte lava flows and hyaloclastite which are overlain in turn by: welded and nonwelded pyroclastic flows, grey aphanite domes, pumice deposits, aphanitic trachyte lava flows, and porphyritic trachyte lava flows.

Aphanitic trachyte

This unit occurs as domes, spires, and flows. It is black on fresh surfaces and rusty brown to yellow on weathered surfaces. It is commonly aphyric, with minor isolated feldspar phenocrysts (<5%), always less than 1 cm in length. It is

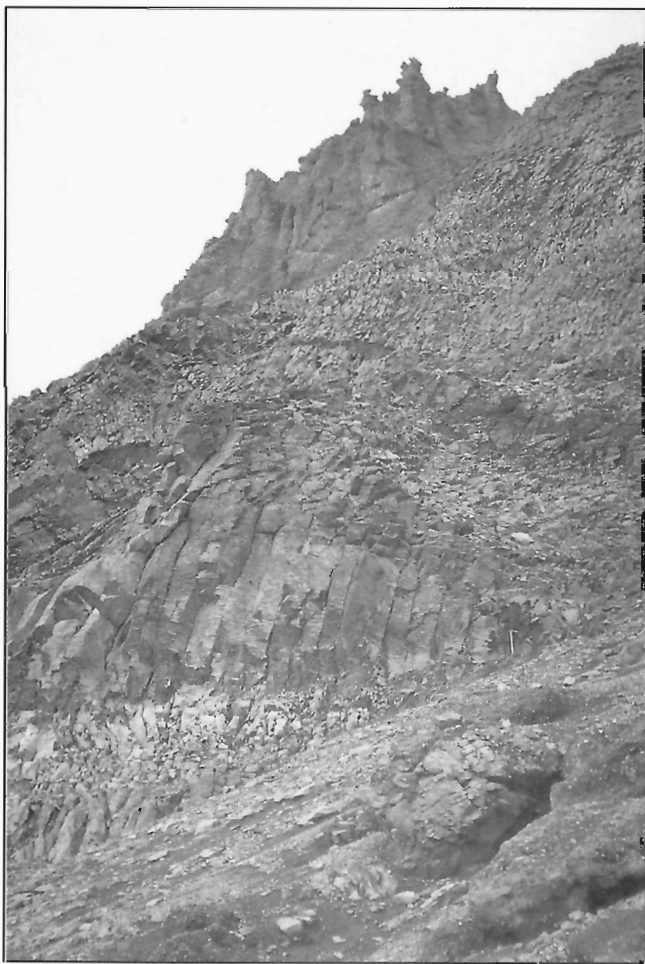


Figure 3. Columnar jointing in aphanitic trachyte on the south side of Hoodoo Mountain. Jointing is vertical near person but is horizontal in upper right of photograph. Hoodoo-forming hyaloclastite makes up the ridge in the background.

moderately magnetic. At least 50% of the exposures show some evidence of columnar jointing (Fig. 3) which is commonly curved and even radial in some cliff exposures.

The aphanitic trachyte forms cliffs up to 200 m high which discontinuously circumscribe Hoodoo Mountain (Fig. 2). Aphanitic trachyte is also found at higher elevations above the cliff-like exposures. Here, aphanitic trachyte is part of a thick package of hyaloclastite which forms the highest exposures occurring on Hoodoo Mountain. Small, highly jointed domes of the aphanite protrude through younger flows of porphyritic trachyte at several locations including: along the northeastern side of NW flow (Fig. 4), immediately south of valley of the hook, and at the southern edge of Twin Glacier.

Five samples collected and radiometrically dated by J.G. Souther and R.L. Armstrong (Canadian Cordillera Geochron File, Armstrong, 1988) ranging from 0.11 ± 0.03 Ma to 0.02 ± 0.01 Ma appear to be aphanitic trachyte based on petrography and the sample locations. The range of ages agrees with field observations which show aphanitic trachytes in several different stratigraphic positions. Relative timing constraints are as follows: 1) the aphanitic trachyte is coeval with some of the hyaloclastite, 2) it underlies and overlies the pyroclastic flows, 3) it is commonly glacially striated, and 4) it is overlain by porphyritic trachyte (Fig. 5).

Hyaloclastite

Monolithologic breccia consisting of greater than 90% fragments of aphanitic trachyte is widespread on Hoodoo Mountain and is tentatively interpreted as hyaloclastite. The hyaloclastite is generally orange-tan to red-orange. It is a clast-supported breccia containing varying proportions of angular to subangular clasts of aphanitic trachyte (Fig. 6). The clasts range in size from less than 0.5 cm to greater than 20 cm and are black on freshly broken surfaces. They are cemented by both silica and iron-rich cements, and some clast

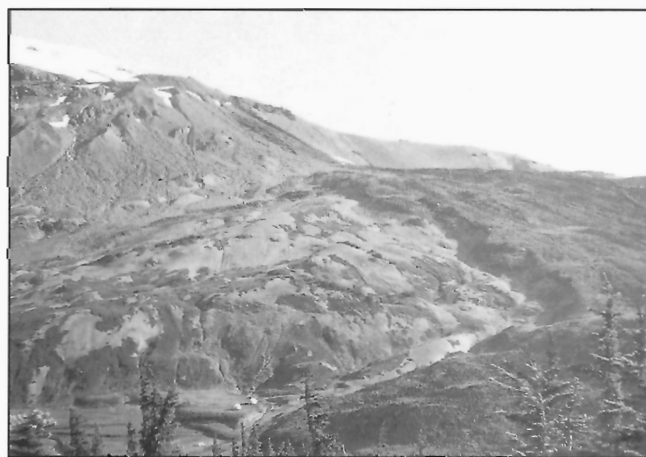


Figure 4. Dome of aphanitic trachyte (light coloured, in centre of photograph) on northwest flank of Hoodoo Mountain overlain by aa lava flow. Elevation difference from the foreground to the edge of the ice cap (upper left hand corner) is 300 m.

surfaces have hematite coatings. A crude layering is present in some areas, particularly at Ship rock. The layering may be the result of subsequent reworking. Outcrops weather to form irregular pillars which are characteristic of Hoodoo Mountain.

Complex, intermingled contact relationships between the breccia and the aphanitic trachyte are very similar to those described by Bergh and Sigvaldason (1991) between basaltic lavas and hyaloclastite in Iceland. Strongly columnar-jointed aphanitic trachyte rests on top of the hyaloclastite (Fig. 7) and occurs as isolated lobes within thick sections of hyaloclastite. The breccia clasts commonly have yellow rims several millimetres thick implying that the clasts have been pervasively altered. The hyaloclastite may have formed during subglacial eruptions of aphanitic trachyte.



Figure 5. Aphanitic trachyte (light coloured) overlain by thin flow of porphyritic trachyte (dark coloured), southeast side of Hoodoo Mountain. Locally, multiple porphyritic trachyte lavas using the same channel form stacks of sheet lava flows (upper left background).

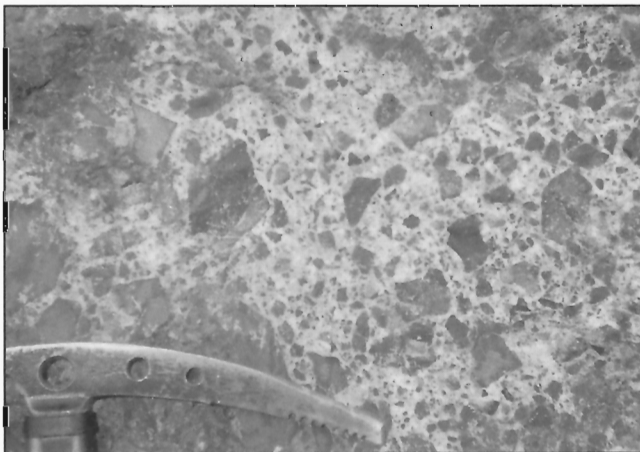


Figure 6. Detail of hyaloclastite showing abundant angular lapilli of aphanitic trachyte in altered matrix. Ice axe head is 35 cm.

Like the aphanitic trachyte, the hyaloclastite occupies more than one stratigraphic position. It occurs both at the base of Hoodoo Mountain and at the top. It overlies and underlies a lithic-rich vitrophyre in the valley of the hook. It is overlain by grey aphanite, pumice deposits, lithic tuff, and porphyritic trachyte lava.

Grey aphanite

The grey aphanite is grey to greenish-grey and is commonly aphyric. It is vesicular and at Pumice point black, glassy flow surfaces are preserved. On the west bank of the upper Hoodoo River, it intrudes the country rock and contains a variety of locally derived xenoliths.

The unit is commonly associated with pumice deposits. The pumice deposits overlie and appear to form a carapace around domes of the grey aphanite. In one locality on the western side of Hoodoo Mountain, the aphanite grades downward into underlying aphanitic trachyte. In the bowl, a dome of the grey aphanite is partially covered by flows of porphyritic trachyte. The aphanite has horizontal glacial striae.

Pumice deposits

The pumice deposits are yellow and are well indurated. They contain angular blocks (fragments of volcanic material greater than 64 mm; Fisher and Schminke, 1984) and lapilli (fragments 2-64 mm in size; Fisher and Schminke, 1984) of partially vesiculated volcanic glass, clasts of grey aphanite, and pumice in a matrix of altered pumice. Pumice fragments are angular to subrounded. Spatter bombs with glassy rinds are rare. The deposit in the upper valley of the hook has vertical slickensides. Fragments of glass and pumice are commonly randomly distributed except along the basal contacts with other units, where lag breccias and crude sorting of volcanic glass lapilli occurs. The lack of good sorting is consistent with the pumice deposits being parts of pyroclastic flows.



Figure 7. Columnar jointed aphanitic trachyte overlying hyaloclastite, south side of Hoodoo Mountain. Aphanitic trachyte overlies and underlies hyaloclastite. Contact (above person) is sharp and irregular.

In the valley of the hook, one of the pumice deposits rests on top of a layer of aphanitic trachyte and a pinched out lens of cobbles derived from a lithic-rich vitrophyre exposed a few hundred metres to the north. Above Pointer ridge, the pumice rests on top of the thick stack of welded ash flows. At Pumice point, the pumice deposit rests on top of grey aphanite with a sharp, irregular contact and is overlain by porphyritic trachyte. The pumice deposits locally have glacial striae.

Pyroclastic flows

The pyroclastic flows vary from grey to yellow to green to red, with black volcanic glass and multicoloured, subrounded accidental and cognate lithic clasts. Welding varies from nonexistent in some units to strongly welded sections that contain fiamme (strongly flattened pumice fragments; Ross and Smith, 1961) and local vitrophyres. The unit includes lithic tuff, welded ignimbrite, and lithic-rich vitrophyre.

Lithic tuff, which is yellow and moderately lithified, underlies several porphyritic trachyte and aphanitic trachyte flows on the northern and western sides of Hoodoo Mountain. It occurs as lenses varying from 1 to 10 m thick within the flows. The lithic tuff contains a diverse population of rounded lithic fragments of various colours and yellow pumice lapilli. A sequence of lithic tuff over 300 m thick occurs at Pointer ridge. Three dark, strongly welded resistant units mid-way up the face of the south valley wall stand in stark contrast to yellow, less-resistant, unwelded layers (Fig. 8). The ice cap above the pyroclastic material is supported by a resistant ledge of dark vitrophyre. Small outcrops of lithic tuff also occur on the western end of the hook.

The ignimbrite is red to green and varies from moderately to strongly welded (Fig. 9). It contains fiamme as well as up to 10% lithic clasts. Crystal fragments are rare. A 70 m thick welded ignimbrite in the valley of the hook contains abundant (30%) round, yellow, red, and green lithic fragments. A vitrophyre forms the central part of the welded ignimbrite and



Figure 8. Pyroclastic flow on north side of Hoodoo Mountain, above Pointer ridge. Lighter coloured sections are non-welded, but the three dark, resistant layers (centre) are strongly welded. The upper part of the flow is capped by a vitrophyre, visible just under the ice (at upper left). Vertical distance from base of lowest unit to ice cap is 275 m.



Figure 9. Welded ignimbrite from the Pointer ridge deposit. Lighter coloured accidental lithic clasts contrast with strongly welded dark pumice fragments (fiamme). Hammer is 37 cm in length.

is overlain by aphanitic trachyte and hyaloclastite. The sharp contact with overlying aphanitic trachyte dips to the west into Hoodoo Mountain. At the Pointer ridge deposit, three strongly welded units of ignimbrite, each approximately 3 m thick, are part of a thicker sequence of unwelded lithic tuff.

Porphyritic trachyte

The golden to grey weathering porphyritic trachyte is distinguished by its large feldspar phenocrysts, commonly greater than 2.5 cm long. The feldspars are strongly aligned with flow directions down the sides of the volcano. Mafic phenocrysts make up less than 10% of the porphyritic trachyte. It is not magnetic. The feldspar in the trachyte is anorthoclase. The porphyritic trachytes commonly have autoliths and locally contain xenoliths, one of which contained olivine(?).

The porphyritic trachyte forms 1-5 m thick lava flows, originating from unexposed subglacial vents. The flows are thinner on slopes up to 30°. Some of the flows appear to be sheet flows (i.e. flows not contained within identifiable channels); others were channelized for part of their descent down the slopes of Hoodoo Mountain. Up to eleven separate lava pulses used the same channel. Flow morphology features found include: 1) basal flow breccia, 2) flow margin breccia, 3) flow levees, 4) sidewall and lava channel tension gashes called riedel shears (Naranjo et al., 1992), 5) autoliths with distinctly different flow alignment of phenocrysts indicating incorporation of blocks from the previous flows or earlier solidified portions of the host flow, and 6) central channel domes also referred to as Armadillo structures (Naranjo et al., 1992). Lava channels are visible from aerial photographs on the south side of Hoodoo Mountain. The lava channel at NW flow is shown in Figure 10. The upper portions of the flows are commonly vesicular and all flows are aa lavas. The flows locally show jointing surfaces perpendicular and parallel to flow.

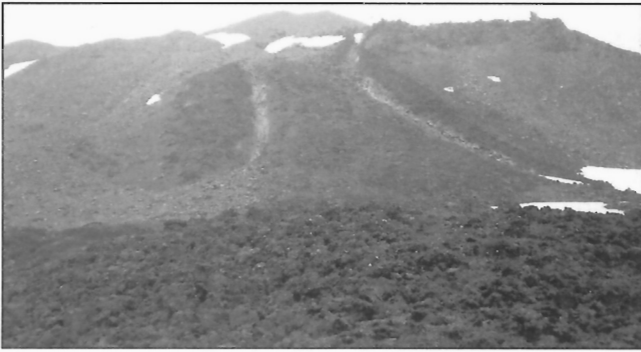


Figure 10. Detail of the lava channel at NW flow, on the northwest corner of Hoodoo Mountain. This channel is approximately 40 m wide, has prominent levees on both sides, and a slightly domed centre (cf. Recent basaltic lava channel, Hauksdóttir et al., 1994).

The porphyritic trachyte is the youngest unit at Hoodoo Mountain volcanic centre. It overlies aphanitic trachyte, hyaloclastite, the pumice deposit at Pumice point, grey aphanite, and one unit of the Little Bear mountain volcanic centre. The eruption age of some of these flows can be qualitatively constrained by the glacial activity associated with Twin and Hoodoo glaciers and the Hoodoo Mountain ice cap. The upper 200 m of most of the trachyte flows have been scoured clean of their rubbly surfaces in contrast to the unglaciated middle and lower parts of the flows. Porphyritic trachyte flows extend beneath the current ice cap along the southeastern flank and extend under the present surface of Twin and Hoodoo glaciers on the eastern and western sides of Hoodoo Mountain. These field relationships suggest that the lavas were erupted in the interglacial period immediately prior to the current interglacial episode. Tree ring ages from the oldest trees on the SW flow set a minimum age for the flow of 180 years (B.C. Hydro, 1985).

STRATIGRAPHY OF LITTLE BEAR MOUNTAIN VOLCANIC CENTRE

Little Bear mountain consists mainly of basaltic breccia containing large clasts and boulders of vesicular olivine basalt. Minor basaltic dykes intrude the summit, and the southeastern edge consists of basaltic hyaloclastite and crystal lithic tuff. The tuff is also exposed along the banks of the south fork of upper Hoodoo River near the confluence with the north fork of upper Hoodoo River.

Basaltic breccia

The breccia is orange-grey and vitrophyric basalt clasts range from 1–20 cm in size. It is volumetrically the most abundant unit at Little Bear mountain. On the southeastern edge of the mountain and the southern lip of the central plateau, cobbles in the basalt breccia define a crude, southward plunging layering. Exposed contacts with the country rock to the west and south are sharp and subvertical.

Basalt dykes

Grey to black olivine basalt occurs as dykes on Little Bear mountain. The basalt contains large plagioclase phenocrysts (greater than 2 cm), olivine, pyroxene, and xenoliths of granite with rims and inclusions of glass. On the northeast flank of the mountain, the dykes are nearly conformable to the layering in the breccia; however, the dykes crosscut the breccia on top of the summit.

Hyaloclastite

Minor orange-tan hyaloclastite occurs on the southeastern side of Little Bear mountain. It contains crystals of plagioclase, olivine, and pyroxene, all generally less than 0.5 cm long. Angular, equant fragments of basaltic glass with a continuous size range from 0.5 cm to less than 0.1 cm form the matrix. The fragmental nature of the glass is interpreted as an ice contact feature.

Crystal lithic tuff

Tan to yellow crystal lithic tuff contains plagioclase, pyroxene, olivine, basalt fragments, and other minor lithic fragments. The tuff exhibits metre-scale laminations and grain size sorting in exposures east of the confluence between the north fork and south fork of the upper Hoodoo River.

SUMMARY OF TIMING CONSTRAINTS

Stratigraphy and geochronology provide evidence for continued volcanic activity at Hoodoo Mountain volcanic centre over the last 110 000 years. Analyses by J.G. Souther and R.L. Armstrong (Canadian Cordilleran Geochron File, Armstrong, 1988) set a minimum age for the oldest aphanitic trachyte flows at 0.11 ± 0.03 Ma. Younger ages of 0.09 ± 0.01 Ma, 0.051 ± 0.015 Ma, and 0.02 ± 0.01 Ma for aphanitic trachyte from other localities around Hoodoo Mountain are corroborated by the stratigraphy defined in this study, which also recognizes several different eruptions of aphanitic trachyte lavas. The SW flow of porphyritic trachyte has a minimum age of 180 years (B.C. Hydro, 1985) based on dating of the oldest trees growing on the lava flow. It rests upon glacial till in the Iskut River valley and must postdate the last main glacial advance down this valley, probably sometime since the end of the last major glaciation in the Canadian Cordillera 10 000 years ago (Clague, 1991). Several other porphyritic trachyte flows on the southern flank of Hoodoo Mountain are also unglaciated, but the oldest porphyritic trachyte flows underlie the ice of Hoodoo and Twin glaciers.

Timing constraints for the formation of the basaltic units of Little Bear mountain volcanic centre are based on field observations. The highest point of this mountain is glacially scoured and has rounded glacial erratics deposited on top of it. The southern flank is overlain by porphyritic trachyte lavas from Hoodoo Mountain volcanic centre. Thus this basaltic centre must be at least as old as the last major glaciation.

CONCLUSIONS

Hoodoo Mountain volcanic centre has a complex history marked by pyroclastic eruptions, lava flows, and subglacial eruptions of peralkaline magmas. The aphanitic trachyte lava flows are strongly jointed and intimately associated with hyaloclastite, which suggests the early history of the centre was dominated by subglacial volcanism. Welded and non-welded pyroclastic flows mark a period of explosive volcanism. The well preserved lava levees, flow breccia, and aa lava flows of porphyritic trachyte formed after the last major glaciation of the Iskut River valley. The adjacent basaltic Little Bear mountain volcanic centre also has ice contact features. The styles of volcanism at Hoodoo Mountain and Little Bear mountain are consistent with those observed at other volcanic centres in the Stikine Volcanic Belt, as is the basalt-trachyte alliance. The possible genetic ties between the basaltic centre of Little Bear mountain and the peralkaline edifice of Hoodoo Mountain, as well as the relationship between these volcanic centres and the other volcanoes in the Stikine Belt, are subjects of future investigations.

ACKNOWLEDGMENTS

We thank Bob Anderson and the GSC (Project 840046) for all technical field support, without which this project would not have been possible. Craig River (104B/11) and Hoodoo Mountain (104B/14) 1:50 000 topographic base maps and aerial photographs were provided by the GSC. Very capable field assistance from Julie Kadar, Darwin Green, Steina Hauksdóttir, Sean Galloway, and Lori Snyder helped tremendously. Mark Stasiuk provided knowledgeable guidance for recognizing lava channels features and describing pyroclastic units. We thank J.G. Souther and R.G. Anderson for thorough manuscript reviews and Bev Vanlier for help with manuscript preparation.

REFERENCES

Anderson, R.G.

- 1993: A Mesozoic stratigraphic and plutonic framework for northwestern Stikinia (Iskut River area), northwestern British Columbia, Canada; in *Mesozoic Paleogeography of the Western United States-II*, (ed.) G. Dunn and K. McDougall; Pacific Section SEPM, Book 71, p. 477-494.

Armstrong, R.L.

- 1988: Mesozoic and early Cenozoic magmatic evolution of the Canadian Cordillera; Geological Society of America, Special Paper 218, p. 55-91.

Bergh, S.G. and Sigvaldason, G.E.

- 1991: Pleistocene mass-flow deposits of basaltic hyaloclastite on a shallow submarine shelf, South Iceland; *Bulletin of Volcanology*, v. 53, p. 597-611.

B.C. Hydro

- 1985: Stikine-Iskut Development, Iskut Canyon and More Creek Projects, 1982-1984; Geotechnical Investigations, Main Report, Volume 1, Report No. H1614. B.C. Hydro Information Centre.

Clague, J.J.

- 1991: Quaternary glaciation and sedimentation, Chapter 12; in *Geology of the Cordilleran Orogen in Canada*, (ed.) H. Gabrielse and C.J. Yorath; Geological Survey of Canada, *Geology of Canada*, no. 4, p. 419-434 (also Geological Society of America, *The Geology of North America*, v. G-2).

Fillipone, J.A. and Ross, J.V.

- 1989: Stratigraphy and structure in the Twin Glacier-Hoodoo Mountain area, northwestern British Columbia (104B/14); in *Geological Fieldwork 1988*; British Columbia Ministry of Energy, Mines and Petroleum Resources, Paper 1989-1, p. 285-292.

Fisher, R.V. and Schminke, H.-U.

- 1984: *Pyroclastic Rocks*; Springer-Verlag, Heidelberg, Germany, 472 p.

Hamilton, T.S.

- 1981: Late Cenozoic alkaline volcanics of the Level Mountain Range, northwestern British Columbia: Geology, petrology and paleomagnetism; Ph.D thesis, University of Alberta, Edmonton, Alberta.

Hauksdóttir, S., Enegren, E.G., and Russell, J.K.

- 1994: Recent basaltic volcanism in the Iskut-Unuk rivers area, northwestern British Columbia; in *Current Research 1994-A*; Geological Survey of Canada.

Kerr, F.A.

- 1948: Lower Stikine and western Iskut river area, British Columbia; Geological Survey of Canada, Memoir 246, 94 p.

Naranjo, J.A., Sparks, R.S.J., Stasiuk, M.V., Moreno, I., and Ablay, G.J.

- 1992: Morphological, structural and textural variations in the 1988-1990 andesite lava of Lonquimay Volcano, Chile; *Geological Magazine*, v. 129, no. 6, p. 657-678.

Ross, C.S. and Smith, R.L.

- 1961: Ash-flow tuffs: Their origin, geologic relations and identification; United States Geological Survey, Professional Paper 366.

Souther, J.G.

- 1990: Hoodoo, Canada; in *Volcanoes of North America*, (ed.) C.A. Wood and J. Kienle; Cambridge University Press, New York, p. 127-128.
1992: The Late Cenozoic Mount Edziza Volcanic Complex, British Columbia; Geological Survey of Canada, Memoir 420, 320 p.

Souther, J.G. and Yorath, C.J.

- 1991: Neogene assemblages, Chapter 10; in *Geology of the Cordilleran Orogen in Canada*, (ed.) H. Gabrielse and C.J. Yorath; Geological Survey of Canada, *Geology of Canada*, no. 4, p. 373-401 (also Geological Society of America, *The Geology of North America*, v. G-2).

Geological Survey of Canada Project 840046

Geology and origins of the Zippa Mountain igneous complex with emphasis on the Zippa Mountain pluton, northern British Columbia

Brian A. Lueck¹ and James K. Russell²

Cordilleran Division

Lueck, B.A. and Russell, J.K., 1994: Geology and origins of the Zippa Mountain igneous complex with emphasis on the Zippa Mountain pluton, northern British Columbia; in Current Research 1994-A; Geological Survey of Canada, p. 77-85.

Abstract: The Zippa Mountain igneous complex comprises three petrologically distinct latest Triassic intrusions: the Zippa Mountain syenite-pyroxenite, Mount Raven diorite, and Seraphim Mountain granite plutons.

Zippa Mountain pluton, a concentrically-zoned, silica undersaturated, bimodal mafic and felsic intrusion intrudes Paleozoic and Triassic rocks of Stikinia and is dominated by syenite, melasyenite, and pyroxenite. Pyroxenite occurs at the pluton margins and grades from mafic syenite to a core of K-feldspar syenite. Aegirine-augite, zoned K-feldspar, biotite, vishnevite-cancrinite, and melanite (Ti-bearing andradite) are major igneous phases accompanied by accessory titanite and apatite. Vishnevite-cancrinite, a complex sulphate- and carbonate-bearing aluminosilicate solid-solution phase, commonly replaced nepheline or leucite.

Trachytic K-feldspar and aligned aegirine-augite crystals and vishnevite-cancrinite-, melanite-, and pyroxene-rich layers in the syenite and pyroxenite define a widespread fabric which, with associated petrographic textures, are interpreted to be cumulate features.

Résumé : Le complexe igné de Zippa Mountain englobe trois intrusions pétrologiquement distinctes, datées du Trias terminal: la syénite-pyroxénite de Zippa Mountain, la diorite de Mount Raven et les plutons granitiques de Seraphim Mountain.

Le pluton de Zippa Mountain, qui est une intrusion sous-saturée en silice, bimodale (mafique et felsique), à zonation concentrique, traverse les roches paléozoïques et triasiques de la Stikinie; il contient principalement de la syénite, de la mélasyérite et de la pyroxénite. La pyroxénite se trouve sur les marges du pluton et passe vers l'intérieur à une syénite mafique et à un noyau de syénite à feldspath potassique. L'augite aegyrinique, le feldspath potassique zoné, la biotite, la cancrinite de variété vishnévite, et la mélanite (andradite titanifère) constituent les phases ignées principales et sont accompagnés de titanite et d'apatite en quantités accessoires. La cancrinite de variété vishnévite, phase complexe représentée par une solution solide alumino-silicatée contenant des sulfates et des carbonates, remplaçait souvent la néphéline ou la leucite.

Dans la syénite et la pyroxénite, la texture trachytique définit par les cristaux de feldspath potassique, les cristaux alignés d'augite aegyrinique, ainsi que les couches riches en cancrinite de variété vishnévite, en mélanite et en pyroxène, définissent une fabrique très répandue qui, de concert avec les textures pétrographiques associées, suggèrent une origine de cumulat.

¹ Mineral Deposit Research Unit, Department of Geological Sciences, University of British Columbia, 6339 Stores Road, Vancouver, British Columbia V6T 1Z4

² Department of Geological Sciences, University of British Columbia, 6339 Stores Road, Vancouver, British Columbia V6T 1Z4

INTRODUCTION

The Zippa Mountain pluton (Fig. 1) occurs in the Iskut River map area, in northern British Columbia (NTS 104B/11), about 10 km southwest of the confluence of the Iskut and Craig rivers. The Mount Raven and Seraphim Mountain plutons are younger, latest Triassic, spatially and temporally associated intrusions (Fig. 2). Together with the Zippa Mountain pluton, they encompass the Zippa Mountain igneous complex. These plutons intrude complexly deformed and metamorphosed Paleozoic limestone and calcareous siltstone of Stikinia.

The Zippa Mountain pluton is elliptical in shape and outcrops over a 3.5 by 5 km area. The intrusion is zoned, layered, characterized by well-developed planar mineral fabrics, and, based on modal mineralogy, is strongly silica undersaturated. These attributes are found in a significant number of other Cordilleran alkaline intrusions (cf. Woodsworth et al., 1991; Lueck et al., 1993). For example, Mesozoic alkaline plutons that are zoned from syenite to pyroxenite, trachytic, and strongly undersaturated occur in both Stikinia and Quesnellia (Lueck et al., 1993). Specific occurrences of this type of alkaline intrusion that are well documented are few but include the Averill (Keep and Russell, 1992) and Rugged Mountain plutons (Neil and Russell, 1993).

This paper presents field observations and a geological map for the Zippa Mountain igneous complex and examines the origins of the intrusive complex. Special emphasis is given to the Zippa Mountain pluton because of its unique mineralogy and structure, which link it to an important, recently recognized suite of zoned alkaline intrusions within the B.C. Cordillera (Neil and Russell, 1993; Lueck et al., 1993; Lueck and Russell, in press). In particular, we seek to elucidate the magmatic processes responsible for the mineralogy, zoning, modal-layering, and mineral fabric found within the Zippa Mountain pluton.

ZIPPA MOUNTAIN IGNEOUS COMPLEX

The Zippa Mountain igneous complex outcrops in a rugged mountainous region characterized by alpine glaciers and ice-fields and well-exposed steep rock faces. The intrusions comprising the igneous complex – Zippa Mountain, Mount Raven, and Seraphim Mountain plutons – were first mapped by Kerr (1948) and further described by Woodsworth et al. (1991) and Anderson (1993). The original descriptions for these sequentially emplaced plutons derive from Anderson (1993).

Zippa Mountain pluton has an age of ~210 Ma based on U-Pb dating of zircon (M.L. Bevier, unpub. data; Anderson et al., 1993). Mount Raven pluton is undated but older than the Seraphim Mountain intrusion which is dated at 213 ± 4 Ma by K-Ar on hornblende (analysis GSC 90-40; R.G. Anderson in Hunt and Roddick, 1991). The Seraphim Mountain pluton

intrudes Triassic Stuhini Group volcanic rocks and also cross-cuts and brecciates rocks of the Mount Raven pluton. Furthermore, field relationships (see below) indicate that the Zippa Mountain pluton is older than the Mount Raven pluton, making it the oldest intrusion recognized in the igneous complex.

Zippa Mountain pluton

The Zippa Mountain pluton is an elliptical laccolith about 14 km² in area comprising three main rock types: pyroxenite, syenite, and mela-syenite (Fig. 2). The pluton is zoned from a pyroxenite border phase, to melasyenite, to trachytic K-feldspar syenite in the core. The silica undersaturated nature of the pluton is manifested in abundant and widespread vishnevite-cancrinite (identified by X-ray diffraction) and melanite garnet showing strong oscillatory zoning (identified optically).

Pyroxenite forms an inwardly-dipping marginal phase which grades through melasyenite to the core syenite (Fig. 2B and 2C). The most extensive rock type is syenite which commonly shows a strong planar alignment of platy K-feldspar. Planar alignments of K-feldspar and acicular pyroxene define a concentric, inward-dipping foliation that shallows

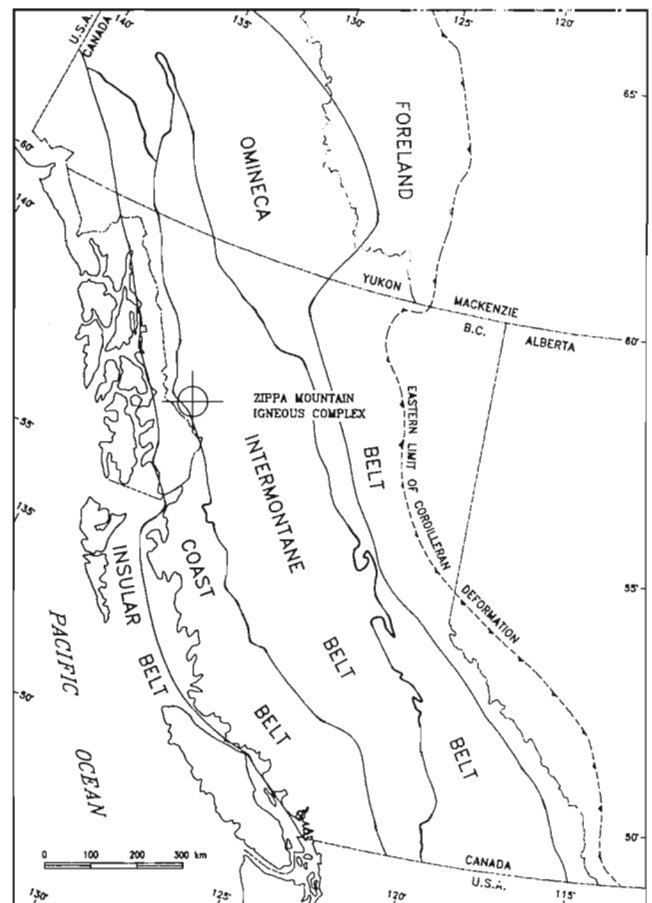
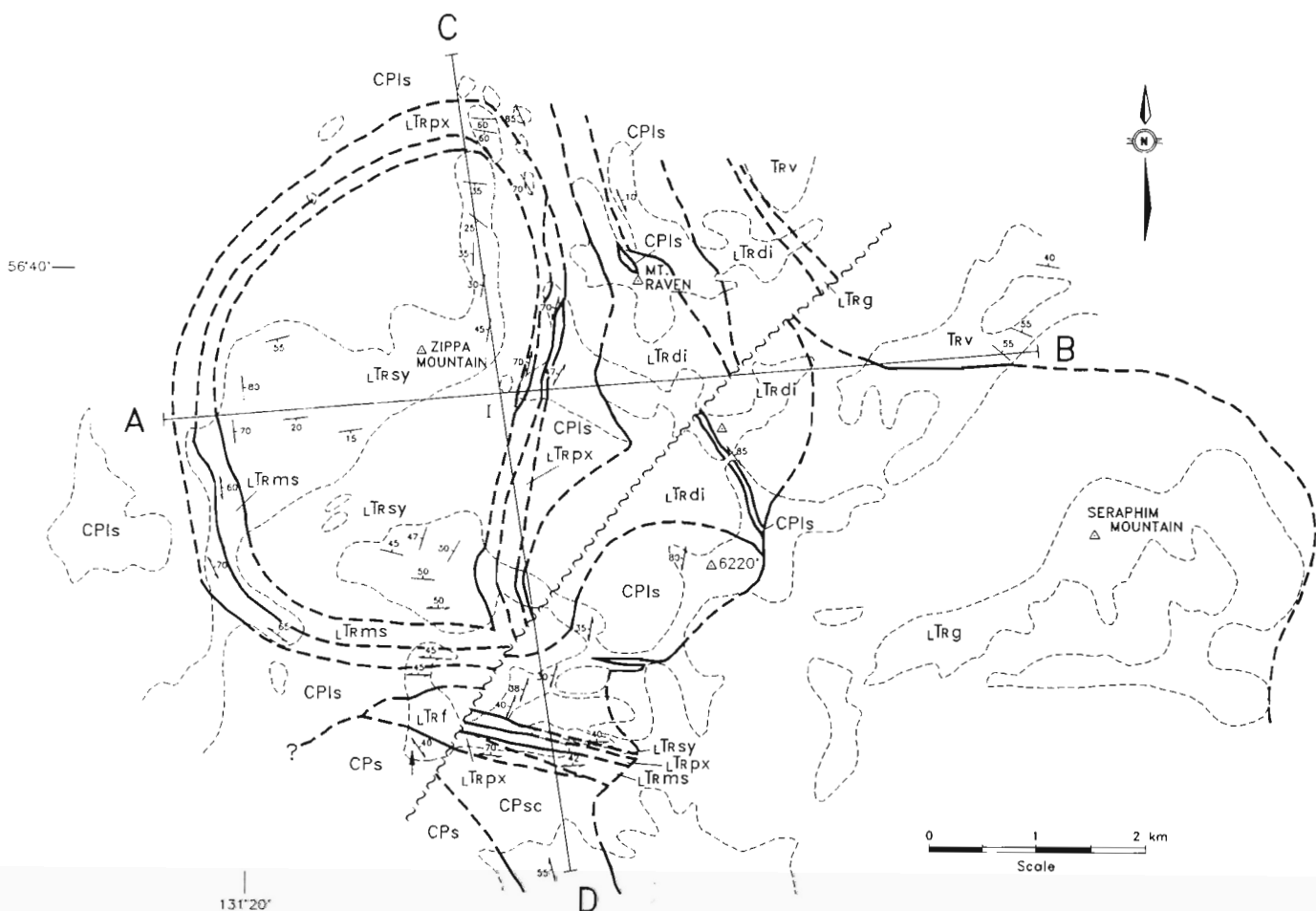


Figure 1. Location map of the Zippa Mountain pluton.



LEGEND

- LTrg Seraphim pluton: equigranular biotite-hornblende granite
- LTrdi Mt. Raven pluton: equigranular or hornblende feldspar porphyritic diorite; local gabbro
- LTrf felsic syenite: equigranular syenite with little or no mafic minerals
- LTrsy Zippa Mtn. K-feldspar syenite: layered and trachytic syenite and vishnevitcancrinite pegmatite
- LTrms Zippa Mtn. mela-syenite: syenite with >40% mafic minerals: pyroxene, melanite and biotite
- LTrpx Zippa Mtn. pyroxenite: equigranular to pegmatitic aegirine-augite pyroxenite
- Trv Stuhini Group: layered tuffaceous volcanic rocks and pyroxene porphyritic flows
- CPIs limestone, calc-silicate rocks, shale, thinly laminated calc-silicate and recrystallized limestone with interbedded calcareous shale
- CPs chert, shale, graphitic shale with interbedded, massive chert
- CPsc schist, phyllite derived from CPs; mica schist at margin of Seraphim pluton

SYMBOLS

- cumulate layering
- transposed layering, schistosity
- mineral lineation
- fault
- geological contact: defined, approximate
- limit of outcrop

Figure 2A. Geology of the Zippa Mountain igneous complex and country rocks.

towards the interior of the intrusion (Fig. 2B and 2C). Large-scale petrological zoning, small-scale mineral layering, and a mappable igneous foliation suggest that these rocks dominantly formed by gravitational settling of minerals crystallizing from a strongly undersaturated alkaline magma.

Pyroxenite

Pyroxenite occurs as a border phase to the pluton and as discrete isolated lenses up to 100 m long within the syenite core. The border phase comprises pale-green to black massive

layers concentrated along the outer pluton margins (Fig. 3). Locally, the pyroxenite border phase is found as lenses <10 m thick interleaved with calc-silicate rock comprising garnet, diopside, wollastonite, and calcite.

Mineralogically, pyroxenite comprises fine grained, acicular, pale green, aegirine-augite (90%) and apatite (10%), subordinate biotite and trace titanite and melanite. Long axes of pyroxene and apatite are co-planar, and produce a strong foliation; within the plane of foliation there is no pronounced lamination (Fig. 4). Biotite, where present, occurs as distinct well-formed euhedral to subhedral crystals set in an

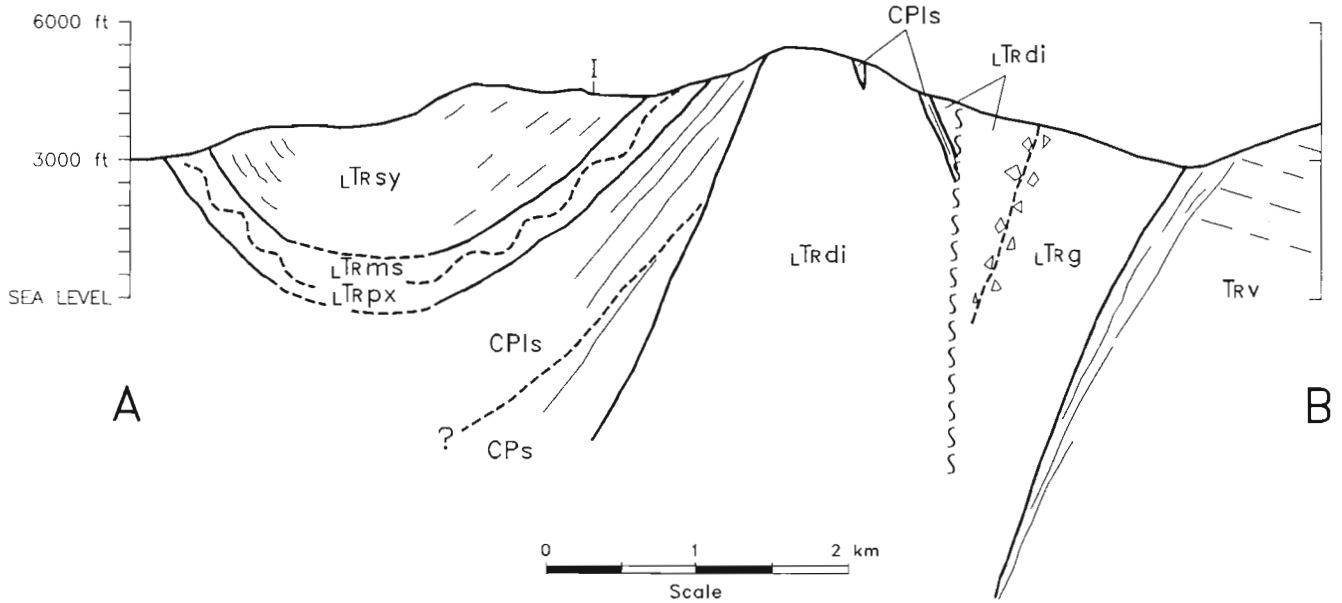


Figure 2B. West to east cross-section (AB). No vertical exaggeration in cross-sections.

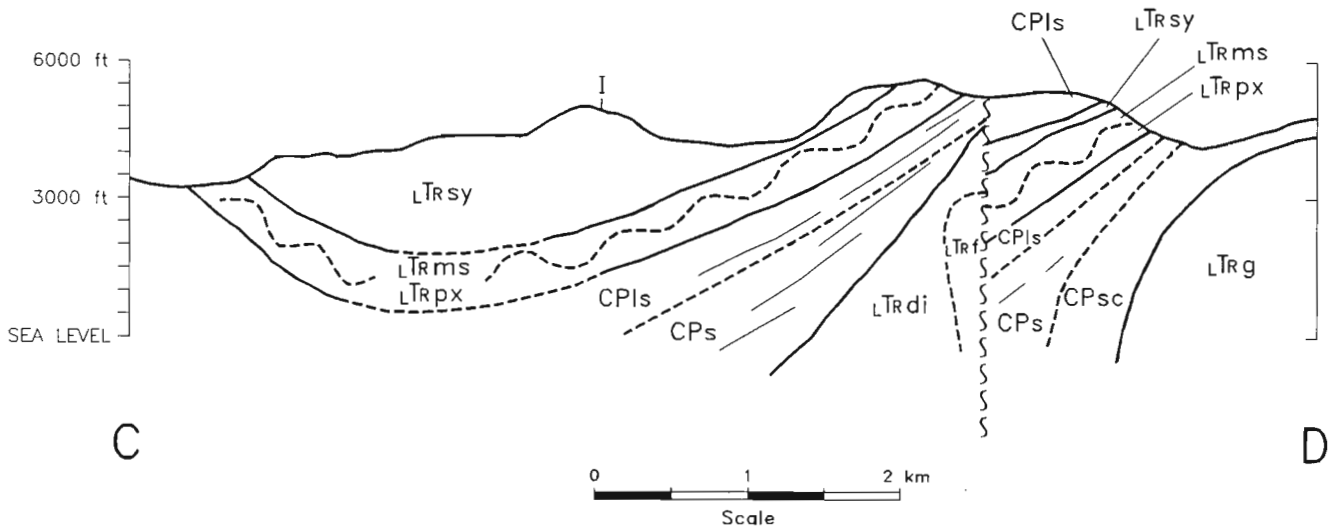


Figure 2C. North to south cross-section (CD). No vertical exaggeration in cross-sections.



Figure 3. Outcrop-scale layering in pyroxenite. Layering results from rhythmic changes in grain size and biotite content.

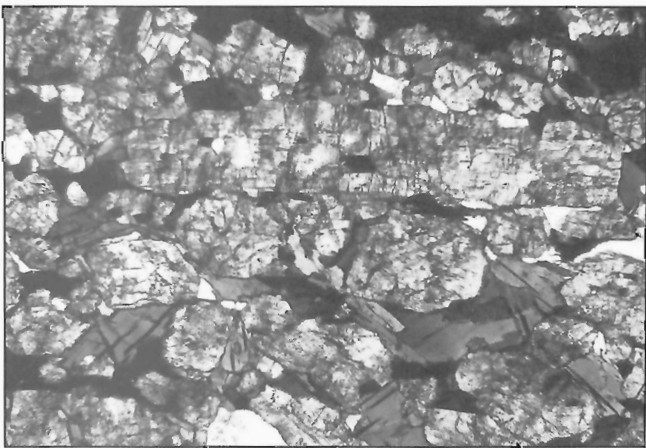


Figure 4. Photomicrograph showing alignment of pyroxene and biotite in pyroxenite cumulate. Clear areas are apatite crystals. Field of view is 5 mm.

interlocking matrix of aegirine-augite crystals. Less commonly, biotite occurs as inclusions within poikilitic pyroxene and melanite.

A pegmatitic phase of pyroxenite is distinguished by megacrysts of aegirine-augite, titanite, and melanite garnet. This pegmatite is only found within the fine grained pyroxenite and melasyenite, where it is abundant and occurs as irregular pockets and stringers. Abundant and large melanite garnet crystals are found within the fine grained pyroxenite where it is in contact with the pegmatite.

Locally, intense, shear-induced deformation has resulted in the development of a strongly foliated biotite schist within the pyroxenite. These schists are distributed near the pluton margins and dip inwards. This tectonic schistose fabric is defined by curvilinear layers of biotite, and thus, is easily distinguished from the pervasive igneous fabrics.

Melasyenite

Melasyenite is an intermediate syenite containing more than 40% mafic minerals. It commonly is found between pyroxenite and syenite and is always found in association with pyroxenite (Fig. 2A-C). Melasyenite ranges in texture from equigranular to pegmatitic and contains aegirine-augite, biotite, melanite (Fig. 5), K-feldspar, and minor titanite and apatite. Equigranular melasyenite approximately comprises 50% K-feldspar, 30% aegirine-augite, 10% biotite, 10% melanite, and trace apatite and titanite. Pegmatitic portions of melasyenite, found along the western margin of the pluton and immediately adjacent to pyroxenite, consist of large (up to 10 cm) K-feldspar megacrysts (55%) in a matrix of aegirine-augite (45%). Poikilitic K-feldspar commonly includes biotite, pyroxene, and melanite.

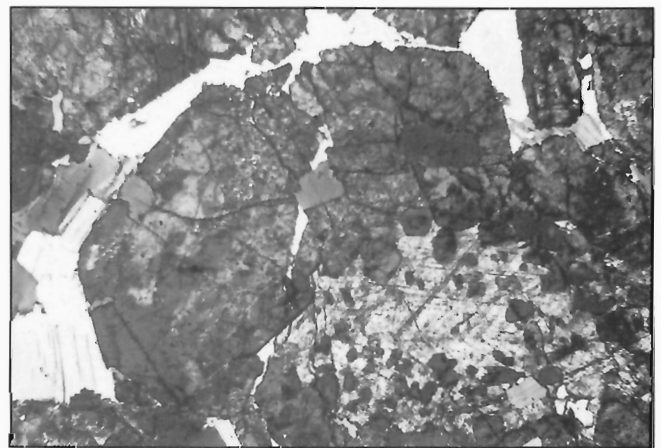


Figure 5. Photomicrograph showing euhedral melanite garnet surrounding a core of titanite; from the melasyenite unit. Field of view is 5 mm.

Syenite

Syenite is the most abundant rock type in the Zippa Mountain pluton. It varies in grain size and texture and is distinguished by abundant grey, strongly zoned, prismatic K-feldspar crystals (Fig. 6). K-feldspar makes up as much as 75% of the rock and subordinate pyroxene, melanite, and biotite make up the remainder. Accessory phases include apatite and titanite. Vishnevite-cancrinite is also an important phase within the pluton. Pegmatitic phases of the syenite dominantly consist of large euhedral books of K-feldspar and significant amounts of vishnevite-cancrinite.

Within the syenite, trachytic K-feldspar defines a mappable fabric which is concentric and conformable with the pluton margins. The fabric dips inward and appears to shallow towards the interior of the intrusion (Fig. 2B-C). The K-feldspar crystals defining the trachytic fabric show no visible strain in thin section, indicating that the fabric is not tectonic. We interpret the fabric as a planar alignment resulting from gravitational settling and compaction on the floor of the magma chamber. The trachytic texture is not always constant in orientation and chaotic patterns of alignment are scattered within the core of the syenite. These areas of chaotic alignment may represent postdepositional disturbances of the cumulates (e.g., slumping events or changes in convection patterns).



Figure 6. Megacrystic K-feldspar syenite.

Vishnevite-cancrinite is a common and abundant constituent of pegmatitic syenite (Fig. 7). It occurs preferentially in layers that vary from a few centimetres to tens of metres in thickness that are unevenly distributed within the pluton; they are significantly more abundant near the melasyenites. Layering generally parallels the trachytic alignment of K-feldspar. The vishnevite-cancrinite occurs as white-weathering, equant, 1-2 cm round aggregates and as finer grained interstitial material (Fig. 7). The larger crystals commonly show hexagonal cross-sectional outlines (Fig. 7) which suggests that vishnevite-cancrinite is pseudomorphic after leucite.

Dykes

All phases of the Zippa Mountain pluton are cut by several compositionally different dykes. Some dykes display well-developed selvages and undoubtedly intruded solidified Zippa Mountain rocks. Other dykes have more ambiguous contact relationships. For example, a group of pegmatitic syenite dykes crosscut pyroxenite, melasyenite, syenite, and the Mount Raven pluton. They lack selvages and are mineralogically similar to the host Zippa Mountain syenite. These

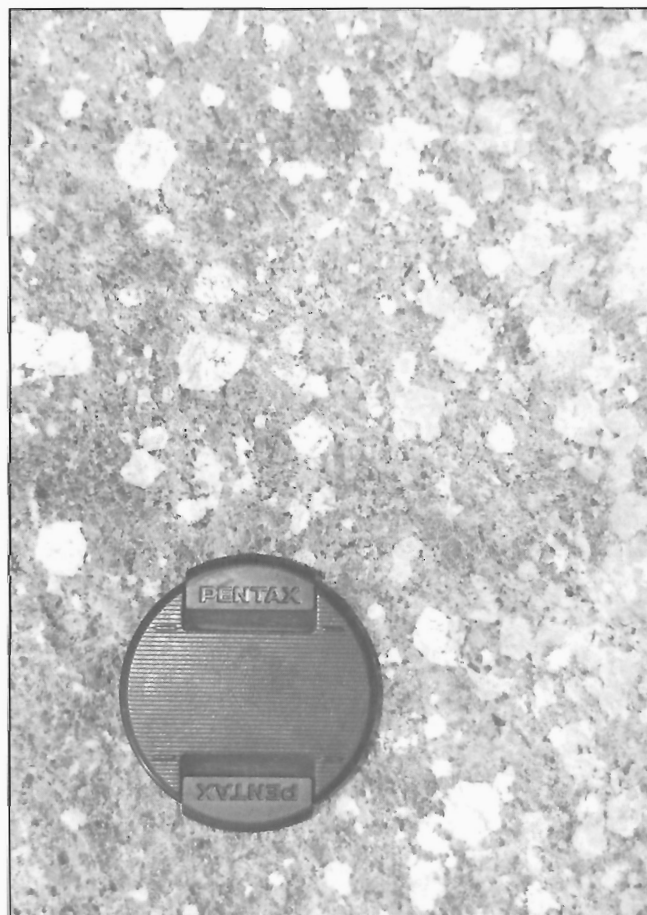


Figure 7. White vishnevite-cancrinite megacrysts in pegmatitic K-feldspar syenite.

pegmatites are inferred to represent late stage dykes derived from the Zippa Mountain magmatic system and emplaced while the cumulate rocks were still hot.

Diorite dykes, mineralogically and texturally similar to Mount Raven intrusive rocks (see below), crosscut cumulate layering. The apparent lack of chilled margins suggests that these dykes also intruded the Zippa Mountain cumulate rocks when the latter were still hot. Altered pyroxene and garnet porphyritic dykes are intermediate in composition and have well-developed chilled margins. These dykes are notable in that they crosscut country rocks and all other members of the Zippa Mountain igneous complex. In contrast, the syenite and diorite dykes, which are probably related to the Zippa Mountain and Mount Raven plutons, respectively, are not observed within the Seraphim Mountain pluton. Lastly, quartz porphyritic dykes crosscut all igneous phases of the Zippa Mountain pluton. These dykes and rocks of the Seraphim Mountain pluton are the only quartz-bearing intrusive rocks.

Mount Raven pluton

The Mount Raven pluton is a fine grained, equigranular diorite to gabbro. The diorite portions of the pluton are approximately 40% hornblende, 30% plagioclase, 10% K-feldspar, 10% relict pyroxene, and trace apatite. Secondary minerals include chlorite and epidote replacing biotite as well as pyrite, calcite, and quartz which occur as disseminations and fracture fillings. Indeed, one of the characteristic traits of the Mount Raven pluton is the presence of a pervasive gossan resulting from the weathering of abundant pyrite. Intensely fractured zones within the pluton contain up to 30% pyrite as disseminations and fracture fillings. Minor interstitial quartz in the rock may be secondary.

The Mount Raven pluton is hosted by the same limestone and calc-silicate country rocks which bound the Zippa Mountain pluton. Contacts between these two plutons do not occur or are not exposed. However, crosscutting relationships between compositionally distinct dykes and the plutons provide a means of establishing relative timings. The Mount Raven pluton is crosscut by pegmatitic dykes which are mineralogically similar to the late-stage dykes observed to crosscut the Zippa Mountain cumulates. Thus, it is older than the youngest portions of the Zippa Mountain pluton. Conversely, the main portion of the Zippa Mountain pluton is intruded by several large mafic dykes which appear mineralogically and texturally related to the Mount Raven pluton. If this is true, the Mount Raven pluton must postdate the early formed Zippa Mountain intrusive rocks.

Seraphim Mountain pluton

The Seraphim Mountain pluton is homogeneous, equigranular granite composed of 30% quartz, 25% plagioclase, 20% alkali feldspar, 20% hornblende, and trace biotite, titanite, and apatite. Secondary phases include chlorite and epidote which replace biotite and hornblende.

At the western margin, the pluton intrudes schist, phyllite, and calc-silicate rocks. Along this margin, contacts between the Seraphim Mountain pluton and country rocks are steeply north- and east-dipping except where the pluton intrudes calc-silicate rocks and forms a sill (Fig. 1).

The Seraphim Mountain intrusion crosscuts and brecciates rocks of the Mount Raven pluton. Blocks of diorite from the Mount Raven pluton and fragments of folded and altered calc-silicate and pyroxene porphyry occur as xenoliths (Fig. 8). Along the eastern margin, the pluton intrudes interbedded pyroxene porphyritic pyroclastic rocks and lavas of the Stuhini Group. The volcanic rocks dip moderately eastward; the contact between the pluton and the volcanic rocks dips steeply westward. Minor granite dykes intrude the older volcanic rocks and parallel the contact.



Figure 8. Xenoliths of diorite, gabbro, pyroxenite, calc-silicate, and pyroxene porphyry in a matrix of Seraphim Mountain granitic rock.

Mineralization

Mineralization in the area occurs at the margins of the Zippa Mountain pluton, within the Mount Raven pluton, and in a northeast-striking vein-fault (Fig. 1). The margins of the Zippa Mountain pluton have varying amounts of pyrite mineralization and minor malachite and chalcopyrite. The Mount Raven pluton is pervasively pyritized and hosts at least one roof pendant containing copper mineralization. Pyritization is widespread and associated with calcite-quartz veinlets within highly fractured diorite.

The northeast striking vein-fault (Fig. 1) crosscuts all units; the southwestern extension is best exposed where it intersects and offsets Zippa Mountain pyroxenite. Here, the fault is manifest by an intense quartz-carbonate alteration zone a few tens of metres wide. To the northeast, the fault crosscuts the Mount Raven pluton in two places. Generally, the fault zone is gossanous due to the presence of pervasive fractures hosting abundant pyrite. In one locale, the fault truncates a limestone roof pendant within the Mount Raven pluton. Here, the fault is pyritized and contains a stockwork of quartz-veins, some of which have abundant chalcopyrite.

DISCUSSION

The Zippa Mountain pluton is one of a group of zoned, silica undersaturated, alkalic plutons which occur throughout the North American Cordillera. They dominantly comprise aegirine-augite pyroxenite and K-feldspar syenite. This pyroxenite-syenite association (Lueck et al., 1993), is petrologically, chemically, and mineralogically unique. The mineralogical characteristics include aegirine-augite, K-feldspar, biotite, melanite, titanite, and apatite as essential phases and hornblende, magnetite, and plagioclase as nonessential and subordinate phases. The presence of feldspathoids and other strongly undersaturated aluminosilicates is implied by the chemical compositions of these rocks; they are all strongly Ne and Lc normative. The fact that these diagnostic minerals have not been reported in many of these intrusions (cf. Neil and Russell, 1993) is probably due to their inherent magmatic instability or susceptibility to alteration.

The Zippa Mountain pluton is an example of this rock suite. It is unique in that it offers unparalleled horizontal and vertical exposure and shows important igneous structures and fabrics related to the origin of the suite. Many of these features are not well-preserved or exposed in other zoned alkaline intrusions (Lueck and Russell, in press) (e.g., Averill and Rugged Mountain intrusions).

The Zippa Mountain pluton is a concentric-zoned, cumulate pluton characterized by: large-scale zonation from pyroxenite margins to syenite interior; fine scale planar alignment of igneous minerals forming concentric inwardly dipping patterns; and mineralogical layering of aegirine-augite, melanite, or vishnevite-cancrinite within syenite and pyroxenite. Two aspects of this intrusion are unique in that they have not been recognized in other similar zoned alkaline intrusions. Firstly, the occurrence of vishnevite-cancrinite (probably after leucite) is important as an indication of the

degree of silica undersaturation. Secondly, the presence of melanite-rich layers within the trachytic syenite suggests that melanite, in addition to being an early crystallization product, was capable of forming cumulate layers. Melanite has previously been recognized as an early crystallization product in these zoned alkaline intrusions (cf. Neil and Russell, 1993). At Zippa Mountain, the presence of rare melanite-rich cumulate layers implies relatively unique magmatic conditions.

CONCLUSIONS

The Zippa Mountain igneous complex comprises three petrologically distinct latest Triassic plutons which intrude Paleozoic Stikinia. The zoned and silica undersaturated Zippa Mountain pluton is, based on field relationships, the oldest member of the complex. It contains aegirine-augite, zoned K-feldspar, biotite, vishnevite-cancrinite, and melanite as major igneous minerals accompanied by accessory titanite and apatite. Trachytic K-feldspar books and aligned aegirine-augite crystals, as well as vishnevite-cancrinite, melanite, and pyroxene-rich layers, define a widespread fabric within the syenite and pyroxenite. This fabric, and the associated petrographic textures, are interpreted to be cumulate in origin.

The Zippa Mountain igneous complex hosts sulphide mineralization in three distinct settings. Within the Zippa Mountain pluton, pyrite and sparse chalcopyrite occur within the mafic border phases and within the calc-silicate country rocks. The Mount Raven pluton has pervasive disseminations and fracture fillings of pyrite. A northeast-trending vein-fault crosscuts the southeast margin of the Zippa Mountain pluton. The vein-fault contains quartz-carbonate veining and some quartz veins contain abundant pyrite and/or chalcopyrite.

ACKNOWLEDGMENTS

Financial and logistical support for this project were provided by the Geological Survey of Canada (Project 840046) and the Mineral Deposit Research Unit (UBC). Special thanks goes to Bob Anderson for his initial encouragement and continuing support and interest in this project. We thank J.A. Roddick for his careful review and Bev Vanlier for her efforts in preparing the manuscript. This paper is Mineral Deposit Research Unit "Copper-Gold Porphyry Project" (MDRU) contribution #P-038.

REFERENCES

- Anderson, R.G.
1993: A Mesozoic stratigraphic and plutonic framework for northwestern Stikinia (Iskut River area), northwestern British Columbia, Canada; in *Mesozoic Paleogeography of the Western United States--II*, (ed.) G. Dunne and K. McDougall; Society of Economic Palaeontologists and Mineralogists, Pacific Section, v. 71, p. 477-494.
- Anderson, R.G., Bevier, M.L., Nadaraju, G., Lewis, P., and Macdonald, J.
1993: Jurassic arc setting for Stikinia's "Golden Triangle" (abstract); Geological Association of Canada-Mineralogical Association of Canada, Programs with Abstracts, v. 18, p. A3.

Hunt, P.A. and Roddick, J.C.

1991: A compilation of K-Ar ages: Report 20; in *Radiogenic Age and Isotope Studies: Report 4*; Geological Survey of Canada, Paper 90-2, p. 122.

Keep, M. and Russell, J.K.

1992: Mesozoic alkaline rock of the Averill plutonic complex; *Canadian Journal of Earth Sciences*, v. 29, p. 2508-2520.

Kerr, F.A.

1948: Lower Stikine and western Iskut River areas, B.C.; Geological Survey of Canada, Memoir 246, 94 p.

Lueck, B.A. and Russell, J.K.

in press: Zoned, silica undersaturated, alkalic plutons of the British Columbia Cordillera; in *Geological Fieldwork 1993*; British Columbia Ministry of Energy, Mines and Petroleum Resources, Paper 1994-1.

Lueck, B.A., Neil, I., and Russell, J.K.

1993: The Rugged Mountain pluton: an example of the melanite bearing pyroxenite-syenite association (abstract); Geological Association of Canada-Mineralogical Association of Canada, Programs with Abstracts, v. 18, p. A61.

Neil, I. and Russell, J.K.

1993: Mineralogy and chemistry of the Rugged Mountain pluton: a melanite-bearing alkaline intrusion; in *Geological Fieldwork 1992*; (ed.) B. Grant and J.M. Newell; British Columbia Ministry of Energy, Mines and Petroleum Resources, Paper 1993-1, p. 149-157.

Woodsworth, G.J., Anderson, R.G., and Armstrong, R.L.

1991: Plutonic Regimes, Chapter 15; in *Geology of the Cordilleran Orogen in Canada*; (ed.) H. Gabrielse and C.J. Yorath; Geological Survey of Canada, *Geology of Canada*, no. 4, p. 491-531 (also *Geological Society of America, The Geology of North America*, no. G-2).

Geological Survey of Canada Project 840046

Northern continuation of the Eastern Waddington Thrust Belt and Tyaughton Trough, Tatla Lake-Bussel Creek map areas, west-central British Columbia¹

P. van der Heyden, P.S. Mustard, and R. Friedman²
Cordilleran Division, Vancouver

van der Heyden, P., Mustard, P.S., and Friedman, R., 1994: Northern continuation of the Eastern Waddington Thrust Belt and Tyaughton Trough, Tatla Lake-Bussel Creek map areas, west-central British Columbia; in Current Research 1994-A; Geological Survey of Canada, p. 87-94.

Abstract: Tatla Lake-Bussel Creek map area may contain the northern terminations of East Waddington Thrust Belt (EWTB) and Tyaughton Trough. Foliated plutons and volcanics of the Jura-Cretaceous Coast belt arc are thrust to the northeast over an Upper Triassic arc succession correlated with Stikine terrane. The arc rocks, in turn, are thrust over marine and nonmarine strata of the Cretaceous Tyaughton Trough, in part derived from a westerly, mixed volcanic-plutonic source. At the northern limit of the thrust belt, the Coast belt is thrust directly on nonmarine Silverquick formation; marine strata of Tyaughton Trough are absent, and the thrust belt is intruded by the ca. 63-67 Ma Klinaklini and McClinchy plutons. Stikine terrane, including the newly dated ca. 220 Ma Sapeye Creek pluton, may underlie Tyaughton Trough between Yalakom and Tchaikazan faults. The area northeast of Yalakom fault is underlain by the Eocene Tatla Lake metamorphic core complex.

Résumé : Les régions cartographiques du lac Tatla et du ruisseau Bussel pourraient contenir les extrémités septentrionales de la zone de chevauchement d'East Waddington et de la cuvette de Tyaughton. Des plutons et des roches volcaniques foliés d'un arc magmatique, remontant au Jurassique-Crétacé et appartenant au Domaine côtier, ont été charriés vers le nord-est, au-dessus d'une succession d'arc située dans le Trias supérieur et corrélée avec le terrane de Stikine. À leur tour, les roches de la succession d'arc du Trias supérieur ont été charriées au-dessus de strates marines et continentales de la cuvette de Tyaughton du Crétacé, qui proviennent partiellement d'une source mixte volcanique-plutonique située à l'ouest. À la limite nord de la zone de plissement, le Domaine côtier a été directement charrié sur la formation continentale de Silverquick; les strates marines de la cuvette de Tyaughton sont inexistantes, et la zone de plissement est traversée par les plutons de Klinaklini et McClinchy, approximativement âgés de 63-67 Ma. Le terrane de Stikine, notamment le pluton de Sapeye Creek nouvellement daté à environ 220 Ma, pourrait être sous-jacent à la cuvette de Tyaughton entre les failles de Yalakom et de Tchaikazan. Le substratum du secteur situé au nord-est de la faille de Yalakom est constitué du complexe à noyau métamorphique de Tatla Lake, d'âge éocène.

¹ Contribution to Canada-British Columbia Agreement on Mineral Development (1991-1995), a subsidiary agreement under the Canada-British Columbia Economic and Regional Development Agreement.

² Department of Geological Sciences, University of British Columbia, 6339 Stores Road, Vancouver, British Columbia V6T 2B4

INTRODUCTION

This report outlines preliminary results of 1:50 000 scale mapping in the Tatla Lake (92N/15) and Bussel Creek (92N/14) map areas (Fig. 1), which straddle the boundary between the Coast and Intermontane belts. The study is a component of the Interior Plateau subprogram, Canada-British Columbia Agreement on Mineral Development 1991-1995, and includes 1:50 000 scale mapping in the Charlotte Lake (93C/3) and Junker Lake (93C/4) map areas (van der Heyden et al., 1993).

The present study area was previously covered as part of a regional study of the northeastern Mt. Waddington area (Tipper, 1969). This study outlined the main lithological subdivisions, focusing on strata deposited in and adjacent to the Jura-Cretaceous Tyaughton Trough, and documented their disruption by southwest-dipping thrust faults and northwest-trending transcurrent faults. More recent mapping south of the present study area (Rusmore and Woodsworth,

1988, 1989, 1991a, 1993) defined the Late Cretaceous (ca. 87-84 Ma) Eastern Waddington Thrust Belt (EWTB), along which the Jura-Cretaceous Coast belt magmatic arc was thrust northeastward over Mesozoic strata of the Tyaughton Trough. Both Tipper (1969) and Rusmore and Woodsworth (1993) showed the Eastern Waddington Thrust Belt projecting into the Tatla Lake-Bussel Creek map area, but its northerly continuation, as well as contact relations and ages of most rock units and structures in the present study area, remained enigmatic.

In Anahim Lake (93C) map area, northwest of the present study area, the eastern Coast belt consists dominantly of Jura-Cretaceous plutonic and metamorphic rocks (van der Heyden, 1990, 1991; van der Heyden et al., 1993); structures are dominated by steeply dipping, northeast-trending ductile fabrics, and the area is disrupted by steeply dipping brittle shear zones. Thrust faults that might correlate with the thrust belt, and rocks correlative with Tyaughton Trough strata, are not present in the Anahim Lake map area.

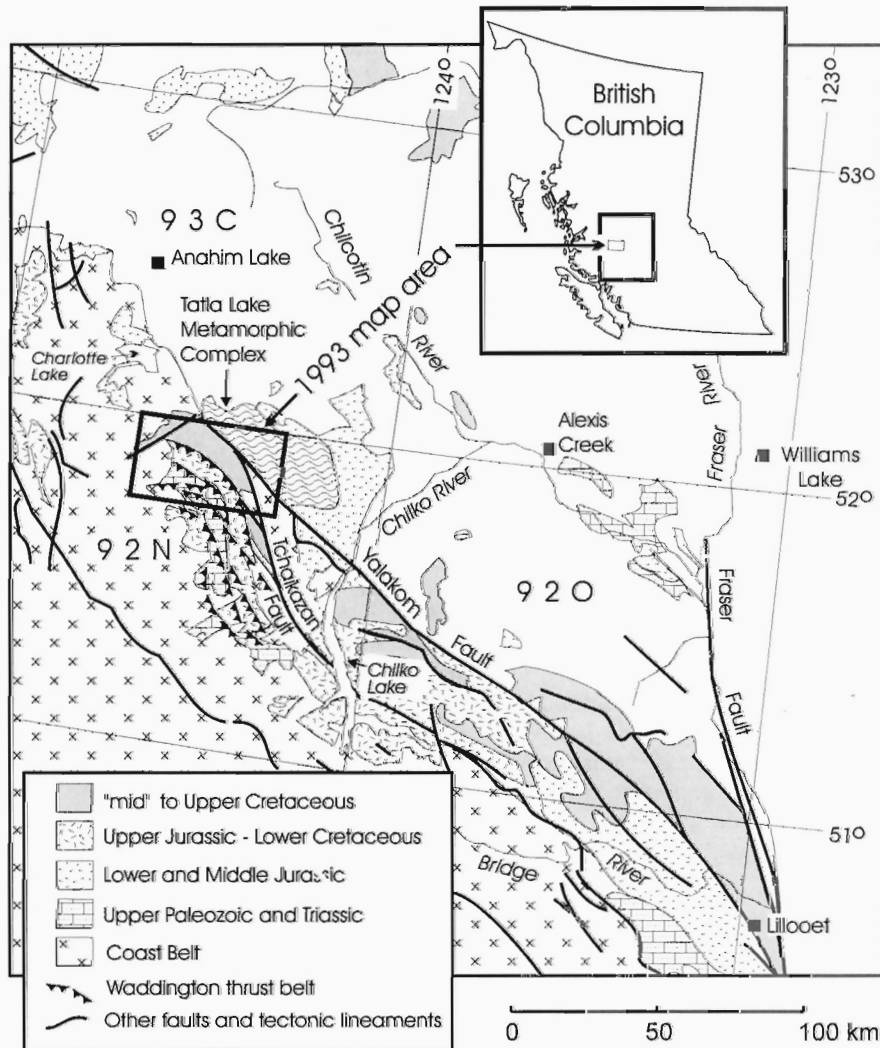


Figure 1. Location of the study area. Geology modified from Wheeler and McFeely (1991), Rusmore and Woodsworth (1993), and other sources.

Current mapping in the Tatla Lake-Bussel Creek area seeks to define the northern extent of the Eastern Waddington Thrust Belt and Tyaughton Trough, to document the stratigraphy and tectonic setting of Mesozoic supracrustal units, and to provide radiometric age constraints on the timing of magmatism and deformation along this segment of the eastern Coast belt. The northeastern part of the Tatla Lake map area was previously mapped in detail by Friedman (1988); Friedman's results are incorporated without revision into the present study. In this paper we briefly describe the major map units and structures of the study area, provide preliminary radiometric dates for several plutonic map units, and discuss the regional implications. The stratigraphy and sedimentology of the area are covered in more detail in a companion paper (Mustard and van der Heyden, 1994). Relationships between most rock units are obscured by thick Quaternary cover and dense vegetation, particularly in the central and eastern parts of the study area; the conclusions reported in this paper should therefore be considered tentative.

RESULTS OF PRESENT MAPPING

The study area can be subdivided into several fault-bounded, west- to northwest-trending domains (Fig. 2). Rocks of the Jura-Cretaceous Coast belt magmatic arc in the southwest are thrust over a strongly imbricated zone consisting of multiple thrust slices of Upper Triassic arc rocks. The arc rocks are thrust over Lower Cretaceous marine strata of Tyaughton Trough, which in turn are thrust over Upper Cretaceous nonmarine strata that record the final stages in the evolution of Tyaughton Trough. Farther northeast, between the trend of the Tchaikazan and Yalakom faults, Cretaceous strata are poorly exposed and relationships between map units are unclear. This area includes Upper Triassic strata intruded by a newly dated Late Triassic pluton. The Eocene Tatla Lake metamorphic core complex underlies the northeastern part of the study area; it is separated from the other domains by the transcurrent Yalakom Fault. All rocks east of and including the imbricate zone are here included in the Intermontane belt.

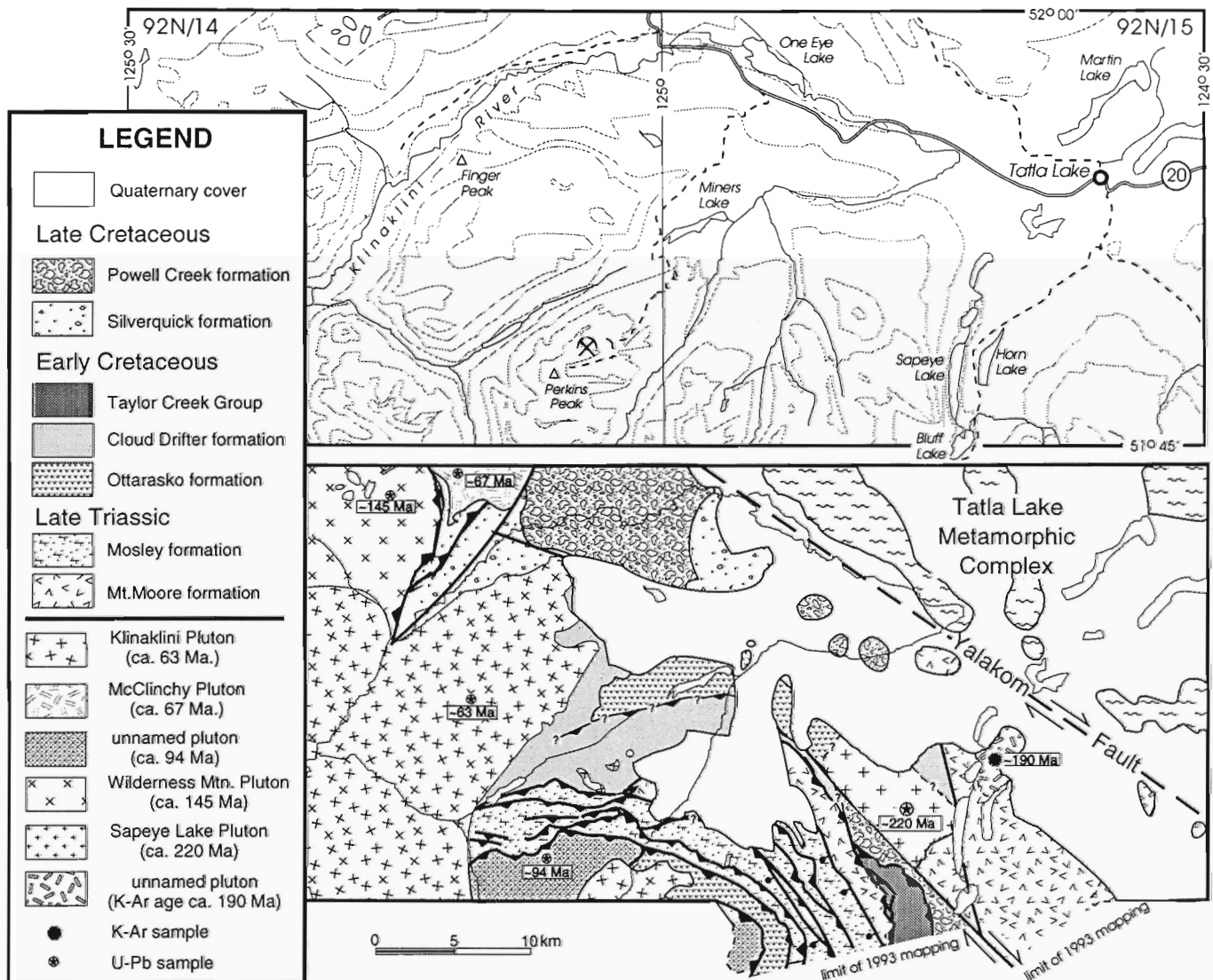


Figure 2. Simplified topography (top) and geology (bottom) of the study area.

Coast belt

The eastern boundary of the Coast belt in the study area is interpreted as a south-southwest-dipping thrust fault which marks the upper boundary of a major imbricate thrust zone (Fig. 2, 3). We correlate the imbricate zone with a similar zone at the base of the Coast belt in the Razorback (92N/10) and Mt. Queen Bess (92N/7) map areas (Rusmore and Woodsworth, 1988, 1989, 1993); as in those areas, the Coast belt rocks in the study area occupy the highest thrust sheet in the Eastern Waddington Thrust Belt. South of Perkins Peak this thrust sheet is dominated by biotite hornblende tonalite with a locally well developed, south-southwest-dipping mylonitic foliation. Zircons from an unfoliated part of the tonalite (Fig. 2) yielded preliminary 94 Ma concordant U-Pb dates, here interpreted as the emplacement age of the pluton. Mylonites are particularly well developed adjacent to the thrust contact with underlying metavolcanic schists and phyllites at the top of the imbricate zone. The thrust changes from a diffuse, south-southwest-dipping ductile shear zone with interdigitated greenschist facies metavolcanic rocks and mylonitic tonalite (Fig. 4) southwest of Perkins Peak, to a sharply defined, south-dipping brittle shear zone separating cataclastic tonalite from low-grade volcanic breccia southeast of Perkins Peak. Tonalite dykes in volcanic breccia near the shear zone are clearly derived from the adjacent pluton, and the shear zone is interpreted as a strongly disrupted intrusive contact. Rare southwest-dipping lineations and slickensides suggest top-to-the-northeast sense of shear.

In the range east of Perkins Peak, rocks closely resembling and here correlated with the 94 Ma tonalite are present only as small, locally sheared but demonstrably intrusive domains within poorly stratified, dominantly felsic volcanoclastic rocks. The southern extent of these plutonic domains is unknown, and their connection with the 94 Ma tonalite south of Perkins Peak is obscured by a younger granodiorite intrusion. The felsic volcanoclastic rocks form the hanging wall of a southwest-dipping brittle shear zone which connects with

the thrust at the base of the Coast belt south of Perkins Peak; volcanoclastic rocks in the footwall of both shear zones are lithologically identical. The 94 Ma tonalite and the felsic volcanic rocks which it is inferred to intrude apparently represent different parts of the same thrust sheet; they are here both included in the Coast belt. We tentatively correlate the felsic volcanoclastic unit with the Early Cretaceous(?) Otterasko formation of Rusmore and Woodsworth (1988, 1989); U-Pb and $^{40}\text{Ar}/^{39}\text{Ar}$ dating of samples from both units is currently in progress. The rocks are dominantly light green, grey, mauve, and lesser maroon-purple lapilli tuffs with angular to subrounded, grey to white rhyolite and dacite(?) clasts that commonly show flowbanding and welded textures. Andesitic(?) feldspar porphyry clasts are also common. Locally the rocks are very coarse grained volcanic breccias and conglomerates, containing clasts up to 40 cm in size. In numerous places the tuffs and breccias contain minor but distinctive rounded to subrounded granitoid cobbles and boulders. A few felsic volcanic flows appear to be interbedded with the volcanoclastic rocks, including light grey and mauve flowbanded rhyolite with local lithophysae. The unit is internally imbricated judging by the presence of several southwest dipping shear zones, and it is severely fractured above the basal thrust.

The northwest corner of the study area is underlain by tonalite of the Wilderness Mountain pluton, a large Middle to Late Jurassic pluton (van der Heyden, 1991; van der Heyden et al., 1993), which we include in the upper Coast belt thrust sheet. It is characterized by a strongly developed, northwest-dipping mylonitic fabric. A relatively undeformed tonalite sample from the northwestern limit of the present map area has yielded a preliminary, concordant 145 Ma zircon U-Pb age (Fig. 2); zircon U-Pb dating of a strongly mylonitic tonalite sample is currently in progress. The contact with adjacent supracrustal rocks is not exposed, but rocks on both sides of the contact are cut by well developed, west- to northwest-dipping brittle shear zones; we tentatively infer the contact to be a major thrust fault.



Figure 3. View southeast from Perkins Peak. Southwest-dipping imbricate zone structurally overlain by ca. 94 Ma mylonitic tonalite in centre, ca. 63 Ma Klinaklini pluton in background. Mountain face in centre is ca. 600 m high.



Figure 4. Upper Triassic(?) metavolcanic schist with stretched 94 Ma tonalite sill, from the imbricate zone south of Perkins Peak.

The upper thrust sheet, the adjacent imbricate zone, and the structurally underlying rocks of the Tyaughton Trough are intruded by the Klinaklini pluton west and north of Perkins Peak, and by the McClinchy pluton north of Klinaklini River. The Klinaklini pluton is dominated by coarse grained tonalite and lesser granodiorite with conspicuous accessory titanite. Zircons from a granodiorite sample (Fig. 2) yielded concordant 63 Ma U-Pb dates, interpreted as the emplacement age of the Klinaklini pluton. Granodiorite and quartz monzonite with local conspicuous K-feldspar megacrysts at the southwestern limit of the study area are probably compositionally distinct phases of the Klinaklini pluton. A satellite granodiorite stock southeast of Perkins Peak has a strongly silicified and pyritized contact aureole; pyrite-galena-quartz boulders found in float near the contact are probably derived from veins related to this intrusion. The McClinchy pluton is dominated by medium grained, locally porphyritic tonalite and granodiorite. Zircons from this pluton (Fig. 2) have yielded concordant U-Pb ages of 67 Ma (V. McNicoll, pers. comm., 1993), comparable to the age of the Klinaklini pluton.

Imbricate zone

The Coast belt is separated from Cretaceous strata of Tyaughton Trough by a major imbricate thrust zone, consisting of multiple thrust-bounded panels of Upper Triassic volcanic and sedimentary rocks. The imbricate zone is about 8 km wide in the Tatla Lake map area, narrows abruptly to about 3 km in the Bussel Creek area near Perkins Peak, and appears to be represented only by a single fault sliver of Upper Triassic(?) volcanic rocks north of Klinaklini River. Upper Triassic strata in the Razorback map area were assigned by Rusmore and Woodsworth (1989, 1991b, 1993) to the late Karnian to early Norian Mt. Moore formation and the late Norian Mosley formation, and correlated with Stikinia. These rocks connect northward with the imbricate zone of the present study; they are described in detail by Mustard and van der Heyden (1994).

We have extended the known outcrop area of the Mosley formation into the range east of Perkins Peak (Fig. 2), based on the presence of a diagnostic redbed unit containing limestone and volcanic cobble conglomerates, as well as a structurally lower single limestone bed with numerous specimens of *Monotis subcircularis* Gabb (E.T. Tozer, pers. comm., 1993), which is associated with volcanic breccias and tuffs that locally contain conspicuous limestone clasts. These rocks were originally mapped as Hauterivian volcanoclastic rocks (Tipper, 1969), but they are clearly continuous with Norian strata exposed in the range to the east. Limestone clasts from the volcanic breccias and conglomerates are being processed for conodonts in an effort to confirm an inferred Upper Triassic source.

The volcanoclastic rocks associated with the *Monotis*-bearing limestone continue into the western part of the range and farther west into the imbricate zone underlying Perkins Peak. Limestone cobbles and interbeds are absent from these rocks, but we believe that they belong to the same Upper Triassic succession. They are dominated by green and lesser maroon-purple volcanic breccia and crystal-lithic lapilli tuff,

with less abundant grey-green feldspar-hornblende porphyry flows. Clasts in the breccias reach 20 cm in diameter, and consist entirely of feldspar porphyry and second-cycle tuffaceous material derived from contemporaneous volcanic flows and tuffs. Rare pyroxenite dykes cut the volcanic rocks southeast of Perkins Peak. We infer that these volcanic rocks represent part of a Late Norian volcanic arc, with contemporaneous sediments of the Mosley formation representing a first-cycle, shallow marine to nonmarine fluvial clastic apron shed off the active arc, as previously suggested by Rusmore and Woodsworth (1991b). We do not rule out the possibility, however, that some of the thrust slices south and east of Perkins Peak belong to the Mt. Moore or Ottarasko formations; these units are all rather similar in appearance.

The entire Upper Triassic succession is stacked into a multitude of map-scale, discontinuous, thrust-bounded sheets or lenses (Fig. 5), some of which contain large folds and overturned sections. Thrust faults are marked by anastomosing phyllitic and sericitic schist and cataclasite zones up to tens of metres thick. Southwest-dipping slickensides and fault grooves, and local northeasterly fold vergence suggest a northeasterly sense of shear. South of Perkins Peak the imbricate zone is extremely gossanous and pyritic schist is common; much of the valley south of Perkins Peak is covered with strongly oxidized ferrocrete breccias. The iron alteration of this area is locally associated with stratiform hematite replacement and quartz-specularite veining in the volcanoclastic rocks (Briton prospect, Minfile # 092N-011). Sheared quartz-calcite-magnetite-malachite-azurite and chlorite-epidote-magnetite veins are locally present in the shear zones. The Pin copper showing (Minfile # 092N-053), southeast of Perkins Peak, characterized by bornite-chalcocopyrite-chalcocite-malachite mineralized float and disseminated chalcocopyrite and malachite in altered volcanic rocks, is also associated with shear zones of the imbricate zone. Several auriferous quartz veins in the study area (Orwill Au-Ag-Cu-Zn-Pb-Sb-Bi prospect, Minfile # 92N-053; Golden Rose Au-As showing, Minfile # 92N-046) also appear to be spatially associated with thrust faults of the imbricate zone.

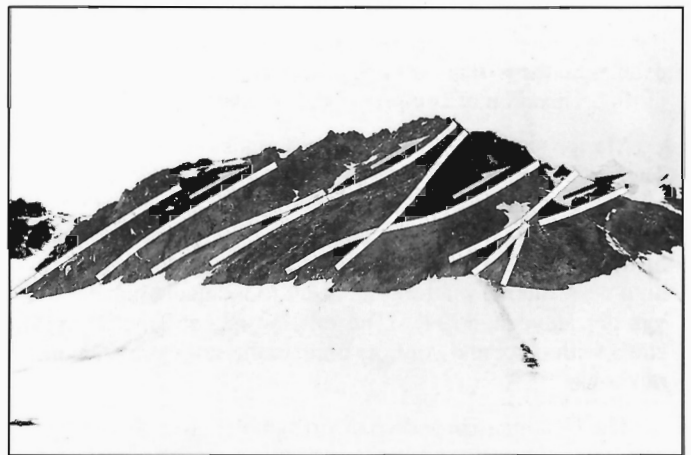


Figure 5. View west at gently south-southwest-dipping thrust slices of the imbricate zone south of Perkins Peak.

Cretaceous Tyaughton Trough

The Tyaughton Trough was defined by Jeletzky and Tipper (1968) as an Upper Jurassic to Upper Cretaceous marine basin flanked by landmasses on the southwest and northeast, situated along the present margin of the southeastern Coast belt. Upper Jurassic and Lower Cretaceous marine sedimentary strata of the basin (Jeletzky and Tipper, 1968) are discontinuously overlain by Upper Cretaceous nonmarine sedimentary and volcanic rocks of the Silverquick and Powell Creek formations (Glover et al., 1987). Jurassic rocks of the Tyaughton Trough, exposed in the Potato Range about 35 km southeast of the study area, do not continue into the Tatla Lake-Bussel Creek map areas. The oldest rocks in the study area which can reasonably be included in the Tyaughton Trough are Hauterivian sedimentary rocks of the informally named Cloud Drifter formation (Rusmore and Woodsworth, 1989; equivalent to map unit 12 of Tipper, 1969).

The Cloud Drifter formation has a minimum thickness of 1500 m and is dominated by sandstone and siltstone, with minor mudstone and conglomerate interbeds. Rare granitoid clasts in the generally volcanic-derived Cloud Drifter formation indicate a mixed volcanic-plutonic source. The unit was probably deposited on a sand-dominated, open clastic shelf, with a southwesterly to westerly source (Mustard and van der Heyden, 1994). Below the thrust north of Perkins Peak (Fig. 6) it is folded into north- to northeast-inclined anticline-syncline pairs; it is probably internally imbricated as well, but generally poor exposure limits detailed mapping of these structures. About 7 km north-northeast of Perkins Peak lithic arenites of the Cloud Drifter formation grade downward into volcanic conglomerate and felsic lapilli tuff, which we correlate with the Ottarasko formation of Rusmore and Woodsworth (1989). The Cloud Drifter and Ottarasko formations may in part be facies equivalents, or the Cloud Drifter formation may be derived in part from erosion of the slightly older Ottarasko formation.

Auriferous arsenopyrite-quartz veins, hosted by small quartz diorite and felsite intrusions near Perkins Peak (Mountain Boss Au-Ag-Cu developed prospect, Minfile # 92N-010; Bluebell Au-graphite prospect, Minfile # 92N-012), occur in fault-bounded lenses in the Cloud Drifter formation below the imbricate zone. The auriferous quartz veins may be late-stage extension veins that formed perpendicular to thrust faults during relaxation of compressional stress.

Marine sandstone, siltstone, and mudstone of the Albian Taylor Creek Group are exposed only west of Bluff Lake, in a fault slice which is thrust over younger rocks of the Powell Creek formation. The unit contains Albian-Cenomanian(?) bivalves (J. Haggart, pers. comm., 1993), and was deposited on a deep marine platform adjacent to a delta (Mustard and van der Heyden, 1994). The relationship of Taylor Creek strata with older and younger units in the study area remains unknown.

The Cenomanian and younger(?), nonmarine Silverquick and Powell Creek formations reflect a major change in tectonic environment from preceding marine conditions in the Tyaughton Trough (Garver, 1992). The areas underlain by these formations in the study area were previously mapped

(Tipper, 1969) as Upper Triassic volcanic rocks and Lower Cretaceous volcanoclastic and sedimentary rocks (Tipper's unit 1, 13, and 16) but they are clearly distinct from units of that age and are here correlated with the nonmarine, informally named Silverquick and Powell Creek formations of Glover et al. (1987). The Silverquick formation in the study area is a thick unit of nonmarine sandstone, conglomerate, and minor mudstone derived from a mixed volcanic-plutonic source (Mustard and van der Heyden, 1994). Some sandstones appear to consist entirely of first-cycle plutonic derivatives; U-Pb dating of detrital zircons from one of these sandstone layers is currently underway. The unit is thought to represent a lower alluvial fan to braidplain environment, with material derived from a westerly, tectonically active source.

The Silverquick formation grades upward into the volcanoclastic Powell Creek formation. This unit is dominated by structureless, green-grey to maroon, volcanoclastic breccias, which were derived from an andesitic source and deposited in a debris flow dominated alluvial fan system (Mustard and van der Heyden, 1994). The combined thickness of both formations in the study area probably exceeds 1250 m. Tipper (1969) suggested that, although deposited over wide areas unrelated to Tyaughton Trough, the greatest accumulation of these nonmarine rocks coincided with the basin axis; these rocks record the final stages in the evolution of the basin (Garver, 1992), and we therefore include these units in Tyaughton Trough.

Late Triassic rocks between the Yalakom and Tchaikazan faults

Rocks between Yalakom and Tchaikazan faults were previously interpreted as Lower Cretaceous volcanic and sedimentary rocks intruded by younger plutons (Tipper, 1969) and, in part, as Upper Cretaceous Kingsvale Group (Rusmore and Woodsworth, 1993). A new, preliminary U-Pb age of ca. 220 Ma for the Sapeye Creek pluton (see Fig. 2 for location),

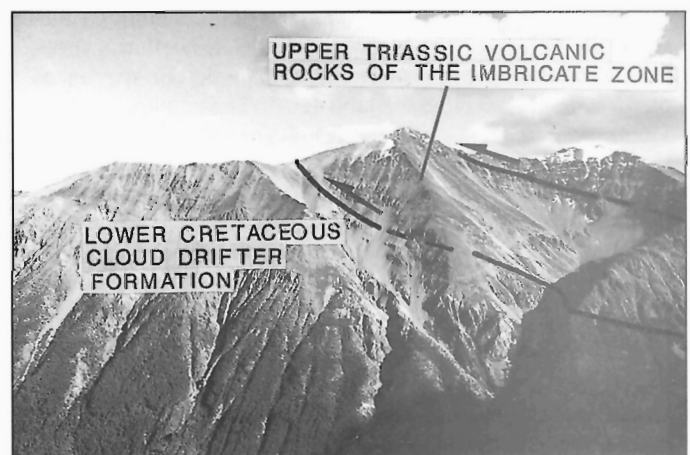


Figure 6. View of the north face of Perkins Peak, with Upper Triassic(?) volcanic and volcanoclastic rocks thrust over Lower Cretaceous Cloud Drifter formation.

together with a previously published 190 Ma hornblende K-Ar date for a similar pluton exposed northeast of Bluff Lake (Friedman and Armstrong, 1988), however, suggest that most of the supracrustal rocks of this area are at least as old as Early Jurassic. With the exception of Lower Cretaceous fossiliferous sediments exposed northwest of Sapeye Lake, volcanic and sedimentary rocks northwest and southeast of Bluff Lake are unambiguously intruded by the older plutons, and we tentatively correlate these rocks with the Upper Triassic Mt. Moore formation. These Upper Triassic strata are described in more detail elsewhere (Mustard and van der Heyden, 1994). They contain a distinctive sedimentary interval with a few fossiliferous limestone beds; corals from these limestones are tentatively assigned to the Upper Triassic (E.T. Tozer, pers. comm., 1993).

Tatla Lake Complex

The northwestern part of the Tatla Lake map area is underlain by crystalline rocks of the Tatla Lake metamorphic complex (TLMC). The complex was not examined in detail during the present study, and no significant new observations were made. The following brief summary of the geology of the complex is based on Friedman (1988, 1992) and Friedman and Armstrong (1988).

The Tatla Lake metamorphic complex is a Eocene mid-crustal core complex that formed in a regional extensional setting. It consists of a core of Cretaceous granoblastic gneiss, migmatic gneiss, and tonalite, overlain by a 1-2.5 km thick Eocene ductile shear zone containing mylonitic orthogneiss, amphibolite facies metasedimentary rocks, and structurally overlying greenschist facies metavolcanic rocks. A ca. 10 km thick missing or strongly attenuated structural section within the ductile shear zone coincides with the transition from amphibolite facies metasedimentary rocks to greenschist facies metavolcanic rocks and correlative low-grade volcanic strata of the upper plate. Low grade rocks of the upper plate are exposed north and east of the Tatla Lake map area; brittle normal faults separating these rocks from the Tatla Lake metamorphic complex are inferred to reflect a late stage in the extensional uplift history, following deformation of the entire core by broad, upright, west- to northwest-trending folds.

The complex and its bounding structures are truncated to the southwest by the Eocene, dextral transcurrent Yalakom fault. The fault itself is not exposed in the Tatla Lake map area, but it is marked by a prominent linear topographic depression and by strongly fractured, veined, and altered outcrops adjacent to its inferred trajectory. Latest motion on the Yalakom fault postdates middle Eocene ductile extensional shear in the complex. Riddell et al. (1993) postulated about 115 km of dextral offset along the Yalakom fault. A truncated western continuation of the complex has not been recognized southwest of the Yalakom fault, and the fault itself has not been observed northwest of the study area.

DISCUSSION

We have demonstrated that the early Late Cretaceous Eastern Waddington Thrust Belt continues at least into the range underlain by Perkins Peak. West of Perkins Peak the thrust belt is intruded by the ca. 63 Ma Klinaklini pluton; at this point the thrust belt trends east-west. There are two possibilities for the continuation of the thrust belt beyond the Klinaklini pluton: to the west, or to the north. West of Klinaklini pluton, Roddick and Tipper (1985) show a steeply south-southwest-dipping structure separating Central Gneiss Complex to the south (their unit nsc) from an Early Cretaceous pluton (their unit IKqd, correlative with the Late Jurassic Wilderness Mountain pluton of this study) to the north, but we do not believe this contact to represent the continuation of Eastern Waddington Thrust Belt. In the thrust belt, rocks of the Coast belt, which locally include Late Jurassic orthogneiss (Rusmore and Woodsworth, 1993), are typically thrust over relatively unmetamorphosed supracrustal rocks. We include the locally strongly mylonitic Wilderness Mountain pluton in the Coast belt, and suggest that the northeast-trending thrust fault which separates it from underlying supracrustal rocks, north of Klinaklini River, represents the northerly continuation of the thrust belt. This fault is intruded by the ca. 67 Ma McClinchy pluton.

Our suggestion for continuation of the thrust belt into northern Bussel Creek map area has several implications and raises further questions. Neither Eastern Waddington Thrust Belt nor Tyaughton Trough strata have been observed farther north (van der Heyden et al., 1993). As previously suggested by Tipper (1969), Tyaughton Trough may have had a northern margin in or near the present study area; Cretaceous marine strata of Tyaughton Trough (Cloud Drifter formation and Taylor Creek Group) are absent north of Klinaklini River, and Jurassic marine strata of Tyaughton Trough (Last Creek formation and Relay Mountain Group) are absent north of Potato Range (ca. 35 km southeast of the study area). The thrust belt appears to coincide, regionally, with the western margin of Tyaughton Trough (Tipper, 1969), and the northern limit of the thrust belt may thus coincide with the northern paleogeographic extent of the Early Cretaceous basin. The otherwise relatively wide imbricate zone of the thrust belt narrows near Perkins Peak and is largely missing north of Klinaklini River, suggesting that the numerous thrusts of the belt merge into only one or two thrusts at the base of the Wilderness Mountain pluton, and that the thrust belt dies out to the north. These distribution patterns may indicate rotational collapse of Tyaughton Trough about a hinge coinciding with its northern termination, in or near the present map area; in such a tectonic scenario the thrust belt might not be expected to continue much beyond the northern basin limit.

Rusmore and Woodsworth (1993) previously correlated the Upper Triassic rocks of the northern Mt. Waddington area with Stikinia. The presence of ca. 220 Ma and 190 Ma plutons associated with Upper Triassic volcanic rocks, north and east

of Bluff Lake, supports Rusmore and Woodsworth's correlation: Late Triassic and Early Jurassic plutons are a common and distinctive element of Stikinia in northern British Columbia (Anderson and Bevier, 1992; Anderson, 1993). The presence of these Upper Triassic rocks between the Yalakom and Tchaikazan faults, together with Early Cretaceous strata of Tyaughton Trough, suggests that the northern margin of the basin was underlain by Stikinia. A similar suggestion was made by Umhoefer (1990), who showed that the correlative Cadwallader terrane (Rusmore, 1987; Umhoefer, 1990) is basement to the Tyaughton Trough farther to the southeast.

ACKNOWLEDGMENTS

We wish to thank Toby Pierce for excellent field assistance during the present mapping project. Mike, Audrey, and Dave King of Whitesaddle Air at Bluff Lake provided outstanding helicopter and fixed wing transportation, logistical support, and general advice. Discussions in the field with Paul Umhoefer, Margi Rusmore, and Glenn Woodsworth clarified numerous aspects of the regional geology. Special thanks go to Peter Brookmeyer of Kleena Kleene for his hospitality and for sharing his knowledge of local access and the geography of the area. Thanks also to Glenn Woodsworth for reviewing the paper, and to Bev Vanlier for editing the final version.

REFERENCES

- Anderson, R.G.**
1993: A Mesozoic stratigraphy and plutonic framework for northwestern Stikinia (Iskut River area), northwestern British Columbia, Canada; in *Mesozoic Paleogeography of the western United States II*, (ed.) G. Dunne and K. McDougall; Pacific Section SEPM, v. 71, p. 477-494.
- Anderson, R.G. and Bevier, M.L.**
1992: New Late Triassic and Early Jurassic U-Pb zircon ages from the Hotailuh Batholith, Cry Lake map area, north-central British Columbia; in *Radiogenic Age and Isotopic Studies: Report 6*; Geological Survey of Canada, Paper 92-2, p. 145-152.
- Friedman, R.M.**
1988: Geology and geochronometry of the Eocene Tatla Lake metamorphic core complex, western edge of the Intermontane Belt, British Columbia; Ph.D. thesis, University of British Columbia, Vancouver, British Columbia, 348 p.
1992: P-T-t path for the lower plate of the Eocene Tatla Lake metamorphic core complex, southwestern Intermontane Belt, British Columbia; *Canadian Journal of Earth Sciences*, v. 29, p. 972-983.
- Friedman, R.M. and Armstrong, R.L.**
1988: The Tatla Lake Metamorphic Complex: an Eocene metamorphic core complex on the southwest edge of the Intermontane Belt, British Columbia; *Tectonics*, v. 7, p. 1141-1166.
- Garver, J.I.**
1992: Provenance of Albian-Cenomanian rocks of the Methow and Tyaughton basins, southern British Columbia: a mid-Cretaceous link between North America and the Insular terrane; *Canadian Journal of Earth Sciences*, v. 29, p. 1274-1295.
- Glover, J.K., Schiarizza, P., and Garver, J.I.**
1987: Geology of the Noaxe Creek map area (92O/2); in *Geological Fieldwork 1987*; British Columbia Ministry of Energy, Mines, and Petroleum Resources, Paper 1988-1, p. 105-123.
- Jeletzky, J.A. and Tipper, H.W.**
1968: Upper Jurassic and Cretaceous rocks of Taseko Lakes map area and their bearing on the geological history of southwestern British Columbia; Geological Survey of Canada, Paper 67-54, 218 p.
- Mustard, P.S. and van der Heyden, P.**
1994: Stratigraphy and sedimentology of the Tatla Lake-Bussel Creek map areas, west-central British Columbia; in *Current Research 1994-A*; Geological Survey of Canada.
- Riddell, J., Schiarizza, P., and Gaba, R.G.**
1993: Geology and mineral occurrences of the Mount Tatlow map area (92O/5,6, and 12); in *Geological Fieldwork 1992*, British Columbia Ministry of Energy, Mines, and Petroleum Resources, Paper 1993-1, p. 37-52.
- Roddick, J.A. and Tipper, H.W.**
1985: Geology, Mount Waddington (92N) map area; Geological Survey of Canada, Open File 1163.
- Rusmore, M.E.**
1987: Geology of the Cadwallader Group and the Intermontane-Insular Superterrane Boundary, southwestern British Columbia; *Canadian Journal of Earth Sciences*, v. 24, p. 2279-2291.
- Rusmore, M.E. and Woodsworth, G.J.**
1988: Eastern margin of the Coast Plutonic Complex, Mount Waddington map area, B.C.; in *Current Research, Part E*; Geological Survey of Canada, Paper 88-1E, p. 185-190.
1989: A note on the Coast-Intermontane Belt transition, Mount Waddington map area, British Columbia; in *Current Research, Part E*; Geological Survey of Canada, Paper 89-1E, p. 163-167.
1991a: Coast Plutonic Complex: a mid-Cretaceous contractional orogen; *Geology*, v. 19, p. 941-944.
1991b: Distribution and tectonic significance of Upper Triassic terranes in the eastern Coast Mountains and adjacent Intermontane Belt, British Columbia; *Canadian Journal of Earth Sciences*, v. 28, p. 532-541.
1993: Geological maps of the Mt. Queen Bess (92N/7) and Razorback Mountain (92N/10) map areas, Coast Mountains, British Columbia; Geological Survey of Canada, Open File 2586, 2 sheets, scale 1:50 000.
- Tipper, H.W.**
1969: Mesozoic and Cenozoic geology of the northeast part of Mt. Waddington map-area (92N), Coast District, British Columbia; Geological Survey of Canada, Paper 68-33, 103 p.
- Umhoefer, P.J.**
1990: Stratigraphy and tectonic setting of the upper part of the Cadwallader terrane, southwestern British Columbia; *Canadian Journal of Earth Sciences*, v. 27, p. 702-711.
- van der Heyden, P.**
1990: Eastern margin of the Coast Belt in west-central British Columbia; in *Current Research, Part E*; Geological Survey of Canada, Paper 90-1E, p. 171-182.
1991: Preliminary U-Pb dates and field observations from the eastern Coast Belt near 52°N, British Columbia; in *Current Research, Part E*; Geological Survey of Canada, Paper 91-1A, p. 79-84.
- van der Heyden, P., Shives, R., Ballantyne, B., Harris, D., Dunn, C., Teskey, D., Plouffe, A., and Hickson, C.**
1993: Overview and preliminary results for the Interior Plateau Program, Canada-British Columbia Agreement on Mineral Development 1991-1995; in *Current Research, Part E*; Geological Survey of Canada, Paper 93-1E, p. 73-79.
- Wheeler, J.O. and McFeely, P.**
1991: Tectonic assemblage map of the Canadian Cordillera and adjacent parts of the United States of America; Geological Survey of Canada, Map 1712, scale 1:2 000 000.

Stratigraphy and sedimentology of the Tatla Lake-Bussel Creek map areas, west-central British Columbia¹

P.S. Mustard and P. van der Heyden
Cordilleran Division, Vancouver

Mustard, P.S. and van der Heyden, P., 1994: Stratigraphy and sedimentology of the Tatla Lake-Bussel Creek map areas, west-central British Columbia; in Current Research 1994-A; Geological Survey of Canada, p. 95-104.

Abstract: In Bussel Creek and Tatla Lake map areas, geology southwest of Yalakom Fault reflects northern continuation of the east Waddington thrust belt, with northwest- to west-trending thrust panels thrust northeast during the late Cretaceous. The highest, most southwest thrust sheets contain Triassic and rare Lower Cretaceous strata. Triassic strata include the Carnian to lower Norian, volcanogenic Mt. Moore formation, and the Norian Mosley formation, a mixed siliciclastic-carbonate nonmarine and shallow marine succession. Central thrust sheets comprise two Early Cretaceous units: the volcanogenic Ottarasko formation and gradationally overlying Cloud Drifter formation, a succession of shelf clastics containing Hauterivian fossils. The northeasterly structural panels contain the youngest units: a single slice of Albian to Cenomanian marine turbidites correlated with the Taylor Creek Group; a nonmarine immature sandstone and conglomerate unit correlated with the Silverquick conglomerate; and a volcanic breccia/conglomerate unit correlated with the Powell Creek volcanics.

Résumé : Dans les régions cartographiques du ruisseau Bussel et du lac Tatla, la géologie du secteur situé au sud-ouest de la faille de Yalakom, caractérisée par des panneaux de charriage de direction nord-ouest à ouest ayant été entraînés vers le nord-est au Crétacé tardif, témoigne du prolongement septentrional de la zone de chevauchement d'East Waddington. Les nappes de charriage les plus hautes, le plus au sud-ouest, contiennent des strates du Trias et, occasionnellement, du Crétacé inférieur. Les strates triasiques comprennent la formation de Mt. Moore, d'origine volcanique, qui s'échelonne du Carnien au Norien inférieur, et la formation de Mosley, du Norien, succession mixte de lithologies silicoclastiques et carbonatées, de milieux continental et épicontinental. Les nappes de charriage de la partie centrale comprennent deux unités qui remontent au Crétacé précoce : la formation d'Ottarasko, d'origine volcanique, et la formation de Cloud Drifter, succession clastique de milieu de plate-forme continentale, à fossiles du Hauterivien, qui la surmonte avec un contact progressif. Les panneaux structuraux situés au nord-est contiennent les unités les plus jeunes : une écaille isolée de turbidites marines d'âge albien à cénomaniens, corrélées avec le Groupe de Taylor Creek; une unité continentale de conglomérat et de grès immatures, corrélée avec le conglomérat de Silverquick; et une unité de brèche volcanique/conglomérat corrélée avec les volcanites de Powell Creek.

¹ Contribution to Canada-British Columbia Agreement on Mineral Development (1991-1995), a subsidiary agreement under the Canada-British Columbia Economic and Regional Development Agreement.

INTRODUCTION

As part of the Canada-British Columbia Mineral Development Agreement, 1:50 000 scale mapping of the Tatla Lake map area (NTS 92N/15), the east half of the Bussel Creek map area (92N/14), and a small part of northern Razorback map area (92N/10) was conducted in 1993 (Fig. 1, 2). Figure 3 summarizes the major lithostratigraphic units, deformation, and intrusive events as currently understood. A companion paper (van der Heyden et al., 1994) focuses on the regional geology, structural setting, and the significance of preliminary radiometric dates from plutons in the study area. This paper concentrates on the stratigraphy and sedimentology of the major lithostratigraphic units.

The main lithostratigraphic units southwest of the Yalakom Fault occur in northwest- to west-trending thrust slices, a northwestern continuation of a late Cretaceous fold and thrust belt (the eastern Waddington thrust belt of Rusmore and Woodsworth, 1991a, in press). Several formations can be identified, with older units (Late Triassic and Early Cretaceous) in upper thrust slices in the southwest and younger units ("mid" to Late Cretaceous) in the most north-easterly thrust slices (Fig. 2). However, out-of-sequence

thrusts occur and a few minor high angle faults have uplifted older assemblages against younger in some places. Pre-thrust intrusions were carried on the thrust sheets, and younger intrusions cut thrust packages.

LITHOSTRATIGRAPHIC UNITS

Upper Triassic

Late Triassic sedimentary and volcanic rocks make up the bulk of complexly interleaved thrust panels in the southwest quarter of the Tatla Lake map area, continuing to the southeast into the Razorback map area and for a short distance to the west into the Bussel Creek and Siva Glacier (92N/11) map areas (Fig. 1, 2, 3). Mapping in the Razorback and Queen Bess map areas prompted Rusmore and Woodsworth (1991b) to recognize two informal formations: the Carnian to lower Norian volcanic-dominated Mt. Moore formation and an overlying Norian sedimentary package they termed the Mosley formation. Our detailed mapping, supplemented by two stratigraphic sections measured in well-exposed areas, supports the Rusmore and Woodsworth divisions and we retain their proposed names.

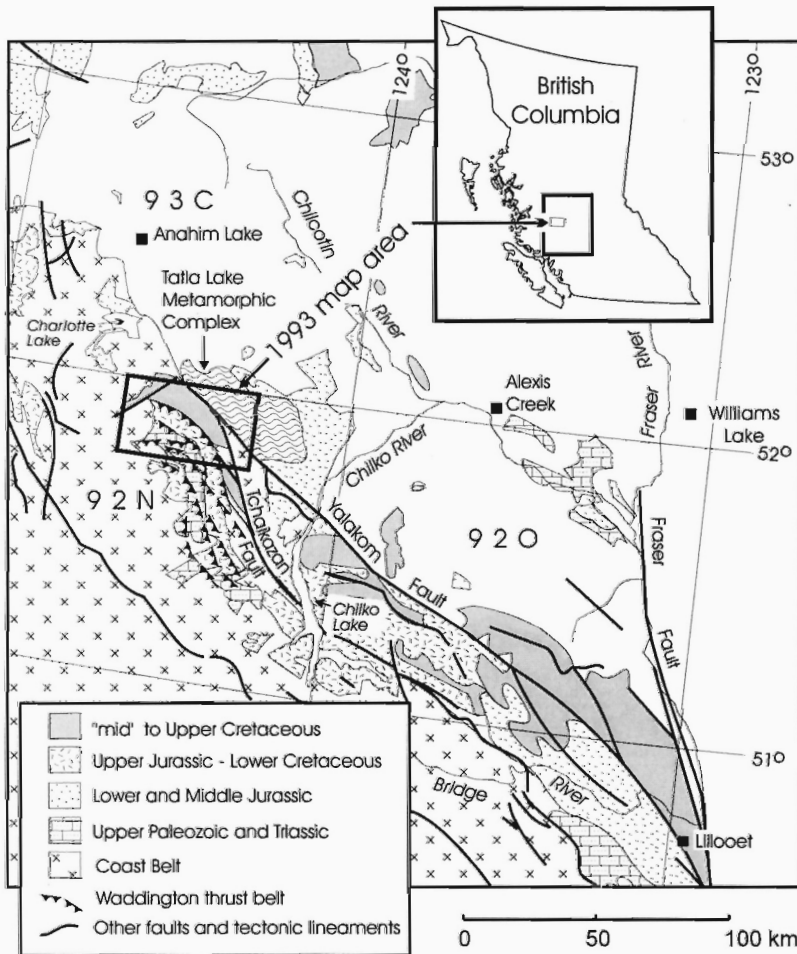


Figure 1. Regional location and geology. Geology modified and greatly simplified from Wheeler and McFeely (1991) with additions from Rusmore and Woodsworth (1993).

Mt. Moore formation

Volcanic and rare interbedded sedimentary rocks of the Mt. Moore formation (map units 1, 2 and 4 of Tipper, 1969) occur in two areas (Fig. 2): as thrust slices within the main imbricated thrust zone in the southwest Tatla Lake and southeast Bussel Creek map areas; and in two outcrop belts offset by the Tchaikazan Fault on the west and east sides of Bluff Lake. The Mt. Moore formation is dominated by mafic to intermediate volcanic breccia, conglomerate, flows, and sills. The breccia and conglomerate comprise angular green to less common maroon volcanic clasts in a green or maroon volcanoclastic matrix. Clasts are identical in composition to flows of this unit with ubiquitous plagioclase and in some places distinctive pyroxene phenocrysts in a fine groundmass. This unit resembles the younger Ottarasko formation, but differs in the presence of pyroxene (augite?) phenocrysts up

to 3 cm long and general absence of hornblende phenocrysts typical of the Ottarasko formation. Rare interbeds of siliceous mudstone and thin-bedded tuffaceous sandstone occur.

Extensive successions of volcanic and interbedded sedimentary rock on the immediate west and east sides of Bluff Lake were originally included by Tipper (1969) in his Lower Cretaceous map unit 13, and later correlated by Rusmore and Woodworth (1993) with the Upper Cretaceous Kingsvale Group. However, preliminary U-Pb dates from the Sapeye Creek pluton (new name) located northwest of Bluff Lake indicate a Late Triassic age (ca. 210-220 Ma) for crystallization. This pluton clearly intrudes the volcanic/sedimentary unit which thus must be no younger than late Triassic. The unit is dominated by massive volcanic breccia to conglomerate and lesser intermediate to mafic volcanic flows similar to those of the Mt. Moore formation and we suggest

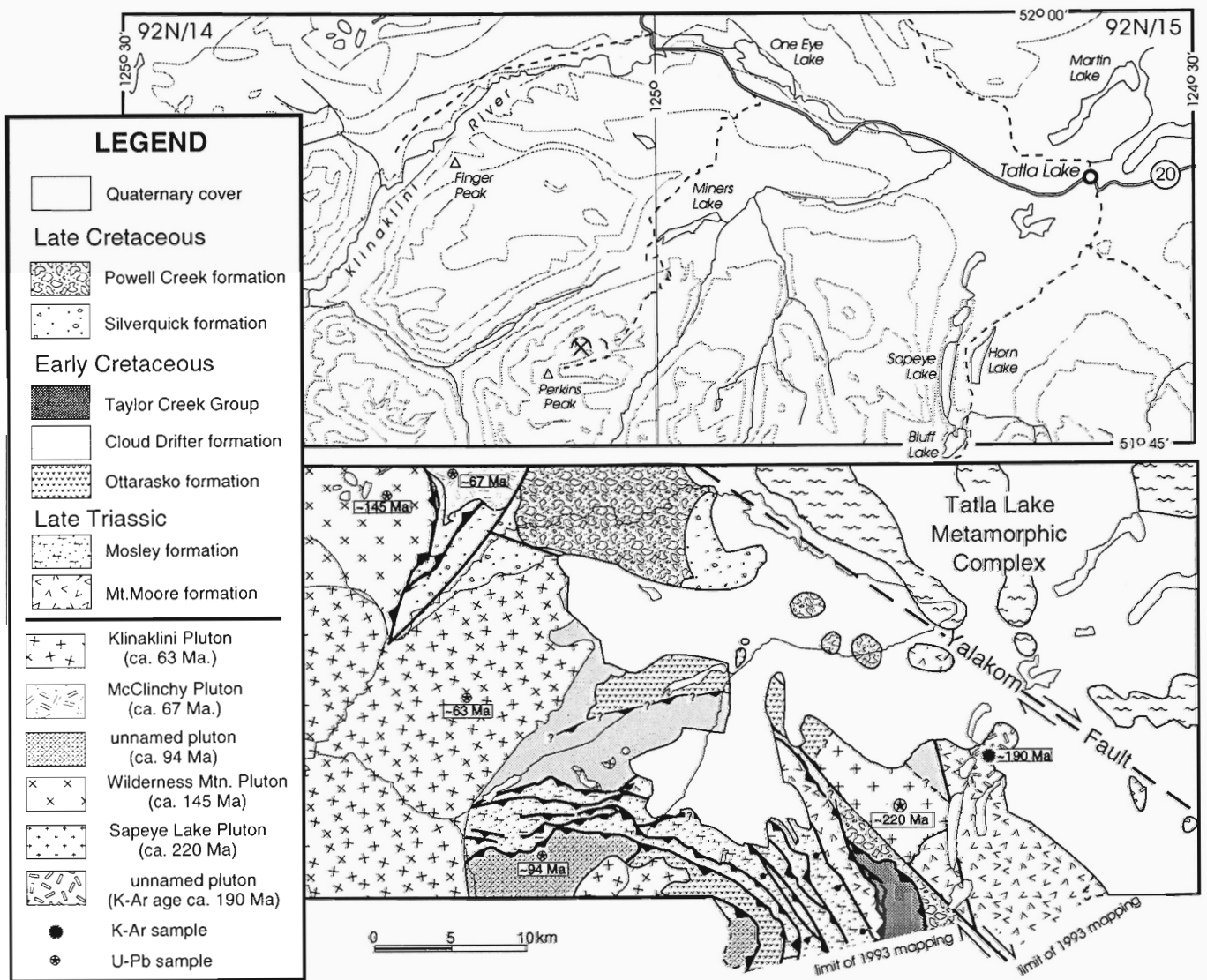


Figure 2. Simplified geology of the project map areas.

this is the most plausible correlation. The main difference from the Mt. Moore formation exposed elsewhere is the presence of a distinctive sedimentary succession several hundred metres thick in the middle of the Bluff Lake volcanic unit. The succession comprises >100 m of vaguely stratified to rarely cross-stratified pebble-cobble conglomerate and coarse sandstone which gradationally overlie volcanoclastic sandstone-mudstone couplets interbedded with intermediate volcanic flows. A few light grey limestone beds <1 m thick occur in this sedimentary succession and contain poorly preserved corals, bivalves, and gastropods. This distinctive, fossil-bearing sedimentary unit was recognized on both sides of the Tchaikazan Fault and thus provides a marker unit, indicating about 7-8 km of apparent dextral strike-slip offset.

The Mt. Moore formation is about 1500 m thick at Bluff Lake, but is everywhere in fault or intrusive contact with other units and thus the true thickness and contact relationships are unknown. The best age control consists of late Carnian to early Norian conodonts recovered from an interbedded limestone lens near Mt. Moore (Rusmore and Woodsworth, 1991b). The intrusive relationship of the Sapeye Creek pluton suggests an early Norian or older age for the Mt. Moore formation in this region, compatible with the age suggested from the Mt. Moore area.

Mosley formation

Most of the Triassic succession in the map area is distinctive dark red to cream-pink siliciclastic sandstone (Fig. 4A). Less abundant grey limestone clastics occur as a mappable, but laterally discontinuous facies within the red unit. The Mosley formation occurs in several thrust slices and no formation contacts are preserved, inhibiting formal formation definition. A measured stratigraphic section in one well-exposed thrust slice documents a minimum thickness of 650 m for this formation, with a thickness exceeding 1 km indicated by the map pattern in other places.

In the best-exposed area of the Mosley formation, a lower facies of massive to faintly laminated grey-brown limestone mudstone to fine grained wackestone is present. Considered by Tipper (1969) a separate map unit (his unit 3), in the Bussel Creek map area this fine carbonate clastic facies is transitional upward and laterally into the other facies of the Mosley formation. The distinctive bivalve *Halobia* was the only fossil found in this facies (GSC localities C-176113, C-101545; identified by E.T. Tozer, Cordilleran Division, pers. comm., 1993). The *Halobia*-bearing carbonate clastic facies changes upward and laterally into a coarse grained, fossil-rich limestone facies which Tipper (1969) also considered a separate map unit (his unit 5). This facies is a distinctive light

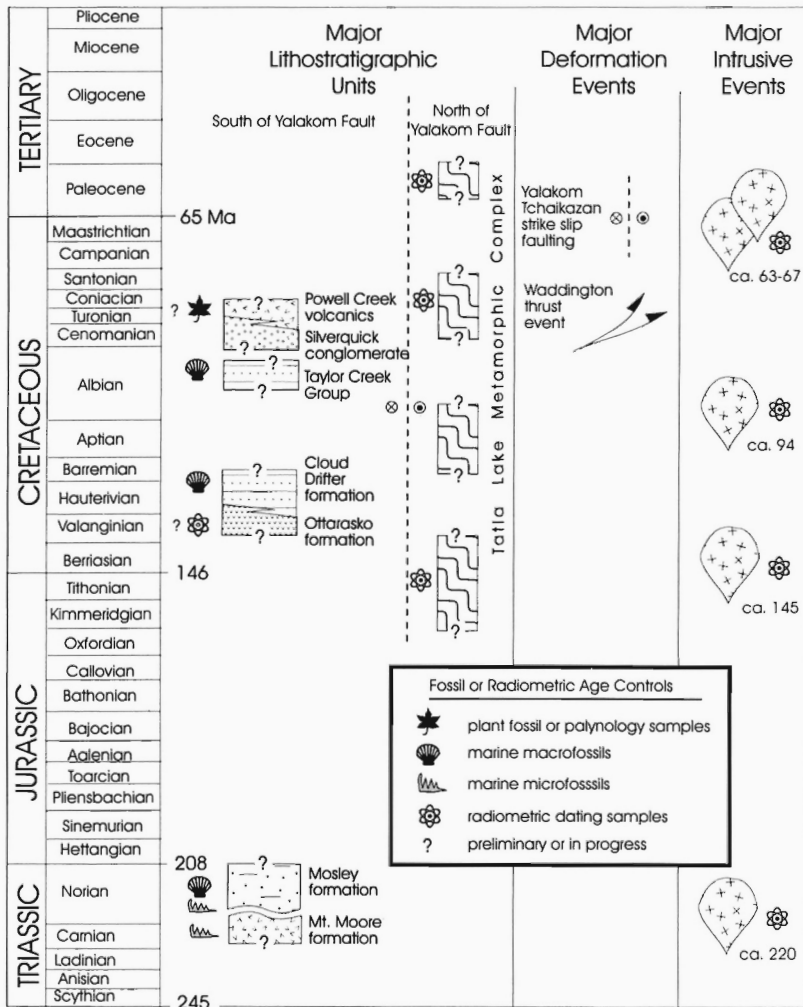


Figure 3. Schematic representation of major lithostratigraphic units, deformation events, and intrusive events in the map area.

grey weathering succession of interbedded limestone wackestone, packstone, and mudstone with abundant bivalves, gastropods and pelecypods occurring either as transported coquina up to a metre thick or in situ shell beds tens of centimetres thick. In one place a 10 m thick bed of both broken and in situ hexacorals, bryozoans, gastropods, and bivalves is preserved in a reef complex traceable laterally for <100 m. Intercalated with the fossil-rich beds are massive to laminated mudstone and laminated to thin-bedded, fine grained wackestone, both containing common shell fragments and *Skolithos* ichnofacies trace fossils (Fig. 4B).

The fossiliferous limestone facies occurs as a discontinuous, but regionally mappable member up to 100 m thick within the dominantly red to cream-pink mixed siliciclastic-carbonate clastic rocks which make up the bulk of the Mosley formation. The contact of the carbonate clastic facies and siliciclastic rocks is gradational over several tens of metres vertically and laterally intertongues. The siliciclastics comprise fine- to coarse-grained tuffaceous lithic arenite which occur in thin to thick beds, commonly normal graded with either gradational caps or interbeds of red to rare green-brown siltstone or silty mudstone. Rare desiccation cracks, bivalve fragments, and simple trace fossils (*Skolithos*, *Diplocraterion*, *Planolites*) are preserved in mudstone interbeds. Mudstone ripups are common. Coarse grained pebbly sandstones and pebble-cobble matrix-supported conglomerates also

occur (Fig. 4C). These coarser rocks include trough cross-bedded, pebbly tuffaceous lithic arenite in sets up to 5 m thick and massive matrix-supported conglomerates up to 10 m thick with volcanic and less common limestone pebbles and cobbles floating randomly in a coarse grained volcanoclastic to tuffaceous lithic wacke matrix. Interbedded with these coarse clastic rocks are fine grained sandstone and mudstone, most commonly red siliciclastic mudstone, but including calcareous mudstone containing rare bivalves and gastropods. In one place a distinctive subaerial exposure surface is preserved between conglomerates with light grey massive limestone replacing older beds (as calcrete) and infilling irregular vertical and horizontal dissolution cavities in the bedded sequence. These minor karstic limestones are identical to many of the limestone clasts found in overlying conglomerate beds.

Features of the non calcareous clastics indicate deposition in a generally nonmarine setting, probably a lower alluvial fan to coarse fan delta or debris apron with a nearby volcanic source area providing the abundant volcanoclastic material. However, the fossiliferous carbonate sandstone-mudstone facies suggest lateral transition to shell banks and rare patch reefs of a marine platform.

Previous fossil collections from the Mosley formation (Tipper, 1969; Rusmore and Woodsworth, 1991b, 1993) indicated an early to late Norian age. New collections include



Figure 4. **A.** Well-exposed Mosley formation north of Mosley Creek. Cliffs are east-facing and expose >500 m of Mosley formation, clastic rocks. **B.** Mosley formation, interbedded fine grained limestone wackestone and packstone with large vertical burrow. **C.** Mosley formation tuffaceous sandstone and conglomerate, typical of the coarser part of the red and cream-pink siliciclastics of this unit. Hammer is 30 cm in length.

Halobia in the lower part of this unit, which suggests a Carnian to early Norian age for the lower Mosley formation. Bivalves from the limestone facies in the central to upper Mosley formation are probably late Norian (GSC locality C-176114; preliminary identifications by E.T. Tozer, pers. comm., 1993). Tipper (1969) also collected the distinctive late Norian bivalve *Monotis subcircularis* from this facies in this area. Although not found in the main Triassic outcrop area during the present project, a single *Monotis* was collected from a Mosley formation limestone bed about 5 km west of the main outcrop area (GSC locality C-202601, identified by E.T. Tozer, pers. comm., 1993).

Lower Cretaceous

Ottarasko formation

Lower Cretaceous strata consist of two regional units, termed map units 12 and 13 by Tipper (1969), but informally designated the Cloud Drifter and Ottarasko formations respectively by Rusmore and Woodsworth (1989, 1993) in map areas to the south, a practice we continue. The volcanic to volcanoclastic Ottarasko formation (Tipper's map unit 13) is preserved beneath the Cloud Drifter formation in the central map area and in one thrust-bound panel in the main imbricate thrust zone in the southwest (Fig. 2). No basal formation contact is known from our map area or from areas to the south, thus the true thickness is unknown, although a thickness exceeding 500 m is suggested by the map patterns and extent.

The Ottarasko formation generally consists of greyish yellow-green to grey-green volcanic breccia and conglomerate with less common intermediate to mafic volcanic flows (rarely pillowed). The volcanic conglomerate and breccia are matrix-supported, poorly stratified to unstratified and massive, with rare pyroclastic bombs (Fig. 5). Most clasts are angular to subround and volcanic composition, with green and red plagioclase porphyry types most common. Rare felsic flows and reworked lapilli tuffs are interbedded with

the felsic component more common in the upper unit. In a few places, interbedded, fine grained tuffaceous sandstone and mudstone occur in sets up to 10 m thick.

On a ridge northwest of Perkins Peak a gradational contact of the Ottarasko formation with the overlying Cloud Drifter formation is preserved, the first documented contact of these formations. Over several hundred metres, Ottarasko formation volcanic conglomerate and thick beds of slightly reworked felsic lapilli tuff gradationally decrease in abundance upward as interbedded thick- to medium-bedded lithic arenite typical of the Cloud Drifter formation increase. The contact is placed where brown-grey lithic sandstone becomes >50% of the unit. This gradational change supports the interpretations of Rusmore and Woodsworth (1988, in press) that these formations are, in part, facies equivalents and the Cloud Drifter sandstone is probably in part derived from erosion of the Ottarasko volcanics.

Cloud Drifter formation

The Cloud Drifter formation, map unit 12 of Tipper (1969), is a thick package of lower Cretaceous sandstone, siltstone, minor mudstone, and conglomerate preserved in the central map area thrust sheets. Fossils collected by Tipper and new collections from this project include common inoceramid bivalves and rare ammonites and belemnites. Poorly preserved carbonaceous plant fragments also occur in some siltstone. All identified fossils indicate a Hauterivian age. The upper contact of the formation is not preserved and thus the true thickness is unknown. The unit is commonly folded into large inclined anticline-syncline pairs which makes thickness estimates difficult. However, a minimum thickness of about 1500 m is suggested in parts of the map area where cross-sections can be drawn with some confidence.

Best exposed on ridges north of Perkins Peak (Fig. 6A), the Cloud Drifter formation is characterized by fine- to medium-grained lithic arenite or wacke in medium to thick beds. These sandstones make up >70% of the unit and in general are massive with rare internal planar or wavy lamina. Beds are non graded or poorly normal graded. Typical sandstone is immature, dominated by volcanic lithic clasts, but with abundant plagioclase and less common potassium feldspar. Hummocky cross-stratification is present in some places, but only identified on exceptionally well-exposed faces (Fig. 6B). Fossils are rare in sandstone and generally restricted to discontinuous bedding parallel layers of inoceramid fragments.

In some places, well-defined fining-upward sequences 10-50 m thick are present with sandstone thick beds changing upward to red-brown massive to faintly laminated siltstone and silty mudstone (Fig. 6A). Contacts between beds are generally non erosive and very slightly loaded.

Conglomerate occurs as irregular beds up to 3 m thick, generally restricted to the lower part of the formation. Most conglomerate beds occur at the base of subtle fining upward sequences or as random isolated beds. Conglomerates include both matrix-supported types with 60-70% pebbles to small cobbles and clast-supported types with 75-90% pebbles and cobbles, both in a coarse- to medium-grained lithic



Figure 5. Ottarasko formation volcanic breccia with rimmed angular cobble in upper left (probably a pyroclastic bomb).

arenite to wacke matrix. Most beds are massive and poorly to moderately sorted with no clast fabric. In some clast-supported conglomerates a vague stratification and poor clast imbrication is preserved with the latter indicating paleoflow in north or northeast directions. Clasts are generally of volcanic composition with intermediate volcanics most common, but both mafic and felsic volcanic clasts occur. Chert is absent; granitoid clasts are rare but present. Inoceramid shell fragments occur in several conglomerate beds.

Most siltstone and mudstone occur as minor interbeds in sandstone-dominant packages, forming <20% of a typical sequence. However, in some areas massive to faintly laminated siltstone and silty mudstone exceed 50 m in thickness with only rare sandstone interbeds. The massive siltstone

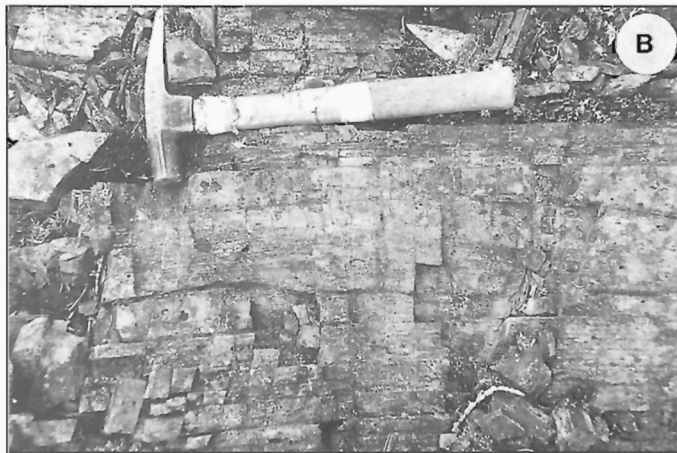


Figure 6. **A.** Well-exposed, northeast-facing cliffs of Cloud Drifter formation north of Perkins Peak. Decimetre-scale fining and thinning upward sandstone-siltstone sequences are apparent in the closest cliffs, some slightly channelized at the base. **B.** Very fine grained sandstone thin beds to thick lamina of the Cloud Drifter formation showing subtle upward curved geometry (in centre below hammer), domal in three dimensional views, and interpreted as hummocky cross-stratification.

facies contain the most abundant and best preserved fossils, with intact inoceramids and rare ammonites up to 30 cm diameter and common broken inoceramid shell material.

The Cloud Drifter formation in this area is interpreted as deposited on a sand-dominated, open clastic shelf. A general lack of high energy or wave structures suggests deposition in relatively deep shelf conditions, although rare hummocky cross-stratification and *Skolithos* ichnofacies indicate at least some deposition above storm wave base. The massive siltstone facies probably formed on sheltered parts of the shelf, although the abundant bivalves indicates open marine conditions. Rare conglomerate beds represent coarse sediment gravity flow deep onto the shelf. The volcanic-rich lithic composition of the sandstone and volcanic-clast dominated conglomerate are compatible with derivation from older Ottarasko formation or exhumed volcanic arc sources, with source areas probably to the southwest or west.

Lower to "Mid" Cretaceous

Taylor Creek Group

Tipper (1969) correlated two sedimentary units in the current map area with the Albian Taylor Creek Group, based on similarity to Taylor Creek Group strata preserved to the southeast and a single fossil locality about 2 km west of Bluff Lake, tentatively assigned an Albian to Cenomanian age (Tipper, 1969, p. 62). Several new fossil collections from the fault-bounded slice directly west of Bluff Lake include numerous bivalves tentatively identified as the inoceramid genus *Birostrina*, common in the Albian and Cenomanian of the western Cordillera (GSC localities C-101535, C-101537, C-101538; preliminary identification by J. Haggart, Cordilleran Division, pers. comm., 1993). This supports correlation of this fault slice with the Taylor Creek Group. However, the sedimentary unit in the western map area, also correlated with the Taylor Creek Group by Tipper, is a nonmarine succession dissimilar to Taylor Creek Group elsewhere which we suggest is more typical of the Late Cretaceous Silverquick conglomerate.

The Taylor Creek Group west of Bluff Lake comprises a generally subvertical succession several hundred metres thick (Fig. 7A), with about 50-60% thick-bedded feldspathic to lithic arenite interbedded with dark grey siltstone and silty mudstone, the latter commonly slightly carbonaceous with common plant debris. Sandstone beds are generally massive to faintly laminated, non graded to poorly normal graded, and medium- to fine-grained, rarely coarse grained (Bouma turbidite types TAE and TABE are common). Tops of beds either grade into, or are sharply overlain by, silty mudstone. Sandstone beds appear laterally continuous for greater than 50 m with bases non erosive, but slightly loaded. Bivalves and rare belemnites occur scattered throughout massive to poorly laminated siltstone or silty mudstone interbeds. Trace fossils also occur and are mostly simple vertical types. Fining- and thinning-upward sequences 10-15 m thick occur in some places, with medium- to thick-bedded sandstone decreasing in abundance and thickness upward as interbeds of siltstone and silty mudstone increase (Fig. 7B).

Deposition in this area is interpreted to reflect a deep marine platformal environment with most sedimentation from turbulent sediment gravity flow. The sand-rich character and abundance of plant debris in many beds may reflect derivation from nearby fluviodeltaic environments, with the sands derived as normal prodelta flows or delta margin failures. Presence of scattered bivalves and trace fossils and lack of preservation of lamina or fine bedding in the massive siltstone and mudstone probably reflects extensive bioturbation.

Upper Cretaceous

Silverquick conglomerate

A thick unit of nonmarine sandstone, conglomerate, and minor mudstone is preserved in the west Klinaklini River valley and well exposed on west-facing cliffs of a prominent ridge locally known as Finger Peak (Fig. 2). The lower contact is not exposed; the upper contact is gradational over several tens of metres into an overlying volcanoclastic and volcanic unit. Leaves in the upper part of the gradational

contact strata were tentatively identified as Cenomanian age (GSC locality 7909; W.A. Bell in Tipper, 1969, p. 95), although Tipper (1969) included this locality in his Lower Cretaceous map unit 13. New collections of leaves and several palynology samples from within the gradational contact are currently being processed.

The lower, sedimentary unit comprises light grey, very coarse- to medium-grained arkosic arenite interbedded with pebble-cobble conglomerate and rare mudstone. The cliffs at Finger Peak expose a continuous section >750 m thick (Fig. 8A). This section is 90-95% sandstone and 5-10% conglomerate. Most beds occur as single, laterally overlapping sheets (each traceable a few hundred metres laterally) with loaded to very slightly erosive bases, and vague internal stratification defined by discontinuous, graded internal sets in an overall normally graded bed generally 30-100 cm thick (Fig. 8B). In some places fining-upward cycles can be defined, each 3-10 m thick. Typically, these have a thin pebble conglomerate or grit sandstone basal layer which is overlain by trough crossbedded coarse- to medium-grained arkosic arenite or wavy planar bedded arenite, all capped by wavy to rippled planar bedded medium- to fine-grained sandstone. These cycles have sharp, irregular curved bases which have eroded tens of centimetres into underlying beds.

Sandstones are immature with abundant subangular plagioclase and potassium feldspar grains and quartz making up the bulk of most sandstone, although volcanic lithic grains are more abundant in the upper part of the formation. Some sandstones have compositions of typical granitoids and appear to be slightly transported grus or other first cycle derivatives of a plutonic source.

Conglomerates are generally clast-supported and moderately sorted with subround to subangular pebbles and cobbles in a coarse grained arkosic arenite matrix. Clast types in the lower part of the sedimentary unit are dominated by felsic plutonic (granitoid) and felsic volcanic compositions with lesser intermediate volcanic and sedimentary clasts (mostly interbasinal sandstone or mudstone ripups). Conglomerate in the upper part of the unit contain more abundant intermediate volcanic clasts although granitoid clasts still make up >10% a typical conglomerate. No chert clasts or other unusual non igneous compositions were identified.

Paleocurrents from imbricated pebbles and sandstone crossbeds define a radial pattern of transport varying from northeast to southeast. This, along with the sedimentary features described above, suggest deposition in a lower alluvial fan to braidplain environment with a western source. Most sandstone are interpreted as sheetflood deposits; the better stratified sandstone and conglomerate suggest braided fluvial deposition with well-defined fining-upward cycles representing main braidplain channels. The immaturity, general coarseness of the unit throughout, and conglomerate clast types suggest an exhumed plutonic-volcanic source immediately west of the deposit. The unit is remarkably consistent in the sandstone-conglomerate bedforms, types, and compositions. This consistency and the coarseness of the deposits suggests continued rejuvenation of a high relief source area, likely reflecting syndepositional faulting in the source area.

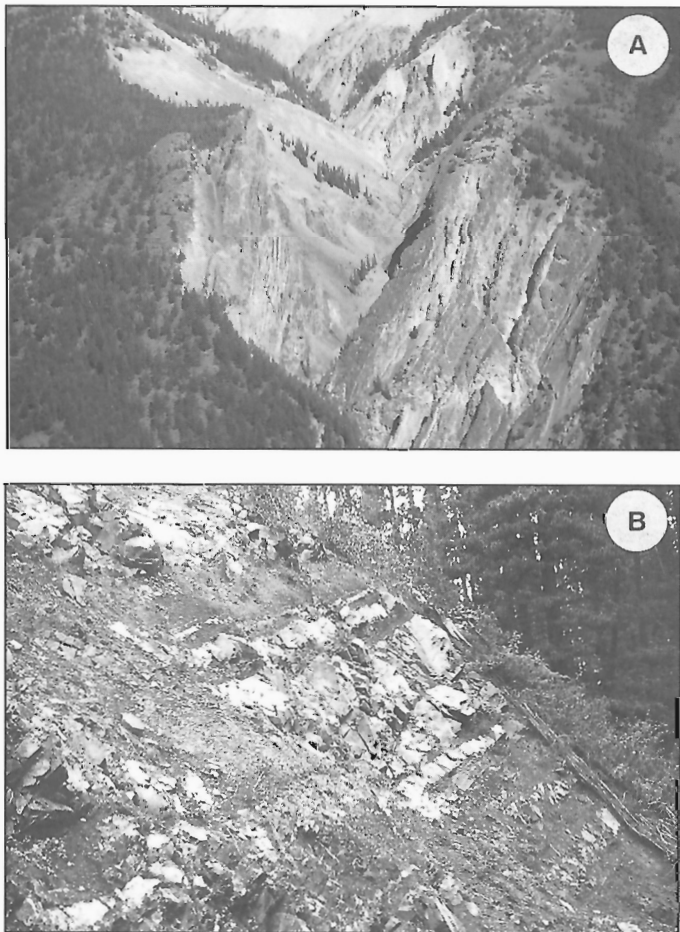


Figure 7. A. Well-exposed canyon of Taylor Creek Group west of Bluff Lake showing typical subvertical sandstone thick beds and interbedded silty mudstone. B. Fining- and thinning-upward sandstone-mudstone cycle about 15 m thick.

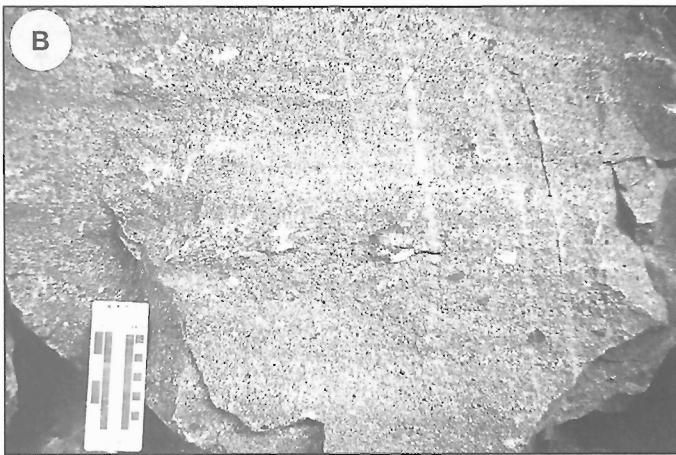


Figure 8 *A.* West-facing cliff face of repetitive sandstone and minor conglomerate beds typical of Silverquick conglomerate. About 250 m of cliff-face is shown in photo. *B.* Coarse grained to pebbly arkosic sandstone of lower Silverquick conglomerate.

This unit was correlated with the Taylor Creek Group by Tipper (1969). However, the nonmarine nature, immaturity, and general contrast with respect to the Taylor Creek Group preserved west of Bluff Lake do not support such correlation. The possible Cenomanian age and gross lithological similarity suggest correlation with the Silverquick conglomerate of areas to the southeast (Mahoney et al., 1992; Garver, 1989; Garver et al., 1989; Glover et al., 1988). The syndimentary faulting control on sedimentation we infer has been suggested for Silverquick conglomerate in other areas (Mahoney et al., 1992; Garver, 1989).

Powell Creek volcanics

As described above, a gradational change over tens of metres marks the contact between the Silverquick conglomerate and an overlying volcanoclastic and volcanic unit we correlate with the Powell Creek volcanics of areas to the southeast. This unit is best exposed in the northeast Bussel Creek and northwest Tatla Lake map areas (Fig. 2). The upper contact is not exposed and probably is cut off by the Yalakom Fault to the northeast. A minimum thickness of several hundred metres (probably >500 m) is suggested from the outcrop extent.

This unit is dominated by matrix-supported volcanoclastic breccia and conglomerate. Bedding is rarely definable with tens to hundreds of metres of apparent thickness of massive, green-grey, medium- to fine-grained volcanoclastic wacke containing 5-30% subangular to angular volcanic pebbles to boulders randomly distributed throughout. Clasts are typically green-grey or less commonly dark red and of intermediate to less common mafic volcanic composition with common plagioclase phenocrysts. Volcanic flows up to several metres thick also occur interbedded with the volcanoclastics. The flows are identical in composition to the volcanoclastic clasts and it is difficult to discern true flows from clast-poor volcanic conglomerate unless outcrop exposure is exceptional. Only in the lower part of the unit are stratified interbeds present. In this gradational contact interval with the underlying sedimentary unit, volcanic conglomerate and rare flows occur interbedded with red-brown siltstone, fine grained lithic arenite, and grey carbonaceous mudstone.

The depositional environment of this volcanoclastic-volcanic unit is interpreted as a nonmarine, debris flow dominated alluvial fan system, part of an area of active volcanism. The tentative Cenomanian age supports correlation with Powell Creek volcanics described in areas to the southeast (Garver, 1989; Glover et al., 1988).

DISCUSSION

Several insights concerning this part of the Coast Belt-Intermontane Belt transition are apparent. Late Triassic strata make up a greater volume of this region than previously believed, including at least one plutonic body cutting

extensive volcanics of the Mt. Moore formation. In addition, the recognition of a distinctive marker horizon on both sides of the Tchaikazan Fault allows an estimate of 7-8 km of apparent dextral strike-slip movement related to this structure. The Mosley formation includes lower Norian mudstone (*Halobia*-bearing unit 3 of Tipper, 1969) and upper Norian limestone and sandstone (units 5 and 6 of Tipper, 1969). Variations in rock type in this formation are facies changes in a continuous, conformable succession.

The recognition of a gradational contact between the Lower Cretaceous Ottarasko and Cloud Drifter formations confirms the interpretations of Rusmore and Woodsworth (1993, 1989) that the Ottarasko formation is older than the Cloud Drifter formation, although probably in part they are lateral equivalents. "Mid"-Cretaceous strata of the Taylor Creek Group are restricted to a fault slice directly west of Bluff Lake. A thick nonmarine alluvial succession previously correlated with the Taylor Creek Group is correlated with the Late Cretaceous Silverquick conglomerate. A gradationally overlying volcanoclastic-volcanic unit is correlated with the Powell Creek volcanics and suggests renewed late Cretaceous volcanism in this area, as previously postulated for southern areas.

ACKNOWLEDGMENTS

Stellar assistance by Toby Pierce was key to completion of the mapping component of this project. Safe, reliable helicopter transport, unflagging logistical support, and sound advice were provided by Mike and Audrey King of Whitesaddle Air. Discussions and outcrop examinations with Margi Rusmore (Occidental College), Glenn Woodsworth (Cordilleran Division), and Paul Umhoefer (Northern Arizona University) contributed to our understanding of the regional geology. Hillary Taylor provided imaginative field assistance for two weeks as part of the GSC Volunteer Program. Manuscript review by Glenn Woodsworth and editing by Bev Vanlier (Cordilleran Division) improved the initial version of this paper.

REFERENCES

- Garver, J.I.**
1989: Basin evolution and source terranes of Albian-Cenomanian rocks in the Tyaughton basin, southern British Columbia: implications for mid-Cretaceous tectonics in the Canadian Cordillera; Ph.D. thesis, University of Washington, Seattle, 227 p.
- Garver, J.I., Schiarizza, P., and Gaba, R.G.**
1989: Stratigraphy and structure of the Eldorado Mountain area, Chilcotin Ranges, southwestern British Columbia; in Geological Fieldwork 1988; British Columbia, Ministry of Energy, Mines and Petroleum Resources, Paper 1989-1, p. 131-144.
- Glover, J.K., Schiarizza, P., and Garver, J.I.**
1988: Geology of the Noaxe Creek map area (92O/02); in Geological Fieldwork 1987; British Columbia, Ministry of Energy, Mines and Petroleum Resources, Paper 1988-1, p. 105-123.
- Mahoney, J.B., Hickson, C.J., van der Heyden, P., and Hunt, J.A.**
1992: The Late Albian-Early Cenomanian Silverquick conglomerate, Gang Ranch area: evidence for active basin tectonism; in Current Research, Part A; Geological Survey of Canada, Paper 92-1A, p. 249-260.
- Rusmore, M.E. and Woodsworth, G.J.**
1988: Eastern margin of the Coast Plutonic Complex, Mount Waddington map area, B.C.; in Current Research, Part E; Geological Survey of Canada, Paper 88-1E, p. 185-190.
1989: A note on the Coast-Intermontane belt transition, Mount Waddington map area, British Columbia; in Current Research, Part E; Geological Survey of Canada, Paper 89-1E, p. 163-167.
1991a: Coast Plutonic Complex: A mid-Cretaceous contractional orogen; Geology, v. 19, p. 941-944.
1991b: Distribution and tectonic significance of Upper Triassic terranes in the eastern Coast Mountains and adjacent Intermontane Belt, British Columbia; Canadian Journal of Earth Sciences, v. 28, p. 532-541.
1993: Geologic maps of the Mt. Queen Bess (92N/7) and Razorback Mountain (92N/10) map areas, Coast Mountains, B.C. 1:50 000; Geological Survey of Canada, Open File 2586.
in press: Evolution of the eastern Waddington thrust belt and its relation to the mid-Cretaceous Coast Mountains arc, western British Columbia; Tectonics.
- Tipper, H.W.**
1969: Mesozoic and Cenozoic geology of the northeast part of Mount Waddington map-area (92N), Coast District, British Columbia; Geological Survey of Canada, Paper 68-33, 103 p.
- van der Heyden, P., Mustard, P., and Friedman, R.**
1994: Northerly continuation of the Eastern Waddington Thrust Belt and Tyaughton Trough, Tatla Lake-Bussel Creek map areas, west-central British Columbia; in Current Research 1994-A; Geological Survey of Canada.
- Wheeler, J.O. and McFeely, P. (comp.)**
1991: Tectonic assemblage map of the Canadian Cordillera and adjacent parts of the United States of America; Geological Survey of Canada, Map 1712A, scale 1:2 000 000.

Preliminary study of Tertiary volcanic stratigraphy in the Clisbako River area, central British Columbia¹

Paul Metcalfe and Catherine J. Hickson
Cordilleran Division, Vancouver

Metcalfe, P. and Hickson, C.J., 1994: Preliminary study of Tertiary volcanic stratigraphy in the Clisbako River area, central British Columbia; in Current Research 1994-A; Geological Survey of Canada, p. 105-108.

Abstract: Three volcanic assemblages are exposed in the Clisbako River area of central British Columbia. The oldest undeformed units in the area are felsic to intermediate volcanic flows and pyroclastic rocks, which host hydrothermal alteration and mineralization. These are overlain by an assemblage of intermediate to mafic lava flows. The area of outcrop of the felsic volcanic rocks and the overlying mafic assemblage is a circular highland area, approximately 40 km in diameter. It is possible that this area is an eroded caldera, partially filled with younger basaltic lavas of the Chilcotin Group.

Résumé : Trois assemblages volcaniques affleurent dans la région de la rivière Clisbako, dans le centre de la Colombie-Britannique. Les unités non déformées les plus anciennes de la région sont constituées de roches pyroclastiques et de coulées volcaniques felsiques à intermédiaires, qui présentent des indices d'altération et de minéralisation hydrothermales. Ces unités sont surmontées d'un assemblage de coulées intermédiaires à mafiques. Le secteur d'affleurement des roches volcaniques felsiques et de l'assemblage mafique sus-jacent forme une zone de hautes terres circulaire d'environ 40 km de diamètre. Il est possible que cette zone soit une caldeira érodée, partiellement remplie de laves basaltiques plus jeunes du Groupe de Chilcotin.

¹ Contribution to Canada-British Columbia Agreement on Mineral Development (1991-1995), a subsidiary agreement under the Canada-British Columbia Economic and Regional Development Agreement.

INTRODUCTION

The primary objective of this project is to identify and correlate Tertiary volcanic rocks within the Interior Plateau as part of the Canada-British Columbia agreement on mineral development, 1991-1995 (van der Heyden et al., 1993). A

preliminary study of Tertiary volcanic stratigraphy in the Clisbako area of central British Columbia (Fig. 1) began in September 1993. The purpose is to determine the stratigraphic succession and petrological relationships of the Early Tertiary felsic volcanic rocks which host epithermal mineralization discovered on the BAEZ and CLISBAKO claim groups, near

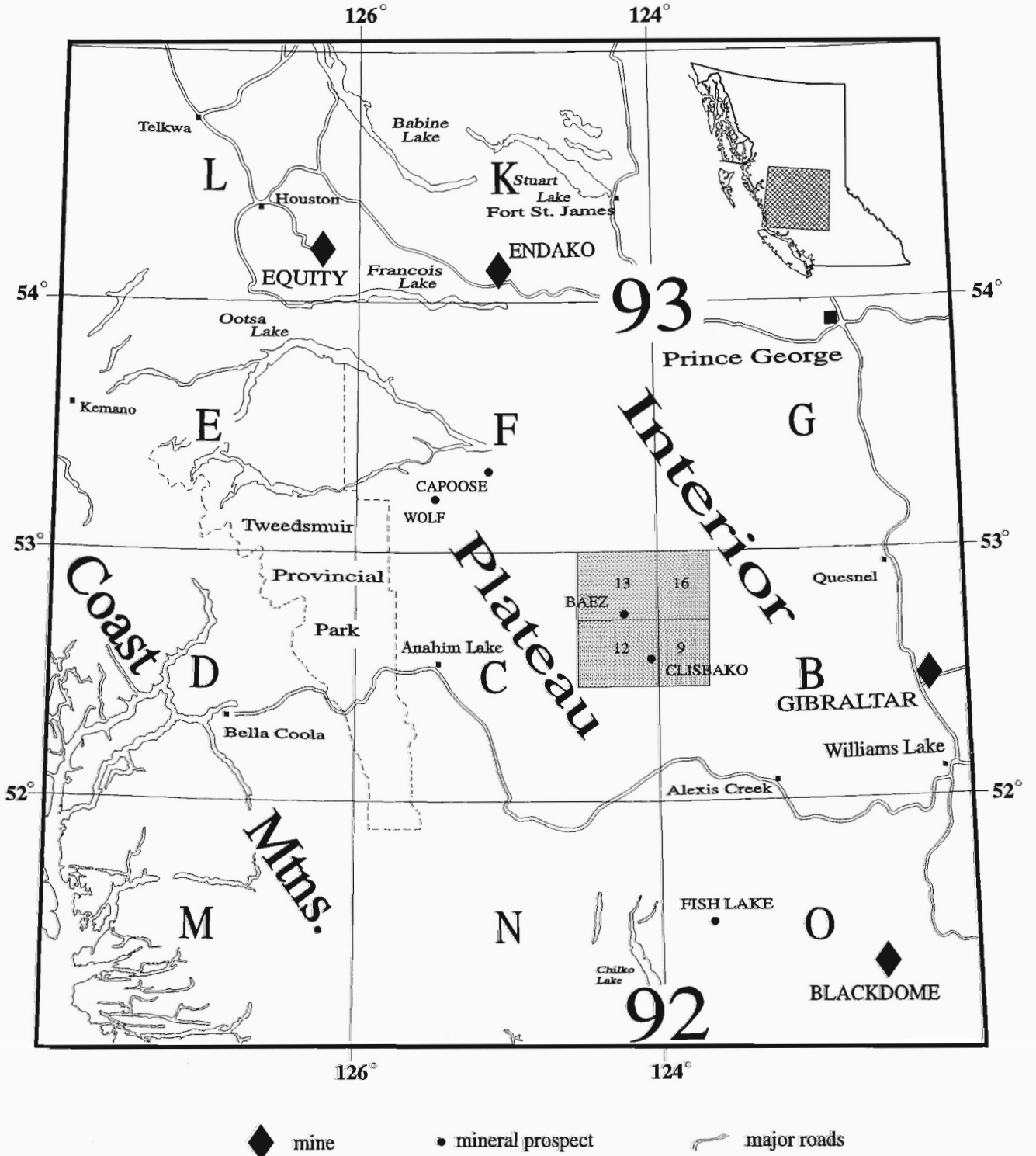


Figure 1. Location of the study area.

the headwaters of the Clisbako River. The study area comprises four 1:50 000 map sheets (93B/12, B/13, C/9, C/16) and is bounded by latitudes 52°30'N and 53°00'N and by longitudes 123°30'W and 124°30'W. The study area forms part of the Chilcotin plateau. Relief is gentle and the area forested. Outcrop is not abundant. The area is accessible by means of numerous logging roads, west from Quesnel and northeast from Anahim Lake. Findings from this study area will be compared with information from Tertiary volcanic rocks exposed to the north in the Nechako River area (93F) and to the south in the Taseko Lakes area (92O).

GEOLOGY

The basement to the Clisbako area consists of intermediate fragmental rocks which differ from other lithologies examined, in that a schistose foliation is present. Scarcity of outcrop precluded comprehensive structural mapping. Tipper (1959, 1969) assigned this assemblage to the Lower Jurassic Hazelton Group, based upon lithological similarity.

The basement rocks are overlain by a succession of felsic volcanic rocks which are the subject of the present study. These rocks underlie the cores of many of the ridges in the study area. This package was identified by Tipper (1959, 1969) as part of the Ootsa Lake Group. These volcanic rocks host many occurrences of hydrothermal alteration, brecciation and mineralization.

Felsic volcanic units, which outcrop in the study area, include four main lithologies. Contacts are rarely exposed and the stratigraphic relationship between the units has not yet been determined. Canyon Mountain, in the south-central portion of the area, is underlain by a felsic to intermediate unit with well-formed biotite and plagioclase phenocrysts. This lithology is poorly exposed, but also occurs as blocks in felsic tuff-breccias and lapilli tuffs in the eastern part of the area; it may be a product of one of the older phases of felsic volcanism.

The most commonly exposed felsic unit consists of black glassy flows with local plagioclase phenocrysts. The unit is structureless but locally it exhibits flow-banding and flow-folding. This lithology is resistant to erosion and, rarely, exhibits cliff exposures with spectacular colonnades as much as 30 m high. In other areas, particularly the northwest part of the study area, blocks of this unit, as much as 2 m in size are included in red- and yellow-weathering flow breccias; these units are as much as 100 m in total thickness.

Towards the centre of the study area scattered and rare outcrops of felsic pyroclastic rocks appear to underlie at least one unit of the black felsic flow breccias. The fragmental rocks are poorly consolidated, recessively weathered and incorporate blocks of both mafic and felsic volcanic rocks. The source of the mafic volcanic rocks is presently unknown.

The felsic and intermediate volcanic package is overlain by a series of intermediate or basaltic lava flows. Several of the ridges, particularly in the far east and west of the study area, are capped by this assemblage. The flows are weakly to

moderately porphyritic, with plagioclase phenocrysts and, less commonly, an altered mafic phase, possibly olivine. The basal contact of this assemblage was not observed, but outcrop relationships suggest that it succeeded eruption of the felsic units. Hydrothermal alteration similar to that observed in the felsic volcanic rocks is also present in some exposures of the ridge-capping assemblage.

Relatively well-exposed basaltic lava flows occur in most of the valleys in the study area. These lavas are distinctively fresh in appearance and commonly show well-developed colonnades and flow tops. They were assigned by Tipper (1959, 1969) to the Miocene Chilcotin Group and described by Mathews (1989). Tipper also noted the presence of a number of small cinder cones in the valleys and on ridge crests, which are probable source vents for the lavas. It is possible that these cones are more abundant than suggested by Tipper's mapping. Their relative ages are not known but this assemblage appears unaffected by hydrothermal alteration. Basaltic eruptions associated with the Anahim volcanic belt extend across the study area to the 7200 Ka Nazko cone (Souther et al., 1987).

SUMMARY

The study area contains three dominant volcanic assemblages, resting upon a deformed volcanic basement of presumed Jurassic age. The oldest undeformed units in the area are felsic to intermediate volcanic flows and fragmental deposits, which host hydrothermal alteration and mineralization. These are capped by intermediate to mafic lava flows.

The outcrop area of the felsic volcanic rocks and the overlying mafic assemblage forms an approximately circular highland area with a diameter of approximately 40 km. The area is eroded to the north, exposing the basement and the central part of the area is a topographic low, partially filled by younger basaltic lavas of the Chilcotin Group. It is possible that the area described was the site of a large composite volcano which underwent caldera formation and subsequent erosion, prior to the eruption of the Chilcotin Group basalts. Implicit in this are the possibilities that the (presently) subeconomic mineralization of the Clisbako area is related to caldera formation and that exploration targets in the area may be masked by the present cover of the Chilcotin Group lavas.

ACKNOWLEDGMENTS

Fieldwork for this project was made possible through the British Columbia – Canada Mineral Development Agreement. The authors are indebted Jim Dawson and to Metall Inc., for providing useful discussions, a base map, and geological information from the Clisbako property; to David Bridge of the Mineral Deposit Research Unit at the University of British Columbia, for his assistance in the field and to Peter van der Heyden for his rapid and thorough critical review of this manuscript.

REFERENCES

Mathews, W.H.

1989: Neogene Chilcotin basalts in south-central British Columbia: geology, ages and geomorphic history; Canadian Journal of Earth Sciences, v. 26, p. 969-982.

Souther, J.G., Clague, J.J., and Mathews, R.W.

1987: Nazko Cone: a Quaternary volcano in the eastern Anahim Belt; Canadian Journal of Earth Sciences, v. 18, p. 2477-2485.

Tipper, H.W.

1959: Geology, Quesnel, British Columbia (93B); Geological Survey of Canada, Map 12-1959, 1" to 4 miles.

1969: Geology, Anahim Lake, British Columbia (93B); Geological Survey of Canada, Map 1202A, 1" to 4 miles.

van der Heyden, P., Shives, R., Ballantyne B., Harris, D., Dunn, C., Teskey, D., Plouffe, A. and Hickson, C.J.

1993: Overview and preliminary results for the Interior Plateau Program, Canada-British Columbia Agreement on Mineral Development 1991-1995; in Current Research, Part E; Geological Survey of Canada, Paper 93-1E, p. 73-79.

Geological Survey of Canada Project 930025

The geology and structure of the Coryell Batholith, southern British Columbia

Patrick Stinson¹ and Philip S. Simony¹

Cordilleran Division

Stinson, P. and Simony, P.S., 1994: The geology and structure of the Coryell Batholith, southern British Columbia; in Current Research 1994-A; Geological Survey of Canada, p. 109-116.

Abstract: The Eocene Coryell Batholith west of Rossland was investigated during the summers of 1992 and 1993. Detailed mapping of the eastern third revealed that it consists of several varieties of syenite and monzonite, as well as fine grained dyke rocks. The shallow dip of the eastern contacts and a large roof pendant indicate that the level of exposure is in the roof zone. Emplacement related foliations are well developed in the northeast portion of the batholith and weakly developed elsewhere. These are subparallel to the margins.

The batholith and its country rocks are cut by north-trending extensional structures concentrated along the western edge of the study area; gently east-dipping mylonite zones are cut by near-vertical brittle faults. East-side-down movement took place along these structural zones. Both the Coryell Batholith and the north-trending structures are manifestations of Eocene extensional tectonics.

Résumé : Le batholite éocène de Coryell, à l'ouest de Rossland, a été étudié en 1992 et 1993. Le levé détaillé du tiers oriental a montré que le batholite est constitué de plusieurs variétés de syénite et de monzonite aussi bien que de dykes microgrenus. Le pendage faible du contact oriental et la présence d'un grand pendentif montrent que le niveau d'affleurement est proche de celui du toit du batholite. Des foliations largement parallèles aux marges du batholite et liées à sa mise en place sont nettes dans la partie nord-est du batholite, mais elles sont faibles ailleurs.

Le batholite et ses roches encaissantes sont recoupés par des structures de distension de direction nord et concentrées le long de la marge occidentale de la région levée. Des zones de mylonite à faible pendage vers l'est sont recoupées par des failles cassantes presque verticales et de direction nord dont les lèvres orientales sont affaissées. Ces structures, aussi bien que le batholite, sont des manifestation d'une distension à l'Éocène.

¹ Department of Geology and Geophysics, The University of Calgary, 2500 University Drive N.W., Calgary, Alberta T2N 1N4

INTRODUCTION

The Rossland-Trail region of the southeastern Omineca Belt is an area with a complex intrusive and structural history. At least five phases of intrusion occur in the Jurassic to Eocene time span. These include the mid-Jurassic Rossland Monzonite, granodiorites of the Nelson suite, including the Trail and Mackie plutons, the Cretaceous Kinnaird Gneiss, and the Eocene College Creek Pluton, Sheppard intrusions, and the Coryell intrusive suites.

The geological framework into which these intrusions were emplaced belongs to the eastern portion of Quesnel Terrane and consists of Paleozoic gneisses overlain by the Pennsylvanian Mount Roberts Formation and the Lower Jurassic Rossland Group of arc volcanics and sediments. Locally, west and south of Rossland, Upper Cretaceous Sophie Mountain conglomerate and the Eocene (?) O.K. volcanics are preserved.

During much of the Eocene the southern Omineca Belt was affected by extension resulting in movement on numerous brittle and ductile faults, and the uprise of metamorphic

core complexes such as the Valhalla Complex northeast of Rossland and the Kettle Complex west of Rossland (Parrish et al., 1988). Two Eocene intrusive suites have been mapped in the Rossland area: the Coryell and Sheppard intrusions.

The Coryell Suite is represented in the Rossland-Trail area by the Coryell Batholith, which extends westward from Rossland to Christina Lake (Fig. 1). It has an outcrop area of about 400 km², and is related to numerous small stocks, extensive north-south felsic dykes, and possibly the O.K. volcanics, which were correlated with the Eocene Marron Volcanics by Little (1982). Coryell syenite from the Valhalla Complex, Greenwood area, and northeast Washington yield U-Pb and K-Ar ages of 51 to 52 Ma (Carr et al., 1987; Carr and Parkinson, 1989; Pearson and Obradovich, 1977; respectively). Coryell intrusions cut the ductile east-directed extensional Valkyr Shear Zone along the west side of the Valhalla Complex (Carr et al., 1987), but they are cut by the west-dipping brittle normal faults to the west of the Kettle Complex (Carr and Parkinson, 1989) and by the east-dipping Kettle Fault. We have also found steep brittle extensional faults in the Coryell Batholith.

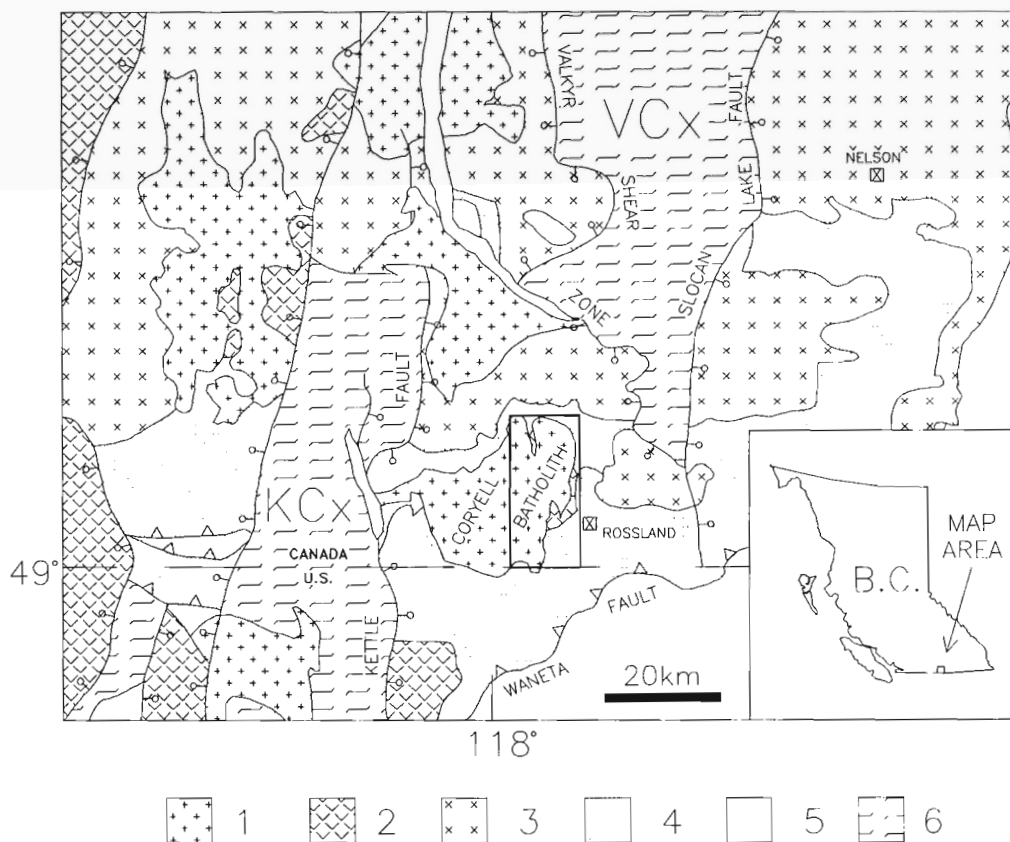


Figure 1. Generalized geology of the Rossland area (modified from Andrew et al., 1991; Little, 1982; Parrish et al., 1988; Wheeler and McFeely, 1991; Yates, 1971). VCx, Valhalla Complex; KCx, Kettle Complex; Lithologies: 1, Eocene (Coryell) syenites; 2, Eocene volcanics; 3, Jurassic to Paleocene intrusions; 4, Paleozoic to Jurassic volcanics and sediments; 5, rocks of North American affinity; 6, gneisses of the Valhalla and Kettle complexes. Area of Figure 2 is indicated by the bold outline.

Earlier geological work in the Rossland area had emphasized the Jurassic intrusions and volcanics which host historically important mineral deposits of the Rossland camp. Previous studies include Drysdale (1915), Little (1982), Fyles (1984), Höy and Andrew (1991), and Höy et al. (1992). Daly (1912) mapped the Coryell Batholith and Rossland area as part of his coverage along the Canada-U.S. border. He distinguished the various intrusive suites, but not the Jurassic and Tertiary volcanic units.

Study of the Coryell Batholith was undertaken to determine its geometry, the relation of the batholith to its country rocks and to extensional structures in the region. The various phases that make up the batholith and their internal relations have never been documented before, yet these relations have to be established to understand the emplacement.

The role of extension in the intrusion of the Coryell Batholith is probable, as extension and intrusion overlap in time. Study of the batholith will enable models of extension to be tested as a mechanism for the emplacement of large volumes of magma (Paterson et al., 1991).

The eastern third of the Coryell Batholith and its country rocks were mapped westward from Highway 3B to the valley of Big Sheep Creek. Road access is fairly good for most of this area. The topography was digitized into AutoCAD (trademark of Autodesk, Inc.) and traverses were entered using Fieldlog (Brodaric and Fyon, 1989).

LITHOLOGY

Rock types in the study area include the syenites and lesser monzonites of the Coryell Batholith and the country rocks they intrude (Fig. 2). These consist of mainly Paleozoic to Eocene sediments, volcanics, and several pre-Coryell intrusive units.

Country rock

The principal country rocks include the Upper Paleozoic Mount Roberts Formation, the Jurassic Rossland Group, Upper Cretaceous Sophie Mountain Formation, and Eocene (?) volcanic rocks herein called the O.K. volcanics following the usage of Fyles (1984). The Coryell Batholith also cuts the western margin of the Jurassic Mackie Pluton.

Clastic and carbonate rocks of Mount Roberts Formation are exposed around the north half of the batholith. Contact metamorphism of impure limestone units has formed epidote-bearing skarns, and in places potentially economic wollastonite deposits. One skarn sample contains scapolite, diopside, actinolite, calcite, and andradite. More common lithologies are black, rusty weathering hornfelsed siltstones, greywackes, coarse sandstones, and pebble conglomerates in the Granite Mountain area. A package of strongly deformed sedimentary rocks east of the O.K. Fault on the east side of the batholith consists of conglomerates (felsic clasts in a darker silty sand matrix) grading upward to the east into sandstones and rusty siltstones. Tops to the east are indicated by rare graded beds. The conglomerates east of the fault have

been assigned to the Elise Formation of Rossland Group by Little (1982) and by Höy and Andrew (1991) but Fyles (1984) included them in the Mount Roberts Formation. This interpretation is preferred here because the conglomerates resemble the Mount Roberts conglomerates, and are interbedded with Mount Roberts sandstones at the foot of Mount Roberts.

Mafic volcanics of the Elise Formation of Rossland Group occur in the southern part of Big Sheep Creek valley, to the north along Lamb Creek, and locally along Highway 3B. These are comparable to Rossland volcanics described from elsewhere in the Rossland area (Little, 1982; Höy and Andrew, 1991). Lithologies in the study area consist of intermediate to mafic crystal-rich tuffs and volcanoclastic conglomerates. In the northwest and southwest corners of the map area Rossland volcanics and Mount Roberts meta-sediments have a strong east-dipping foliation and down-dip lineation, and are intruded by Coryell dykes parallel to this fabric.

South of Rossland, near latitude 49°N, conglomerates of the Upper Cretaceous Sophie Mountain Formation are intruded by Coryell dykes. Sophie Mountain Formation consists of clast-supported quartzite boulder conglomerates that are distinct from the heterolithic conglomerates of the Jurassic Elise Formation which they unconformably overlie. Rare mudstone beds in the Sophie Mountain Formation have yielded Late Cretaceous plant fragments (Little, 1982).

Igneous rocks intruded by the Coryell Batholith include granodiorites, diorites, quartz-feldspar porphyry, and serpentinite. Granodiorite and diorite occur as xenoliths in the medium grained monzonite unit of the batholith and are probably derived from the Jurassic Mackie Pluton to the northeast of Coryell Batholith (Crowe, 1981). A 4-5 km² body of quartz-feldspar porphyry occurs on the batholith's southeastern margin, and is intruded by dykes related to the batholith and andesitic dykes probably related to the O.K. volcanics. The quartz-feldspar porphyry cuts the Elise Formation (Little, 1982), is in fault contact with the serpentinite body to its east, but no relationship was observed with the Sophie Mountain conglomerate. Little (1982) speculated that the quartz-feldspar porphyry was Early Cretaceous, which is likely, as map relations suggest that the quartz-feldspar porphyry and the Elise Formation are unconformably overlain by the Upper Cretaceous conglomerate. The origin and emplacement of the serpentinites are poorly understood; they are in fault-contact with all units except for both the coarse grained and hypabyssal phases of the batholith which intrude them. They are very strongly deformed and sheared; probably they were emplaced during thrusting in the Jurassic accretionary event before being placed against the O.K. volcanics by pre-batholith normal faults.

The O.K. volcanics form a large, gently west-dipping panel along the eastern margin of the batholith bounded on the east by the west-dipping O.K. Fault. Also a large roof pendant of O.K. volcanics makes up the top 300 m of Old Glory Mountain. The base of this volcanic package was mapped by Little (1982) in two roof pendants within the northern portion of the batholith, north of Old Glory Mountain. There he identified white arkosic tuffs overlying

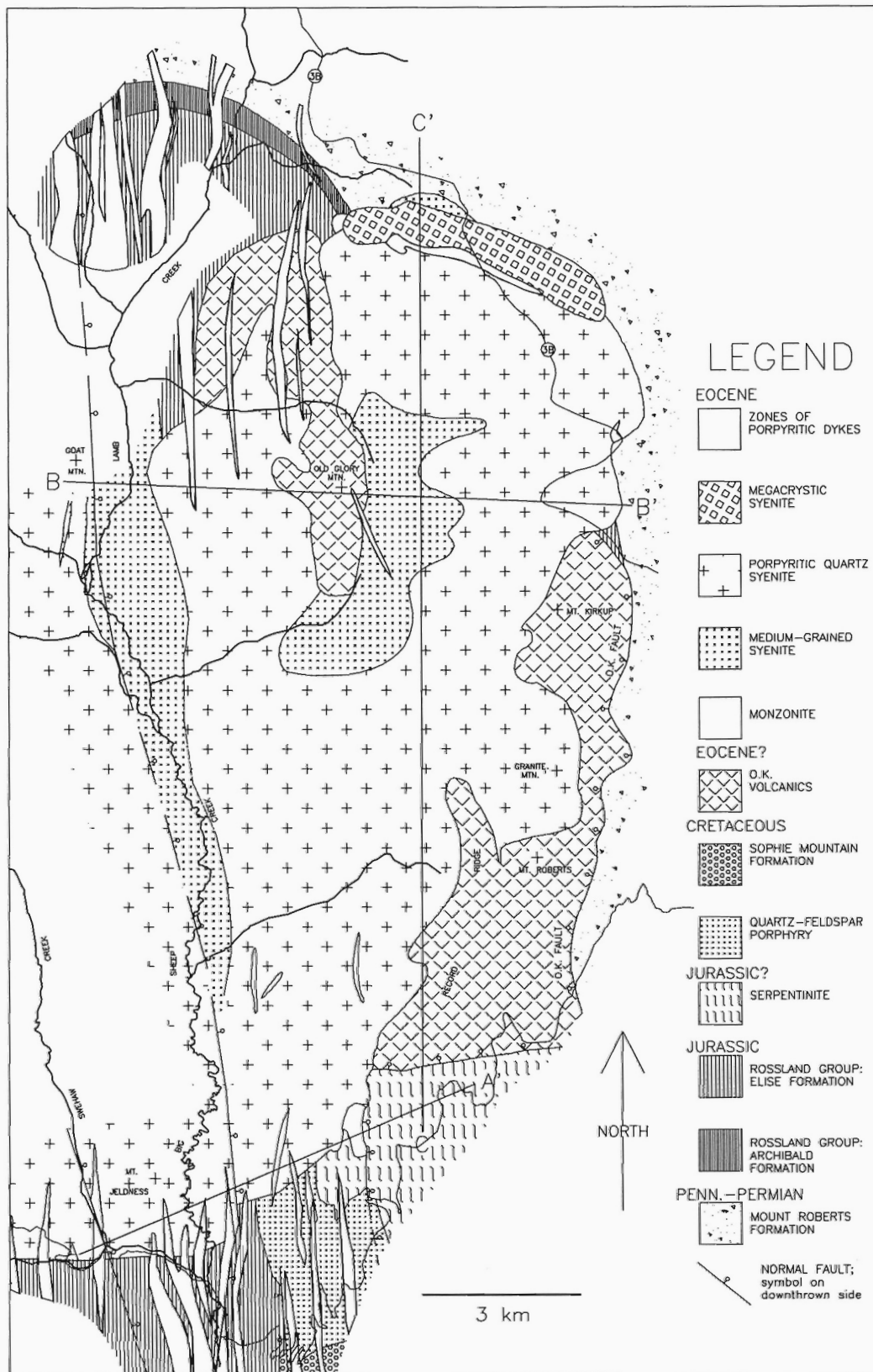


Figure 2. Geological map of the eastern third of the Coryell Batholith. Areas indicated as being porphyritic syenite dykes represent regions where dykes make up 50 to 100% of the outcrop.

the Rossland Group and correlated these with the Eocene Kettle River Formation which underlies the Marron Formation in the Greenwood map area to the west (Little, 1983). Our mapping revealed these and other similar fragmental rocks to be interbedded with O.K. lavas, suggesting that the Kettle River Formation is not present in this area. The panel of O.K. volcanics on the east side of the batholith dips and faces west. Its base is not exposed due to truncation by the O.K. Fault, and the top is lost to erosion. The exposed stratigraphic thickness ranges from 450 to 900 m. The base of the O.K. volcanics is present in two locations in the study area: a small roof pendant northwest of Old Glory Mountain where it unconformably overlies shales of the upper Rossland Group (Hall Formation), and an isolated body in the south where it overlies serpentinite unconformably.

The O.K. volcanics consist of felsic to intermediate lava flows and tuffs, and epiclastic sandstones and conglomerates. Where exposure is good, individual flows are 5 to 15 m thick, locally autobrecciated, and have irregular or clinkery tops with rare thin sediment accumulations in the depressions. Compositionally they range from trachytic to andesitic, and are usually porphyritic. Only one rhyolite lava was seen but clasts of rhyolite lava occur in several conglomerate horizons. The remainder of the sections are made up of volcaniclastic sandstones and conglomerates with some interbedded tuffs and lapilli tuffs. Base-surge deposits were identified in some areas based on the presence of accretionary lapilli-bearing horizons and rare dune-forms in thinly bedded tuffs. Possible air-fall tuffs and scoria-flow deposits were also recognized.

There appear to be wide facies variations across and along strike; no correlations were possible from one ridge to the next, neither of individual units nor of packages of units. Based on the thickness and intermediate composition of

individual lava flows they are unlikely to have been voluminous or fluidal enough to extend across neighbouring ridges 1 to 2 km apart. Hydrothermal alteration is extensive so chemical variations or trends are unlikely to have been preserved.

Recent work in this area (Little, 1982) has treated this volcanic package as being part of the Eocene Marron Formation, a mildly alkaline volcanic package in the Tertiary volcano-sedimentary succession mapped near Pentiction (Church, 1973). This correlation was based on similarity between several thin sections of lavas from the Tertiary volcanics near Rossland and the Marron Formation near Pentiction (Little, 1982). This correlation is unlikely considering the great distance between these localities, even with restoration of Eocene extension, and the fact that the O.K. volcanics are clearly of local derivation. They may, however, be part of the Eocene Pentiction Group (Church, 1982) which represents an episode of widespread variably alkaline volcanism occurring over south-central British Columbia and north-eastern Washington, of which the Marron and Kettle River formations are part. Coryell or similar intrusive rocks outcrop over much of this area and are probably broadly related to this volcanism. In the Rossland area some early units of the Coryell Batholith may be comagmatic with some of the O.K. volcanics, but this has yet to be demonstrated. In this study area, however, the age of the O.K. volcanics are only constrained to being older than middle Eocene (when they were intruded by the batholith) and younger than the widespread Late Jurassic deformation and plutonism.

Late rare lamprophyre and other mafic dykes occur in the study area, cutting the Mount Roberts Formation, the O.K. volcanics, and many of the batholith phases, including the earlier porphyritic syenite dykes. They also intrude along the

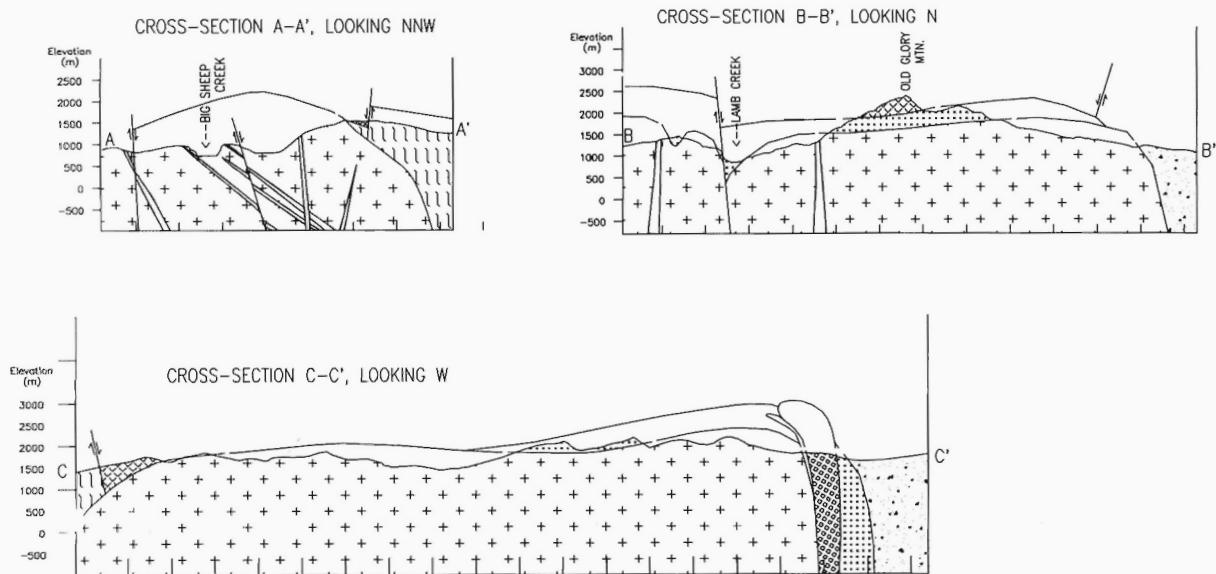


Figure 3. Cross-sections across the map area. Section locations are shown in Figure 2. Contacts above ground level are projected from outcrops near the lines of section. Symbols are the same as in Figure 2.

O.K. Fault Zone in places, and are common all through the Rossland-Trail area including the underground workings of the Rossland gold mines (Drysdale, 1915, p. 30-34). They are therefore among the youngest rocks in the study.

Coryell Batholith intrusive phases

The Coryell Batholith consists of several coarse grained intrusive phases, mainly syenite and monzonite. Although the main phases of the batholith in the study area are coarse grained, many dyke phases are seen, especially along Big Sheep Creek and Lamb Creek.

By far the most voluminous phase is porphyritic quartz syenite. This unit underlies almost the entire mapped area of the batholith, except around Old Glory Mountain, where it is capped by medium grained syenite, which in turn is capped by the large roof pendant of O.K. volcanics (Fig. 3). The porphyritic quartz syenite has a hypidiomorphic texture with stubby orthoclase phenocrysts up to 3 cm long; it includes 8 to 15% hornblende, and 4 to 5% interstitial quartz. It is homogeneous and free of enclaves, except for local small ovoid dioritic autoliths and weak schlieren. The north half of the unit has a foliation defined by alignment of orthoclase phenocrysts. It varies in intensity from weak near Granite Mountain to strong in the northeast. In thin section the strong fabric is shown to have developed in the solid state, with orthoclase phenocrysts and the other constituents having undulose extinction and in places being thoroughly recrystallized. This foliation is subparallel to, and most intense near, the margins of the unit suggesting the fabric is related to emplacement. Where the fabric is weaker and more irregular the phenocrysts and matrix are unstrained, suggesting that this might represent an original magmatic foliation subparallel to the margins of the body, but with a steeper dip.

Medium grained syenite occurs as a flat-lying sheet overlying porphyritic quartz syenite near the middle of the map area, in isolated exposures in the northeastern part of the batholith, and along portions of the eastern side of Big Sheep Creek valley. It has a hypidiomorphic granular, seriate texture, locally porphyritic. It is distinguished from quartz syenite by having a higher colour index (approx. 20), less quartz, and a high sphene content (2-3%). An antirapakivi texture (orthoclase overgrowing oligoclase) is common and well-developed. Both syenite units have somewhat gradational contacts with one another. Medium grained syenite occurs as a rootless flat-lying sheet in the roof of the quartz syenite pluton, which suggests that it is a roof pendant.

Megacrystic syenite forms an elongate pluton about 2 km long along the northeastern margin of the batholith. It consists of around 30% euhedral tabular orthoclase megacrysts 2 to 6 cm long in a fine- to medium-grained quartz syenite groundmass. The colour index is approximately 10, the main mafic minerals being subequal amounts of hornblende and biotite. Megacrysts contain minor inclusions of oligoclase and biotite. The unstrained megacrysts define a strong foliation and

the groundmass in which they are suspended is unstrained. This suggests that the foliation is magmatic (see Paterson et al., 1991). This foliation is subparallel to the long axis of the body, as well as to the fabric in the adjacent outcrops of porphyritic quartz syenite.

Three varieties of monzonite make up a screen that separates the megacrystic syenite body from the main porphyritic quartz syenite body. These consist of medium grained monzonite, biotite monzonite, and augite biotite monzonite. The medium grained monzonite is characterized by recessively weathering ovoid mafic clots up to 6 mm across. Near its western limit it is xenolithic, containing sedimentary, volcanic, and igneous xenoliths 5 cm to 3 m across which are commonly partially assimilated. The other monzonites are both coarse grained and are characterized by biotite flakes up to 2 cm across. They are distinguished on the basis of different proportions of mafic minerals; biotite monzonite contains 15% biotite, 5% augite, and <1% hornblende; augite biotite monzonite contains up to 20% each of biotite and augite, about 5% each of olivine and enstatite, and 1-2% hornblende. These two units are both recrystallized, with 0.5 to 2 cm unstrained flakes of biotite having overgrown locally developed layering in the augite monzonite. This may have occurred when the monzonites were heated during the intrusion of the syenites.

Two phases of felsic fine grained porphyritic intrusives occur in and near the batholith. Fine grained porphyritic syenite occurs as 0.5 to 5 m wide dykes crosscutting all other units. Although concentrated in the area surrounding Big Sheep Creek Valley, they occur over the entire map area. Many of the dykes strike north and dip steeply. They have a fine- to very fine-grained syenitic groundmass with around 40% phenocrysts of orthoclase, plagioclase, and biotite. The other common variety is porphyritic syenite, or trachyte, which contains glomerocrysts of feldspar, and occasional embayed quartz phenocrysts in a fine- to medium-grained groundmass dominated by orthoclase with lesser oligoclase. It has a distinctive pink or green-brown colour due to clayey alteration of feldspars and mafic minerals. It has been mapped around the north and south ends of Big Sheep Creek valley, typically as 3 to 40(+) m wide dykes cutting the batholith and the country rock.

STRUCTURE

The two principal structural elements in the study area are the Coryell Batholith and the extensional faults. To the east of Coryell Batholith, a complex sequence of Jurassic and younger fold and fault structures has been recognized (Little, 1982; Simony, 1979; Höy and Andrew, 1991) but it is difficult to decipher the structures into which the batholith was emplaced. At depth the batholith must have penetrated the west-dipping Mesozoic thrust structures and the down-dip continuation of the Valkyr Shear Zone (Carr et al., 1987).

The batholith is composite, consisting of several intrusive units. The eastern portion of the batholith is dominated by the north-trending porphyritic quartz syenite body (Fig. 2). As illustrated in the cross-sections of Figure 3, the roof of that large pluton is in part preserved in the Old Glory Mountain and Record Ridge areas. A panel of east-dipping and east-facing O.K. volcanics making up the top of Old Glory Mountain is a remnant of the roof. This panel is underlain by medium grained syenite forming a gently dipping "cap". If the steeply dipping band of medium grained syenite along the east side of Big Sheep Creek valley was continuous with the "cap" prior to erosion, then it outlines the steep west wall of the quartz syenite pluton. Porphyritic quartz syenite on the west side of Big Sheep Creek would then form part of another, but closely related, unit of the batholith.

Along the north and south boundaries of the quartz syenite body swarms of closely spaced or sheeted north-striking and steeply dipping dykes of porphyritic trachyte and micro-syenite represent continuations of the batholith. Near the 49th parallel these dykes occupy steeply east-dipping foliations within the Rosslund volcanics.

The porphyritic quartz syenite body is bounded at its northeast limit by monzonite which forms a steeply dipping screen separating the quartz syenite pluton from a small mass of megacrystic syenite. Both syenite bodies invaded the monzonite, but the megacrystic phase is interpreted to be younger than the quartz syenite because both the latter and the monzonites of the screen have solid-state foliations. Orthoclase in the megacrystic body is aligned by magmatic flow parallel to the walls of the body, but no foliation has been imposed on the groundmass.

Syenitic, intermediate, mafic, and lamprophyric dykes are widespread in the area. In the Coryell Batholith and its immediate vicinity syenitic dykes are particularly abundant and are probably related to the batholith. The majority of the dykes strike north and have very steep dips. The dykes cut the O.K. volcanics, and all older rocks, and at least the earlier phases of the batholith. Intermediate, hornblende-phyric dykes related to the O.K. volcanics are common near the O.K. Fault Zone and the directly underlying Mount Roberts Formation, but not in the syenites.

Deformation during and after the intrusion of the batholith was of two principal styles. Ductile shearing before and somewhat after the intrusion of porphyritic quartz syenite was important in the southern part of Big Sheep Creek valley, at the 49th parallel. West-dipping ductile faulting (O.K. Fault and others) also predated the intrusion of the quartz syenite. Late brittle faulting postdates all rock units and is concentrated in the valleys of Big Sheep Creek and Swehaw Creek.

In the southwestern corner of the Big Sheep Creek valley, near the 49th parallel, a penetrative ductile fabric characterizes the Rosslund Group volcanics. This fabric strikes north and dips moderately to the east, with a strong down-dip lineation. Late porphyritic syenite dykes were intruded parallel to this fabric and are undeformed. Within the foliated volcanics post-tectonic amphibole porphyroblasts have overgrown

the fabric as a result of heating by the abundant microsyenite dykes related to the large porphyritic quartz syenite pluton to the north.

In the batholith just to the north of the foliated volcanics along Big Sheep Creek there are discrete ductile shear zones up to 10 m wide whose planar-linear fabric is parallel to that of the volcanics. These shears cut the otherwise undeformed batholith and are not parallel to the weak east-trending magmatic foliation in this region of the batholith. Kinematic indicators (winged porphyroclasts and rare mica fish) in these shears indicate hanging-wall-down to the east. The shear zones in the batholith indicate that the shearing strain that affected the Rosslund volcanics continued until after the intrusion and early consolidation of the porphyritic quartz syenite body.

In the study area the extensional faulting can be divided into two sets, separated in time by the intrusion of the porphyritic quartz syenite of the batholith.

An earlier set of west-dipping normal faults such as the O.K. Fault and the faults bounding the serpentinite body predate the intrusion of the porphyritic quartz syenite body. The O.K. Fault is exposed on the southeast corner of Granite Mountain, where it is a healed fault zone 5-10 cm wide with a 2 m wide zone of mylonitic foliation around it. This zone crosscuts, at a low angle, the strong foliation in the footwall Mount Roberts conglomerates. Fyles (1984) mapped this fault and several more to the east; he estimated that the O.K. Fault had a net slip of 600 to 1000 m. This fault appears to terminate northward against the batholith. The faults bounding the serpentinite body are unexposed, but they are probably similar, as a parallel zone of strong foliation occurs in the adjacent serpentinite.

The later set of faults, including the Big Sheep Creek and Swehaw Creek faults, cut the porphyritic quartz syenite pluton. On either side of the linear valley of Swehaw Creek there are zones where the syenite is locally crushed. In these crushed zones feldspar grains are crossed by microcracks and outcrops are laced with chlorite- and epidote-coated fractures, some of which display slickenlines (grooves and chlorite mineral fibres). In thin section this zone is seen to consist of protocataclastite with strong calcite-chlorite alteration. This indicates significantly lower P-T conditions than in the nearby shear zones in the syenite where hornblende is stable. Orientation of the slickensided surfaces is variable, but most have steep east or west dips with slickenlines pitching 70 to 90 degrees. Tracing the fault zone across topography also suggests near vertical dips.

A zone of crushed rocks including a distinct 10 to 20 m wide fracture zone crosses the low ridge of syenite in Big Sheep Creek valley just north of latitude 49°. The crushed zones are similar to those near Swehaw Creek. Crush zones were also discovered along the steep east flank of Goat Mountain and along the east side of the valley west of Record Ridge where monzonite is apparently offset against medium grained syenite to the east. Therefore the southern straight segment of Big Sheep Creek probably follows the trace of a

steep fault. Slickenside surfaces and fracture zones with cataclasis suggest a near-vertical dip; and slickenlines have steep pitches implying that motion was largely dip-slip.

The Swehaw and Big Sheep Creek faults are possibly fault strands in a broad zone extending through the centre of the batholith. It is on the east side of these faults that the O.K. volcanics are preserved in the roof of the batholith, and that the unconformity underlying the Upper Cretaceous Sophie Mountain Formation is lowest. These suggest east-side-down motion on the brittle faults, as on the older ductile shear zones. These faults probably belong to the set of north-striking faults, such as the Kettle and Slocan Lake faults, formed during the Eocene extension (Parrish et al., 1988).

CONCLUSIONS

The Coryell Batholith is a large composite quartz syenite, syenite, and monzonite intrusion. A homogeneous porphyritic quartz syenite pluton makes up most of the mapped area. Older sedimentary and volcanic country rocks and the earlier Coryell syenite and monzonite phases make up roof pendants or overlie the porphyritic quartz syenite body's outward-dipping contacts. Megacrystic syenite forms a late, 2 km long pluton on the northeast margin of the quartz syenite body. North-south striking porphyritic syenitic dykes are abundant in the coarse grained intrusives and surrounding country rocks.

The most significant structures, aside from the batholith itself, are east-dipping ductile mylonite zones and later steep brittle faults. A zone of strong ductile deformation in Jurassic volcanics in the southwestern part of the map area continues into the batholith as discrete shear zones, suggesting that deformation at least partly postdated intrusion. This was followed by brittle faults along the same trend. Several criteria give an east-side down sense to both episodes of deformation. The structural style in this area is compatible with Eocene extensional deformation elsewhere in the southern Omineca Belt.

ACKNOWLEDGMENTS

The authors would like to acknowledge the valuable assistance of Richard Guthrie and John Van Ham in the field during the last two summers. Discussions with Sharon Carr (Carleton University), Dan Werhle (Vangold Resources), David Pattison, Charles Ferguson, Jim Vogl (all of the University of Calgary) were very helpful. The computer mapping lab of the Department of Geology and Geophysics at the University of Calgary under the supervision of T.M. Gordon was of great assistance in this project. This paper was greatly improved by a critical review by J.O. Wheeler. Research was supported by NSERC operating grants and EMR research agreements held by Philip Simony.

REFERENCES

- Andrew, K.P.E., Höy, T., and Simony, P.S.**
1991: Geology of the Trail map area, southeastern British Columbia; British Columbia Ministry of Energy, Mines, and Petroleum Resources, Open File 1991-16.
- Brodaric, B. and Fyon, J.A.**
1989: OGS FIELDLOG: A microcomputer-based methodology to store, process, and display map-related data; Ontario Geological Survey, Open File Report 5709, 73 p. and 1 diskette.
- Carr, S.D. and Parkinson, D.L.**
1989: Eocene stratigraphy, the age of the Coryell Batholith, and extensional faults in the Granby Valley, southern British Columbia; in Current Research, Part E; Geological Survey of Canada, Paper 89-1E, p. 79-87.
- Carr, S.D., Parrish, R., and Brown, R.L.**
1987: Eocene structural development of the Valhalla Complex, southeastern British Columbia; *Tectonics*, v. 6, p. 175-196.
- Church, B.N.**
1973: Geology of the White Lake Basin; British Columbia Department of Mines and Petroleum Resources, Bulletin 61, 120 p.
1982: Notes on the Penticton Group: a progress report on a new stratigraphic division of the Tertiary, south-central British Columbia; in Geological Fieldwork 1981; British Columbia Ministry of Energy, Mines, and Petroleum Resources, Paper 1982-1, p. 12-16.
- Crowe, G.G.**
1981: The structure and evolution of the Mackie Plutonic Complex, southern British Columbia; M.Sc. thesis, University of Calgary, Alberta, 154 p.
- Daly, R.A.**
1912: North America Cordillera; Forty-ninth Parallel; Geological Survey of Canada, Memoir 38, pts. 1, 2, and 3.
- Drysdale, C.W.**
1915: Geology and ore deposits of Rosslund, British Columbia; Geological Survey of Canada, Memoir 77.
- Fyles, J.T.**
1984: Geological setting of the Rosslund Mining Camp; British Columbia Ministry of Energy, Mines, and Petroleum Resources, Bulletin 74.
- Höy, T., Dunne, K.P.E., and Wehrle, D.**
1992: Tectonic and stratigraphic controls of gold-copper mineralization in the Rosslund Camp, southeastern British Columbia; in Geological Fieldwork 1991; British Columbia Ministry of Energy, Mines, and Petroleum Resources, Paper 1992-1, p. 261-272.
- Höy, T. and Andrew, K.P.E.**
1991: Geology of the Rosslund area, southeastern British Columbia; in Geological Fieldwork 1990; British Columbia Ministry of Energy, Mines, and Petroleum Resources, Paper 1991-1, p. 21-31.
- Little, H.W.**
1982: Geology of the Rosslund-Trail map-area, British Columbia; Geological Survey of Canada, Paper 79-26.
1983: Geology of the Greenwood map-area, British Columbia; Geological Survey of Canada, Paper 79-29.
- Parrish, R.R., Carr, S.D., and Parkinson, D.L.**
1988: Eocene extensional tectonics and geochronology of the southern Omineca Belt, British Columbia and Washington; *Tectonics*, v. 7, p. 181-212.
- Paterson, S.R., Vernon, R.H., and Fowler, T.K., Jr.**
1991: Aureole tectonics; in Contact Metamorphism, *Reviews in Mineralogy*, v. 26, Mineralogical Society of America, p. 673-722.
- Pearson, R.C. and Obradovich, J.D.**
1977: Eocene rocks in Northeast Washington - radiometric ages and correlation; United States Geological Survey, Bulletin 1433.
- Simony, P.S.**
1979: Pre-Carboniferous gneisses near Trail, British Columbia; Canadian Journal of Earth Sciences, v. 16, p. 1-11.
- Wheeler, J.O. and McFeely, P.**
1991: Tectonic assemblage map of the Canadian Cordillera and adjacent parts of the United States of America; Geologic Survey of Canada, Map 1712A, Scale 1:2 000 000.
- Yates, R.G.**
1971: Geologic map of the Northport Quadrangle, Washington; United States Geological Survey, Miscellaneous Geological Investigations Map I-603.

A new regional mapping project in Vernon map area, British Columbia

Robert I. Thompson and Kenneth L. Daughtry¹
Cordilleran Division, Vancouver

Thompson, R.I. and Daughtry, K.L., 1994: A new regional mapping project in Vernon map area, British Columbia; in Current Research 1994-A; Geological Survey of Canada, p. 117-122.

Abstract: In Vernon map area (82L) at least two stratigraphic assemblages link Quesnel terrane, Kootenay terrane and undivided metamorphic assemblages: 1) a Windermere-like biotite/hornblende-feldspar-quartz assemblage; and 2) a carbonaceous schist, phyllite, argillite assemblage.

Volcanic rocks, east of Vernon, thought to be Triassic and unconformable on older strata are likely part of an Eocene succession emplaced during crustal extension.

Eocene crustal extension was distributed across a broad area along steeply dipping faults; the horizontal component across north Okanagan Valley amounts to a few kilometres.

Metallic mineral deposit types include porphyry copper and molybdenum, Kuroko-type volcanogenic massive sulphide, skarn copper and gold, mesothermal gold, silver, and base metal veins, epithermal gold and silver veins and breccias, placer gold, and podiform chromite.

Nonmetallic mineral occurrences include granite, sand and gravel, limestone, marble, gypsum, clay, asbestos, soapstone, coal, agate, opal, jasper, wollastonite, fluorite, palagonite, silica, and kyanite.

Résumé : Dans la région cartographique de Vernon (82L), au moins deux assemblages stratigraphiques lient entre eux le terrane de Quesnel, le terrane de Kootenay et des assemblages métamorphiques non divisés : 1) un assemblage à biotite/hornblende-feldspath-quartz s'apparentant à ceux du Supergroupe de Windermere; et 2) un assemblage de schiste carboné, de phyllade et d'argilite.

Les roches volcaniques situées à l'est de Vernon, sans doute d'âge triasique et reposant en discordance sur des strates plus anciennes, font probablement partie d'une succession d'âge éocène dont la mise en place a eu lieu pendant un épisode de distension crustale.

La distension de la croûte survenue à l'Éocène s'est effectuée sur une vaste étendue par l'entremise de failles de fort pendage; la composante horizontale de cette distension, le long d'un transect situé au nord de la vallée de l'Okanagan, s'établit à quelques kilomètres.

Les types de gîtes minéraux métallifères sont notamment des gîtes de cuivre et de molybdène porphyriques; des sulfures massifs volcanogènes de type Kuroko; des skarns cuprifères et aurifères; des gîtes filoniens mésothermaux de cuivre, d'or et de métaux communs; des gîtes filoniens et bréchiformes épithermaux d'or et d'argent; des placers aurifères; et des gîtes lenticulaires de chromite.

Les indices de substances non métalliques sont composés de granite, de sables et graviers, de calcaire, de marbre, de gypse, d'argile, d'amiante, de stéatite, de charbon, d'agate, d'opale, de jaspe, de wollastonite, de fluorine, de palagonite, de silice et de kyanite.

¹ Discovery Consultants, P.O. Box 933, Vernon, British Columbia V1T 6M8

INTRODUCTION

Vernon project represents a renewed focus by the Cordilleran Division of GSC on the bedrock geology and resource endowment of south-central British Columbia.

The Vernon map area, the region of current focus, sits astride the north Okanagan Valley, a region rich in natural resources. Lumber, pulp, beef, and fruit are mainstays of a local economy that continues to grow and diversify as tourism and recreation, light industry, and urban development play increasingly significant roles. There is mineral potential but no current mineral production. This could easily change however, past exploration efforts have demonstrated significant occurrences of volcanogenic massive sulphides, epithermal gold, and stratiform base metals.

As people continue to move to and invest in the Okanagan Valley, land use planning becomes increasingly important. Assuring reliable and adequate sources of clean water, minimizing the environmental impact of landfills, providing for the safe disposal of effluent, and restricting urban development to areas without slope stability hazards or in the path of infrequent flash floods, are some of the challenges facing city and town councils and the professionals advising them. Similar challenges face provincial land use planners as they try to balance the need for resource development, such as mining and forestry, with recreational needs, and the preservation of a robust ecology.

A sound geological database is essential if planning is to be comprehensive. This project will contribute bedrock maps at a working scale of 1:50 000 and compiled at 1:250 000 scale; this framework will be integrated with other databases including geophysics, silt geochemistry, surficial geology, and hydrogeology. Final products will be in hard copy and electronic forms so that different user groups can tailor output to specific needs.

This project builds on the considerable contributions of others. Two regional compilations are especially noteworthy: GSC Memoir 296 by A.G. Jones (1959) and GSC Open File 637 by A.V. Okulitch (1979). They have made sure our work is "cut out for us".

GEOLOGICAL SETTING

Two geological terranes abut each other in Vernon map area, Kootenay on the northeast and Quesnel on the west; on the southeast are "undivided metamorphic assemblages" that have been excluded from terrane classification (Wheeler and McFeely, 1992). Quesnel Terrane is composed of Upper Triassic and Lower Jurassic arc volcanic rocks and associated volcanoclastic rocks overlain by Jurassic arc-derived clastic rocks; the assemblage was accreted to the North American margin during Jurassic time. Kootenay Terrane is a succession of deformed and metamorphosed clastic sedimentary rocks with subordinate volcanic and carbonate strata; the succession was intruded by Ordovician, Devonian, and Mississippian age plutons. Unlike Quesnel Terrane rocks which are exotic with respect to North America, Kootenay Terrane

rocks have a strong affinity to ancestral North America; they were probably deposited at, or close to, the ancestral margin. The region of "undivided metamorphic assemblages" defines a large re-entrant extending from Vernon, east to at least Slocan Lake, and then south to the Canada-U.S.A. border. Fault-bounded blocks of Quesnel rocks are interpreted to follow the trace of the re-entrant.

The town of Vernon is at the boundary between the three assemblages and is a good place to investigate the character of the terrane boundary, and to look for possible stratigraphic links to discriminate between pre- and post-accretion history. It is important to establish whether any of the undivided metamorphic assemblages, as yet excluded from terrane classification, have affinities with Kootenay or possibly Quesnel rocks.

Terrane accretion accompanied Jurassic and Cretaceous mountain building that saw imbrication of the continental terrace wedge, metamorphism, and wholesale eastward displacement of Kootenay Terrane on the order of 200 km. Regional compilations for the Vernon map area show few thrust faults or large recumbent (isoclinal) folds of the kind normally associated with the core zone of an alpine-type mountain belt. Refined internal stratigraphy may help determine whether such structures are present.

Crustal extension early in the Tertiary, postdated, for the most part, thrust faulting and folding associated with Jurassic, Cretaceous, and early Tertiary mountain building. The Okanagan Valley-Eagle River Fault is a west-side-down listric normal fault that follows southern Okanagan Lake and apparently continues north-northeast bisecting Vernon map area from Wood Lake to Mara Lake where the fault bends northeast to follow the trace of the Eagle River. Estimates of fault displacement across southern Okanagan Lake is tens of kilometres. Fortunately there is sufficient geological control along an east-west transect through Vernon to constrain the geometry and magnitude of Early Tertiary extension thereby placing limits on the nature of the Okanagan Valley-Eagle River structure in this part of the Vernon map area.

1993 Coverage

Work was confined to the Oyama (82L/3) and Vernon (82L/6) 1:50 000 map areas.

STRATIGRAPHY

Biotite/hornblende-feldspar-quartz assemblage

At the lowest structural and presumably stratigraphic level, on the east side of Kalamalka Lake, is a thick biotite and/or hornblende feldspar-quartz semi-schist interlayered with 1 to 10 m thick units of foliated feldspar-quartz "grit" (Fig. 1). The latter can be traced for kilometres; the units have sharp contacts, compositional homogeneity, and are foliated. On weathered surfaces, coarse sand- to grit-sized feldspar grains weather prominently, showing a tightly packed equigranular texture. Individual feldspar grains have well defined boundaries and grain size is independent of proximity to unit boundaries. The more pelitic semi-schists are finer grained and more

compositionally diverse than foliated feldspar-quartz layers. A white "marble" marker unit has been traced several kilometres within the succession. The unit, about 20 to 40 m thick, is a metamorphosed calcareous quartzite/siliceous marble with one or more layers of feldspar-quartz grit. Hornblende-rich "greenstone" lenses and layers are present. Pegmatite is common and occurs as crosscutting dykes, folded dykes and sills, and irregular intrafolial layers.

Thickness of the biotite/hornblende-feldspar-quartz assemblage cannot be estimated until internal structure is better understood.

Age of the protolith is inferred to be late Proterozoic.

This assemblage is part of the "granitoid gneiss, schist, phyllite, slate unit" of Jones (1959); the "dioritic gneiss, amphibolite unit" of Okulitch (1979); and the "undifferentiated metamorphic assemblage (protolith unknown)" of Wheeler and

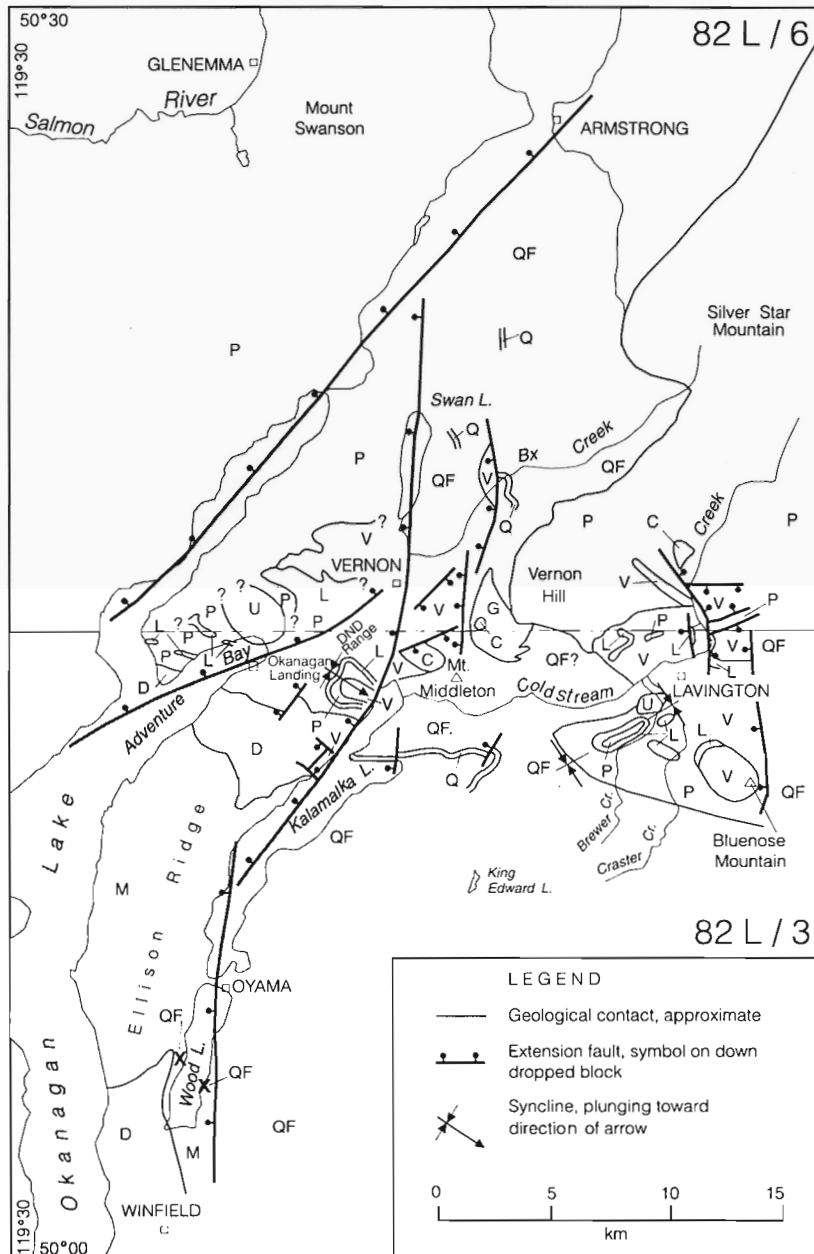


Figure 1. Generalized geological map for parts of 82L/3,6. QF – biotite/hornblende-feldspar-quartz assemblage and quartzite, schist, greenstone assemblage; Q – calcareous quartzite marker unit within QF; P – carbonaceous phyllite- and L – limestone (Permian)-assemblage; V – volcanic breccia- and C – conglomerate-assemblage (Eocene); D – foliated diorite (Jurassic); G – foliated biotite granite (Jurassic?); M – unfoliated syenite and porphyritic granodiorite (late Cretaceous and Eocene); U – ultramafic intrusions.

McFeely (1992). For four reasons, the succession east of Kalamalka Lake is interpreted as metamorphosed Windermere Group sandstone and pelite: overall compositional homogeneity dominated by feldspar, quartz, and biotite/hornblende; great thickness yet lack of good internal stratigraphy; presence of feldspathic "grit" units with stratigraphic continuity; and stratigraphic position at the base of known Paleozoic stratigraphy. The abundance of feldspathic "grit" may signify proximity to a source terrain.

Quartzite, schist, greenstone assemblage

Quartzite and micaceous quartzite interlayered with biotite and/or hornblende quartz-feldspar schist separates the coarser and older feldspathic grit and pelite from younger Paleozoic rocks (Fig. 1). It is mapped along the base and west-facing slope of Vernon Hill, can be traced northward across BX Creek into the base of Silver Star Mountain, and has been recognized in the Brewer Creek area southeast of Lavington where it is interbedded with, and overlain by, foliated, fine grained greenstone.

The thickness of the succession probably doesn't exceed 500 m.

The age is unknown but these rocks are assumed to be Windermere.

Carbonaceous schist, phyllite, limestone assemblage

A carbonaceous metasedimentary assemblage of phyllite, graphitic schist, siliceous argillite, and argillaceous chert is widespread from the west side of north Okanagan Lake east to the Trinity Valley and from the south slopes of Coldstream Valley north beyond Silver Star Mountain (Fig. 1). Volcanic rocks form a minor part. One to 5 m thick flows of foliated and altered andesitic(?) porphyry were mapped near Becker Lake, and sheared, fine grained greenstone occurs near Adventure Bay.

A distinctive recrystallized limestone forms a continuous and useful time-stratigraphic marker within the carbonaceous assemblage. This Permian-aged carbonate (Jones, 1959) has been mapped from west of Okanagan Lake to the base of Bluenose Mountain south of Lavington, including both sides of the Coldstream Valley. The limestone lacks primary sedimentary features except occasional feeding burrows. Crinoid stems are present in most massive exposures, recognizable as lighter-coloured cylindrical features, some of which weather out; rarely, slight silicification indicates presence of coral-like features.

Mapping by Okulitch (1979) and Jones (1959) suggests the carbonaceous assemblage extends into adjacent 1:50 000 scale map areas.

Thickness of the assemblage is difficult to estimate but thickness of the Permian limestone within it is no more than 50 m. Jones (1959) estimated a total thickness of approximately 25 000 ft (8000 m): 8000 ft. (2500 m) of argillite overlain by 8000 ft. (2500 m) of andesitic volcanics succeeded by 10 000 ft. (3200 m) of limestone.

The volcanic succession of Jones (1959), discussed below, occurs above the carbonaceous assemblage and is separated from it by an erosional unconformity.

Age of the carbonaceous assemblage probably ranges from Carboniferous to Triassic. Constraints are the Permian limestone marker unit and Triassic limestone that occurs east of Lumby (Okulitch and Cameron, 1976).

Volcanic breccia, conglomerate assemblage

An assemblage of massive volcanic breccia with subordinate conglomerate facies was mapped from north of Okanagan Landing through the town of Vernon to the east side of Kalamalka Lake. A second set of exposures extends along the north side of the Coldstream Valley to Lavington and south of Lavington at Bluenose Mountain (Fig. 1). These volcanics are broadly folded and fault-bounded, and considered here to be part of a succession of Eocene volcanics erupted during crustal extension. Jones (1959) mapped part of the succession as Paleozoic and the remainder as Tertiary; Okulitch (1979) considered part of the succession Triassic (Nicola Group) and the remainder Tertiary.

This volcanic succession, mapped previously as two separate units, can be traced continuously from one to the other. It lacks structural and metamorphic imprints of older assemblages, suggesting it was deposited after metamorphism and penetrative deformation. An Eocene age is suggested on the basis of gross lithology and similarity with nearby Eocene exposures in Vernon townsite, at Bluenose Mountain, and west of Coldstream Creek.

The unconformity separating the volcanics from underlying rocks is erosional with metres, if not more, of relief. It has been the focus of previous investigations (Preto, 1964; Read and Okulitch, 1977) and correlated with a mid-Triassic unconformity having regional extent. However, where the unconformity can be dated paleontologically, along the Salmon River about 40 km west of Vernon town site, the overlying fossiliferous Triassic succession consists of conglomerate, argillite, basic and vitric tuff, greywacke, and calcarenite, a succession more typical of the eastern clastic facies of the Nicola Group and bearing little resemblance to the massive breccias mapped in and around Vernon town site.

Miocene(?) conglomerate unit

The north-flowing creek that drains King Edward Lake also cuts through a conglomerate that underlies younger Miocene basalt flows. The conglomerate can be traced about a kilometre along the valley wall, is not more than 80 m thick, and probably represents a coarse fluvial unit; it is not continuous beneath the overlying volcanic flows but has been observed east of King Edward Creek for several kilometres and southeast of Oyama. Clasts consist, for the most part, of rounded quartz and feldspar-quartz granitoid in a yellow-brown-weathering matrix of quartz, feldspar grit, and sand. Some placer gold has been recovered from this unit.

Miocene and younger volcanic assemblage

Columnar jointed, aphyric and olivine phyric basalt flows and rhyolite flows cap the Thompson Plateau. Unlike the older Eocene(?) volcanic assemblage, these flows are essentially flat lying.

Intrusive rocks

There is a plethora of intrusive rocks with a wide variety of compositions and ages. The most obvious and areally extensive are the foliated diorite, quartz diorite, and granodiorite of the Nelson plutonic suite of Jurassic age cut by unfoliated pink and buff weathering syenite and quartz monzonite of Eocene age (named Coryell Syenite in Penticton map area to the south). They are intruded by mafic dykes especially near the contacts between them. The ridge separating Okanagan from Wood and Kalamalka lakes is dominated by these plutonic suites. A third suite comprising unfoliated biotite granite containing feldspar megacrysts (Okanagan Batholith of Cretaceous age) is present but has not been separated from the pink syenite suite.

Foliated diorite and granodiorite intrudes the biotite/hornblende-feldspar-quartz assemblage especially near the southern limits of Oyama map area. In areas where foliation is intense, discriminating the diorite from the biotite/hornblende feldspar-quartz assemblage is difficult.

Foliated diorite also forms small intrusions at Craster Creek 3 km south of Lavington; here the intrusions are cut by gold bearing quartz veins occupying a steeply dipping fracture zone (Kalamalka Property, Minfile No. 082LSW050).

A foliated, light grey biotite granite intrudes the micaceous quartzite assemblage on the west-facing lower slopes of Vernon Hill. This intrusion is a large lens-shaped body within the compositional layering of enveloping metasedimentary rocks. Small granite intrusions similar in texture and composition occur near the peak of Silver Star Mountain.

Two occurrences of foliated and altered ultramafic rocks, possibly small lens-shaped bodies, occur near Becker Lake.

Two ultramafic intrusions, one immediately north of Okanagan Landing and the other crossing the lower reaches of Brewer Creek, are medium to coarse crystalline and unfoliated; fine crystalline microdiorite(?) is common at the margins. These intrusions are distinct from the occasional foliated and altered ultramafic rocks noted above. Some quartz veins within the ultramafic bodies are gold bearing.

Small, unfoliated, crosscutting feldspar porphyry dykes occur sporadically.

STRUCTURE

No major contractional structures have been mapped. On Vernon Hill, the oldest rocks are at the bottom, the youngest at the top; this is true for the south side of Coldstream Valley between Kalamalka Lake and Lavington. A penetrative foliation – schistosity in the feldspar-quartz rich assemblages

and cleavage in the carbonaceous assemblage – affects all units older than the presumed Eocene volcanic breccia, conglomerate assemblage. An east-trending mineral lineation defined, most often, by alignment of micas or amphiboles, is common. Upright mesoscopic folds are rarely observed probably because of poor exposure. Some thin pegmatitic layers within the biotite/hornblende-feldspar-quartz assemblage outline complex folds that appear related to intrafolial flow.

Upright, gentle folds are outlined by the Permian limestone marker unit within the carbonaceous assemblage. One east-trending syncline traverses Craster and Brewer creeks south of Lavington; another plunges eastward into Kalamalka Lake at the Department of National Defense Range and Training Reserve.

Tertiary extension faults

North-northeast trending extension faults coincide with Kalamalka Lake, and each of the two arms at the northern termination of Okanagan Lake. Dips are relatively steep and total extension is estimated as 5 km or less. The Permian limestone marker, which can be mapped across each of the blocks west of Kalamalka Lake constrains both the geometry and displacement across the faults. Other steeply dipping faults are present. For example Mount Middleton, at the north end of Kalamalka Lake is fault-bounded; the headwaters of - Coldstream Creek traces a north-trending east-side-down fault; the west margin of Vernon Hill is bounded by a west-side-down extension fault.

If the Okanagan Valley-Eagle River Fault follows Wood Lake and Kalamalka Lake, it dips relatively steeply having a throw of less than 1 km; total east-west extension would be 5 km at most. Presence of biotite-feldspar-quartz schist belonging to the biotite/hornblende feldspar-quartz assemblage on both east and west sides of Wood Lake, near water level, suggests the fault has minor displacement there.

Timing

Rocks older than the volcanic breccia, conglomerate assemblage are metamorphosed and foliated. Because the diorite and granodiorite of the Nelson Plutonic Suite are foliated, some deformation must have accompanied and/or postdated emplacement of the plutons. As conglomerate associated with the volcanic breccia assemblage contains foliated, randomly oriented metasedimentary and plutonic clasts, regional penetrative deformation and metamorphism predates deposition of the conglomerate. This leaves a period between the mid-Jurassic and the Eocene for this deformation.

Contradictory evidence comes from Salmon River. Here, Read and Okulitch (1977) mapped a pre-upper Triassic conglomerate containing randomly oriented clasts of older strata that are metamorphosed and foliated, whereas upper Triassic strata overlying the conglomerate are neither foliated nor regionally metamorphosed. Their data suggest regional metamorphism and deformation sometime between the Permian and the late Triassic.

As for extension, the volcanic breccia, conglomerate assemblage has dips up to 40 degrees and is cut by extension faults. The overlying Miocene and younger volcanic flows have very gentle regional dips. Extension occurred during and after deposition of the volcanic breccias.

RESOURCE POTENTIAL

Metallogenic overview

The diverse tectonic history of the Vernon map area, evident in the juxtaposition of the different rock assemblages, is mirrored in this diversity of mineral deposits. Each important rock assemblage is characterized by a distinct assemblage of mineral deposit types.

In the Kootenay Terrane, older metasedimentary rocks with affinity to North America host sedimentary-exhalative zinc+lead±silver±copper deposits, whereas the younger Palaeozoic volcanic and sedimentary rocks related to continental margin rifting and early arc development host (Besshi-type) volcanogenic massive sulphide mineralization.

The carbonaceous phyllite, limestone, and associated volcanic rock assemblage contains numerous mesothermal gold±silver vein occurrences as well as gold skarns. Also, almost all of the Tertiary and Quaternary placer gold deposits are spatially related to this assemblage.

Island-arc related rocks of the Quesnel Terrane host occurrences of Kuroko-type volcanogenic massive sulphide mineralization and copper+gold skarns. In one locality, a high-level alkaline intrusion, related to the Nicola Group volcanic rocks, carries alkalic porphyry copper+gold mineralization.

Along the (presumed) suture zone between the Quesnel and Kootenay Terranes, ophiolitic rocks contain podiform chromite, asbestos, nickel, and talc occurrences.

In the Mesozoic plutonic rocks of the Quesnel Terrane, both porphyry copper-molybdenum and porphyry molybdenum occurrences are common, including the Brenda Mine, a major past-producer which is a short distance outside the southwest part of the map area. In contrast, only minor porphyry molybdenum mineralization is known in Mesozoic plutonic rocks of the Kootenay Terrane. Granitic rocks in both terranes host mesothermal vein gold occurrences.

Post-accretionary Eocene overlap assemblage rocks are characterized by a distinct assemblage of mineral deposit types, including coal in basal sedimentary units, epithermal gold and gold-silver mineralization related to extensional structures, opal, jasper, and agate occurrences in both sedimentary and volcanic units, and minor sediment-hosted uranium occurrences.

The overlap assemblage also includes plateau basalt flows of Miocene age which overlie buried fluvial channel deposits containing minor uranium mineralization.

Current production

At present, mining activity is restricted to gypsum at Falkland, ornamental marble near Mabel Lake, granite near Vernon and Oyama, alumina at Buse Lake, limestone near Kelowna, numerous sand and gravel operations, and minor placer gold and gemstone production.

Current exploration

In recent years, systematic mineral exploration activity has focused on volcanogenic massive sulphides in rocks of the Eagle Bay Formation, epithermal gold in Eocene volcanic units and their underlying basement rocks, sedimentary exhalative deposits in lower Paleozoic and Proterozoic sedimentary rocks, and skarn gold in Paleozoic and Triassic rocks.

Southwest quadrant, Vernon map area (82L)

The southwest quadrant of Vernon map area contains a diverse array of mineral occurrences. Metallic mineral deposit types include porphyry copper and molybdenum, Kuroko-type volcanogenic massive sulphide, skarn copper and gold, mesothermal gold, silver and base metal veins, epithermal gold and silver veins and breccias, placer gold, and podiform chromite.

Documented nonmetallic mineral occurrences include granite ornamental and building stone, sand and gravel, limestone, marble, hydrothermal gypsum, clay, asbestos, soapstone, coal, agate, opal, jasper, wollastonite, fluorite, palagonite, silica, and kyanite.

REFERENCES

- Jones, A.G.**
1959: Vernon map-area, British Columbia; Geological Survey of Canada, Memoir 296, 186 p.
- Okulitch, A.V.**
1979: Lithology, stratigraphy, structure and mineral occurrences of the Thompson-Shuswap-Okanagan area, British Columbia; Geological Survey of Canada, Open File 637.
- Okulitch, A.V. and Cameron, B.E.B.**
1976: Stratigraphic revisions of the Nicola, Cache Creek, and Mount Ida groups, based on conodont collections for the western margin of the Shuswap Metamorphic Complex, south-central British Columbia; Canadian Journal of Earth Sciences, v. 13, p. 44-53.
- Preto, V.A.**
1964: Structural relationships between the Shuswap Terrane and the Cache Creek Group in southern British Columbia; M.Sc. thesis, University of British Columbia, Vancouver, British Columbia.
- Read, P.B. and Okulitch, A.V.**
1977: The Triassic unconformity of south-central British Columbia; Canadian Journal of Earth Sciences, v. 14, p. 606-638.
- Wheeler, J.O. and McFeely, P.**
1992: Tectonic assemblage map of the Canadian Cordillera and adjacent parts of the United States; Geological Survey of Canada, Map 1212A, scale 1:2 000 000.

Was the depositional environment of the Sullivan Zn-Pb deposit in British Columbia marine or lacustrine and how saline was it?: a summary of the data

F.W. Chandler and G.A. Zieg¹
Continental Geoscience Division

Chandler, F.W. and Zieg, G.A., 1994: Was the depositional environment of the Sullivan Zn-Pb deposit in British Columbia marine or lacustrine and how saline was it?: a summary of the data; in Current Research 1994-A; Geological Survey of Canada, p. 123-130.

Abstract: Published information and new sedimentological data suggest that the mid-Proterozoic Aldridge Formation of British Columbia and the correlative Prichard Formation in the United States, were deposited in a tidal sea of normal salinity, with perhaps hypersaline bottom water and under a hot dry climate.

Evidence comes from various broadly correlative formations: the Aldridge, Prichard, Fort Steele, LaHood, Waterton, Altyn, Chamberlain, Newland and ?Yellowjacket. It includes opposed crossbedding and ripples, syneresis cracked tidal bedding, simple sulphate – evaporite mineral composition, abundant scapolite, chamosite, dry-climate alluvial fan sediments, geochemical and isotopic data and a moderate index of weathering. The marine environment of the Sullivan appears to be in contrast to some major mid-Proterozoic Australian SEDEX deposits.

Résumé : L'information publiée et de nouvelles données sédimentologiques semblent indiquer que la Formation d'Aldridge (Protérozoïque moyen), en Colombie-Britannique, et la formation correlative de Prichard, aux États-Unis, se sont déposées dans une mer soumise à des marées, aux eaux de salinité normale, avec peut-être des eaux de fond hypersalines, dans des conditions climatiques chaudes et arides.

Les indices viennent de diverses formations globalement corrélatives, à savoir les formations d'Aldridge, de Prichard, de Fort Steele, de LaHood, de Waterton, d'Altyn, de Chamberlain, de Newland et de Yellowjacket?. Ces indices sont : des stratifications obliques et des rides de sens inverse d'une strate à l'autre; des couches à figures de rétractation sous-aquatique formées dans la zone de battement des marées; un assemblage de sulfates et d'évaporites présentant une composition minérale simple; de la scapolite en abondance; la présence de chamosite; des sédiments de cône de déjection déposés dans un climat aride; les données géochimiques et isotopiques; et un indice modéré d'altération météorique. Le milieu marin du gisement de Sullivan paraît très différent de celui qui caractérise certains importants gisements australiens de type SEDEX du Protérozoïque moyen.

¹ Cominco American Limited, East 15120 Euclid Ave, Spokane, Washington, 99216-1896

INTRODUCTION

The Sullivan Deposit at Kimberley, British Columbia (Fig. 1), is a world-class 160M tonne SEDEX lead-zinc deposit (Hamilton et al., 1983). Because the ore reserves of the mine are almost exhausted, much valuable information at the mine will shortly become lost when the mine closes. In order to document the ore body and its environment as fully as possible before this event, an international research program was formed. Led by John Lydon of the Geological Survey of Canada, it includes staff of the United States Geological Survey, the British Columbia Ministry of Energy, Mines and Petroleum Resources and several universities.

This report focuses on two unresolved related questions: (a) whether the lower Belt basin was marine or lacustrine (Winston, 1986, p. 542) and (b) whether evaporites formed in the basin (see Hietanen, 1967; Leitch, 1992; White, 1977). These questions are important because of the role of brines as ore fluids. In order to seek clues to the salinity of the water in which the Aldridge Formation was deposited, the literature was searched for evidence of salinity e.g. chamosite, glauconite, evaporites, syneresis cracks (Allen, 1982; Plummer and Gostin, 1981), tidally influenced rippled bedding (Reineck and Wunderlich, 1968) and herringbone crossbedding (Klein, 1977, fig. 3-5). Some reported exposures were checked and relevant formations were examined for new data.

The Belt/Purcell Supergroup occupies a broadly north-northwest striking belt mainly in Montana and Idaho and extending north into British Columbia and Alberta (Fig. 1). It consists of four divisions: (a) the lower Belt, dated at 1.48 Ga (Höy, 1989), (b) the Ravalli Group, (c) the middle

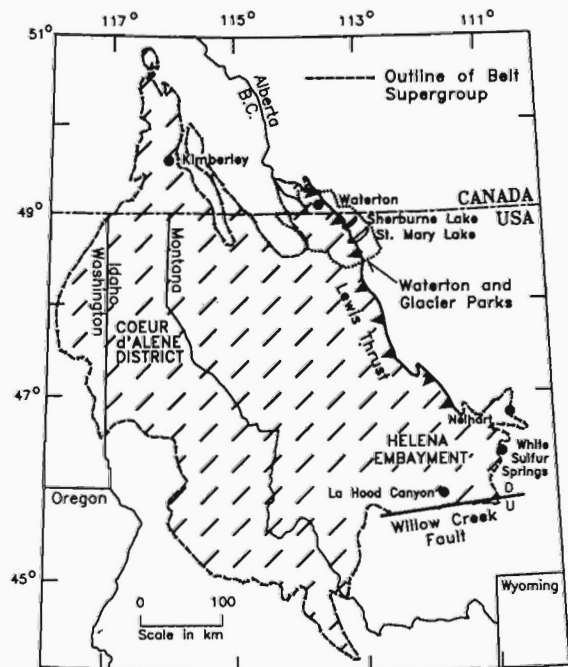


Figure 1. Distribution of Belt-Purcell Supergroup and location map to show sites discussed in text.

Belt carbonate unit, and (d) the Missoula Group. The lower Belt includes a mainly turbiditic unit, termed the Prichard Formation (Fig. 2) in the United States (Cressman, 1989) and the Aldridge Formation in Canada (Höy, 1993). Other broadly correlative formations in the lower Belt include: in Waterton and Glacier National parks, the Waterton and overlying Altyn and Appekunny formations; east of Kimberley, British Columbia, the Fort Steele; in the Helena Embayment, the Neihart, LaHood, Chamberlain and Newland, and in Idaho, possibly the Yellowjacket (Ekren, 1988; Harrison, 1972; Höy, 1993; Winston, 1986, fig. 4, 5). These mainly shallow water and alluvial correlative formations formed the focus of this study because coastal to alluvial sediments are more likely to retain a sedimentological imprint of paleosalinity, tidal activity and paleoclimate than would deep water turbidites.

ENVIRONMENTAL INDICATORS IN THE LOWER BELT SUPERGROUP

The Aldridge and Prichard formations

The Aldridge Formation of British Columbia is a 2-4 km thick (Höy, 1993) sequence of quartzofeldspathic wackes (Cressman, 1989; Shaw et al., 1993), divided into three parts: lower fine grained turbidites, middle, mainly quartz wackes, and a shoaling, non-turbiditic, upper argillaceous part (Höy, 1993). The Sullivan lead-zinc deposit was formed at the boundary between the lower and middle parts (Höy et al., 1991). Leitch (1992) inferred from saline (15-27 wt%) fluid inclusions a relation between saline fluids and the Sullivan deposit and the possibility that evaporites might be present at depth. Höy et al. (1993) reported crystal casts with the swallow tail form of selenite from the middle member of the Aldridge Formation, near Kimberley (Fig. 1).

The >6 km thick Prichard Formation forms the bulk of the lower Belt turbidite sequence. Cressman (1989) divided it into a muddy turbidite facies and a broadly correlative sandy turbidite facies to its northwest. From the middle of the muddy facies (member E) Cressman (1989, p. 20) reported hummocky crossbedding, desiccation cracks and mud chip breccias. Finch and Baldwin (1984) also identified shallow water to emergent units, some with mud cracks, in the Prichard.

| | WEST MONTANA - IDAHO | SOUTHERN BRITISH COLUMBIA | INTER-NATIONAL BORDER | NORTH HELENA EMBAYMENT | SOUTH HELENA EMBAYMENT |
|-------------------------------|----------------------|---------------------------|-----------------------|--|---|
| Lower Belt-Purcell Supergroup | Prichard Fm | Aldridge Fm | Altyn Fm | Newland Fm | Newland Fm |
| | | Fort Steele Fm | Waterton Fm | Chamberlain Fm | Chamberlain Fm |
| | | | | Neihart Fm | LaHood Fm |
| PRE-BELT CRYSTALLINE ROCKS | Base | not | exposed | NONCONFORMITY | NONCONFORMITY |
| | | | | A 7 L A -5 L S L S L L S 7 A L A L | 5 L S A L 7 L S L S L L A L S L A 7 |

Figure 2. Stratigraphic correlations in the lower part of the Belt-Purcell Supergroup, USA-Canada, after Harrison (1972).

Hobbs et al. (1965) reported mud cracks in the Coeur d'Alene district, Idaho, from the base of the upper Prichard to the top of the Belt section. But an illustration by Hobbs et al. (1965, fig. 4), of some of these mudcracks strongly resembles syneresis cracks, and casts doubt on the identification of the mudcracks. This latter interpretation is supported by the report (Cressman, 1989) of syneresis cracks from a transition member at the top of the Prichard Formation (placed in the Creston Formation of Canada, pers. comm., J.E. Reesor, in Cressman, 1989, p. 35).

Hietanen (1967) suggested that scapolite in the lowest part of the Prichard Formation in Idaho was derived from marginal marine evaporites. The credibility of this suggestion is supported by the above report of shallow water facies in the Prichard. Also of interest here are reports of scapolite (Modreski, 1985; Evans, 1993) and of both mud cracks (Ekren, 1988, p. 2) and syneresis cracks (Modreski, 1985, fig. R4) in the Yellowjacket Formation of Idaho, because of its possible correlation with the lower Prichard Formation (Ekren, 1988).

Fort Steele Formation

Quartzite of the >2000 m thick Fort Steele Formation is exposed several kilometres east of Kimberley (Fig. 1) (Höy, 1979) and may be correlative with (Hamilton et al., 1983; Paul Ransom, pers. comm., 1993) or underlie (Finch and Baldwin, 1984; Höy, 1993) the lowest Aldridge Formation.

Höy (1993) used mud cracks to support braided fluvial deposition. Herringbone crossbeds and polymodal paleocurrents indicated to Delaney (1981) and Legun (pers. comm., 1993), tidal marine deposition for at least part of the formation. In the upper 80 m of the Fort Steele Formation (drill core # E91-4 of Kootenay Exploration, Cominco-Canada), syneresis cracks are common in lenticular bedded and wavy (Reineck and Wunderlich, 1968) bedded sandstone and mudstone. Notably absent in the core and exposure seen by the senior author, were such features common in Precambrian fluvial sandstones such as mud cracks, reddening or mud pebbles.

Neihart and Chamberlain formations

The 215 m thick Neihart Formation is known only from a small area on the northern side of the Helena Embayment where it overlies gneissic basement (Ross, 1963). It has been correlated with the Fort Steele Formation (Harrison, 1972). Interpretation of the depositional environment was not possible from examination of the almost massive quartzite immediately south of the town of Neihart on the east side of Highway 89.

Locally, the Neihart is overlain by 750 m of interbedded black siltstone and wavy and flaser bedded sandstone of the Chamberlain Formation. Exposure along a forest road south of Neihart, about 250 m above the base of the Chamberlain Formation showed well developed syneresis cracks (Fig. 3).

LaHood Formation

The LaHood Formation is a sequence of pebbly arkose and arkosic paraconglomerate, up to 3 km thick, equivalent to at least the Prichard Formation (McMannis, 1963) and possibly a source for Prichard turbidites (Tom Chadwick and Bruce Otto, pers. comm., 1993). It lies north of the south bounding fault system of the Helena embayment in western Montana (Fig. 1). McMannis (1963) and Foster (1993) interpreted the formation as moderately deep water turbidites. Boyce (1975) proposed an arid alluvial fan-delta complex in which conglomerates are interpreted as debris flows, characteristic of a dry-climate alluvial fan (McGowen, 1974).

Tom Chadwick (pers. comm., 1993) concluded that the drab bulk of the LaHood was deposited in a submarine fan (see also Foster, 1993 and Foster et al., 1993). Two small red paraconglomerate-rich areas of exposure, one in LaHood Canyon, also seen by the writers, and another to the south, across the basin bounding fault zone (Foster et al., 1993, fig. 1) where the LaHood overlies gneissic basement, Chadwick interpreted as of dry-climate alluvial fan origin.

Waterton Formation

The Waterton Formation and the overlying Albyn Formation are the lowest Belt formations exposed near the international border in the eastern Rocky Mountains, where they form the base of the Cretaceous Lewis thrust sheet (Fig. 1). The Waterton Formation, 133 m thick, contains two shallow subtidal to supratidal, streaked (sic.) members. They consist of interbedded buff weathering algal dolomite and blue-grey weathering limestone with mud cracks, edgewise conglomerate, elongate stromatolites and silicified gypsum casts (Hill and Mountjoy, 1984).



Figure 3. Syneresis cracks, Chamberlain Formation, Neihart, Montana. GSC 1993-233B

The upper streaked member was examined by the senior author in four sections along the Akamina Highway, that runs northwest from the town of Waterton. Only one pair of opposed current ripples was found. Numerous samples of chert nodules and bedded chert were collected to search for evidence of evaporites. Quartz vugs with internal platy (box work) structure, reminiscent of replaced sulphate evaporite nodules (White, 1984), were also collected.

Altyn Formation

The Altyn Formation, correlative with the Newland Limestone (White, 1984) is divided into five informal members. The lowest and middle consist of shallowing upward, subtidal to supratidal cycles. The cycles consist of basal, subtidal, crossbedded siliciclastic-dolarenites, overlain by intertidal stromatolitic and smooth algal mat dolomite, with siliciclastic arenite-filled channels. Supratidal conditions were evidenced by mud cracks and by dolomitization of the stromatolites. Paleomagnetic data from the literature, evaporites (see below) and dolomitization persuaded White (1984) that the Altyn Formation was deposited on a coastal sabkha at a trailing continental margin and in a dry tropical environment like Shark Bay or the Persian Gulf.

The lowest member is well exposed on Appekunny Creek and in adjacent cliffs, just below Appekunny Falls, at the west end of Sherburne Lake (Fig. 1). The middle member is exposed on the north shore of St. Mary Lake, near Rising Sun (Whipple, 1992).

Features that point to a tidal as opposed to saline lacustrine environment are bimodal cross lamination in the tidal channel sands and polymodal planar crossbeds from the subtidal arenites (White, 1984). Reexamination of these crossbeds on the shore of St. Mary Lake, showed numerous examples of herringbone (Klein, 1977) crossbeds (Fig. 4). Silica pseudomorphs after both anhydrite nodules and gypsum crystals, quartz vugs, remnant inclusions of the two evaporite minerals and flamboyant quartz and length slow chalcedony in the subtidal arenite and stromatolite dolomite (White, 1977, 1984) are added evidence of evaporitic conditions during deposition (White, 1984). Associated amoeboid black chert preserves laminae of stromatolites and is therefore not likely to have replaced evaporite nodules.

The only evidence of evaporites reported by White (1984) from the middle member is chert or quartz vugs (Fig. 5) with a reticulate network of quartz crystals that could be pseudomorphing anhydrite laths. The senior author found the vugs to be commonly ovoid and lie in groups extended in bedding surfaces. They lie mainly in the dolarenite, rarely in stromatolitic dolomite. Some in the dolarenite units have a subdued star shape, reminiscent of modern clusters of gypsum rosettes found in sabkhas (Masson, 1955). They may be surrounded by a hematite halo locally containing pyrite. Ovoid to irregular quartz nodules in dolarenite of the middle member contain rhombic pits up to 1.5 cm across, with an interfacial angle of 110°, similar to that of calcite. Calcite crystals, of similar form to the rhombic cavities were found in siliceous nodules in the basal member on Appekunny Creek. The above pyrite probably

formed by reduction of evaporite sulphate nodules, a likely precursor of the vugs; the calcite may have formed from the displaced Ca.

Newland Formation

This south thickening, 610 to 2898 m formation (Zieg, 1986), though mainly siliciclastic, is also termed the Newland limestone. It is exposed along the northern margin of the Helena Embayment. The lower part consists of pelagic basinal calcareous shale with turbidites near the top. The upper part consists of two cycles in which carbonate leads up to shale and rippled siltstone. Zieg interpreted the cycles to represent shoaling from basin slope to mid shelf. At the Zieg ranch several kilometres west of White Sulphur Springs Montana (Fig. 1), the upper member of the lower cycle consists of rippled and flaggy fine sand and siltstone with flaser and parallel bedding and several sets of opposed current ripples, likely indicative of reversing tidal currents. Stromatolite-like

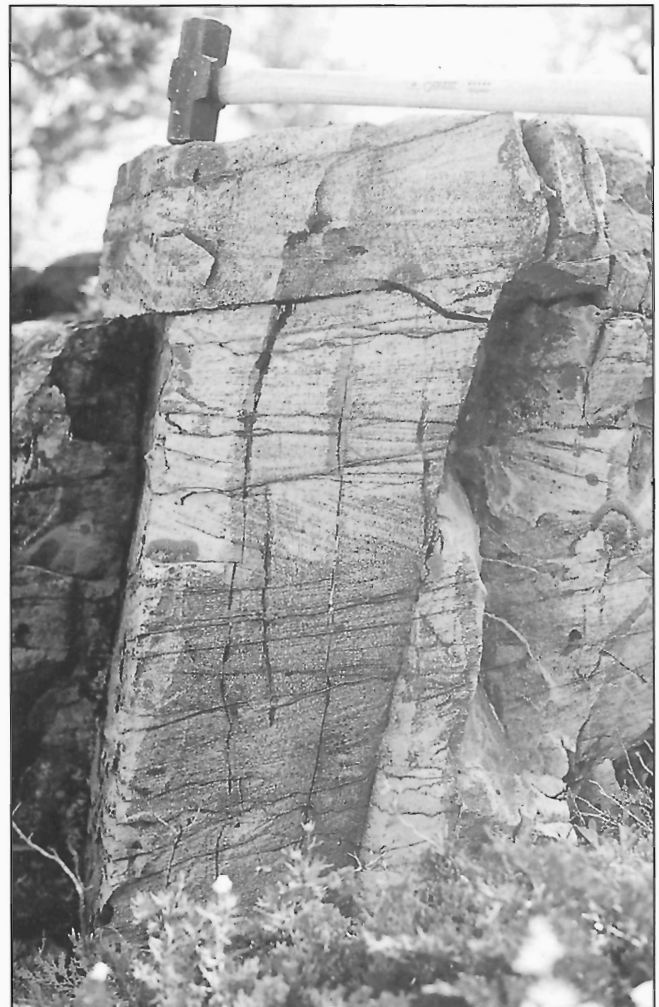


Figure 4. *Opposed (herringbone) planar crossbeds, evidence of tidal currents, member C, Altyn Formation, Glacier National Park, Montana. GSC 1993-233E*



Figure 5. Quartz vug after sulphate evaporite nodule, basal member, Altyn Formation, Appekunny Creek, Glacier National Park, Montana. GSC 1993-233A

structures named *Newlandia* (see Horodyski, 1993), well developed in the carbonate of the lower cycle, are similar to structures in carbonate of the LaHood Formation, interpreted by Boyce (1975, plates 9, 10) as possibly of evaporitic origin. The writers interpret *Newlandia* as of inorganic (possibly structural-solution) origin and unlike any evaporite related structures that they have observed (see also Horodyski, 1993; Zieg, 1981). Furthermore, this observation supports correlation of the upper Newland with the LaHood Formation. Barite crystals and nodules with textural similarities to sulphate evaporites were reported from the Newland Formation by Strauss and Schieber (1990).

DISCUSSION

Cressman (1989) considered that a river the size of the Mississippi, draining into an enclosed basin and a fan the size of the Prichard fan accumulating in a lake, are "not credible concepts".

Opposed tidal currents, if more or less equal in strength, can form stacked crossbeds of opposed inclination (herringbone crossbedding), or polymodal current roses (Klein, 1977). McMechan (1981) reported locally abundant herringbone crossbedding and poly- to bimodal current roses (McMechan, fig. 9) from the Creston Formation, that directly overlies the Aldridge Formation in southeastern British Columbia. Herringbone crossbeds in the Fort Steele

(Delaney, 1981; Legun, pers. comm., 1993) and in the Altyn Formation are strongly suggestive of tidal, i.e. marine deposition of these formations. Evans (1993) reported bi-directional crossbeds and interlayered quartzite and argillite interlayered on 1 cm scale "pinch and swell couple and couplet types", with syneresis cracks, from the Yellowjacket Formation, a possible correlative of the Prichard Formation. The bedding style of the interbedded quartzite and siltstone is reminiscent of tidal wavy bedding of Reineck and Wunderlich (1968).

Opposed crossbeds in fluvial deposits have been cited as evidence of the unreliability of herringbone crossbeds as an indicator of tidal currents in the Belt Supergroup (Winston, 1986, p. 457). However abundant evidence of sabkha deposition in the Altyn Formation (White, 1984) obviates fluvial deposition for that unit.

Rippled bedding can reflect tidal influence in two ways. First, as opposed cross laminations, second, as sand ripples formed during current and wave action, interlaminated to thinly interbedded with mud deposited during slack water (Klein, 1977, p. 15; Reineck and Wunderlich, 1968). White (1984) reported opposed cross lamination in tidal channel arenites in the Altyn Formation. Further, opposed cross laminations were seen in flaser bedded and parallel bedded fine grained sandstone and shale of the Newland Formation at White Sulphur Springs, Montana. Thinly interbedded mudstone and rippled siltstone of lenticular, wavy and flaser types, associated with syneresis cracks and with opposed ripples in some cases, in the Fort Steele, Chamberlain, Yellowjacket, and Newland formations (Reineck and Wunderlich, 1968) are reminiscent of tidal bedding.

Syneresis cracks are reported from the lower Aldridge, lower Prichard, upper Fort Steele, lower Chamberlain and Yellowjacket formations. In most of these formations the cracks occur in unoxidized sediments, are less complete than subaerial desiccation cracks and appear "ptygmatic" in vertical section. These features are interpreted as subaqueous shrinkage cracks in clays interbedded with sandstone. They appear to be favoured by saline environments, including salt lakes (e.g. Rooney et al., 1969), but not restricted to them (Allen, 1982, p. 553; Collinson and Thompson, 1982, p. 140; Plummer and Gostin, 1981).

Evaporites and meta-evaporites have been reported from a number of lower Belt formations (Evans, 1993; Hill and Mountjoy, 1984; Hietanen, 1967; Strauss and Schieber, 1990; White, 1984). Pyrite in quartz nodules in the Altyn Formation supports origin of the pyrite by sulphate reduction. The wide range of evaporite minerals such as analcime or trona, which occur in alkali lakes (Milton and Eugster, 1959; Rooney et al., 1969) or shortite (a sodium carbonate-bicarbonate), which cannot be precipitated from normal sea water (Muir, 1983, p. 164), have not been reported from the lower Belt Supergroup (Schieber, 1993) or found by the writers. Bedded and nodular chert in the Waterton and Altyn formations, lacks the reticulate surface pattern (Hay, 1968) or macroscopic crystal casts (Eugster, 1969) characteristic of chert formed after evaporite minerals of alkaline lakes. Evidence of shallow water deposition of parts of the Prichard Formation fits with

Hietanen's (1967) interpretation of scapolite in the formation being formed from marginal marine evaporites. Microfossils from chert of the Newland Formation (Horodyski, 1993) originated in offshore waters that appear not to have been hypersaline. This is in keeping with the absence so far, of reports of bedded evaporites, an indicator of hypersaline standing water, in the lower Belt. We stress that the nodular evaporites discussed here merely indicate evaporative coastal conditions. It would be important to determine whether the scapolite in the Prichard Formation is bedded or of sabkha type. Possible evidence of deep hypersaline water is the report of crystal casts (Höy et al., 1993) with the swallow tail form of selenite from the middle member of the Aldridge Formation.

Schieber (1993), used mass balance calculations to infer that the Belt basin had an oceanic connection. The high sulphur/carbon ratio in turbidites of the lower part of the Aldridge Formation (also Goodfellow, pers. comm., 1993) and from the Chamberlain and Newland formations of the Helena Embayment, as well as the high degree of sulphidation of iron in these formations (Lyons, 1993) indicated a marine rather than a fresh water environment. Both oxygeniferous and euxinic settings may be represented. A bimodal positive sulphur isotopic composition for the Newland and Chamberlain formations was interpreted by Lyons (1993) as caused by two pyrite-forming processes ((a) hydrothermal and (b) bacterial sulphate reduction), similar to the modern red Sea. Overlap of bacterial sulphide and sulphate isotopic ratios for the lower Newland suggested that the basin was marked by periods of isolation. Chamosite, a mineral common in warmer, modern, shallow, shelf seas, (Johnson, 1978) in the Newland Formation (Schieber, 1993) is also suggestive of marine deposition.

Evidence of the hot dry climatic conditions conducive to formation of sabkha evaporites in Prichard/Aldridge time (White, 1977) comes also from both paleomagnetic data (in White, 1984) and from the alluvial fan part of the LaHood Formation where relative abundance of mud flows suggests that the fan was formed under a dry climate. Further the chemical index of alteration (CIA) of the Belt Supergroup is 65-70 and varies little. In comparison with the average Archean shield of northwestern Ontario (CIA = 49.5), Pleistocene varved clays (CIA = 60-65), Early Proterozoic varvites (CIA = ~55-65) and the average shale (CIA = 70-75) (Nesbitt and Young, 1982), the CIA of the Belt indicates moderate chemical weathering (Schieber, 1993) in keeping with a dry climate.

ECONOMIC IMPLICATIONS

The Sullivan deposit belongs to a class of very large sediment hosted exhalative (SEDEX) base metal deposits. Most authors (Large, 1983; Sangster, 1990) have favoured a seafloor syn-sedimentary origin for them, with brines involved in their genesis (Morganti, 1988; Neudert and Russell, 1981), and evaporites characteristic of the host rocks of major examples (Muir, 1983) or of associated shelf successions (Large, 1983). Evidence of close association of evaporites with the Sullivan deposit is tenuous. Russel (1991) advocated stratified, tropical lakes or seas as settings for SEDEX

deposits: the major middle Proterozoic (1680-1690 Ma) SEDEX deposits of northern Australia (HYC or McArthur, Dugald River, Lady Loretta, Mt. Isa, Hilton) have been interpreted as formed in saline lakes (Muir, 1983; Neudert and Russell, 1981). Muir (1983) referred to trona casts and shortite, sodium minerals that form in alkaline lakes. But Eugster (1987), noting the bedded barite with the Lady Loretta Deposit classes it as a marine SEDEX deposit.

CONCLUSIONS

Whereas there is evidence that most of the Australian deposits formed in saline lacustrine environments, evidence presented here, suggests that the Sullivan deposit formed in a low latitude marine environment under a dry climate. Although the open sea was probably not hypersaline, there is limited evidence of hypersaline deep bottom water and broadly contemporaneous coastal evaporites formed in the Belt Basin.

ACKNOWLEDGMENTS

Thanks are due to Paul Ransom of Cominco Exploration Canada, Trygve Höy of British Columbia Department of Mines, Cameron Allen of Cominco American, Bruce Otto and Tom Chadwick, Consulting Geologists, Willie Williams of the Institute of Sedimentary and Petroleum Geology, Calgary, staff of Waterton National Park, Alberta and Glacier Park Montana, and of Cominco Inc. of Kimberley, British Columbia for sharing their expertise and for tendering a variety of logistical support. Reviews by Craig Leitch, Rob Rainbird and Bob Taylor significantly improved the manuscript.

Special thanks are due to Charlie Jefferson and John Scoates of the Mineral Deposits Division of the Geological Survey of Canada for their moral support. Most important were the essential financial support of John Lydon of the Geological Survey of Canada and the unstinted hospitality of Cominco American.

REFERENCES

- Allen, J.R.L.**
1982: Sedimentary structures, their character and physical basis; in *Developments in Sedimentology*, 30B, v. II, Springer (Pub.), 663 p.
- Boyce, R.L.**
1975: Depositional systems in the LaHood Formation, Belt Supergroup, Precambrian, southwestern Montana; Ph.D. thesis, University of Texas, Austin Texas, 247 p.
- Collinson, J.D. and Thompson, D.B.**
1982: Sedimentary Structures; Allen and Unwin, 194 p.
- Cressman, E.R.**
1989: Reconnaissance stratigraphy of the Prichard Formation (middle Proterozoic) and the early development of the belt Basin, Washington, Idaho and Montana; United States Geological Survey, Professional paper 1490, 80 p.
- Delaney, G.**
1981: 1981 Sullivan exploration annual internal report, research; Consolidated Mining and Smelting Company, Kimberley, British Columbia, p 12.

- Ekren, E.B.**
1988: Stratigraphic and structural relations of the Hoodoo Quartzite and the Yellowjacket Formations of middle Proterozoic age from Hoodoo Creek eastward to Mount Taylor, central Idaho; United States Geological Survey, Bulletin 1570, 17 p.
- Eugster, H.P.**
1969: Inorganic bedded cherts from the Magadi Area, Kenya; Contributions to Mineralogy and Petrology, v. 22, p. 1-31.
1987: Depositional models for the sediment-hosted Cu-Zn-Pb deposits of N. Australia; International Congress on the Geology, Structure, Mineralization and Economics of the Pacific Rim, 1987, Australasian Institute of Mining and Metallurgy, p. 119-122.
- Evans, K.V.**
1993: The Yellowjacket Formation of east-central Idaho; Belt Association Inc., Belt Symposium III, August 14-21, 1993, Program and Abstracts.
- Finch, J.C. and Baldwin, D.O.**
1984: Stratigraphy of the Prichard Formation, Belt Supergroup; in The Belt, Special Publication 90, Montana Bureau of Mines and Geology, Abstracts with Summaries, Belt Symposium II, 1983, p. 5-7.
- Foster, F.**
1993: Some observations regarding formation correlations and regional paleogeography of the southern Helena Embayment; Belt Association Inc., Belt Symposium III, August 14-21, 1993, Program and Abstracts.
- Foster, F., Chadwick, T., and Nilsen, T.**
1993: Paleodepositional setting and sedimentary mineralization in Belt Supergroup rocks of the Whitehall, Montana area; Belt Association Inc., Belt Symposium III, August 14-21, 1993, Program and Abstracts.
- Hamilton, J.M., Delaney, G.D., Hauser, R.L., and Ransom, P.W.**
1983: Geology of the Sullivan Deposit, Kimberley, B.C., Canada; in Sediment-hosted Stratiform Lead-Zinc Deposits, D.F. Sangster (ed.); Mineralogical Association of Canada, Short Course Notes, p. 31-83.
- Harrison, J.E.**
1972: Precambrian Belt Basin of northwestern United States: its geometry, sedimentation and, and copper occurrences; Geological Society of America Bulletin, v. 83, p. 1215-1240.
- Hay, R.L.**
1968: Chert and its sodium-silicate precursors in sodium-carbonate lakes of East Africa; Contributions to Mineralogy and Petrology, v. 17, p. 255-274.
- Hietanen, A.**
1967: Scapolite in the Belt Series in the St. Joe-Clearwater region, Idaho; Geological Society of America, Special Paper 86, 56 p.
- Hill, R. and Mountjoy, E.W.**
1984: Stratigraphy and sedimentology of the Waterton Formation, Belt-Purcell Supergroup, Waterton Lakes National Park, southwest Alberta; in Northwest Montana and adjacent Canada, Montana Geological Society, 1984 Field Conference and Symposium, p. 91-100.
- Hobbs, W., Griggs, A.B., Wallace, R.E., and Campbell, A.B.**
1965: Geology of the Coeur d'Alene District, Shoshone County, Idaho; United States Geological Survey, Professional Paper 478, 139 p.
- Horodyski, R.J.**
1993: Paleontology of the Belt Supergroup; Belt Association Inc., Belt Symposium III, August 14-21, 1993, Program and Abstracts.
- Höy, T.**
1979: Geology of the Estella – Kootenay King area, Hughes Range, southeastern British Columbia; British Columbia Ministry of Energy, Mines and Petroleum Resources, Preliminary map 36, 1: 50 000 scale.
1989: The age, chemistry, and tectonic setting of the Middle Proterozoic Moyie sills, Purcell Supergroup, southeastern British Columbia; Canadian Journal of Earth Sciences, v. 26, p. 2305-2317.
1993: Geology of the Purcell Supergroup in the Fernie west-half map-area, southeastern British Columbia; British Columbia Ministry of Energy, Mines and Petroleum Resources, Bulletin 84, 157 p.
- Höy, T., Berg, N., Delaney, G.D., Fyles, J.T., McMurdo, D., and Ransom, P.W.**
1991: The Sullivan Ore Body, in Geology and regional setting of major mineral deposits in southern British IAGOD Symposium, Field Trip Guidebook, Geological Survey of Canada, Open File 2167, p. 29-43.
- Höy, T., Dunne, K., and Wilton, P.**
1993: Massive sulfide and precious metal deposits in southeastern British Columbia; Geological Association of Canada, Mineralogical Association of Canada, Joint Annual Meeting, 1993, Field trip A-7, 74 p.
- Johnson, H.D.**
1978: Shallow Siliciclastic Seas; in Sedimentary Environments and Facies, H.G. Reading (ed.); Elsevier, p. 207-258.
- Klein, G. de Vries**
1977: Clastic tidal facies; CEPSCO: Continuing Education Publishing Company, Champaign, Illinois, 149 p.
- Large, D.E.**
1983: Sediment-hosted massive sulphide lead-zinc deposits: an empirical model; in Sediment-hosted Stratiform Lead-Zinc Deposits, D.F. Sangster (ed.), Mineralogical Association of Canada, Short Course p. 1-29.
- Leitch, C.H.B.**
1992: A progress report of fluid inclusion studies of veins from the vent zone, Sullivan stratiform sediment-hosted Zn-Pb deposit, British Columbia; in Current Research, Part E; Geological Survey of Canada, Paper 92-1E, p. 71-82.
- Lyons, T.W.**
1993: Geochemical constraints on paleoenvironments within the Belt Supergroup (middle Proterozoic), Montana: preliminary results; Belt Association Inc., Belt Symposium III, August 14-21, 1993, Program and Abstracts.
- Masson, P.H.**
1955: An occurrence of gypsum in southwest Texas; Journal of Sedimentary Petrology, v. 25, p. 72-77.
- McGowen, J.H.**
1974: Alluvial fans and fan deltas: processes and facies (abstract); Geological Society of America, Abstracts with Programs, v. 6/2, p. 116-7.
- McMannis, W.J.**
1963: LaHood Formation – a coarse facies of the Belt Series in southwestern Montana; Geological Society of America Bulletin, v. 74, p. 407-436.
- McMechan, M.E.**
1981: The middle Proterozoic Purcell Supergroup in the southwestern Rocky and southeastern Purcell Mountains, British Columbia and the initiation of the Cordilleran miogeocline, southern Canada and adjacent United States; Bulletin of Canadian Petroleum Geology, v. 29, p. 583-621.
- Milton, C. and Eugster, H.P.**
1959: Mineral assemblages of the Green River Formation; in Researches in Geochemistry, P.H. Abelson, (ed.); Wiley and Sons, Pub., p. 118-150.
- Modreski, P.J.**
1985: Stratabound cobalt-copper deposits in the Middle Proterozoic Yellowjacket Formation in and near the Challis Quadrangle; United States Geological Survey, Bulletin 1658, Chapter R, p. 203-221.
- Morganti, J.M.**
1988: Sedimentary-type stratiform ore deposits: some models and a new classification; in Ore Deposit Models, R.G. Roberts and P.A. Sheahan, (ed.), Geoscience Canada Reprint Series 3, p. 67-77.
- Muir, M.D.**
1983: Depositional environments of host rocks to northern Australian lead-zinc deposits, with special reference to McArthur River; in Sediment-hosted Stratiform Lead-Zinc Deposits, D.F. Sangster (ed.); Mineralogical Association of Canada, Short Course, p. 141-174.
- Nesbitt, B.W. and Young, G.M.**
1982: Early Proterozoic climates and plate motions inferred from major element chemistry of lutites; Nature, v. 299, p. 715-717.
- Neudert, M.K. and Russell, R.E.**
1981: Shallow water and hypersaline features from the Middle Proterozoic Mt. Isa Sequence; Nature, v. 293, p. 284-286.
- Plummer, P.S. and Gostin, V.A.**
1981: Shrinkage cracks: desiccation or syncretism?; Journal of Sedimentary Petrology, v. 51, p. 1147-1156.
- Reineck, H.E. and Wunderlich, F.**
1968: Classification and origin of flaser and lenticular bedding; Sedimentology, v. 11, p. 99-104.
- Rooney, T.P., Jones, B.F., and Neal, J.T.**
1969: Magadiite from Alkaline Lake Oregon; American Mineralogist, v. 54, p. 1034-1043.

Ross, C.P.

1963: The Belt Series in Montana; United States Geological Survey, Professional Paper 346, 122 p.

Russel, M.J.

1991: SEDEX deposits: back-tracking the systems; Abstracts with Programs, Annual meeting, Geological Society of America, v. 23/5, p. A20-21.

Sangster, D.F.

1990: Mississippi Valley-type and sedex lead-zinc deposits: a comparative examination; Transactions of the Institution of Mining and Metallurgy, Section B, Applied Earth Sciences, v. 99, p. B21-B42.

Schieber, J.

1993: A survey of sedimentologic, geochemical and mineralogical features of the Belt Series and their bearing on the lacustrine vs. marine debate; Belt Association Inc., Belt Symposium III, August 14-21, 1993, Program and Abstracts.

Shaw, D.R., Hodgson, C.J., Leitch, C.H.B., and Turner, R.J.W.

1993: Geochemistry of albite-chlorite-pyrite and chlorite-pyrrhotite alteration, Sullivan Zn-Pb deposit, British Columbia; in Current Research, Part A; Geological Survey of Canada, Paper 93-1A, p. 109-118.

Strauss, H. and Schieber, J.

1990: A sulfur isotope study of pyrite genesis: the mid-Proterozoic Newland Formation, Belt Supergroup, Montana; *Geochimica et Cosmochimica Acta*, v. 54, p. 197-204.

Whipple, J.W.

1992: Geologic map of Glacier National Park, Montana; United States Geological Survey, Map I-1508-F, 1:100 000 scale.

White, B.

1977: Silicified evaporites from the middle Proterozoic Altyn Formation, lower Belt Supergroup of Montana (abstract); Geological Society of America, Abstracts with Programs, v. 9/7, p. 1223-1224.

1984: Stromatolites and associated facies in shallowing-upward cycles from the middle Proterozoic Altyn Formation of Glacier National Park, Montana; *Precambrian Research*, v. 24, p. 1-26.

Winston, D.

1986: Evidence for intracratonic, fluvial and Lacustrine Settings of Middle to Late Proterozoic basins of western U.S.A.; in *Mid-Proterozoic Laurentia-Baltica*, C.F. Gower, T. Rivers, B. Ryan (ed.); Geological Association of Canada, Special Paper 38, p. 535-564.

Zieg, G.A.

1981: The stratigraphy, sedimentology and diagenesis of the Precambrian Upper Newland Limestone, central Montana; M.Sc thesis, University of Montana, 182 p.

1986: Stratigraphy and sedimentology of the middle Proterozoic upper Newland Limestone; in *Belt Supergroup: A guide to the Proterozoic rocks of Western Montana and adjacent areas*; Montana Bureau of Mines and Geology, Special Publication 94, p. 125-141.

Geological Survey of Canada Project 770063

Field evidence for Early Proterozoic tectonism in core gneisses of Frenchman Cap dome, Monashee complex, southern Canadian Cordillera

James L. Crowley¹ and Peter M. Schaubs¹
Cordilleran Division

Crowley, J.L. and Schaubs, P.M., 1994: Field evidence for Early Proterozoic tectonism in core gneisses of Frenchman Cap dome, Monashee complex, southern Canadian Cordillera; in Current Research 1994-A; Geological Survey of Canada, p. 131-141.

Abstract: Early Proterozoic migmatization and deformation were identified in core gneisses of Frenchman Cap dome during recent fieldwork. The principle evidence is that granite dykes which were previously estimated as Early Proterozoic age postdate the oldest migmatitic and gneissic fabric (S1) in the core gneisses. The dykes and S1 are interpreted as predating the overlying cover gneisses because the dykes, which occur throughout the core, do not intrude the cover. The dykes are deformed by F2 folds, yet they are not transposed into the dominant S2 fabric and are neither migmatitic nor gneissic. Recognition of S1 and the deformation state of the dykes suggest that core gneisses were less affected by Phanerozoic tectonism than cover gneisses at higher levels. These field interpretations corroborate previously-obtained isotopic data. Various rock types from all levels were sampled for a U-Pb geochronological study that attempts to refine ages of protolith and tectonism.

Résumé : Un épisode de migmatisation et de déformation remontant au Protérozoïque précoce a été reconnu dans les gneiss du noyau du dôme de Frenchman Cap lors de travaux récents sur le terrain. Le principal indice est que les dykes de granite dont l'âge avait été fixé au Protérozoïque précoce sont postérieurs à la structure migmatitique et gneissique la plus ancienne (S1) relevée dans les gneiss du noyau. Les dykes et S1 seraient antérieurs aux gneiss de couverture sus-jacents parce que les dykes, qui s'observent partout dans le noyau, ne pénètrent pas les roches de couverture. Les dykes sont déformés par des plis F2, bien que n'étant pas transposés pour autant dans la structure S2, et ne sont ni migmatitiques ni gneissiques. La reconnaissance de S1 et l'état de déformation des dykes indiquent que les gneiss du noyau ont été moins touchés par l'activité tectonique du Phanérozoïque que les gneiss de couverture à des niveaux supérieurs. Ces interprétations établies sur le terrain corroborent les données isotopiques recueillies auparavant. Divers types de roches de tous les niveaux ont été échantillonnés en vue d'une étude géochronologique U-Pb visant à préciser les âges du protolite et de l'activité tectonique.

¹ Department of Earth Sciences and Ottawa-Carleton Geoscience Centre, Carleton University, Ottawa, Ontario K1S 5B6

INTRODUCTION

Frenchman Cap and Thor-Odin domes in the northern and southern Monashee complex, respectively (Fig. 1, 2), are cored by Early Proterozoic orthogneiss and older paragneiss (Wanless and Reesor, 1975; Armstrong et al., 1991; Parkinson, 1991) which are interpreted as westernmost exposures of the North American craton in the southern Canadian Cordillera. These core gneisses are unconformably overlain by metasedimentary-dominated cover gneisses, which were mapped on the north flank of Frenchman Cap dome by Wheeler (1965), McMillan (1973), Psutka (1978), Brown (1980), Journeay (1986), Hoy (1987), and Scammell and Brown (1990). Cover gneisses are bounded above by a thrust fault, the Monashee décollement (Brown, 1980; Journeay,

1986), which transported the Selkirk allochthon in its hanging wall at least 80 km to the east (Read and Brown, 1981). Although previous U-Pb geochronology in Frenchman Cap dome has approximated ages of a few core orthogneiss bodies (Armstrong et al., 1991) and the age of a metamorphic event in the cover gneisses in the vicinity of the Monashee décollement (Journeay and Parrish, 1989; R.R. Parrish, unpublished data, pers. comm., 1991), there is uncertainty in the ages of (1) older deformation and metamorphism in core and cover gneisses, (2) deposition of core and cover paragneisses, and (3) intrusive and extrusive magmatism in the cover. The ages of these rocks and tectonic events in Frenchman Cap dome have important implications for reconstruction of the southern Omineca Belt.

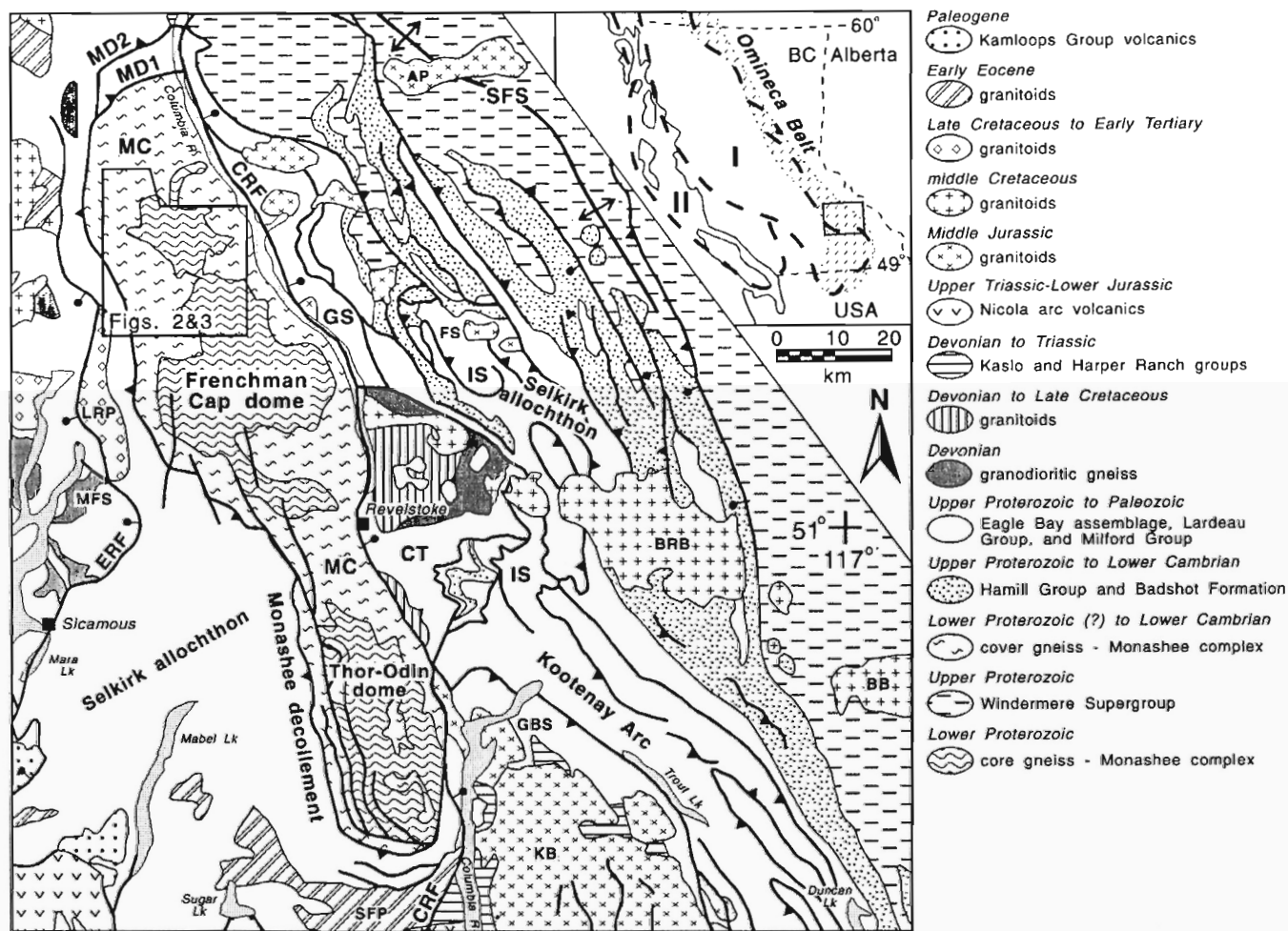


Figure 1. Tectonic map of southeastern British Columbia, modified after Wheeler and McFeely (1991). Box in inset map locates this map with respect to the Omineca Belt and Superterrane I (Intermontane) and II (Insular) of Monger et al. (1982). The Monashee décollement (MD1, MD2) is underlain by the Monashee complex (MC) and overlain by the Selkirk allochthon, which east of the complex is composed of the Clachnacudainn terrane (CT), Goldstream slice (GS), and Illecillewaet slice (IS). The Selkirk fan structure (SFS) lies in the northern Selkirk Mountains. Tertiary normal faults are Columbia River fault (CRF) and Eagle River fault (ERF). Granitoid bodies are Adamant pluton (AP), Battle Range batholith (BRB), Bugaboo batholith (BB), Fang stock (FS), Galena Bay stock (GBS), Kuskanax batholith (KB), Long Ridge pluton (LRP), Mount Fowler suite (MFS), and South Fosthall pluton (SFP).

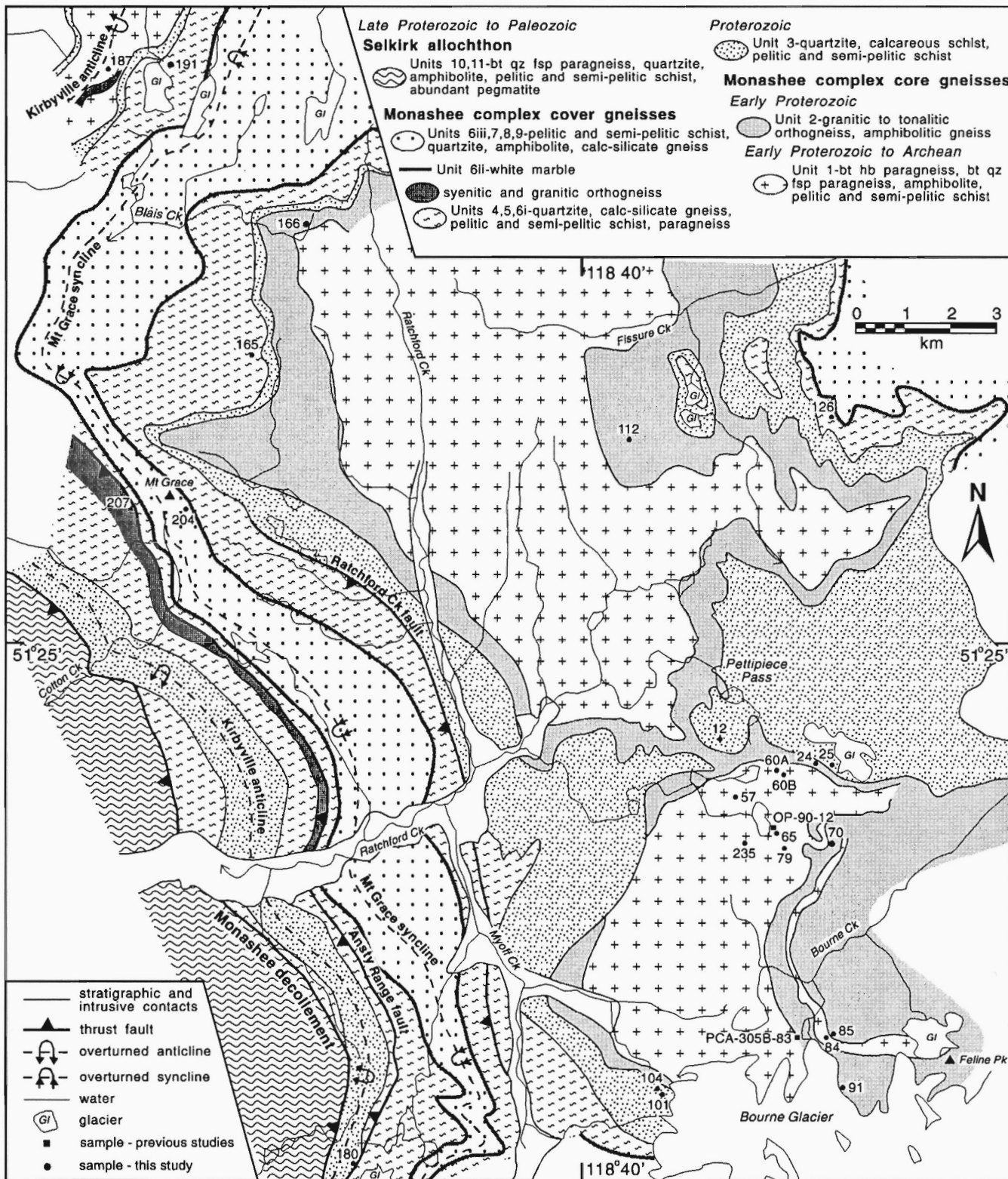


Figure 2. Geology of the north flank of Frenchman Cap dome after Wheeler (1965), McMillan (1973), Psutka (1978), Brown (1980), Journey (1986), and Hoy (1987). Unit names in legend are those used by Journey. Potential geochronology sample localities that are discussed in text are shown.

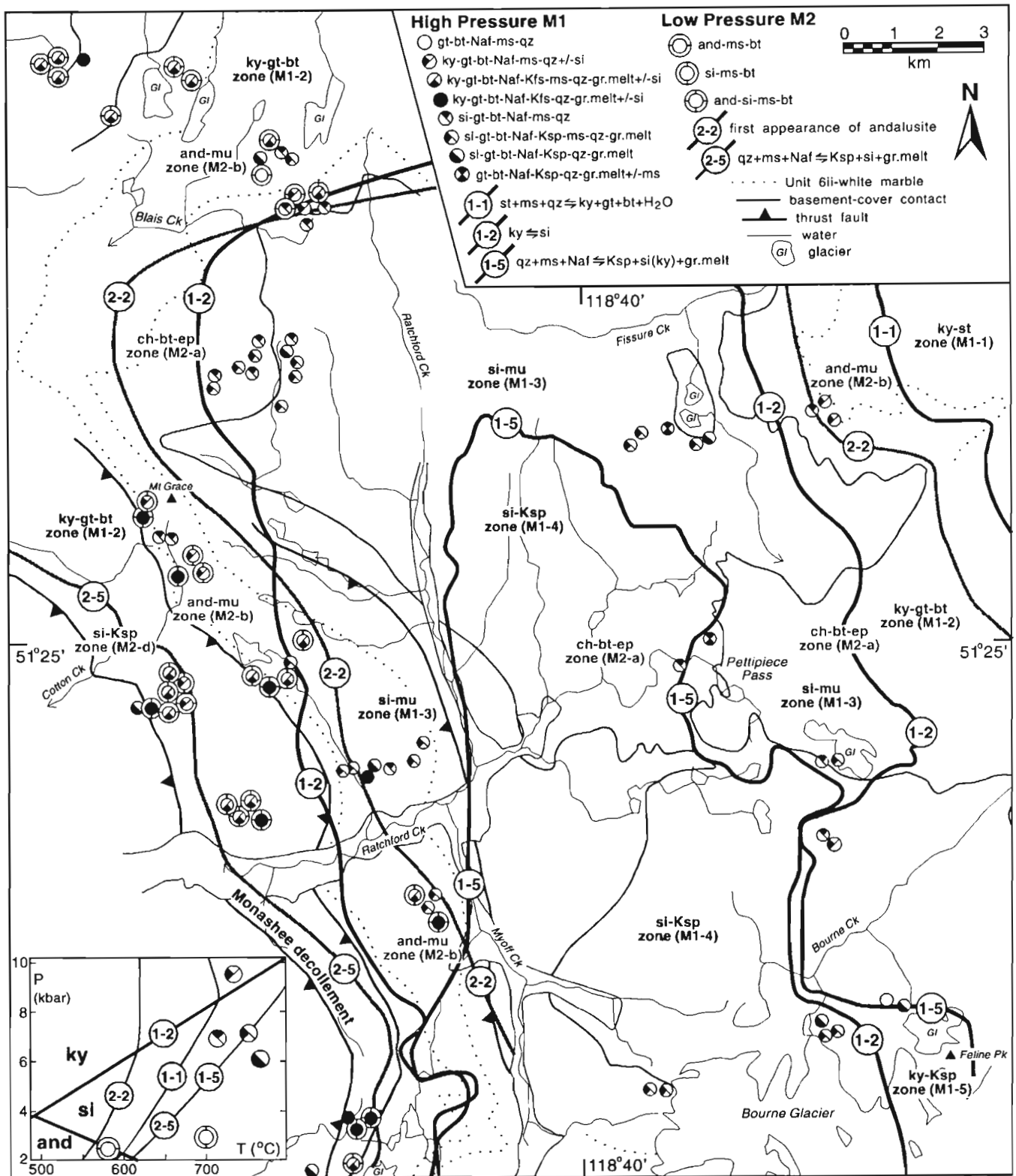


Figure 3. Metamorphic isograds and zones mapped by Journeay (1986) on the north flank of Frenchman Cap dome. Mineral assemblages are those mapped by this study and symbols depicting assemblages are those used by Journeay. P-T grid is from Spear and Cheney (1989). Mineral abbreviations are andalusite (and), biotite (bt), granitic melt (gr.melt), K-feldspar (Ksp), kyanite (ky), garnet (gt), muscovite (mu), Na-feldspar (Naf), quartz (qz), sillimanite (si), and staurolite (st).

The goal of this project is to estimate ages of protolith, magmatism, metamorphism, and deformation on the north flank of Frenchman Cap dome (Fig. 2) through mapping and U-Pb geochronology. Fieldwork in 1993 consisted of collecting samples and documenting their field relationships. This paper presents the pertinent relationships, after setting them in a regional context by briefly outlining previously collected data, the resulting interpretations, and reasons why the determination of ages of protolith and tectonism is significant to understanding the southern Omineca Belt.

PREVIOUS AGE ESTIMATES

This discussion is restricted to previous age estimates from Frenchman Cap dome (refer to Wanless and Reesor (1975), Duncan (1982), Coleman (1990), and Parkinson (1991) for data from Thor-Odin dome).

Journey (1986) provided petrological evidence for a normal Barrovian metamorphism (M1) in the Ratchford Creek map area that was overprinted by an inverted Buchan metamorphism (M2). Figure 3 delineates isograds resulting from each event. Journey interpreted M1 as occurring at high pressure during to slightly after Middle Jurassic east-directed displacement on the Monashee décollement (MD1) and second phase folds in the dome. The inferred Middle Jurassic age for M1 was based on correlation of M1 isograds across the décollement into the Kootenay Arc, where Archibald et al. (1983) documented Middle Jurassic high pressure metamorphism and plutonism, and on the estimated age of MD1. Journey postulated that the inverted M2 was synchronous with to slightly younger than Late Cretaceous to early Tertiary east-directed thrusting on the Monashee décollement (MD2). M2 was interpreted as a result of ramping of increasingly hotter and deeper tectonic levels of the Selkirk allochthon onto the cooler and shallower levels of the Monashee complex. The age assigned to M2 was based on the time required to exhume Frenchman Cap dome by 12-15 km from depths attained during a Middle Jurassic M1 given exhumation rates of 0.1-0.2 mm/a (uplift rates in Kootenay Arc for this time period as determined by Archibald et al., 1983). This discussion points out that Journey's inferred ages of M1 and M2 are not based on U-Pb geochronological data from the dome.

Armstrong et al. (1991) reported that Frenchman Cap dome core gneisses contain highly radiogenic Sr that scatters about a 2206 ± 117 Ma (1 sigma) Rb-Sr isochron, Sm-Nd whole-rock and crustal-residence (T_{DM}) ages of ~ 2.3 Ga, and mafic-felsic layering that is the same Early Proterozoic age as the rocks themselves. Zircon fractions from three orthogneiss samples have U-Pb ages that lie on chords with upper intercepts (inferred to be minimum time of crystallization) of 2066-2103 Ma. Granite described by Armstrong et al. as "little deformed, essentially postkinematic" (p. 1186) from the toe of Bourne Glacier (sample PCA-305B-83) yielded data that was interpreted as indicating either intrusion or metamorphism at 1851 ± 8 Ma; the presence of xenocrystic zircon made interpretations uncertain. The lack of major Pb-loss in monazite suggested that the granite was not reheated to migmatite-forming conditions after monazite

growth. Armstrong et al. concluded that core gneisses were little affected after the Early Proterozoic because there is no consistent isotopic pattern indicating, or even suggesting Late Proterozoic or younger magmatism, metamorphism, or migmatization.

Further evidence for Early Proterozoic metamorphism in core gneisses is found in unpublished Early Proterozoic titanite and zircon U-Pb ages (R.R. Parrish, unpublished data, pers. comm., 1991) from amphibolite sample OP-90-12 that is interlayered with augen orthogneiss south of Pettipiece Pass (Fig. 2). Zircons have a morphology suggesting that they grew during metamorphism. A moderate degree of Pb-loss in titanite implies that the sample was not subjected to upper amphibolite facies conditions after titanite growth. Other monazite and zircon U-Pb ages (Journey and Parrish, 1989; R.R. Parrish, unpublished data, pers. comm., 1991) indicate that on the west and northwest flanks of the dome (1) there was an early Tertiary metamorphic event in kyanite-bearing cover gneisses in the vicinity of the Monashee décollement and (2) early Tertiary pegmatites cut across fabrics in the footwall of the décollement.

These reconnaissance isotopic studies in Frenchman Cap dome suggest that the most recent significant metamorphism is Early Proterozoic age in the core and early Tertiary age in the cover in the vicinity of the Monashee décollement. No available data suggest that major metamorphism or deformation occurred between these ages.

SIGNIFICANCE OF THE AGE ESTIMATES

Protolith ages and ages of tectonism in Frenchman Cap dome have significant bearing on tectonic reconstruction of the southern Omineca Belt. Magmatic ages of the core gneisses allow for comparison with tectono-stratigraphic belts on the Canadian Shield and protolith ages of the cover gneisses assist in correlation with rocks above the Monashee décollement. Ages of tectonism have bearing on the mechanism, timing, and amount of exhumation in the southern Omineca Belt. Parrish et al. (1988) postulated that Eocene extension is the main cause of present crustal architecture of the Shuswap metamorphic complex. This model implies that the crust was more than 50 km thick prior to extension, the Shuswap complex was not exposed to erosion prior to the Eocene, and that it was tectonically denuded and exhumed on Eocene normal faults. Another model proposes that Eocene extension played a subordinate role in exhumation of Frenchman Cap dome (Journey, 1986; Brown et al., 1986; Brown and Journey, 1987). This model contends that major (12-15 km) pre-M2 (pre-Late Cretaceous to early Tertiary) erosional exhumation occurred during ramping within Frenchman Cap dome, during transfer of displacement from MD1 to deeper, foreland-stepping thrusts. Additional post-M2 exhumation of the dome could have resulted from erosion during ramping on deeper-level thrust faults or from displacement on extensional faults, or from a combination of the two. Two requirements of the exhumation mechanism necessary to preserve the inverted M2 gradient (before it was erased by conductive heat transfer within the crust) are that it was rapid and

occurred during or immediately after MD2 thrusting. Because extension on the Eocene Columbia River and Eagle River faults was required by geochronological data to have occurred more than 10 Ma after the proposed age of M2, some of the post-M2 exhumation was attributed to erosion that occurred during ramping of the dome onto two deeper foreland-stepping thrusts. The compressional model attributes final exhumation (6-10 km) and cooling to extensional faulting that is linked to the gravitational collapse of the uplifted crustal welt.

Revelation that metamorphic zircon overgrowths from kyanite-bearing cover gneisses in the immediate footwall of the Monashee décollement on the northwest flank of the dome are Late Paleocene-Early Eocene age (Journey and Parrish, 1989; R.R. Parrish, unpublished data, pers. comm., 1991) suggested to Journey and Parrish (1989) that M2 is this age. This age assignment led them to contend that extensional faulting played a significant role in post-M2 exhumation.

FIELD RELATIONSHIPS

Notes on terminology: (1) lithologic units referred to below and in Figure 2 are named according to Journey’s (1986) terminology; (2) deformation and metamorphic events, fold generations, and deformation fabrics are numbered according to our observations and do not necessarily correspond to previous workers’ terminology; and (3) events, phases, and fabrics in the core are number differently from those in the cover for reasons given below.

Core gneisses of Frenchman Cap dome

Orthogneiss and younger intrusives

Previous workers mapped core orthogneiss as intrusive into core paragneiss. No localities were found in which this relationship could be proven because the contacts between major orthogneiss bodies and paragneiss units are concordant with the transposed layering in the paragneiss. The regional-scale discordance between the orthogneiss bodies and paragneiss units is not considered as evidence for an intrusive relationship because discordancy results from both intrusive and unconformable contacts. Perhaps the best argument for an intrusive relationship is that thin and irregularly distributed layers of paragneiss within orthogneiss are probably deformed metasedimentary xenoliths rather than infolds. In order to better constrain the magmatic age of the major core orthogneiss bodies, the coarse augen orthogneiss (unit 2d, sample 65) mapped by Journey as the youngest body was sampled for U-Pb geochronology. Locations of potential geochronology samples are shown in Figure 2. Sample 187 is biotite hornblende granodioritic orthogneiss in the core of the Kirbyville anticline that was collected to determine whether core orthogneiss in this outlier is coeval with orthogneiss in the centre of the dome.

All major orthogneiss bodies contain the oldest observed fabric (S1). S1 is interpreted to have developed during the oldest recognizable deformation (D1) and metamorphism (M1) because it is gneissic and migmatitic (Fig. 4, 5, 6 depict S1 and its relationship to younger intrusives and deformation). S1 is rarely seen because it is typically transposed by second phase (F2) folds into the dominant, axial planar,

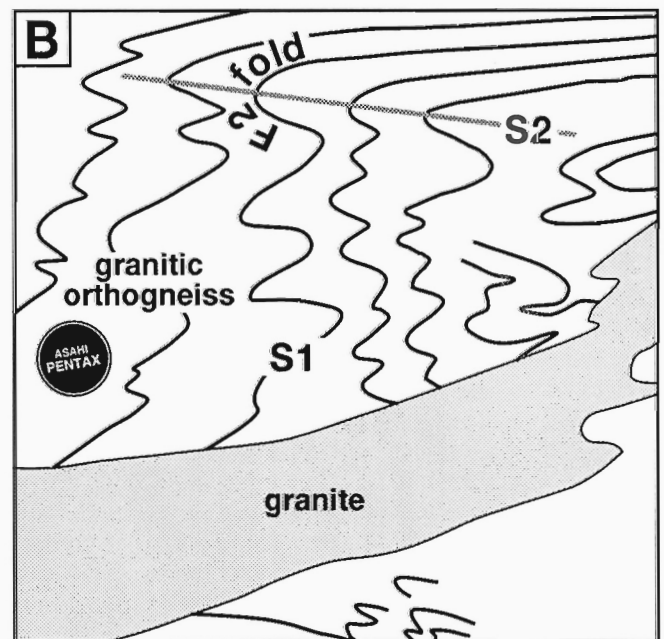
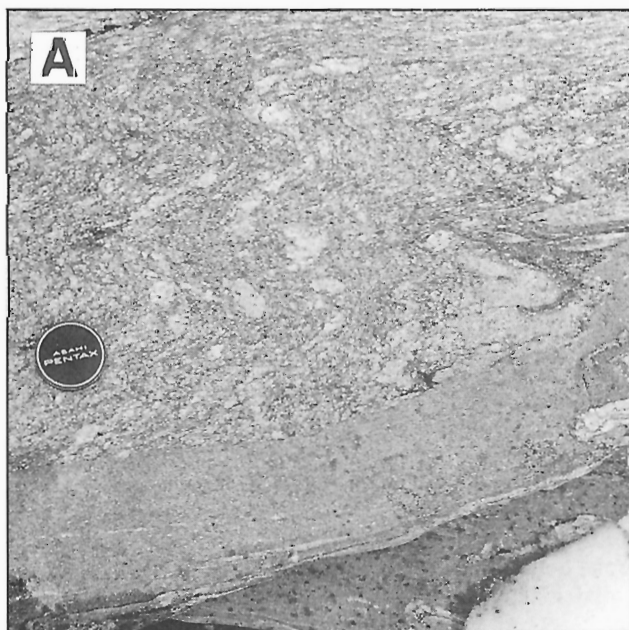


Figure 4. Photograph (A) and sketch (B) of migmatitic and gneissic S1 in core granitic orthogneiss (unit 2a) that is deformed by F2 folds and truncated by a granite dyke (similar to sample 60B). Note that F2 folds also deform the dyke to the right. The granite is thought to be Early Proterozoic age for reasons given in text. South of Pettipiece Pass.

second fabric (S2); S1 is only seen folded around F2 fold hinges in localities where F2 transposition is incomplete (Fig. 4, 5, 6). F2 folds are tight, overturned to recumbent, and have hinge lines that parallel the west-southwest-trending, stretching and mineral lineations. Third phase (F3) folds are northeast-verging, open, and upright to overturned postmetamorphic structures in the Pettipiece Pass area. F3 folds are pervasive in the cover gneisses and die out downward into the core gneisses.

In outcrops south of Pettipiece Pass intrusive contacts of homogeneous grey medium grained granite dykes with poorly defined linear and planar deformation fabrics truncate S1 in adjacent orthogneiss (Fig. 4). The dykes, in contrast to the orthogneiss, are neither migmatitic nor gneissic. They are deformed by F2 folds yet are not boudinaged or transposed into S2; intrusive contacts are discordant to S2, more so in F2 fold hinges and less so in the limbs (Fig. 4, 7). These

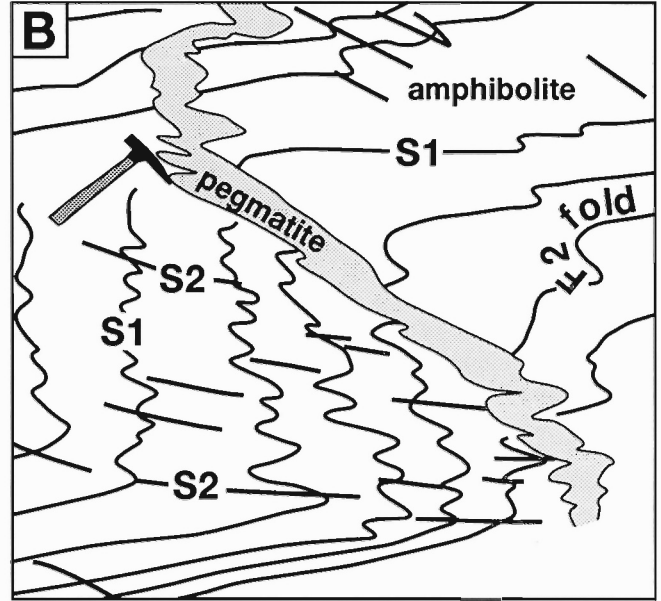


Figure 5. Photograph (A) and sketch (B) of migmatitic and gneissic S1 in core amphibolite that is deformed by F2 folds and truncated by a pegmatite dyke (similar to sample 60A), which is also deformed by F2 folds. South of Pettipiece Pass.

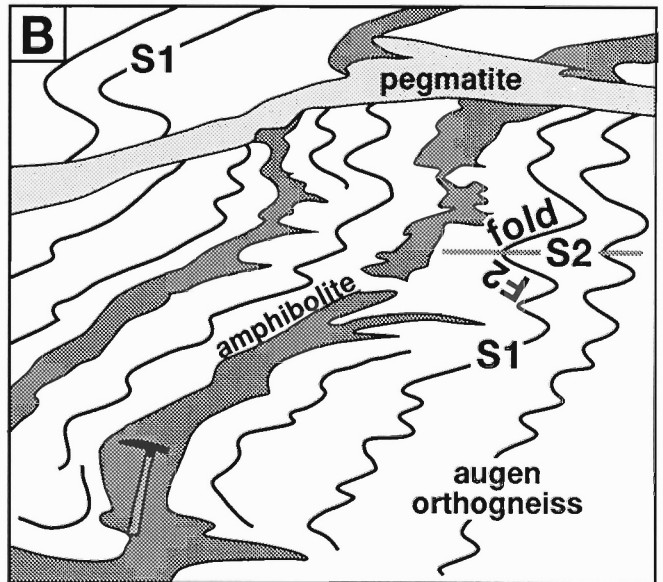
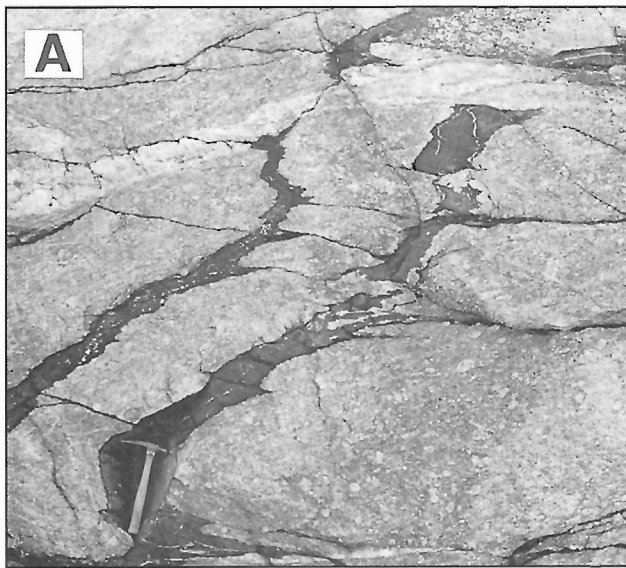


Figure 6. Photograph (A) and sketch (B) of core amphibolite dykes (sample 79) that are parallel with S1 in the host augen orthogneiss (unit 2d), deformed by F2 folds, and truncated by pegmatite. Sample 79 was collected from fold hinge upon which hammer lies. These relationships indicate that the amphibolite predates development of S1. South of Pettipiece Pass.



Figure 7. Intrusive contacts of a granite dyke (similar to sample 60B) are discordant to S2 seen in the host augen orthogneiss (unit 2d) and deformed by F2 folds. These relationships indicate that the dyke was involved in F2 folding yet was not transposed into S2. Toe of Bourne Glacier.

relationships suggest that deformation and metamorphism, which occurred in the core after intrusion of the dykes, were not intense enough to transpose or migmatize the dykes.

All granite dykes that we observed as intrusive into the core between D1 and D2 have similar grain size, colour, and composition, and are therefore interpreted to be part of the same magmatic phase of approximately the same age. We consider the dykes to be older than the cover gneisses because they intrude up to the highest structural levels in the core but do not intrude the cover. This interpretation is significant because it requires that M1 and D1 in the core predate deposition of the cover gneisses. Journeay (1986) also noted a stage of migmatization that is restricted to the core. Our interpretation of the antiquity of the granite is consistent with the observation that the "little deformed, essentially postkinematic" granite from the toe of Bourne Glacier (sample PCA-305B-83) which yielded data interpreted by Armstrong et al. (1991) as indicating intrusion or metamorphism at 1851 Ma appears to part of this magmatic phase. We make this correlation because granite at the sample locality intruded core gneisses between D1 and D2, and has similar grain size, colour, and composition as post-D1/pre-D2 granite seen elsewhere.

Sample 60B is a granite dyke collected south of Pettipiece Pass for igneous zircon and monazite which will potentially determine whether the granite is indeed Early Proterozoic. Samples 60A and 84 are pegmatite dykes which intruded the granite between D1 and D2 (Fig. 5). We could not determine whether these pegmatites predate the cover gneisses because pegmatite occurs in both core and cover and all generations appear similar. Sample 235 is an amphibolite layer which truncates S1 yet is folded by F2 folds. Crystallization ages from these samples will be upper limits on D1 and the

associated M1 migmatization and lower limits on D2. The age of the granite dyke will be a lower limit on deposition of the cover gneisses. Sample 79 is an amphibolite layer that is concordant with S1 and truncated by granite dykes and pegmatite (Fig. 6). Because concordancy with S1 requires that it predates D1, its crystallization age will be a lower age limit on M1 and D1.

Samples 57 and 91 are post-D2 pegmatites which contain no deformation fabrics and are not affected by F2 folds. Their relationship to F3 folds is unknown because there are no F3 folds in the vicinity of the samples.

Paragneiss

As also noted by Journeay (1986), metamorphic mineral assemblages in the core pelitic schist (unit 1p) are identical to those in the nearest cover schist. Figure 3 shows that the typical core assemblage is garnet-sillimanite-biotite \pm muscovite \pm granitic melt and the muscovite-out isograd is continuous from core into cover. These observations require that either minerals in the core and cover grew during the same event or that an event that affected the cover coincidentally attained the same metamorphic grade as one restricted to the core.

In an attempt to differentiate ages of metamorphism in the core and cover (different ages are predicted from field relationships outlined above) and to test Armstrong et al.'s (1991) suggestion that Phanerozoic metamorphism did not greatly affect the deeper parts of the dome, pelitic schist samples 24, 70, 85, 112, and 166 were collected for monazite and/or zircon dating. Figures 2 and 3 show that they were collected near cover samples with identical assemblages, requiring that sample pairs experienced similar P-T conditions during their shared metamorphism. It is expected that U-Pb ages will not record the inverted, lower pressure metamorphic overprint (M2 of Journeay, 1986) seen at higher structural levels because the samples occur in Journeay's chlorite-biotite-epidote M2-a zone (Fig. 3).

Unconformity between core and cover gneisses

The contact between the core gneisses and basal quartzite (unit 3q1) of the cover gneisses was interpreted as unconformable by previous workers. This interpretation is supported by 1990-2007 Ma detrital zircon ^{207}Pb - ^{206}Pb ages obtained from the basal quartzite on the west flank of Frenchman Cap dome by Ross and Parrish (1991); ages are similar to those from the core orthogneiss. Our best field evidence for an unconformity is the fact that core orthogneiss does not intrude the cover. Quartz pebble conglomerate which overlies the core elsewhere in the Monashee complex was not observed. Instead, clean and micaceous quartzite typically occurs at the base and is interbedded with metre-wide quartz grit layers. Thin (0.3-1 m) quartz pebble conglomerate layers were locally seen ~10 m above the contact. South of Pettipiece Pass the basal quartzite lies upon migmatitic biotite schist in the core (Fig. 8) that is locally strongly sheared in 1-2 m wide zones.



Figure 8. Unconformity between core and cover gneisses south of Pettipiece Pass. Basal micaceous quartzite of the cover (unit 3q1) overlies biotite schist of the core. F3 folds deform the contact.

Cover gneisses of Frenchman Cap dome

Samples 25, 126, and 165 were collected in the cover pelitic schist in an attempt to date the high pressure metamorphism (M1 of Journeay, 1986). It is expected that monazite and zircon ages from these samples will record the high pressure metamorphism rather than the low pressure overprint because they occur below the zone of andalusite overprint (M2-b of Journeay, 1986). Our mapping of metamorphic mineral assemblages in cover pelitic schist mostly agrees with Journeay's mapping.

Similar to the core gneisses, the cover gneisses south of Pettipiece Pass contain a migmatitic S1 that is typically transposed by F2 folds into the axial planar, dominant S2 (Fig. 9). F2 folds in the cover gneisses at this structural level have the same style and orientation as F2 folds in the core and S2 in the cover is concordant with S2 in the core. Journeay (1986) considered F2 folds everywhere to be coeval. Structural relationships, however, present us with a conundrum because S1 in the core predates deposition of the cover gneisses for reasons given above concerning the granite dykes (sample 60B) which do not intrude the cover. There are three obvious possible explanations for this conundrum. One possibility is that S1 in the cover is coeval with S2 in the core, requiring that F2 folds in the cover are younger than and

unrelated to F2 folds in the core, regardless of their similar geometry and orientation. Because the only folds (F3 folds) that affect S2 in the core are continuous across the unconformity, an implication of this scenario is that F2 folds in the cover did not greatly affect the core. A second possibility is that F2 folds in the core and cover are indeed coeval. Because F2 folds in the core are apparently the oldest structures that deform S1 in the core, an implication of this scenario is that F1 folds in the cover did not greatly affect the core. Such scenarios require that the unconformity separates structural levels, with cover gneisses being strongly deformed while the core remained relatively unaffected. A third possibility is that enough displacement occurred along the unconformity to juxtapose different structural levels. This problem obviously requires further study.

Samples 12, 180, and 191 were collected from different structural levels in an attempt to determine whether the dominant outcrop-scale folds in the cover are coeval. We interpret such folds that occur in the relatively low structural level (immediately above the core gneisses) in the Pettipiece Pass area as F2 folds because they deform only one pre-existing fabric (S1). S1 is seen at this structural level because D2 transposition was not complete. We do not assign a generation to the dominant folds in higher structural levels because only one, undoubtedly transposed, fabric is seen. Most leucosome and pegmatite layers at this level are also transposed into the dominant fabric. We have not sufficiently mapped the area between Pettipiece Pass and the higher structural levels to confidently correlate the dominant fabric in all levels. Journeay (1986) interpreted F2 folds that he mapped as the dominant outcrop-scale structures that are coeval from the core to the immediate footwall of the Monashee décollement.



Figure 9. Migmatitic S1 in cover pelitic schist (near sample 101, unit 3p) is deformed by F2 folds. S1 in the core (Fig. 4, 7, 8) is thought to be older than S1 in the cover for reasons given in the text, yet they have the same relationships to metamorphism and are deformed by F2 folds that have similar geometry and orientation.

Sample 12 is late-D2 pegmatite from immediately above the core south of Pettipiece Pass that was being transposed into concordancy with S2 when D2 ceased. This interpretation is made because a few pegmatite layers of this generation are concordant with S2 and most are slightly to moderately discordant and boudinaged. Sample 191 is folded, kyanite-bearing leucosome within cover schist on the east limb of the Kirbyville anticline. Sample 180 is leucosome that is deformed by the dominant fold set within kyanite- and sillimanite-bearing cover schist in the immediate footwall of the Monashee décollement.

Samples 204 and 207 were collected with hopes of better estimating the age of the cover gneisses. Previous geochronology is interpreted as indicating that the basal quartzite (unit 3) is pre-740 Ma (Parrish and Scammell, 1988) and the middle of the sequence (Cottonbelt Pb-Zn deposit, unit 6iii) is Lower Cambrian (Hoy and Godwin, 1988). Sample 204 is quartz pebble conglomerate at the base of unit 7, from which detrital zircons will reveal source ages and allow for comparison with ages obtained from the basal quartzite by Ross and Parrish (1991). Sample 207 is granitic orthogneiss on the west flank of Mount Grace that lies 200-300 m structurally above the Cottonbelt Pb-Zn deposit. It contains the same deformation fabrics seen in adjacent paragneiss and its lower (east) boundary is concordant with these fabrics. Other intrusives associated with it include leucogranitic and granodioritic orthogneiss. Journeay (1986) placed the Anstey Range thrust fault beneath the orthogneiss and Hoy (1987) placed a thrust fault above it. Upon observing the lower contact directly west of Mount Grace, we found that it lies ~200 m farther east than as mapped by Hoy and concluded that there is no firm evidence for either an intrusive or faulted contact. It is hoped that ages from these samples could reveal one or more unconformities in the cover gneisses that have yet to be noticed.

SUMMARY

This paper presents field relationships in the Pettipiece Pass area corroborating Armstrong et al.'s (1991) isotopic data which suggest that core gneisses of Frenchman Cap dome were migmatized and deformed in the Early Proterozoic. Field relationship indicate that this tectonism occurred prior to deposition of the cover gneisses. Field and isotopic data also suggest that core gneisses were not as affected by Phanerozoic tectonism as cover gneisses were at higher structural levels. Further refinements of the age of tectonism in all levels of the dome are required before description and explanation of such a tectonic scenario can be proposed.

ACKNOWLEDGMENTS

Fieldwork was supported by the Continental Geoscience Division of the Geological Survey of Canada and NSERC Operating Grant 42512 to R.R. Parrish. NSERC Operating Grant 2693 to R.L. Brown supplied a computer. This project is a Ph.D. thesis undertaken by JLC at Carleton University

and co-supervised by R.R. Parrish and R.L. Brown, who are thanked for their input during mapping. J.M. Journeay is thanked for reviewing the manuscript.

REFERENCES

- Archibald, D.A., Glover, J.K., Price, R.A., Farrar, E., and Carmichael, D.O.**
1983: Geochronology and tectonic implications of magmatism and metamorphism, southern Kootenay Arc and neighboring regions, southeastern British Columbia, Part I: Jurassic to mid-Cretaceous; *Canadian Journal of Earth Sciences*, v. 20, p. 1891-1913.
- Armstrong, R.L., Parrish, R.R., van der Heyden, P., Scott, K., Runkle, D., and Brown, R.L.**
1991: Early Proterozoic basement exposures in the southern Canadian Cordillera: core gneiss of Frenchman Cap, Unit I of the Grand Forks Gneiss and Vaseux Formation; *Canadian Journal of Earth Sciences*, v. 28, p. 1169-1201.
- Brown, R.L.**
1980: Frenchman Cap Dome, Shuswap Complex, British Columbia; in *Current Research, Part A; Geological Survey of Canada, Paper 80-1A*, p. 47-51.
- Brown, R.L. and Journeay, J.M.**
1987: Tectonic denudation of the Shuswap metamorphic terrane of southeastern British Columbia; *Geology*, v. 15, p. 142-146.
- Brown, R.L., Journeay, J.M., Lane, L.S., Murphy, D.C., and Rees, C.J.**
1986: Obduction, backfolding and piggyback thrusting in the metamorphic hinterland of the southeastern Canadian Cordillera; *Journal of Structural Geology*, v. 8, p. 225-268.
- Coleman, V.J.**
1990: The Monashee décollement at Cariboo Alp and regional kinematic indicators, southeastern British Columbia; M.Sc. thesis, Carleton University, Ottawa, Ontario, 112 p.
- Duncan, I.J.**
1982: The evolution of the Thor-Odin gneiss dome and related geochronological studies; Ph.D. thesis, University of British Columbia, Vancouver.
- Hoy, T.**
1987: Geology of the Cottonbelt lead-zinc magnetite layer, carbonatites and alkalic rocks in the Mount Grace area, Frenchman Cap dome, southeastern British Columbia; *British Columbia Ministry of Energy, Mines, and Petroleum Resources, Bulletin 80*, 99 p.
- Hoy, T. and Godwin, C.I.**
1988: Significance of a Cambrian date from galena lead-isotope data for the stratiform Cottonbelt deposit in the Monashee complex, southeastern British Columbia; *Canadian Journal of Earth Sciences*, v. 25, p. 1534-1541.
- Journeay, J.M.**
1986: Stratigraphy, internal strain, and thermo-tectonic evolution of northern Frenchman Cap dome, an exhumed basement duplex structure, Omineca hinterland, southeastern Canadian Cordillera; Ph.D. thesis, Queen's University, Kingston, Ontario.
- Journeay, J.M. and Parrish, R.R.**
1989: The Shuswap thrust; sole fault to a metamorphic-plutonic complex of Late Cretaceous-early Tertiary age, southern Omineca Belt, British Columbia; *Abstracts with Programs, Geological Society of America, Cordilleran Section*.
- McMillan, W.J.**
1973: Petrology and structure of the west flank, Frenchman's Cap dome, near Revelstoke, British Columbia; *Geological Survey of Canada, Paper 71-29*.
- Monger, J.W.H., Price, R.A., and Tempelman-Kluit, D.J.**
1982: Tectonic accretion and the origin of the two major metamorphic and plutonic belts in the Canadian Cordillera; *Geology*, v. 10, p. 70-75.
- Parkinson, D.**
1991: Age and isotopic character of Early Proterozoic basement gneisses in the southern Monashee complex, southeastern British Columbia; *Canadian Journal of Earth Sciences*, v. 28, p. 1159-1168.

Parrish, R.R. and Scammell, R.J.

1988: The age of the Mount Copeland Syenite Gneiss and its metamorphic zircons, Monashee Complex, southeastern British Columbia; in Radiogenic Age and Isotopic Studies: Report 2; Geological Survey of Canada, Paper 88-2, p. 21-28.

Parrish, R.R., Carr, S.D., and Parkinson, D.L.

1988: Eocene extensional tectonics and geochronology of the southern Omineca Belt, British Columbia and Washington; Tectonics, v. 7, p. 181-212.

Psutka, J.F.

1978: Structural setting of the Downie slide, northeast flank of the Frenchman Cap gneiss dome, Shuswap Complex, southeastern British Columbia; M.Sc. thesis, Carleton University, Ottawa, Ontario.

Reag, P.B. and Brown, R.L.

1981: Columbia River fault zone: southeastern margin of the Shuswap and Monashee complexes, southern British Columbia; Canadian Journal of Earth Sciences, v. 18, p. 1127-1145.

Ross, G.M. and Parrish, R.R.

1991: Detrital zircon geochronology of metasedimentary rocks in the southern Omineca Belt, Canadian Cordillera; Canadian Journal of Earth Sciences, v. 28, p. 1254-1270.

Scammell, R.J. and Brown, R.L.

1990: Cover gneisses of the Monashee terrane: a record of synsedimentary rifting in the North American Cordillera; Canadian Journal of Earth Sciences, v. 27, p. 712-726.

Spear, F.S. and Cheney, J.T.

1989: A petrogenetic grid for pelitic schists in the system SiO₂-Al₂O₃-FeO-MgO-K₂O-H₂O; Contributions to Mineralogy and Petrology, v. 101, p. 149-164.

Wanless, R.K. and Reesor, J.E.

1975: Precambrian zircon age of orthogneiss in the Shuswap metamorphic complex, British Columbia; Canadian Journal of Earth Sciences, v. 12, p. 326-332.

Wheeler, J.O.

1965: Big Bend map area, British Columbia (82N east half); Geological Survey of Canada, Paper 64-32.

Wheeler, J.O. and McFeely, P. (compilers)

1991: Tectonic assemblage map of the Canadian Cordillera and adjacent parts of the United States of America; Geological Survey of Canada, Map 1712A, scale 1:2 000 000.

NSERC Operating Grant 42512

Geology of Big Bar map area, British Columbia: facies distribution in the Jackass Mountain Group¹

C.J. Hickson, J.B. Mahoney², and P. Read³

Cordilleran Division, Vancouver

Hickson, C.J., Mahoney, J.B., and Read, P., 1994: Geology of Big Bar map area, British Columbia: facies distribution in the Jackass Mountain Group; in Current Research 1994-A; Geological Survey of Canada, p. 143-150.

Abstract: The Big Bar map area (920/1) is situated between the Fraser fault system on the east and the Yalakom fault system on the southwest, and is underlain mainly by clastic sedimentary rocks of the Lower Cretaceous Jackass Mountain Group, as well as extensive exposures of Miocene-Pliocene Chilcotin Group basalt, Eocene volcanic rocks, Lower Cretaceous Spences Bridge Group volcanic rocks, Middle Jurassic Dewdney Creek Formation sedimentary rocks, Permian to Lower Jurassic(?) Cache Creek Complex, and Permian(?) Shulaps Complex mélange. Geological mapping of the area has resulted in a more complete understanding of the facies distribution of the Lower Cretaceous Jackass Mountain Group, which here is subdivided into four informal members, including: 1) green feldspathic litharenite facies; 2) polymictic conglomerate facies; 3) massive litharenite facies; and 4) bedded sandstone and siltstone facies. These facies are laterally and vertically gradational and the group generally fines both upsection and to the west.

Résumé : La région cartographique de Big Bar (920/1) est située entre le système de failles du Fraser, à l'est, et le système de failles de Yalakom, au sud-ouest, et son sous-sol est composé de roches sédimentaires clastiques du Groupe de Jackass Mountain (Crétacé inférieur) ainsi que de vastes affleurements de basalte du Groupe de Chilcotin (Miocène-Pliocène), de roches volcaniques éocènes, de roches volcaniques du Groupe de Spences Bridge (Crétacé inférieur), de roches sédimentaires de la Formation de Dewdney Creek (Jurassique moyen), du complexe de Cache Creek (Permien-Jurassique inférieur?) et d'un mélange du complexe de Shulaps (Permien?). La cartographie géologique de la région a permis de mieux établir la répartition des faciès du Groupe de Jackass Mountain du Crétacé inférieur, qui est ici subdivisé en quatre membre informels : 1) le faciès de litharénite feldspathique de couleur verte; 2) le faciès de conglomérat polygénique; 3) le faciès de litharénite massive; 4) le faciès de grès et de siltstone stratifiés. Ces faciès présentent des contacts progressifs, tant latéraux que verticaux, et les unités du groupe ont généralement un grain plus fin vers le haut de la coupe stratigraphique et vers l'ouest.

¹ Contribution to Frontier Geoscience Program Chilcotin-Nechako Hydrocarbon Province

² Department of Geological Sciences, University of British Columbia, 6339 Stores Road, Vancouver, British Columbia V6T 1Z4

³ Geotex Consultants Limited, #1200-100 West Pender Street, Vancouver, British Columbia V6B 1R8

INTRODUCTION

Mapping of Big Bar map area (92O/1) completes mapping in Taseko Lakes (92O). This fieldwork started in 1990 as part of the Frontier Geoscience Program (Hickson, 1990). Previous fieldwork covered the northeastern sector (Hickson et al., 1991; Read, 1992, 1993), central part (Hickson, 1992; Mahoney et al., 1992; van der Heyden and Metcalfe, 1992) and the northwest quadrant (Hickson and Higman, 1993; Hickson, 1993). Also, a surficial mapping component addressed not only distribution of surficial deposits (Broster and Huntley, 1992), but also glacial flow patterns over the entire Taseko Lakes map area (Huntley and Broster, 1993).

This report presents the findings of 1993 fieldwork, and compilation and discussion of earlier work, including Trettin (1961), Tipper (1978), Read (1988), and Schiarizza et al. (1990). This season's mapping in 92O/1 (Fig. 1) concentrated on the stratigraphy of the Jackass Mountain Group. Mapping along the Fraser River, completed by Read (1988), and that in extreme southwest corner by Schiarizza et al. (1990), were part of the 1985-1990 Provincial-Federal Mineral Development Agreement (MDA).

STRATIGRAPHY

Paleozoic to Mesozoic

Shulaps Complex

The Permian(?) Shulaps Complex (**Psm**; Fig. 1) is poorly exposed west of the Yalakom Fault, in the southwestern part of the map area (Schiarizza et al., 1990). The unit weathers recessively; the best exposures are in roadcuts east of the Yalakom River and on the ridge between the Yalakom River and Blue Creek. In this area, the Shulaps Complex is a serpentinite mélange primarily consisting of boudins of serpentinite, gabbro, and amphibolite in a talc schist and serpentinite matrix. Foliations trend northwest, parallel to the trend of the Yalakom Fault, and dip steeply to the east. West of the map area, Schiarizza et al. (1990) mapped the serpentinite mélange as structurally overlain by mantle harzburgite along Peridotite Creek. They describe these rocks as forming the eastern limb of a broad synform that encompasses the entire Shulaps Complex.

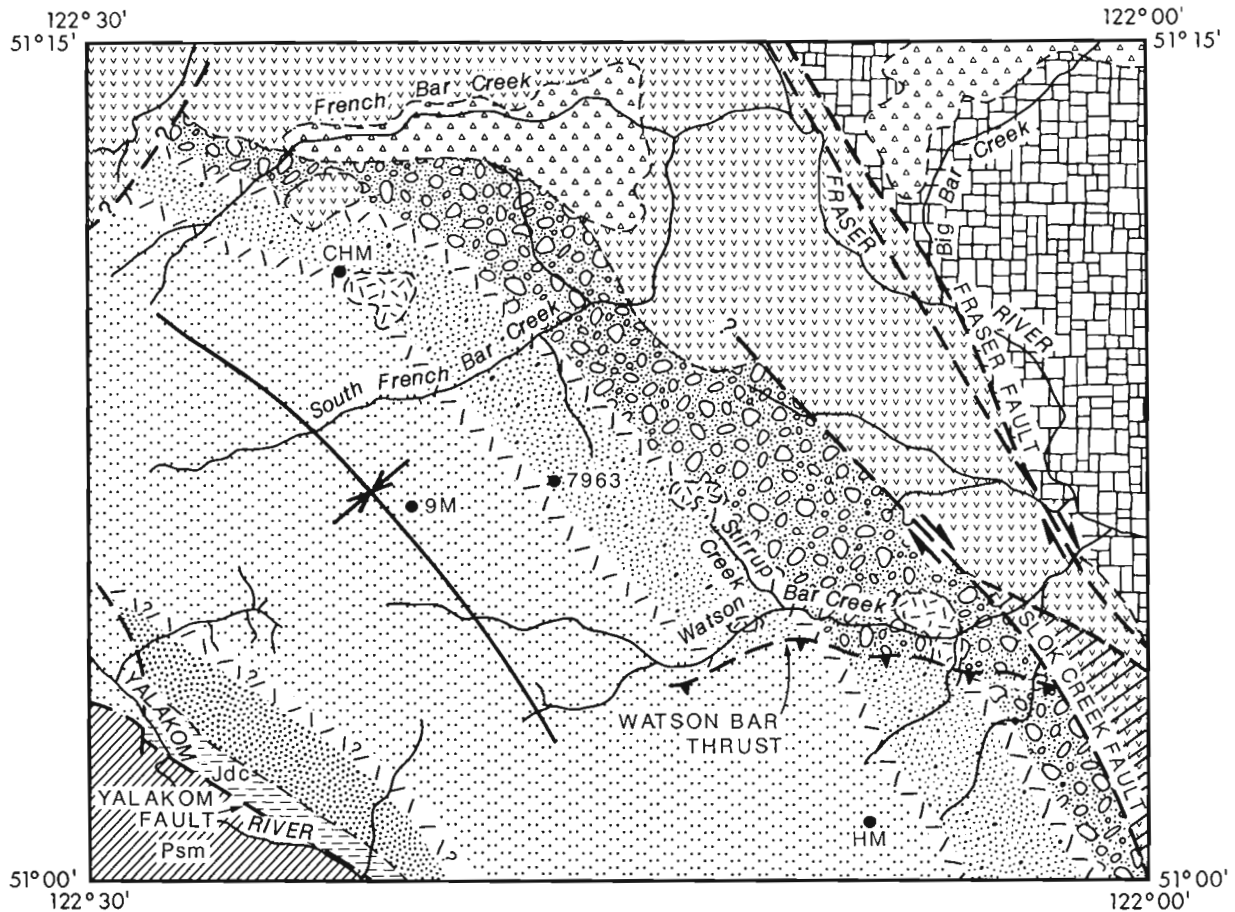


Figure 1. Schematic geological map of the Big Bar map area (92O/1). Location symbols include: CHM=China Head Mountain; 9M=Nine Mile Ridge; 7963=Peak 7963; HM=Hogback Mountain.

Cache Creek Complex

In the map area, limited exposures of Cache Creek Complex (**PJcc**; Fig. 1) (Monger and McMillan, 1989) occur along the Fraser River, east of the Fraser fault. The Cache Creek Complex exposed here is sediment dominated and contains grey phyllite, varicoloured ribbon chert, siltstone, greywacke, and minor limestone and greenstone. The Cache Creek Complex in this area is believed to range from Permian to Upper Triassic and possibly Lower Jurassic(?).

Mesozoic

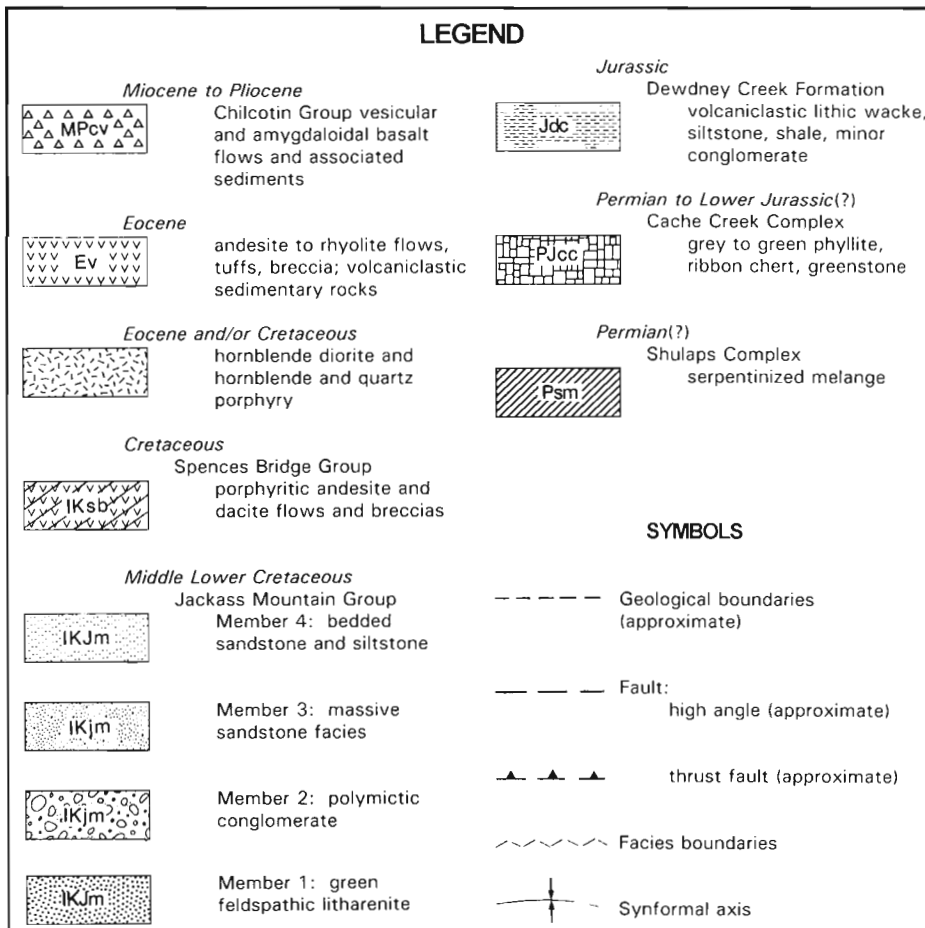
Jurassic

Dewdney Creek Formation

Middle Jurassic siltstone, argillite, and minor volcanic sandstone and conglomerate are exposed along the northeast side of the Yalakom fault, on the east side of the Yalakom River, in the southwestern portion of the map area. These strata have been subject to a confusing array of nomenclature. The unit was originally mapped as the Lower Cretaceous Lillooet Group by Duffell and McTaggart (1952). Leech (1953) reported new fossil localities, and mapped the unit as a Middle Jurassic volcanic sandstone. Trettin (1961) and Frebold et al. (1969) retained the name Lillooet Group but reported new Middle Jurassic biostratigraphy. Woodsworth (1977) mapped the unit as the Upper Jurassic-Lower Cretaceous

Relay Mountain Group, and Tipper (1978) correlated the unit with the Tyaughton Group. Schiarizza et al. (1989) avoided the confusing nomenclature, and simply mapped the unit as an unnamed mid-Jurassic volcanic sandstone. Mahoney (1992, 1993) showed that Middle Jurassic strata exposed north of Lillooet correlate with the western distal facies of the Dewdney Creek Formation, and represent a portion of the formation offset by the dextral Fraser fault system.

The Middle Jurassic Dewdney Creek Formation (**Jdc**; Fig. 1) (Mahoney, 1993) in this area consists of thin bedded argillite and siltstone interbedded with medium- to thick-bedded volcanic sandstone and granule to pebble conglomerate. Although the recessively weathering argillite and siltstone are volumetrically more abundant, the sandstone and conglomerate form prominent lenticular ribs that locally dominate the outcrop belt. Coarse grained strata are in cyclic coarsening and thickening/fining and thinning upward sequences, separated by thick sequences of fine siltstone and argillite with abundant sedimentary structures indicative of turbidite deposition. The base of the formation is not exposed, and the lower contact of the formation is the Yalakom fault. The formation is disconformably overlain by the Jackass Mountain Group. The maximum thickness is estimated to be 800 m. Based on numerous ammonite fossils found on the east side of the Yalakom River, above the confluence with Blue Creek, the age of the formation is constrained as Aalenian to Bajocian (Frebold et al., 1969; Mahoney, 1992).



Jackass Mountain Group

The Lower Cretaceous Jackass Mountain Group (IKjm; Fig. 1) is well exposed and volumetrically the most significant unit in the central and eastern Camelsfoot Range. It forms the central part of a ~150 km long, southward-tapering wedge of mainly coarse grained volcanic sandstone and polymictic conglomerate exposed between the Yalakom and Fraser fault systems. It forms a broad, asymmetric synclinalorium; the base of the unit is exposed in steeply dipping beds on the western limb, east of the Yalakom River, and the upper part is exposed in moderately west-dipping beds in the eastern limb. The unit lies disconformably above the Middle Jurassic Dewdney Creek Formation and the present erosion surface forms the top of the group in this area. The Jackass Mountain Group is generally nonfossiliferous, but has yielded Barremian to Albian bivalves, ammonites, and belemnites, particularly from the basal part of the group (Duffell and McTaggart, 1952; P. Schiarizza, pers. comm., 1993).

In the Camelsfoot Range, the Jackass Mountain Group can be subdivided into four informal members (Fig. 1) that are laterally and vertically gradational. These members are as follows:

Member 1 - green feldspathic litharenite: The basal member consists of medium- to thick-bedded (0.5-1 m), structureless, medium- to coarse-grained feldspathic litharenite that contains primarily moderate- to well-sorted angular to subangular grains of volcanic lithics, plagioclase feldspar, quartz, and subordinate chert fragments. The quartz content locally approaches 15%, and angular red chert clasts (<0.25 cm) are locally dispersed within the unit. The unit is conspicuously green and has a conchoidal fracture pattern. Intercalated with the arenite are thin beds of brown siltstone and parallel and cross laminated, fine grained arenite. These fine interbeds are locally scoured and incorporated as rip-up clasts into the base of overlying sandstone beds. Bivalve shells and fragments are found locally within this member.

Schiarizza et al. (1990) report a thin basal polymictic conglomerate bed containing abundant plutonic debris near the disconformity with underlying Middle Jurassic strata. Little or no angular discordance exists between the Jackass Mountain Group and underlying Middle Jurassic strata.

Member 2 - polymictic conglomerate: Member 2 consists of pebble to boulder polymictic conglomerate and coarse grained feldspathic lithic arenite. The conglomerate is generally matrix supported. Clasts are ellipsoidal to spherical and consist of subrounded to rounded clasts of granodiorite, foliated granodiorite, gneiss, intermediate volcanic rocks, and chert (Fig. 2). Maximum clast size observed was 40-50 cm in diameter. The conglomerate fabric ranges from internal disorganization to crude stratification defined by imbrication of clasts. Conglomeratic intervals consist of 10-30 m of amalgamated thick bedded (1-2 m) conglomerate and intercalated coarse grained feldspathic lithic arenite. Boulder lag deposits occur locally. Beds vary between lenticular to laterally continuous and appear to be both channelized and unchannelized. Scour features and rip-up clasts are common

near the base of conglomerate beds. The upper portions of the beds are very crudely stratified and graded. Conglomerate beds grade upward into coarse grained to pebbly feldspathic lithic arenite.

Polymictic conglomerate forms a northwest-trending belt on the eastern side of the map area (Fig. 1). The unit is well exposed on the east end of China Head Mountain ridge, on the ridges north and east of Stirrup Creek, on the north side of Watson Bar Creek, and south and east of Hogback Mountain. Member 2 decreases in grain size and becomes sandier to the west. The grain size distribution and clast composition suggest a northeast source supplying clasts from the Mt. Lytton, Eagle, and the Cache Creek complexes (Monger, 1989). This paleogeography is consistent with that suggested by Kleinspehn (1982).

Member 3 - massive sandstone facies: Member 3 is mainly thick bedded to massive, medium- to coarse-grained feldspathic lithic and volcanic lithic arenite, which are pebbly in part, with intercalated medium- to thick-bedded pebble conglomerate and thin bedded, fine grained sandstone and siltstone (Fig. 3). The sandstone is moderately to moderately well sorted, grain supported, and contains subangular to subrounded grains of volcanic lithics, sericitized plagioclase, plutonic and metamorphic quartz (locally up to 15-20%), chert, and metamorphic lithics. Matrix is generally lacking, although locally the sandstone appears to be lithic wacke.

The unit is massive and structureless but close examination reveals thick bedded sandstone containing internal amalgamation surfaces defined by subtle changes in grain size, sorting, minor scour surfaces, and rip-up clast intervals. Rip-up clast intervals are common, and consist of angular to subrounded pebbles to cobbles of white to light yellow siltstone in a sandstone matrix near the base of structureless sandstone beds. Minor thin bedded (1-4 cm) light yellow siltstone interbeds occur within amalgamated sandstone intervals, but are commonly scoured by overlying sandstone beds. Subtle grading is common within sandstone beds, and faint, crude parallel laminae occur locally near the top of thick

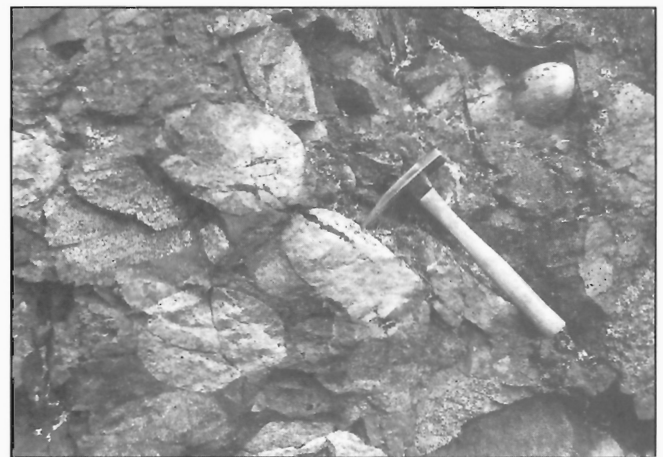


Figure 2. Photograph of polymictic conglomerate facies of Member 2, Jackass Mountain Group.

sandstone beds. Beds are tabular and laterally continuous. Amalgamated sandstone intervals attain thicknesses of 50-100 m, and intercalated thin- to medium-bedded, fine grained sandstone and siltstone locally attain 5-10 m. Channel features and planar crossbeds occur locally near the top of the unit, below the contact with the overlying thin- to medium-bedded member 4. The lower contact of the unit is placed above the uppermost thick conglomerate unit in member 2, and the upper contact is placed at the top of the uppermost thick amalgamated sandstone interval.

Member 4 - bedded sandstone and siltstone facies: Member 4 consists primarily of intercalated, thin- to medium-bedded, fine- to medium-grained sandstone and thin bedded parallel laminated siltstone and mudstone (Fig. 4). The sandstone is primarily fine- to medium-grained, well sorted lithic feldspathic arenite to wacke. It consists of moderately well-



Figure 3. Photograph of thick bedded, laterally continuous, medium- to coarse-grained volcanic sandstone of Member 3, Jackass Mountain Group. Note thin bedded intervals separating thick sandstone sequences.



Figure 4. Photograph of thin to medium bedded sandstone and siltstone of Member 4, Jackass Mountain Group.

to well-sorted angular to subangular grains of plagioclase, quartz, hornblende, and chert, and subangular to subrounded grains of volcanic and metamorphic lithics. Sedimentary structures include parallel laminae, normal grading, basal scour features, and rare planar cross-sets and convolute laminae. Sandstone beds are commonly gradationally overlain by thin bedded (1-5 cm) parallel laminated siltstone and mudstone. Siltstone is thin bedded, laterally continuous, locally bioturbated, and displays parallel laminae, cross laminae, and minor convolute laminae. The sandstone and siltstone beds tend to form intercalated couplets; 10-20 cm of sandstone, overlain by 1-5 cm siltstone to mudstone. Thin bedded, normally graded, fine grained sandstone locally amalgamates to 1 to 3 m, and is locally interbedded with both medium- to thick-bedded, coarse grained sandstone that contains basal scour features and rip-up clast intervals, and minor polymictic pebble conglomerate and thin bedded sandy limestone. The lower contact of member 4 is placed at the last appearance of thick (>5 m) amalgamated sandstone beds of member 3 and is well exposed on the east end of Nine Mile Ridge, in the saddle south of peak 7963. The top of the unit is the present erosion surface.

These four facies are both laterally and vertically gradational with each other. In general, the Jackass Mountain Group fines upward and to the west (Fig. 1). The Jackass Mountain Group was produced by mass sediment gravity flows and is interpreted to represent deposition in both the lower channelized and unchannelized parts of a submarine fan system. Jackass Mountain Group strata define a cyclic stratigraphic sequence that coarsens upward from a marine, green, moderately well sorted, sandstone into a polymictic conglomerate and then fines upward into massive sandstone overlain by thin- to medium-bedded sandstone and siltstone. This coarsening then fining upward sequence differs from that described by Kleinspehn (1982), who suggested the Jackass Mountain Group is a coarsening upward sequence.

Schiarizza (in press) subdivides the Jackass Mountain Group in the southwest corner of 92O/1 into a basal Barremian-Aptian lithic sandstone (IKJMy1) and an overlying Albian arkosic sandstone (IKJMy2). Mapping in 92O/1 suggests that the Barremian-Aptian unit corresponds to member 1 and the overlying Albian unit to members 2, 3, and 4.

Cretaceous

Spences Bridge Group

Porphyritic plagioclase andesite and dacite(?) flows and breccia correlated with the Spences Bridge Group (IKsb; Fig. 1) (Hickson et al., 1991) form a wedge bounded on the west by the Slok Creek fault, on the east by the Fraser fault, and truncated to the north by a splay of the Fraser fault (Fig. 1). Most volcanic rocks in this unit are andesitic to dacitic(?) and distinguishable from Eocene and younger volcanic rocks by their green to maroon colour, alteration of groundmass and phenocrysts, and ubiquitous small laths (1 x 2 mm) of altered (commonly cored and zoned) plagioclase feldspar crystals with few if any other phenocrysts. Particularly diagnostic is extensive veining and amygdaloidal infilling.

Tertiary to Quaternary

Eocene

Eocene volcanic rocks in 920/1 (Ev, Fig. 1) typically lack alteration of groundmass and phenocryst assemblages, are vesicular, lack amygdaloids and veins, and are simply jointed. The Eocene assemblage includes a variety of volcanic and sedimentary rock types. Eocene rocks are only exposed north and northeast of the Slok Creek fault. It is apparent that oblique slip, down to the east, on the Slok Creek fault and associated structures preserve Eocene volcanic strata on the east side of the fault, and that coeval strata on the west side of the fault have been eroded. Near Lone Cabin Creek (920/8) and French Bar Creek, Eocene volcanic rocks depositionally overlie Lower Cretaceous Jackass Mountain Group sedimentary rocks and amygdaloidal, andesitic Lower Cretaceous volcanic rocks.

East of the Fraser fault, in the southeastern sector of the map area, "Swiss-cheese" weathering cliffs of aphanitic grey breccia, bentonitic brown andesite and white rhyolitic lapilli tuff and minor flows (unit Evdx; Read, 1988) form a westerly dipping succession unconformably above the Permian Cache Creek Group.

West of the Fraser fault, the Eocene succession consists mainly of varicoloured aphanitic volcanic rocks ranging from andesite to rhyolite flows, breccia, and tuff with intercalated tuffaceous sediment. These volcanic rocks are capped by a sedimentary sequence consisting of a distinctive volcanic conglomerate (unit Ecg; Read, 1988) and bentonitic siltstone and shale (unit Ep; Read, 1988).

Most of the Eocene volcanic rocks are aphanitic andesite and dacite flows (unit Evd; Read, 1988) with lesser quantities of poorly bedded, grey-, brown-, and maroon-weathering tephra (unit Evdx; Read, 1988). The most extensive exposures are in the lower part of French Bar Creek, with approximately 1000 m of aphanitic, locally plagiophyric, andesite and dacite flows. These flows usually have platy jointing or flow layering suggesting that the Eocene volcanic rocks form a gently east-dipping homocline truncated on the east by the Fraser Fault.

Rhyolitic rocks are common throughout the volcanic succession, but are locally restricted and diminish westward at the expense of widespread grey aphanitic dacite and some andesite flows (Read, 1988). A subhorizontal sheet of porphyritic (quartz, sanidine), columnar-jointed rhyolite, up to a few hundred metres thick, underlies the ridge near the major forestry road connecting Watson Bar and Ward Creek. Glassy and locally perlitic rhyolite flows containing sparse biotite, hornblende, augite, and plagioclase phenocrysts form a flow-layered sequence up to a few hundred metres thick and a few kilometres long, north of Watson Bar Creek and French Bar Creek. The rocks vary from pale green and flesh through grey to dark grey. Medium grey, chocolate-brown, and maroon-red aphyric andesite and dacite tephra and thin flows intercalate rhyolite units and tuffaceous sediments.

Tuffaceous sediments (unit Etf; Read, 1988) range from a lithic rich sandstone or siltstone composed of varicoloured andesite and dacite lithics to an ashy white, lithic quartz sandstone,

derived from rhyolite. The sediments, particularly those with abundant andesite and dacite detritus, are bentonitic. The tuffaceous sediments form a northwest-trending lens truncated on the south by the Slok Creek fault near Watson Bar Creek. These sediments are surrounded and probably overlain by Eocene volcanic rocks in all other directions. The base of the tuffaceous sediments is not exposed; the minimum thickness is 200 m. The sediments and surrounding volcanic rocks occupy the core of a northwest-trending, northeast vergent, asymmetric, doubly plunging anticline. The tuffaceous sediments underlie the thick conglomerate-bearing late Eocene sedimentary rocks, but their stratigraphic position within the Eocene volcanic succession is unknown.

Miocene to Pliocene

Chilcotin Group Basalt

Flows of the Chilcotin Group Basalt (MPcv; Fig. 1) are laterally extensive over the northern part of the map area. These flows form capping plateaus on ridge tops, and locally fill paleovalleys such as French Bar Creek. Prominent knobs south of French Bar Creek may be feeders to the flows. The flows are subaerial, vesicular to dense, olivinephyric basalt associated with minor basal breccia.

PLUTONIC ROCKS

On the eastern flank of the Camelsfoot Range, 3 small stocks intrude Jackass Mountain Group on the western side of the Slok Creek fault (Fig. 1). These stocks are aligned along a northwest trend, suggesting possible structural control on emplacement. The age of these intrusions is unknown but radiometric dating is underway. The China Head stock is white to light grey, medium grained, equigranular hornblende diorite containing conspicuously zoned plagioclase, visible in hand sample. The unit is fresh and unaltered; contact metamorphic effects are minimal. Of the 3 stocks, this one may be the youngest, possibly Eocene in age.

Two stocks in the Stirrup Creek area are believed to be related, and vary from a plagioclase hornblende porphyry to hornblende diorite. They are medium- to coarse-grained, display local alignment of hornblende phenocrysts, and locally have chilled margins. Rocks of the Jackass Mountain Group are hornfelsed adjacent to the intrusions, and the stock in the headwaters of Stirrup Creek is associated with epithermal mineralization (Fig. 1). A complex, multiphase intrusion is structurally deformed and hydrothermally altered in the lower plate of the Watson Bar Thrust, in the lower parts of Watson Bar Creek. This intrusion consists of two units: a hornblende porphyry and a quartz porphyry, both of which are cut by fine grained felsic dykes and quartzphyric dykes. The intrusion is medium grained, altered (bleached white or limonitic stained red), sheared, and shattered.

STRUCTURE

The Fraser fault system is the largest fault system crossing the map area, and comprises an imbricate zone several kilometres wide (Fig. 1). The Slok Creek fault is a strand of the Fraser fault, originating from it southeast of the map area near Lillooet. Subhorizontal slickensides on both the Fraser and Slok Creek faults indicate that the latest movements were strike-slip. Both faults display intense brecciation and shear fabrics. The Slok Creek fault separates Eocene volcanic rocks and Lower Cretaceous volcanic strata on the east from Lower Cretaceous sedimentary rocks of the Jackass Mountain Group on the west. The absence of Eocene strata west of the fault suggests motion was post-Eocene, downthrown to the east, with a minimum displacement of 1000+ m.

Near Watson Bar, the Slok Creek fault cuts an imbricate zone of south-southeast-dipping low angle thrust faults of which the main fault is termed the Watson Bar Thrust (Fig. 1). It separates an upper plate of Jackass Mountain Group rocks from a lower plate of Jackass Mountain Group rocks and small Cretaceous(?) dioritic plutons. The fault is easily recognizable on the south side of Watson Bar Creek as a highly disrupted, iron-stained zone approximately 500 m thick. Within the zone, deformation of the Jackass Mountain Group is lithologically controlled. Competent sandstones are brecciated and fractured, and less competent siltstone beds localize shear zones, zeolite veining, and common bedding parallel shears zones. Plutons within the fault zone are highly altered, including kaolinitic alteration of feldspars and oxidation of hornblende. They are cut by south-dipping fracture zones, and shearing is locally concentrated along intrusive contacts. The age of the faulting is constrained as post-early Late Cretaceous, the age of the Jackass Mountain Group, and pre-Oligocene, the age of Slok Creek fault which cuts the fault on the east. The orientation of the fault suggests that it may be an accommodation structure associated with movement on the Fraser fault system (J.M. Journeay, pers. comm., 1993).

ACKNOWLEDGMENTS

This work was funded under project #890039, part of the Frontier Geoscience Program. Mapping by P. Read of part of 92O/1 was funded under an MDA 1985-1990 grant to assess the industrial mineral potential of Eocene rocks along the Fraser River. The authors wish to thank Ms. L. Snyder and Dr. M. Weston, volunteers, for capable field assistance. H.W. Tipper is thanked for a useful review of the manuscript.

REFERENCES

- Broster, B.E. and Huntley, D.H.**
1992: Quaternary stratigraphy in the east-central Taseko Lakes area, British Columbia; *in* Current Research, Part A; Geological Survey of Canada, Paper 92-1A, p. 237-241.
- Duffell, S. and McTaggart, K.C.**
1952: Ashcroft map-area, British Columbia; Geological Survey of Canada, Memoir 262, 122 p.
- Frebold, H., Tipper, H.W., and Coates, J.A.**
1969: Toarcian and Bajocian rocks and guide ammonites from southwestern British Columbia; Geological Survey of Canada, Paper 67-10, 55 p.
- Hickson, C.J.**
1990: A new Frontier Geoscience Project: Chilcotin-Nechako region, central British Columbia; *in* Current Research, Part F; Geological Survey of Canada, Paper 90-1F, p. 115-120.
1992: An update on the Chilcotin-Nechako Project and mapping in the Taseko Lakes area, west-central British Columbia; *in* Current Research, Part A; Geological Survey of Canada, Paper 92-1A, p. 129-135.
1993: Geology of the northwest quadrant, Taseko Lakes map area (92O), west-central British Columbia; Geological Survey of Canada, Open File 2695, map and extended legend.
- Hickson, C.J. and Higman, S.**
1993: Geology of the northwest quadrant, Taseko Lakes map area, west-central British Columbia; *in* Current Research, Part A; Geological Survey of Canada, Paper 93-1A, p. 63-76.
- Hickson, C.J., Read, P., Mathews, W.H., Hunt, J.A., Johansson, G., and Rouse, G.E.**
1991: Revised geological mapping of northeastern Taseko Lakes map area, British Columbia; *in* Current Research, Part A; Geological Survey of Canada, Paper 91-1A, p. 207-217.
- Huntley, D.H. and Broster, B.E.**
1993: Glacier flow patterns of the Cordilleran Ice Sheet during the Fraser Glaciation, Taseko Lakes map area, British Columbia; *in* Current Research, Part A; Geological Survey of Canada, Paper 93-1A, p. 167-172.
- Kleinspehn, K.L.**
1982: Cretaceous sedimentation and tectonics, Tyaughton-Methow Basin, southwestern British Columbia; Ph.D. thesis, Princeton University, New Jersey, 184 p.
- Leech, J.B.**
1953: Geology and mineral deposits of the Shulaps Range, southwestern British Columbia; British Columbia Department of Mines, Bulletin no. 32, 54 p.
- Mahoney, J.B.**
1992: Middle Jurassic stratigraphy of the Lillooet area, south-central British Columbia; *in* Current Research, Part A; Geological Survey of Canada, Paper 92-1A, p. 243-248.
1993: Facies reconstructions in the Lower to Middle Jurassic Ladner Group, southern British Columbia; *in* Current Research, Part A; Geological Survey of Canada, Paper 93-1A, p. 173-182.
- Mahoney, J.B., Hickson, C.J., van der Heyden, P., and Hunt, J.A.**
1992: The Late Albian-Early Cenomanian Silverquick conglomerate, Gang Ranch area: evidence for active basin tectonism; *in* Current Research, Part A; Geological Survey of Canada, Paper 92-1A, p. 249-260.
- Monger, J.W.H.**
1989: Geology, Hope, British Columbia; Geological Survey of Canada, Map 41-1989, sheet 1, scale 1:25 000.
- Monger, J.W.H. and McMillan, W.J.**
1989: Geology, Ashcroft, British Columbia; Geological Survey of Canada, Map 41-1989, sheet 1, scale 1:250 000.
- Read, P.**
1988: Tertiary stratigraphy and industrial minerals, Fraser River: Lytton to Gang Ranch, southwestern British Columbia (92I/5, 92I/12, 92I/13, 92J/16, 92O/1, 92O/8, 92P/4); British Columbia Ministry of Energy, Mines and Petroleum Resources, Open File map 1988-29.
1992: Geology of parts of Riske Creek and Alkali Lake areas, British Columbia; *in* Current Research, Part A; Geological Survey of Canada, Paper 92-1A, p. 105-112.
1993: Geology of northeast Taseko Lakes map area, southwestern British Columbia; *in* Current Research, Part A; Geological Survey of Canada, Paper 93-1A, p. 159-166.
- Schiarizza, P.**
in press: Geology of the Taseko-Bridge River area, NTS 92O/1,2,3; 92J/15, 16; British Columbia Ministry of Energy, Mines and Petroleum Resources.
- Schiarizza, P., Gaba, R.G., Coleman, M., Garver, J.I., and Glover, J.K.**
1990: Geology and mineral occurrences of the Yalakom River area (92O/1, 92J/15,16), British Columbia; *in* Geological Fieldwork 1989; British Columbia Ministry of Energy, Mines and Petroleum Resources, Paper 1990-1, p. 53-72.

- Schiarizza, P., Gaba, R.G., Garver, J.I., Glover, J.K., Church, B.N., Umhoefer, P.J., Lynch, T., Sajgalik, P.P., Safton, K.E., Archibald, D.A., Calon, T., MacLean, M., Hanna, M.J., Riddell, J.M., and James, D.A.R.**
1989: Geology of the Tyughton Creek area; British Columbia Ministry of Energy, Mines and Petroleum Resources, Open File 1989-4.
- Tipper, H.W.**
1978: Taseko Lakes (920) map-area; Geological Survey of Canada, Open File 534.
- Trettin, H.P.**
1961: Geology of the Fraser River Valley between Lillooet and Big Bar Creek; British Columbia Ministry of Energy, Mines and Petroleum Resources, Bulletin 44, 109 p.

- van der Heyden, P. and Metcalfe, S.**
1992: Geology of the Piltz Peak plutonic complex, northwestern Churn Creek map area, British Columbia; in Current Research, Part A; Geological Survey of Canada, Paper 92-1A, p. 113-119.
- Woodworth, G.J.**
1977: Pemberton (92J) map area; Geological Survey of Canada, Open File 482.

Geological Survey of Canada Project 890039

Preliminary studies of Recent volcanic deposits in southwestern British Columbia using ground penetrating radar

M.V. Stasiuk¹ and J.K. Russell²
Cordilleran Division

Stasiuk, M.V. and Russell, J.K., 1994: Preliminary studies of Recent volcanic deposits in southwestern British Columbia using ground penetrating radar; in Current Research 1994-A; Geological Survey of Canada, p. 151-157.

Abstract: Ground penetrating radar data were collected from traverses over five well-exposed, Recent volcanic rock deposits from Mount Meager volcano and the Cheakamus valley, in southwestern British Columbia. The traverses overlie pyroclastic and lava flow deposits, including: a thick accumulation of pumice talus, a welded glassy lava breccia, a bed of airfall pumice, a pyroclastic block and ash flow, and a basalt lava flow. The volcanic rocks are dacite and basalt in composition and glassy to holocrystalline. Data were collected via a *pulseEKKO IV* ground penetrating radar system with a focused radar signal of 100 MHz. Other experimental conditions varied: i) sample intervals were 0.5 to 1.0 m, ii) ground penetrating radar data was collected with total time windows of 512 or 2048 ns, iii) the number of stacks used was between 64 and 512. Preliminary results suggest that ground penetrating radar is an effective means of delineating important stratigraphic contacts and can resolve complex internal structures in young volcanic deposits.

Résumé : Des données ont été recueillies par géoradar le long de profils passant au-dessus de cinq dépôts de roches volcaniques holocènes bien exposées du volcan du mont Meager et de la vallée Cheakamus, dans le sud-ouest de la Colombie-Britannique. Ces profils passent au-dessus de dépôts pyroclastiques et de coulées de lave, dont une épaisse accumulation d'éboulis de ponces, une brèche de lave vitreuse à fragments soudés, une couche de ponces de retombée, une coulée pyroclastique de blocs et de cendre et une coulée de lave basaltique. Les roches volcaniques sont composées de dacite et de basalte et leur texture varie de vitreuse à holocristalline. Les données ont été recueillies par géoradar *pulseEKKO IV* produisant un signal radar focalisé de 100 MHz. Les autres conditions expérimentales ont été variables : i) les intervalles d'échantillonnage ont été de 0,5 à 1,0 m, ii) les données recueillies par géoradar ont donné des fenêtres d'un temps total de 512 ou de 2 048 ns, iii) le nombre de sommations utilisées a varié entre 64 et 512. Les résultats préliminaires indiquent que le géoradar est un moyen efficace de délimiter les contacts stratigraphiques importants et de reconstituer les structures internes complexes dans les dépôts volcaniques récents.

¹ Laboratoire de Physique de Magmatique, Université de Paris, Paris, France

² Department of Geological Sciences, University of British Columbia, 6339 Stores Road, Vancouver, British Columbia V6T 1Z4

INTRODUCTION

Stratigraphic and facies problems related to Recent volcanic deposits are complicated by the fact that deposits are commonly poorly exposed. Information on the physical properties, distributions, thicknesses, and internal structures of Recent deposits typically derives from a few dissected outcrops which offer significant vertical and horizontal exposure. Modern volcanic eruption deposits are even less likely to be dissected, leaving volcanologists with only surfaces of deposits to work with. As a result, there are large uncertainties associated with geological maps of volcanic deposits. These uncertainties relate to variations in thicknesses and facies, estimates of eruption volumes, or interpretations of eruptive style.

Ground penetrating radar (GPR) is a highly portable geophysical method with which information on the thickness, physical character, and internal structure of deposits can be obtained immediately in the field, with a minimum of data processing (e.g., Davis and Annan, 1989; Smith and Jol, 1992). In locations where exposure is poor, GPR provides an alternative to expensive direct sampling methods (e.g., drilling or excavation). Volcanic deposits are particularly appropriate for the use of GPR because they are typically thin (<100 m) and can comprise mainly glass. Their thinness permits the radar pulses to see through their entire vertical dimension, and the glassy nature also facilitates deep penetration by the electromagnetic radiation.

Ground penetrating radar data were collected along five traverses overlying volcanic deposits from Mount Meager (e.g., Read, 1977a, b) and the Cheakamus Valley (Green et al., 1988), southwest of Whistler (Fig. 1). The traverse sites selected have excellent cross-sectional exposure allowing direct comparison between GPR data profiles and structures observed within the deposits. The sites chosen cover a variety of volcanic deposit types. These are summarized in Table 1 with each GPR traverse (Fig. 1). Mount Meager volcanic deposits have been described in detail by (Stasiuk and Russell, 1990; Stasiuk et al., in press). Deposit types include: 1) a thick accumulation of pumice talus on the south side of the Lillooet River, 2) densely welded glassy lava breccia dissected by the Lillooet River, 3) thinly vegetated airfall pumice deposits exposed on a set of switchbacks on logging roads on the north side of the Lillooet River, 4) pyroclastic block and ash flow underlying lahar, and 5) a valley-filling basalt lava flow.

Our preliminary results suggest that GPR surveys could be used routinely in studies of modern volcanic eruption deposits or other poorly dissected older volcanic rock bodies. In particular, this geophysical method provides the means to map deposits away from well-exposed locations and reveal significant variations in thickness, internal structure, or physical property (e.g., Davis and Annan, 1989; Pilon et al., 1991; Smith and Jol, 1992).

EXPERIMENTAL TECHNIQUE

A pulseEKKO IV (*pEIV*) ground penetrating radar system was used for each survey, employing a focused radar signal of 100 MHz. Transmitter and receiver were connected to a laptop computer by optical cable and controlled via *pEIV* software. Surveys were run within a few metres of the steep slopes and cliffs which exposed the deposits in cross-section. This practice ensured that received signals could be correlated directly with features seen in the deposit exposures. The focused radar beam reduced significant reflections produced from the abrupt edges of the deposits. Specific details of the deposits are discussed below.

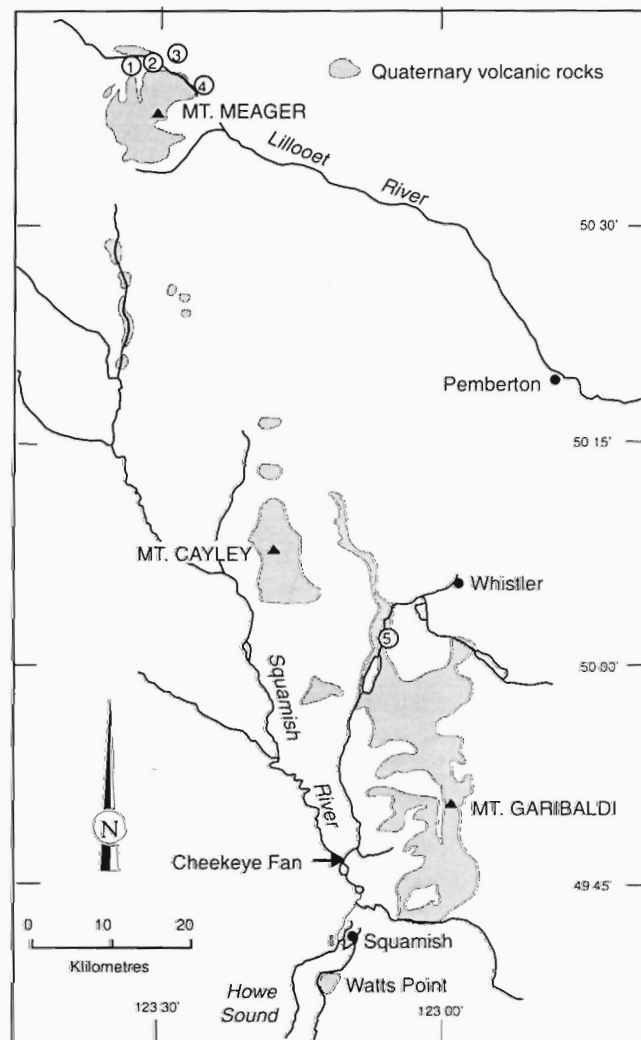


Figure 1. Locations of ground penetrating radar traverses situated at Mount Meager (1 to 4) and in the Cheakamus valley (5). Also shown is distribution of other Quaternary volcanoes and other volcanic rocks. Numbered traverse sites include: 1) pumice talus cone, 2) welded lava breccia, 3) airfall pumice deposit, 4) pyroclastic flow deposit, and 5) basalt lava flow.

The system was sufficiently portable to be operated over irregular terrain. Indeed, survey lines were carried out successfully over talus, fallen trees, a small bridge over a river, and through thin brush and forest. Each survey line comprises a series of evenly-spaced readings, where both the transmitter and receiver were moved to a new position for each point. Experimental and sampling details for each GPR traverse are summarized in Table 2. At each point the received signal was stacked, typically between 64 and 512, to reduce random noise over time windows of between 512 and 2048 ns (Table 2). The signal was collected without gain, but for interpretation and presentation (see below), data were examined with no gain, constant gain or automatic gain control

(AGC)-standard options within the *pEIV* software package. Increased gain enhanced deeper reflecting surfaces but saturated the shallow signal by amplifying scatter and noise from shallow levels. By systematically increasing gain, reflecting surfaces at ever-deeper levels can be resolved.

The signal traces recorded along a single GPR traverse are best displayed side by side, forming a profile analogous to a vertical cross-section parallel to the survey line. Reflections which are continuous from trace to trace can then be detected more easily by eye. This concept is illustrated in Figure 3 using GPR data collected from Site 4, the traverse over a pyroclastic flow from Mount Meager.

Table 1. Brief descriptions of deposits found at Sites 1-5 (Fig. 1). Additional details are in Stasiuk et al. (in press).

| Site | Deposit Type/Exposure | Outcrop | Rock Type | Other Descriptors |
|------|---|--|--|---|
| 1 | Pumice talus cone; toe of cone is dissected by Lillooet River | Well-layered and cross-laminated, moderately well-sorted, unconsolidated, reworked pumice | dacite pumice lapilli | Deposit is a thick apron of reworked pumice overlying rock avalanche deposit |
| 2 | Welded, glassy, lava breccia; Lillooet River cuts gorge through deposit | Well-indurated, monolithologic glassy porphyritic lava breccia filling paleo-Lillooet River valley | dacite lava breccia | The deposit is layered due to variable degrees of welding and crude variations in jointing, clast size and clast to matrix ratios |
| 3 | Airfall pumice deposit; exposed in switchbacks on logging road | Well-sorted, matrix-poor, massive, unconsolidated, airfall pumice deposit | dacite pumice lapilli | Upper portions of deposit are reworked and crudely laminated |
| 4 | Pyroclastic flow deposit; dissected by Lillooet River | Unsorted, chaotic, block and ash-rich, unconsolidated pyroclastic flow | dacite pumice blocks, lapilli and ash | Charred trees are common; deposit sits below moderately well-stratified reworked debris flows and above old forest floor |
| 5 | Basalt lava flow; highway road cut | Massive, poorly jointed, fine-grained basalt flow | olivine plagioclase porphyritic basalt | Lava is 3-6 m thick, has one joint colonnade from top to bottom (0.7 m in diameter); vesicular base overlies scoriaceous breccia and glacial till |

Table 2. Summary of GPR traverses, collection and processing conditions*, and pertinent field measurements.

| Site | Filename MMgpr-xx | Deposit Thickness (m) | Time Window (ns)/Stacks | Traces | Traverse Description |
|------|-------------------|-----------------------|-------------------------|--------|---|
| 1 | 18 | 115 | 512/256 | 51 | 50 m; 1 m spacing; runs W to E |
| 2a | 25 | 13.5 exposed but >100 | 2048/512 | 37 | 36 m; 1 m spacing; runs E to W (parallel to gorge) |
| 2b | 16 | >100 | 2048/512 | 67 | 66 m; 1 m spacing; runs N to S (to and 4.4 m above site 2a) |
| 3 | 14 | 3.58 | 512/128 | 52 | 51 m; 1 m spacing; runs W to E |
| 4 | 10-11a | 16 | 512/64 | 192 | 191 m; 1 m spacing; runs W to E |
| 5 | 20 | 3 - 6 | 512/128 | 81 | 40 m; 0.5 m spacing; runs N to S |

* Preliminary GPR profiles converted travel times to depths using a velocity of 0.1 m/ns.

TRAVERSE SITE DESCRIPTIONS

Site 1: pumice talus cone

Steep, 100 m high cliffs form the south banks of the Lillooet River, east and slightly north of Plinth Peak, near a washed-out bridge. These stream-eroded bluffs comprise thick, pumice-rich fragmental and unconsolidated deposits exhibiting complex, overlapping, lensoidal internal stratigraphy. The deposit represents an accumulation of pumice which formed by slumping from steep slopes during eruption of the Mount Meager volcano 2350a (Stevenson, 1946; Nasmith et al., 1967; Stasiuk et al., in press). The accumulated material forms a very heterogeneous deposit; metre-scale variations from coarse to fine grained, well-sorted layers to beds of coarse pumice clasts with fine grained matrix are typical. This package of reworked pumice-rich pyroclastic material overlies an older unconsolidated, matrix-rich rock avalanche deposit.

The GPR traverse follows a logging road situated on the bench defining the top of the bluffs (Table 2). Along this traverse, the deposit varies gradually in thickness but is easily 80 m thick.

Site 2: welded lava breccia

Upstream (50-200 m) from Lillooet Falls, erosion by the Lillooet River has created a narrow gorge cutting through a thick unit of welded dacite lava breccia (Table 1). Ground penetrating radar data for the lava breccia were collected along two traverses; the traverses were oriented both parallel and perpendicular to the Lillooet River gorge (Table 2). The lava breccia comprises angular lava fragments in a fine grained matrix. Both fragments and matrix are dominantly glass, the latter representing finely comminuted lava pieces. Overall the deposit is glassy, has less than 20% phenocrysts, is strongly indurated, variably jointed and massive to crudely

Figure 2.

Field aspects of GPR site 4. Upper photograph (a) shows entire span of survey over deposit (looking east) with buried horizontal flat forest floor marked by subtle break in slope and black stump in middle of photograph. Lower photograph (b) shows scale of layering and heterogeneous nature of deposit, including charred logs and large pumice blocks (note blocks collected at base of cliff).



layered; layering is horizontal. Stasiuk et al. (in press) have proposed welding of hot lava-avalanche debris, episodically-emplaced into the paleo-Lillooet River valley as the origin of the deposit.

At this location the minimum observed thickness of the welded lava breccia is 13.5 m, however, downstream at Lillooet Falls, a 100-140 m high cliff exposes the entire deposit. This exposure best constrains the total thickness of the welded lava breccia and clearly shows the deposits internal structure. The deposit appears to comprise four horizontal cooling units of similar thickness (about 25 m each), defined by abrupt changes in the jointing patterns. In outcrop, the tops and bases of the cooling units are commonly marked by horizontal lines of vegetation along the cliff walls, presumably indicating that the interfaces are more permeable to water. Thinner, more numerous, and somewhat more subtle layers appear to result from variations in the clast size and concentration and variations in the degree of welding.

Site 3: airfall pumice deposit

An airfall pumice deposit associated with a 2350a eruption of the Mount Meager volcanic complex occurs at locality 3 (Table 1). Angular dacitic pumice fragments form a loose framework which lacks fine matrix material. The deposit has little to no internal structure although the top 10% is commonly slightly reworked and crudely layered. Detailed descriptions are in Stasiuk et al. (in press). The measured thickness of the deposit is 3.8 m, although the thickness varies somewhat because of postdepositional erosion and slumping. The GPR data were collected along a 50 m traverse over the airfall pumice deposit above a logging road (Table 2).

Site 4: pyroclastic flow section

Downstream from Mount Meager, near the confluence of the Lillooet River and Pebble Creek, is a 20 m high stream-dissected bluff (Fig. 2a) containing unconsolidated pyroclastic deposits (Stasiuk et al., in press). A 191 m long GPR traverse was run along a flat bench immediately above this bluff (Table 2). The underlying stratigraphy includes a package, 20-25 m in thickness, topped by thinly laminated stream deposits and a mudflow deposit which thins along the exposure (Fig. 2b). Most of the section comprises two pyroclastic block and ash flow deposits (Stasiuk et al., in press). The pyroclastic flow deposits are chaotic, unstructured, virtually unsorted mixtures of large (0.5-1 m) blocks of pumice, pumice lapilli, and abundant ash-lapilli sized matrix. Locally, the pyroclastic flow contains abundant charred logs, stumps, and branches. Preliminary GPR results for this traverse are shown (Fig. 3) and discussed below.

Site 5: Cheakamus Valley basalt lava

The last GPR survey was carried out on a basaltic lava flow which is exposed in cross-section along a roadcut on Highway 99, north of Brandywine Falls provincial park (Fig. 1, Table 1). The basaltic lava is holocrystalline rather than

glassy and generally massive (Green et al., 1988). The lava is 3-6 m thick and has a poorly-indurated, irregular, basal lava breccia. The lava and breccia overlie clay-rich glacial till. The lava flow is columnar jointed with single columns, 0.7 m in diameter extending the entire flow thickness.

PRELIMINARY GPR PROFILES FOR SITE 4

The GPR survey over the pyroclastic flow deposits (Site 4) was 191 m long (Table 2). Seven individual line segments (Fig. 3a) were oriented roughly parallel to the face of the bluff (Fig. 2a). Ground penetrating radar data were collected at 1 m spacings and the resulting profiles are shown in Figure 3. Travel times (left vertical axis, Fig. 3) are converted to depths (right vertical axis, Fig. 3) using a velocity of 0.1 m/ns. The radar profiles shown have undergone no signal processing (e.g., migration, etc.) other than applying different AGC gains. Specifically, the radar profiles in Figure 3 (b, c, and d) result from the application of sequentially stronger gains of 0.001, 0.008, and 0.02. Each radar profile is shown at 4 times vertical exaggeration. For comparison, the radar profile generated with the highest AGC gain (0.02) is also shown without vertical exaggeration (Fig. 3e). As gain is increased the radar profiles show reflectors at ever greater depths to a maximum of approximately 16-17 m. This depth and reflector correspond to the level of the old forest floor upon which the younger volcanic eruption products are deposited. There are no reflectors seen beneath this layer because the contact is a well-developed soil horizon. The conductive character of this layer probably ensures rapid dissipation of the radar signal.

Other features, in addition to the pronounced basal contact, visible in Figure 3 include the upper finely-layered sediments which thin to the right. Left-dipping structures in the middle of the section are seen in both field and in the GPR profiles (cf. Fig. 2b and 3d or 3e). As gain increases the GPR profiles become rather noisy; we infer that the noise is, in part, due to suspended 1 m diameter pumice blocks and concentrations of logs. These are preliminary results which we are currently reanalyzing with better velocity estimates and more detailed examination of the stratigraphic section.

DISCUSSION

The results presented here are very preliminary, however, even using unmigrated sections it is clear that ground penetrating radar has considerable potential for aiding mapping of young volcanic deposits. The study of these types of deposits is significantly improved using GPR techniques because these deposits typically blanket topography and fill in valleys; this makes it difficult to determine distributions, thicknesses, volumes, or the nature of internal variations. The few radar results shown in Figure 3 indicate that thicknesses and internal structures of volcanic deposits can be clearly elucidated. Such information obtained in the field, without requiring office time for data processing is extremely valuable. Data processing can enhance the images and the apparent attitudes of dipping strata (e.g., correcting for "dip moveout").

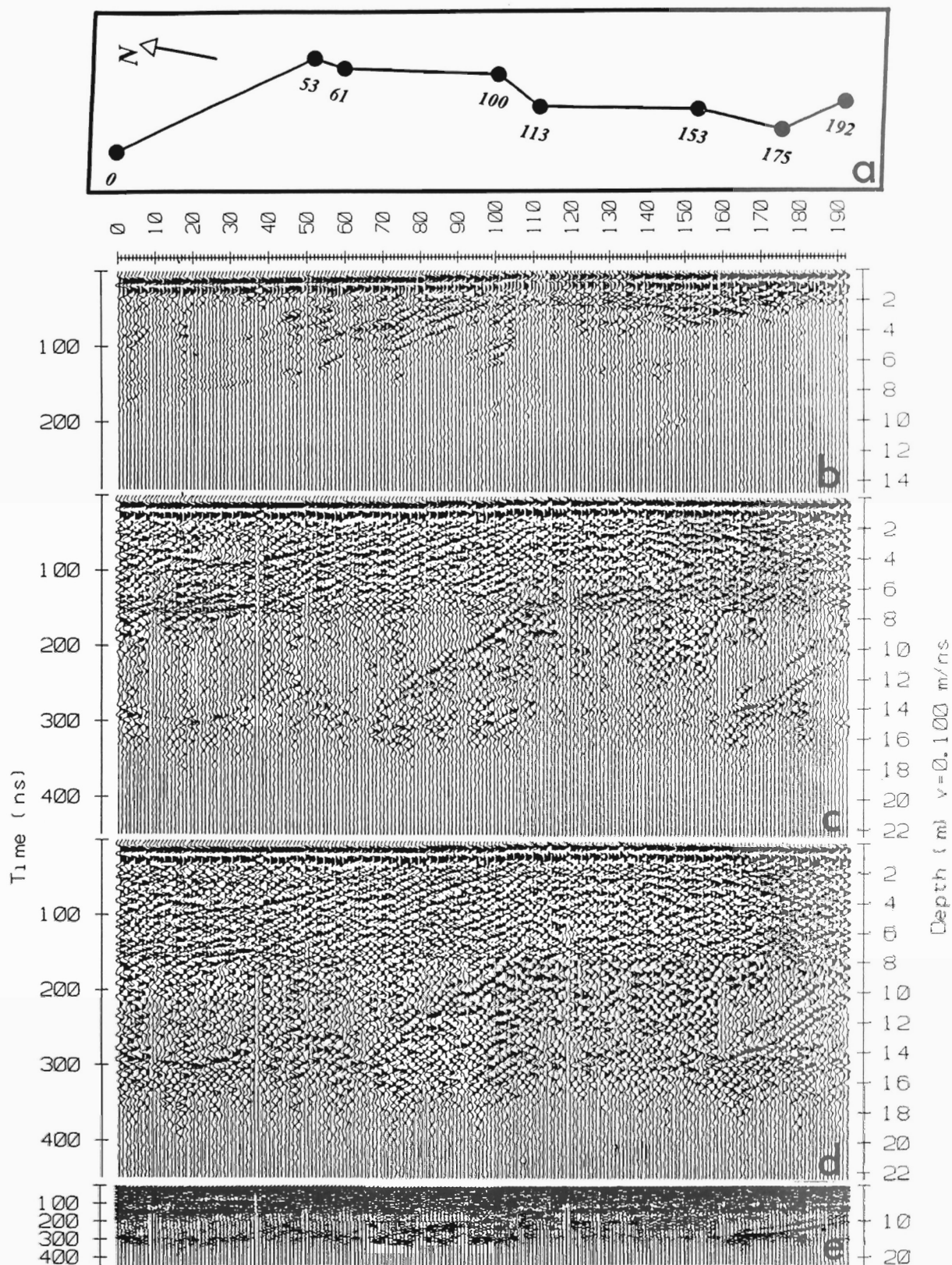


Figure 3. Radar profiles for pyroclastic flow section (Site 4). Entire traverse comprises 7 traverse segments which crudely parallel the cliff face (a). GPR results are shown with 4 times vertical exaggeration and gains of (b) 0.001, (c) 0.008, and (d) 0.02, and (e) with no vertical exaggeration and a gain of 0.02.

The relatively shallow depth of penetration of the radar does not represent a major barrier to its use for volcanic deposits since they are commonly thin (e.g., less than 20 m). Furthermore, preliminary results suggest that glassy deposits are relatively transparent to radar and hence thick glassy volcanic deposits might also be studied effectively with GPR.

ACKNOWLEDGMENTS

Pertinent field logistical costs were covered by EMR contract #23254-3-1032/01-XSB. Ancillary research costs were born by NSERC operating grant A0820 (JKR). We also wish to acknowledge Dr. R.J. Knight for access to her GPR and Jane Rea and Mike Knoll for practical instruction and beneficial discussions. Data reduction and presentation were facilitated by the *pulseEKKO IV* User's Guide and PC-based programs supplied by Sensors and Software Inc. The manuscript was significantly improved with a timely reviews and editing by Dr. C.J. Hickson and Bev Vanlier. All results and interpretations presented herein, represent the views of the authors, alone.

REFERENCES

- Davis, J.L. and Annan, A.P.**
1989: Ground-penetrating radar for high-resolution mapping of soil and rock stratigraphy; *Geophysical Prospecting*, v. 37, p. 531-551.
- Green, N.L., Armstrong, R.L., Harakal, J.E., Souther, J.G., and Read, P.B.**
1988: Eruptive history and K-Ar geochronology of the late Cenozoic Garibaldi volcanic belt, southwestern British Columbia; *Geological Society America Bulletin*, v. 100, p. 563-579.
- Nasmith, H., Mathews, W.H., and Rouse, G.E.**
1967: Bridge River ash and some other Recent ash beds in British Columbia; *Canadian Journal Earth Sciences*, v. 4, p. 163-170.
- Pilon, J.A., Grieve, R.A.F., and Sharpton, V.L.**
1991: The subsurface character of Meteor Crater, Arizona, as determined by ground-probing radar; *Journal of Geophysical Research*, v. 96, p. 15 563-15 576.
- Read, P.B.**
1977a: Meager Creek volcanic complex, southwestern British Columbia; in Report of Activities, Part A; Geological Survey of Canada, Paper 77-1A, p. 277-281.
1977b: Geology of Meager Creek geothermal area, British Columbia; Geological Survey of Canada, Open File 603.
- Smith, D.G. and Jol, H.M.**
1992: Ground-penetrating radar investigation of a Lake Bonneville delta, Provo level, Brigham City, Utah; *Geology*, v. 20, p. 1083-1086.
- Stasiuk, M.V. and Russell, J.K.**
1990: The Bridge River assemblage in the Meager Mountain volcanic complex, southwestern British Columbia; in Current Research, Part E; Geological Survey of Canada, Paper 90-1E, p. 153-157.
- Stasiuk, M.V., Russell, J.K., and Hickson, C.J.**
in press: Influence of magma chemistry on eruption behaviour from the distribution and nature of the 2350 B.P. eruption products of Mount Meager, British Columbia; Geological Survey of Canada, Open File.
- Stevenson, L.S.**
1946: Pumice from Haylmore, Bridge River, British Columbia; *American Mineralogist*, v. 32, p. 547-551.

Geological Survey of Canada Project 930008

Turonian (Upper Cretaceous) strata and biochronology of southern Gulf Islands, British Columbia

James W. Haggart
Cordilleran Division, Vancouver

Haggart, J.W., 1994: Turonian (Upper Cretaceous) strata and biochronology of southern Gulf Islands, British Columbia; in Current Research 1994-A; Geological Survey of Canada, p. 159-164.

Abstract: The stratigraphic assignment of Cretaceous rocks of the southernmost Gulf Islands is revised: rocks on Sidney Island and several other islands adjacent to the northeast Saanich Peninsula of Vancouver Island are assigned to the Sidney Island Formation. Strata of the formation include conglomerate, sandstone, and siltstone, and reflect marine transgression in the region. The Sidney Island Formation ranges in age from Early to Middle Turonian, based on ammonites and inoceramid bivalves. Stratigraphic and structural relations of the formation with strata of the basal Nanaimo Group (Comox Formation) are presently uncertain. Strata of the formation appear to be unrelated to Cretaceous thrust faulting in the nearby San Juan Islands.

Résumé : L'attribution stratigraphique des roches du Crétacé des îles Gulf méridionales est révisée : les roches de l'île Sidney et de plusieurs autres îles voisines de la partie nord-est de la péninsule Saanich, de l'île de Vancouver, sont attribuées à la Formation de Sidney Island. Les couches de la formation sont composées de conglomérat, de grès et de siltstone, et témoignent d'une transgression marine dans la région. La Formation de Sidney Island, d'après l'étude d'ammonites et de bivalves d'inocéramides, remonte au Turonien précoce à moyen. Les relations stratigraphiques et structurales entre la formation et les couches de la partie basale du Groupe de Nanaimo (Formation de Comox) sont actuellement indéterminées. Les couches de la formation ne semblent pas présenter de lien avec l'activité de chevauchement qui s'est déroulée au Crétacé dans les îles San Juan situées à proximité.

INTRODUCTION

The Cretaceous Nanaimo Group of southwestern British Columbia contains diverse and well-preserved mollusc faunas, splendidly displayed in well-exposed stratigraphic succession. Many different studies of Nanaimo Group rocks have been undertaken (summarized in Mustard, in press), examining stratigraphy, fossil content, structure, and geochemistry; the stratigraphic scheme established by Muller and Jeletzky (1970) has served as the basic framework for most of these studies.

Based on marine macrofossils, the age of the Nanaimo Group, as defined by Muller and Jeletzky (1970), ranges from Santonian (later part) to Maastrichtian. The basal unit of the standard Nanaimo Group section, the Comox Formation, consists of nonmarine, marginal-marine, and fully marine deposits, which grade upward into deeper-water shelf and submarine fan facies (Haslam and younger formations). The

age of the oldest Comox Formation rocks is poorly constrained, reflecting their nonmarine to marginal-marine origin and poorly fossiliferous nature.

Recent studies of rocks assigned to the Nanaimo Group on the southernmost margin of the basin has revealed that older rocks are present at some localities. Popenoe et al. (1987) first suggested that Turonian strata might be present in the basin, on the basis of a distinctive gastropod fauna found on Sidney Island (Fig. 1). Haggart (1991a) subsequently collected ammonites and bivalves which indicated that the lower Sidney Island beds are of Early Turonian age, significantly older than the typical Nanaimo Group succession. Recent collections reported herein have demonstrated Middle Turonian strata on Sidney Island as well.

Collectively, these southern outcrops comprise a sequence of strata distinct from the typical lower Nanaimo Group succession. These strata are described more fully in this report and are herein named the Sidney Island formation (formal definition pending).

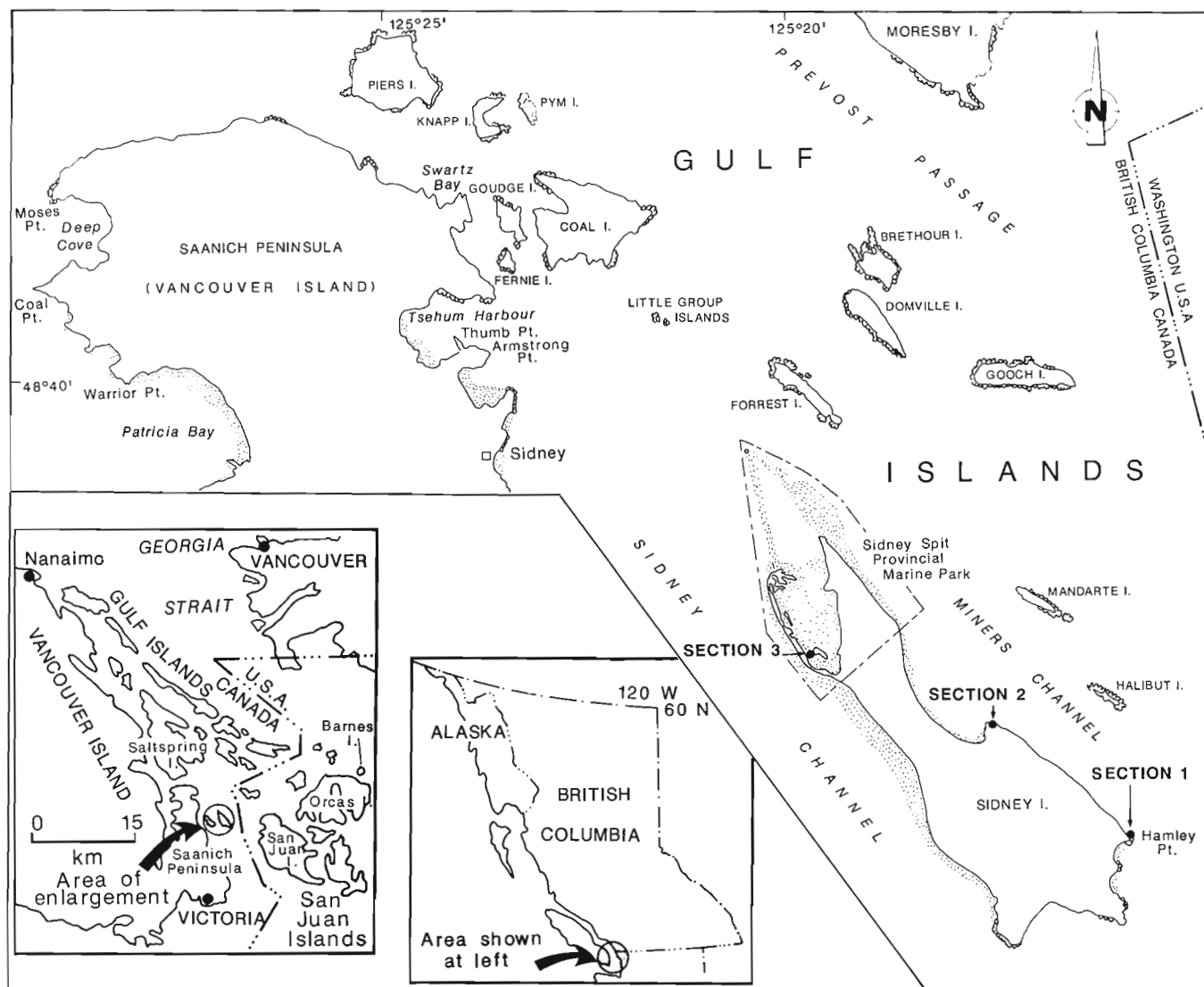


Figure 1. Location map showing principal locations discussed in text.

LITHOSTRATIGRAPHY OF SIDNEY ISLAND FORMATION

The name Sidney Island formation is taken from Sidney Island, where the type section (section 1) of the formation is found (Fig. 1). All Cretaceous strata which outcrop on Sidney Island are herein assigned to the formation. These rocks were previously correlated with the Comox Formation by Muller (1983), who lacked fossil control on their age. England (1989) subsequently assigned the Sidney Island strata to the Tzuhalem and Saanich members of the Benson (=Comox) Formation. Haggart (1991a) described the exposures at Hamley Point and noted the dissimilarity of those rocks with typical Comox Formation strata.

The best exposures of the Sidney Island formation are at Hamley Point on the most easterly point of the island, and comprise the type section. Along-strike exposures of the upper part of the formation are continuous for about 2.75 km along the shore northwest from Hamley Point, to a large bay in the middle of the east side of the island; a second section through the formation (section 2) is found on the south side of this bay. A small exposure of the formation is also found at the northwest end of Sidney Island, on the small island in the bay at Sidney Spit Marine Park (section 3). In addition, the formation is exposed on the nearby Halibut and Mandarte islands.

The base of the Cretaceous section is not seen at the type locale, but outcrops of highly deformed and altered metavolcanics are found several hundred metres to the southwest; at section 2, the Cretaceous strata are seen to nonconformably overlie the metavolcanic rocks. All these basement rocks were mapped as Jurassic age, Saanich Granodiorite by Muller (1983), but are herein considered as probably correlative with the unnamed volcanic unit of Permian and/or Triassic age mapped by Muller (1983) underlying Cretaceous rocks in Tsehum Harbour on Saanich Peninsula (Fig. 1). Kachelmeyer (1978) considered these basement rocks to be Late Triassic to Early Jurassic Bonanza Volcanics.

The youngest strata in all sections of the formation studied on Sidney, Halibut, and Mandarte islands plunge into the water; thus, no contact of the formation with overlying strata can be seen.

Strata of the Sidney Island formation comprise a fining-upward marine sequence (Haggart, 1991a; Fig. 2). The base of the type section consists of medium- to coarse-grained,

massive to cross-stratified sandstone, locally with floating pebbles and cobbles. Lenses of subangular to mostly well-rounded, cobble to boulder conglomerate, up to several metres in thickness and several tens of metres in length, are found within the sandstone succession. The lower part of the formation grades upward into hummocky-cross-stratified sandstone and siltstone.

All strata of the formation are fossiliferous. The lowest beds include robust marine bivalves (including trigoniids and inceramids), gastropods, and rare ammonite fragments; the fauna and sedimentary structures indicate a very shallow-water, inner shelf environment. The overlying siltstones and hummocky cross-stratified, fine grained sandstones include common ammonites, and represent somewhat deeper-marine, probably mid-shelf environments.

Sidney Island formation strata exposed on Halibut and Mandarte islands are similar to those seen on Sidney Island and include lower conglomerates and sandstones grading upward into fine grained sandstone and siltstone. The base of the formation is not exposed on either of these islands, but several large (to 80 cm), angular boulders of greenstone are found in the lowest beds on Halibut Island, suggesting stratigraphic proximity of the basement rocks. The repetition of Sidney Island formation stratigraphy on Mandarte and Halibut islands, north of the type section, is considered to reflect structural repetition of the section along one or more thrust faults hidden beneath the waters of Miners Channel.

BIOSTRATIGRAPHY OF SIDNEY ISLAND FORMATION

Faunas of Early and Middle Turonian age have been collected from the Sidney Island formation. Haggart (1991a) described collections made from the lower part of the type section of the formation. Additional collections have subsequently been made from higher beds on the island and at other localities.

Mytiloides ex gr. labiatus fauna

The lower beds of the Sidney Island formation on Sidney Island have produced abundant gastropods, inoceramid and trigoniid bivalves, and ammonites. The stratigraphically lowest, fossiliferous beds at the type section include the inoceramid bivalve *Mytiloides ex gr. labiatus*, the trigoniid

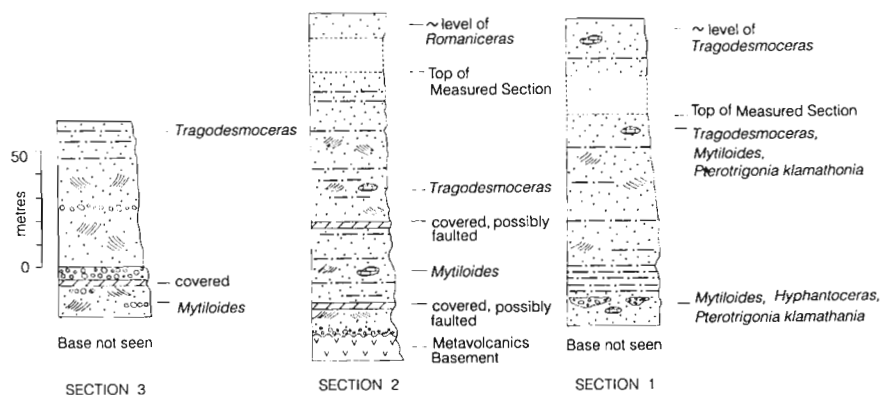


Figure 2.

Schematic stratigraphic sections of the Sidney Island formation, Sidney Island. Section locations shown in Figure 1.

bivalves *Pterotrigonia klamathonia* and *Litschkovitrigonia* sp., the gastropod *Gyrodos dowelli*, and fragments of ammonites; the fauna is indicative of the Lower Turonian.

***Tragodesmoceras ashlandicum* fauna**

Somewhat higher strata in the formation are characterized by the ammonite *Tragodesmoceras ashlandicum*, also indicative of the Lower Turonian. Other ammonites are associated with *T. ashlandicum*, including tetragonitids and phylloceratids, and numerous bivalve and gastropod taxa are locally common as well. Trigoniid bivalves are noticeably rare, reflecting the somewhat deeper-water nature of these deposits.

Tragodesmoceras? sp. has also been collected from the uppermost beds of Mandarte Island (GSC loc. 85513), suggesting that these beds are likely of Early Turonian age as well.

***Romaniceras* sp. fauna**

Mollusc fossils are relatively sparse in the upper beds of the Sidney Island formation; however, several additional specimens have been collected on the northeast shore of Sidney Island. The stratigraphically highest beds on the island (GSC loc. C-197029) yielded the Turonian ammonite *Romaniceras* sp., probably the subgenus *Yubariceras*. *Romaniceras* is a cosmopolitan genus, characteristic of Middle Turonian deposits around the globe.

No fossils younger than Middle Turonian have been identified in any sections assigned to the Sidney Island formation. Thus, the age range of the formation as presently known is Early to Middle Turonian.

COMPARISON WITH COMOX FORMATION

Strata of the Sidney Island formation outcrop east of, and are lithologically distinct from, exposures of the Comox Formation exposed nearby in the southern Gulf Islands, especially those on Forrest, Coal, and Goudge islands (Fig. 1), as well as other islands adjacent to the northeastern Saanich Peninsula. Kachelmeyer (1978), Ward (1978), and England (1989) have all described Comox Formation strata in this area in detail, and the author has visited numerous localities as well.

The available evidence indicates that the lower part of the Comox Formation in this region is a stratigraphically-complex succession of marginal-marine to nonmarine sandstone, siltstone, and carbonaceous mudstone, locally rich in coal, and probably several hundred metres in total thickness. Macrofossils are uncommon but found locally in the coarser units, and include robust, shallow-water trigoniids and other bivalves, and gastropods. The finer grained units, interstratified with the sandstones, include silty mudstone with nonmarine gastropods, abundant plant debris, including stems and leaves, and coalified stumps and coal seams to several centimetres thick.

The lower Comox Formation deposits likely reflect heterogeneous sedimentation in shifting, nonmarine to marginal-marine environments. The uppermost part of the formation reflects the transition to shallow-water, but fully-marine, deposition. It is from this fully-marine, upper part of the Comox Formation that ammonites have previously been collected, giving a late Santonian age for the strata (Muller and Jeletzky, 1970). The age of the lower part of the formation in southern Gulf Islands is still problematic (see discussion below).

The Comox Formation in the southernmost Gulf Islands appears to be locally more complex stratigraphically than farther to the northwest, where marine facies appear to predominate through most of the section. For example, on Saltspring Island (Fig. 1) the base of the Comox Formation consists of shallow-marine sandstones which directly overlie metavolcanics (Haggart, 1991b).

TURONIAN BIOCHRONOLOGY

Turonian deposits are uncommon in coastal British Columbia, and Turonian fossils are rare. Poorly fossiliferous and structurally disrupted Turonian strata are present on northern Vancouver Island (Jeletzky, 1977) and Queen Charlotte Islands (McLearn, 1972; Haggart, 1991c). In addition, poorly studied deposits of probable Late Turonian age are known from the San Juan Islands (Garver, 1988). Thus, the Sidney Island formation provides especially valuable data for the development of Turonian biochronology of western British Columbia and North America (Fig. 3).

| | | CHARACTERISTIC MOLLUSC TAXA | LITHOLOGIC UNITS | |
|------------------|-----------|-----------------------------|---|---|
| UPPER CRETACEOUS | SANTONIAN | Upper | <i>Sphenoceras schmidtii</i> Haslam Formation | |
| | | Lower | <i>Eubostriochoceras elongatum</i> Comox Formation | |
| | CONIACIAN | | No Marine Fossils yet Identified | Non-marine Comox Formation ? |
| | | | | ---? ---? ---? ---? ---? ---? ---? ---? ---? ---? |
| | TURONIAN | Upper | <i>Reesidites</i> sp. | *Barnes Island mudstone* |
| | | Middle | <i>Romaniceras</i> sp. | ? ---? ---? ---? ---? ---? ---? ---? ---? ---? |
| | | Lower | <i>Tragodesmoceras</i> sp. <i>Mytiloides</i> ex. gr. <i>labiatus</i> | Sidney Island Formation |

Figure 3. Stratigraphic and biochronologic framework for Upper Cretaceous strata of the southern Gulf Islands region, based on this report, Muller and Jeletzky (1970), and Garver (1988).

Early Turonian

Earliest Turonian time in the Sidney Island formation is represented by the cosmopolitan inoceramid bivalve group *Mytiloides* ex gr. *labiatus*. This group is widespread on Pacific-slope North America, known previously from California (Matsumoto, 1960; Jones and Bailey, 1973; Sliter et al., 1984; author's collections), Queen Charlotte Islands (Riccardi, 1981; Haggart, 1991c), and elsewhere. Overlying the beds with *M. ex gr. labiatus*, and associated with the inoceramid in its highest levels, is the ammonite assemblage dominated by *Tragodesmoceras ashlandicum*. The minimal stratigraphic overlap of these two taxa in the collections from Sidney Island suggests that *T. ashlandicum* ranges higher into the Lower Turonian than *M. ex gr. labiatus*. Support for this interpretation comes from California where *T. ashlandicum* is found in Early Turonian deposits younger than the beds containing *labiatus*-group inoceramids (Matsumoto, 1959; Haggart, 1986).

Middle Turonian

Middle Turonian time in the southern Gulf Islands region is represented by the ammonite genus *Romaniceras*, a cosmopolitan indicator of the Middle Turonian in California and Japan, and most regions of the globe (Matsumoto, 1959; Matsumoto and Suekane, 1987). *Romaniceras* has also been collected from structurally-disrupted strata on the northern coast of Vancouver Island (Jeletzky, 1977).

Late Turonian

Although *labiatus* group inoceramids are known from Queen Charlotte Islands, no younger Turonian fossils have yet been found there, and it would appear that much of Late Turonian time in the Insular Belt is characterized by progradation of coarse clastic systems (Haggart, 1993; J.W. Haggart, unpub. data). Upper Turonian strata have been recognized in the San Juan Islands of northwestern Washington State, however. P.D. Ward (in Garver, 1988; pers. comm., 1985, 1990, 1993) has identified the ammonite *Reesidites* and the foraminifer *Globotruncana helvetica*, from mudstones exposed on Barnes Island in the northeastern San Juan Islands (Fig. 1). Ammonites closely allied to *Reesidites* are found in the Upper Turonian of California (Matsumoto, 1959); *Reesidites* itself is known from Japan and is considered a cosmopolitan indicator of the Upper Turonian (Matsumoto, 1984).

Thus, a three-fold subdivision can be established for Turonian time in the southwestern British Columbia/northwestern Washington State region. *Mytiloides* ex gr. *labiatus* and *Tragodesmoceras* represent Early Turonian age deposits, *Romaniceras* the Middle Turonian, and *Reesidites* the Late Turonian.

STRATIGRAPHIC AND PALEOGEOGRAPHIC IMPLICATIONS

Strata of the Sidney Island formation represent shallow-marine deposition during Early and Middle Turonian time. These strata are temporally and lithologically distinct from strata of the basal Nanaimo Group present in the region and have important implications for basin stratigraphy and paleogeography.

Age of the basal Comox Formation

The age of Comox Formation in the southernmost Gulf Islands is problematic. To date, most interpretations of the age of this unit have recognized its stratigraphic position conformably beneath fossiliferous marine rocks of the Haslam Formation bearing the Late Santonian index ammonite *Didymoceras (Eubostriochoceras) elongatum*. Indeed, Haslam Formation turbiditic mudstone with the index fossil outcrops just to the north of Comox Formation strata on Piers and Pym islands, and on the northern tip of the Saanich Peninsula (Kachelmeyer, 1978; Ward, 1976, 1978).

Little faunal data bearing on the age of the lower part of the Comox Formation in the study area are presently available. However, molluscs collected from the northeastern side of Goudge Island (GSC loc. C-140507) include poorly preserved trigonid bivalves tentatively identified as *Pterotrigonia* cf. *klamathonia*, suggesting at least the possibility of a Turonian to earliest Coniacian age (Jones, 1960) for this locality. These strata on Goudge Island appear to represent a higher level within the Comox Formation, perhaps indicating that the basal part of the formation may range down into the Coniacian or even Turonian; all strata on Goudge Island are, however, lithologically distinct from the Sidney Island formation.

Correlations with other units

It is tempting to correlate the basal, nonmarine Comox Formation strata which outcrop in the vicinity of northern Saanich Peninsula, with the shallow-marine rocks of the Sidney Island formation to the east; however, given the poor constraints at present on the age of the basal Comox Formation in this region, precise depositional and paleogeographic relationships of the two units is uncertain.

Indeed, the Sidney Island formation may be more closely related to the Upper Turonian Barnes Island mudstones. Sidney Island formation strata reflect marine inundation and transgression, progressing from shallow to deeper-water deposits through Early and Middle Turonian time. The transition to deep-water mudstone deposition in Late Turonian time would be a natural continuation of this transgressive trend. The possibility exists that the Sidney Island formation and Barnes Island mudstones may not be directly related to the rest of the Nanaimo Group sequence exposed to the north and west.

The basal deposits of the Nanaimo Group, and by implication, the Turonian deposits of the Sidney Island formation, have been interpreted as the initial deposits of sedimentation which accumulated adjacent to a thrust system to eastward,

in the Coast Mountains and San Juan Islands (Brandon et al., 1988; Mustard, in press). However, there is little evidence in the preserved stratigraphic record of the Sidney Island formation which suggests a position of sedimentation proximal to active thrusting (e.g., no more than 5 km from thrusts on San Juan Island according to Brandon et al., 1988). The shallow marine strata of the formation are relatively mature, well-sorted, and laterally continuous; they form a thin stratigraphic section and do not exhibit significant lateral variations in clast size, sorting, or facies, as would be expected in molasse deposits accumulating directly adjacent to a significant thrust system.

The possibility exists that strata of the Sidney Island formation accumulated prior to initial thrusting in the San Juan Islands region (≈ 100 -84 Ma or latest Albian to Late Santonian/Early Campanian; Brandon et al., 1988). Alternatively, Turonian rocks of the southernmost Gulf Islands may have been brought to their present position close to the San Juan Islands Thrust by transport along one or more faults running subparallel to the San Juan Fault on southern Vancouver Island; at least 50 km of left-lateral offset has occurred along this fault since ≈ 39 -40 Ma (Fairchild and Cowan, 1982).

ACKNOWLEDGMENTS

Captain Ted Aubrey is thanked for expert boatmanship. Although not in agreement with several of the conclusions, Peter Mustard contributed a thoughtful review of the manuscript and is thanked for such.

REFERENCES

- Brandon, M.T., Cowan, D.S., and Vance, J.A.**
1988: The Late Cretaceous San Juan Thrust System, San Juan Islands, Washington; Geological Society of America, Special Paper 221, Boulder, Colorado, 81 p.
- England, T.D.J.**
1989: Late Cretaceous to Paleogene evolution of the Georgia Basin, southwestern British Columbia; Ph.D. thesis, Memorial University of Newfoundland, St. John's, Newfoundland, 481 p.
- Fairchild, L.H. and Cowan, D.S.**
1982: Structure, petrology, and tectonic history of the Leech River complex northwest of Victoria, Vancouver Island; Canadian Journal of Earth Sciences, v. 19, p. 1817-1835.
- Garver, J.**
1988: Stratigraphy, depositional setting, and tectonic significance of the clastic cover to the Fidalgo Ophiolite, San Juan Islands, Washington; Canadian Journal of Earth Sciences, v. 25, p. 417-432.
- Haggart, J.W.**
1986: Stratigraphy of the Redding Formation of north-central California and its bearing on Late Cretaceous paleogeography; in Cretaceous Stratigraphy, Western North America, (ed.) P.L. Abbott; Society of Economic Paleontologists and Mineralogists, Pacific Section, Book 46, p. 161-178.
1991a: A new assessment of the age of the basal Nanaimo Group, Gulf Islands, British Columbia; in Current Research, Part E; Geological Survey of Canada, Paper 91-1E, p. 77-82.
1991b: Biostratigraphy of the Upper Cretaceous Nanaimo Group, Gulf Islands, British Columbia; in A Field Guide to the Paleontology of Southwestern Canada, (ed.) P.L. Smith; Geological Association of Canada, Cordilleran Section, p. 222-257.
1991c: A synthesis of Cretaceous stratigraphy, Queen Charlotte Islands, British Columbia; in Evolution and Hydrocarbon Potential of the Queen Charlotte Basin, British Columbia, (ed.) G.J. Woodsworth; Geological Survey of Canada, Paper 90-10, p. 253-277.
- Haggart, J.W. (cont.)**
1993: Latest Jurassic and Cretaceous paleogeography of the northern Insular Belt, British Columbia; in Mesozoic Paleogeography of the Western United States - II, (ed.) G.C. Dunne and K.A. McDougall; Society of Economic Paleontologists and Mineralogists, Pacific Section, Book 71, p. 463-475.
- Jeletzky, J.A.**
1977: Mid-Cretaceous (Aptian to Coniacian) history of Pacific slope of Canada; Palaeontological Society of Japan, Special Papers, no. 21, p. 97-126, pl. 3.
- Jones, D.L.**
1960: Pelecypods of the genus *Pterotrignia* from the west coast of North America; Journal of Paleontology, v. 34, p. 433-439, pls. 59-60.
- Jones, D.L. and Bailey, E.H.**
1973: Preliminary biostratigraphic map, Colyear Springs Quadrangle, California; United States Geological Survey, Miscellaneous Field Studies Map MF 517, 1 sheet, scale 1:48 000.
- Kachelmeyer, J.M.**
1978: Bedrock geology of the North Saanich-Cobble Hill area, British Columbia, Canada; M.Sc. thesis, Oregon State University, Portland, Oregon, 153 p.
- Matsumoto, T.**
1959: Upper Cretaceous ammonites of California. Part II; Kyushu University, Memoirs of the Faculty of Science, Series D (Geology), Special Volume 1, 172 p., 41 pls.
1960: Upper Cretaceous ammonites of California. Part III; Memoirs of the Faculty of Science, Kyushu University, Series D (Geology), Special Volume 2, 204 p., 1 pl.
1984: The so-called Turonian-Coniacian boundary in Japan; Geological Society of Denmark, Bulletin, v. 33, p. 171-181.
- Matsumoto, T. and Suekane, T.**
1987: Some acanthoceratid ammonites from the Yubari Mountains, Hokkaido - Part I; Science Report of the Yokosuka City Museum, no. 35, p. 1-14, pls. 1-4.
- McLearn, F.H.**
1972: Ammonoids of the Lower Cretaceous Sandstone member of the Haida Formation, Skidegate Inlet, Queen Charlotte Islands, western British Columbia; Geological Survey of Canada, Bulletin 188, 78 p., 45 pls.
- Muller, J.E.**
1983: Geology, Victoria, west of Sixth Meridian, British Columbia; Geological Survey of Canada, Map 1553A, 1 sheet, scale 1:100 000.
- Muller, J.E. and Jeletzky, J.A.**
1970: Geology of the Upper Cretaceous Nanaimo Group, Vancouver Island and Gulf Islands, British Columbia; Geological Survey of Canada, Paper 69-25, 77 p.
- Mustard, P.S.**
in press: The Upper Cretaceous Nanaimo Group, Georgia Basin, southwestern British Columbia; in Geology of southwestern British Columbia, (ed.) J.W.H. Monger; Geological Survey of Canada.
- Popenoe, W.P., Saul, L.R., and Susuki, T.**
1987: Gyrodiform gastropods from the Pacific coast Cretaceous and Paleocene; Journal of Paleontology, v. 61, p. 70-100.
- Riccardi, A.C.**
1981: An Upper Cretaceous ammonite and inoceramids from the Honna Formation, Queen Charlotte Islands, British Columbia; in Current Research, Part C; Geological Survey of Canada, Paper 81-1C, p. 1-8, 1 pl.
- Sliter, W.V., Jones, D.L., and Throckmorton, C.K.**
1984: Age and correlation of the Cretaceous Hornbrook Formation, Oregon and California; in Geology of the Upper Cretaceous Hornbrook Formation, Oregon and California, (ed.) T.H. Nilsen; Society of Economic Paleontologists and Mineralogists, Pacific Section, Special Volume 42, p. 89-98.
- Ward, P.D.**
1976: Stratigraphy, paleoecology and functional morphology of heteromorph ammonites of the Upper Cretaceous Nanaimo Group, British Columbia and Washington; Ph.D. thesis, McMaster University, Hamilton, Ontario, 194 p.
1978: Revisions to the stratigraphy and biochronology of the Upper Cretaceous Nanaimo Group, British Columbia and Washington State; Canadian Journal of Earth Sciences, v. 15, p. 405-423.

Cayoosh Assemblage: regional correlations and implications for terrane linkages in the southern Coast Belt, British Columbia

J.M. Journeay and J.B. Mahoney¹
Cordilleran Division, Vancouver

Journeay, J.M. and Mahoney, J.B., 1994: Cayoosh Assemblage: regional correlations and implications for terrane linkages in the southern Coast Belt, British Columbia; in Current Research 1994-A; Geological Survey of Canada, p. 165-175.

Abstract: The Cayoosh Assemblage is an upward-coarsening succession of metamorphosed phyllitic argillite, siltstone, and sandstone that conformably overlies oceanic rocks of the Bridge River Complex. The age and regional distribution of these rocks suggest that the Bridge River ocean was long-lived, and remained open to marine sedimentation until Late Jurassic or Early Cretaceous time. New stratigraphic and paleontological data suggest that outboard terranes, including the Cadwallader and Harrison island arc complexes, may have been linked prior to accretion along the continental margin. Coarsening-upward clastic successions near the top of the Cayoosh Assemblage overlap these outboard terranes and record the final stages of terrane accretion along the ancestral continental margin.

Résumé : L'Assemblage de Cayoosh est une succession à cycle négatif d'argilite, de siltstone et de grès métamorphisés, qui surmonte en concordance les roches océaniques du complexe de Bridge River. L'âge et la distribution régionale de ces roches indiquent que l'océan de Bridge River a eu une existence de longue durée et est demeuré ouvert à la sédimentation marine jusqu'à la fin du Jurassique ou au début du Crétacé. De nouvelles données stratigraphiques et paléontologiques indiquent que des terranes situés au large, dont les complexes d'arc insulaire de Cadwallader et de Harrison, auraient pu être reliés avant leur accrétion à la marge continentale. Les successions détritiques à cycle négatif, près du sommet de l'Assemblage de Cayoosh, recouvrent ces terranes extracôtiers et témoignent des derniers stades de l'accrétion des terranes à la protomarge continentale.

¹ Department of Geological Sciences, University of British Columbia, 6339 Stores Road, Vancouver, British Columbia V6T 2B4

INTRODUCTION

Conceptual tectonic models of the western Canadian Cordillera, as it may have appeared in early to middle Jurassic time, portray ancestral terranes of the Coast and Insular belts as an array of island arc festoons and oceanic plateaus situated outboard of an accretionary/fore-arc complex (Monger et al., 1982; van der Heyden, 1992), a setting similar to that of the present southwest Pacific plate margin.

Outboard terranes of the northern Coast Belt (54°-60°N), which include Wrangellia and Alexander island arc complexes (Fig. 1), appear to have remained outboard of the ancestral continental margin throughout much of the Jurassic. Mississippian to Callovian (ca. 330-160 Ma) pelagic cherts of the Bridge River Complex and overlying Early Jurassic(?)

Belt) by Middle to Late Jurassic time. During the final stages of accretion, the zone of active subduction shifted westward from the Cache Creek suture to the outboard margin of the Insular superterrane, leading to the development of a post-Middle Jurassic accretionary/fore-arc complex (Chugach terrane) and an Andean-style magmatic arc (van der Heyden, 1992).

Terranes of the southern Coast Belt (49°-54°N), which include island arc assemblages of Wrangellia, Cadwallader, and Harrison terranes and oceanic rocks of the Bridge River terrane (Fig. 1), appear to have remained outboard of the ancestral continental margin throughout much of the Jurassic. Mississippian to Callovian (ca. 330-160 Ma) pelagic cherts of the Bridge River Complex and overlying Early Jurassic(?)

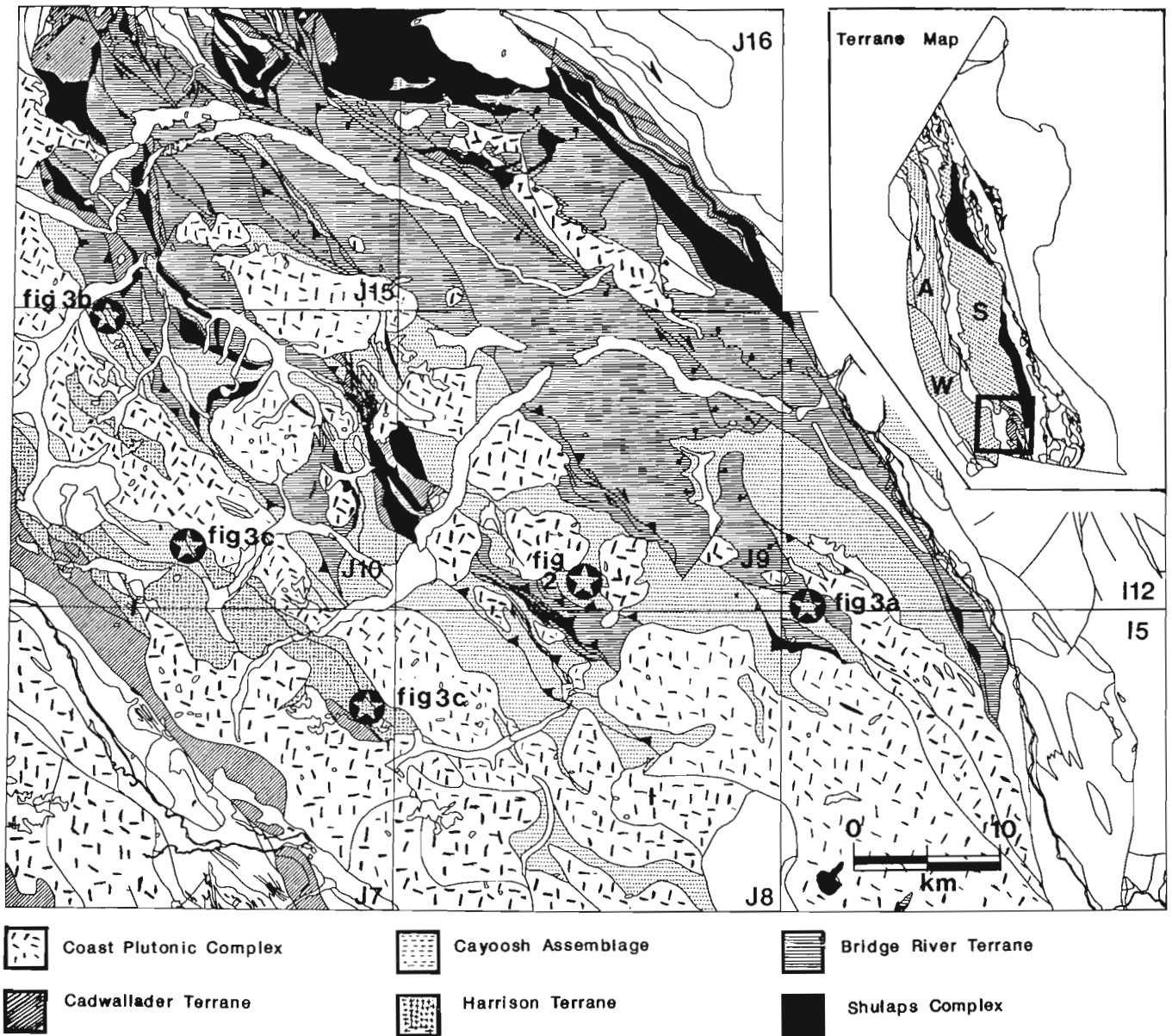


Figure 1. Tectonic setting (inset) and regional geology of the eastern Coast Belt. W: Wrangellia terrane; A: Alexander terrane; S: Stikinia terrane.

to Early Cretaceous(?) fine grained, clastic rocks of the Cayoosh Assemblage suggest that the Bridge River ocean remained open to marine sedimentation until Early Cretaceous time (Journeay and Northcote, 1992; Cordey and Schiarizza, 1993; Mahoney and Journeay, 1993). Early to mid-Cretaceous fluvial conglomerates and shallow marine clastic rocks (Gambier, Taylor Creek, and Jackass Mountain groups) form the oldest demonstrable overlap assemblage among terranes in the southern Coast Belt, and indicate that outboard terranes were stratigraphically linked prior to the onset of crustal shortening and large-scale crustal imbrication (Journeay and Friedman, 1993). However, it is not clear whether these outboard terranes were amalgamated prior to the Early Cretaceous and situated near the ancestral continental margin in a marginal basin setting, or whether they may have been added incrementally as part an accretionary/fore-arc complex in response to ongoing post-middle Jurassic subduction of the Bridge River ocean.

To address this question, we have focused our investigations on the internal stratigraphy and regional distribution of Jurassic and Cretaceous clastic successions that overlie oceanic rocks of the Bridge River Complex and associated island arc assemblages of the Cadwallader and Harrison terranes. These include turbidites and upward-coarsening clastic successions of the Cayoosh Assemblage, coarse clastic and shallow marine successions of the Tyaughton and Relay Mountain groups, and fine grained marine and volcanoclastic successions of the Mysterious and Billhook Creek formations, respectively. Fieldwork during the 1993 season involved 1:50 000 scale mapping in the Cadwallader and Cayoosh ranges of the eastern Coast Belt (92J/7, 92J/8, 92J/9, 92J/10, 92I/5, and 92I/12; Fig. 1), and detailed stratigraphic and sedimentological studies of the Cayoosh Assemblage.

CAYOOSH ASSEMBLAGE

The Cayoosh Assemblage is an upward-coarsening succession of metamorphosed phyllitic argillite, siltstone, and sandstone that conformably overlies interbedded greenstone, chert, and phyllitic argillite of the Bridge River Complex (Fig. 1; Journeay and Northcote, 1992; Journeay, 1993; Mahoney and Journeay, 1993). Primary sedimentary structures and stratigraphic relationships are preserved, but have been modified by the effects of penetrative deformation and regional metamorphism associated with Alpine-style folding and large-scale imbrication of the eastern Coast Belt (Journeay and Friedman, 1993). These structural and metamorphic complexities preclude accurate estimates of primary stratigraphic thicknesses or detailed reconstructions of sedimentation patterns and basin configuration. However, the integrity and lateral continuity of regional lithofacies lead us to conclude that the Cayoosh Assemblage is a stratigraphically coherent succession that preserves a record of Jurassic and Early Cretaceous sedimentation during the final stages in the evolution of the Bridge River ocean.

Stratigraphy

We have subdivided the Cayoosh Assemblage into five distinct lithofacies (Fig. 2). In ascending stratigraphic order, these include: graphitic phyllite, siltstone, and sandstone (unit 1), tuffaceous phyllite, graphitic phyllite, minor lapilli tuff, and tuff breccia (unit 2), graphitic phyllite, siltstone, limestone, and volcanoclastic sandstone (unit 3), graphitic siltstone, shale, phyllite, arkosic sandstone, and quartzite (unit 4), and thin-bedded graphitic phyllite, siltstone, and volcanoclastic sandstone (unit 5). For the purposes of discussion, we have used a standard rock column format to summarize and to describe the internal stratigraphy of the Cayoosh Assemblage (Fig. 2). This column is compiled from measured structural sections in reference localities of the Cayoosh Assemblage and does not indicate primary stratigraphic thickness.

This stratigraphy represents a more detailed subdivision of the Cayoosh Assemblage than that initially proposed by Mahoney and Journeay (1993). Neocomian sandstones and siltstones of unit 5, initially included in the upper siltstone/quartz-rich sandstone succession of the Cayoosh Assemblage, are here recognized as a distinct lithofacies. Fluvial conglomerate, initially included as the uppermost member of the Cayoosh Assemblage, is interpreted to unconformably overlie fossiliferous sandstones of unit 5 in the vicinity of Mount Brew. This conglomerate represents a fundamental change in depositional environment, and has been split out as a separate stratigraphic unit. Clast compositions and the occurrence of Late Jurassic granitoid boulders (ca. 151 Ma; V. McNicoll, pers. comm., 1992) suggest correlation with Early Cretaceous conglomerate of the Jackass Mountain Group. Detailed descriptions of the Cayoosh Assemblage in its type locality are reported by Mahoney and Journeay (1993). The following is a brief synopsis.

Interlayered greenstone, ribbon chert, limestone, calcareous greenschist, and graphitic phyllite of the Bridge River Complex grade upward with apparent conformity into a succession of graphitic siltstone, phyllite, greywacke and thin-bedded turbidites of the Cayoosh Assemblage (unit 1). The basal contact of the Cayoosh Assemblage is defined at the top of the stratigraphically highest chert horizon, and is locally marked by a thin, intra-formational pebble conglomerate containing clasts of limestone, siliceous argillite, and chert. Thinly laminated tuffaceous siltstone occurs near the top of this succession and signals an important change in provenance.

Unit 2 is characterized by thick (2-60 m) horizons of metamorphosed light to dark green, medium- and thick-bedded tuff, lapilli tuff, and tuff breccia, which occur as distinct layers in a succession of graphitic phyllite and siltstone. These pyroclastic rocks represent a minor (10-25%) but stratigraphically important component of the section. They record distinct pulses of volcanic activity in a basin characterized by thick accumulations of fine grained sediments. Both lower and upper boundaries of this succession are gradational.

Unit 3 comprises a thick (500-600 m) succession of fine- to coarse-grained volcanic sandstone and siltstone (30-35%) interlayered with graphitic phyllite (55-65%) and thin bands

Cayoosh Assemblage Stratigraphy

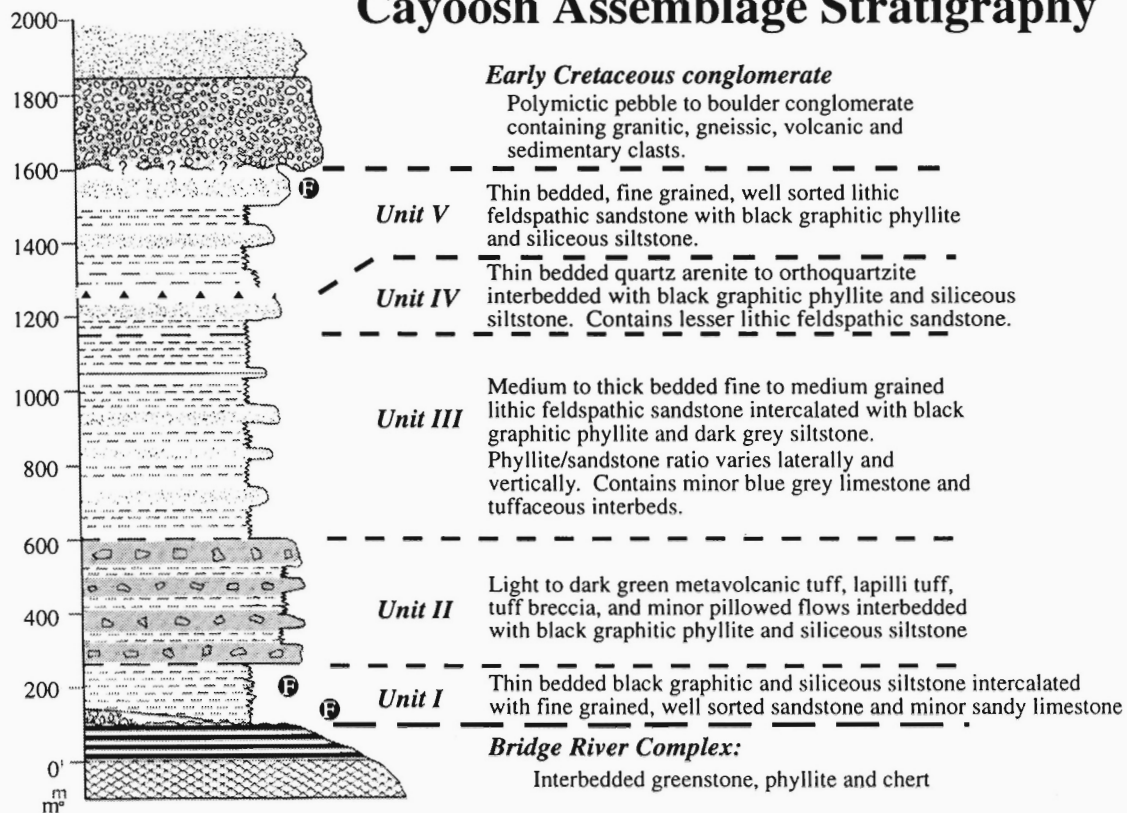


Figure 2. Schematic stratigraphic section of the Cayoosh Assemblage, as compiled from measured structural sections in the Melvin Creek and Mount Brew regions.

of limestone (5%). Sandstone horizons consist primarily of interlayered feldspathic arenite and greywacke with intercalations of thinly laminated siltstone. Horizons of quartz-rich feldspathic arenite occur near the top of the unit, suggesting that the Cayoosh Assemblage may have received detritus from multiple source regions. Sandstone intervals vary in thickness (50-100 m) and lateral extent throughout the unit, and are interpreted to be lenticular in cross-section and lobate in plan view. They define a cyclic coarsening- and thickening-upward/fining- and thinning-upward succession, with the highest proportion of sandstone occurring near the middle of the unit. Pyritiferous shale and siltstone near the top of unit 3 grade upward into feldspathic sandstone, similar in appearance to those of unit 1, but containing a higher proportion of detrital quartz.

Unit 4 is characterized by the presence of a quartz-rich clastic facies in, what is otherwise, a thick and monotonous succession of graphitic siltstone, shale, and phyllite. Thin, light grey and white laminae, interpreted as tuffaceous ash layers, are locally abundant and attest to continued volcanic activity. Sandstone horizons consist primarily of thin- and thick-bedded, fine- to coarse-grained, quartz-rich feldspathic arenite, orthoquartzite, and thinly laminated phyllitic quartzite. Feldspathic arenite beds are 5-8 m thick, locally graded and contain basal shale rip-up clasts. Quartzite horizons, which represent an unusual but very distinctive component of the upper Cayoosh Assemblage, consist primarily of quartz

with lesser amounts of detrital feldspar and hornblende (Fig. 4). The appearance of compositionally mature quartz-rich detritus in this part of the section suggests a continental influence. Provenance studies, including systematic petrography and U-Pb analysis of detrital zircon, are underway.

Quartz-rich clastic rocks of unit 4 grade upward into a thick (200-300 m) sequence of thin-bedded graphitic phyllite, siltstone, and fine- and medium-grained volcanoclastic sandstone (unit 5). Near Mount Brew, this section coarsens upward into a sequence of interlayered calcareous sandstone, phyllite, and green lithic feldspathic arenite. This upper clastic section is interpreted to be unconformably overlain by fluvial conglomerate, tentatively correlated with Early Cretaceous conglomerates of the Jackass Mountain Group. The upward coarsening trend and the occurrence of fossiliferous shallow marine sandstone near the top of unit 5 signal an important change in depositional environment, and may reflect the end of marine sedimentation in the Cayoosh Assemblage.

Age and regional distribution

Available age constraints indicate that the Cayoosh Assemblage probably ranges from Early Jurassic(?) to Early Cretaceous (Journeay and Northcote, 1992; Mahoney and Journeay, 1993). Basal turbidites in the type locality of

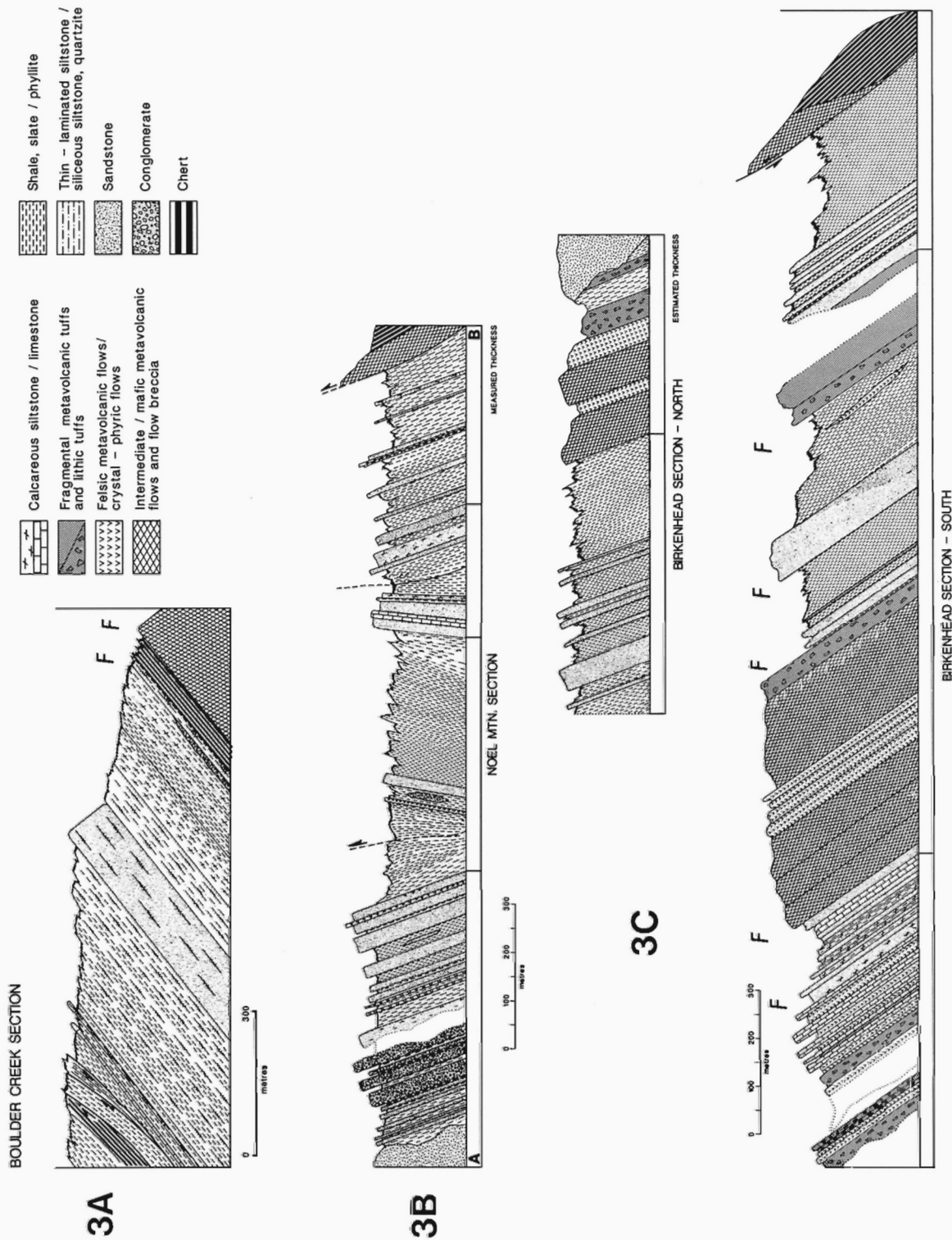


Figure 3. (A) Geological setting and stratigraphy of the Boulder Creek section. (B) Geological setting and stratigraphy of the Noel Mountain section. (C) Geological setting and stratigraphy of the Birkenhead section.

Melvin Creek overlies Upper Triassic (Norian) limestone-bearing oceanic rocks of the Bridge River Complex with apparent conformity. The uppermost clastic facies of the Cayoosh Assemblage (unit 5) contains shallow marine volcanic sandstones that yield bivalves (*Buchia*) of Early Neocomian age (Duffell and McTaggart, 1952).

In its type locality, the Cayoosh Assemblage occupies the core of a regional southwest-verging syncline, the limbs of which are cut by southwest-directed thrusts of the Bralorne and Downton Creek fault zones (Fig. 1). The axis of this syncline extends more than 100 km along strike to the southeast from the mining district of Bralorne, across the Cayoosh and Lillooet ranges into the Fraser Canyon, where it is cut by dextral transcurrent faults of the Fraser River fault system. In the course of systematic 1:50 000 scale mapping of stratified rocks in the eastern Coast Belt (Fig. 1; Journeay and Northcote, 1992; Journeay, 1993), we have expanded the outcrop belt of the Cayoosh Assemblage to include imbricated panels of fine grained metasedimentary rocks in both upper and lower plates of the Bralorne Fault (previously mapped as Noel Formation and Chism Creek Schist, respectively). Reconnaissance work in the region north of Carpenter Lake, and mapping by Schiarizza et al. (1989), suggest that clastic rocks of the Cayoosh Assemblage may also extend northward into the Chilcotin Mountains to include graphitic phyllite, siltstone, and sandstone successions presently mapped as part of the Bridge River Complex.

NEW DATA AND INTERPRETATIONS

Stratigraphic relations, the apparent age range, and regional distribution of the Cayoosh Assemblage in the eastern Coast Belt suggest that clastic sedimentation, derived in part from volcanic source terranes, was active in parts of the Bridge River ocean throughout much of the Jurassic. However, stratigraphic linkages between fine grained clastic successions of the Cayoosh Assemblage and outboard island arc assemblages (Wrangellia, Cadwallader and Harrison terranes) remain tenuous. Contact relationships are obscured by an array of postaccretionary thrust and strike-slip faults, which have imbricated and shuffled the eastern Coast Belt since Early Cretaceous time (Schiarizza et al., 1989; Journeay et al., 1992; Journeay and Friedman, 1993), and by eastward-younging batholithic suites of the Coast Plutonic Complex (Friedman and Armstrong, in press). Although isolated by faults and surrounded by plutons, the stratigraphic components of this geological puzzle continue to yield surprising and important new bits of information.

Boulder Creek Section

The Boulder Creek section (Fig. 3A) is well exposed at the southeast end of the Bridge River mélange belt (Journeay et al., 1992; Monger and Journeay, 1992). It is flanked to the west by the Downton Creek Fault, and to the east by

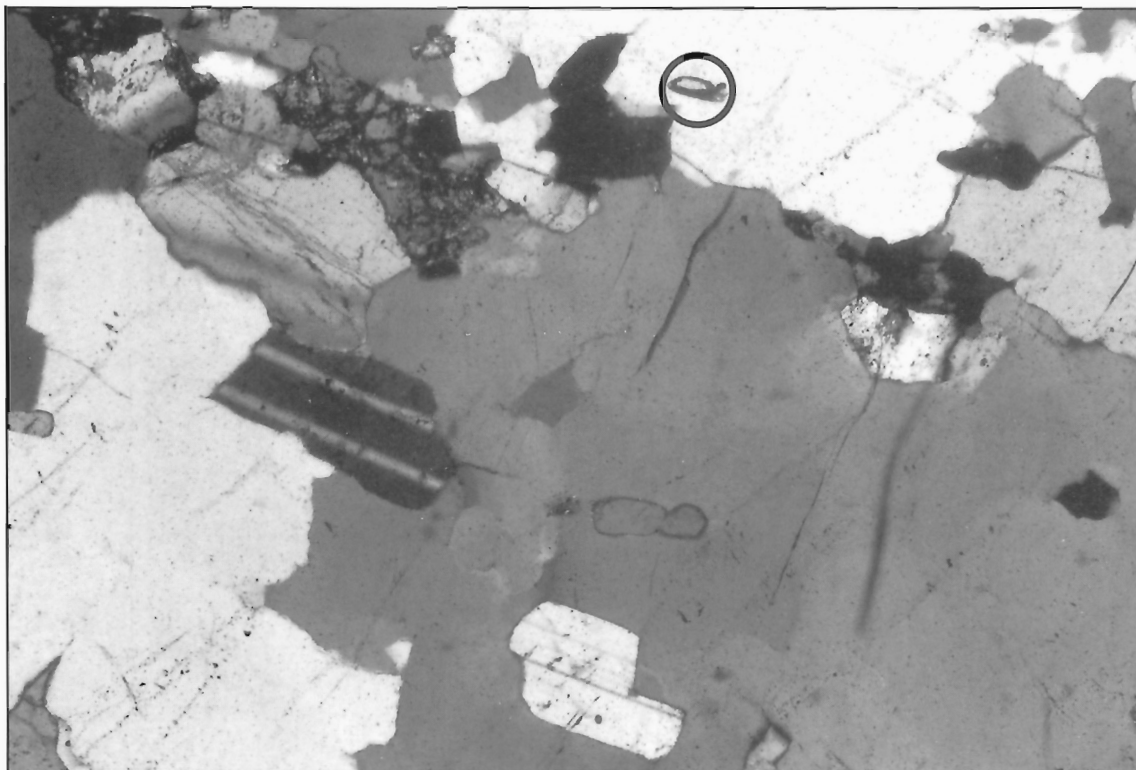


Figure 4. Photomicrograph of quartz-rich clastic facies. Note recrystallized quartz surrounding plagioclase feldspar. Subhedral zircon grain is circled.

low-angle mylonites of the Cayoosh Creek Fault. Imbricated fault slivers of greenstone, chert, limestone, and siltstone, locally containing pods of Upper Triassic (Norian) limestone, characterize the lower part of this section. The highest of these fault slivers contains a stratigraphically coherent panel of interlayered greenstone and chert which grades upward into a thick succession of siltstone, shale, and phyllite of the Cayoosh Assemblage. The contact, defined at the top of the highest chert horizon of the Bridge River Complex, is concordant and locally marked by thin lenses of chert pebble conglomerate. Siliceous argillite and thin bedded turbidites (125 m) at the base of the clastic succession grade upwards into a 75 m thick sequence of interbedded graphitic siltstone and phyllite containing 0.5 to 1.0 m thick horizons of chloritic (metatuffaceous) siltstone. This sequence coarsens upwards into a thick succession (90 m) of immature, medium- to thick-bedded volcanoclastic sandstone, dark grey siltstone, and metatuffaceous phyllite. Sandstones at the top of this clastic succession are, in turn, overlain by an upward-fining succession (200 m) of monotonous dark grey and black graphitic siltstone and phyllite, locally containing thin horizons of metatuffaceous siltstone and limestone. Imbricate fault slivers of greenstone, chert, and siltstone mark the southeast end of this section.

Stratigraphic similarities and lithological associations suggest to us a direct correlation of the Boulder Creek section with both the lower members of the Cayoosh Assemblage (units 1-3; compare Fig. 2 and 3A), and with the Lower to Middle Jurassic Ladner Group (Boston Bar and Dewdney Creek formations), which occurs along strike to the southeast (Fig. 1). Radiolaria extracted from siliceous argillite and siltstone at base of the Boulder Creek section are recrystallized, but include forms that are found in Upper Triassic and Lower Jurassic cherts of the Bridge River Complex (F. Cordey, pers. comm., 1993). Elsewhere in the Bridge River Complex, Cordey and Schiarizza (1993) have documented radiolarian cherts and associated siltstones that are as young as late Middle Jurassic (Callovian). These data suggest to us a complex and protracted history of basin evolution in which parts of the Bridge River ocean began to receive clastic detritus in the Late Triassic/Early Jurassic while other parts of the basin, presumably more distal, remained open to deep water sedimentation until late Middle Jurassic time. The implication is that the Cayoosh Assemblage may represent a time transgressive basin margin succession.

Noel Mountain section

The Noel Mountain section comprises a western assemblage of interlayered siltstone, sandstone and conglomerate, and an eastern assemblage of fine grained volcanoclastic sandstone, siltstone, and phyllite (Journeay, 1993; Fig. 3B).

The western assemblage is an upright panel of siltstone, thin- and thick-bedded greywacke, quartz-rich feldspathic arenite, and heterolithic conglomerate. Thick lenses of conglomerate in the middle of the section mark the transition from a lower coarsening-upward succession of fine grained volcanic sandstone and siltstone into an overlying, fining-upward succession of sandstone, siltstone, and phyllite.

Conglomerate horizons include both pebble- and boulder-sized clasts of quartz-rich sandstone, volcanic wacke, limestone, chert, and both fine grained volcanic and coarse grained plutonic rock. Conglomerates and the overlying, fining-upward clastic succession are interpreted to be part of the Early Cretaceous Taylor Creek Group (Rusmore, 1985; Woodsworth, 1977), which is well-exposed along strike to the northwest. The coarsening-upward succession of quartz-rich sandstones and siltstones that underly these conglomerates is interpreted to be part of the upper Cayoosh Assemblage (units 4 and/or 5).

The eastern assemblage is a thick (400-450 m) succession of thin bedded, dark grey graphitic shale, siltstone, phyllite, and fine grained volcanic sandstone, locally interlayered with feldspathic and calcareous wacke and thin, but distinctive lenses of dark grey limestone, limestone pebble conglomerate, and calcareous siltstone. Graded turbidites at the base of the section, locally containing thin horizons of light grey tuffaceous siltstone, calcareous wacke, and pebble conglomerate, grade upward into monotonous dark grey phyllite and siltstone (220 m). Fine grained volcanic sandstone at the top of this siltstone succession coarsens upward into 140 m of thick bedded, fine grained volcanic sandstone and siltstone. Stratigraphic repetition of this sandstone/siltstone facies, together with dip reversals of the dominant bedding-parallel foliation (S₁) and stratigraphic reversals of thin limestone pebble conglomerate horizons to the east, are interpreted to be the result of tight and isoclinal (F₂) folding (Fig. 3B). These folds are overturned to the southwest and appear to be localized in the footwall of the Bralorne Fault, a regional southwest-directed thrust system of Late Cretaceous age (Rusmore, 1985; Journeay et al., 1992; Journeay, 1993). Stratigraphic facing directions along the limbs of these second generation folds imply that the entire eastern Noel Mountain section must have been structurally overturned prior to F₂ folding and fault imbrication. We have traced this overturned panel of siltstone and volcanic sandstone northwestward across Green Mountain into the Downton Lake region. It appears to be the overturned limb of an alpine-scale, southwest-verging recumbent nappe structure.

The age of the eastern Noel Mountain section is unknown. The association of volcanic sandstone, calcareous siltstone, and thin horizons of limestone pebble conglomerate suggests a possible correlation with fine grained Late Triassic volcanoclastic rocks of the Hurley Formation (Cadwallader Group; Rusmore, 1985; Woodsworth, 1977; Journeay, 1993). However, the overall thickness of this succession, the abundance of thick volcanic sandstone and graphitic siltstone/phyllite successions, local occurrences of stretched pelecypods (*Buchia*?) and gastropods, and the notable absence of conodonts or thick limestone horizons anywhere in the section, suggest that a correlation with lower and middle members (units 2/3) of the Cayoosh Assemblage is more likely. This interpretation is corroborated by the investigations of Cairnes (1937), who documented a conformable relationship between thin bedded siltstones exposed along Noel Creek (Eastern Noel Mountain section) and underlying cherts of the Bridge River Group (Fergusson Series), a relationship similar to that documented in the type section of the Cayoosh Assemblage

(Journey and Northcote, 1992; Mahoney and Journey, 1993). Cairnes assigned these siltstones and shales to what he defined as the Noel Formation and proposed correlations with other siltstone/sandstone successions in the region, including those exposed along Cadwallader Creek and in the vicinity of Bralorne and Gun Lake. We support these correlations and propose that other siltstone/sandstone successions mapped by Cairnes (1937) as Noel Formation be included as part of the Cayoosh Assemblage. These correlations, coupled with regional stratigraphic and structural continuity, suggest a potential tie between the Cayoosh Assemblage and fine grained clastic rocks of the Last Creek formation and lower Relay Mountain Group, which overlie Triassic arc assemblages of the Cadwallader Group along strike to the north (Schiarizza et al., 1989).

Birkenhead section

The Birkenhead section is a northeast-dipping panel of inter-layered massive and fragmental volcanic flows and associated volcanoclastic rocks that grade upward into a succession of volcanic sandstone, siltstone, and phyllite (Fig. 3C; Journey, 1993). The section locally contains ammonite and bivalve forms of probable Late Triassic and Early Jurassic age, and has been included as part of the Cadwallader terrane (Cadwallader and Tyaughton groups; Woodsworth, 1977). Fieldwork during the 1993 season involved 1:50 000 scale mapping and detailed stratigraphic studies in a region extending northward from Cayoosh Mountain to the Birkenhead River (Fig. 1). These studies, initially aimed at investigating a stratigraphic tie between basal turbidites of the Cayoosh Assemblage (unit 1) and Lower Jurassic siltstones of the Last Creek formation, have uncovered exciting new evidence, including new fossil data and a previously undescribed volcanic succession, that require significant revision of existing correlations.

Fragmental volcanic rocks at the base of this section occupy the core of a regional southwest-verging anticlinal nappe (Birkenhead Anticline), the axial surface of which extends northwestward from Cayoosh Mountain to the west end of Birkenhead Lake (Fig. 1). The lowest portion of this section comprises a thick (220 m) sequence of dark green and maroon feldsparphyric flows, flow breccias, and associated fragmental lithic tuffs. Overlying these massive volcanics is a thick (150 m) succession of interlayered felsic metavolcanic flows, calcareous sandstone, and recrystallized limestone. This transitional facies grades upward into a thick (150 m) sequence of dark grey volcanoclastic sandstone, sandy limestone, and dark grey siltstone, locally containing corals and bivalves of probable Late Triassic age (Fig. 3C). Stratigraphic similarities and available age constraints suggest that these volcanic and sedimentary successions represent the Upper Triassic Pioneer and Hurley formations of the Cadwallader Group (Woodsworth, 1977).

Overlying this Upper Triassic arc assemblage with apparent conformity is a thick (450 m) succession of green and dark green metavolcanic flows, porphyritic flows and tuffs, locally containing light grey, fine grained felsic metavolcanic flows (50-80 m) and lesser amounts of fine grained volcanoclastic

sandstone and siltstone (Fig. 3C). Pyroclastic rocks at the top of this section are gradational upward into a 400-450 m thick succession of volcanoclastic sandstone, siltstone, shale, and phyllite, locally containing tuffaceous interbeds and intermediate volcanic flows. The contact between this volcanic succession and overlying volcanoclastic sequence is well exposed along the north and east flanks of Cayoosh Mountain, and can be traced northwestward to Gates Lake and into ridges west of Birkenhead Peak. This same section is overturned along the east flank of the Birkenhead River valley (Journey, 1993) and may correlate with volcanic and volcanoclastic successions that overlie Upper Triassic arc assemblages of the Cadwallader Group in the Tenquille Lake region (Grizzly Pass section of Journey, 1993).

Ammonite forms at the base of the volcanic section (Fig. 5) are characterized by distinctive ornamentation that suggest a probable lower to middle Toarcian age (H.W. Tipper and G. Jakobs, pers. comm., 1993). Bivalves that occur within sandstone of the overlying volcanoclastic succession (Fig. 6) resemble pelecypods collected by G.J. Woodsworth and interpreted by T.P. Poulton as trigoniid forms of probable Middle Toarcian to Bajocian age. The internal stratigraphy and age range of this arc assemblage is similar to that of the Middle Jurassic Harrison Lake Formation (Arthur et al., 1993), and suggests to us a probable correlation. This interpretation extends the known limits of the Harrison terrane northward and eastward into the imbricate zone of the Coast Belt Thrust System (Journey and Friedman, 1993), and implies a potential link between Harrison and Cadwallader terranes.

Intermediate and felsic metavolcanic flows mark the boundary between this Middle Jurassic arc sequence and overlying volcanoclastic sandstones, siltstones, and phyllites of the upper Birkenhead section (Fig. 3C). The contact between these two units is exposed along the margin of the Mt. Rohr pluton, near Birkenhead Peak, and appears to be conformable. The lower 80 to 100 m of this succession are characterized by interlayered volcanic sandstone, tuffaceous siltstone, and thinly laminated calcareous and graphitic siltstone. Sandstone horizons are fine- to medium-grained, thin- and thick-bedded (0.5-2 m), and include both immature feldspathic wacke and moderately well-sorted feldspathic arenite. This sandstone/siltstone facies fines upwards into a thick (250 m) succession of graphitic siltstone and phyllite. This upward-fining clastic succession is flanked to the east by imbricate fault slivers of the Bridge River Complex, and is repeated on the overturned limb of the Birkenhead Anticline, where it is apparently truncated by the Birkenhead River Fault. Stratigraphic relations suggest that this upper clastic succession is younger than Middle Jurassic, and may be correlative with either fine grained sedimentary rocks of the Callovian Mysterious Creek Formation (Harrison Terrane) or with undated volcanic sandstone/siltstone successions (units 3-5) of the Cayoosh Assemblage. Associations with quartz-rich meta-sandstones and conglomerates, which occur along strike to the northwest in roof pendants of the Mt. Rohr pluton, support the latter of these two interpretations. This correlation provides a potential link between outboard terranes (Cadwallader and Harrison arc assemblages) and clastic



Figure 5. Lower to Middle Toarcian ammonite collected from the middle unit of the Birkenhead section. Sample found by Jan Daly and identified by Howard Tipper and Giselle Jakobs. See Figure 5 for location.



Figure 6. Late Toarcian to Bajocian bivalves collected from the middle unit of the Birkenhead section.

Regional Correlations and Terrane Linkages

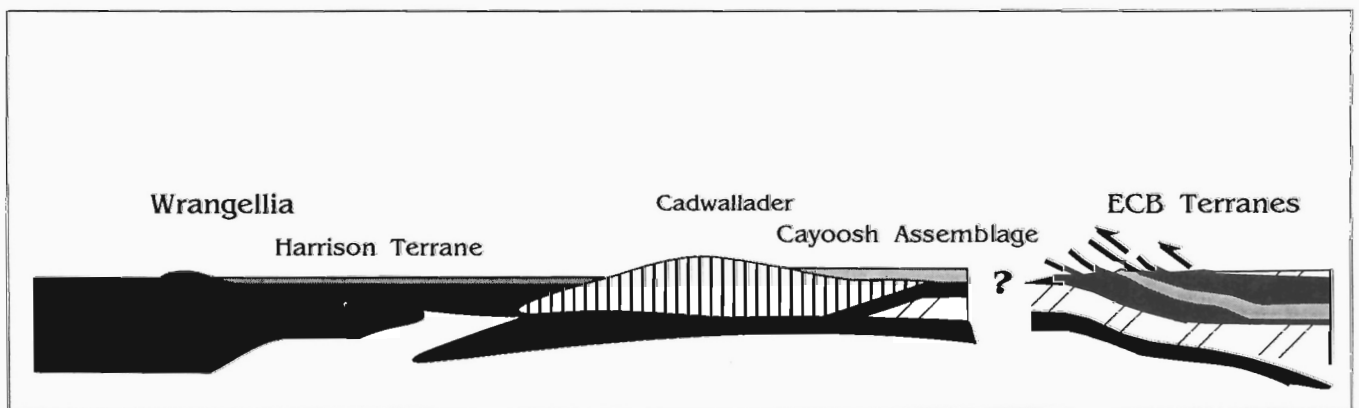
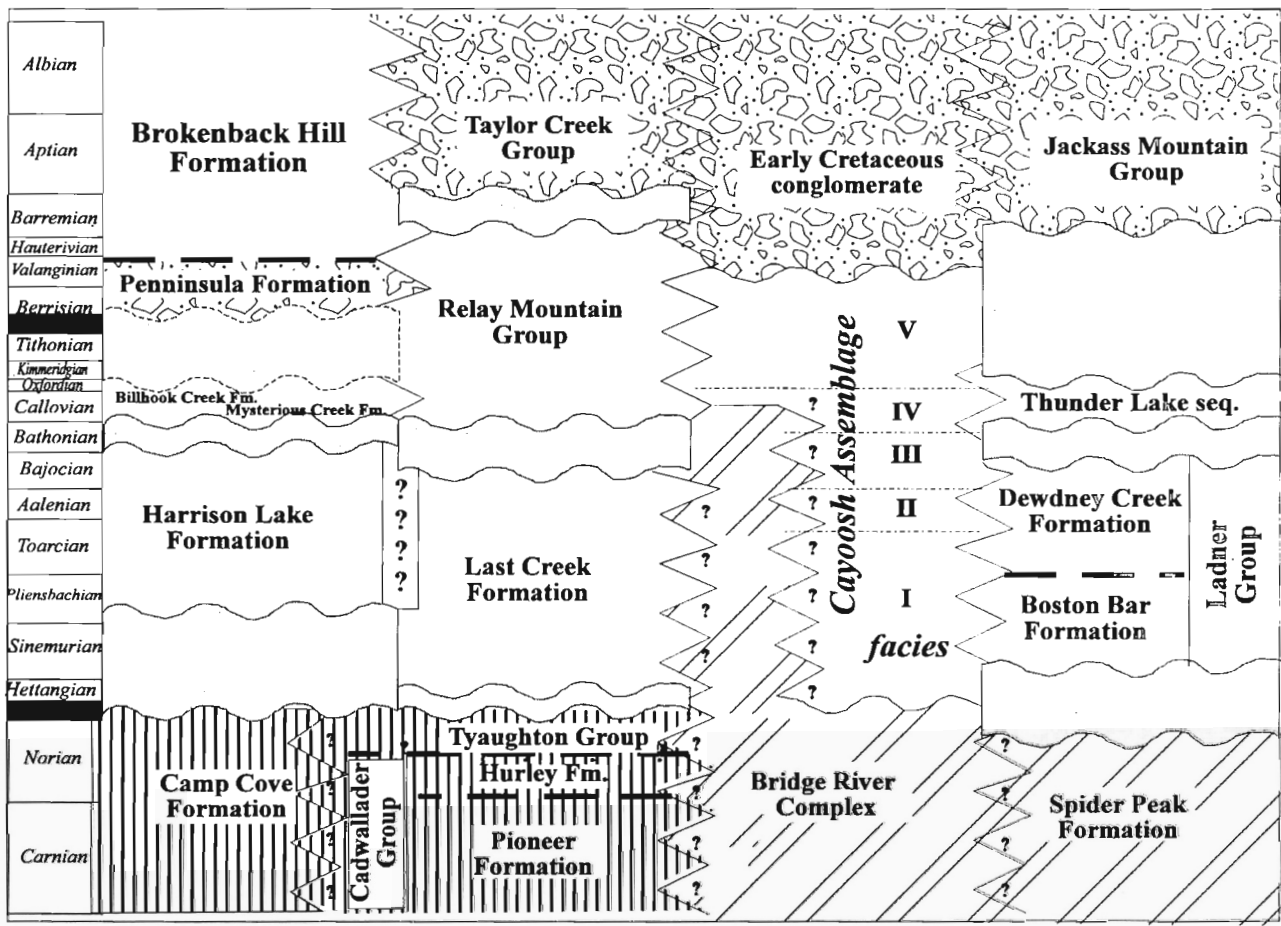


Figure 7. Proposed regional stratigraphic correlation of Jurassic basin successions in the eastern Coast Belt.

successions that overlie oceanic rocks of the Bridge River terrane, and may represent a stratigraphic bridge that predates final accretion along the continental margin and subsequent onlap of Early Cretaceous conglomerate.

SUMMARY AND CONCLUSIONS

Stratigraphic relationships documented in this and previous reports (Journeay and Northcote, 1992; Journeay, 1993; Mahoney and Journeay, 1993) have established the Cayoosh Assemblage as a coherent stratigraphic succession that conformably overlies oceanic rocks of the Bridge River Complex. Stratigraphic associations and available age constraints support a correlation with Lower and Middle Jurassic rocks of the Ladner Group (Methow basin) and with clastic successions that overlie Triassic and Middle Jurassic island arc assemblages of the Cadwallader and Harrison terranes (see Fig. 7). Stratigraphic ties with Jurassic clastic successions of the Last Creek formation and Relay Mountain Group are probable, but have not yet been established.

These correlations suggest to us a complex basin evolution in which parts of the Bridge River ocean began to receive clastic detritus in the Late Triassic/Early Jurassic, while other parts of the basin, presumably more distal, remained open to pelagic sedimentation until late Middle Jurassic time. Quartz-rich sandstone and upward-coarsening clastic successions of the Cayoosh Assemblage (units 4 and 5), the youngest of which are Early Cretaceous, reflect the arrival and/or emergence of both crystalline and volcanic source terranes and the closure of the Bridge River ocean.

Stratigraphic relationships and new paleontological data in the Birkenhead section suggest a disconformable relationship between the Upper Triassic Cadwallader arc and overlying Middle Jurassic rocks of the Harrison Lake Formation. Along strike to the south, this Middle Jurassic arc overlaps Triassic rocks of the Camp Cove Formation (Arthur et al., 1993). This implies the Cadwallader Group and Camp Cove Formation are either part of the same Triassic arc complex, or fragments of separate terranes that were amalgamated prior to the development of the Harrison Lake arc in Middle Jurassic time. Linkages between clastic successions at the top of the Birkenhead section and the upper Cayoosh Assemblage suggest that this Middle Jurassic arc most likely formed along the outboard margin of the ancestral Bridge River ocean.

ACKNOWLEDGMENTS

Our ideas have evolved through many stimulating discussions with Jim Monger, Howard Tipper, Glenn Woodsworth, Peter van der Heyden, Paul Schiarizza, Bill McClelland and Fabrice Cordey. Fieldwork was carried out with volunteer assistance from Jan Daly. Her mountaineering skills and keen eyes led the way through the Birkenhead section and to important new fossil localities. We are grateful to Howard Tipper, Giselle Jakobs, and Fabrice Cordey for sharing the

preliminary results of their biostratigraphic investigations. Will Husby provided valuable photographic documentation of fossil collections from the Birkenhead section.

REFERENCES

- Arthur, A.J., Smith, P.L., Monger, J.W.H., and Tipper, H.W.**
1993: Mesozoic stratigraphy and Jurassic paleontology west of Harrison Lake, southwestern British Columbia; Geological Survey of Canada, Bulletin 441, 62 p.
- Cairnes, C.E.**
1937: Geology and mineral deposits of the Bridge River mining camp, British Columbia; Geological Survey of Canada, Memoir 213, 140 p.
- Cordey, F. and Schiarizza, P.**
1993: Long-lived Panthalassic remnant: The Bridge River accretionary complex, Canadian Cordillera; *Geology*, v. 21, p. 263-266.
- Duffell, S. and McTaggart, K.C.**
1952: Ashcroft map area, British Columbia; Geological Survey of Canada, Paper 67-10, 55 p.
- Friedman, R.M. and Armstrong, R.L.**
in press: Jurassic and Cretaceous geochronology of the southern Coast Belt, southern British Columbia, 49-50 degrees N; Geological Society of America in Jurassic magmatism in the western North American Cordillera, (ed.) D. Miller; Memoir.
- Journeay, J.M.**
1993: Tectonic assemblages of the Eastern Coast Belt, southwestern British Columbia: Implications for the history and mechanisms of terrane accretion; in *Current Research, Part A*; Geological Survey of Canada, Paper 93-1A, p. 221-233.
- Journeay, J.M. and Friedman, R.M.**
1993: The Coast Belt Thrust System: evidence of Late Cretaceous shortening in the Coast Belt of SW British Columbia; *Tectonics*, v. 12, no. 3, p. 756-775.
- Journeay, J.M. and Northcote, B.R.**
1992: Tectonic assemblages of the Southern Coast Belt, SW British Columbia; in *Current Research, Part A*; Geological Survey of Canada, Paper 92-1A, p. 215-224.
- Journeay, J.M., Sanders, C., Van-Konijnenburg, J.-H., and Jasma, M.**
1992: Fault systems of the eastern Coast Belt, southwest British Columbia; in *Current Research, Part A*; Geological Survey of Canada, Paper 92-1A, p. 225-235.
- Mahoney, J.B. and Journeay, J.M.**
1993: The Cayoosh Assemblage, southwestern British Columbia: last vestige of the Bridge River ocean; in *Current Research, Part A*; Geological Survey of Canada, Paper 93-1A, p. 235-244.
- Monger, J.W.H. and Journeay, J.M.**
1992: Guide to the geology and tectonic evolution of the southern Coast Belt: A field guide to accompany the Penrose Conference on the "Tectonic Evolution of the Coast Mountain Orogen", May 1992, 97 p.
- Monger, J.W.H., Price, R.A., and Tempelman-Kluit, D.J.**
1982: Tectonic accretion and the origin of two major metamorphic and plutonic belts in the Canadian Cordillera; *Geology*, v. 10, p. 70-75.
- Rusmore, M.E.**
1985: Geology and tectonic significance of the Upper Triassic Cadwallader Group and its surrounding faults, southwestern British Columbia; Ph.D. thesis, University of Washington, Seattle, 170 p.
- Schiarizza, P., Gaba, R.G., Glover, J.K., and Garver, J.I.**
1989: Geology and mineral occurrences of the Tyaughton Creek area (92 O/2, 92 J/15); in *Geological Fieldwork 1988*; British Columbia Ministry of Energy, Mines and Petroleum Resources, Paper 1989-1, p. 115-130.
- van der Heyden, P.**
1992: A Middle Jurassic to Early Tertiary Andean-Sierran Arc Model for the Coast Belt of British Columbia; *Tectonics*, v. 11, no. 1, p. 82-97.
- Woodsworth, G.J.**
1977: Pemberton (92J) map area, British Columbia; Geological Survey of Canada, Open File 482.

Late Cretaceous to Paleogene cooling adjacent to strike-slip faults in the Bridge River area, southern British Columbia, based on fission-track and ^{40}Ar - ^{39}Ar analyses

John I. Garver¹, Doug A. Archibald² and William F. Van Order, Jr.¹
Cordilleran Division

Garver, J.I., Archibald, D.A., and Van Order, W.F., Jr., 1994: Late Cretaceous to Paleogene cooling adjacent to strike-slip faults in the Bridge River area, southern British Columbia, based on fission-track and ^{40}Ar - ^{39}Ar analyses; in Current Research 1994-A; Geological Survey of Canada, p. 177-183.

Abstract: Zircon fission-track (ZFT) ages and ^{40}Ar - ^{39}Ar ages on biotite and hornblende are used to constrain the timing of low-temperature cooling in the Bridge River area of southern British Columbia. Cooling ages at ~78-75 Ma and ~55-52 Ma (ZFT), from the Dickson and Bendor plutons respectively, may be related to either normal cooling of high-level plutons by conduction or to cooling induced by erosional or tectonic denudation, possibly driven by strike-slip faulting. Zircon fission track ages of rocks cut by the Marshall Creek fault, and from rocks in the footwall of the fault system indicate movement must have occurred during the interval ~43 to 39.5 Ma. This episode of movement on the Marshall Creek fault may be kinematically related to dextral strike-slip faulting on the Fraser fault system.

Résumé : La datation du zircon par la méthode des traces de fission (TFZ) et les âges $^{40}\text{Ar}/^{39}\text{Ar}$ sur biotite et sur hornblende permettent de préciser les limites dans le temps de l'épisode de refroidissement à basse température reconnu dans la région de Bridge River, dans le sud de la Colombie-Britannique. Les âges de refroidissement, évalués à 78-75 Ma et à 55-52 Ma (TFZ), pour les plutons de Dickson et de Bendor respectivement, pourraient être liés soit à un refroidissement normal par conduction de plutons mis en place à faible profondeur, soit à un refroidissement dû à une dénudation érosionnelle ou tectonique, causée peut-être par le jeu de décrochements. Les âges obtenus par la méthode des traces de fission sur zircon des roches traversées par la faille et des roches du mur du système de failles indiquent que le mouvement a dû se produire dans l'intervalle de 43 à 39,5 Ma. Cet épisode de mouvement dans la faille de Marshall Creek pourrait être relié cinématiquement au décrochement dextre s'étant produit dans le système de failles du Fraser.

¹ Department of Geology, Union College, Schenectady, New York 12308-2311

² Department of Geological Sciences, Queen's University, Kingston, Ontario K7L 3N6

INTRODUCTION

The Bridge River area is located on the eastern flank of the Coast Range, about 200 km north of Vancouver, British Columbia, and is located between the Insular terrane to the west and the Intermontane terrane to the east (Fig. 1). The area is underlain by several distinct tectonostratigraphic terranes, which are blanketed by upper Middle Jurassic to upper Cretaceous strata of the Tyaughton basin. The basement terranes and the basin strata are intruded by plutonic rocks which represent the eastern margin of the Coast Plutonic Complex (Roddick and Hutchison, 1973; Woodsworth, 1977; Monger and Journeay, 1992). These igneous rocks are important in that they provide some of the only constraints on the timing of structural development in the area. The Tyaughton basin strata are interpreted to rest unconformably on volcanic and volcanic-rich sedimentary rocks of the Upper Triassic Cadwallader terrane (Schiarizza et al., 1989, 1990 and references therein). Structurally interleaved with the Cadwallader terrane and strata of the Tyaughton basin is the Bridge River Complex, which is composed of highly deformed oceanic rocks that range in age from Mississippian to Middle Jurassic

based on radiolarians and conodonts from chert and limestone (Cordey and Schiarizza, 1993). Clastic rocks of the Cayoosh assemblage, which may be Jura-Cretaceous in age, may rest unconformably on rocks of the Bridge River Complex (Fig. 1; Monger and Journeay, 1992).

Cretaceous to Paleogene contraction and strike-slip faulting dominate the regional structural pattern, and considerable controversy surrounds the timing and style of deformation. Mid-Cretaceous orogenesis involved significant northeast-southwest and east-west contraction, but the role of contemporaneous strike-slip faulting is uncertain. Directly to the south of our area, Journeay and Friedman (1993) have documented a distinct period of west-vergent contraction that occurred between ~97 to 91 Ma. In the Bridge River area, mid-Cretaceous contraction was followed by a discrete phase of strike-slip faulting (Schiarizza et al., 1989, 1990; Garver et al., 1989; Garver, 1991). An important and unresolved question, in terms of the regional geology of this area, centres around the timing of initiation, duration, and magnitude of strike-slip faulting. Umhoefer and Schiarizza (1992) have proposed that slip on strike-slip faults stepped from southwest

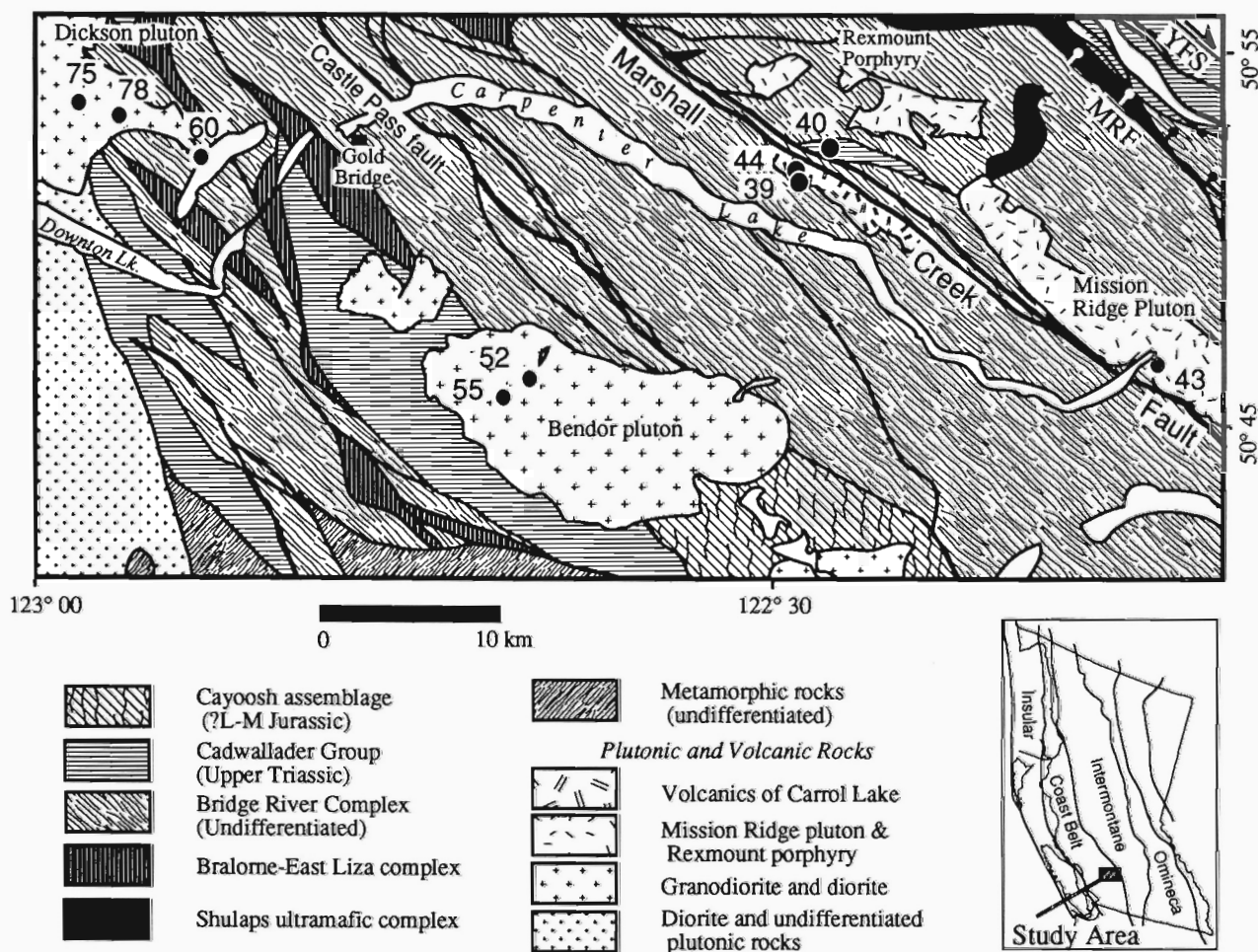


Figure 1. Location and generalized geology of the study area showing zircon fission-track ages. See Table 1 for ages and units; Ar-Ar ages are in Table 2. Figure modified from Monger and Journeay (1992).

to northeast as the system accommodated transfer of movement from the northwest-trending Yalakom fault system to the north-trending Fraser-Straight Creek fault system.

Zircon fission track (ZFT) age determination allows us to estimate the time at which rocks have cooled below about $240 \pm 40^\circ\text{C}$ (Brandon and Vance, 1992), and the Ar-Ar total fusion dates reported here correspond to cooling below about $280 \pm 40^\circ\text{C}$ for biotite and about $500 \pm 50^\circ\text{C}$ for hornblende, although the closure in both systems is dependent on the rate of cooling. Previous work indicates that the low-temperature cooling of the Coast Plutonic Complex (CPC) occurred at relatively slow rates in the early Tertiary, but cooling adjacent to the strike-slip faults in the Bridge River area occurred much more rapidly (Parrish, 1983). The location of our study area allows us to examine the cooling from the eastern flank of the Coast Plutonic Complex into and across this strike-slip fault system.

SAMPLING AND LABORATORY METHODS

Fission-track dating

For zircon fission-track analysis, our procedures for sample preparation and dating are similar to those outlined in Naeser (1976) for the external detector method. The Zeta method was used to provide calibration to an age standard and glass dosimeters were used in all irradiation packages (Wagner and van den Haute, 1992). The dated zircon fractions, which were non-magnetic with grain sizes between +200 and -60 mesh, were mounted in FEP Teflon, polished, and etched at 225°C for 12 to 20 hours. Low-uranium muscovite flakes were affixed to the Teflon mounts and the mounts were irradiated at the Oregon State nuclear reactor using a nominal fluence of 2×10^{15} neutrons/cm². The CN-5 glass standard, which was placed at the top, middle, and bottom of the irradiation

tube, was used to monitor the fluence. Zircon mounts of the Fish Canyon Tuff were also irradiated and were used to determine a Zeta factor for JIG and WFV (see Table 1). Fission tracks were counted at 1250X using an oil immersion objective on an Olympus BH-2 petrographic microscope. The ages, Zeta factors, glass dosimeter densities were calculated using the computer programs of Brandon and Vance (1992).

Ar-Ar analysis

Unknowns and flux monitors (standards) were irradiated with fast neutrons at the McMaster nuclear reactor for 29 hours. Although monitors were spaced throughout the irradiation container, J-values for the samples were determined by comparison to values from a well-characterized sample (TL88-17); calibration to the flux monitors may change these ages slightly and as a result the Ar-Ar total fusion ages in this report should be considered preliminary. The ultra-high vacuum, stainless steel argon extraction system is operated on-line to a substantially modified A.E.I. MS-10 mass-spectrometer run in the static mode. Measured mass-spectrometric ratios were extrapolated to zero time, corrected to a $^{40}\text{Ar}/^{39}\text{Ar}$ atmospheric ratio of 295.5 and corrected for neutron induced ^{40}Ar from potassium and ^{39}Ar and ^{36}Ar from calcium. Dates and errors are calculated according to the methods of Dalrymple et al. (1981) and the constants used are those recommended by Steiger and Jäger (1977). The errors shown in Table 2 represent the analytical precision at 2% assuming a J-value error of zero.

RESULTS

Our fission track data and Ar-Ar data are from three principal regions in the Bridge River area: the Dickson peak area in the western part of the area, the Eldorado pluton and the Bendor

Table 1. Summary of zircon fission track (ZFT) data.

| Number | Unit/Area | Elev. | | | ρ^d $\times 10^6 \text{ cm}^{-2}$ | N | $\chi^2\%$ | U (ppm) | Pooled age | Mean Age | |
|--------|-----------|---------------------|-------|------|---|-------|------------|------------|------------|-----------------|-----------------|
| | | | Ns | Ni | | | | | | | |
| 1 | WV-08 | Unk. ss; Carrol Lk. | 4020' | 1464 | 1468 | 2.289 | 10 | 29.7 | 229 | 39.1 ± 5.1 | 39.8 ± 5.6 |
| 2 | WV-07 | Rhy vx; Carrol Lk. | 5120' | 1068 | 965 | 2.296 | 9 | 80.4 | 369 | 43.5 ± 6.1 | 43.5 ± 5.4 |
| 3 | WV-06 | Hurley Cg. clast | 7120' | 366 | 366 | 2.307 | 6 | 85.8 | 159 | 39.5 ± 7.5 | 39.3 ± 5.9 |
| 4 | JG - 01 | Bendor; tarn | 6300' | 925 | 789 | 2.777 | 7 | 8.2 | 242 | 52.0 ± 6.4 | 52.1 ± 8.2 |
| 5 | JG - 02 | Bendor; ridge crest | 8150' | 947 | 775 | 2.791 | 9 | 51.9 | 199 | 54.5 ± 6.7 | 55.1 ± 6.2 |
| 6 | JG - 03 | Mission Rdg. Plut. | 2000' | 883 | 926 | 2.806 | 7 | 2.9 | 356 | 42.8 ± 5.1 | 42.9 ± 7.4 |
| 7 | JG - 04 | Dickson; Slim Ck. | 4490' | 861 | 416 | 2.749 | 7 | 11.1 | 206 | 90.7 ± 13.2 | 94.3 ± 19.4 |
| 8 | JG - 05 | Dickson; Roxy Ck. | 5940' | 937 | 627 | 3.271 | 7 | 42.2 | 220 | 78.0 ± 9.8 | 80.6 ± 11.0 |
| 9 | JG - 06 | Dickson Pk. | 7560' | 1133 | 761 | 3.140 | 10 | 95.3 | 224 | 74.6 ± 8.8 | 75.4 ± 8.8 |
| 10 | JG - 08 | Dickson; Gun Lk. | 2820' | 894 | 794 | 3.324 | 7 | 32.1 | 401 | 59.8 ± 7.3 | 61.0 ± 7.8 |

Notes: ZFT ages calculated using the Zeta method of calibration (see text). Counting parameters as follows: 1) Van Order (WV samples) Zeta = 346.26 ± 15.36 (± 1 se); 2) Garver (JG) Zeta = 320.97 ± 7.79 (± 1 se). Ns = number of spontaneous tracks; Ni = number of induced tracks. ρ^d = density of tracks on the glass dosimeter extrapolated to the position of the sample. $\chi^2\%$ is the probability (%) that grain ages are representative of a single population; the χ^2 test is failed when the probability falls below 5%. The pooled age (age calculated from the total Ns/Ni) is preferred when the sample passes the χ^2 test, and the mean age (mean of individual grain ages) is used when the sample fails χ^2 . For both the Mean age and the Pooled age, the error shown is the 95% confidence interval.

Table 2. Summary Ar-Ar total fusion data.

| Number | Unit/Area | Mineral | Grain size | Mass | $^{40}\text{Ar}/^{39}\text{Ar}$ | $^{36}\text{Ar}/^{39}\text{Ar}$ | $^{37}\text{Ar}/^{39}\text{Ar}$ | Vol $^{39}\text{Ar}^1$ | % ^{40}Ar rad | Age ($\pm 2\sigma$) |
|---------|---------------------|---------|------------|------|---------------------------------|---------------------------------|---------------------------------|------------------------|------------------------|-----------------------|
| JG - 01 | Bendor; tarn | biotite | 40/60 | 45 | 5.670 | 0.0018 | 0.017 | 17.268 | 91.79 | 64.36 \pm 0.34 |
| JG - 02 | Bendor; ridge crest | biotite | 60/80 | 74 | 6.288 | 0.0062 | 7.816 | 2.118 | 71.10 | 62.86 \pm 1.79 |
| JG - 02 | " " | hnb | +40 | 59 | 5.527 | 0.0012 | 0.039 | 20.110 | 93.60 | 63.99 \pm 0.28 |
| JG - 04 | Dickson; Slim Ck. | biotite | +40 | 56 | 7.782 | 0.0011 | 0.016 | 21.662 | 95.75 | 91.35 \pm 0.21 |

Note: Dates are calculated relative to a previous age determination on TL87-17 (biotite). For these data 47 mg of a 40/60 mesh split of TL88-17 gave an age of 67.06 ($^{40}\text{Ar}/^{39}\text{Ar} = 5.927$; $^{36}\text{Ar}/^{39}\text{Ar} = 0.0017$; Vol $^{39}\text{Ar} = 17.286$; % ^{40}Ar rad = 91.50). J values used for all samples are 7.0150e3. (1) Vol ^{39}Ar is in units of E-08 cm³.

Range in the south-central part of the study area, and rocks along the Marshall Creek fault northeast of Carpenter Lake (Fig. 1).

Dickson pluton

The Dickson pluton is composed of granodiorite to diorite. Two samples from high elevations yield zircon fission track ages within error of one another: one from the southern flank of Dickson Peak (7560'), gave an age of 74.6 \pm 8.8 Ma, and a second sample from the upper reaches of Roxy Creek (5940') gave an age of 78.0 \pm 9.8 Ma (Table 1). A sample from a small arm of the pluton at a low elevation (2820') (Woodsworth, 1977), has a zircon fission track age of 59.8 \pm 7.3 Ma (Table 1). An Ar-Ar total fusion age of 91.35 \pm 0.21 Ma on biotite and a zircon fission track age of 90.7 \pm 13.2 Ma were obtained from a sample collected at the edge of the pluton along Slim Creek (just off the northwest corner of Fig. 1; 4490'; Tables 1, 2).

Eldorado pluton

The main intrusion of the Eldorado pluton is a biotite-hornblende granodiorite but smaller related stocks and a wide alteration zone are present in this area (Garver et al., 1989). A sample from the centre of the pluton gives a $^{40}\text{Ar}/^{39}\text{Ar}$ plateau age on biotite of 67.05 \pm 0.88 Ma (D.A. Archibald, unpub. data). The excellent plateau age, and the presence of zircon, apatite, biotite, and amphibole, make this sample a possible candidate for an age standard.

Bendor pluton

One of several granodioritic plutons in the Bendor Range, the Bendor pluton is a biotite-hornblende granodiorite that is the largest in the suite of Bendor intrusions (Roddick and Hutchison, 1973). Our zircon fission track data from different elevations indicate cooling below the zircon closure temperature at about 55-52 Ma (Table 1). We obtained a younger age (52.0 \pm 6.4 Ma) from a low elevation sample (~6300') and a slightly older age (54.5 \pm 6.7 Ma) from a sample taken from a nearby ridge crest (~8150'). Three Ar-Ar total fusion ages are from these same two samples (Table 2); both samples yield biotite ages within error of each other with an average age of ~63.5 Ma, and a hornblende age of ~64 Ma (Table 2).

Mission Ridge pluton and adjacent rocks

We sampled rocks on both sides of the northwest-trending Marshall Creek fault (MCF) to better constrain the timing of movement (Van Order, 1993). On the southwest side of the fault, in the Carrol Lake area, a zircon fission track age of ~39 Ma was obtained from detrital zircon from the lithic arkosic sandstones that are interbedded with and underlie rhyolitic and dacitic pyroclastic rocks (unit 12 of Roddick and Hutchison, 1973). Because these sandstones contain a significant percentage of felsic volcanic fragments, we suggest that this age represents a maximum age of deposition. In this same stratigraphic section, a zircon fission track age of 43.5 Ma was obtained from the overlying volcanics. As an age of this stratigraphic section, we favour the age of the volcanics (~43.5 Ma) over the age obtained from the detrital zircon because of problems associated with variable etch properties of detrital fission track samples. On the northeast side of the fault, we have obtained a zircon fission track age of 39.5 \pm 7.5 Ma from a granitic clast in metamorphosed conglomerates of the Upper Triassic Hurley Formation (Schiarrizza et al., 1990). Zircons from the Mission Ridge pluton, at the Terzaghi Dam, yield a mean zircon fission track age of 42.9 \pm 7.4 Ma.

DISCUSSION OF AGE DATA

Dickson pluton

The Dickson pluton, at the western edge of the study area and at the eastern edge of the Coast Plutonic Complex, has a U-Pb age of 92.4 \pm 0.3 Ma (Parrish, 1991). The Ar-Ar total fusion age of ~91 Ma on biotite and a zircon fission track age of 90.7 \pm 13.2 Ma are close to the crystallization age of the pluton. These ages indicate rapid cooling, presumably at the border of the pluton, at a relatively high level (<~9 km - the approximate closure depth of fission-tracks in zircon). Zircon fission track ages in the centre of the pluton and from low elevations (JG-5, 6, 8) indicate cooling below the zircon closure temperature at about 78 to 60 Ma. Farther to the northwest, Archibald et al. (1989) reported an Ar-Ar total fusion ages of 82 Ma (hornblende) and 71.8 Ma (biotite) from what has been mapped as the same plutonic body. An Ar-Ar total fusion age of 78 Ma (sericite) was obtained from the alteration zone around the pluton. The Dickson pluton is

presently poorly mapped, and it is not clear if the plutonic body as mapped is composite or if younger plutons are present.

Bendor and Eldorado plutons

Friedman and Armstrong (in press) reported a discordant U-Pb crystallization age of $64 \pm 11/-2$ Ma for the Bendor pluton; the fractions cluster below concordia and the age is difficult to interpret. The actual crystallization age may be similar to the age of the Eldorado pluton (~67 Ma). Our Ar-Ar total fusion ages of ~63.5 (biotite) and ~64 Ma (hornblende) indicate very rapid cooling during this time, suggesting crystallization and cooling at shallow levels. A K-Ar age of ~59.5 Ma (biotite - Wanless et al., 1978) from the centre of the pluton is slightly younger than our Ar-Ar total fusion age on biotite. Both zircon fission track samples, taken from different elevations, give ages that are within analytical error.

Mission Ridge pluton and adjacent rocks

The Mission Ridge pluton, which intrudes metamorphic rocks of the Bridge River Complex ("Bridge River schist"), lies in the footwall to the low-angle Mission Ridge fault and the high-angle Marshall Creek fault. The map relations, kinematics, and timing constraints of these faults have been recently studied by Coleman and Parrish (1991) and Schiarizza et al. (1990). The Mission Ridge fault separates high-level, low-grade rocks of the Bridge River Complex (and overlying sedimentary rocks) in the hanging wall, from the Bridge River schists and intrusives in the footwall; the footwall was exhumed during movement on both faults (Coleman and Parrish, 1991). The Marshall Creek fault cuts the Mission Ridge pluton which has a U-Pb date of 47.4 ± 0.3 Ma (Coleman and Parrish, 1991). An $^{40}\text{Ar}-^{39}\text{Ar}$ age of 46.4 Ma on biotite from a high elevation (~8600') biotite reaction zone, in a footwall position at the southern edge of the Shulaps ultramafic complex (Archibald et al., 1991), indicates cooling that was perhaps related to tectonic denudation caused by movement on the MRF (Coleman and Parrish, 1991). The Marshall Creek fault juxtaposes low-grade rocks of the Bridge River Complex and unconformably overlying Tertiary(?) volcanics and sedimentary rocks on the southwest against Bridge River schists and metamorphosed rocks of the Cadwallader Group on the northeast (Schiarizza et al., 1990). In the Carrol Lake area, the Marshall Creek fault cuts Tertiary volcanic and underlying sedimentary rocks, which rest unconformably on the underlying Bridge River Complex.

Our zircon fission track ages indicate that faulting must have, in part, postdated the deposition of the volcanic and sedimentary rocks at 43.5 Ma. Likewise, the zircon fission track ages of 39.5 Ma and 42.9 Ma on the granite clast and the Mission Ridge pluton respectively, indicate cooling of the footwall rocks at this time. Together, these data indicate movement of and cooling along the Marshall Creek fault between ~43.5 Ma and 39.5 to 43 Ma; this timing constraint is one of our most significant findings. To bring rocks on the

northeast side of the fault towards the surface, dip-slip movement was likely, but the amount of strike-slip movement is uncertain.

DISCUSSION

Our cooling ages young from southwest to northeast across the study area. Our interpretation of all these data, however, is complicated by the fact that our cooling ages are from plutonic rocks that also young from southwest to northeast. For this reason, we are in the difficult position of determining whether these ages reflect either post-intrusion thermal decay or denudation of overlying rocks and subsequent downward movement of low-temperature isotherms.

In the case of the Bendor and Dickson plutons, the zircon fission track ages could represent: 1) post-intrusion cooling by conduction at high levels in the crust (above the closure temperature of zircon); or 2) cooling induced by either erosional or tectonic denudation. We cannot rule out either option 1 or 2 above, but our ongoing studies using fission track and Ar-Ar dating of other mineral phases may shed additional light on this problem. However, the presence of a vertical thermal gradient, as suggested by younger ages at lower elevations in the Dickson and Bendor plutons, suggests cooling proceeded downward when zircon passed through its closure temperature. This pattern of cooling suggests, but is not diagnostic of, cooling by either erosional or tectonic denudation.

The Castle Pass fault, which is interpreted to be a strike-slip fault, is intruded by the 67 Ma Eldorado pluton, which is just north of the limit of our study area in Figure 1 (Garver et al., 1989; Schiarizza et al., 1989; Garver, 1991), but cuts rocks as young as 94 Ma (Silverquick conglomerate - see Garver and Brandon, in press). Strike-slip faulting, therefore, affected the rocks in the western part of the map area sometime between 94-67 Ma. Two of the four zircon fission track ages from the Dickson pluton (78-75 Ma) fall within this permissible age range of strike-slip faulting. Amphibole from a hornblende porphyry dyke near the Yalakom fault system, gives an age of ~76 Ma ($^{40}\text{Ar}/^{39}\text{Ar}$; Archibald et al., 1990). Likewise, low-temperature cooling ages near the Dickson pluton in the Warner Pass area (Archibald et al., 1989) give ages between 78 and 72 Ma. Therefore, the zircon fission track and Ar-Ar data suggest a period of cooling and dyke emplacement during the interval between ~78-72 Ma. These cooling ages could be linked to either the initiation of dextral transpression, and cooling that may have been driven by uplift and denudation, or post-orogenic uplift and denudation following the regionally significant mid-Cretaceous contractional episode, or both. The oldest zircon fission track age (~91 Ma) is from rocks at the edge of the pluton and presumably represents rapid cooling at the edge of the pluton, or possibly cooling of a separate unrecognized plutonic body. The youngest zircon fission track age (~60 Ma) is from a very low elevation and therefore may have been deeper than the other samples during cooling; this young age may be related to a separate cooling event that is preserved in the Bendor Range (see below).

Umhoefer and Schiarizza (1992) argued that the Late Cretaceous to early Tertiary strike-slip faults in the Bridge River area evolved as a transfer zone between movement on the northwest-trending Yalakom fault system and related faults in Washington state. They suggested that the region experienced a change from transpression to transtension at about 58 Ma, coincident with a change to rapid and oblique convergence of the Kula plate and the North American plate; they note, for example, that northwest along the Yalakom fault system, ~58 Ma cooling and extension occurred in the Tatla Lake metamorphic complex (Friedman and Armstrong, 1988). It is possible that both the K-Ar age of ~59.5 Ma and the zircon fission track ages of ~55-52 Ma from the Bendor Range, and the zircon fission track ages of ~60 Ma from the Dickson pluton record cooling associated with uplift and erosion that may have been controlled by vertical movements of crustal blocks separated by dextral strike-slip faults.

From data collected in the Bridge River Canyon area, Coleman and Parrish (1991) suggest that about 100 km of dextral movement on the Fraser fault (nearby to the east) occurred after 46.5 Ma, but before intrusion of a 34 Ma phase of the Chilliwack batholith (see Tepper, 1991). Umhoefer and Schiarizza (1992) postulated that at ~47 Ma, the Straight Creek fault in Washington state, was the active southern continuation of the Yalakom fault system. As faulting progressed, ~110 km of dextral offset on the Straight Creek fault was transferred to ~20 km on the Marshall Creek fault-Yalakom fault system and ~90 km on the Fraser fault. Our data from rocks along the Marshall Creek fault and below the Mission Ridge fault indicate that rapid cooling occurred between 43 and 39 Ma. We suggest, as have others, that the latest movement on the Marshall Creek was kinematically linked to movement on the Fraser fault to the east (Coleman and Parrish, 1991; Umhoefer and Schiarizza, 1992), and that our low-temperature cooling ages from rocks adjacent to the Marshall Creek fault date an episode of dip-slip movement (northeast side up) driven by dextral slip on the Fraser fault. Therefore, our data suggest that an episode of movement on the Marshall Creek fault, and probably the Fraser fault, occurred between 43.5-39 Ma. Our ongoing studies using fission-track dating of apatite and ^{40}Ar - ^{39}Ar analyses of biotite and K-spar will allow us to better resolve the spatial and temporal aspects of low-temperature cooling in this area.

ACKNOWLEDGMENTS

We gratefully acknowledge financial support for this project by a EMR grant #322 from the GSC to DAA and JIG. The geochron lab at Queens University is supported by an NSERC operating grant to E. Farrar. This project was also financially supported by the Union College Faculty Research Fund (JIG), and the Union College Internal Education Fund (WFV). We thank Peter van der Heyden for a thorough manuscript review.

REFERENCES

- Archibald, D.A., Glover, J.K., and Schiarizza, P.**
1989: Preliminary report on $^{40}\text{Ar}/^{39}\text{Ar}$ geochronology of the Warner Pass (92O/3) and Noaxe Creek (92O/2) map areas; in Geological Fieldwork 1988; British Columbia Ministry of Energy, Mines, and Petroleum Resources, Paper 1989-1, p. 145-151.
- Archibald, D.A., Schiarizza, P., and Garver, J.I.**
1990: $^{40}\text{Ar}/^{39}\text{Ar}$ dating and the timing of deformation and metamorphism in the Bridge River terrane, southwestern British Columbia (92O/02; 92J/15); in Geological Fieldwork 1989; British Columbia Ministry of Energy, Mines, and Petroleum Resources, Paper 1990-1, p. 45-51.
1991: $^{40}\text{Ar}/^{39}\text{Ar}$ evidence for the age of igneous and metamorphic events in the Bridge River and Shulaps complexes, southwestern British Columbia; in Geological Fieldwork 1990; British Columbia Ministry of Energy, Mines, and Petroleum Resources, Paper 1991-1, p. 75-83.
- Brandon, M.T. and Vance, J.A.**
1992: New statistical methods for analysis of fission-track grain-age distributions with applications to detrital zircon ages from the Olympic subduction complex, western Washington state; *American Journal of Science*, v. 292, p. 565-636.
- Coleman, M. and Parrish, R.R.**
1991: Eocene dextral strike-slip and extensional faulting in the Bridge River terrane, southwest British Columbia; *Tectonics*, v. 10, no. 6, p. 1222-1238.
- Cordey, F. and Schiarizza, P.**
1993: Long-lived Panthalassic remnant: the Bridge River accretionary complex, Canadian Cordillera; *Geology*, v. 21, p. 263-266.
- Dalrymple, G.B., Alexander, E.C., Jr., Lanphere, M.A., and Kraker, G.P.**
1981: Irradiation of samples for $^{40}\text{Ar}/^{39}\text{Ar}$ dating using the Geological Survey TRIGA Reactor; United States Geological Survey, Professional Paper 1176, 55 p.
- Friedman, R.M. and Armstrong, R.L.**
1988: Tatla Lake metamorphic complex: an Eocene metamorphic core complex on the southwest edge of the Intermontane Belt of British Columbia; *Tectonics*, v. 7, p. 1141-1166.
in press: Jurassic and Cretaceous geochronology of the southern Coast Belt, B.C., 49-51°N; in *Jurassic Magmatism in the Cordillera*, (ed.) D. Miller; Geological Society of America Memoir.
- Garver, J.I.**
1991: Kinematic analysis and timing of structures in the Bridge River Complex and overlying Cretaceous sedimentary rocks, Cinnabar Creek area, southwestern British Columbia (92J/15); in Geological Fieldwork 1990; British Columbia Ministry of Energy, Mines, and Petroleum Resources, Paper 1991-1, p. 65-74.
- Garver, J.I. and Brandon, M.T.**
in press: Fission-track ages of detrital zircons from Cretaceous strata, southern British Columbia: implications for the Baja BC hypothesis; *Tectonics*.
- Garver, J.I., Schiarizza, P., and Gaba, R.G.**
1989: Stratigraphy and structure of the Eldorado Mountain area, Cariboo-Chilcotin mountains, southern B.C. (92O/02, 92J/15); in Geological Fieldwork 1988; British Columbia Ministry of Energy, Mines, and Petroleum Resources, Paper 1989-1, p. 131-143.
- Journey, J.M. and Friedman, R.M.**
1993: The Coast Belt thrust system: evidence of Late Cretaceous shortening in southwest British Columbia; *Tectonics*, v. 12, no. 3, p. 756-775.
- Monger, J.W.H. and Journey, J.M.**
1992: Guide to the geology and the tectonic evolution of the southern Coast Belt: a field guide to accompany the Penrose Conference on "Tectonic evolution of the Coast Mountains orogen", Bowen Island, B.C.; Geological Survey of Canada, Vancouver, B.C., 97 p.
- Naeser, C.W.**
1976: Fission-track dating; United States Geological Survey, Open-file Report 76-190, 65 p.

Parrish, R.R.

1983: Cenozoic thermal evolution and tectonics of the Coast Mountains of British Columbia 1: Fission-track dating, apparent uplift rates and patterns of uplift; *Tectonics*, v. 2, p. 601-631.

1991: U-Pb ages for Cretaceous plutons in the Coast belt of southern BC; in *Radiogenic Age and Isotopic Studies; Report 5; Geological Survey of Canada, Paper 91-2*, p. 109-113.

Roddick, J.A. and Hutchison, W.W.

1973: Pemberton (east half) map area, British Columbia; *Geological Survey of Canada, Paper 73-17*, 21 p.

Schiarizza, P., Gaba, R.G., Glover, J.K., and Garver, J.I.

1989: Geology of the Tyaughton Creek area (92O/02, 03, 92J/15, 16); in *Geological Fieldwork 1988; British Columbia Ministry of Energy, Mines, and Petroleum Resources, Paper 1989-1*, p. 115-130.

Schiarizza, P., Gaba, R.J., Coleman, M., Garver, J.I., and Glover, J.K.

1990: Geology and mineral occurrences of the Yalakom River area (92O/1,2, 92J/15,16); in *Geological Fieldwork 1989; British Columbia Ministry of Energy, Mines, and Petroleum Resources, Paper 1990-1*, p. 53-72.

Steiger, R.H. and Jäger, E.

1977: Subcommittee on geochronology: Convention on the use of decay constants in Geo- and Cosmo-chronology; *Earth and Planetary Science Letters*, v. 36, p. 359-362.

Tepper, J.H.

1991: Petrology of mafic plutons and their role in granitoid genesis, Chilliwack batholith, North Cascades, Washington; Ph.D. thesis, University of Washington, Seattle, 307 p.

Umhoefer, P.J. and Schiarizza, P.

1992: Timing and offset on strike-slip faults in the SE Coast Belt, B.C., and WA, and 40-80 Ma fault reconstructions; *Geological Society of America, Abstracts with Programs*, v. 25, p. 156.

Van Order, W.F., Jr.

1993: Fission-track evidence for Late Eocene uplift of the Shulaps Range due to movement on the Marshall Creek fault, British Columbia, Canada; B.Sc. thesis, Union College, Schenectady, New York, 39 p.

Wagner, G. and van den Haute, P.

1992: Fission track dating; Kluwer Academic Press, Solid Earth Sciences Library, Volume 6, Dordrecht, The Netherlands, 285 p.

Wanless, R.K., Stevens, R.D., Lachance, G.R., and Delabio, R.N.

1978: Age determinations and geological studies, K-Ar isotopic ages, Report 13; *Geological Survey of Canada, Paper 77-2*, 60 p.

Woodworth, G.J.

1977: Pemberton (92J) map area, British Columbia; *Geological Survey of Canada, Open File 482*.

Energy, Mines and Resources grant 322

The Ice River Complex, British Columbia

T.D. Peterson and K.L. Currie

Continental Geoscience Division

Peterson, T.D. and Currie, K.L., 1994: The Ice River Complex, British Columbia; in Current Research 1994-A; Geological Survey of Canada, p. 185-192.

Abstract: The Devonian (~360 Ma) Ice River Complex, a large, well-exposed ijolite-carbonatite-syenite intrusion in southeastern British Columbia, consists of a feldspar-poor series (ijolite-carbonatite) and a slightly younger feldspar-rich series (melanocratic to leucocratic nepheline syenite). Melanocratic rocks of the feldspar-poor series contain perovskite, while those with higher silica activity (feldspar-rich series) do not. The feldspar-poor series at Aquila Ridge forms a swarm of northwest-trending dykes with many screens of fenitized limestone. Some of these dykes contain macrocrysts (≤ 6 cm) of olivine, clinopyroxene zoned from chrome diopside cores to titanite rims, and phlogopite, consistent with an alkaline ultramafic parental magma. The excellent exposure, favourable mineralogy, and unusual tectonic setting (passive margin) make the Ice River Complex a prime site for research on the generation, differentiation, and emplacement of alkaline mafic intrusions.

Résumé : Le complexe d'Ice River du Dévonien (360 Ma), vaste intrusion bien exposée d'ijolite-carbonatite-syérite dans le sud-est de la Colombie-Britannique, est composé d'une série pauvre en feldspath (ijolite-carbonatite) et d'une série riche en feldspath (syérite à néphéline mélanocrate à leucocrate), légèrement plus récente. Les roches mélanocrates de la série pauvre en feldspath contiennent de la pérovskite, tandis que celles qui présentent une plus forte teneur en silice (série riche en feldspath) n'en contiennent pas. La série pauvre en feldspath, à la crête Aquila, forme un essaim de dykes de direction nord-ouest au contact desquels s'observent de nombreux écrans de calcaire fénitisé. Certains dykes contiennent des phénocristaux (6 cm) d'olivine, de clinopyroxène zoné (noyau de diopside chromifère passant à une bordure de titano-augite) et de phlogopite, ce qui est compatible avec un magma parental de composition ultramafique alcaline. La qualité de ses affleurements, sa minéralogie favorable et son cadre tectonique inhabituel (marge passive) font du complexe d'Ice River un site de première importance pour la recherche sur la formation, la différenciation et la mise en place d'intrusions mafiques alcalines.

INTRODUCTION

The Ice River alkaline complex forms a U-shaped mass of ijolite, carbonatite, and syenite underlying about 30 km² of the main ranges of the Rocky Mountains south of Field, British Columbia (Fig. 1). Because of the variety of lithologies and superb exposure across parts of three ranges, the complex offers a unique opportunity to study the petrogeny and emplacement of alkaline rocks. However difficult access, complicated by its location in Yoho National Park, and heavy precipitation have hindered detailed study of the complex, although the disposition of the main phases has been accurately known since the classic mapping by Allan (1914). Allan's work was revised and updated by Currie (1975) after Rapson (1963) demonstrated the presence of an igneous carbonatite body (as opposed to the limestone inclusion mapped by Allan) within the ijolite. The complex, emplaced mainly into Ordovician limestone (Ottertail Formation) in Devonian time (368 ± 4 Ma, Parrish et al., 1987; 357 Ma by U-Pb (perovskite), L. Heaman, pers. comm., 1991), underwent Laramide deformation, but most portions of it appear pristine, although the work of Parrish et al. (1987) shows that chemical and isotopic disturbance is widespread. The

evolution and emplacement of the complex are not well understood. Currie (1975) concluded that the complex was emplaced mainly as a sill-like mass with subordinate dykes and plugs, and that diverse compositions were derived from a single parental magma by various combinations of fractional crystallization, and silicate/carbonate and silicate/silicate liquid immiscibility.

Further work by Peterson (1983) substantiated Currie's petrological subdivisions, but raised questions regarding the emplacement mechanisms and the role of liquid immiscibility. This paper summarizes the results from 3 days of study by the authors at the north end of Aquila Ridge (Fig. 2) and attempts to identify outstanding problems which must be addressed in future studies of this complex.

This study led to the following conclusions:

1. the ijolite and nepheline syenite arose from separate magma batches; the nepheline syenite magma may have been contaminated by silica-rich Archean basement or upper Proterozoic sedimentary rocks;
2. the carbonatite body is a dyke swarm which dramatically expands within the Aquila Ridge ijolites;

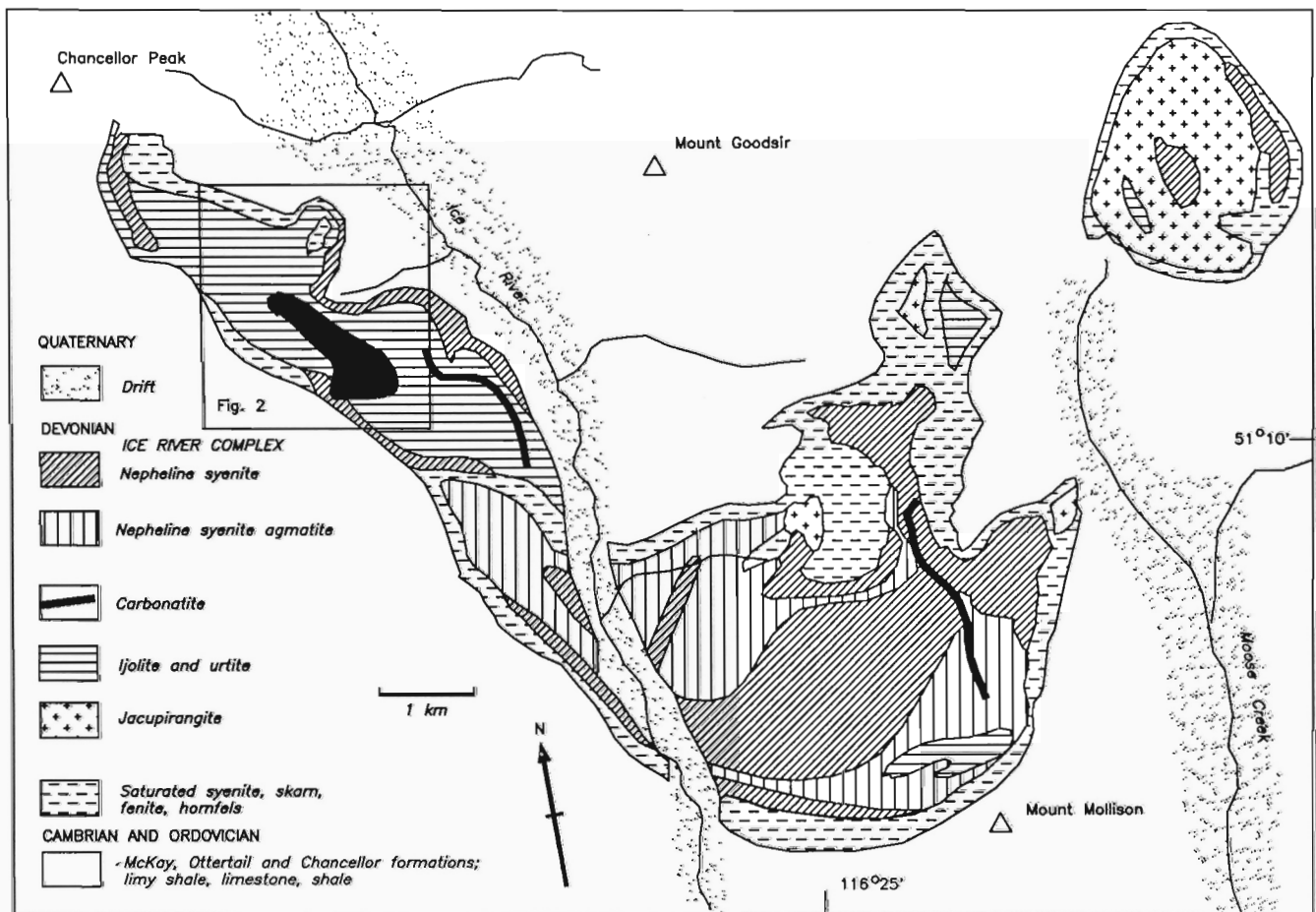


Figure 1. Location and simplified geology of the Ice River Complex. The area of Figure 2 is shown by the heavy lines.

3. the Aquila Ridge ijolite body consists mainly of dykes and contains a large volume of strongly metasomatized and partially melted screens of country rock (the "zeolite syenites" of Currie, 1975); and
4. Dyke rocks rich in macrocrysts of olivine, augite, and phlogopite indicate that nephelinite magma was parental to the ijolite.

The carbonatite body of Garnet Cirque

The carbonatite, a relatively homogeneous body, weathering dark reddish-brown to black due to its high Fe content (see Currie 1975 for analyses), is exposed on the south wall of Garnet Cirque. From the opposite wall of the cirque, the cross-section forms a triangular mass of dark rocks with crude internal layering or zonation (Fig. 3) narrowing from 750 m across the top, to less than 150 m at its partly covered base. Numerous carbonatite dykes exposed on the floor and north wall of the cirque trend south-southeast toward this body, suggesting that it is either a source of the dykes, or formed by coalescence of dykes.

The carbonatite body contains numerous leucocratic, anastomosing veins ≤ 30 cm thick consisting mainly of natrolite ($\text{Na}_2\text{Si}_3\text{Al}_2\text{O}_{10} \cdot 2\text{H}_2\text{O}$), occasionally with melanocratic margins of Fe-serpentine (berthierine). Euhedral, twinned phenocrysts of tetranatrolite (a high-temperature tetragonal polymorph of natrolite) plus magnetite and berthierine were identified in other carbonatite dykes of this complex by Peterson (1983) who suggested the natrolite veins could form by liquid immiscibility between hydrous silicate and carbonatite melts, with natrolite forming a liquidus phase common to both melts.

The Ice River carbonatite is substantially richer in Fe (present as ankerite, siderite, and Fe-oxides and silicates) than most other carbonatites (which are usually dominated by calcite or dolomite). Iron-rich carbonatites must, in general, have a protracted differentiation history, since liquids of this composition cannot arise from the mantle or by liquid immiscibility from reasonable magma compositions (Kjarsgaard and Peterson, 1991).

Ijolite body of Aquila Ridge

Currie (1975) mapped the ijolite body of Aquila Ridge as a layered sill, with melanocratic rocks concentrated near the bottom (northeast edge). The north wall of Garnet Cirque is laced with ijolitic dykes which parallel both carbonatite dykes and the trend of Aquila Ridge, suggesting that the northwest-southeast elongation of the ijolite body may reflect emplacement of a large number of diverse subparallel dykes. Diverse dykes and incorporation of numerous screens of country rock could produce the observed extreme local variation in rock types. Layering of any type is difficult to discern in mountainside exposures of the ijolites, but some internal divisions within the Aquila Ridge ijolite body can be recognized. Wollastonite-bearing ijolites are concentrated in the topographically highest portions of the body, as noted by Currie (1975), while the most primitive and silica-undersaturated rocks, typically perovskite-rich pyroxenite cumulates, are concentrated along the northeastern edge of the body (corresponding to the "floor" in a sill model). If the ijolite body is a dyke complex, either similar (gravitational?) differentiation has taken place within many dykes, or some unknown mechanism has segregated dykes to produce the observed disposition.

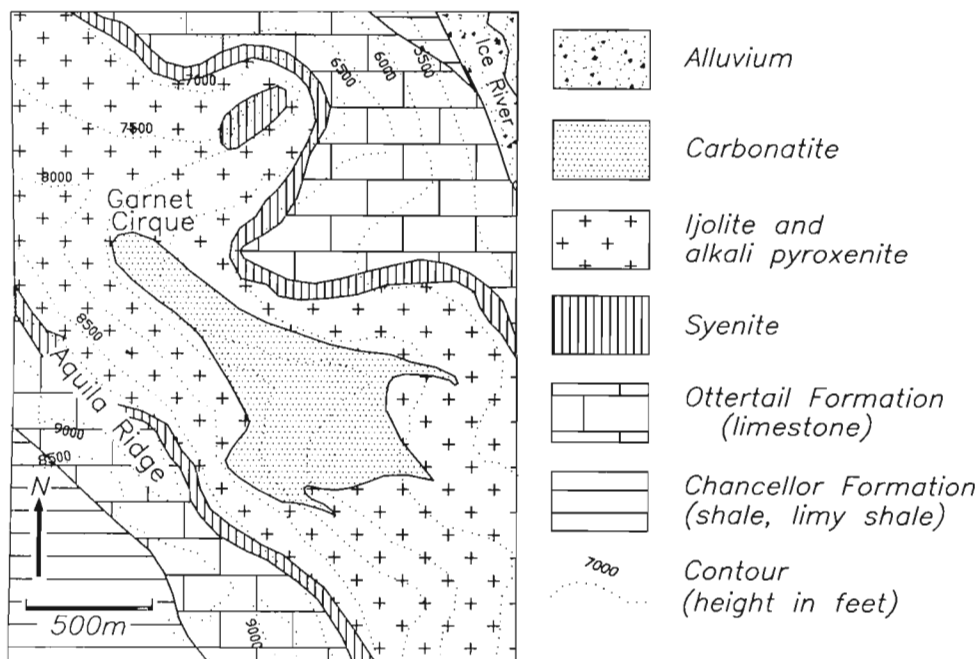


Figure 2. Geological sketch of Garnet Cirque. Aquila Ridge is the southeast-trending mountain spine overlooking the cirque (after Currie, 1975).



Figure 3. The carbonatite body (dark grey) at Garnet Cirque viewed from the north. Note how the body narrows at the base where a feeder system is presumed to exist. Crude layering parallel to the contacts can be distinguished, a common feature in carbonatite intrusions probably resulting from subsolidus deformation of soft carbonate rock. The edges of the carbonatite along the ridge crest are marked by (added) heavy black lines.

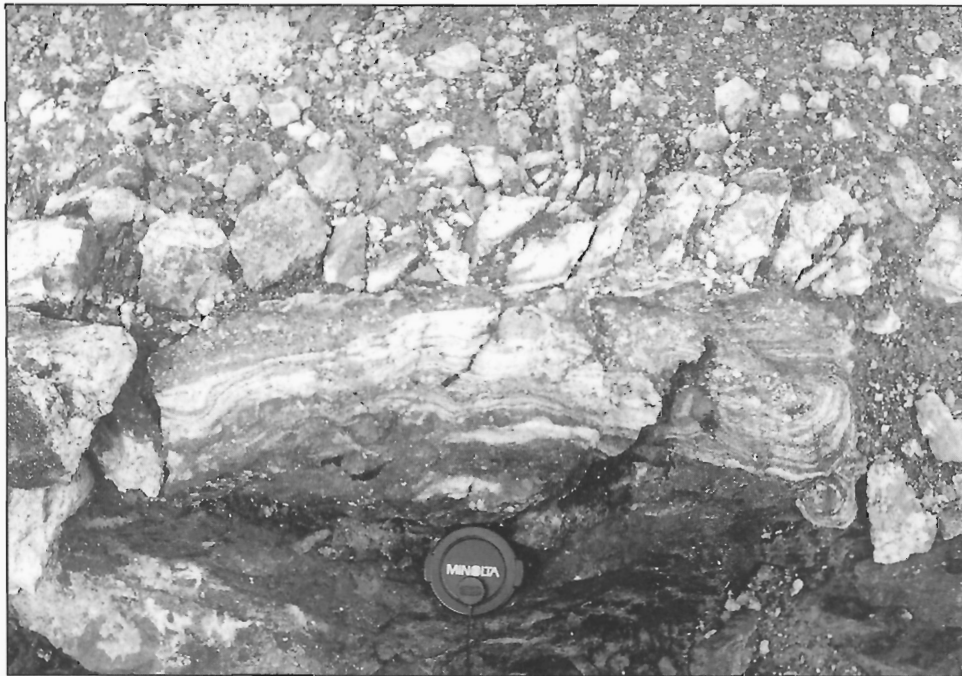


Figure 4. Typical layered fenite from the ridge north of Garnet Cirque. Note the contorted layering (relict bedding?), possibly indicative of some partial melting.

Fenitization

Carbonatites normally intrude SiO₂-rich country rocks. Metasomatism accompanying such emplacement (fenitization) has been described by numerous authors. In many cases fenitization may be so extreme that primary igneous rocks cannot be distinguished from the fenites, except by isotopic studies. The Ice River Complex presents an unusual example of the emplacement of carbonatite into silica-poor dolomitic limestones.

Fenitization of country rocks adjacent to the intrusion was minimal, possibly because the limestone was relatively plastic and tended to confine the metasomatising fluids within, or close to, the pluton. We recognize three types of fenitization in Garnet Cirque. The most common type of fenitization involves alteration of thin limestone screens within the ijolite to zeolites+aegirine. These screens, less than 1 m thick, commonly exhibit strongly contorted, centimetre-scale layering possibly reflecting bedding in the protolith (Fig. 4). Zeolite-rich portions of the fenite screens weather to distinctive white to pink or red. Large bodies (up to 1 km long) of zeolite-rich "syenite" in the ijolite (Currie, 1975) may represent bodies of coalesced, melted fenites. The limestone fenites commonly have 1-2 cm thick glimmerite (phlogopite-rich) rims produced by reaction with the alkaline magmas.

A second type of metasomatic effect can be observed along the top of the ridge forming the north wall of Garnet Cirque, an area intruded by numerous carbonatite dykes (Fig. 5). Pegmatitic dykes of ijolite and urtite (leucocratic ijolite) contain large (≤ 20 cm) "sprays" of acicular ferrobustamite (iron-rich wollastonite, Currie, 1975) in an altered, grey-green nepheline+pyroxene matrix. These rocks were interpreted by Currie (1975) as a late igneous differentiation product, genetically related to the carbonatite. However wollastonite is extremely rare as a phenocryst phase in magmas of similar composition (Peterson, 1989), and von Eckermann (1948) interpreted wollastonite-bearing rocks at the classic Alnö intrusion of Sweden as an important product of metasomatic alteration. We therefore consider a secondary origin for the wollastonite ijolites to be possible, with growth of ferrobustamite blades induced by introduction of Ca from the carbonatites. If this is the correct explanation, metasomatism must have taken place above the inversion temperature from the wollastonite to ferrobustamite structure. As with many other phenomena around alkaline complexes, sharp distinction of igneous and metasomatic processes may be difficult and unrealistic.

A third possible type of fenitization is displayed at the top of the north wall of Garnet Cirque. A cap of pegmatitic syenite composed of alkali feldspar+minor pyroxene overlies an ijolite-carbonatite dyke swarm, forming part of the "contact syenite" of Currie (1975). This contact syenite, spatially, texturally, and mineralogically distinct from the nepheline syenites, is the only critically silica-saturated rock of the complex, and displays a crude, metre-scale fissility (Fig. 6) which parallels bedding in the country rocks nearest to the syenite cap. We tentatively interpret this body to be the

product of isochoric replacement of country rock, although why the resulting rock is so different from the banded fenites is unclear.

Dyke rocks

Lamprophyre dykes, with phenocrysts of phlogopite plus minor olivine and clinopyroxene, were described by Currie (1975) and interpreted as representative of the primary magma of the complex. We discovered three new dyke lithologies which contain primitive phenocryst phases. Dykes exposed at about 7000 feet altitude on the north wall of the cirque (Fig. 7; sample IRD-1) contain olivine macrocrysts (≤ 2 cm) normally zoned from Fo₇₂ to Fo₆₈ (Table 1), as well as phenocrysts of aluminous titanite, magnetite, and apatite, in a matrix of poikilitic kaersutite and phlogopite (Table 2). Boulders of dykes found on the floor of the cirque



Figure 5. The ridge north of Garnet Cirque looking northeast. A fenite screen (white) is located near the hammer. The arrows point to three carbonatite dykes cutting the ridge at a high angle. The double arrow indicates the thickness of the contact syenite cap over the ijolites. Note the layering in the syenite dipping to the right at about 45°. Near the contact with the ijolites the syenite contains many dikes of ijolite and carbonatite.

Table 1. Olivine and clinopyroxene compositions in dyke rocks.

| sample | IRD-1 | IRD-1 | IRD-2 | IRD-3 | IRD-3 | IRD-4 ¹ | IRD-4 ¹ |
|--------------------------------|-------|-------|--------|-------|-------|--------------------|--------------------|
| mineral | ol | ol | cpx | cpx | cpx | cpx | cpx |
| location | core | rim | pcryst | core | rim | core | rim |
| SiO ₂ | 37.57 | 37.02 | 50.42 | 46.93 | 45.70 | 51.28 | 48.85 |
| TiO ₂ | 0.04 | 0.03 | 4.16 | 1.22 | 2.71 | 0.50 | 1.61 |
| Al ₂ O ₃ | 0.00 | 18.41 | 3.65 | 3.12 | 7.55 | 4.23 | 5.95 |
| Cr ₂ O ₃ | 0.00 | 0.00 | 0.04 | 0.00 | 0.04 | 1.59 | 0.40 |
| FeO | 25.38 | 28.10 | 6.16 | 20.26 | 6.47 | 3.76 | 4.40 |
| MnO | 0.57 | 0.83 | 0.16 | 0.77 | 0.15 | 0.10 | 0.10 |
| MgO | 35.17 | 33.09 | 13.25 | 4.23 | 12.13 | 16.92 | 14.57 |
| CaO | 0.32 | 0.45 | 23.37 | 21.24 | 22.70 | 18.34 | 21.57 |
| Na ₂ O | 0.00 | 0.00 | 0.58 | 1.06 | 0.46 | 0.92 | 0.53 |
| ¹ macrocryst | | | | | | | |

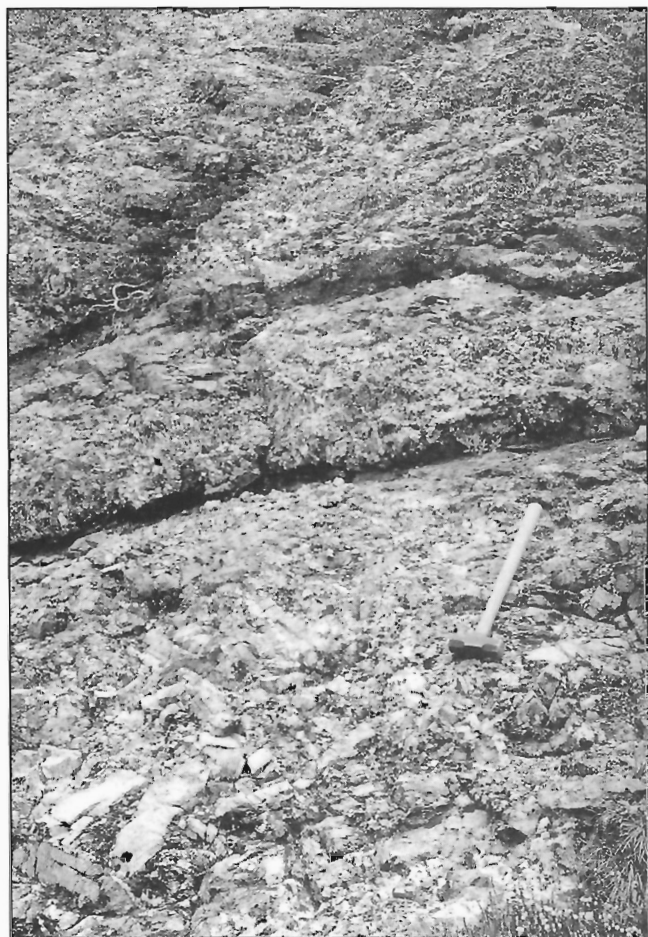


Figure 6. Closeup of the contact syenite. Note the large size of some individual feldspar crystals, and the crude metre-scale layering that is interpreted as bedding in limestone (not carbonatite) that was metasomatised by underlying igneous rocks.



Figure 7. Lamprophyre (nephelinitic) dyke, north wall of Garnet Cirque. The dyke is oriented parallel to the long axis of the Aquila Ridge ijolite body, as were nearly all others encountered in this area.

Table 2. Amphiboles in dyke rocks.

| | IRD-1 secondary | IRD-1 primary | IRD-4 secondary |
|--------------------------------|--------------------|------------------|--------------------|
| SiO ₂ | 39.17 | 41.08 | 53.95 |
| TiO ₂ | 0.17 | 3.34 | 0.73 |
| Al ₂ O ₃ | 12.77 | 11.84 | 1.31 |
| Cr ₂ O ₃ | 0.06 | 0.08 | 0.12 |
| FeO | 21.56 | 20.55 | 12.73 |
| MnO | 0.27 | 0.18 | 0.14 |
| MgO | 7.26 | 13.10 | 15.37 |
| CaO | 9.54 | 11.48 | 2.40 |
| Na ₂ O | 4.12 | 2.59 | 7.30 |
| K ₂ O | 0.63 | 1.41 | 0.85 |

contains phenocrysts of augite normally zoned to titanite, plus an abundance of xenocrysts and xenoliths derived from the country rock and intrusive complex (Table 1, sample IRD-3). Sample IRD-4 contains macrocrysts of clinopyroxene (≤ 6 cm) with cores of chrome diopside (Table 1) and rims of aluminous, moderately Ti-rich augite, in a matrix of phlogopite, clinopyroxene, magnetite, and apatite. Secondary amphiboles replacing primary kaersutite have much higher Na/K and Fe/Mg. Secondary sodic amphibole replacing a limestone xenolith in IRD-4 has high Mg/Fe, probably reflecting the presence of dolomite in the limestone (Table 2).

The olivine and pyroxene macrocrysts are readily interpreted as phenocrysts or xenocrysts derived from the upper mantle. The chrome diopside macrocrysts are probably high-pressure megacrysts. The assemblage restricts possible compositions of primary melts (which can not be satisfactorily determined by chemical analysis of our samples) to those in which olivine+augite is a near-liquidus assemblage, and phlogopite+kaersutite appears at lower temperatures (and pressures?). Such assemblages are typical of volatile-rich (H, F, CO₂) alkaline magmas with broadly olivine nephelinitic compositions. Such compositions commonly crystallize to ultramafic lamprophyres, but the presence of lamprophyric texture is an artifact of crystallization conditions which were only rarely realized in the Ice River Complex. The widespread presence of perovskite in the ultramafic dykes suggests that magma compositions were too poor in silica to crystallize feldspar, even at appropriate pressures, and the presence of a differentiation series (ijolite-urtite) poor in feldspar suggests that differentiation did not increase silica activity sufficiently to stabilize significant amounts of feldspar. The feldspar-rich parts of the complex must have formed from a magma of higher silica activity, either a magma from a different source or a magma contaminated by addition of a siliceous component.

TECTONIC SETTING

According to conventional wisdom, carbonatite-bearing intrusions are usually emplaced within active intracontinental fault zones, many of which are embryonic rifts. However, the Ice River Complex was emplaced at the edge of a continental

shelf where sedimentary facies changed from shallow-water carbonates to deeper-water shales (Aitken, 1971). Several other carbonatite bodies of similar age are found north of Ice River in a similar setting, notably the Aley dolomite carbonatite (Mader, 1987; Pell and Höy, 1989). The standard model of passive upwelling beneath an extensional zone to produce CO₂-rich alkaline magma can be applied to these carbonatite bodies, if their emplacement resulted from limited extension coinciding with the Devonian initiation of strike-slip motion between North America and the Pacific basin (Eisbacher, 1983). Assuming little or no rotation of the complex during Tertiary folding and thrusting, the northwest-southeast orientation of the Aquila Ridge dyke suite should approximate the direction of first slippage along a major fault zone to the west. Since that time numerous allochthonous terranes have docked with western North America, isolating the carbonatite intrusions from the continental margin.

DISCUSSION

Our interpretation of the Ice River Complex emphasizes the possible role of metasomatism in producing a wide spectrum of rock types, some of which can only be distinguished with difficulty from genuine igneous rocks. The interpretation is readily testable by additional mapping, and by stable and radiogenic isotope studies of critical rock types. The Ice River Complex exhibits little fenitization relative to most other intrusions of this type (many of which have been interpreted as comprised almost entirely of remelted fenites). This minimal igneous-country rock interaction may account for the apparently exceptionally pristine nature of the Ice River Complex.

The relationships between syenites and ijolites in alkaline intrusions (and phonolites and nephelinites in corresponding volcanic suites) are complex, and cannot be reduced to any single set of processes (Bell and Peterson, 1991). Melanocratic syenites of the Ice River Complex contain their own distinctive suite of high-Ti and hydrous mafic minerals (titanite and kaersutite, versus perovskite and phlogopite in the ijolites). We consider it probable that the syenites crystallized from a magma with higher silica activity than the magma parental to the ijolite suite, possibly a magma of generally alkali basaltic composition. This interpretation would be confirmed if the nepheline syenites are isotopically distinguishable from the ijolites and carbonatites. The magma parental to the nepheline syenites could have arisen either as a completely separate entity from the magma parental to the ijolite series, or as a cognate magma which assimilated siliceous material, either from continental basement below the complex, or possibly from siliceous sedimentary host rocks.

Our observations on the prevalence of dykes in the western parts of the Ice River Complex suggest that the rest of the complex needs to be re-examined in order to define more closely the form and mechanism of emplacement of the pluton. It can no longer be assumed that the complex represents a single pluton of simple shape. Because of the superb three-dimensional exposure of the Ice River Complex, it may

be possible to determine the form and sequence of intrusive phases with sufficient accuracy to serve as a model for other alkaline complexes.

The megacryst suite in the dyke rocks will provide information on the state of the upper mantle beneath the continental margin in the mid-Paleozoic. Contrasts in isotopic composition between macrocrysts and later phenocryst phases should provide a measure of crust-magma interaction, a notoriously difficult parameter to estimate in alkaline intrusions.

ACKNOWLEDGMENTS

The authors thank the Rangers of Yoho National Park for their co-operation, and the pilots of Canadian Helicopters for flying under difficult conditions. The manuscript has been much improved by the comments of critical reader B.A. Kjarsgaard.

REFERENCES

- Aitken, J.D.**
1971: Control of lower Paleozoic sedimentary facies by the Kicking Horse Rim, southern Rocky Mountains, Canada; *Bulletin of the Canadian Society of Petroleum Geologists*, v. 19, p. 557-569.
- Allen, J.A.**
1914: Geology of the Field map-area, British Columbia and Alberta; Geological Survey of Canada, Memoir 55.
- Bell, K. and Peterson, T.D.**
1991: Nd and Sr isotope systematics of Shombole volcano, East Africa, and the links between nephelinites, phonolites, and carbonatites; *Geology*, v. 19, p. 582-585.
- Currie, K.L.**
1975: The geology and petrology of the Ice River alkaline complex, British Columbia; Geological Survey of Canada, Bulletin 245, 68 p.
- Eisbacher, G.H.**
1983: Devonian-Mississippian sinistral transcurrent faulting along the cratonic margin of western North America: a hypothesis; *Geology*, v. 11, p. 7-10.
- Kjarsgaard, B.A. and Peterson, T.D.**
1991: Nephelinite-carbonatite liquid immiscibility at Shombole volcano, East Africa: petrographic and experimental evidence; *Mineralogy and Petrology*, v. 43, p. 293-314.
- Mader, U.K.**
1987: The Aley carbonatite complex, northern Rocky Mountains, British Columbia; British Columbia Ministry of Energy, Mines and Petroleum Resources 1986, Paper 1987-1, p. 283-288.
- Parrish, R.R., Heinrich, S., and Archibald, D.**
1987: Age of the Ice River complex, southeastern British Columbia; Geological Survey of Canada, Paper 87-2, p. 33-37.
- Pell, J. and Höy, T.**
1989: Carbonatites in a continental margin environment - the Canadian Cordillera; in *Carbonatites: Genesis and Evolution*, (ed.) K. Bell; Unwin Hyman, London, p. 200-220.
- Peterson, T.D.**
1983: A study of the mineralogy and petrology of the Ice River alkaline complex, Yoho National Park; B.Sc. thesis, University of Calgary, Calgary, Alberta.
1989: Peralkaline nephelinites II. Low pressure fractionation and the hypersodic lavas of Oldoinyo Lengai; *Contributions to Mineralogy and Petrology*, v. 102, p. 336-346.
- Rapson, J.E.**
1963: Age and aspects of metamorphism connected with the Ice River Complex, British Columbia; *Bulletin of the Canadian Society of Petroleum Geologists*, v. 11, p. 116-124.
- von Eckermann, H.**
1948: The alkaline district of Alnö Island; *Sveriges Geologiska Undersökning*, no. 36.

Geological Survey of Canada Project 680071

A gravitational origin for the Hell Creek 'fault', British Columbia

John J. Clague and Stephen G. Evans¹
Terrain Sciences Division, Vancouver

Clague, J.J. and Evans, S.G., 1994: A gravitational origin for the Hell Creek 'fault', British Columbia; in Current Research 1994-A; Geological Survey of Canada, p. 193-200.

Abstract: The Hell Creek 'fault', located northwest of Lillooet, British Columbia, has been thought to be a neotectonic feature. However, its close association with antisllope scarps and deep-seated landslides in highly deformed and foliated rocks of the Bridge River complex argues for a gravitational, rather than tectonic, origin. The segmented antisllope scarp that constitutes the Hell Creek structure occurs near the contact between highly deformed and broken metasedimentary rocks (part of the Bridge River complex) and more competent igneous rocks (Mission Ridge pluton). It was produced, during the Holocene, by complex slow landsliding and attendant slope extension. The Hell Creek 'fault', although incapable of generating an earthquake, does reflect deep-seated slope instability that is a potential hazard to development in the Bridge River valley below the site. Similar features are common throughout the southern Coast Mountains and record widespread slope deformation in the region.

Résumé : La «faille» de Hell Creek, située au nord-ouest de Lillooet, en Colombie-Britannique, était considérée de nature néotectonique. Cependant, son étroite association avec des escarpements à regard opposé à celui de la pente naturelle et des glissements de grande profondeur dans des roches très déformées et foliées du complexe de Bridge River font pencher en faveur d'une origine gravitaire plutôt que tectonique. L'escarpement segmenté à regard inverse qui constitue la structure de Hell Creek est situé près du contact entre des roches métasédimentaires très déformées et fragmentées (faisant partie du complexe de Bridge River) et des roches ignées plus compétentes (pluton de Mission Ridge). Il a été produit, à l'Holocène, par des glissements de terrain complexes et lents, accompagnés d'une extension concomitante du talus d'éboulis. La «faille» de Hell Creek, quoique incapable de provoquer un tremblement de terre, indique une instabilité profonde des pentes qui pourrait constituer un danger pour des travaux d'aménagement dans la vallée de la rivière Bridge à des altitudes plus basses. Des structures semblables sont nombreuses dans le sud de la chaîne Côtière et elles révèlent une déformation étendue des pentes dans la région.

¹ Terrain Sciences Division, Ottawa

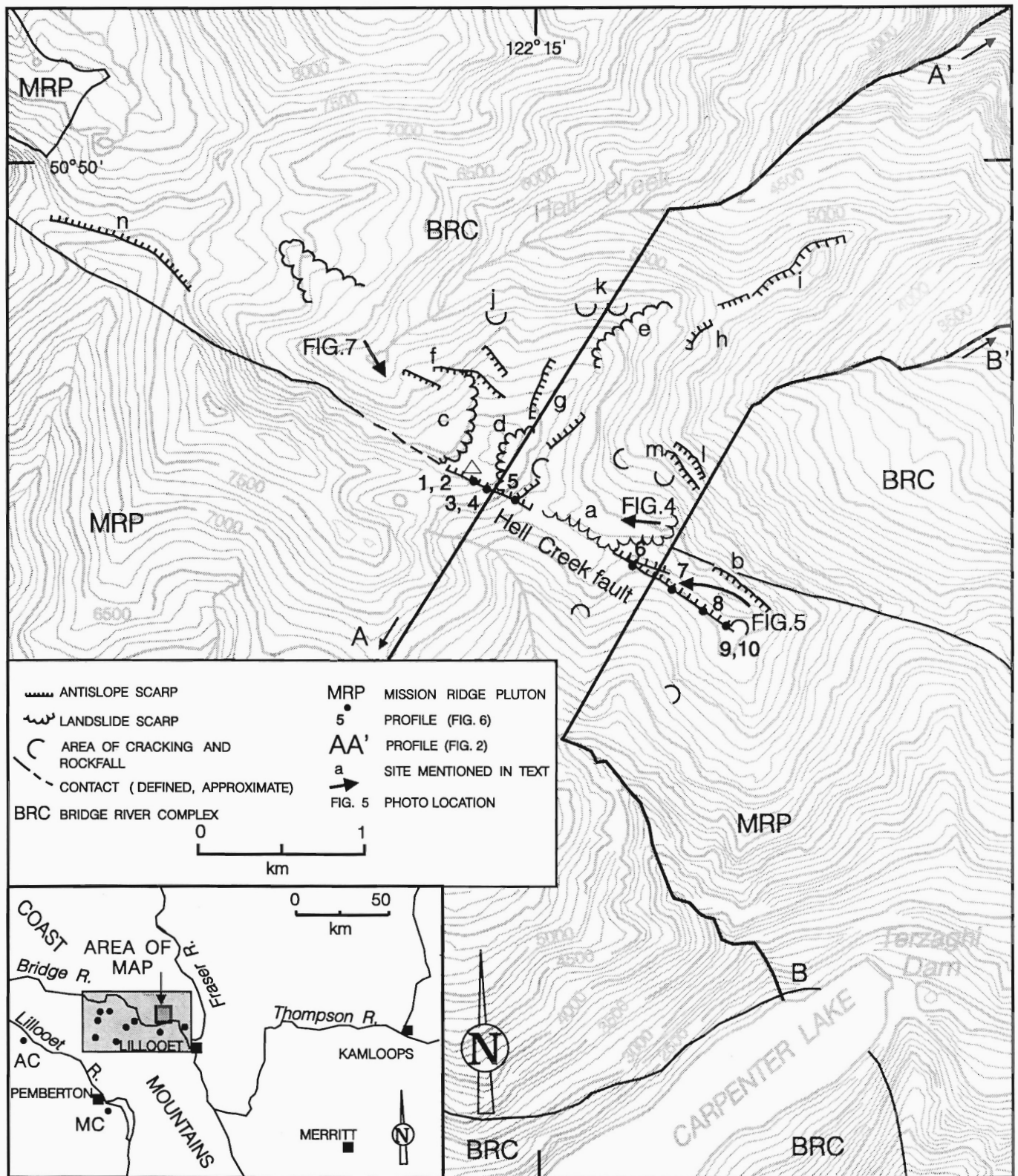


Figure 1. Map showing locations of the Hell Creek 'fault', related gravitational features, topographic profiles, and photographs. The triangle indicates the same locality in Figures 1, 3, 4, 5, and 7. Topographic contour interval = 100 ft. (30.5 m). Inset shows locations of other features (dots) in the Bridge River area (box) that are similar to the Hell Creek fault, as well as the Affliction Creek (AC) and Mount Currie (MC) structures (see text).

INTRODUCTION

The high seismicity (Milne et al., 1978), elevation, and relief of southwestern British Columbia indicate that the region is tectonically active. In spite of this, few active faults have been identified in this part of the Cordillera. In fact, aside from faults at present-day plate boundaries in the eastern North Pacific Ocean, there is only one structure in southwestern British Columbia that is widely believed to be active – the Hell Creek 'fault' near Lillooet (Fig. 1). (For convenience and in keeping with past usage, the structure is referred to as the Hell Creek 'fault' throughout the paper; no tectonic connotation, however, is implied.)

The Hell Creek fault was first identified in 1970 by J.A. Roddick and W.W. Hutchison of the Geological Survey of Canada. They observed on airphotos a 2 km long scarp on a high ridge in the eastern Coast Mountains. This feature displaces bedrock and Quaternary sediments and was shown on their geological map of the Pemberton area as a "Recent fault" (Roddick and Hutchison, 1973). Later, Slemmons et al. (1978) briefly described and interpreted the Hell Creek fault. They postulated three phases of displacement during the Holocene and suggested that the structure could generate a large earthquake in the future.

The Hell Creek fault is only 2 km from Terzaghi Dam, which impounds Carpenter Lake and is an important hydroelectric facility (Fig. 1). Because the dam might be damaged by a moderate or large local earthquake, the seismic capability of the Hell Creek fault is of more than academic interest. We argue in this paper that the structure is gravitational in origin and consequently is incapable of generating an earthquake, although a major landslide into Carpenter Lake clearly would have serious consequences.

GEOLOGICAL SETTING

The Hell Creek fault is located in an area of high relief and steep slopes (Fig. 1, 2) in the eastern Coast Mountains near the boundary between the Intermontane and Insular superterrane. This part of the Cordillera comprises several fragments of crust, or terranes, that originated in oceanic and island arc settings and subsequently were accreted to North America (Potter, 1986).

The area is underlain, in part, by Mississippian to Middle Jurassic phyllite, schist, greenstone, chert, marble, and serpentinite of the Bridge River complex (Potter, 1986; Cordey and Schiarizza, 1993). The rocks have been metamorphosed from greenschist to lower amphibolite facies. Low grade (prehnite-pumpellyite facies) rocks are highly broken and chaotic, whereas higher grade rocks have a more orderly structure. The Bridge River complex in the vicinity of the Hell Creek fault consists largely of phyllite, siliceous phyllite, and metachert and is intruded by hornblende-biotite-quartz-feldspar porphyry and biotite granodiorite, part of the Mission Ridge pluton of early Tertiary age (Fig. 1; Potter, 1983; Schiarizza et al., 1989, 1990; Coleman and Parrish, 1991).

Structures produced by subduction-related deformation and metamorphism are found locally in Triassic blueschists and Middle Jurassic or younger mélangé of the Bridge River complex (Garver et al., 1989; Schiarizza et al., 1989, 1990). The brittle faulting and lenticularity of lithological units that characterize the Bridge River sequence may be a result of this early deformational history (Schiarizza et al., 1990).

Numerous northwest-trending faults postdate these old structures and record a complex history of mid-Cretaceous to Tertiary compressional, strike-slip, and extensional

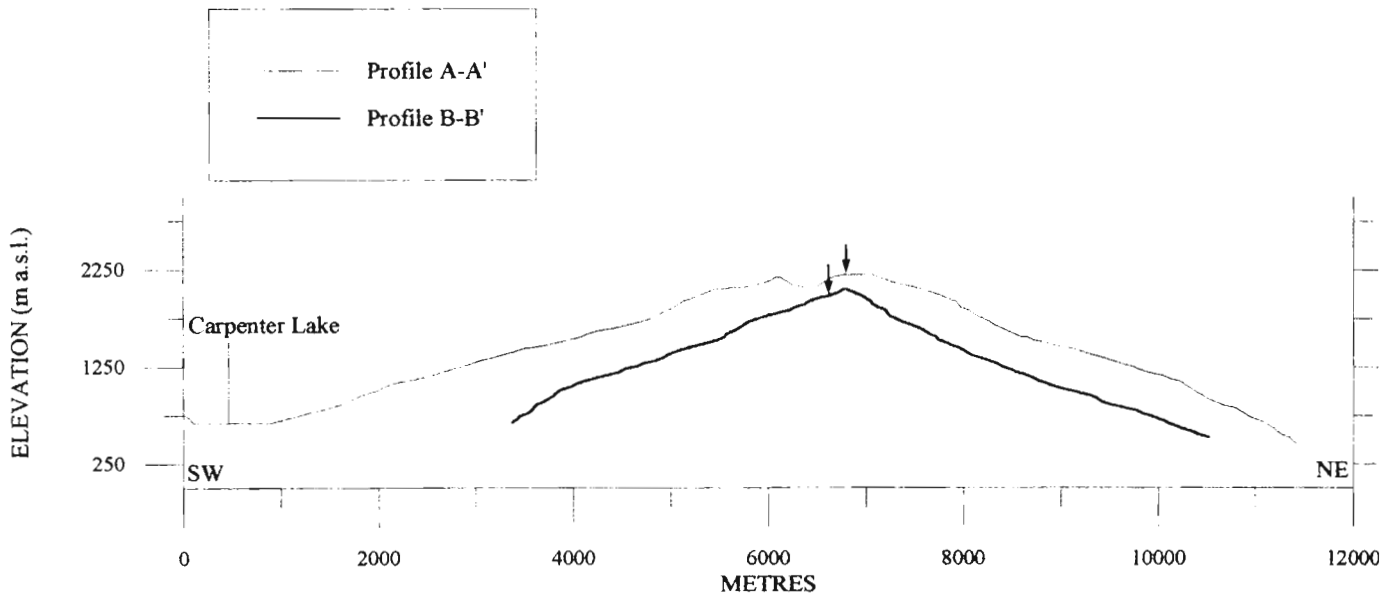


Figure 2. Representative topographic profiles across the ridge followed by the Hell Creek fault (see Fig. 1 for locations). Arrows show the position of the fault on the profiles.

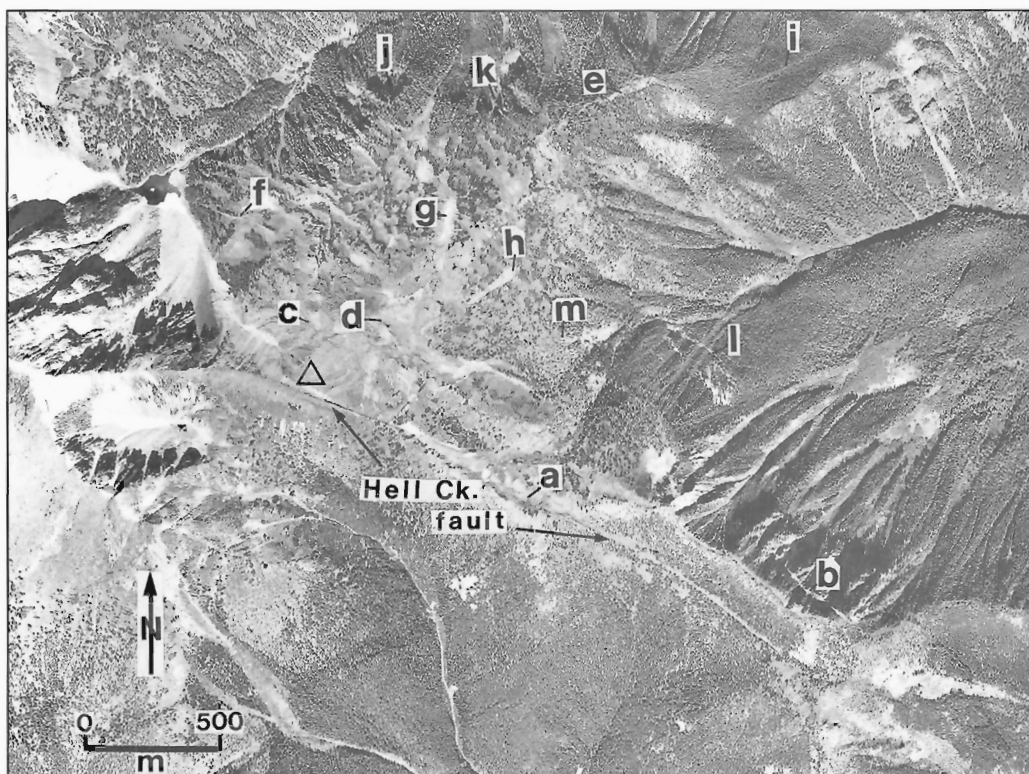


Figure 3. Vertical aerial photograph of the study area. The lettered features and triangle correspond to those in Figure 1 (see text for discussion). Province of British Columbia airphoto BC7788-062.



Figure 4. The Hell Creek fault; aerial view west (see Fig. 1 for location). The headscarp of a large slump that separates the two sections of the fault is visible in the lower left (arrow). See Figure 5 and Slemmons et al. (1978, Fig. 5-7) for other photographs of the Hell Creek fault.



Figure 5. Antislope scarp near the southeast end of the Hell Creek fault; view west-northwest (see Fig. 1 for location).

deformation (Schiarizza et al., 1989, 1990; Coleman and Parrish, 1991; Journeay et al., 1992). Late Cretaceous, south-westerly directed thrusting was followed, in early Tertiary time, by dextral strike-slip faulting. Subsequent extensional faulting is recorded in a major northeast-dipping normal fault east of Hell Creek and in late vertical displacements to the southwest. These structures are offset by late Eocene, dextral strike-slip faults of the Fraser Fault system which strike north to north-northwest (Monger, 1989).

DESCRIPTION

The Hell Creek fault extends 2 km in a west-northwest direction along a high ridge north of Carpenter Lake (Fig. 1, 3). It ranges in elevation from 2170 m a.s.l. at its northwest end to 1980 m a.s.l. on the southeast where it terminates on a steep slope above Bridge River (610 m a.s.l.). We found no geomorphic evidence (e.g., scarps or lineaments) that the structure crosses Bridge River valley and continues southeast to the vicinity of Fraser River, as suggested by Slemmons et al. (1978, p. 57).

The Hell Creek fault can be divided into two sections that differ in orientation by about 10° and are separated by the headscarp of a landslide in phyllites of the Bridge River complex (a in Fig. 1; Fig. 4). Southeast of the landslide, the structure occurs within intrusive rocks of the Mission Ridge pluton and is delineated by a slightly arcuate ($< 5^\circ$), north-east-facing, antislope scarp in bedrock and till (Fig. 5). This scarp is inclined up to 35° ; its height decreases towards the northwest from 6 m to a few tens of centimetres (Fig. 6).

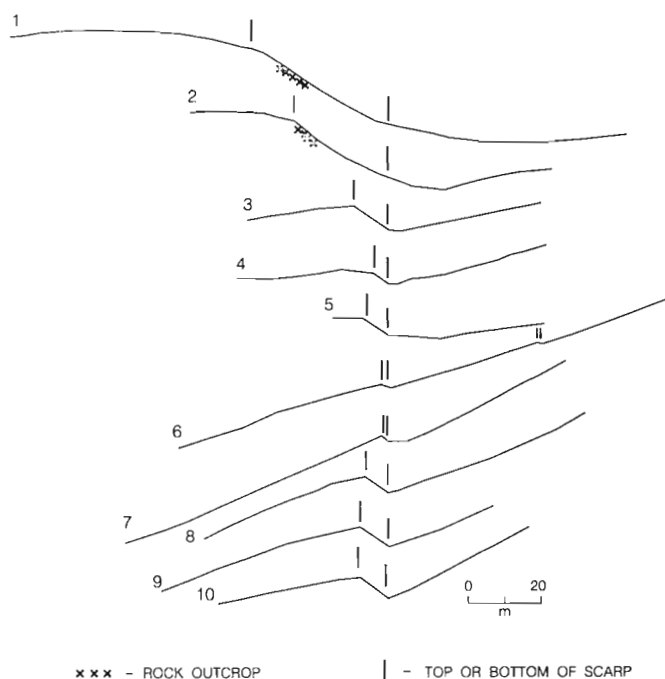


Figure 6. Topographic profiles across the Hell Creek fault (see Fig. 1 for location). Each profile is parallel to the slope.



Figure 7. Large slump in highly deformed rocks of the Bridge River complex northeast of the Hell Creek fault; aerial view southeast (see Fig. 1 for location).

Slopes above and below the scarp are inclined 10-30° (Fig. 6). A parallel antislope scarp, which faces the opposite direction (southwest), is present on the opposite side of the ridge at about the same elevation (b, Fig. 1). A low (<20 cm), subdued scarp branches off the main antislope scarp just southeast of the above-mentioned landslide. Tension cracks and fresh rockfall were noted below the southeast section of the Hell Creek fault and near the crest of the ridge above it, suggesting that the slopes in this area are unstable.

The second, northwest, section of the Hell Creek fault is located at or near the contact between the Mission Ridge pluton and the Bridge River complex. It is marked by a 4-22 m high antislope scarp inclined 30-40° north-northeast (triangle in Fig. 1, 3, 4, 5, and 7). Slopes above and below this part of the structure are more gentle than those to the southeast. The terrain to the northeast shows abundant evidence of large-scale downslope movement of Bridge River phyllites: landslide headscarps (c, d, e, Fig. 1), antislope scarps (f, g, h, i), and fresh rockfall (j, k); the unnamed lake at the head of Hell Creek is impounded by a large slump (Fig. 1, 7). Antislope scarps and fresh rockfall also occur below the headscarp of the landslide that separates the two sections of the Hell Creek fault (l, m, Fig. 1).

The antislope scarp that delineates the Hell Creek structure can be traced northwest into a steep slope at the head of Hell Creek. This slope coincides with the contact between the Mission Ridge pluton and Bridge River complex.

A subdued antislope scarp, a few tens of centimetres high and approximately 1.5 km long, extends across a gentle mountain slope 3 km west-northwest of the Hell Creek fault (n, Fig. 1). This scarp has approximately the same strike as the Hell Creek structure, but is separated laterally from it.

Rock fabric appears to control the orientation of the Hell Creek fault. Foliation and conspicuous joints within the Bridge River complex and Mission Ridge pluton are parallel or subparallel to the trace of the structure and dip to the north-northeast (Fig. 8).

INTERPRETATION

Evidence presented above indicates that the Hell Creek fault is a complex gravitational structure controlled by local rock lithology and fabric. It is located at and near the contact between two rock units of very different competence: jointed porphyritic and granitic rocks of the Mission Ridge pluton and foliated, pervasively faulted and fractured phyllites of the Bridge River complex.

There is abundant geomorphic evidence of large-scale landsliding in rocks of the Bridge River complex northeast of the Hell Creek fault. Much of the terrain in this area appears to have slumped and sagged towards lower elevations. This is particularly evident on the northeast-trending ridge just south of Hell Creek. Antislope scarps are present on both flanks of this ridge, and part of the ridge crest is marked by headscarps of deep-seated slumps and sags (Fig. 1). Most of these features are oriented almost perpendicular to the Hell Creek fault and are restricted to the area northeast of it. This part of the fault is interpreted to be a backstop for gravitational deformation that has affected the Bridge River complex. It coincides, in part, with the headscarp of a large slump that has displaced Bridge River rocks to the northeast (a, Fig. 1) and, in part, with an antislope scarp produced by sagging of the aforementioned northeast-trending ridge (Fig. 9a). The Hell Creek fault in this area is subparallel to the local rock fabric (Fig. 8A).

The southeast section of the Hell Creek fault is entirely within the Mission Ridge pluton. It comprises two branches delineated by scarps that dip upslope, i.e. to the north-northeast. The more northerly of the two is short and inconspicuous, but is otherwise similar to the main scarp a short distance to the south. The latter is slightly curved and parallels the crest of the ridge about 150 m to the northeast; it also is parallel to a major joint set within the Mission Ridge pluton (Fig. 8B), suggesting gravitational control. A gravitational origin for this section of the Hell Creek fault is supported by the presence of a parallel antislope scarp on the opposite side of the ridge at about the same elevation. The two scarps dip in opposite directions (i.e., upslope), but are otherwise identical. We conclude that they are genetically related and record gravitational spreading of the ridge, with the crest having subsided relative to the flanks (Fig. 9b). Fresh rockfall, both at the crest of the ridge and on its southwest flank, support this notion and indicate that movement may be continuing.

Similar structures are common elsewhere in the southern Coast Mountains of British Columbia; those that have been examined and reported in the literature (Affliction Creek – Bovis, 1982; Mount Currie – Evans, 1987) have been ascribed to gravitational processes and not tectonism. These

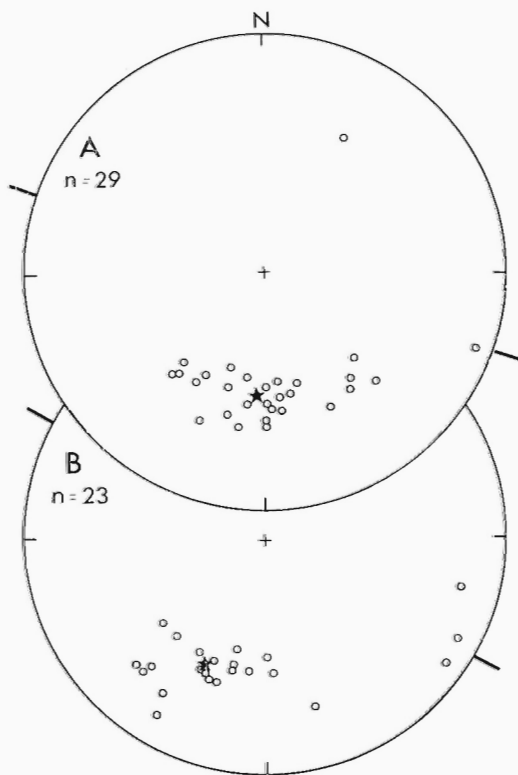


Figure 8. Stereographic projections of poles (open circles) to foliation and joints in the Bridge River complex and Mission Ridge pluton along the two sections of the Hell Creek fault; the projections are equal-area, lower hemisphere plots. **A)** Northwestern section, striking 290° (tick mark); peak pole position (star) = $186^\circ/44^\circ$. **B)** Southeastern section, striking 300° ; peak pole position = $207^\circ/38^\circ$. The data, although limited, suggest that the Hell Creek fault is parallel or subparallel to the strike of the rock fabric.

features also are found in many other mountain areas and have been described and interpreted as gravitational features by Zischinsky (1969), Tabor (1971), Radbruch-Hall et al. (1976), Mahr (1977), Radbruch-Hall (1978), Savage and Varnes (1987), and Thorsen (1992), among others.

Glacial sediments deposited between 15 000 and 12 000 years ago, during the last (Fraser) glaciation, are offset by all antislope scarps in the study area. This indicates that the Hell Creek fault and related gravitational structures are latest Pleistocene or Holocene in age. The steepness of the scarps (up to 40°) and the lack of significant amounts of colluvium in adjacent troughs argue for at least some movement during the late Holocene. The presence of fresh rockfall on slopes above and below the Hell Creek fault suggests that the gravitational movements that formed the antislope scarps may be continuing.

IMPLICATIONS

A gravitational origin for the Hell Creek fault has important implications for earthquake hazard assessment in the Bridge River area. We conclude, contrary to Slemmons et al. (1978),

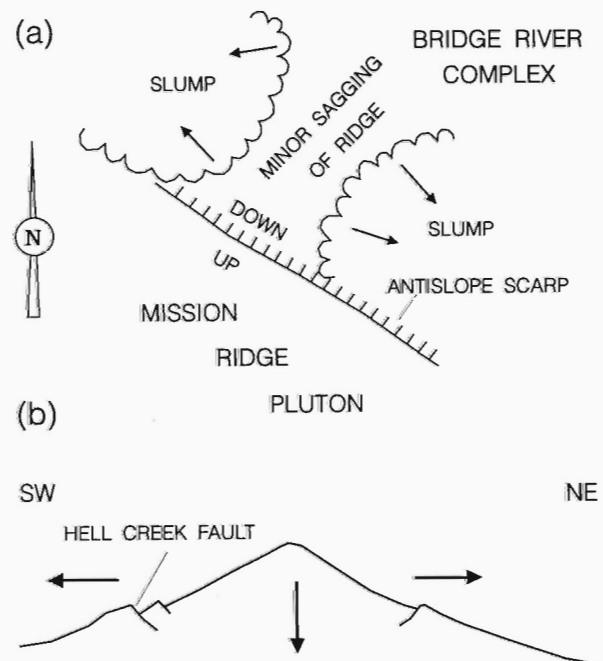


Figure 9. Schematic diagrams illustrating the proposed gravitational origin of the Hell Creek fault; **a)** Plan showing slumping and sagging of highly deformed Bridge River phyllite adjacent to more competent granitic rocks of the Mission Ridge pluton (vicinity of section A-A', Fig. 1). These movements produced the antislope scarp that delineates the northwestern part of the Hell Creek structure. **b)** Cross-section of the ridge underlain by Mission Ridge plutonic rocks at the southeast end of the structure (near section B-B', Fig. 1). Antislope scarps on opposite sides of the ridge suggest extension and minor subsidence of the crest relative to the flanks.

that the Hell Creek fault is not a potential source of earthquakes. This, however, does not deny the possibility that destructive earthquakes may occur in the area in the future, or that there are seismically capable faults that have not yet been recognized. A large earthquake could occur on a blind structure that has no surface expression or on an old fault that is presumed to be inactive.

Attempts to better understand the relationship between historical seismicity and crustal structure in British Columbia are vexed by the fact that few active faults have not been identified in this region. As we have shown, the Hell Creek fault, the only onshore structure in southwestern British Columbia generally thought to be active, is in fact a gravitational feature. We are reluctant, however, to conclude that there are no active surface faults in the region, even though large earthquakes of the historic period (A.D. 1872 and 1946) apparently produced no surface rupturing. There almost certainly are Holocene faults in southwestern British Columbia, but these will be difficult to locate in the high-relief, forested terrain that dominates the region. In the future, it may be possible to identify these structures from the loci of precisely located earthquakes.

Our identification of the Hell Creek fault as a gravitational structure also has implications for landslide hazard assessment. Some of the rocks of the Bridge River complex are highly unstable and susceptible to landsliding. Deformation similar to that at Hell Creek is found at many places in the Bridge River area (Fig. 1 inset) and is characterized by deep-seated slumping and sagging, toppling, and the formation of antislope scarps. Slopes at Hell Creek and at other sites where there are antislope scarps may be deforming today. An important unanswered question is whether slow deformation of this type could, at some future date, trigger a catastrophic rock avalanche that would reach a developed valley floor. Given the high relief and widespread evidence of instability in the Bridge River area, catastrophic slope failures probably should be viewed as a greater local hazard than earthquakes. Perhaps the worst-case scenario is that a large earthquake would trigger such landslides.

ACKNOWLEDGMENTS

Tonia Williams drafted several of the figures. J. Adams and J.W.H. Monger reviewed the paper and contributed to its improvement. Field work was partially funded by PERD (Program on Energy, Research and Development) Project no. 61254.

REFERENCES

- Bovis, M.J.**
1982: Uphill-facing (antislope) scarps in the Coast Mountains, southwest British Columbia; *Geological Society of America Bulletin*, v. 93, p. 804-812.
- Coleman, M.E. and Parrish, R.R.**
1991: Eocene dextral strike-slip and extensional faulting in the Bridge River terrane, southwest British Columbia; *Tectonics*, v. 10, p. 1222-1238.
- Cordey, F. and Schiarizza, P.**
1993: Long-lived Panthalassic remnant: The Bridge River accretionary complex, Canadian Cordillera; *Geology*, v. 21, p. 263-266.
- Evans, S.G.**
1987: Surface displacement and massive toppling on the northeast ridge of Mount Currie, British Columbia; in *Current Research, Part A*; Geological Survey of Canada, Paper 87-1A, p. 181-189.
- Garver, J.I., Schiarizza, P., and Gaba, R.G.**
1989: Stratigraphy and structure of the Eldorado Mountain area, Chilcotin Ranges, southwestern British Columbia (92O/2 and 92J/15); in *Geological Fieldwork 1988*; British Columbia Ministry of Energy, Mines and Petroleum Resources, Paper 1989-1, p. 131-143.
- Journey, J.M., Sanders, C., Van-Konijnenburg, J.-H., and Jaasma, M.**
1992: Fault systems of the Eastern Coast Belt, southwest British Columbia; in *Current Research, Part A*; Geological Survey of Canada, Paper 92-1A, p. 225-235.
- Mahr, T.**
1977: Deep-reaching gravitational deformations of high mountain slopes; *International Association of Engineering Geology Bulletin*, no. 16, p. 121-127.
- Milne, W.G., Rogers, G.C., Riddihough, R.P., McMechan, G.A., and Hyndman, R.D.**
1978: Seismicity of western Canada; *Canadian Journal of Earth Sciences*, v. 15, p. 1170-1193.
- Monger, J.W.H.**
1989: Geology of Hope and Ashcroft map areas, British Columbia; Geological Survey of Canada, Maps 41-1989 and 42-1989, scale 1:250 000.
- Potter, C.J.**
1983: Geology of the Bridge River complex, southern Shulaps Range, British Columbia; Ph.D. thesis, University of Washington, Seattle, Washington, 192 p.
1986: Origin, accretion, and postaccretionary evolution of the Bridge River terrane, southwest British Columbia; *Tectonics*, v. 5, p. 1027-1041.
- Radbruch-Hall, D.H.**
1978: Gravitational creep of rock masses on slopes; in *Rockslides and Avalanches, 1, Natural Phenomena* [Developments in Geotechnical Engineering 14A], (ed.) B. Voight; Elsevier Scientific Publishing Co., Amsterdam, p. 607-657.
- Radbruch-Hall, D.H., Varnes, D.J., and Savage, W.Z.**
1976: Gravitational spreading of steep-sided ridges ("Sackung") in western United States; *International Association of Engineering Geology Bulletin*, no. 14, p. 23-35.
- Roddick, J.A. and Hutchison, W.W.**
1973: Pemberton (east half) map area, British Columbia; Geological Survey of Canada, Map 13-1973, scale 1:250 000.
- Savage, W.Z. and Varnes, D.J.**
1987: Mechanics of gravitational spreading of steep-sided ridges ("Sackung"); *International Association of Engineering Geology Bulletin*, no. 35, p. 31-36.
- Schiarizza, P., Gaba, R.G., Coleman, M., Garver, J.I., and Glover, J.K.**
1990: Geology and mineral occurrences of the Yalakom River area (92O/1,2, 92J/15,16); in *Geological Fieldwork 1989*; British Columbia Ministry of Energy, Mines and Petroleum Resources, Paper 1990-1, p. 53-72.
- Schiarizza, P., Gaba, R.G., Glover, J.K., and Garver, J.I.**
1989: Geology and mineral occurrences of the Tyaughton Creek area (92O/2, 92J/15,16); in *Geological Fieldwork 1988*; British Columbia Ministry of Energy, Mines and Petroleum Resources, Paper 1989-1, p. 115-130.
- Slemmons, D.B., Carver, G.C., Glass, C.E., Trexler, D.T., and Tillson, D.D.**
1978: Remote sensing analysis of fault activity and lineament pattern of the epicentral region of the 1872 Pacific Northwest earthquake; in *Proceedings of the Third International Conference on Basement Tectonics*, (ed.) D.W. O'Leary and J.L. Earle; Basement Tectonics Committee, Denver, Colorado, p. 51-63.
- Tabor, R.W.**
1971: Origin of ridge-top depressions by large-scale creep in the Olympic Mountains, Washington; *Geological Society of America Bulletin*, v. 82, p. 1811-1822.
- Thorsen, G.W.**
1992: Splitting and sagging mountains; *Washington Geologic Newsletter*, v. 17, no. 4, p. 3-13.
- Zischinsky, U.**
1969: Über Sackungen; *Rock Mechanics*, v. 1, p. 30-52.

An overview of the Vancouver-Fraser Valley hydrogeology project, southern British Columbia

Brian D. Ricketts and Lionel E. Jackson, Jr.¹

Cordilleran Division, Vancouver

Ricketts, B.D. and Jackson, L.E., Jr., 1994: An overview of the Vancouver-Fraser Valley hydrogeology project, southern British Columbia; in Current Research 1994-A; Geological Survey of Canada, p. 201-206.

Abstract: A new hydrogeology project aims at delineating and characterizing aquifers and groundwater flow in the Greater Vancouver and lower Fraser Valley regions. Important aspects of the project are summarized, in particular the groundwater database, and experimental geophysical (ground penetrating radar, seismic and EM) and geochemical techniques. Preliminary sedimentological studies in the Brookwood unconfined aquifer are provided to calibrate the ground penetrating radar data.

Résumé : Un nouveau projet d'hydrogéologie a été mis sur pied pour délimiter et caractériser les aquifères et l'écoulement des eaux souterraines dans les régions du Grand Vancouver et de la basse vallée du Fraser. Les aspects importants du projet sont présentés, en mettant l'accent sur la base de données sur les eaux souterraines et les techniques géophysiques (géoradar, méthodes sismiques et électromagnétiques) et géochimiques expérimentales. Les études sédimentologiques préliminaires dans l'aquifère à nappe libre de Brookwood servent à étalonner les données géoradar.

¹ Terrain Sciences Division, Vancouver

INTRODUCTION

In April 1993, the Geological Survey of Canada launched a hydrogeological program to delineate and characterize the geology of major aquifers, groundwater flow, discharge and recharge, and water chemistry, in rapidly growing regions of Canada. Two projects initiating the program are the Oak Ridges Moraine north of Toronto, and the Vancouver lower mainland – Fraser Valley.

Rationale

Rapid urban, industrial and agricultural growth in the greater Vancouver area, requires rational planning by all levels of government to deal with the increasing demand for potable water. The protection of existing groundwater resources, and the exploration for and utilization of new sources, depend on a sound understanding of the regional hydrogeological framework. Factors such as groundwater mining, salt water intrusion and contaminant plume migration can only be properly assessed if the regional hydrogeological architecture is understood. Better understanding of groundwater flow will also provide a more accurate basis for identifying potential contaminant flow paths, thereby reducing the cost of remediation programs.

The Vancouver study area initially includes the two townships of Surrey and Langley, south to the international border (Fig. 1). This area was chosen because it contains a high proportion of domestic groundwater users, in addition to agricultural (e.g., irrigation) and industrial uses such as fish hatcheries. Furthermore, contamination of groundwater by agriculturally derived nitrates and pesticides is of increasing concern in several unconfined aquifers (e.g., Liebscher et al., 1992). There are about 4000 water wells in the initial study area which will form the backbone of the hydrogeology database.

THE DATABASE

There are two components to the Vancouver-Fraser Valley hydrogeology database: existing water well and chemistry information that is scattered among several government agencies and private companies, and new data. A great deal of information is available from existing water well records, most of which have been provided by the Water Management Branch of the B.C. Ministry of Environment, Lands and Parks; well and test drilling records have also been provided by Environment Canada and gravel pit operators. These records contain lithological and hydrological data, which

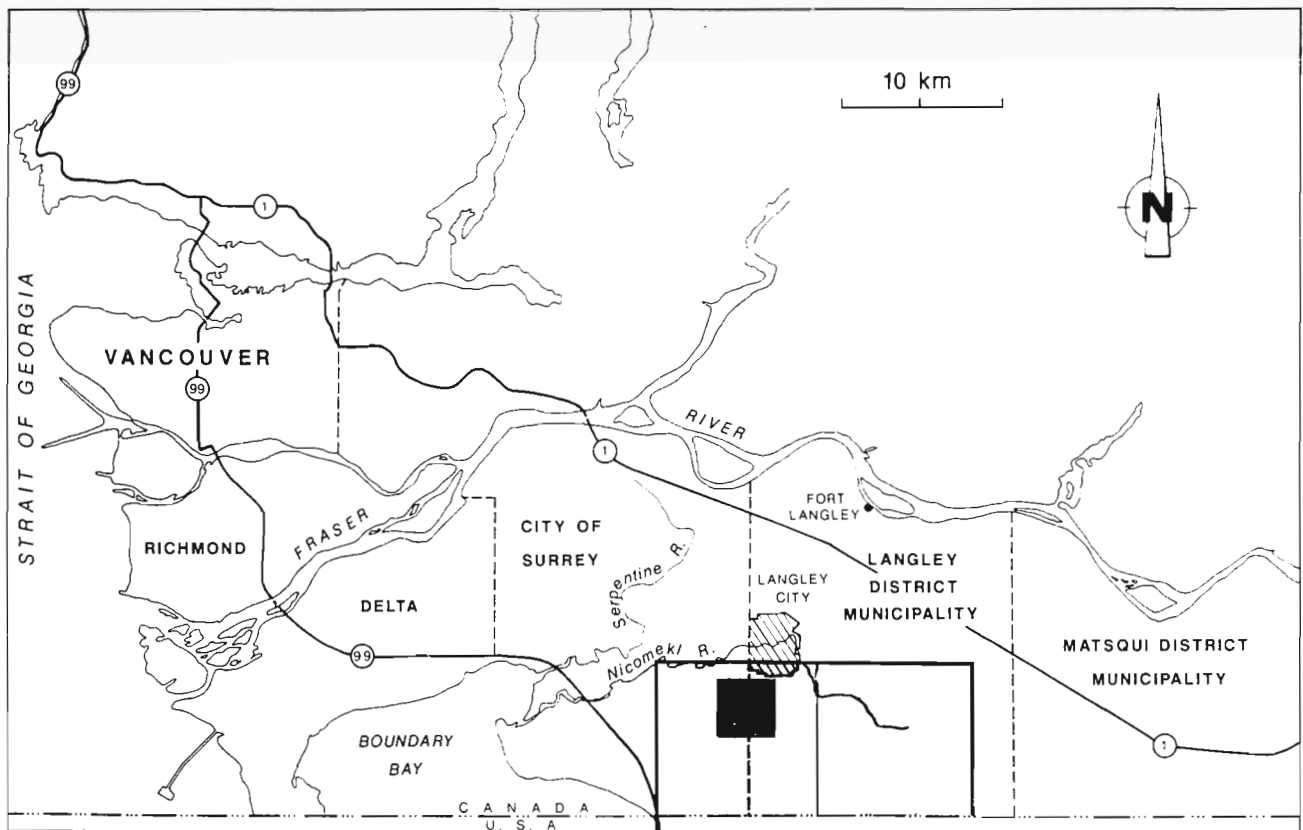


Figure 1. Location of initial Vancouver-Fraser Valley hydrogeology project study area. The location of Figure 2 is marked by the black square.

have been converted to a dBASE structure (details in Woodsworth and Ricketts, 1994). Few water well records in British Columbia are located by NTS coordinates. Consequently, all well locations have been digitized, with the coordinates added to a location database file. The various dBASE files will in turn be exported to ARC/INFO®, together with coverages such as digital elevation, surface geology, water chemistry, weather and land use.

Various geophysical techniques, stratigraphic test drilling and piezometer arrays will be used to generate new data, to test the integrity of existing well records, and to provide a more comprehensive picture of the three dimensional hydro-stratigraphic architecture.

Ground penetrating radar

Ground Penetrating Radar (GPR) experiments were successfully conducted over the Brookwood unconfined aquifer, part of the postglacial outwash complex known as Sumas Drift (Armstrong, 1981, 1984; Halstead, 1986, Fig. 1, 2), to determine the following (see Rae et al., 1994):

- i. can GPR be used to examine an aquifer's sedimentological and stratigraphic organization, which in turn provide clues to such factors as hydraulic conductivity, and
- ii. is the method useful for imaging the water table, and/or contaminant plumes?

Three dimensional GPR modelling was also conducted at the Stokes municipal gravel pit in Surrey, where there is good control on the depth of the water table, and some control on the stratigraphy in pit-wall exposures (Fig. 2).

Future experiments

High resolution reflection seismic experiments will be conducted in 1994, co-ordinated by S. Pullen, Terrain Sciences Division, following some of the transects in the GPR experiments. The GPR, which generally images to a maximum depth of 15-20 m, will compliment the deeper penetrating seismic surveys. It is anticipated that some electromagnetic experiments, co-ordinated by M. Best, Pacific Geoscience Centre will also be conducted. Some stratigraphic drilling is anticipated along certain transects to calibrate seismic, GPR and existing well records.

Geochemistry

Water chemistry data are currently being assembled from different external sources (e.g., Environment Canada) to determine sample distribution and data integrity. The data will be added to ARC/INFO® coverages. The primary aim is to map broad compositional facies and establish base-line composition trends. A program has been initiated by G. Hall, Mineral Resources Division that examines rare-earth elements for identifying sources of deep and shallow groundwater. An analytical program for identifying possible natural and anthropogenic hydrocarbons is also underway, coordinated by L. Snowdon, Institute of Sedimentary and Petroleum

Geology, Calgary. These 'fingerprinting' techniques will help, in addition to the other hydrogeological/geophysical methods, identify groundwater sources and flow paths.

PRELIMINARY SEDIMENTOLOGICAL STUDIES

Exposures of Quaternary glaciogenic deposits over most of the Fraser Valley are confined to some stream beds and gravel pits. Preliminary investigations were made in an area of Sumas Drift deposits known locally as the Brookwood aquifer (Fig. 2), to provide the sedimentological criteria for interpreting GPR experiments.

The Sumas Drift was deposited during the late Fraser Glaciation as outwash sand and gravel interfingering with lodgement and flow tills and glaciolacustrine clay (Armstrong, 1981, 1984; Armstrong and Hicoek, 1980; Halstead, 1986). Total thickness ranges from about 40 m, to zero at erosional pinchout margins. It is underlain primarily

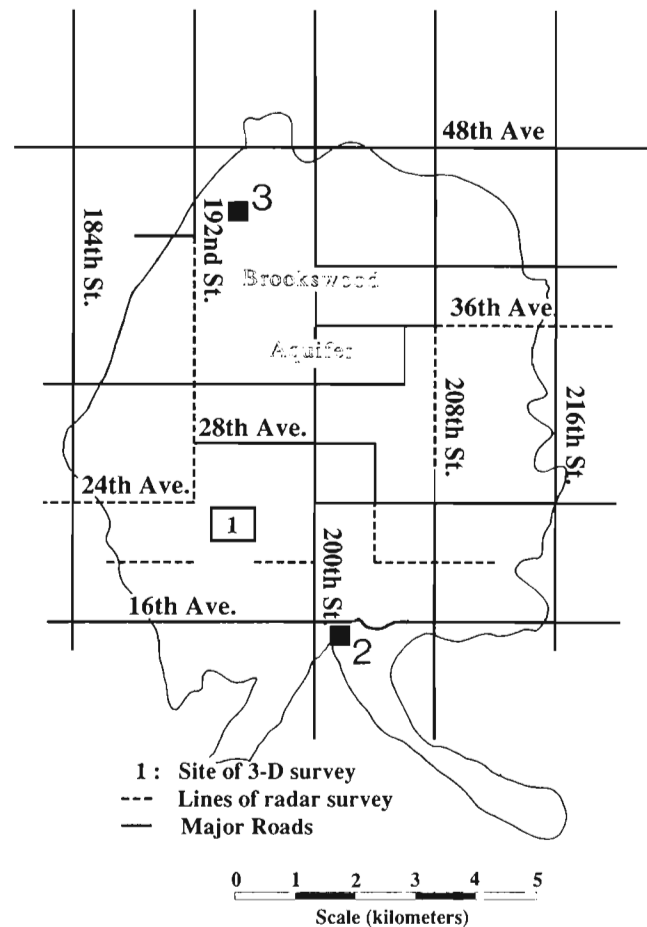


Figure 2. Map showing location of GPR transects and gravel pits: 1. Stokes municipal pit, 2. Harmony Pit, 3. 192nd Street pit.

by glaciomarine clay and till of the Fort Langley Formation. Similar stratigraphic and sedimentological associations occur in the adjacent, but hydraulically unconnected Aldergrove and Abbotsford aquifers (e.g., Clague and Luternauer, 1982).

Lithological records from water wells penetrating the aquifer indicate a high degree of lateral and vertical stratigraphic variability. The lithological heterogeneity typical of the Sumas Drift (Armstrong, 1981; Halstead, 1957) is illustrated in two pit exposures (Fig. 2). In the 'Stokes' municipal pit (Fig. 3) a lower unit (A) consists of south-southwest dipping (5-8°), rippled sand foresets that interfinger with clay layers and lenses, locally disrupted by small, synsedimentary extensional faults. An important sedimentary association in the sand-mud foresets is flaser and lenticular bedding. The mud-sand foresets are typical of point bars, and with the ripple bedforms suggesting a possible tidal influence in an estuarine point bar setting. Planar and trough crossbedded sand and gravelly sand (B) overlies unit A with up to 1.5 m erosional relief. Pebbles average about 1 cm, with a maximum of 4 cm. Unit C consists of coarse pebble and cobble gravel, with maximum clast size up to 15 cm. Foresets, 2 m thick, dip south

at 12-15° and locally are cut by cobble-filled channels and sand lenses. Clay rip-ups are present locally. Both units B and C are typical of braided stream deposits, the large foresets representing transverse bars. The foresets correspond to the dipping layers imaged by the GPR survey (Rae et al., 1994, Fig. 6).

Steeply dipping, gravel and sand layers appear to be common in other pit exposures, not only in the Brookwood aquifer, but also the Abbotsford aquifer. Foresets up to 5 m thick, dipping 20-25°, and overlain by crossbedded sand 1-2 m thick appear to be more diagnostic of foreset-topset organization in fan deltas (Fig. 4). Gravitational failure is common in sandier foresets, usually expressed as small, rotational listric or extensional faults. North to northwest-dipping foresets in a second pit (Fig. 5), 2.5-3 m thick, are made up of alternating clay layers 10-20 cm thick and containing some lenticular bedding, and sand layers up to a metre thick. Crossbeds in the sands are draped by clay veneers. Like the point bar deposits in Stokes pit, there is a possibility of tidal influence although the glaciofluvial influence seems to have been greater. The diamicton overlying the foreset unit shows

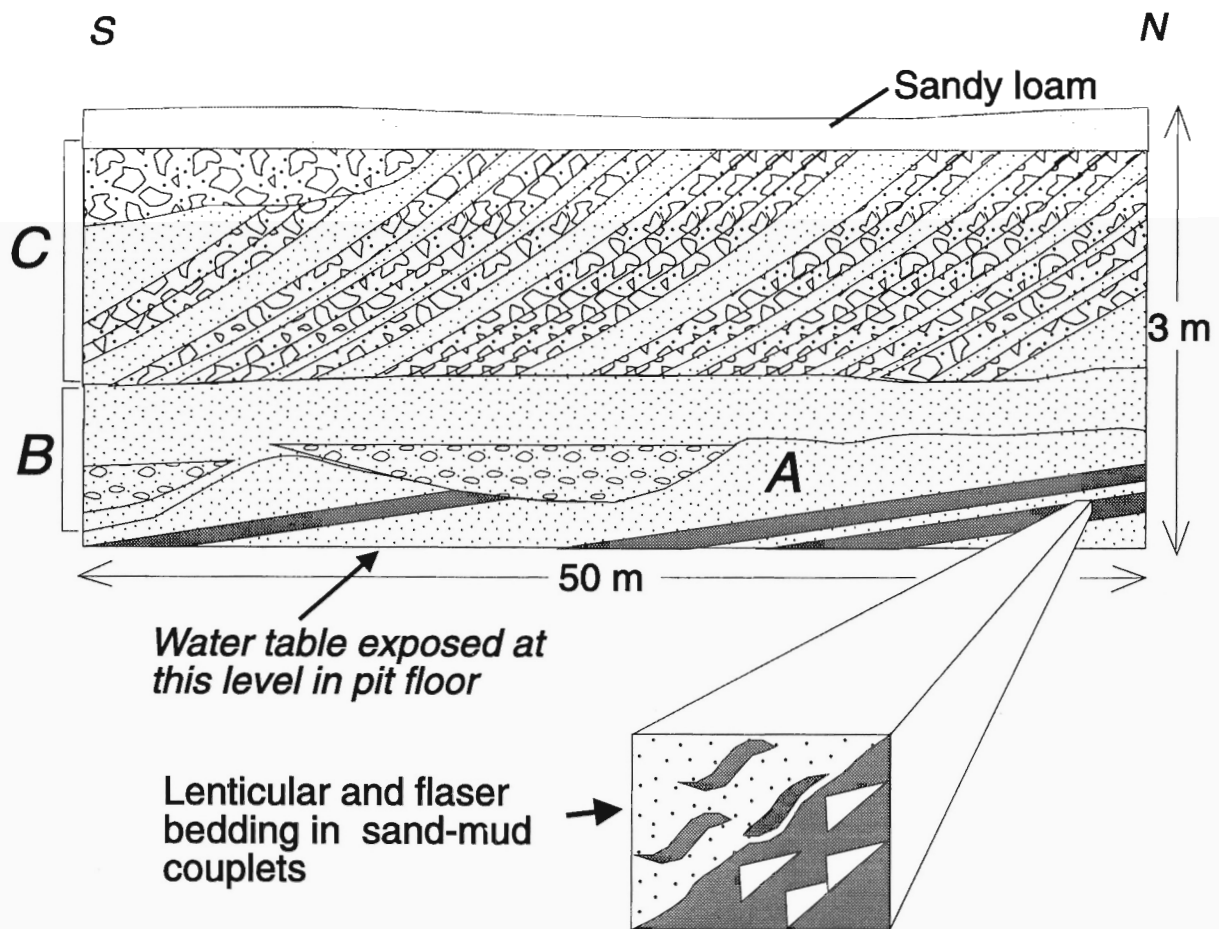


Figure 3. Sketch of exposure along the west wall of Stokes pit showing the tripartite stratigraphic division and the position of the water table. This section is adjacent the grid used for 3-D GPR modelling (Rae et al., 1994, Fig. 6).



Figure 4. Possible fan delta topset and foreset deposits in a gravel pit, south of 16th Avenue, just east of Campbell River. Measuring pole in feet.

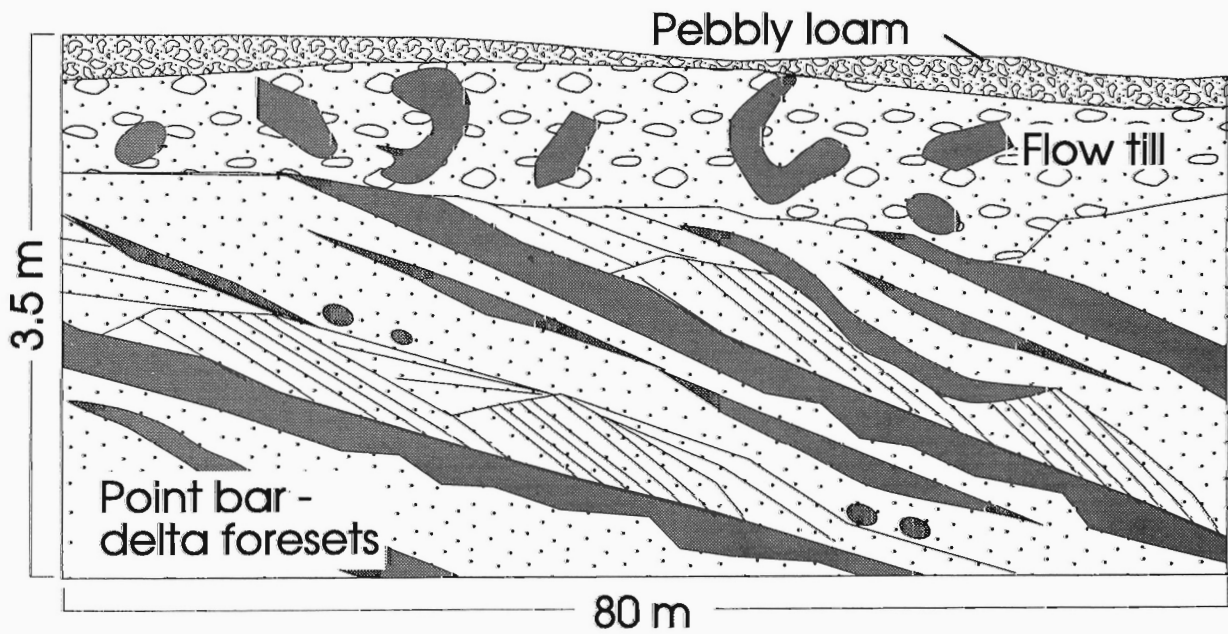


Figure 5. Sketch of large sand-clay foreset couplets, possibly of point bar origin exposed in gravel pit near the northwest margin of Brookwood aquifer, east of 192nd Street.

considerable internal disruption, having several plastically deformed sandy layers and large clay rip-ups, suggesting a possible flow-till formed during local ice advance.

ACKNOWLEDGMENTS

The initiation of this project results from discussions over the past two years with many people representing federal, provincial and municipal government agencies, and the private sector. In particular, Hugh Liebscher of Environment Canada, and Paul Matysek and Peter Bobrowsky (B.C. Geological Survey Branch) were instrumental in getting us to think about the regional aspects of groundwater. Rodney Zimmerman (Water Management Branch, B.C. Ministry of Environment, Lands and Parks) provided the project with its first batch of water well data. Ideas, adjustments, constructive criticisms of the project, and new data have come from many quarters: Bob Turner, Glenn Woodsworth, John Clague and John Luternauer (GSC Vancouver); Carl Halstead; John Philion, Steve Martin and Kerry Schneider (B.C. Ministry of Health); Ken Bennett (Township of Surrey); Peter Scales and Neil Calver (Township of Langley); Tom Heath (Greater Vancouver Regional District); John Psutka (B.C. Hydro); John Gartner, David Osmond, Robert Dickin and Tony Sperling (Gartner Lee); David Tiplady (Piteau Associates); Graham Rawlings (Golder Associates); Mike Davies (Klohn-Crippen Ltd.); Hugh Harris (ERM Ltd.); Jim Britton (Dynamic Oil); Marvin Breyfogle (Dandelion Geothermal); Dick Campanella (Civil Engineering, UBC), Rosemary Knight and Jane Rea (Astronomy and Geophysics, UBC), and Mike Roberts (Geography, SFU). Wayne Clifton (Stokes Pit, Surrey), Terry Schoeppe (Harmony Gravel Pit, 16th Ave.), Gary Breaks (192nd St. Gravel pit), and Ron Bruhaug (Central Aggregate) are thanked for access to pit exposures.

Bob Turner is thanked for reviewing the manuscript, and Raelyn Crossley for providing field and office assistance during the summer.

REFERENCES

- Armstrong, J.E.**
 1981: Post-Vashon Wisconsin glaciation, Fraser Lowland, British Columbia; Geological Survey of Canada, Bulletin 322, 34 p.
 1984: Environmental and engineering applications of the surficial geology of the Fraser Lowland, British Columbia; Geological Survey of Canada, Paper 83-23, 54 p.
- Armstrong, J.E. and Hicock, S.R.**
 1980: Surficial geology, New Westminster, British Columbia; Geological Survey of Canada, Map 1484A, scale 1:50 000.
- Clague, J.J. and Luternauer, J.L.**
 1982: Excursion 30A: Late Quaternary sedimentary environments, southwestern British Columbia; International Association of Sedimentologists, 11th International Congress on Sedimentology (Hamilton), Field Excursion Guidebook, 167 p.
- Halstead, E.C.**
 1957: Ground-water resources of Langley Municipality, British Columbia; Geological Survey of Canada, Water Supply Paper No. 327.
 1986: Ground water supply - Fraser Lowland, British Columbia; National Hydrology Research Institute Paper No. 26, Inland Waters Directorate, Environment Canada, Scientific Series No. 145, 80 p.
- Liebscher, H., Hii, B., and McNaughton, D.**
 1992: Nitrates and pesticides in the Abbotsford aquifer, southwestern British Columbia; Environment Canada, 83 p.
- Rea, J., Knight, R., and Ricketts, B.D.**
 1994: Ground penetrating radar survey of the Brookwood aquifer, Fraser Valley, British Columbia; in Current Research 1994-A; Geological Survey of Canada, Paper 94-1A.
- Woodsworth, G.J. and Ricketts, B.D.**
 1994: A digital database for Fraser Valley groundwater data; in Current Research 1994-A; Geological Survey of Canada.

A digital database for groundwater data, Fraser Valley, British Columbia

G.J. Woodsworth and Brian D. Ricketts
Cordilleran Division, Vancouver

Woodsworth, G.J. and Ricketts, B.D., 1994: A digital database for groundwater data, Fraser Valley, British Columbia; in Current Research 1994-A; Geological Survey of Canada, p. 207-210.

Abstract: We describe a flexible and expandable relational database that is being developed and used in the Cordilleran Division for groundwater data. The database contains location, well details, and driller's logs for about 4000 wells in the Langley and Surrey regions of the Fraser Valley, British Columbia.

Résumé : Nous décrivons une base de données relationnelles, flexible et extensible, qui est actuellement mise au point et exploitée par la Division de la Cordillère pour gérer les données sur les eaux souterraines. Cette base de données renferme les coordonnées de localisation, les détails sur les puits, et les journaux de sondage d'environ 4 000 puits implantés dans les régions de Langley et de Surrey dans la vallée du Fraser en Colombie-Britannique.

INTRODUCTION

In 1993, the GSC began a study of the regional hydrogeological framework of the Vancouver-Fraser Valley region of southwestern British Columbia (Ricketts and Jackson, 1994). A strategic part of this project is the preparation of a comprehensive database for the existing hydrogeological data for the region. This note describes the preliminary design and structure of this database.

The initial study area includes the townships of Langley and Surrey. Records for about 4000 water wells in this area were made available in hard copy and on diskette in Word-Perfect form by the Water Management Branch of the B.C. Ministry of Environment, Lands and Parks. These records, although convenient print-outs of the data, are not directly suitable for use in GIS systems or structured databases. The records have no well-defined structure, making complex search-and-retrieval operations and export of comma-delimited files difficult. NTS coordinates and latitudes and longitudes are absent, precluding efficient use of the data in a GIS system.

The water well records were converted into dBase 4 format using a series of utility programs. UTM coordinates were generated by digitizing locations from location maps provided by the Water Management Branch. When complete, the dBase files will be exported to ArcInfo format and combined with digital elevation models, surface geology, chemistry, and other data to form a comprehensive database.

DATABASE DESIGN AND STRUCTURE

The database uses a relational system of three dBase files. This database is based on the CASP system for biostratigraphic data (Weston et al., 1991) which is successfully being used in the Cordilleran Division of the GSC. The groundwater system is designed for flexibility and expendability and to meet the guidelines suggested by the Federal-Provincial Working Group on Groundwater (1991). Location information is stored in one file (WELL_LOC.DBF); general information about each well is in another (WELL_SUM.DBF); and the driller's logs, where available, are in a third (WELL_LOG.DBF). The main advantages of this design over a single "flat" file is that it is more efficient use of disk space than a flat file, particularly in handling the driller's logs; it allows multiple wells at any locality; and it is very easy to add new modules such as water chemistry. Each file is linked to the others by one or more common fields. Brief descriptions of these files follow.

The structures of the three files that constitute the database system are outline below. Column headings are:

No. Field number

Name Field name

FT Field type, where C=character; N=numeric; D=date; M=memo

Len. Field length, in characters

Dec. Number of decimals (numeric fields only)

File: WELL_LOC.DBF

This file contains detailed geographic data for each locality, with one record per locality. Fields are available for "absolute" locations using UTM coordinates, latitude and longitude, elevation, and for "cultural" locations using street address, township, and city or municipality. A memo field allows for additional free-form data. The field LINK1 gives a link between this file and the others; LINK1 is an integer value that is unique to a given locality.

| No. | Name | FT | Len. | Dec. | Description |
|-----|------------|----|------|------|---|
| 1 | TRIM_MAP | C | 9 | | Digital TRIM map number |
| 2 | LINK1 | N | 5 | 0 | Unique number for this location (linking field) |
| 3 | LAND_DIST1 | C | 3 | | Land district (numeric code) |
| 4 | LAND_DIST2 | C | 25 | | Land district (full name) |
| 5 | DRAIN_BASN | C | 25 | | Drainage basin |
| 6 | TOWNSHIP | C | 3 | | Township |
| 7 | SECTION | C | 3 | | Section |
| 8 | IND_RESERV | C | 4 | | Indian reserve |
| 9 | ISLAND | C | 20 | | Island name |
| 10 | OWNER_NAME | C | 36 | | Name of registered land owner |
| 11 | STREET_ADD | C | 36 | | Street address of this locality |
| 12 | CITY | C | 20 | | City name |
| 13 | UTM_ZONE | N | 11 | 0 | UTM zone (1 or 2 digits) |
| 14 | UTM_EAST | N | 10 | 0 | UTM easting (6 digits) |
| 15 | UTM_NORTH | N | 12 | 0 | UTM northing (7 digits) |
| 16 | UTM_DATUM | C | 12 | | UTM datum used, such as NAD 27 |
| 17 | LAT_DEG | N | 9 | 0 | Latitude, degrees |
| 18 | LAT_MIN | N | 8 | | Latitude, minutes |
| 19 | LAT_SEC | N | 9 | 2 | Latitude, seconds |
| 20 | LONG_DEG | N | 11 | 0 | Longitude, degrees |
| 21 | LONG_MIN | N | 10 | | Longitude, minutes |
| 22 | LONG_SEC | N | 11 | 2 | Longitude, seconds |
| 23 | LOC_ACCUR | C | 1 | | Code for precision or accuracy of location |
| 24 | ELEVATION | N | 11 | 1 | Elevation (metres) |
| 25 | ELEV_DATUM | C | 30 | | Datum used for elevation |
| 26 | ELEV_ACCUR | C | 1 | | Code for precision or accuracy of elevation |
| 27 | LOC_VER | C | 1 | | Has location been verified on ground? |
| 28 | LOCA_NOTE | M | 10 | | Remarks on location |

Total record length: 357 characters

File: WELL_SUM.DBF

This file contains details about the wells, using one record per well; much of this data is taken directly from the Ministry of Environment records. Fields 29-47 indicate the presence or absence of specific data. A memo field allows for additional free-form data that pertain to the well as a whole. The field LINK1 gives a link between this file and the others; LINK1 is an integer value that is unique to a given locality. The field LINK2 is an integer value unique for a given well; this field links to other files lower in the hierarchy.

| No. | Name | FT | Len. | Dec. | Description |
|---|------------|----|------|------|---|
| 1 | WELL_NUMB | C | 20 | | MOE well number |
| 2 | LINK1 | C | 5 | | Locality linking field |
| 3 | LINK2 | C | 5 | | Unique number for this well (linking field) |
| 4 | DEPTH_TOTA | N | 6 | 1 | Total depth of the well |
| 5 | FEET_METRE | C | 1 | | Units of measure for hole depth (M=metres, F=feet) |
| 6 | ORIG_UNITS | C | 1 | | Original units of measure (M=metres; F=feet) |
| 7 | HOLE_ANGLE | N | 2 | 0 | Angle of the hole; 0 = vertical |
| 8 | HOLE_AZIM | N | 3 | 0 | Azimuth of hole, if not vertical, in degrees |
| 9 | PROJECT | C | 36 | | Project name, for wells that are part of a larger program |
| 10 | CONTRACTOR | C | 36 | | Name of drilling contractor |
| 11 | CONST_DATE | D | 8 | | Date of well construction |
| 12 | CONST_METH | C | 20 | | Construction method (e.g., rotary) |
| 13 | DRILLFLUID | C | 2 | | Drilling fluid used, if any (2-letter code) |
| 14 | CASING_MAT | C | 2 | | Casing material (2-letter code) |
| 15 | HOLE_DIAM | N | 4 | 1 | Hole diameter (cm) |
| 16 | M_WATER | N | 5 | 1 | Depth to water (metres) |
| 17 | M_WATERTAB | N | 5 | 1 | Depth to water table (metres) |
| 18 | M_STATLEVL | N | 5 | 1 | Static level (metres) |
| 19 | M_BEDROCK | N | 5 | 1 | Depth to bedrock (metres) |
| 20 | ARTES_FLOW | N | 10 | 1 | Artesian flow (litres/second) |
| 21 | WELL_YIELD | N | 10 | 1 | Well yield (litres/second) |
| 22 | SCREEN_FRM | N | 5 | 1 | Screened from (metres) |
| 23 | SCREEN_TO | N | 5 | 1 | Screened to (metres) |
| 24 | OTH_SCREEN | C | 1 | | Other screens (Y, N) |
| 25 | SLOT_SIZE | C | 3 | 1 | Slot size (cm) |
| 26 | AQUIF_LITH | C | 20 | | Aquifer lithology |
| 27 | WELL_USE | C | 20 | | Well use |
| 28 | WATER_UTIL | C | 20 | | Water use |
| Each of the fields below indicates if this data was collected or not (Y, N) | | | | | |
| 29 | PUMP_TEST | C | 1 | | Pump test |
| 30 | GRWAT_REPT | C | 1 | | Groundwater report |
| 31 | SIEVE_ANAL | C | 1 | | Sieve analysis |
| 32 | FILTER_PAK | C | 1 | | Filter pack |
| 33 | SCREEN_DET | C | 1 | | Screen details |

| No. | Name | FT | Len. | Dec. | Description |
|-----|-------------|----|------|------|------------------------------|
| 34 | CHEM_LAB | C | 1 | | Water chemistry (laboratory) |
| 35 | CHEM_FIELD | C | 1 | | Water chemistry (field) |
| 36 | CHEM_SITE | C | 1 | | Water chemistry (site) |
| 37 | OTHR_TEST | C | 20 | | Other tests |
| 38 | PIEZOMETER | C | 1 | | Piezometer data |
| 39 | DRILLERLOG | C | 1 | | Driller's log |
| 40 | LITHOL_LOG | C | 1 | | Lithological log |
| 41 | GAMMA_LOG | C | 1 | | Gamma log |
| 42 | RESIST_LOG | C | 1 | | Resistivity log |
| 43 | SP_LOG | C | 1 | | Self-potential log |
| 44 | GATHERM_LOG | C | 1 | | Geothermal log |
| 45 | GCHEMI_LOG | C | 1 | | Geochemical log |
| 46 | CALIPR_LOG | C | 1 | | Calliper log |
| 47 | TIME_LOG | C | 1 | | Drilling time log |
| 48 | DATA_SOURC | C | 128 | | Sources of data |
| 49 | WELL_NOTE | M | 10 | | Other remarks on this hole |

Total record length: 461 characters

File: WELL_LOG.DBF

This file contains the driller's log, if any, using one record per each interval described by the drillers. This data is taken directly from the Ministry of Environment records, without any interpretation and only minor clean-up of spelling and formatting. A memo field allows for additional free-form data that pertain to this interval. The fields LINK1 and LINK2 are as described above. The field LINK3 is an integer value unique to each record in the file and allows for links to future modules in the database system.

| No. | Name | FT | Len. | Dec. | Description |
|-----|------------|----|------|------|--|
| 1 | WELL_NUMB | C | 20 | | MOE well number |
| 2 | LINK1 | C | 5 | | Locality linking field |
| 3 | LINK2 | C | 5 | | Unique number for this well (linking field) |
| 4 | LINK3 | C | 5 | | Unique number for this depth interval |
| 5 | DEPTH_FROM | N | 5 | 1 | Starting depth for this interval (metres) |
| 6 | DEPTH_TO | N | 5 | 1 | Ending depth for this interval (metres) |
| 7 | LITHOL | C | 48 | | Lithology (from driller's log) |
| 8 | H2O_BEARNG | C | 1 | | Water-bearing (Y, N) |
| 9 | MATERIAL | C | 48 | | Material (from driller's log) |
| 10 | DESCRIPT | C | 48 | | Description (from driller's log) |
| 11 | COLOUR | C | 12 | | Colour (from driller's log) |
| 12 | CORING | C | 1 | | Coring done? |
| 13 | LOG_NOTE | M | 10 | | Notes on the driller's log for this interval |

Total record length: 213 characters

ACKNOWLEDGMENTS

We thank Rodney Zimmerman of the Water Management Branch of the B.C. Ministry of Environment, Lands and Parks for supplying the WordPerfect groundwater data. Useful discussions on the structure of the database came from John Luternauer (GSC Vancouver) and Pat Monahan (Pacific Geoscience Centre). Digitizing was done by Bertrand Groulx and Raelyn Crossley.

REFERENCES

- Federal-Provincial Working Group on Groundwater**
1991: Groundwater Data Management; Office of the Groundwater Advisor, Inland Waters Directorate, Environment Canada, 76 p.
- Ricketts, B.D. and Jackson, L.E.**
1994: Hydrogeology, Vancouver-Fraser Valley, southern British Columbia; in Current Research 1994-A; Geological Survey of Canada.
- Weston, M.L., Woodsworth, G.J., Orchard, M.J., and Johns, M.J.**
1991: Design of an electronic database for biostratigraphic data; in Evolution and Hydrocarbon Potential of the Queen Charlotte Basin, British Columbia, (ed.) G.J. Woodsworth; Geological Survey of Canada, Paper 90-10, p. 545-554.

Geological Survey of Canada Projects 930035 and 930039

Ground-penetrating radar survey of the Brookwood aquifer, Fraser Valley, British Columbia

Jane Rea¹, Rosemary Knight¹, and Brian D. Ricketts
Cordilleran Division, Vancouver

Rea, J., Knight, R., and Ricketts, B.D., 1994: Ground-penetrating radar survey of the Brookwood aquifer, Fraser Valley, British Columbia; in Current Research 1994-A; Geological Survey of Canada, p. 211-216.

Abstract: A ground penetrating radar (GPR) study has been conducted over the Brookwood aquifer in the Fraser Valley, southwestern British Columbia. Twelve kilometres of data were collected to assess the usefulness of GPR as a means of characterizing the stratigraphic architecture of the Brookwood aquifer. Existing well data in the area are compared with the GPR results. Over most of the study area, the signal penetration depth was 10 to 20 m. Strong reflections are visible from the water table and from lithological contacts identified from well data. Smaller scale reflections provide information about the spatial heterogeneity within stratigraphic units (e.g., large scale crossbedding). One three-dimensional survey (50 m x 25 m) was conducted and the data displayed using 3-D visualization techniques. The 3-D data set is a useful means of illustrating the geometry of sedimentary structures and potential anisotropy in aquifers.

Résumé : Un levé par géoradar a été réalisé au-dessus de l'aquifère de Brookwood dans la vallée du Fraser, dans le sud-ouest de la Colombie-Britannique. Des données ont été recueillies sur douze kilomètres pour évaluer l'utilité du géoradar pour caractériser l'architecture stratigraphique de l'aquifère de Brookwood. Les données de puits actuelles sont comparées aux données géoradar. Sur la majeure partie de la région à l'étude, la profondeur de pénétration du signal a varié de 10 à 20 m. De fortes réflexions sont visibles au niveau de la surface de la nappe d'eau souterraine et au niveau de contacts lithologiques reconnus dans les données de puits. Des réflexions à plus petite échelle renseignent sur l'hétérogénéité spatiale au sein des unités stratigraphiques (p. ex. stratification oblique à grande échelle). Un levé tridimensionnel (50 m x 25 m) a été réalisé et les données ont été visualisées en trois dimensions. Ces données tridimensionnelles constituent un moyen utile d'illustrer la géométrie des structures sédimentaires et l'anisotropie potentielle dans les aquifères.

¹ Department of Geophysics and Astronomy, University of British Columbia, Vancouver, British Columbia V6T 1W5

INTRODUCTION

Analysis of the regional stratigraphic framework of aquifers, groundwater flow, discharge, and recharge in the Vancouver lower mainland-Fraser Valley region, is one of two hydrogeology projects initiated in 1993 by the Geological Survey of Canada, (see Ricketts and Jackson, 1994; Woodsworth and Ricketts, 1994). Ground penetrating radar (GPR) is being used as an integral part of this study to determine the architecture of unconfined aquifers in the Surrey and Langley townships (Fig. 1). Imaging of the water table along the transects will also provide constraints for regional mapping of this potentiometric surface.

Ground penetrating radar is a geophysical technique ideally suited for shallow hydrogeological applications. Emitted electromagnetic waves are reflected at the boundary between two materials with different dielectric constants. Because most stratigraphic units have different dielectric

constants, a GPR survey can be used to image near-surface stratigraphy. The dielectric constant of water (80) is much higher than that of air and most earth materials. This contrast can produce a strong reflection from the water table in GPR surveys. For an in-depth discussion of GPR principles and methods, refer to Davis and Annan (1989).

An important consideration in conducting a GPR survey is the depth to which the subsurface can be imaged. Depth of penetration is dependent upon the materials through which the electromagnetic waves travel. In aquifers consisting of sand and gravel the depth of penetration is commonly 10-25 m. Conductive materials, such as clays or saline groundwater, dissipate the electromagnetic energy and severely attenuate the reflected signal. However, attenuation of the radar signal can be used to advantage, for example to locate units of high clay content, salt water intrusion, or contaminated groundwater plumes.

SURVEY LOCATION

The Brookwood aquifer is an unconfined aquifer covering an area of about 35 km², that straddles the Surrey-Langley municipality boundary (Fig. 1). It is a component of the Sumas Drift, deposited during the late Fraser Glaciation as outwash sand and gravel, with interfingering lodgement and flow tills, and glaciolacustrine clay (Armstrong, 1981, 1984; Halstead, 1986). Total aquifer thickness ranges from about 40 m, to zero at erosional pinchout margins. Correlative outwash 'fans' in Fraser Valley include the Abbotsford and Aldergrove aquifers.

The primary objective of the survey was to determine whether the subsurface stratigraphy could be mapped with GPR to help constrain the factors governing groundwater flow. A total of 12 km of radar data were collected and calibrated with lithological and static water level data from nearby wells; water table levels were used only from wells penetrating and producing from the Brookwood aquifer. The GPR survey includes one 3-D survey to examine local sedimentological complexities in greater detail.

DESCRIPTION OF EQUIPMENT AND DATA ACQUISITION PROCEDURE

The radar data were obtained using a *PulseEKKO IV* ground penetrating radar unit with 100 MHz antennas. The unit consists of:

1. a transmitting antenna and its electronics,
2. a receiving antenna and its electronics,
3. a control box; and
4. a portable computer (386, 20MHz)

Two types of surveys are carried out in GPR: reflection surveys, and common mid-point surveys (CMPs). Reflection surveys provide a profile of the subsurface. Common mid-point surveys are used to determine the velocity of the

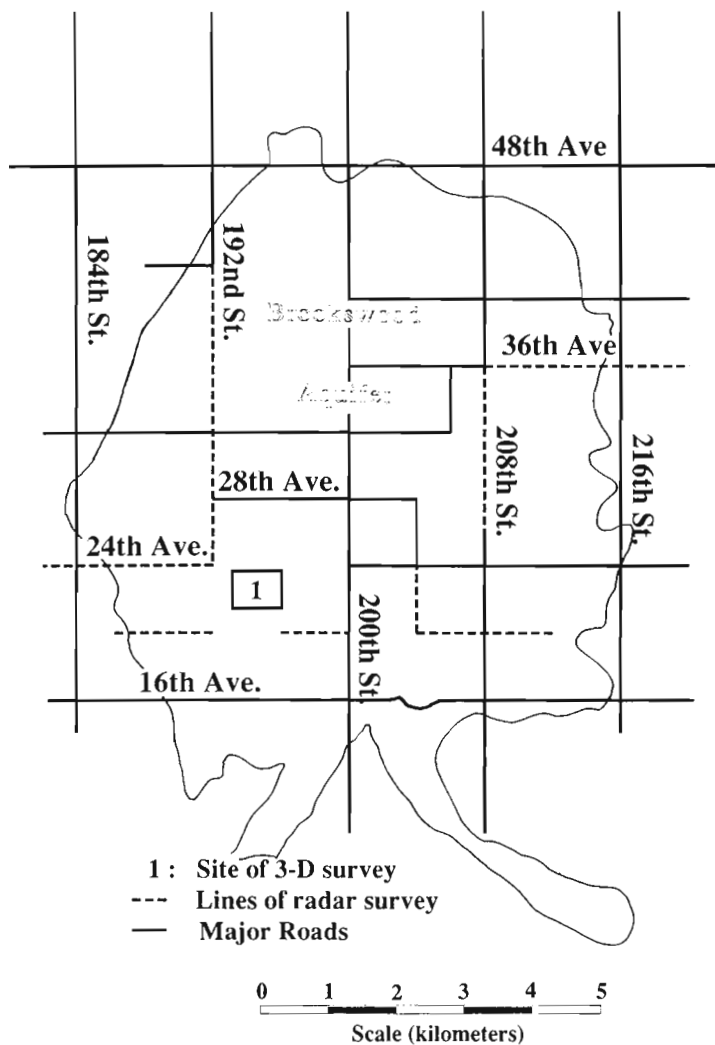


Figure 1. Location map of radar survey, also showing the outline of Brookwood aquifer (from Armstrong and Hicock, 1980).

electromagnetic waves in the subsurface and are a means of converting the time plot provided by a reflection survey to a more useful depth plot.

A reflection survey is carried out with the antennas parallel to one another, a fixed distance apart. A sounding is taken, and the antennas are then moved to the next station. The distance between stations is usually between 0.25 m and 2.0 m. The choice of station spacing depends on the desired resolution of the features in the subsurface, with closer station spacing producing radar images of higher resolution.

A short line was surveyed at three different station spacings (0.25, 0.5, and 1.0 m) to determine the appropriate station spacing to be used over the present study area (Fig. 2). It is clear that the resolution of dipping reflectors improves with decreasing station spacing. At 1 m spacing very little structure is visible except for a horizontal reflector at 0.1 μ s. In comparison, the 0.25 m spacing profile shows many more reflectors including what appears to be crossbedding between 15 and 30 m on the horizontal scale at a reflection time of 0.15 to 0.20 μ s. A station spacing of 0.5 m was selected as a compromise between resolution and time required for data acquisition.

Detailed resolution cannot be achieved in areas of high clay content where limited penetration precludes the detection of any subsurface structure (e.g., till or glaciolacustrine deposits). Where it is important to determine the extent of such clay bodies, because of their potential influence on groundwater flow, station spacing was increased to 1 m.

The spacing between the receiver and transmitter is determined at the beginning of a reflection survey. Antennas must not be so close together that there is an electronic saturation of the receiver, and not so far apart that near surface events are distorted by normal moveout. The antenna separation required to avoid saturation depends upon the type of material in the subsurface. In this survey, the most favourable antenna separation was found to be 0.6 m. The antennas must be kept at least 5 m from the computer to avoid electrical interference.

A common mid-point survey is conducted by placing the antennas approximately 20 cm apart on either side of a fixed centre point. A sounding is taken and the antennas are moved apart in equal steps, a sounding being taken at each step. The results of this type of survey can be analyzed to determine the velocities of different layers in the subsurface.

The radar unit time window (the length of time the receiver "listens" for reflected energy) was set to 512 ns; for longer times the signal-to-noise ratio becomes too low for reliable data interpretation. The *PulseEKKO* radar unit stacks the response from multiple transmitter signals in order to increase the signal-to-noise ratio. It has been found that a stack of 64 is optimal.

Most lines were collected on the gravel shoulder of roads crossing the aquifer. Where the shoulder was paved, signal penetration was decreased. Where possible, quiet side streets were chosen to minimize traffic and other cultural noise (underground pipes, etc.).

DATA PROCESSING

Processing of the ground penetrating radar data is carried out on a Sun work-station using a seismic processing package developed by Inverse Theory and Applications (ITA). The following steps are routinely followed during processing:

1. Data transfer: Data from the laptop computer are converted to SEG-Y format (a standard geophysical data format) and transferred to a Sun work-station.

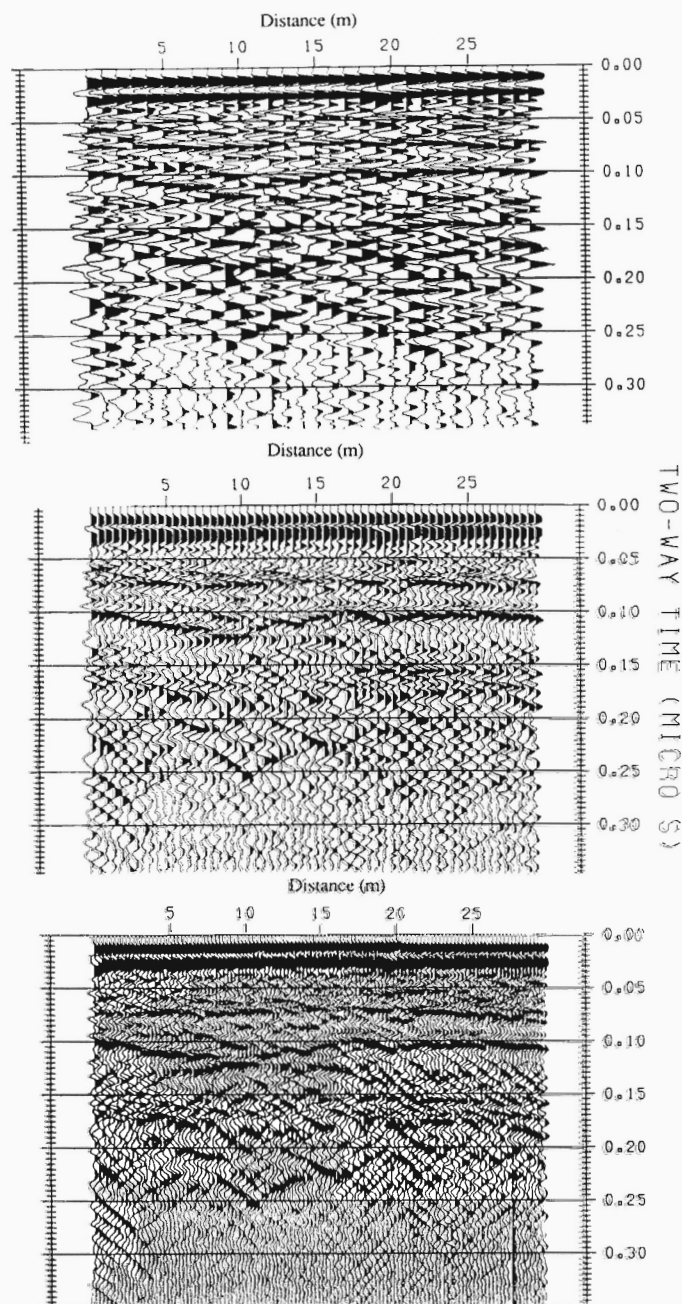


Figure 2. Three radar surveys over the same line with three different station spacings: 0.25 m, 0.5 m, and 1.0 m, showing improvement in resolution with closer spacing.

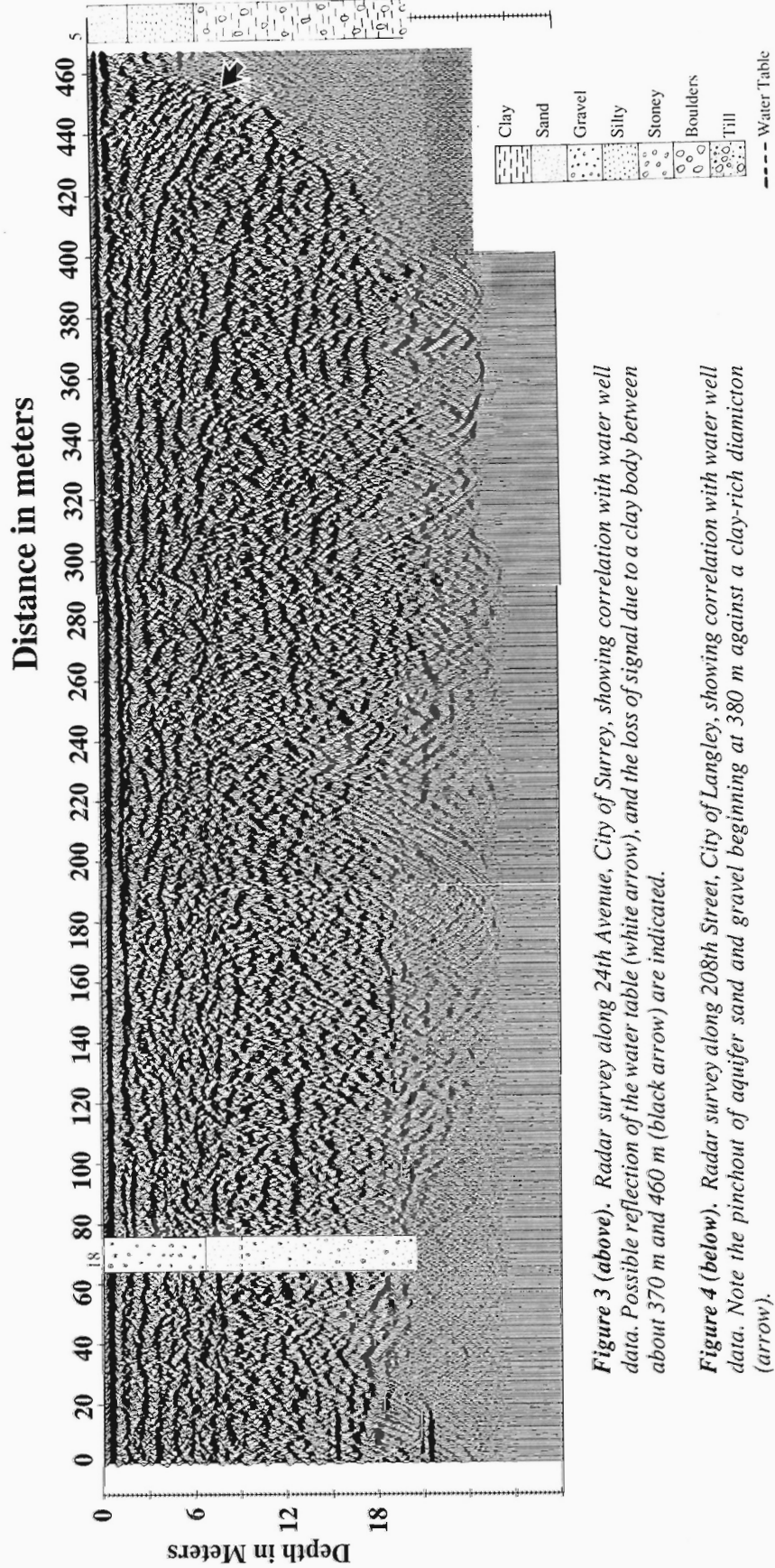
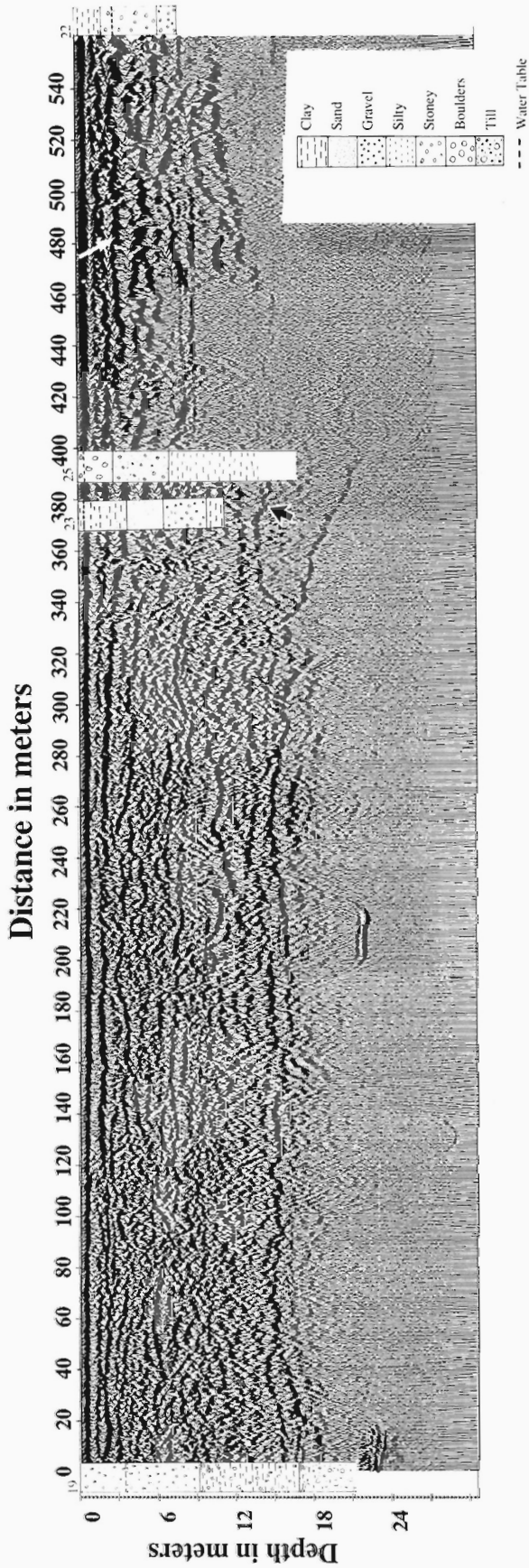


Figure 3 (above). Radar survey along 24th Avenue, City of Surrey, showing correlation with water well data. Possible reflection of the water table (white arrow), and the loss of signal due to a clay body between about 370 m and 460 m (black arrow) are indicated.

Figure 4 (below). Radar survey along 208th Street, City of Langley, showing correlation with water well data. Note the pinchout of aquifer sand and gravel beginning at 380 m against a clay-rich diamicton (arrow).

2. Time zero correction: The time at which the first signal from the transmitter reaches the receiver antenna, is designated as "time-zero". The time zero point may occur at a different time from trace to trace due to warming of the electronics or other noise factors. This drift must be corrected so that the first arrivals seen in the data occur at the same time.
3. Median filtering: The data must be filtered to remove any dc offset or signal "wow". The wow is a distorting effect caused by saturation of the electronics.
4. Gain: An automatic gain control gain is applied to the data to enhance reflections of lower amplitude. This gain operates by amplifying the signal within a given window to its maximum value.
5. Bandpass filtering: A bandpass filter with corner frequencies of 10, 15, 185, and 200 MHz is applied to the data to reject some of the high frequency noise and produce a cleaner signal.
6. Velocity calculations: Common mid-point surveys (CMPs) are collected at regular intervals along the survey lines. Velocity calculations completed to date show some variation in velocity, from 0.1 to 0.06 m/ns. This corresponds to dielectric constants between 10 and 25, consistent with materials from saturated silt to saturated sand.
7. Migration: The data are migrated in order to collapse any diffraction patterns and move dipping reflectors to their true subsurface locations. Velocities obtained from common mid-point surveys are used in the migration routines.

RESULTS

Two dimensional sections

Figure 1 shows the transects used for data collection. A continuous north-south line provides a nearly complete cross-section of the aquifer. A series of shorter east-west transects were collected in the southern half of the aquifer. The northern section of the aquifer is more densely populated and cultural noise precludes data collection in this area. Several lines have also been collected on outlying segments of the main Brookwood aquifer in an attempt to determine whether the stratigraphic architecture of these segments differ from those of the main aquifer.

Imaging stratigraphy

Initial correlation was carried out along two transects on the eastern side of the Brookwood aquifer. The transect along 24th Avenue east from 208th Street is shown in Figure 3 combined with data from nearby wells. The maximum depth of penetration is about 20 m. The first two strong continuous reflectors correspond to the air and ground arrivals and contain no useful information, however there is a lot of detail visible in the region below 1.5 m. At the beginning of the

profile (0 m) there is a strong reflection at a depth of 16 m. This correlates with data from well 19 which indicates a transition from gravel and clay to till. Beginning at 370 m, and continuing to 460 m along the profile, there is a distinct decrease in penetration depth corresponding to the presence of a clay lens, which is also recorded in wells 23 and 25. Channel structures are also imaged between 200 m and 300 m horizontal distance, at about 8-10 m depth.

The north-south transect along 208th Street (just south of 24th Avenue; Fig. 4) shows clearly the aquifer pinching out, or overlapping a clay-rich unit; penetration decreases to 2 m at the end of the profile (460 m). The presence of a pinchout in this area is confirmed by data from well 5. Also notable are the large foresets that dip into the clay-till confining unit.

Determining the depth to the water table

A strong reflection from the water table is clearly visible in many of the sections obtained. An example is shown in Figure 3. There is a strong, continuous reflector at a depth of 3 m at a horizontal distance of about 420 to 570 m along the profile. Correlation with well 22 indicates that this reflector corresponds to the water table; the data from wells 23 and 25 are ambiguous.

In Figure 5 data collected along the top of the Stokes gravel pit, about 3 to 3.5 m above the exposed water table, show a discontinuous reflector corresponding to a similar depth. The quality of the data here is lower than that collected from the roadside surveys, possibly due to the proximity to the cliff face and the heavy vegetation cover along the cliff top. Discontinuities in the reflector may be a result of interference from diffraction patterns or observed, large scale foresets crosscutting the water table.

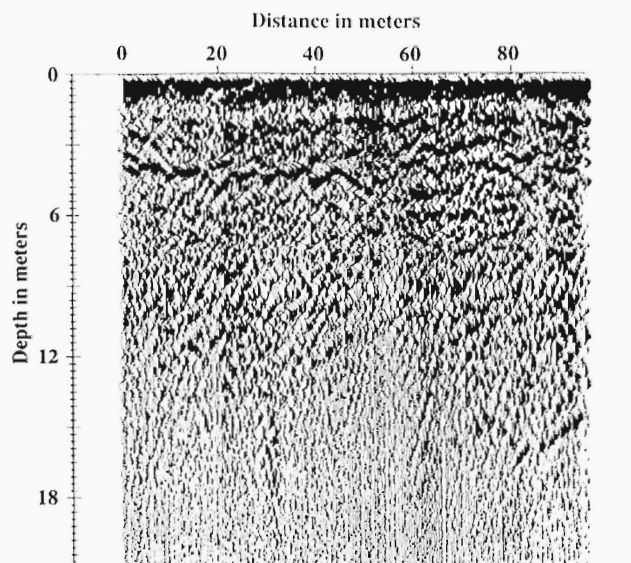


Figure 5. Radar survey in the Surrey municipal gravel pit showing possible reflection from the water table between 3 and 4 m depth.

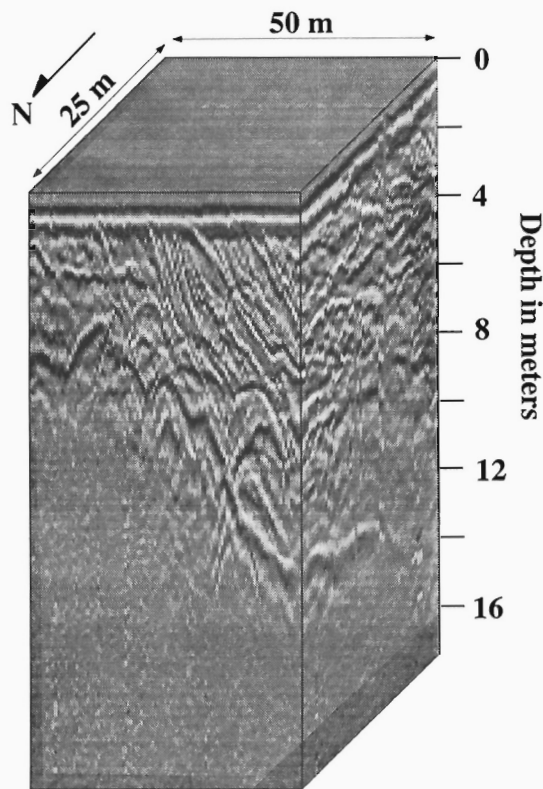


Figure 6. Results of 3-D survey in the Surrey municipal gravel pit. The imaged foresets (exaggerated dips in the model) dip 8° to 10° northwest in nearby pit exposures. Depth in metres.

Three-dimensional section

A 3-D radar data set was collected in the Langley municipal gravel pit (Fig. 1). The 25 m by 50 m survey was located in the southwest corner of the gravel pit in an area that had been excavated almost to the water table. Water was visible in ditches about 0.5 m from the surface on the north, west, and south sides of the pit. Fifty-one, parallel survey lines, spaced 0.5 m apart were collected to create a 0.5 m square grid spacing. The total length of the survey was 2.55 km and the total number of soundings was 5151. The CMPs from the gravel pit give a velocity of about 0.08 m/ns, corresponding to a dielectric constant of 14.

The data (Fig. 6) show generally southwest-dipping sand and gravel layers. The depth of penetration is 12 m on the western side of the survey, decreasing to 6 m on the eastern side. Interbedded clay and sand in delta or estuarine point-bar foresets (see Ricketts and Jackson, 1994) are exposed just north of the survey grid, which possibly account for the decreased penetration. To further investigate this transition in penetration, we collected an additional line of data east from the 3-D grid. The results show a variation in depth of penetration which correspond to the clay lens exposed in the trench. We are currently developing methods of calculating the true dip of sedimentary layers from the 3-D radar images.

CONCLUSIONS

Based on the results obtained to date, we conclude that ground penetrating radar is useful for:

1. Regional mapping of unconfined, coarse grained aquifers, with more precise definition of aquifer boundaries.
2. Imaging the stratigraphy of an aquifer and providing a means of correlating lithological information obtained from wells and outcrops.
3. Providing better definition of aquifer heterogeneity.
4. Mapping the water table in an aquifer. Regular measurements along selected transects would provide details of seasonal variations in water table depth.
5. Imaging an aquifer in 3-D, enabling a more detailed analysis of the structure of the aquifer, the degree of anisotropy, and the possibility of calculating true dip of sedimentary layering.

ACKNOWLEDGMENTS

John Amor is thanked for his invaluable aid in the processing and visualization of the radar data. Hugh Liebscher (Environment Canada) is thanked for valuable discussions and advice. Rodney Zimmerman, Groundwater Section, B.C. Ministry of Environment, Lands and Parks kindly supplied water well information. Field assistants were Parisa Jourabchi and Paulette Tercier. John Luternauer provided a thorough review of the manuscript.

REFERENCES

- Armstrong, J.E.**
1981: Post-Vashon Wisconsin glaciation, Fraser Lowland, British Columbia; Geological Survey of Canada, Bulletin 322, 34 p.
1984: Environmental and engineering applications of the surficial geology of the Fraser Lowland, British Columbia; Geological Survey of Canada, Paper 83-23, 54 p.
- Armstrong, J.E. and Hicock, S.R.**
1980: Surficial geology, New Westminster, British Columbia; Geological Survey of Canada, Map 1484A, scale 1:50 000.
- Davis, J.L. and Annan, A.P.**
1989: Ground-penetrating radar for high resolution mapping of soil and rock stratigraphy; *Geophysical Prospecting*, v. 37, p. 531-551.
- Halstead, E.C.**
1986: Ground water supply – Fraser Lowland, British Columbia; National Hydrology Research Institute Paper No. 26, Inland Waters Directorate, Environment Canada, Scientific Series No. 145, 80 p.
- Ricketts, B.D. and Jackson, L.E.**
1994: An overview of the Vancouver-Fraser Valley hydrogeology project, southern British Columbia; in *Current Research 1994-A*; Geological Survey of Canada.
- Woodsworth, G.J. and Ricketts, B.D.**
1994: A digital database for groundwater data, Fraser Valley, British Columbia; in *Current Research 1994-A*; Geological Survey of Canada.

Preliminary studies of currents on Sturgeon Bank, Fraser River delta, British Columbia

Tracey D. Feeney¹
Cordilleran Division

Feeney, T.D., 1994: Preliminary studies of currents on Sturgeon Bank, Fraser River delta, British Columbia; in Current Research 1994-A; Geological Survey of Canada, p. 217-224.

Abstract: Current velocity and directional data are critical to the study of sediment movement on the intertidal area of Sturgeon Bank. Data collected using InterOcean S4 current meters for one month at five stations show that currents on the bank are highly variable in both speed and direction. In general, flow is bidirectional with flooding currents on the outer bank (seaward) having higher average velocities, while currents on the inner bank (shoreward) show no preferred orientation or peak velocity measurements. Current meters deployed adjacent to coastal structures or tidal channels reveal data which reflect these interferences. Measuring physical processes in this environment is a difficult task and rarely attempted but this valuable information can assist in the analysis of sediment dynamics in an important part of the deltaic environment.

Résumé : Les données sur la vitesse et la direction des courants sont d'une importance cruciale pour l'étude des mouvements de sédiments dans la zone intertidale du banc Sturgeon. Les données recueillies par courantomètre *InterOcean S4* pendant un mois à cinq stations indiquent que les courants sur le banc sont très variables en vitesse et en direction. En général, l'écoulement est bidirectionnel mais les courants de flot sur la partie externe du banc (vers le large) présentent des vitesses moyennes plus élevées tandis que les courants sur la partie interne du banc (vers le continent) n'indiquent aucune orientation préférentielle ni vitesse de pointe. Les courantomètres déployés près des ouvrages côtiers ou des chenaux de marée produisent des données qui reflètent ces interférences. La mesure des processus physiques dans cet environnement est une tâche difficile qui a rarement été mise à l'essai, mais ces informations valables peuvent aider à analyser la dynamique des mouvements de sédiments dans une partie importante du milieu deltaïque.

¹ Department of Oceanography, University of British Columbia, 6270 University Boulevard, Vancouver, British Columbia V6T 1Z4

INTRODUCTION

The study of sediment dynamics in the marine environment provides locations of erosion, deposition, and pathways of sediment migration. This knowledge allows determination of the stability of the environment, the sediment budget, and the pathways of pollutants associated with these sediments. Deltas are dynamic environments with physical processes such as waves, tides, and river runoff contributing to their ever-changing morphology. In order to understand the sediment dynamics associated with the deltaic environment, a knowledge of the physical processes at work is needed. This is difficult primarily because the bank is exposed for long periods due to tides. This limits methods traditionally used in the study of physical oceanography because the equipment is designed for sampling in water and not air. The presence of shifting tidal channels and man-made structures complicate the problem even more.

STURGEON BANK

Sturgeon Bank is an intertidal sand and mud flat located on the western front of the Fraser River delta in British Columbia (Fig. 1). It extends 13 km from the north arm to the main arm of the Fraser River and is 6 km wide on average. The effects of jetty construction,

in addition to those of pollutant discharge on Sturgeon Bank, make it an important area for studying the physical processes involved in sediment dynamics. Sturgeon Bank is an important habitat for a variety of marine and freshwater species and it protects a highly productive brackish marsh at its landward edge, so monitoring effects on this environment is essential. Although the Fraser River is discharged primarily north of the north arm jetty and south of the Steveston jetty (Fig. 2), approximately 5% of the total river flow is discharged on to Sturgeon Bank through the middle arm (Luternauer and Murray, 1973). Maximum water wave heights of 1.52 m and average heights of 0.6 m have been documented for the area (Hoos and Packman, 1974). Mixed semidiurnal tides rise as high as 4.8 m above chart datum (Canadian Hydrographics Service, 1972; Thomson, 1977). Surface currents on the seaward edge of Sturgeon Bank flow north at rates ranging from 2.6 to 5.1 cm/s while currents below the surface average 2.6 cm/s, but range from 1.5 to 5.1 cm/s (Giovando and Tabata, 1970; Tabata et al., 1971).

PREVIOUS WORK

An annular field flume called the Sea Carousel was deployed at 10 stations (Fig. 2) on Sturgeon Bank to determine sediment response to currents (C.L. Amos, pers. comm., 1993). The flume was lowered to the seafloor at high tide and a current of known velocity was created in the annulus and then incrementally increased. Optical backscatter imagers

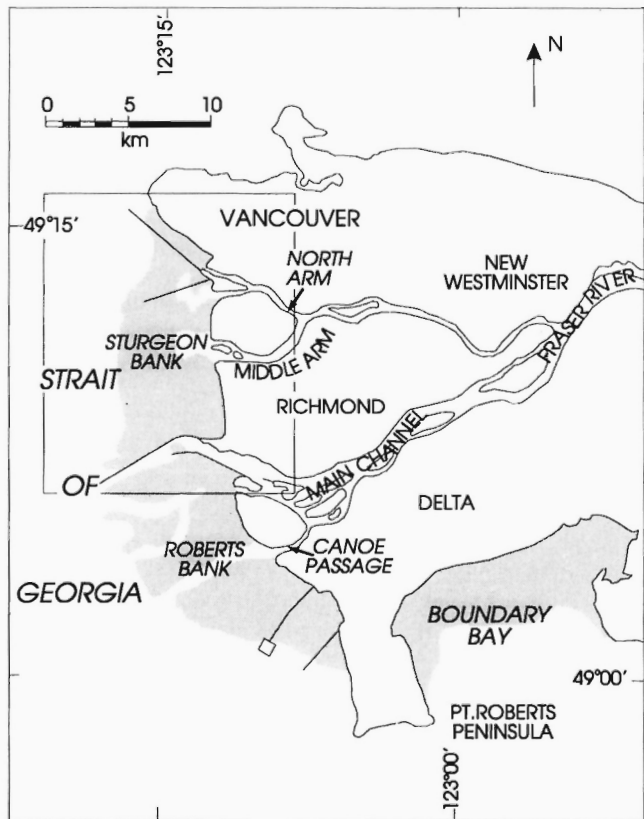


Figure 1. The Fraser River delta, British Columbia. The study area, Sturgeon Bank, is enclosed within the box.

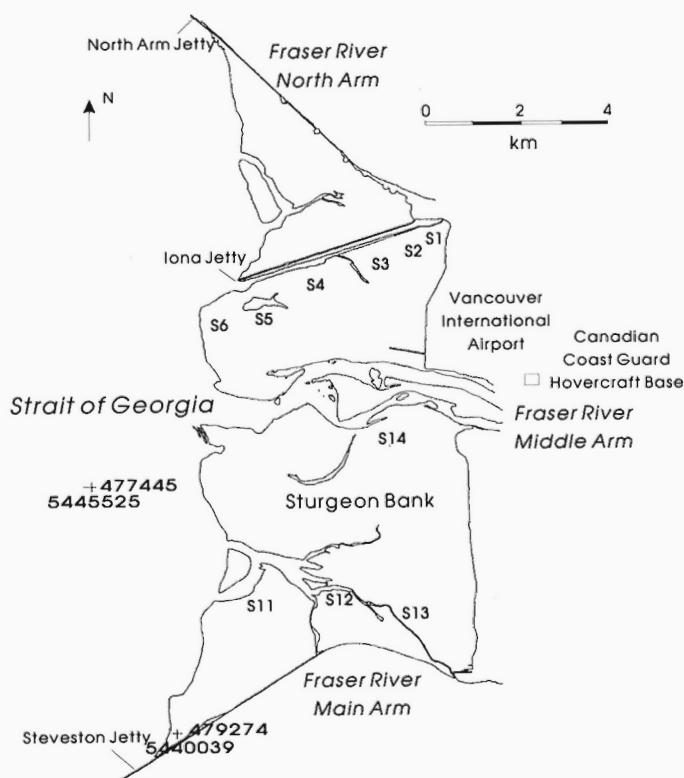


Figure 2. Station location for Sea Carousel and current meter data collection. Only stations 2, 4, 6, 12, and 14 results have been examined in this paper.

measured the amount of sediment in suspension at each velocity and thus provided the volume of sediment eroded from the bottom. See Amos et al. (1992) for a detailed process description. Sea Carousel results include values for the critical threshold for erosion and deposition. This study attempts to determine the real current velocities on Sturgeon Bank so that the Sea Carousel results can be calibrated.

CURRENT VELOCITY

Current velocity acquisition

In order to determine current properties on the bank, six InterOcean S4 current meters were deployed at the Sea Carousel stations for one month, (locations on Fig. 2) using the Canadian Coast Guard hovercraft. Station 4 was occupied for two months. S4 current meters are an excellent tool for analyzing currents in shallow water because they allow the effects of waves to be filtered out upon processing so that only tidal effects may be seen.

The current meters were calibrated in the laboratory for salinity, temperature, direction, and velocity. They were also cold temperature tested to ensure they would continue data collection if temperatures on the bank decreased. Aluminum poles, 1-1.5 m in length, were screwed into the base of the current meter and then shoved, by hand, into the sediments. A plexiglass plate was placed on the rod 30 cm below the base of the current meter to ensure that it did not sink further into the sediments over the month of deployment. The electrodes were wiped down with ethanol prior to leaving the site and then care was taken not to splash them with the hovercraft as it moved away. Each current meter was programmed to sample every 1.5 seconds for speed and direction of currents. After 10 data entries (15 seconds) an additional line of information including conductivity, temperature, density, salinity, the speed of sound and in some cases the depth and tilt angle of the instrument, were recorded. This data was only recorded every 15 seconds to preserve more memory in the internal S4 computer for current velocity and direction measurements. This procedure was repeated 3 more times (a total of 1 minute) after which the instrument shut itself off for the following 59 minutes. On the next hour, the S4 would "wake up" and begin sampling again at a rate of 1.5 seconds for one more minute, recording additional data at the end of every 15 seconds. This continued from May 7, 1993 at 14:00 to June 3, 1993 at 08:00 (PST). After one month the current meters were removed, the data was extracted and the current meter re-initialized so that it could be redeployed at the other stations. The data collected during the second month of this survey will not be examined this paper. The first months' data was carefully analyzed to determine when the tide was at a sufficient height to cover the electrodes on the current meter. This was possible because the current meter deployed at station 4 was equipped with a pressure sensor to measure depth of inundation. The depths at station 4 acted as a guide to determine the times when current meters at the other stations were inundated. Data from station 4 was not used unless a depth of 0.5 m was recorded which ensured that the electrodes collecting the measurements were sufficiently in

the water. Data collected at station 6 and 12, was not used unless a depth of 0.1 m was being recorded at station 4. For station 2 and 14, data was not used unless a depth of 1 m was being recorded at station 4. Conductivity measurements assisted in the determination of S4 exposure or inundation. Ignoring the first hour of data collected with good conductivity measurements and keeping the data collected one hour after this ensured that no questionable data was included. This procedure was closely followed but rare exceptions were made as it seemed that tides did not rise and fall at the same rate at different stations.

Data presentation

Current directional data for stations 2, 4, 6, 12, and 14 were divided into 10° increments and plotted as frequency of occurrence in Figures 3-7. Both a rose diagram and frequency histogram were produced for ease in data visualization. The population of the data used in the generation is given in the legend. Data collected from current meters situated on the inner tidal flat will have a smaller population because of the shorter period of inundation. The maximum percentage in one 10° class interval is given in the legend and the mean percentage is based on the percentage values in each petal or cell. Standard statistics of deviation and trend were calculated using methods of Davis (1986). A confidence interval of 95% was used throughout the calculations. It should be noted that R-mag, the resultant of the vector mean standardized to range between 0 and 1, is useful for unidirectional flow but when flow is bidirectional or multidirectional, as it is under the influence of waves and tides, the use of R-mag becomes limited.

After the data had been divided into 10° class intervals, their associated velocities were averaged and plotted on Figures 3 to 7. Although rose diagrams are an excellent way of representing current direction, they provide no information on the magnitude of the current speeds related to these orientations. Including another variable in rose plots was considered difficult to visualize. Plotting a frequency histogram below a velocity graph shows the current velocities associated with their directions. It should be noted that current velocities for each class interval may exceed or fall below mean velocities to a large extent. Currents generated by waves may have single velocities several times that of the mean. In terms of sediment dynamics, average velocity values may not be a useful variable to measure because sediment transport utilizes velocities over a certain threshold.

RESULTS

Current plots for station 2 show no strongly preferred orientation for currents (Fig. 3). This station is close to the shoreward edge of the bank, a place tides reach infrequently. It is, therefore, not surprising to find current directions quite scattered, probably reflecting very low net sediment movement in this area. Average current velocities at this station are consistent with direction results. Velocities show no distinct increase or decrease in any preferred orientation and velocities in all directions average 6 cm/s.

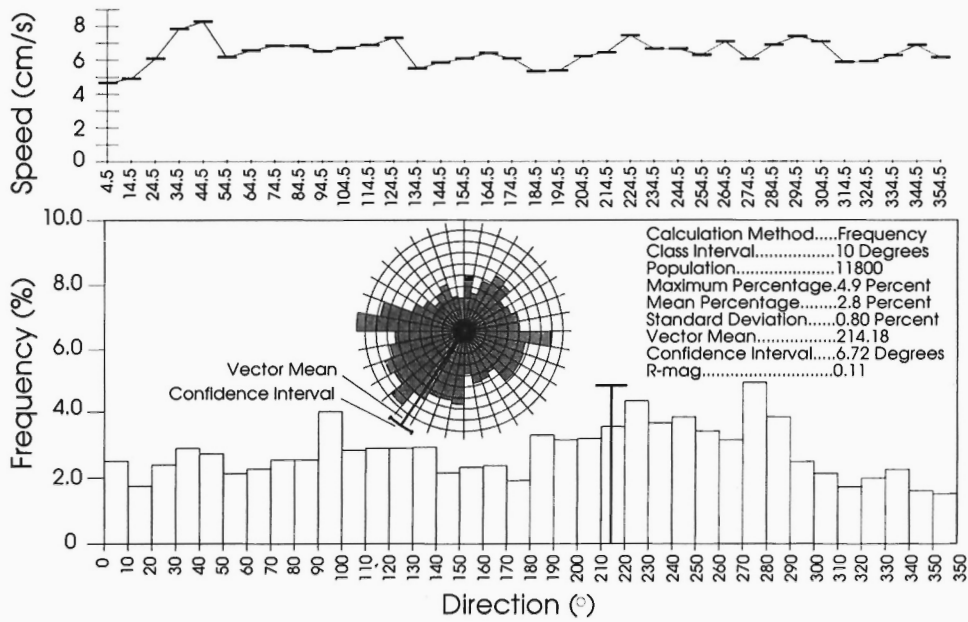


Figure 3. Current speed and frequency of flow direction over 10° intervals for station 2. Horizontal bars in the current speed profile indicate the class interval in which the data was averaged. Statistics were calculated using methods by Davis (1986).

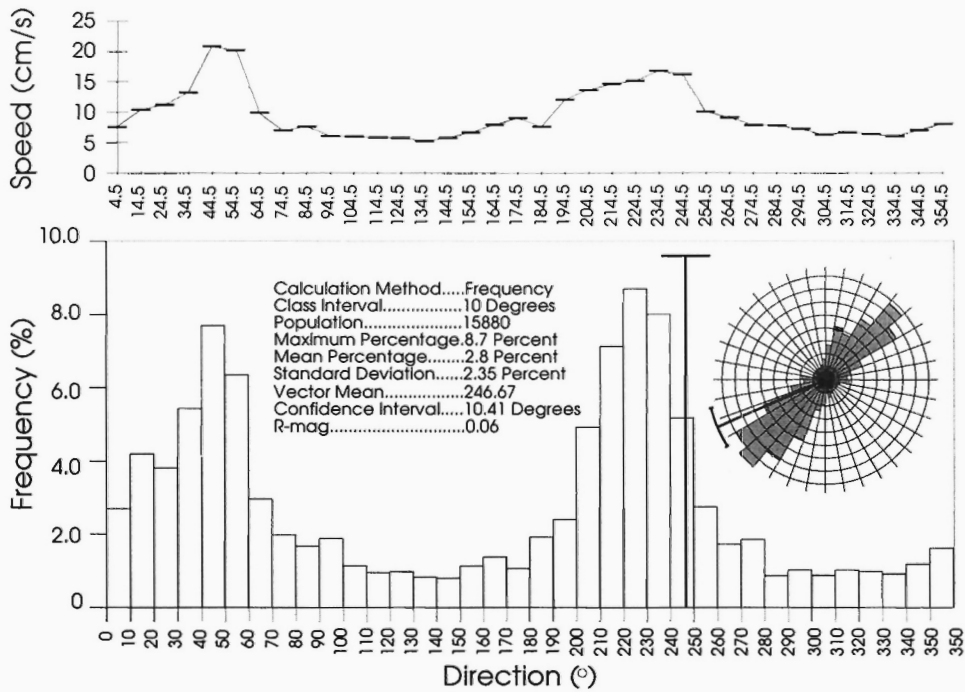


Figure 4. Current speed and frequency of flow direction over 10° intervals for station 4. Horizontal bars in the current speed profile indicate the class interval in which the data was averaged.

Data from station 4 shows marked trends in both current velocity and direction as is expected from a station in the middle of the bank. The strong bidirectional flood and ebb tidal directions can be seen in the rose diagram with the frequency of ebb directions being slightly higher than those of the flood directions (Fig. 4). The frequency histogram and the average current velocity profile are used to demonstrate the higher current velocities associated with the flood tide. Worth noting is the sharp peak in velocity in the flood direction, 22 cm/s, versus the lower, more broad peak in the ebb direction, approximately 18 cm/s (i.e. the flood tide is more focused in one direction than the ebb). The net direction is seaward and the flows are oriented at approximately 50° and 230° for the flood and ebb tide, respectively.

In contrast, station 6 direction measurements show bidirectional tidal type flow with dominant flow directions approximately 90° for the flood and 250° for the ebb (Fig. 5). The net direction of flow is shoreward. Current velocity measurements are highest here because this station is located at the outer edge of the bank. Average velocities reach 23-24 cm/s on both the flood and ebb tide and maintain velocities over 12 cm/s throughout most of the tidal cycle.

Station 12 results are similar to those at station 6 with the exception of a dominant southward flow being present (Fig. 6). The bidirectional tidal influences are recognizable but a substantial amount of flow heads south toward the Steveston jetty. Current velocities measured here are lower than at station 6, but are similar in that two peaks in the flood and ebb directions and be seen. Like station 4, the flood velocity peak is slightly higher (18 cm/s) with a more focused orientation than the ebb velocity peak (14 cm/s).

Results from station 14 show net current directions shoreward with very little contribution in the ebb tidal direction (Fig. 7). There is a reasonable amount of scattering which, like station 2, is not surprising due to the position of station 14 on the bank. Velocity measurements at station 14, however, are almost twice as high in the seaward direction as they are in the shoreward direction. Peaks of 15 cm/s for the ebb tide versus 7-10 cm/s for the flood tide were found.

DISCUSSION

Directional information for stations 2, 4, 6, 12, and 14 indicate that flow on Sturgeon Bank is variable (summarized on Fig. 8). Stations on the eastern edge (shoreward) of the bank (2 and 14) show large scattering in directional data and low and essentially constant velocities through the range of directions. One minor exception is the high velocity in the seaward direction at station 14. Because the frequency of flow in this direction is low, these speeds must only be reached for short times during the tidal cycle. Station 14 is adjacent to the middle arm of the Fraser River, the flow of which, although only 5% of the total Fraser River flow, must be substantial at low tides to produce these large current velocities.

Net current directions on the middle and outer bank stations demonstrate a strong bidirectional component of flow due to the tides, however these directions vary from station to station. Station 4 demonstrates bidirectional flow in a northeast/southwest direction, where as both station 6 and station 12 exhibit east/west flow directions normal to the edge of the bank. Station 12 has an additional component of

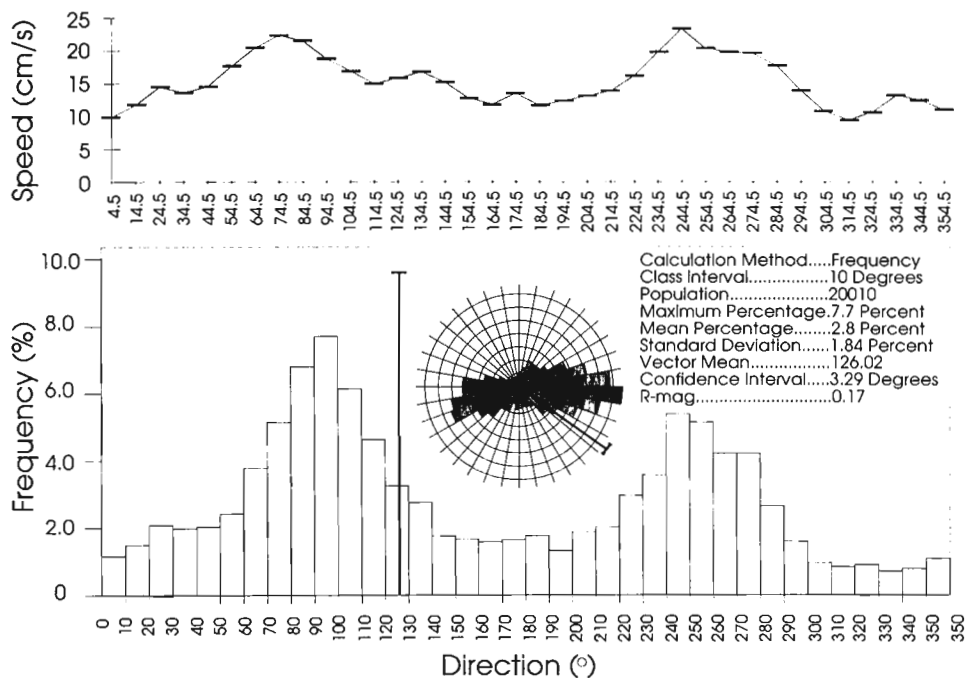


Figure 5. Current speed and frequency of flow direction over 10° intervals for station 6. Horizontal bars in the current speed profile indicate the class interval in which the data was averaged.

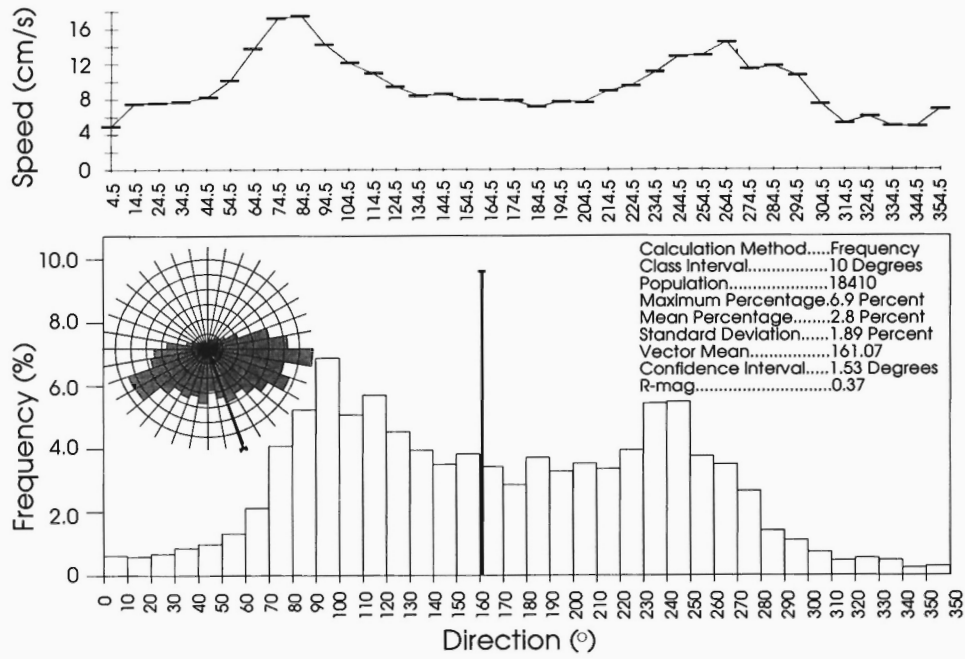


Figure 6. Current speed and frequency of flow direction over 10° intervals for station 12. Horizontal bars in the current speed profile indicate the class interval in which the data was averaged.

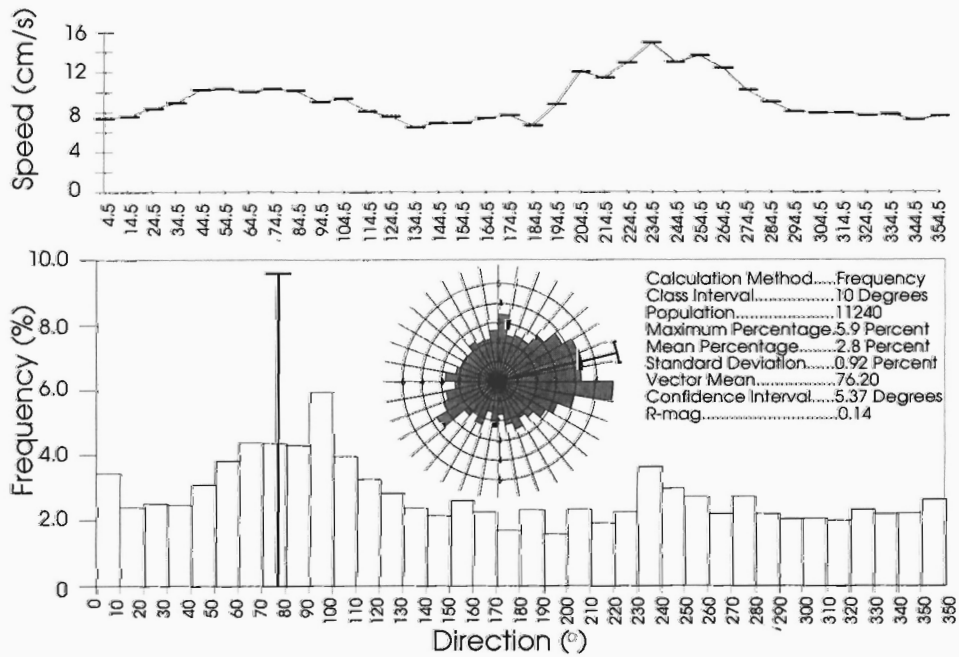


Figure 7. Current speed and frequency of flow direction over 10° intervals for station 14. Horizontal bars in the current speed profile indicate the class interval in which the data was averaged.

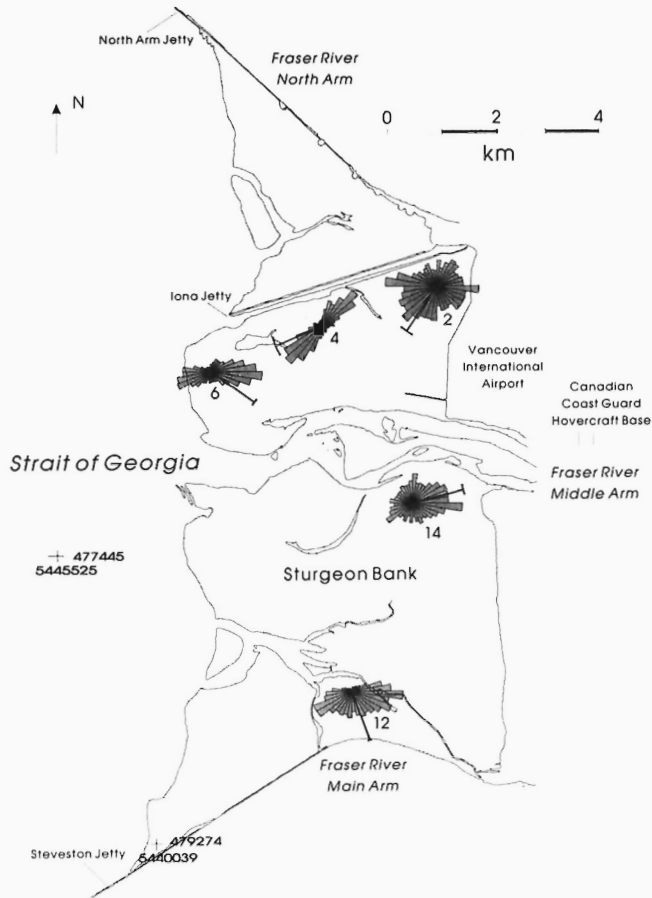


Figure 8. Summary of flow directions on Sturgeon Bank using rose diagrams from stations 2, 4, 6, 12, and 14. Frequency scales have been removed for ease in visualization.

flow to the south which has not yet been explained. The data also reveals a trend of higher velocities in the northern portion of the bank. This observation is not well defined and will need the support data from the stations not yet analyzed to confirm this hypothesis. It should be noted that the vector mean is not an absolute current direction. From the rose diagrams, the dominant direction of flow can be seen and minor variations in flow direction can change the position of the vector mean considerably. The analysis of surface currents at the seaward edge of Sturgeon Bank conclude that currents flow north at 2.6 to 5.1 cm/s and that currents below the surface range from 1.5 to 5.1 cm/s (Giovando and Tabata, 1970; Tabata et al., 1971). These results are not consistent with the results obtained from this survey where average velocities at the edge of the bank are commonly three times higher than those observed in the previous study. Current meters used in this study measured currents 50 cm from the seabed surface rather than the sea surface, so the results of the two studies can not be directly compared.

Data from stations 1, 3, 5, 11, 13, and the second deployment of station 4 has not yet been analyzed and may contribute additional information to these initial studies. Time series plots of salinity, and temperature measurements would also provide data useful in understanding the physical processes on Sturgeon Bank.

CONCLUSIONS

Studying the physical processes on an intertidal flat has rarely been attempted because of the many outside variables that evolve when trying to analyze the data. Coastal structures, channel migration, and exposure time all make analyzing the effects of waves, tides, and river runoff on intertidal deltas a difficult task. InterOcean S4 current meters are a useful tool for determining the net current directions and their magnitude of flow. Current meter studies on Sturgeon Bank, to date, imply variable conditions throughout the bank thus making extrapolation across the bank difficult. Current measurements determined are therefore only useful within short distances from where they were taken.

In general, current flow directions on Sturgeon Bank are bidirectional with a dominant increase in velocity for the flooding tide and possibly higher velocities in the northern portion of the bank. The flooding tide also shows less random orientations in its net current direction. This is only one step in determining the flow characteristics on Sturgeon Bank, but the information is valuable because this type of study has not previously been attempted. In situ suspended sediment concentrations across the bank as well as an accurate topographic map of the bank are additional tools that will enable us to calibrate the results of the Sea Carousel model to determine the stability of Sturgeon Bank, its sediment budget, and the pathways of sediment on its surface.

ACKNOWLEDGMENTS

The author would like to thank Steve Pond who loaned the current meters and spent hours in the lab calibrating them. If not for his rigorous testing, the data may never have been collected in such a difficult environment. John Luternauer provided the funding for this survey and Paul LeBlond supplied the expertise on methods of current meter analysis. The members of the Canadian Coast Guard hovercraft search and rescue unit made sampling on the delta much easier; they were patient, always cheerful and willing to monitor the condition of the current meters on the bank whenever they could. Peter Mustard spent hours assisting writing programs to reduce the data and critically reviewed the paper. Hugh McLean assisted in the deployment and recovery of the current meters. A special thank-you goes to Bev Vanlier whose patience was appreciated.

REFERENCES

- Amos, C.L., Grant, J., Daborn, G.R., and Black, K.**
1992: Sea Carousel - A benthic annular flume; *Estuarine Coastal Shelf Science*, v. 34, p. 557-577.
- Canadian Hydrographic Service**
1972: Canadian tide and current tables (Juan de Fuca and Georgia Strait); v. 5, p. 14.
- Davis, D.C.**
1986: *Statistics and Data Analysis in Geology*; Wiley, New York, 646 p.
- Giovando, L.P. and Tabata, S.**
1970: Measurements of surface flow in the Strait of Georgia by means of free-floating current-followers; Fisheries Research Board of Canada Technical Report 163, 69 p.
- Hoos, L.M. and Packman, G.A.**
1974: The Fraser River estuary: status of environmental knowledge to 1974; Canada Department of the Environment Regional Board, Pacific Region, Special Estuary Series No. 1, 518 p.
- Luternauer, J.L. and Murray, J.W.**
1973: Sedimentation on the western delta-front of the lower Fraser River, British Columbia; *Canadian Journal of Earth Sciences*, v. 10, p. 1642-1663.
- Tabata, S., Giovando, L.F., and Devlin, D.**
1971: Current velocities in the vicinity of the Greater Vancouver Sewerage and Drainage District's Iona Island Outfall, 1968; Fisheries Research Board of Canada Technical Report 263, 110 p.
- Thomson, R.E.**
1977: The oceanographic setting of the Fraser River delta front; unpubl. manuscript, Institute of Ocean Sciences, Patricia Bay.

Geological Survey of Canada Project 860022

Two centimetre-level Global Positioning System surveys of intertidal habitat, Fraser River delta, British Columbia

Jennifer A. Aitken¹ and Tracey D. Feeney¹
Cordilleran Division

Aitken, J.A. and Feeney, T.D., 1994: Two centimetre-level Global Positioning System surveys of intertidal habitat, Fraser River delta, British Columbia; in Current Research 1994-A; Geological Survey of Canada, p. 225-230.

Abstract: The purpose of this study was to establish a highly accurate surveying method suited to delta habitats. A four day survey in the lower Fraser River delta employed Global Positioning System (GPS) survey techniques and Canadian Coast Guard Search and Rescue hovercraft. The survey was conducted in two parts: elevation data were obtained in twelve transects between Iona and Steveston jetties and a survey in Ladner Marsh used GPS positions to reference vegetation samples. The post processed GPS positions are accurate to 10 cm or less in three dimensions. This approach is suited for surveying intertidal areas which are difficult to access and are not represented on bathymetric and topographic maps in detail.

Résumé : Cette étude a pour objet d'élaborer une méthode de levé très précise adapté aux habitats situés dans les deltas. Pour un levé de quatre jours dans le delta du bas Fraser (Colombie-Britannique), on a eu recours à des techniques faisant appel au système de positionnement global (SPG) et à un aéroglisseur de recherche et de sauvetage de la Garde côtière canadienne. Le levé a été réalisé en deux parties : les données sur l'altitude ont été obtenues suivant douze profils entre les digues d'Iona et de Steveston, et un levé a été réalisé dans le marais Ladner en employant les positions établies par SPG pour localiser les points de prélèvement d'échantillons de végétation. Les positions établies par SPG, suite à un traitement des données, sont exactes à plus ou moins 10 cm dans les trois dimensions. Cette méthode est adaptée à la réalisation de levés dans les zones intertidales qui sont difficiles d'accès et qui ne sont pas représentées en détail sur les cartes bathymétriques et topographiques.

¹ Department of Oceanography, University of British Columbia, 6270 University Boulevard, Vancouver, British Columbia V6T 1Z4

INTRODUCTION

The study of sediment dynamics and its effect on beach morphology is a difficult one. Large intertidal areas are relatively unstudied because of the short window of access between successive tides, coupled with inhospitable working conditions including waist deep mud and densely packed marsh vegetation. Intertidal flats may form as a result of delta progradation and in these cases river flow as well as the physical processes such as waves and tides will effect the sediment dynamics. Rivers may also serve as source of pollutants that can be deposited on tidal flats.

An approach is needed to cover large, difficult to access areas in a short time with a high degree of precision. The resulting positions can be used to map and monitor changes in elevation, sediment volume, to reference ground truth observations, and as input for digital terrain models (Morton and Leach, 1993). Mapping and monitoring have been limited to airphoto and discrete ground sampling. These techniques are time consuming and expensive, are often spatially inaccurate, and subject to human interpretation.

A full overview of the Global Positioning System is beyond the scope of this paper, and the reader is referred to Leick (1990) or Wells et al. (1987). Morton and Leach (1993) provided an introduction for a kinematic GPS survey of beach sediments. This paper focuses on a GPS survey conducted July 30-August 2 (corresponding to day of year 211-214) of Sturgeon Bank and the Ladner Marsh Estuary (Fig. 1).

STURGEON BANK STUDY AREA

The intertidal areas of Sturgeon Bank and Roberts Bank on the Fraser River delta (Fig. 1) protect a highly productive marsh on the landward edge and are important habitats for fish and waterfowl. Sturgeon Bank was chosen as the primary focus for this study because it has been the site of sewage discharge and because of concerns with the stability of the western delta front (Luternauer, 1980; Medley, 1978; Medley and Luternauer, 1976). The Iona sewage treatment plant discharged Vancouver's sewage directly onto Sturgeon Bank until 1987, when the outfall was moved to 100 m depth on the delta slope. Sturgeon Bank extends 13 km from the North Arm jetty in the north to the Steveston jetty in the south and is 6 km wide on average (Hoos and Packman, 1974). The marsh accounts for approximately 8% of the area; sand and mud flats account for the remaining area. Shallow tidal channels and large scale bedforms are present throughout the bank (Medley and Luternauer, 1976). Documenting the short term changes in morphology will demonstrate the extent of channel migration across the tidal flats as well as the migration of polluted sediments. Long term monitoring of morphological changes show whether the bank is stable. The livelihood of the marsh is dependent on these changes. Long term morphological changes may also assist in assessing the outcome of sea level rise due to global warming.

Attempts have been made in the past to map the morphology of the intertidal areas on the Fraser River delta (Medley and Luternauer, 1976). Aerial photography was used to map the incoming tide as a contour line (Tupper, 1977). Although effective to date, aircraft costs to fly for an entire incoming tide make this a prohibitively expensive procedure. In addition, the time needed to complete successive flight lines allows the tide to move substantial distances so the resultant contour lines are never stationary. Ground-truthing the precise depth of these contours is also difficult because winds on or off shore will shift their position. Additional problems include the scarcity of extreme low tides, the occurrence of winter extreme low tides at night and the need for a clear day with little wind. The largest source of error in this method is the determination of the position of the tidal line by human interpretation. Sections of the tidal flats remain wet-looking all the time and the exact position of the tidal line often is ambiguous. Although a topographic map of Sturgeon bank was produced using this method (Tupper, 1977), the repeatability of this study is limited because of the many conditions which must be satisfied for successful contouring and the ambiguity in line positioning. Traditional surveying techniques have also been employed with some success but the size of Sturgeon Bank also limits this method. Shore-parallel transects 9 km long (the distance between the Iona and Steveston jetties) would be impossible to complete in the short time the tide is out, whereas shore-normal transects must pass through a muddy bank where it is not unusual to sink above the knees.

The survey method of this study is not weather dependent, is not ambiguous and can be repeated at any time for monitoring changes in bank morphology. The Canadian Coast Guard hovercraft was used for this study because of its proximity to the delta and its manoeuvrability on both the water and land. The GPS survey technique provides highly accurate three-dimensional positions at a rapid data rate (one position per second). This technique allows monitoring of changes over time to determine areas of erosion, deposition and sediment migration. The position information can be directly incorporated into a GIS (Geographical Information System) to create one dimensional profiles, a two-dimensional contour map and a three-dimensional perspective.

GPS METHOD

Differential GPS involves the use of two receivers collecting data simultaneously; one receiver over a known reference point and one receiver on an unknown point (static) or on a moving platform (kinematic). The GPS solution is affected by error in the satellite orbits, satellite clocks, receiver clocks, and deliberate signal degradation by the U.S. Department of Defense (Selective Availability, or SA) (Wells et al., 1987). When the reference receiver is over a known reference point the receiver determines the error in the satellite signals and in post processing these corrections are applied to the second receiver, provided the second receiver is within a given range (in this application <50 km). Differential kinematic GPS

allows position determination at the centimetre level (post processed) with accuracies of 0.5 cm plus one to two parts-per-million (ppm) of the baseline (Remondi, 1985).

GPS SURVEY PROCEDURE

Preparation

Two geodetic quality GPS receivers and two GPS antennas (one specifically for mobile data collection) were used. An antenna mount fabricated for the hovercraft consisted of a 10 foot board equipped with a removable 5/8" bolt. The board extended approximately 1.3 m to the side, beyond the

hovercraft's inflatable skirt. The extension allowed antenna height measurement while the hovercraft was at full inflation. In future processing, the antenna height will be subtracted from the GPS position to obtain the ground position.

Prior to mobile data collection an accessible reference point was established at the Canadian Coast Guard Station (CGS), Vancouver International Airport. The reference point co-ordinates were determined via a static differential survey tied to a first order survey marker in Steveston, approximately 9 km distant. The reference position is accurate relative to the Steveston marker at the sub-centimetre level. The accuracy of all mobile GPS solutions are relative to the established reference co-ordinates.

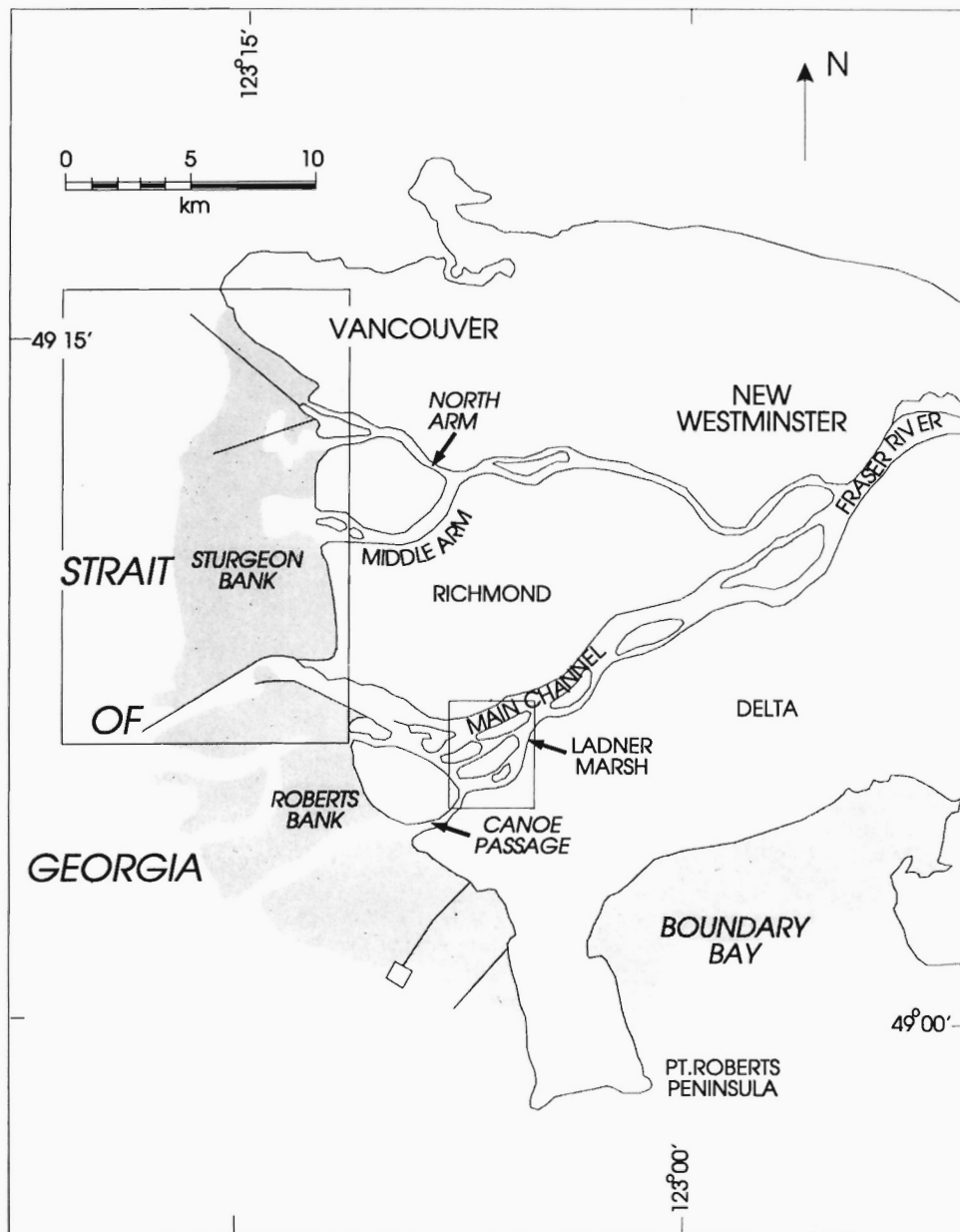


Figure 1. Fraser River delta, B.C. Large box encloses Sturgeon Bank survey area, small box encloses Ladner Marsh survey area.

Kinematic survey technique

The primary observable in centimetre-level kinematic positioning is the carrier phase. The carrier phase observable is the difference between the phase of the incoming carrier wave (from the satellite) and the phase generated inside the receiver (Morton and Leach, 1993). To precisely apply the corrections from the reference receiver to the mobile data, the baseline between the two GPS antennas, expressed as the exact number of carrier phase cycles, must be determined. This requires a few minutes of static data collection while the mobile antenna is over an initial starting or "index" point. When the baseline is fixed, the exact number of cycles of the carrier phase between the reference and mobile antenna is known and any subsequent motion is measured as the change in this cycle count (Fig 2). After indexing, the mobile solution requires that both receivers maintain continuous phase lock on a minimum of four common satellites throughout the survey.

Loss of phase lock with the satellite signal (a "cycle slip") can cause the solution to lose the correct integer number of cycles and hence the correct distance to that satellite. The solution must have the correct integer for at least four satellites throughout the solution in order to solve four equations (latitude, longitude, ellipsoid height, and time).

Kinematic survey #1

The first two surveys on DOY 211 and 212 were conducted to obtain ground elevations of Sturgeon Bank. The survey was thus conducted at very low tide.

The GPS solution provides a position for the antenna. To obtain the ground positions, the height of the antenna mounted on the hovercraft was measured before and after the survey. Height was fixed by keeping the hovercraft at full inflation during height measurement and while collecting transect positions. The index point was marked during height measurement. Because of horizontal drift due to wind and engine vibration, the hovercraft was stabilized with a forklift and a truck during indexing and height measurement. Antenna height was measured before and after data collection and varied -4.9 cm (DOY 211) and +6.4 cm (DOY 212).

The hovercraft traversed twelve transects between the Iona and Steveston jetties, spaced approximately 500 m apart (Fig. 3). Speed averaged 25 knots and each transect took an average of 10 minutes, providing close to 600 data points for each of the twelve transects. Survey time was 2 hours 14 minutes (DOY 211) and one hour 55 minutes (DOY 212).

Kinematic survey #2

The objective of the DOY 213 and 214 surveys was to provide precise in situ positions of vegetation species to ground truth airborne spectral imagery. In this application the elevations were less important than the latitude and longitude, and hovercraft height was not measured. The survey was conducted at high tide to allow access to vegetation growing on the banks of deep (approximately 4 m) tidal channels.

Data collection began with the mobile antenna on a survey tripod over an established index. The baseline between the mobile and reference antennas was fixed and the antenna was

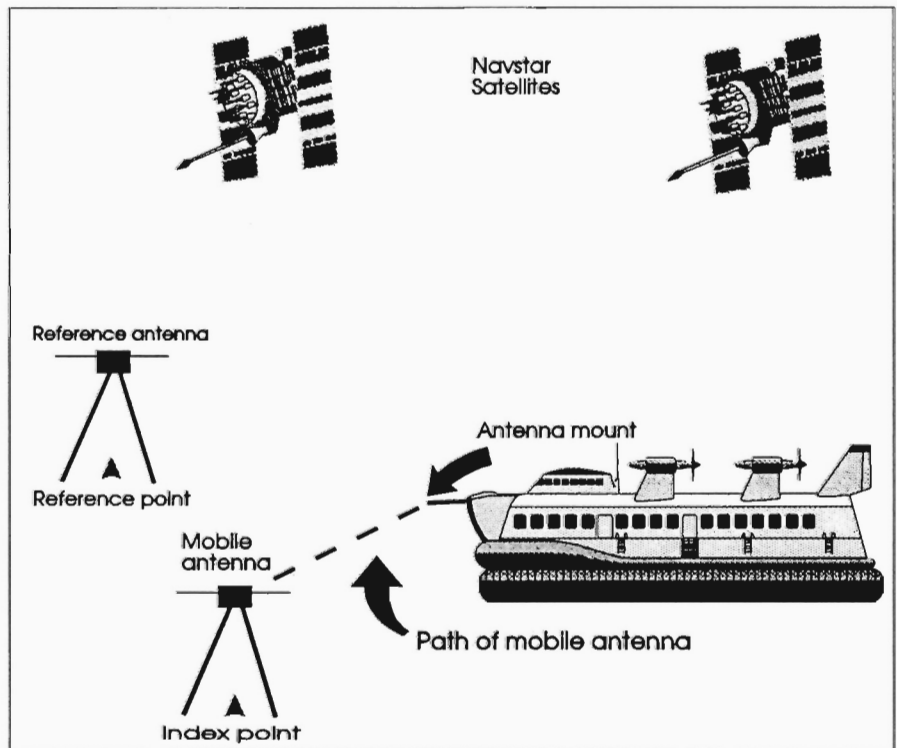


Figure 2.

Experiment configuration for DOY 213 and 214. Mobile antenna is indexed to fix baseline with reference. Path of mobile antenna represents one position per second.

moved to the hovercraft, which then travelled from CGS to Ladner Marsh (Fig. 1). Vegetation positions were obtained by stopping the hovercraft to collect samples, and by running transects through areas of homogenous vegetation (e.g., cattail beds).

DOY 213 survey took two hours 16 minutes and DOY 214 took one hour 14 minutes. During the two day survey over 890 discrete points were related to samples of 13 vegetation species.

Processing

Kinematic data were processed with the U.S. National Geodetic Survey OMNI processing software. The solution files contain the starting index position for the mobile antenna and an independent position solution for each second of data collection. The position solutions are expressed as delta values from the starting position. Thus, for each epoch the mobile antenna is over the index, the delta values are zero or close to zero, and during reoccupation of the index the delta values should again be zero or close to zero.

All positions are referenced to the WGS84 co-ordinate system. Elevations are height above the WGS84 ellipsoid model.

SURVEY RESULTS

The accumulated errors for DOY 213 are 0.2 cm north latitude, 0.8 cm east longitude and 0.1 cm height. For DOY 214 the accumulated errors are 2.2 cm north, 0.7 cm east, and 4.4 cm height. These were the residual errors in the kinematic solution after the initial index position was reoccupied.

On DOY 211 and 212, cycle slips in the mobile data caused tracking to drop below the required minimum of four satellites, effectively ending the survey before the index was reoccupied. This occurred near the end of each survey and no important data were lost. The error in the DOY 211 and 212 surveys are determined from the requirements of the post processing software. The solution algorithm cannot solve for a position unless the carrier phase is known to within

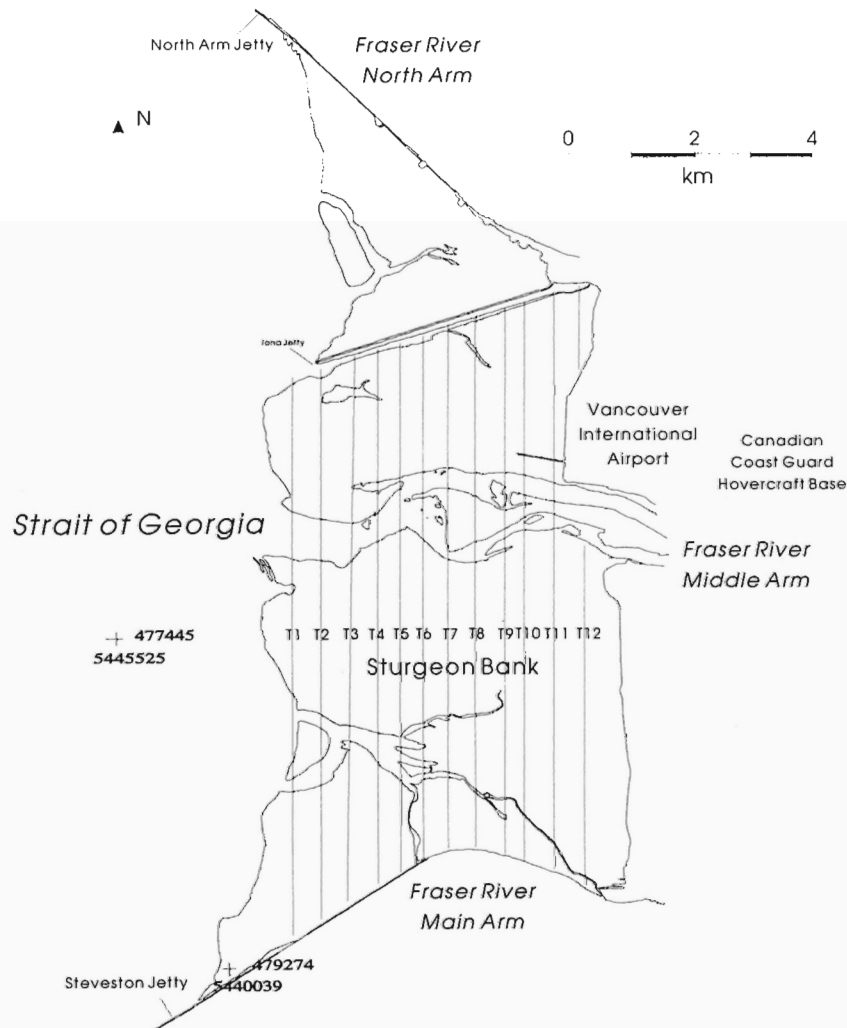


Figure 3. Approximate location of transect lines on Sturgeon Bank.

1/2 wavelength. The wavelength is 19 cm, therefore, the mobile positions are accurate to within 10 cm (M. Leach, Applied Research Laboratories, Austin, Texas, pers. comm., 1993).

DISCUSSION

This discussion focuses on factors which affected the accuracy of the GPS solution: indexing procedure, hovercraft speed, cycle slips, and the use of dual frequency receivers.

Indexing while measuring hovercraft height proved difficult. Despite stabilizing the hovercraft with both vehicle and forklift, horizontal drift hindered the accurate marking of the index point. It is easier to begin over a marked index and then transferring the antenna to the hovercraft. Spatial inaccuracies in occupying the index can result in a drift in what may appear to be good solutions.

Speeds above 40 knots require further stabilization of the hovercraft's antenna mount, as vibration at high speeds is thought to have contributed to the large number of cycle slips on DOY 213 and 214. Dual frequency receivers were used and the second frequency, which did not suffer the same amount of cycle slips, was used for DOY 213 and 214 solutions. Dual frequency receivers are recommended even for short baselines (<50 km) to provide data redundancy.

Cycle slips can also be caused by sharp sudden turns and by blockage of the satellite signal. On DOY 211 a sharp turn at the end of the survey caused the tracking to drop to less than four satellites, thus terminating the solution before the index could be reoccupied. On DOY 212, when returning to the hovercraft station, the vehicle came too close to the hanger and again the tracking dropped to three satellites. Provided the solution drops to three satellites only once, the solution can be processed backwards from the end up to that point, but if this happens more than once, the data between data epochs with less than 3 satellites are lost.

Current developments in processing software focus on fixing cycle slips, a procedure known as "on the fly" ambiguity resolution (G. Mader, National Geodetic Survey, pers. comm., 1993). When this processing technique is fully operational, initial cycle ambiguity can be resolved at any epoch and the kinematic survey will be less constrained by cycle slips and the need to index will be eliminated. This processing capability will have significant impact on the ease and accuracy of differential kinematic surveys.

In conclusion, this study demonstrates that kinematic surveys can provide a high density of positions at the centimetre level. The GPS equipment is easily adapted to vehicles like the hovercraft which are specifically designed for particular environments. These positions can be used for contour

maps and three dimensional models. Future GPS surveys can be compared to track sediment movement and changes in vegetation distribution.

ACKNOWLEDGMENTS

The members of the Canadian Coast Guard Search and Rescue, Hovercraft Unit provided cheerful assistance, patience and expertise. This study is indebted to Paul LeBlond from the Department of Oceanography at U.B.C. for covering the cost of the GPS equipment rental and to Stuart Nimmo of the Department of Fisheries and Oceans for costs of hovercraft fuel. John Luternauer from the Geological Survey of Canada provided the impetus for this survey. Rob Stevens contributed greatly to data collection. The authors thank Peter Mustard for the paper review and Bev Vanlier for her guidance.

REFERENCES

- Hoos, L.M. and Packman, G.A.**
1974: The Fraser River Estuary – status of environmental knowledge to 1974; Report of the Estuary Working Group, Environment Canada, Regional Board, Pacific Region, Special Estuary series no. 1, 518 p.
- Leick, A.**
1990: GPS Satellite Surveying; New York, Wiley, 352 p.
- Luternauer, J.L.**
1980: Genesis of morphologic features on the western delta front of the Fraser River, British Columbia – status of knowledge; in *The Coastline of Canada*, (ed.) S.B. McCann; Geological Survey of Canada, Paper 80-10, p. 381-396.
- Medley, E.**
1978: Dendritic channels and tidal flat erosion, west of Steveston, Fraser River delta, British Columbia; B.A.Sc. thesis, University of British Columbia, Department of Geological Sciences, Vancouver, 70 p.
- Medley, E. and Luternauer, J.L.**
1976: Use of aerial photographs to map sediment distribution and to identify historical changes on a tidal flat; in *Report of Activities, Part C*; Geological Survey of Canada, Paper 76-1C, p. 293-304.
- Morton, R.A. and Leach, M.P.**
1993: Monitoring beach changes using GPS surveying techniques; *Journal of Coastal Research*, v. 9, no. 3, p. 701-720.
- Remondi, B.W.**
1985: Performing centimetre-level surveys in seconds with GPS carrier phase: Initial results; *Journal of the Institute of Navigation*, v. 32, p. 194-208.
- Tupper, W.A.**
1977: A photogrammetric study of the morphology of the Fraser River delta intertidal zone; unpublished report for the Geological Survey of Canada for marine sciences section, Pacific Region, British Columbia Institute of Technology, 35 p.
- Wells, D.E., Beck, N., Delikaraoglou, D., Kleusberg, A., Krakiwsky, E.J., Lachapelle, G., Langley, R.B., Nakiboglu, M., Schwarz, K.P., Tranquilla, J.M., and Vanicek, P.**
1987: Guide to GPS Positioning; Canadian GPS Associates, Fredericton, New Brunswick.

Regional geology of the Cardston map area, Alberta¹

Daniel Lebel

Institute of Sedimentary and Petroleum Geology, Calgary

Lebel, D., 1994: Regional geology of the Cardston map area, Alberta; in Current Research 1994-A; Geological Survey of Canada, p. 231-236.

Abstract: Regional mapping of the Cardston area has recognized the southern extension of several new Upper Cretaceous stratigraphic units recently defined in the Crowsnest Pass area. They comprise the Lees Lake, Burmis and Pakowki formations (Alberta Group) and the Connelly Creek, Lundbreck and Drywood Creek formations (Belly River Group).

The eastern edge of the Rocky Mountain Foothills underlies the Cardston area. The Foothills in this area consist of a series of southwest-dipping, northeast-verging thrust faults deforming Upper Cretaceous strata. Although no major southwest-verging thrust fault was mapped near the edge of the Foothills belt, structural relationships observed on some outcrops and at the regional scale suggest the presence of a triangle zone with a complex kinematic history.

Résumé : La cartographie régionale de la région de Cardston a permis d'établir le prolongement vers le sud des unités stratigraphiques du Crétacé supérieur nouvellement définies dans la région de Crowsnest Pass. Celles-ci comprennent les formations de Lees Lake, de Burmis et de Pakowki (Groupe d'Alberta), ainsi que les formations de Connelly Creek, de Lundbreck et de Drywood Creek (Groupe de Belly River).

La marge est des contreforts des montagnes Rocheuses (Foothills) traverse la région de Cardston. Les Foothills de cette région consistent en une série de failles de chevauchement à pendage sud-ouest et à vergence nord-est impliquant des strates du Crétacé supérieur. Malgré qu'aucune faille de chevauchement importante à vergence sud-ouest n'ait été cartographiée aux abords de la marge est des Foothills, les relations structurales observées à certains affleurements et à l'échelle régionale laissent suggérer la présence d'une zone triangulaire ayant eu une histoire cinématique complexe.

¹ Southern Alberta NATMAP Program

INTRODUCTION

Bedrock mapping of the Cardston area (Fig. 1) represents one of the initial geological mapping projects of the new Southern Alberta NATMAP Program. This five-year project (1993-1998) will produce a new digital geoscience database for the eastern edge of the Cordillera in southern Alberta, comprising new bedrock geological maps and new cross-sections of subsurface structure established in co-operation with the petroleum industry using proprietary seismic information. New maps of the Quaternary geology will also be produced (Jackson, 1994). Field observations in the Cardston area have been designed with the building of such a digital database in mind, using a comprehensive data collection system including coded information about surveyed outcrops, rock lithologies (including composition, grain size, colour, sedimentary structures and bed thickness), and structural measurements. In the future, this information will be available interactively through the graphic interface of a Geographical Information System (GIS) product. Additional databases will include data about exploration wells, thermal maturation, fossil collections, till geochemistry, mineral deposits, rock analysis, measured stratigraphic sections and areal limits of previous work with bibliographical references.

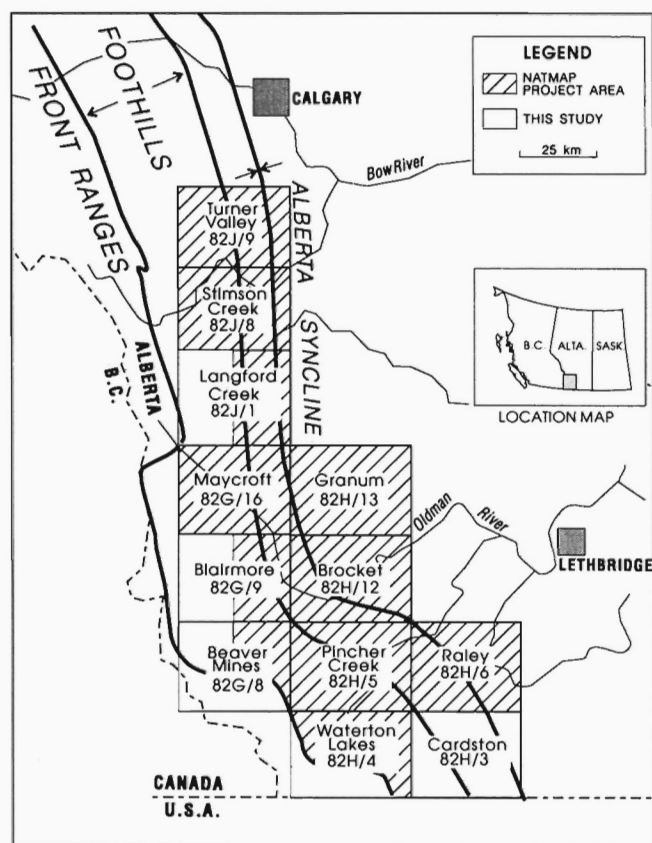


Figure 1. Location of the study area and the Southern Alberta NATMAP Program.

The Cardston map area (NTS 82H/3, Fig. 1) overlaps the southern Alberta Foothills and Alberta Plains geological divisions and lies immediately north of the Canada-U.S.A. border. The eastern part of the area is marked by the Alberta Syncline and the western flank of the Bow Island (Sweetgrass) Arch. Quaternary deposits are extensive in the area, and relief generally is less than 300 m. Good exposures are found along the banks of St. Mary River and Lee Creek (Fig. 2).

The Foothills belt in the western part of the area was previously mapped in detail (1: 31 680 scale) by Williams (1949). Remapping of the area was required to apply the new stratigraphic units within the Alberta and Belly River groups recognized recently by Jerzykiewicz and Norris (1993, in press) in the Crowsnest Pass (Blairmore) area to the north; to utilize recent petroleum industry seismic and well data; to construct cross-sections to create a new digital geological database; and to apply a modern kinematic framework. Geological mapping was conducted for two months in the summer of 1993. Observations were plotted on air photographs (1: 30 000 scale) and all data were compiled on a 1: 50 000 scale digital topographic base map. Available well and seismic data will be used in the future to outline the structure of the area at depth.

STRATIGRAPHY

Only Upper Cretaceous rocks are exposed in the Cardston map area (Fig. 2). The lower part of this segment of the regional stratigraphic column has been revised and redefined by Jerzykiewicz and Norris (1993, in press). Their six new stratigraphic units are used herein. The six new units overlying the Wapiabi Formation are, in stratigraphic order: the Lees Lake, Burmis and Pakowki formations (upper Alberta Group, Campanian), and the Connelly Creek, Lundbreck and Drywood Creek formations (Belly River Group, Campanian). Four other formations overlie the Belly River Group: the Bearpaw Formation (Uppermost Campanian), the Blood Reserve and the St. Mary River formations (Lower to Mid-Maastrichtian), and the Willow Creek Formation (Upper Maastrichtian) (Fig. 2, 3). Previously, Williams (1949) used the base of the Burmis Formation for the base of his Belly River Formation which ranged to the base of the Bearpaw Formation.

The Wapiabi Formation consists of dark grey marine shales and minor thin bedded siltstone, fine grained sandstone and calcareous sandstone. No complete section of this unit is exposed but it is estimated to be 154 m in the adjacent Waterton and Pincher Creek map areas (Douglas, 1951, 1952).

The Lees Lake Formation consists of a dark grey marine mudstone interbedded with light grey sandstone showing sedimentary structures typical of turbidity current deposits (e.g. Bouma sequence, syndimentary folding). This unit is in transitional contact with the underlying Wapiabi Formation. It is usually poorly exposed in the Cardston area. The best exposure is found along Lee Creek, in the immediate hanging wall of the Ockey thrust (Fig. 2) where its measured thickness is 74 m. The turbidites observed in this formation have been interpreted as symptomatic of the early Laramide tectonic activity (Jerzykiewicz and Norris, 1993, in press).

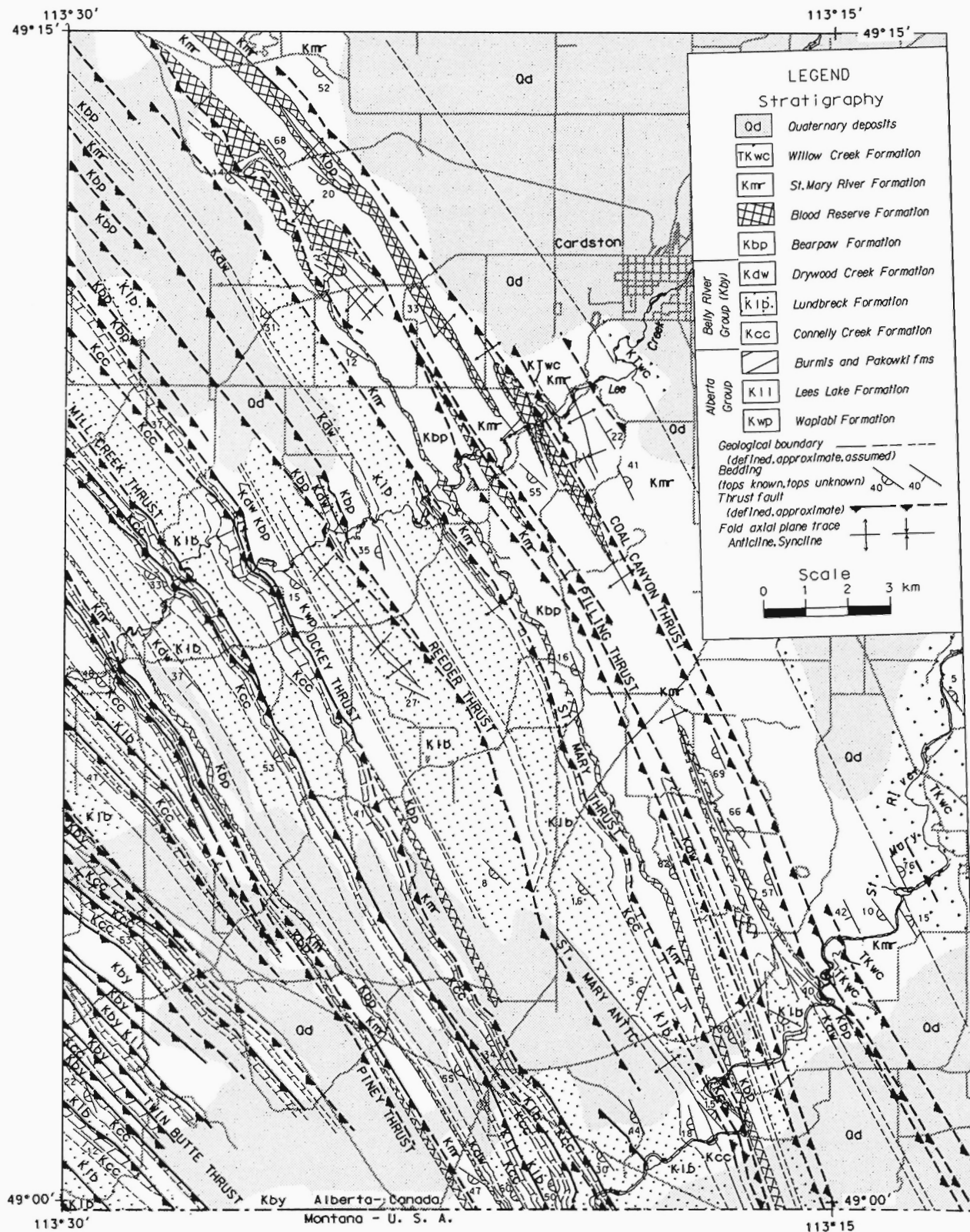


Figure 2. Geological map of the west half of the Cardston map area (NTS 82 H13).

The Burmis Formation is in sharp contact with the underlying Lees Lake Formation. It consists of fine grained, light grey, resistant sandstone forming persistent ridges throughout the area. This unit is characterized by 1 to 3 m cycles of crossbedded, light grey weathering, and soft sandstone beds, capped by more resistant 30 cm to 1 m thick brown weathering concretionary and iron-bearing calcareous sandstone beds. These beds are locally associated with lenses of magnetite-bearing sandstone. These lenses have also been observed near Crowsnest Pass and described by Mellon (1961). Wood prints and fragments are locally observed. The Burmis Formation varies from 20 to 43 m thick. It has been interpreted as a marine shoreline deposit (Williams, 1949) situated ahead of a strand plain (Rosenthal and Walker, 1987) within a large delta system fed by a distributary channel throughout the Crowsnest re-entrant (Jerzykiewicz and Norris, in press).

The overlying Pakowki Formation is a recessive, dark greenish grey marine shale, only observed in outcrop along the St. Mary River, where it is about 10 m thick. The top of this unit marks the contact between the Alberta Group and the overlying Belly River Group (Jerzykiewicz and Norris, in press).

The Connelly Creek Formation is composed of concretionary fine- to medium-grained, grey to greenish grey sandstone, showing crossbedding and commonly wood, plants and coaly fragments. This unit is more recessive than the Burmis Formation because its sandstones are usually not well cemented and are interbedded with 10 cm to 3 m thick mudstone intervals. Locally, coquinas composed of freshwater gastropods are exposed near the top of the unit. The Connelly Creek Formation is rarely well exposed. Good exposures are found along Lee Creek in the hanging wall of the Ockey thrust, and along the St. Mary River (Fig. 2). Thicknesses of close to 100 m were measured in both places. This unit is interpreted as a fluvial sediment deposited on the upper delta-plain (Jerzykiewicz and Norris, in press).

The Lundbreck Formation is composed mainly of greenish grey mudstone, and is recognized by the common occurrence of concretions and continuous layers of limestone of pedogenic origin (Jerzykiewicz and Sweet, 1988; Jerzykiewicz and Norris, in press). A few fine- to coarse-grained channelized sandstone bodies, usually less than 5 m thick, are also present, embedded within the caliche-bearing mudstone. No complete section of the Lundbreck Formation has been observed in the Cardston area, but preliminary structure cross-sections suggest a thickness of between 300 and 500 m. This formation is interpreted as a terrestrial alluvial fan deposit (Jerzykiewicz and Norris, in press).

The Drywood Creek Formation is composed of fine grained sandstone interbedded with about an equal proportion of greenish grey mudstone beds. The sandstone beds are mostly less than 1 m thick, and show current ripples, parallel laminations, crossbedding, wood fragments and some concretions. The unit locally contains coaly lenses or coal beds up to 2 m thick, as exposed in the hanging wall of the Reeder thrust, along Lee Creek (Fig. 2). The formation is estimated to be at least 50 m thick. The upper contact is situated at the base of an oyster-bearing coquina within the Bearpaw Formation. The Drywood Creek formation is interpreted as a transitional

facies between the alluvial plain facies of the Lundbreck Formation and the open marine sediments of the Bearpaw Formation (Jerzykiewicz and Norris, in press).

The Bearpaw Formation consists of dark brownish grey marine mudstones, interbedded with a few very fine- to fine-grained, thin sandstone beds. A number of rusty limestone concretions, up to 1 m in diameter are also present at several horizons. The thickness of the formation is difficult to assess because it is commonly folded and crosscut by thrust faults and is rarely completely exposed. The thickest observed section measures about 80 m, along the St. Mary River, in the hanging wall of the Coal Canyon thrust.

The Blood Reserve Formation is characterized by a resistant fine- to medium-grained, light grey sandstone, which appears as massive or crossbedded, 1 to 3 m thick beds. A distinctive feature is the presence of oyster-bearing coquina

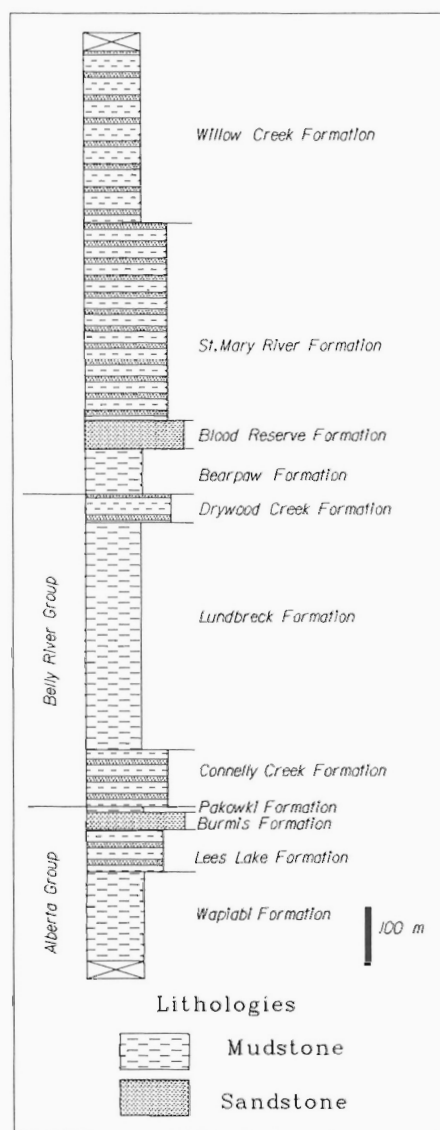


Figure 3. Schematic stratigraphic column of the Cardston area.

beds up to 3 m thick that interfinger with the sandstone layers or lenses. Laterally, these coquina lenses can disappear abruptly and are thin in most locations. Other coquina and some coal beds present in the lower part of the overlying St. Mary River Formation also serve as useful key beds to map the Blood Reserve Formation, which varies in thickness from 30 to 80 m. The formation is interpreted as a marine shoreline facies (Williams, 1949; Nadon, 1988).

The St. Mary River Formation is composed of fine grained, light greenish grey sandstone interbedded with greenish grey mudstone (Fig. 3). The proportion and thickness of the sandstone beds vary from small and thin bedded in the lower and upper part of the formation to dominant and thick bedded in the central part. This central part is also characterized by large, channel-fill sandstone bodies, showing crossbedding and current ripples, and with rip-up clasts and fresh water molluscs at the base of some of the beds. This unit is best exposed along the St. Mary River below the Coal Canyon Thrust (Fig. 2). Its thickness is estimated to be about 350 m (Williams, 1949). The St. Mary River Formation is interpreted as a fluvial deposit (Nadon, 1988).

The contact between the Willow Creek Formation and the St. Mary River Formation is defined by the first appearance of a buff weathering, fine grained sandstone associated with red, green and dark grey mudstones. The Willow Creek Formation is characterized by a predominantly pelitic composition in which green, red, and dark grey mudstones are represented in about the same proportions. Fine grained, buff weathering sandstone in channel-fills makes up the remaining 25 to 40 per cent of the formation. The dark grey mudstone layers bear caliche nodules, which appear to have been transported and redeposited by debris flows. The upper part of the Willow Creek Formation, dominated by greenish grey mud-

stones (T. Jerzykiewicz, pers. comm., 1993) of Early Paleocene age, is not exposed in the Cardston area. The estimated preserved thickness of this formation is 300 m.

STRUCTURAL GEOMETRY OF THE FOOTHILLS FROM SURFACE GEOLOGY

The general structure of the Foothills Belt in the Cardston area comprises a series of northeast-verging, southwest-dipping thrust sheets. Most of the faults are recognized by successive structural repeats of the resistant sandstones of the Burmis and/or Blood Reserve formations. From southwest to northeast, some of the more prominent faults have been labeled Twin Butte, Piney, Mill Creek, Ockey, St. Mary and Coal Canyon thrusts (Fig. 2).

Geometry of the frontal zone

For most of the Foothills of the Canadian Cordillera, a triangle zone is usually recognized, where a west-verging panel overlies the edge of the deformed belt along an upper décollement (Jones, 1982; Price, 1986; P.A. MacKay, unpub. thesis, 1991; D. Lebel, unpub. thesis, 1993). In the Cardston area and farther south in Montana (Mudge and Earhart, 1983) no such triangle zone has been discussed or recognized to date in the scientific literature. At the eastern edge of the Foothills belt in the Cardston area, most important faults are northeast-verging and only a few west-verging backthrusts with relatively small displacement are observed. Only a few kilometres to the northwest of the Cardston map area, cross-sections presented by Gordy et al. (1977, fig. 11b, 14), based on well and seismic data interpretation, suggest that the triangle zone still exists

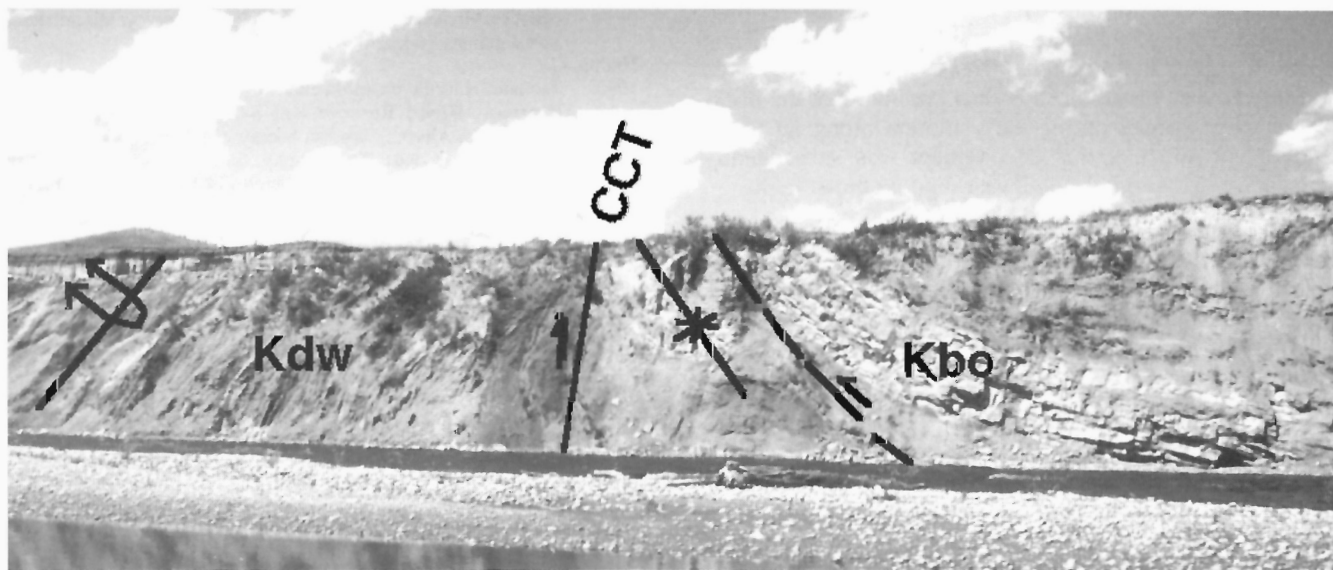


Figure 4. Coal Canyon Thrust (CCT) as observed along the St. Mary River, upstream from Coal Canyon Creek. Note the opposite vergence of structures on opposite sides of the Coal Canyon thrust. Kdw, Drywood Creek Formation; Kbo, Blood Reserve Formation; CCT, Coal Canyon Thrust. UTM location: 335372, 5434403.

there with an upper décollement panel showing significant displacement. Field observations suggest that a triangle zone may have been present in the Cardston area for a period of time but most backthrusts have now been crosscut by east-verging faults.

Between the Ockey Thrust and the edge of the deformed belt to the east (Fig. 2), several macroscopic and mesoscopic folds are encountered, ranging from broad to tight. These folds are usually upright or overturned towards the northeast. Such folds are found in the hanging wall of the Pilling and Coal Canyon thrusts (Fig. 2) and are sometimes associated with backthrusts.

A good example is found along the St. Mary River, upstream from Coal Canyon Creek (Fig. 2, 4). There, the Drywood Creek Formation wraps around a northeast-verging overturned fold which is thrustured over the Blood Reserve Formation along the steeply dipping Coal Canyon Thrust (Fig. 4). In the footwall of this thrust, Blood Reserve Formation is duplicated along a minor southwest-verging, shallow northeast-dipping thrust associated with a southwest-verging asymmetric anticline-syncline fold pair. The opposing vergence of the folds found on each side of the Coal Canyon Thrust suggests that they were formed within different kinematic regimes. Because older beds are found on the west side than on the east side of the Coal Canyon Thrust, it favours the idea that this fault has crosscut the southwest-verging structures found in its footwall.

Locally southwest-verging and northeast-dipping thrust faults (backthrusts) are also found on the northeast limb of some of the upright folds. For example, along the St. Mary River, the St. Mary Anticline (Fig. 2) is a broad fold involving the Lees Lake, Burmis and Connelly Creek formations. The northeast limb of this anticline displays two subtle backthrusts involving the Connelly Creek Formation. A few hundred metres east of these faults, the northeast-verging, southwest-dipping St. Mary thrust fault displays a significant throw, bringing the Connelly Creek Formation over the St. Mary River Formation. It is thus possible that the backthrusts were formed during early motion along an upper décollement and that this décollement was subsequently crosscut by east-verging, southwest-dipping thrust faults.

It is worth noting that macroscopic folds are restricted to the zone situated near the edge of the Foothills belt in the Cardston area. The influence of the triangle zone kinematics upon the formation of these folds is not determined yet, but it is possible that these folds are related to the tightening of structures situated underneath an upper décollement panel prior to the appearance of steep, northeast-verging thrusts crosscutting this décollement.

Future work will involve examining seismic data in conjunction with deep exploration wells to follow the trajectories of the various thrust faults and thrust sheets at depth within the Mesozoic and Paleozoic sequences. This should provide a better understanding of the evolution and regional kinematic history of the frontal zone of the Foothills in the Cardston area.

ACKNOWLEDGMENTS

I wish to thank Gerren Saskiw for his assistance during the 1993 field season, and Margot McMechan for her helpful comments during the preparation of this paper.

REFERENCES

- Douglas, R.J.W.**
1951: Preliminary Map, Pincher Creek, Alberta; Geological Survey of Canada, Paper 51-22.
1952: Preliminary Map, Waterton, Alberta; Geological Survey of Canada, Paper 52-10.
- Gordy, P.L., Frey, F.R., and Norris, D.K.**
1977: Geological guide for the CSPG 1977 Waterton-Glacier Park Field Conference; Canadian Society of Petroleum Geologists, Calgary, Alberta, Canada, 93 p.
- Jackson, L.**
1994: Quaternary geology and terrain inventory, Foothills and adjacent Plains, southwestern Alberta: some new insights into the last two glaciations; in Current Research, 1994-A; Geological Survey of Canada.
- Jerzykiewicz, T. and Norris, D.K.**
1993: Evolution of the Laramide foredeep and adjacent thrust belt in southern Alberta; Geological Survey of Canada, Open File 2663, 96 p.
in press: Belly River Delta in the Crownsnest Embayment of the Colorado Sea, southern Canadian Cordillera; Cretaceous Research.
- Jerzykiewicz, T. and Sweet, A.R.**
1988: Sedimentological and palynological evidence of regional climatic changes in the Campanian to Paleocene sediments of the Rocky Mountain Foothills, Canada; Sedimentary Geology, v. 59, p. 29-76.
- Jones, P.B.**
1982: Oil and gas beneath east-dipping underthrust faults in the Alberta Foothills; in Geological Studies in the Cordilleran Thrust Belt, (ed.) R.B. Powers; Rocky Mountain Association of Geologists, v.1, p. 61-74.
- Mellon, G.B.**
1961: Sedimentary magnetite deposits of the Crownsnest Pass region, southwestern Alberta; Research Council of Alberta, Bulletin 9, 98 p.
- Mudge, M.R. and Earhart, R.L.**
1983: Bedrock geologic map of part of the northern disturbed belt, Lewis and Clark, Teton, Pondera, Glacier, Flathead, Cascade, and Powell counties, Montana; United States Geological Survey, Miscellaneous Investigations Series, Map I-1375.
- Nadon, G.**
1988: Tectonic controls on sedimentation within a foreland basin: the Bearpaw, Blood Reserve and St. Mary River formations, southwestern Alberta; Canadian Society of Petroleum Geologists field guide to Sequences, Stratigraphy, Sedimentology: Surface and Subsurface Technical Meeting, September 14-16, Calgary, Alberta, 84 p.
- Price, R.A.**
1986: The southeastern Canadian Cordillera: thrust faulting, tectonic wedging, and delamination of the lithosphere; Journal of Structural Geology, v. 8, p. 239-254.
- Rosenthal, L.R.P. and Walker, R.G.**
1987: Lateral and vertical facies sequences in the Upper Cretaceous Chungo Member, Wapiabi Formation, southern Alberta; Canadian Journal of Earth Sciences, v. 24, p. 771-783.
- Williams, E.P.**
1949: Preliminary Map, Cardston, Alberta; Geological Survey of Canada, Paper 49-3.

Geological Survey of Canada Project 930006

Quaternary geology and terrain inventory, Foothills and adjacent plains, southwestern Alberta: some new insights into the last two glaciations¹

Lionel E. Jackson, Jr.

Terrain Sciences Division, Vancouver

Jackson, L.E., Jr., 1994: Quaternary geology and terrain inventory, Foothills and adjacent plains, southwestern Alberta: some new insights into the last two glaciations; in Current Research 1994-A; Geological Survey of Canada, p. 237-242.

Abstract: The limits of the (last) Erratics Train Glaciation can be easily traced along the Foothills south of Highwood River. Its alpine glaciation was restricted to valley glaciers and cirques in the Plateau Mountain area. Till deposited during the penultimate Willow Creek Glaciation, however, is restricted to valley bottoms and flat topped ridges. The possibility that these were two distinct glaciations separated by tens or hundreds of thousands of years is strongly suggested by: differences in depths of weathering between tills deposited during the Willow Creek and Erratics Train glaciations; extensive erosion of Willow Creek till from all but level sites; low relief on till surfaces, abundant ventifacts and paucity of kettle lakes on Willow Creek Glaciation surfaces relative to Erratics Train Glaciation surfaces; and the eroded state of cirques that fed Willow Creek glaciers in the Foothills. Paleomagnetism and fossil periglacial features are being tested as tools for stratigraphic correlation and demonstration of the significant hiatus between Willow Creek and Erratics Train glaciations.

Résumé : Les limites de la (dernière) Glaciation d'Erratics Train peuvent facilement être suivies le long des Foothills, au sud de la rivière Highwood. Cette glaciation alpine a été limitée à des glaciers de vallée et de cirque dans la région du mont Plateau. Le till déposé pendant la pénultième Glaciation de Willow Creek est confiné au fond des vallées et aux crêtes à sommet plat. La possibilité que la Glaciation d'Erratics Train et la Glaciation de Willow Creek soient deux glaciations distinctes séparées par des dizaines ou des centaines de milliers d'années ressort nettement : des différences dans la profondeur d'altération des tills attribués à ces deux glaciations; de l'érosion étendue du till associé à la Glaciation de Willow Creek, qui est disparu partout sauf sur les surfaces horizontales; du faible relief des surfaces des tills, de l'abondance des cailloux façonnés par le vent et de la rareté des lacs de kettle sur les surfaces affectées par la Glaciation de Willow Creek par rapport à celles de la Glaciation d'Erratics Train; et de l'érosion des cirques qui ont alimenté les glaciers de la Glaciation de Willow Creek dans les Foothills. Le paléomagnétisme et les caractéristiques périglaciaires fossiles font l'objet d'une vérification comme outils de corrélation stratigraphique et de démonstration de l'existence d'un hiatus important entre la Glaciation de Willow Creek et la Glaciation d'Erratics Train.

¹ Southern Alberta NATMAP Program

INTRODUCTION

Field mapping of the surficial geology of the Foothills of southwestern Alberta and contiguous areas of the Interior Plains and the Rocky Mountain Front Ranges was undertaken during July and August 1993, as part of Canada's National Geoscience Mapping Program (NATMAP) aimed at the bedrock and surficial geology of this region. A total of thirteen 1:50 000 areas will be mapped over three field seasons as part of this project (Fig. 1). The project also incorporates sampling of the geochemistry and carbonate content of glacial till. These have applications in mineral exploration and evaluation of the potential of acid rain to damage soil and surface and ground waters.

Surficial geology mapping has a wide range of applications in land use planning and natural resource protection and conservation in the Foothills region. Examples include the siting of sanitary landfills, protection of wells from pollution, augmentation of existing sand and gravel inventories, more characterization of soil textures, and a complete inventory of landslides in the region, the principal geological hazard. Protection of ground water is of particular concern because of drought conditions in recent years.

Maps produced by this and all mapping projects under NATMAP will be available as computer files as well as traditional paper products. In addition, all field notes will be available as interactive database files. The formats of map and database files are currently being decided. Maps are being prepared as AutoCAD release 12 drawings and field notes have been entered into FIELDLOG, an interactive database developed by the Geological Survey of Canada and the Ontario Geological Survey. Tables listing such variables as lithology, sample description, and stratigraphy are linked by field station number.

The surficial geology of the region is presently mapped at a scale of 1:250 000 from work dating from the 1950s and 1960s. Remapping this region at a more detailed scale will result in both maps and an understanding of the surficial geology that are more accurate, detailed, and useful. Furthermore, the record of multiple, overlapping glaciations of the Foothills by the Laurentide and Rocky Mountain provenance ice sheets (e.g., Dawson, 1885; Dawson and McConnell, 1895; Douglas, 1950; Stalker, 1963; Alley, 1973) needs to be re-examined in light of the significant increase in the understanding of glacial sediments and stratigraphy gained over the past three decades through the study of contemporary glacial sedimentary environments. Sediment correlation and dating

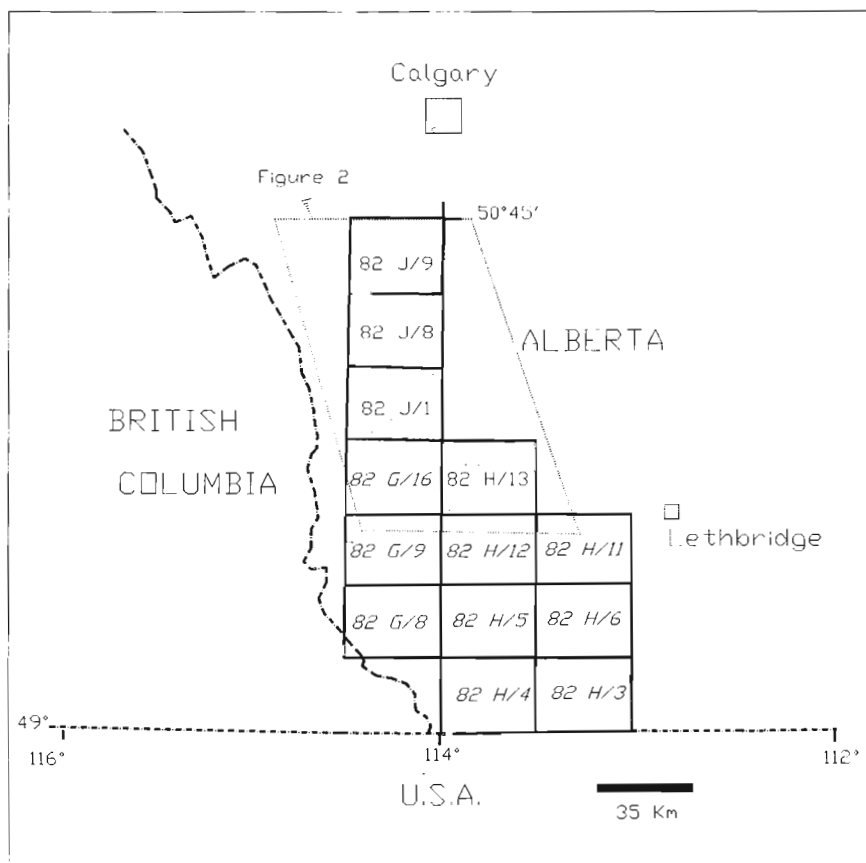


Figure 1. Area to be covered by terrain inventory mapping as a part of the Southern Alberta NATMAP Program. Stippled areas were covered during the 1993 field season.

techniques, such as paleomagnetism, have not been applied to the exposures of tills and interstratified sediments exposed in major valleys in the region. Key exposures of sediments thought to represent multiple glaciations will be re-examined by new techniques to improve correlation and allow a detailed understanding of Foothills glacial history.

ERRATICS TRAIN AND WILLOW CREEK GLACIATIONS

Four areas were mapped during 1993, including 82 J/1 (Langford Creek), 82 J/8 (Stimson Creek), 82 J/9 (Turner Valley), and 82 H/13 (Granum). Deposits from the last two glaciations are distributed widely within these map areas. These two glaciations have been named the Erratics Train (the younger) and the Willow Creek (the older) glaciations by Jackson (1980). The Erratics Train Glaciation was named for the Foothills Erratics Train, a narrow belt of large, angular quartzite boulders which have their source in the Rocky Mountains near Jasper (Stalker, 1956; Mountjoy, 1958; Roed et al., 1967; Jackson, 1993). The Foothills Erratics Train marks approximately the former boundary between ice of the Laurentide Ice Sheet and montane provenance glacial ice during the last (Late Wisconsinan) glaciation.

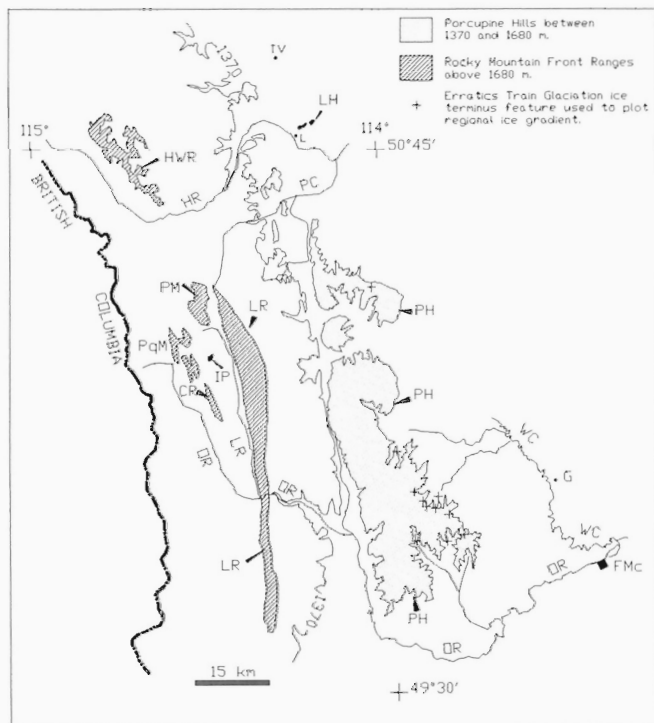


Figure 2. Geographic reference map of areas covered during the 1993 field season. The 1370 m contour approximates the eastern edge of the Foothills. Towns and cities: L, Longview; TV, Turner Valley; G, Granum; FMc, Fort MacLeod. Rivers: LR, Livingstone River; OR, Oldman River; WC, Willow Creek; PC, Pekisko Creek; HR, Highwood River. Mountains: LH, Longview Hill; HWR, Highwood Range; PM, Plateau Mountain; PqM, Pasque Mountain; IP, Isola Peak; CR, Cabin Ridge; PH, Porcupine Hills.

The Willow Creek Glaciation (WCG) was named by Jackson (1980) for the glaciation that deposited till, glaciofluvial and glacial lake deposits in the upper Willow Creek basin above the limits of the Erratics Train Glaciation (Douglas, 1950; Alley, 1973; Alley and Harris, 1974). It is equivalent to the "Glacial Episode 2" term used informally by Alley (1973) and Harrison (1976)

Erratics Train Glaciation

During the Erratics Train Glaciation (ETG), coalesced glacial ice from the Rocky Mountains (bearing the Foothills Erratics Train) and the Laurentide ice sheet travelled south and southwest along the Foothills. It pushed up Foothills valleys that were free of ice (Jackson, 1980; Jackson et al., 1989). In the Turner Valley and Stimson Creek map areas (82 J/9 and 82 J/8), most of the terrain north of the Highwood River was covered by glacial ice. Clasts of purple banded quartzite of the Gog Group and equivalent formations, in addition to the Foothills Erratics Train, mark the extent of ice from the Rocky Mountain Main Ranges. Main Ranges quartzite clasts are found atop Longview Hill and similar Foothills' ridges in excess of 1400 m. The quartzite is lacking in deposits of the Willow Creek Glaciation which are entirely of Rocky Mountain Front Ranges origin. South of Highwood River in 82 J/8, 82 J/1 and 82 H/13, the limits of the Erratics Train Glaciation extend up valleys within the Foothills and Porcupine Hills. This digitate limit can be traced clearly on the ground and on airphotos by the upper limits of: unweathered and continuous till, well defined former ice-walled channels, deltas graded to ice-dammed lakes, abundant kettle lakes, hummocky moraine, and cross divide channels.

In the basins of Stimson and Pekisko creeks where regional slope toward the Interior Plains is gentle, ice pushed well into the Foothills but reached an elevation of only about 1400 m. However, farther east and south, ice reached 1460 m at the north end of the more precipitously rising Porcupine Hills. The upper limit of Erratics Train Glaciation ice can be clearly traced along the eastern margin of the Porcupine Hills in 82 H/13; it descends from 1460 m at the north margin to 1400 m at the south end, a descent of about 0.7 m/km (Fig. 2). Along the south side of the Porcupine Hills, where the ice pushed into the broad lowland of the Oldman River valley and its tributaries, the gradient markedly increased by a factor of about 10. Completion of this mapping project should provide data to contour the Laurentide Ice Sheet during Erratics Train Glaciation in the vicinity of the Foothills and aid in the modelling of its paleoflow dynamics.

Within the map areas that include the Rocky Mountain Front Ranges, alpine glaciation during Erratics Train Glaciation was confined to the Plateau Mountain area which supported cirque and local valley glaciers. Figure 3A plots the orientation of cirques, within 45° divisions of the compass, and elevations of cirque floors which were active during the Erratics Train Glaciation in the Plateau Mountain area in 82 J/1 and 82 J/8 and in the Highwood Range immediately west of 82 J/9. These cirques lack dendritic drainage systems (characteristic of cirques active only during Willow Creek Glaciation) and clearly fed valley glaciers which advanced

from the cirques. The lower limit of cirques at about 2050 m elevation provides an estimate of the firm line in the Foothills during Erratics Train Glaciation. Cirques active during Willow Creek Glaciation and below 2050 m were not reoccupied during Erratics Train Glaciation. The extent to which valley glaciers advanced from Plateau Mountain was quite asymmetric. Ice descended to about 1830 m on the south-oriented Livingstone River valley and about 1600 m in upper Pekisko Creek on the north side of Plateau Mountain.

Willow Creek Glaciation

Till from the Willow Creek Glaciation (WCG) is preserved only on nearly level sites such as valley bottoms or flat-topped ridges (which are common in the Porcupine Hills) or where it has been buried beneath Erratics Train Glaciation sediments. Relief on morainal surfaces is usually less than 2 m over distances of 10 m or more. Kettle lakes are rare and very small relative to those seen within the limits of Erratics Train Glaciation. The difference in depth of weathering between tills deposited during the two glaciations is significant. Most of the clasts found within till along the east side of the Porcupine Hills are friable sandstones and shales of the early Tertiary and upper Cretaceous Porcupine Hills, Willow Creek and St. Mary River formations. Although these are largely disaggregated within the upper 50 cm in Erratics Train till,

clasts are readily recognizable. In contrast, excavation of at least 60 cm is required before any recognizable clasts of local bedrock are discernable or erratic pebbles from the Canadian Shield are seen in abundance in areas underlain by Willow Creek till. Clasts encountered down to this depth are usually wind sculpted pebbles (ventifacts). These clasts are also found within the upper 10 to 20 cm of recognizable till suggesting that significant overturning and mixing of the till sediments has occurred through agencies such as frost activity or bioturbation. Ventifacts rarely occur within the Erratics Train Glaciation limit and then only at the limit where catabatic winds were funnelled through cross divide gaps.

Observations on the distribution and lithology of sediments deposited during Willow Creek Glaciation largely corroborate the observations and conclusions of Douglas (1950), Alley (1973), Alley and Harris (1974), and Day (1971). Willow Creek Glaciation was a significantly more extensive glaciation than the Erratics Train Glaciation. The firm line dropped to at least 1680 m in the Foothills, based on the lowest elevation of cirques seen within the map areas (Fig. 3B). This produced a significantly different pattern of ice flow from that of the subsequent Erratics Train Glaciation. Till with uniquely Front Ranges and Foothills pebble lithology is exposed along the Highwood River 45 km east of the nearest cirque (Fig. 4). Whereas the Livingstone River valley south of Plateau Mountain was ice-free during Erratics Train

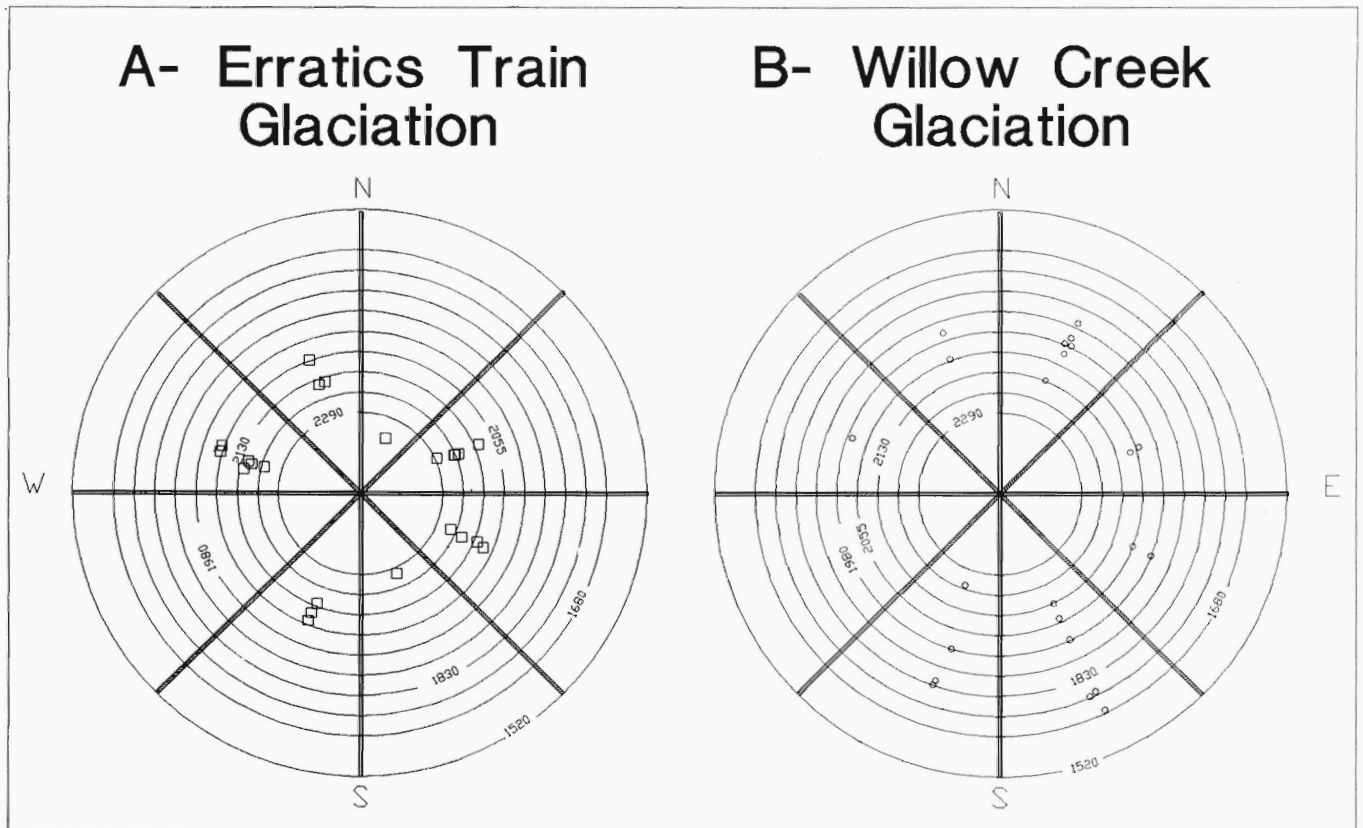


Figure 3. Orientation and cirque-floor elevations of cirques active during (A) Erratics Train Glaciation and (B) Willow Creek Glaciation.

Glaciation, erratics within passes in the Livingstone Range document more than 350 m of ice which filled the valley and the Pasque Mountain-Isola Peak-Cabin Ridge area east of the valley and supported an extensive ice cap which sculpted the alpine glacial landforms that characterize the area. Ice spilled eastward across the Livingstone Range into the upper Willow Creek basin. It is not known how far to the east montane ice advanced in Willow Creek basin because evidence has been removed by subsequent advances from the east. Erratics from the Front Ranges cap ridges south of Chain Lakes Reservoir more than 100 m above the valley floor.

Laurentide till can be found as a continuous blanket on flat-topped ridges up to about 1550 to 1560 m along the eastern side of the Porcupine Hills. The 1560 m elevation is the upper limit of apparently fluvially cut gaps on ridges along eastern and northern margins of the Porcupine Hills. Above 1560 m, the hills are marked by tor-like features on ridges and scattered sorted-stone polygons occur on flat or gently sloping sites. However, sufficient control is not available on the upper limit of Willow Creek deposits to define the slope of the Laurentide Ice Sheet along the east side of the Porcupine Hills during the Willow Creek Glaciation.

Alley (1973) and Alley and Harris (1974) concluded that the culmination of advances of Laurentide and montane ice were out of phase during Willow Creek Glaciation (their "Glacial Episode 2"). Field observations corroborate this conclusion. Montane ice had to have been in retreat to permit the advance of Laurentide ice across the Porcupine Hills along the Willow Creek valley, and the ponding of Glacial Lake Westrup and Glacial Lake Oldman (Douglas, 1950; Alley and Harris, 1974) in the valley system between the Porcupine Hills and Livingstone Range.

AGE OF WILLOW CREEK GLACIATION AND PALEOMAGNETIC INVESTIGATIONS

No absolute ages are available for Willow Creek Glaciation but the possibility that it and Erratics Train Glaciation were two distinct glaciations separated by tens or hundreds of thousands of years is strongly suggested by: differences in depths of weathering of till; extensive erosion of till from all but level sites; low relief on till surfaces; abundant ventifacts and lack of kettle lakes between these two glaciations; and the

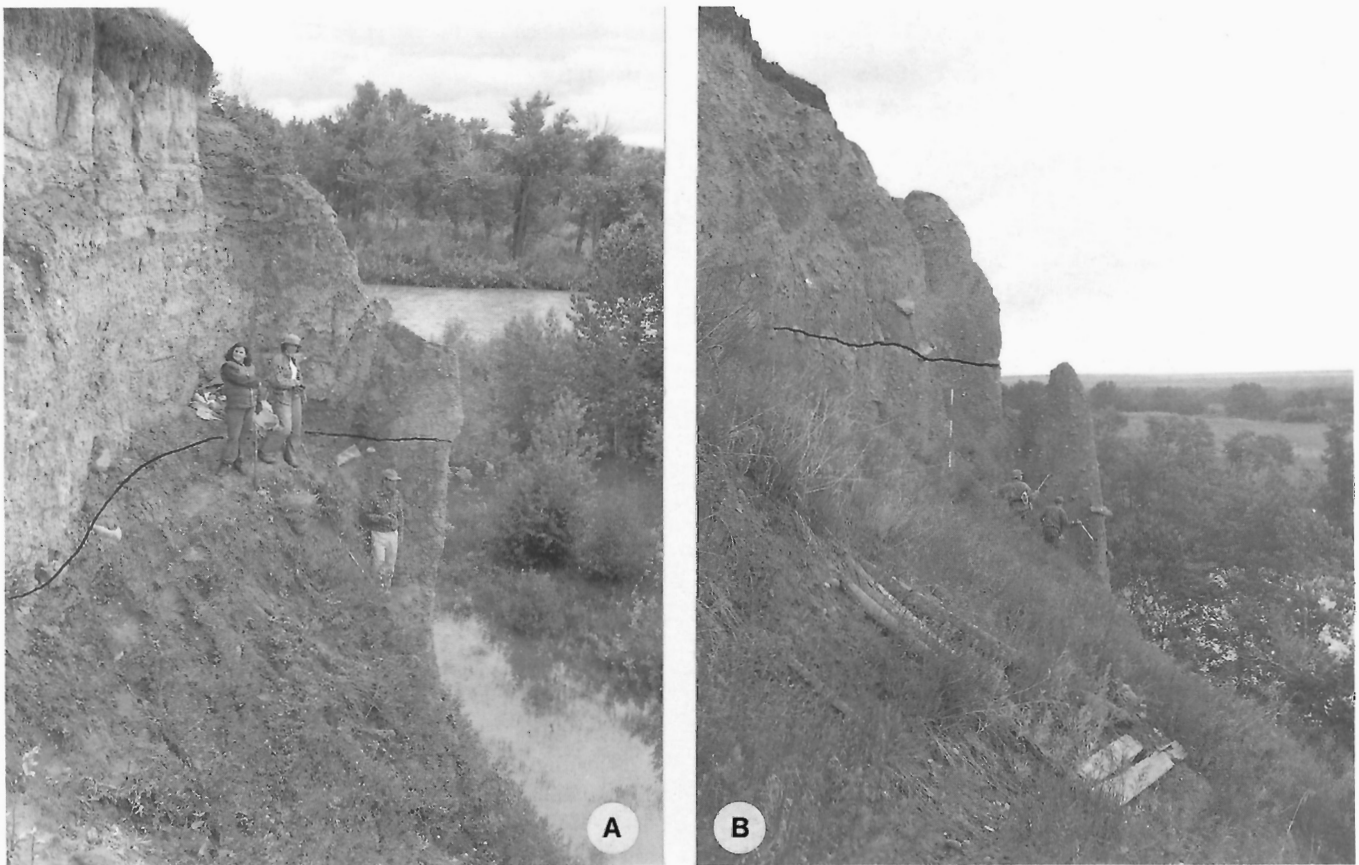


Figure 4. Till exposures with Front Ranges provenance correlated to the Willow Creek Glaciation along the Highwood River (A-UTM 11U 712500, 5604500; B-11U 708200, 5600700). They are overlain (line indicates contact) by till deposited during Erratics Train Glaciation which contains shield pebbles and purple-banded quartzites from the Main Ranges. The two tills have strong fabrics that parallel the Highwood River valley and are separated by sheared erosional contacts denoted by the line.

eroded state of cirques that fed Willow Creek glaciers in the Foothills. An observation of a periglacial feature noted may further indicate that Willow Creek sediments experienced at least one period of permafrost climatic conditions since their deposition. A well developed example of an ice wedge pseudomorph (a cast of an ice wedge) was noted in a Willow Creek Glaciation deltaic gravel at 1420 m elevation in the upper part of the Willow Creek basin (UTM 11U 695600, 5554200; Fig. 5). Ventifacts are common along the top of the exposure. To the author's knowledge, similar features have not been recorded within gravels deposited during the late Wisconsinan in the Foothills or elsewhere in southern Alberta. The presence or absence of such features will be of particular interest in examining gravels within the limits of these two glaciations during subsequent field seasons.



Figure 5. Ice-wedge pseudomorph developed within a former delta graded to Glacial Lake Westrup, a glacial lake ponded during the Willow Creek Glaciation. A dotted line has been drawn along the boundary between the sandy fill and the surrounding gravels. Divisions on the pole are approximately 30 cm.

An experiment was initiated during the field work in co-operation with R.W. Barendregt of the University of Lethbridge to determine the paleofields recorded within tills and lacustrine sediments of Erratics Train and Willow Creek glaciations. Assuming both were deposited during the Bruhnes normal Chron and that the data are suitable, they will be compared statistically in order to demonstrate whether sufficient secular variations have occurred to resolve them as separate glaciations and to determine if some measure of age difference can be assigned.

REFERENCES

- Alley, N.F.**
1973: Glacial stratigraphy and the limits of the Rocky Mountain and Laurentide ice sheets in southwestern Alberta, Canada; *Bulletin of the Canadian Society of Petroleum Geology*, v. 21, p. 153-177.
- Alley, N.F. and Harris, S.A.**
1974: Pleistocene glacial lake sequences in the Foothills, southwestern Alberta, Canada; *Canadian Journal of Earth Sciences*, v. 11, p. 1220-1235.
- Dawson, G.M.**
1885: Report on the region in the vicinity of the Bow and Belly Rivers, North West Territory; Geological and Natural History Survey of Canada, Report of Progress 1882-1883-1884, p. 1-169C.
- Dawson, G.M. and McConnell, R.G.**
1895: Glacial deposits of southwestern Alberta in the vicinity of the Rocky Mountains; *Bulletin of the Geological Society of America*, v. 7, p. 31-66.
- Day, D.L.**
1971: The glacial geomorphology of the Trout Creek area, Porcupine Hills, southwestern Alberta; MSc. thesis, Department of Geography, University of Calgary, Alberta, 158 p.
- Douglas, R.J.W.**
1950: Callum Creek, Langford Creek, and Gap map areas, Alberta; Geological Survey of Canada, Memoir 255, 124 p.
- Harrison, J.E.**
1976: Evolution of a landscape – the Quaternary Period in Waterton Lakes National Park; Geological Survey of Canada, Miscellaneous Report 26, p. 1-33.
- Jackson, L.E., Jr.**
1980: Glacial stratigraphy and history of the Alberta portion of the Kananaskis Lake map area; *Canadian Journal of Earth Sciences*, v. 17, p. 459-477.
1993: The Foothills Erratics Train: key to the Quaternary history of the Alberta Foothills; in *The Palliser Triangle*, (ed.) R.W. Barendregt, M.C. Wilson, and F.J. Jankunis; University of Lethbridge, Alberta, p. 63-76.
- Jackson, L.E., Jr., Rutter, N.W., Hughes, O.L., and Clague, J.J.**
1989: Glaciated fringe (Quaternary stratigraphy and history, the Canadian Cordillera); in Chapter 1 of *Quaternary Geology of Canada and Greenland*, (ed.) R.J. Fulton; Geological Survey of Canada, Geology of Canada no. 1 (also Geological Society of America, *The Geology of North America*, v. K-1).
- Mountjoy, E.W.**
1958: Jasper area, Alberta – A source of the Foothills Erratics Train; *Journal of the Alberta Society of Petroleum Geologists*, v. 6, p. 218-226.
- Roed, M.A., Mountjoy, E.M., and Rutter, N.W.**
1967: The Athabasca Valley erratics train, Alberta and Pleistocene ice movements across the continental divide; *Canadian Journal of Earth Sciences*, v. 4, p. 625-632.
- Stalker, A., MacS.**
1956: The erratics train, Foothills of Alberta; Geological Survey of Canada, Bulletin 37, 28 p.
1963: Quaternary stratigraphy in southern Alberta; Geological Survey of Canada, Paper 62-34, 52 p.

AUTHOR INDEX

| | | | |
|----------------------------|----------|------------------------------|-----------------|
| Aitken, J.A. | 225 | Journey, J.M. | 165 |
| Anderson, R.G. | 45 | Knight, R. | 211 |
| Archibald, D.A. | 177 | Lebel, D. | 231 |
| Brent, D. | 1 | Lewis, P.D. | 37 |
| Bull, K.F. | 45 | Lowe, C. | 19 |
| Chandler, F.W. | 123 | Lueck, B.A. | 77 |
| Clague, J.J. | 193 | Macdonald, A.J. | 37 |
| Crowley, J.L. | 131 | Mahoney, J.B. | 143, 165 |
| Currie, K.L. | 185 | Metcalfe, P. | 105 |
| Daubeny, P.H. | 45 | Mustard, P.S. | 87, 95 |
| Daughtry, K.L. | 117 | Patterson, K. | 25 |
| Davies, A.G.S. | 37 | Peterson, T.D. | 185 |
| Edwards, B.R. | 69 | Rea, J. | 211 |
| Enegren, E.G. | 57 | Read, P. | 143 |
| Evans, S.G. | 193 | Ricketts, B.D. | 201, 207, 211 |
| Feeny, T.D. | 217, 225 | Roots, C. | 1 |
| Friedman, R. | 87 | Russell, J.K. | 57, 69, 77, 151 |
| Garver, J.I. | 177 | Schaubs, P.M. | 131 |
| Gordey, S.P. | 11 | Seemann, D.A. | 19 |
| Green, D. | 25 | Simony, P.S. | 109 |
| Greig, C.J. | 45 | Stasiuk, M.V. | 151 |
| Gunning, M.H. | 25 | Stevens, R.A. | 11 |
| Haggart, J.W. | 159 | Stinson, P. | 109 |
| Halliday, D.W. | 19 | Thompson, R.I. | 117 |
| Hauksdóttir, S. | 57 | van der Heyden, P. | 87, 95 |
| Hearty, D.B. | 19 | Van Order, W.F., Jr. | 177 |
| Hickson, C.J. | 105, 143 | Woodsworth, G.J. | 207 |
| Hinderman, T.K. | 45 | Zieg, G.A. | 123 |
| Jackson, L.E., Jr. | 201, 237 | | |

NOTE TO CONTRIBUTORS

Submissions to the Discussion section of Current Research are welcome from both the staff of the Geological Survey of Canada and from the public. Discussions are limited to 6 double-spaced typewritten pages (about 1500 words) and are subject to review by the Chief Scientific Editor. Discussions are restricted to the scientific content of Geological Survey reports. General discussions concerning sector or government policy will not be accepted. All manuscripts must be computer word-processed on an IBM compatible system and must be submitted with a diskette using WordPerfect 5.0 or 5.1. Illustrations will be accepted only if, in the opinion of the editor, they are considered essential. In any case no redrafting will be undertaken and reproducible copy must accompany the original submissions. Discussion is limited to recent reports (not more than 2 years old) and may be in either English or French. Every effort is made to include both Discussion and Reply in the same issue. Current Research is published in January and July. Submissions should be sent to the Chief Scientific Editor, Geological Survey of Canada, 601 Booth Street, Ottawa, Canada, K1A 0E8.

AVIS AUX AUTEURS D'ARTICLES

Nous encourageons tant le personnel de la Commission géologique que le grand public à nous faire parvenir des articles destinés à la section discussion de la publication Recherches en cours. Le texte doit comprendre au plus six pages dactylographiées à double interligne (environ 1500 mots), texte qui peut faire l'objet d'un réexamen par le rédacteur scientifique en chef. Les discussions doivent se limiter au contenu scientifique des rapports de la Commission géologique. Les discussions générales sur le Secteur ou les politiques gouvernementales ne seront pas acceptées. Le texte doit être soumis à un traitement de texte informatisé par un système IBM compatible et enregistré sur disquette WordPerfect 5.0 ou 5.1. Les illustrations ne seront acceptées que dans la mesure où, selon l'opinion du rédacteur, elles seront considérées comme essentielles. Aucune retouche ne sera faite au texte et dans tous les cas, une copie qui puisse être reproduite doit accompagner le texte original. Les discussions en français ou en anglais doivent se limiter aux rapports récents (au plus de 2 ans). On s'efforcera de faire coïncider les articles destinés aux rubriques discussions et réponses dans le même numéro. La publication Recherches en cours paraît en janvier et en juillet. Les articles doivent être envoyés au rédacteur en chef scientifique, Commission géologique du Canada, 601, rue Booth, Ottawa, Canada, K1A 0E8.

Geological Survey of Canada Current Research, is released twice a year, in January and July. The four parts published in January 1994 (Current Research 1994- A to D) are listed below and can be purchased separately.

Recherches en cours, une publication de la Commission géologique du Canada, est publiée deux fois par année, en janvier et en juillet. Les quatre parties publiées en janvier 1994 (Recherches en cours 1994-A à D) sont énumérées ci-dessous et sont vendues séparément.

Part A: Cordillera and Pacific Margin
Partie A : Cordillère et marge du Pacifique

Part B: Interior Plains and Arctic Canada
Partie B : Plaines intérieures et région arctique du Canada

Part C: Canadian Shield
Partie C : Bouclier canadien

Part D: Eastern Canada and national and general programs
Partie D : Est du Canada et programmes nationaux et généraux